Journal of Biological Regulators & Homeostatic Agents
Volume 29, No. 1, January - March, 2015

CONTENTS

EDITORIAL

CAN VITAMIN A MEDIATE IMMUNITY AND INFLAMMATION?

E. SPINAS[1], A. SAGGINI[2], S.K. KRITAS[3], G. CERULLI[4], A. CARAFFA[5], P. ANTINOLFI[5], A. PANTALONE[6], A. FRYDAS[7], M. TEI[4], A. SPEZIALI[4], R. SAGGINI[8], F. PANDOLFI[9] and P. CONTI[10]

[1]Department of Surgery and Odontostomatological Sciences, University of Cagliari, Italy; [2]Department of Dermatology, University of Rome Tor Vergata, Rome, Italy; [3]Department of Microbiology and Infectious Diseases, School of Veterinary Medicine, Aristotle University of Thessaloniki, Macedonia, Greece; [4]Nicola's Foundation, Onlus, Arezzo, Italy; [5]Orthopedic Division, University of Perugia, Perugia, Italy; [6]Orthopedic Division, University of Chieti-Pescara, Chieti, Italy; [7]Aristotelian University, Thessaloniki, Greece; [8]Department of Neurosciences and Imaging, Faculty of Medicine and Surgery, G. d'Annunzio University Chieti-Pescara, Chieti, Italy; [9]Catholic University of Rome, Italy; [10]Immunology Division, Postgraduate Medical School, University of Chieti-Pescara, Chieti, Italy.

Received November 5, 2015 – Accepted February 27, 2015

Vitamins are natural components of foods and are organic compounds distinct from fat, carbohydrates and proteins. Vitamin A is the generic descriptor for compounds with the qualitative biological activity of retinol. Unlike beta-carotene, vitamin A is not an antioxidant and its benefit is related to possible boosting of immune reactions. The effect of vitamin A on immune function is wide-reaching and its deficiency appears to affect immunity in several ways. Innate and adaptive immune responses are affected in some way by lack of vitamin A. Retinoids seem to act on differentiation of lymphocytes, antibody production, phagocytosis of macrophages, NK, Treg, and T helper cell activity. In addition, in humans, signs of a vitamin A deficiency also include the dysregulation of cytokine/chemokine generation and release. However, excess of vitamin A has been demonstrated to have toxic effects in most species studied. Here we summarize some important effects of vitamin A in immunity and inflammation.

In 2600 B.C. beriberi was recognized in China and is probably the earliest documented vitamin deficiency disorder, and in 130-200 A.D. Soranus Ephesius provided a classical description of rickets. In 1492-1600 world exploration was threatened by scurvy, and Magellan lost four-fifths of his crew and Vasco da Gama lost 100 of his 160 men to this disease. Menkel J.F. in 1810 reported that malnourished patients were suffering from atrophy of the thymus. In 1951, Rickes and co-workers in the United States and Smith in England isolated vitamin B12, the last vitamin discovery, while the first was vitamin A in the twentieth century. The existence of nutritive factors such as vitamins and the beginning of the

Key words:vitamins, immunity, inflammation, cytokines, chemokines

Mailing address:
Prof. Enrico Spinas,
Department of Surgery and Odontostomatological Sciences,
University of Cagliari,
Cso Vittorio Emanuele 340,
09123 Cagliari, Italy
Tel.: +39 330412295
e-mail: enricospinas@tiscali.it

0393-974X (2015)

study of vitamins began in the twentieth century. In the early 1900's many scientists realized that diet does not consist only of carbohydrate, fat, protein and salt, but there had to be something else. The grouping of food is based on the nutrients they share. The vegetable group can provide several minerals along with folate, vitamin E, vitamin K and vitamin A; while fruit offers vitamin C, and potassium.

Nowadays, in developing countries malnutrition afflicts millions of people which affects the immune system and impairs the normal immune functions. Human nutrition deficiency including vitamins, occurs in endemic proportion in many developing countries and constitutes a serious health hazard (1). In addition, it is well known that infections are more common in under-nourished than in well-nourished persons.

Vitamins have pleiotropic functions in immune responses and cellular homeostasis and their activity is exerted through several action mechanisms. They are complex organic compounds required in micro or milligrams per day in diet to perform a normal physiological life. Certain vitamins are synthesized by the intestinal tract bacteria in adequate amounts necessary to our body. Vitamins are divided into two groups: a) water soluble and b) fat soluble. The first include the B-complex vitamins, and vitamin C, while the latter are vitamins A, D, E and K. Vitamins have also been identified by describing a function or its source and are necessary for normal synthesis and breakdown of body carbohydrates, fats and proteins.

Vitamins and other dietary components may influence various elements of several pathophysiological mechanisms and malnutrition may contribute in predisposing to immune disorders, while altered nutrition may be useful in therapy of such diseases. Therefore, vitamins and nutritional components have a strong influence on the immune system and several diseases induce dysregulation of the immune system, including immune cells and cytokine/chemokine generation (2). Vitamin deficiency is especially prominent in the elderly and might contribute to increased morbidity and mortality (3). Supplementation of high pharmacologic doses of vitamins may be useful for improving immune responses.

Authors suggest that dietary vitamins show improvements of inflammatory diseases in experimental animal models (4). They also recommend that a diet high in vitamins somehow plays a causal role in diseases, by reducing stiffness, swollen joints, joint pain, time to fatigue, the use of non-steroidal anti-inflammatory drugs and increasing grip strength and improved pulmonary function. Therefore, an increase in vitamin intake may be of benefit in inflammatory diseases and improve exercise capacity.

Vitamins are immunoregulatory compounds and have been suggested to have anti-inflammatory properties by inhibiting the products of arachidonic acid cascade such as prostaglandins (PGE2 and TXB2), and leukotrienes (LTB4 and SRS-A). They are also believed to inhibit pro-inflammatory and immune regulatory mediators, such as cytokines/ chemokines. However, some studies reported that they do not influence the concentration of cytokines in serum but did report decreased TNF-alpha and IL-8 levels (5).

Vitamins and their receptors have immunoregulatory and agonist activities influencing cytokine production. Cytokines are principal mediators of inflammatory and immune reactions and constitute a major class of proteins which enhance the functions of phagocytes, activate T lymphocytes and stimulate inflammatory responses (6). Chemokines are a large family of low molecular weight cytokines which provoke movement and migration of leukocytes (7). Vitamins may not only favour the induction of regulatory T cells (CD4+ CD25+), but can also enhance their recruitment to inflammatory sites, favoring the transcription and production of cytokines and chemokines (8).

It is well known that vitamins are important regulators of immunity and inflammation in addition to their role in cell homeostasis and metabolism. In particular, several vitamins exert pluripotent effects on adaptive immune functions such as T-cell activation and on the innate immune system which comprises macrophages and dendritic cells which are sentinels of the immune system and represent a heterogeneous cell population and induce and regulate T-cell responses (8). In addition, they can promote the development of regulatory T cells (Treg) with suppressive activity (9).

VITAMIN A

Vitamin A is found in foods of both plant and

SIGNS OF VITAMIN DEFICIENCY

- Growth inhibition
- Dermatitis, alopecia
- Weakness
- Hepatic diseases (steatosis)
- Ataxia
- Atrophy of the thymus
- Affects the immune system and impairs normal immune functions
- Affects cellular homeostasis
- Contributes to immune disorders and alters nutrition
- Favours pro-inflammatory properties
- Lack of modulation of cell proliferation and differentiation
- Regulates the generation of prostaglandins PGE2, TXB2, leukotriene B4 and SRS-A
- Regulates TNF-alpha and IL-8 levels
- Regulates Treg (CD4+ CD25+)
- Inhibition of synthesis and breakdown of the body carbohydrates, fats and proteins
- Failure of differentiation of epithelial cells
- Lack of regulation of neutrophils, monocytes, macrophages, NK cells, and lymphocytes
- Lack of effects on immune-cell precursors
- Lack of effect of antioxidant effects
- Lack of effect on reversing effects of damaged DNA and boosting immunity
- Lack of effect on phagocytic activity of macrophages
- Lack of effect on $CD11b^{+}$ dendritic cell progenitors in tissues
- Lack of effect on pro-inflammatory mediators like IL-6 and IFN-γ generated by T cell
- Lack of effect on production of anti-inflammatory mediator IL-4
- Lack of effect on mediation on production of Treg
- Lack of effect on Alzheimer's disease
- Lack of effect on chemokine CXCL10 (IP10), and lower IL-6 and IL-17
- Lack of effect on the inducing expression of FoxP3 in CD4 positive T cells
- Lack of effect on ROS
- Lack of effect on up-regulation of chemokine CCR3 transcription
- Lack of effect on endothelial inflammation
- Lack of effect on NADPH oxidase and NF-κB-dependent pathways
- Lack of effect on reducing MCP-1 generation

animal origin and is also needed for normal growth and reproduction. This vitamin itself does not occur in plant products but its precursor, carotene is present in several forms. Vitamin A includes retinol which binds the retinol binding protein and is transported through the circulatory system.

Vitamin A is converted to active retinoids by a series of oxidative reactions *in vivo*. Retinoids are

able to modulate cell proliferation, differentiation and morphogenesis. Vitamin A is known to be an essential nutrient which plays a vital role in vision, and its deficiency causes the skin to become dry and rough, and increases susceptibility to infectious diseases, because the linings of the gastrointestinal and respiratory tracts are damaged and cannot act effectively as barriers to keep bacteria from entering the body. Vitamin A participates in both innate and adaptive immune response induced by biological and non-biological insults and is important for a variety of biological functions including the development of healthy immune responses. Its derivatives (13-cis retinoic acid) are used to treat skin disorders such as acne. Research has shown that people who have a high intake of beta-carotene which has antioxidant properties, are less likely to develop cancer. In addition, vitamin A has also the possibility of reversing the effects of damaged DNA and boosting immunity.

In modulating innate immunity, vitamin A plays an important role on the regulation of neutrophils, monocytes, macrophages, natural killer (NK) cells, lymphocytes, and their precursors. Furthermore, it seems particularly determinant in the generation and duplication of $CD11b^+$ dendritic cell progenitors in tissues that perform protective functions and prevents the entry of microorganisms, increasing phagocytic activity of macrophages (10). However, these authors reported that vitamin A also elevated inflammatory cytokines such as TNF, and IL-1 beta and stimulated arachidonic acid cascade PGE2.

Recent data show that respiratory tract epithelial cells support vitamin A-mediated IgA production, and encourage the clinical testing of vitamin A supplements in vitamin A-deficient populations to improve mucosal immune responses toward respiratory tract pathogens (11).

Vitamin A along with D inhibit pro-inflammatory mediators like IL-6 and IFN-γ generated by T cells, and increase T-cell production of anti-inflammatory mediators, such as IL-4 and probably IL-10. In addition, it mediates the production of Tregs (12).

Metabolite of vitamin A, such as carotenoids (*trans*-retinoic acid), act on the cell by activating nuclear receptors namely retinoic acid receptors α, β and γ, and retinoid x receptors α, β, and *γ;* these effects activate or inhibit different genes and influence several pathways, including cellular metabolism and biosynthesis (13). The inflammatory response is always almost mediated by pro-inflammatory cytokines such as TNFα, IL1β, IL6, IL-33, etc. and chemokines as well as acute phase proteins, reactive nitrogen and oxygen species.

Supplementation of vitamin A induces an increase in the number of NK cells, inflammatory chemokine CXCL10 (IP10), lowers IL-6 and IL-17 in the circulatory system and decreases monocyte-derived ROS (10). ROS generated from activated leukocytes or from other sources may affect various biological molecules, provoking tissue damage that may have been prevented by vitamin A supplementation. Moreover, trans-retinoic acids and TGF-β1 may induce the expression of FoxP3 in CD4 positive T cells.

Retinoids, which are the sole specific vitamin A transporter in blood, are active metabolites of vitamin A that participate in a variety of biological processes. Current consensus holds that retinoids have an important role in the central nervous system, since retinoid receptors are expressed in the brain areas such as retrosplenial areas, hippocampus, and cortex.

Ueki S, et al. reported that retinoids participate in the differentiation of granulocyte and immunity and up-regulate the chemokine CCR3 transcription in retinoid-stimulated eosinophils using gene microarray, suggesting an important role of these compounds in the tissue accumulation of eosinophils (14). Other authors such as Farjo KM, et al. found that elevated levels of serum retinol-binding protein 4, the transport protein for retinol in the blood circulation, induce significant endothelial inflammation in human endothelial cells, showing that retinol-binding protein 4-mediated endothelial inflammation acts via NADPH oxidase- and NF-κB-dependent pathways (15).

Retinoids affect immunity in several ways and seem to act on the differentiation of lymphocyte subsets and phagocytosis of macrophages. They also affect the immune-surveillance of activated natural killer cells and T-helper cells, and influence the generation of cytokines/chemokines by immune cells. Vitamin A deficiency results in a failure of differentiation of epithelial cells without impairment of proliferation and squamous metaplastic changes

morphologically similar to pre-cancerous lesions.

Retinoids possess an anti-inflammatory effect *in vitro* and *in vivo* animal models with cellular protective action, probably by suppression of inflammatory cytokines/chemokines and other inflammatory mediators. Authors reported that retinoic acids, active metabolites of vitamin A, interact with TGF-beta to promote the differentiation of Treg, playing an important role in maintaining cellular homeostasis (16). Retinoids are currently in clinical use for the treatment of acne vulgaris, neuroblastoma, acute pro-myelocytic leukemia and psoriasis. Therefore, targeting their receptors, retinoids may reverse the above-mentioned inflammatory diseases.

We can conclude that vitamin A is an immune and inflammatory regulator (17), even if its exact role remains to be determined.

REFERENCES

1. Spinas E, Saggini A, Kritas SK, et al. Obesity, inflammation and neurological alterations. Eur J Inflamm 2014; 12:415-18.
2. Levine M. New concepts in the biology and biochemistry of ascorbic acid. N Engl J Med 1986; 314(14):892-902.
3. Venturini L, Perna S, Sardi F. Alzheimer's disease: from genes to nutrition. Eur J Inflamm 2014; 2:405-14.
4. Tardif JC. Antioxidants and atherosclerosis: emerging drug therapies. Curr Atheroscler Rep 2005; 7(1):71-7.
5. Stubbs JR, Idiculla A, Slusser J, et al. Cholecalciferol supplementation alters calcitriol-responsive monocyte proteins and decreases inflammatory cytokines in ESRD. J Am Soc Nephrol 2010; 21(2):353-61.
6. Spinas E, Kritas SK, Saggini A, et al. Role of mast cells in atherosclerosis: a classical inflammatory disease. Int J Immunopathol Pharmacol 2014; 27(4):517-21.
7. Kritas SK, Saggini A, Cerulli G, et al. Neuropeptide NGF mediates neuro-immune response and inflammation through mast cell activation. J Biol Regul Homeost Agents 2014; 28(2):177-81.
8. Gordon JR, Ma Y, Churchman L, Gordon SA, Dawicki W. Regulatory dendritic cells for immunotherapy in immunologic diseases. Front Immunol 2014; 5:7.
9. Shaik-Dasthagirisaheb YB, Varvara G, Murmura G. Role of vitamins D, E and C in immunity and inflammation. J Biol Regul Homeost Agents 2013; 27(2):291-5.
10. Weiskirchen R, Tacke F. Cellular and molecular functions of hepatic stellate cells in inflammatory responses and liver immunology. Hepatobiliary Surg Nutr 2014; 3(6):344-63.
11. Rudraraju R, Jones BG, Surman SL. Respiratory tract epithelial cells express retinaldehyde dehydrogenase ALDH1A and enhance IgA production by stimulated B cells in the presence of vitamin A. PLoS One 2014; 9(1):e86554.
12. Røsjø E, Myhr KM, Løken-Amsrud KI, et al. Increasing serum levels of vitamin A, D and E are associated with alterations of different inflammation markers in patients with multiple sclerosis. J Neuroimmunol 2014; 271(1-2):60-5.
13. Sodhi RK, Singh N. Retinoids as potential targets for Alzheimer's disease. Pharmacol Biochem Behav 2014; 120:117-23.
14. Ueki S, Nishikawa J, Yamauchi Y, et al. Retinoic acids up-regulate functional eosinophil-driving receptor CCR3. Allergy 2013; 68(7):953-6.
15. Farjo KM, Farjo RA, Halsey S, Moiseyev G, Ma JX. Retinol-binding protein 4 induces inflammation in human endothelial cells by an NADPH oxidase- and nuclear factor kappa B-dependent and retinol-independent mechanism. Mol Cell Biol 2012; 32(24):5103-15.
16. Seo GY, Jang YS, Kim HA, et al. Retinoic acid, acting as a highly specific IgA isotype switch factor, cooperates with TGF-β1 to enhance the overall IgA response. J Leukoc Biol 2013; 94(2):325-35.
17. Malek HA, Shata A. Effect of a high dose of vitamin D on a rabbit model of atherosclerosis. Int J Immunopathol Pharmacol 2014; 27(2):195-201.

DEVELOPMENT OF TWO *SALMONELLA*-BASED ORAL VACCINES AGAINST HUMAN RESPIRATORY SYNCYTIAL VIRUS

F. AZIZI JALILIAN[1,2], K. YUSOFF[1], S. SUHAIMI[1], R. AMINI[3], Z. SEKAWI[4] and F. JAHANSHIRI[1]

[1]Department of Microbiology, Faculty of Biotechnology and Biomolecular Sciences, Universiti Putra Malaysia, Malaysia; [2]Department of Medical Microbiology, Faculty of Medicine, Hamedan University of Medical Sciences, Hamedan, Iran; [3]Department of Microbiology, Faculty of Sciences, Islamic Azad University, Hamedan, Iran; [4]Department of Medical Microbiology, Faculty of Medicine and Health Sciences, Universiti Putra Malaysia, Malaysia.

Received April 25, 2014 – Accepted November 27, 2014

Human respiratory syncytial virus is the most common cause of bronchiolitis and other respiratory infections in infants and the elderly worldwide. We have developed two new oral vaccines using *Salmonella typhi* TY21a to carry and express the immunogenic epitopes of RSV fusion (F) and attachment (G) glycoproteins on its surface, separately. To evaluate the efficacy of the designed vaccines, BALB/c mice were orally immunized and then infected with RSV. Immune response analyses showed that cell-mediated, mucosal and humoral immunity in the vaccinated mice were significantly enhanced compared to the control group. Both vaccines generated a balanced Th1/Th2 immune response which is crucial for efficiency of vaccines against RSV. Furthermore, histopathological examination proved that these vaccines were safe as they did not cause any Th2-associated adverse effects in the lungs of RSV-infected mice. The findings of this research suggest that *Salmonella*-F and *Salmonella*-G vaccine candidates may have strong potential to prevent RSV infection.

Human respiratory syncytial virus is the leading cause of serious lower respiratory tract complications among infants and young children worldwide (1). This virus infects more than 70% of children in the first year of life and 100% of children by the age of 2 (2), where about 3% of infants under the age of 1 develop severe bronchiolitis or pneumonia which may result in hospitalization (3). RSV genome encodes for 11 proteins (4), of which F and G surface glycoproteins together with NS1 and NS2 non-structural proteins are key viral components involved not only in evasion of the host immune response but also in its infective cycle (5, 6).

The G protein, the major RSV attachment protein, is able to elicit neutralizing antibodies and mucosal immunity with the main epitope located between residues 124-226 (7, 8). The F protein is responsible for viral penetration and fusion of infected cells, which lead to syncytium formation. The F protein plays a pivotal role in protection against RSV infection by producing high titers of neutralizing antibodies and RSV-specific cytotoxic and T-helper lymphocytes (9). The antigenic region of the RSV F protein is located between residues 209-575 (10).

Key words: respiratory syncytium virus, immune response, th1, th2, cytokines, Salmonella, vaccine

Mailing address: Dr. Fatemeh Jahanshiri,
Department of Microbiology,
Faculty of Biotechnology & Biomolecular Sciences,
Universiti Putra Malaysia,
43400 UPM, Serdang, Selangor, Malaysia
Tel.: +603-89466724 Fax: +60389472595
e-mail: f.jahanshiri@gmail.com

0393-974X (2015)

Despite clear need and extensive research there is no vaccine against RSV. The development of an effective and safe vaccine has faced obstacles such as weak immunogenicity of RSV (11) and the immaturity of infants' immune systems and the presence of maternal antibodies as interfering agents against vaccination (12). Besides, the effects of some vaccines such as formalin-inactivated RSV induces a Th2-dominant response, which results in enhancement of the disease after exposure to natural infection (11-13).

Studies have shown that a protective and safe vaccine should be able to raise RSV-specific neutralizing antibodies, cell-mediated immunity, mucosal immunity and more importantly elicits a balanced Th1/Th2 immune response (14-16).

In regard to development of efficient RSV vaccines, a few Gram-positive and Gram-negative bacteria, including *Staphylococcus aureus* (17), and *Salmonella* (18, 19) have been investigated for their ability and potential to be used as recombinant live vectors for delivering heterologous antigens. Among different bacteria *Salmonella typhi* Ty21a has gained attention as it is a safe vaccine strain (20). This facultative intracellular bacterium can colonize inside the intestines and proliferate in the gut-associated lymphoid tissue, systemically spreading to the liver and spleen. It has been shown that recombinant *Salmonella typhi* Ty21a expressing bacterial or viral antigens, is able to elicit a potent cellular, mucosal and humoral immunity in immunized animals (21, 22). To display antigenic determinants on the surface of *Salmonella,* different transporter proteins have been examined such as ice-nucleation protein (Inp), derived from *Pseudomonas syringae* (23).

In this study, RSV F and G immunogenic domains were fused to Inp, cloned into an expression plasmid (pKMS) and surface-displayed on *Salmonella typhi* Ty21a, separately. Live recombinant *S. typhi* Ty21a cells harboring pKMSInak-F or pKMSInak-G were used as vaccines.

MATERIALS AND METHODS

Cell and virus culture

Human respiratory syncytial virus strain A2 was purchased from American Type Culture Collection (ATCC# VR-1540) and propagated in Vero cells. Vero cells were grown in tissue culture flasks in RPMI-1640 supplemented with antibiotics and 10% FBS. RSV with multiplicity of infection (MOI) of 4:1 was added to the flask and virus adsorption was carried out at 37°C for 1:30 h with 5% CO_2. RPMI supplemented with 2% FBS was added to the flask and infected cells were observed for cytopathic effects (CPE) for an additional 4-5 days. RSV-infected cells were harvested using a scraper and centrifuged at 2500 x g for 10 min at 4°C to remove cellular debris, then stored at -80°C until further use.

RT-PCR

Total RNA was isolated from the RSV stocks using the ZR viral RNA kit (Zymo Research, USA). RT-PCR was performed to amplify the F and G immunogenic domains. Reverse transcription was carried out at 45°C for 45 min, followed by 94°C for 4 min to inactivate AMV RT and RNA/cDNA/Primer denaturation. Then PCR was carried out, consisting of 40 cycles of denaturation at 94°C for 30 s, annealing at 57°C (for the RSV- F domain), 62°C (for the RSV-G domain) for 30 s and extension at 68°C for 2 min. The RSV-G specific forward (5' cgcggatccaacctgcaacccacaacag 3') and reverse (5' cccaagcttttaggtacttcctttggtttagtg 3') primers, and the RSV-F forward (5' cgcggatccaagcaaagctgcagcatatc 3') and reverse (5' cccaagctttatcagttactaaatgcaat 3') primers, containing *Bam*HI (forward) and *Hind*III (reverse) restriction sites, respectively, were used in amplification. The products of RT-PCR, which corresponded to 124-226 residues for the RSV-G protein and 209-575 residues for RSV-F protein were purified from LE agarose gel using a gel purification kit. The pKMSInak vector (donated by Prof. Zainul, Universiti Sains Malaysia), which already contained the Inp fragment as a protein transporter, and the purified DNA fragments were subjected to *Bam*HI and *Hin*dIII restriction enzyme digestions, followed by gel purification and subsequently used for cloning (data not shown). These recombinant plasmids named pKMSInak-G and pKMSInak-F, were then transformed into *Salmonella typhi* TY21a using the electroporation method, as described elsewhere. *Salmonella* cells carrying pKMSInak-G and pKMSInak-F plasmids were designated as *Salmonela*-G and *Salmonella*-F, respectively, and used as vaccine candidates.

Plasmid stability test

This test was performed to verify the persistence of a plasmid in dividing bacteria. The bacteria were cultured on antibiotic-free media for 20 days, which was equal to roughly 200 generations. Then, a 10^{-3}dillution of bacteria for each passage was prepared and cultured on agar plates without antibiotic and containing antibiotic to determine the number of live and antibiotic-resistant bacteria (which

contained the plasmids). The number of CFU (Colony Forming Unit) was multiplied by the dilution factor and 100% to obtain the percentage of bacteria containing plasmids.

Surface Display of RSV-G and RSV-F Proteins
Indirect immunofluorescence

To determine the expression of the F or G protein on the *Salmonella* surface, indirect immunofluorescence assay (IFA) was performed. Briefly, a single colony of an overnight culture was harvested, resuspended in normal saline and fixed on a coverslip using 2.5% paraformaldehyde for 25 min. Blocking was carried out in PBS containing 1% of FBS for 15 min. Coverslips were washed twice with 500 µl of PBS, then incubated with mouse polyclonal antibody against RSV at a dilution of 1:100 in PBS for 1 h. Washing was performed three times, each with 500 µl of PBS for 10 min to remove unbound antibodies. Surface-bound antibodies were detected by incubation with a FITC-conjugated goat anti-mouse secondary antibody for 1 h. The coverslips were washed three times for 10 min with 500 µl of PBS, and the labeled bacteria were visualized by oil-immersion fluorescence microscopy with a FITC filter .

Preparation of outer membrane proteins

To confirm the expression of recombinant proteins on the *Salmonella* surface, bacterial outer membranes were fractionated by a modified sarkosyl method (24). Briefly, overnight recombinant *Salmonella* cells were harvested from agar plates, washed twice with PBS, concentrated by centrifugation and resuspended in PBS to a density corresponding to an OD600 value of 10. Then, the suspension was sonicated on ice with 20 pulses of 35 s each, at maximum intensity, followed by a 1 min interval after each pulse. The intact cells were removed from the disrupted cells by centrifugation at 7000 x g for 10 min at 4°C. The supernatant was centrifuged at 100,000 x g for 45 min at 4°C. The supernatant, which contained the cytoplasmic and periplasmic fractions, was removed. The pellet was treated with 1% (V/V) of l-laurylsarcosinate at 4°C for 1 h to solubilize the inner membrane proteins. Then, the solution was subjected to centrifugation at 100,000 x g for 30 min at 4°C to separate the outer membrane proteins, which were pelleted and resuspended in 350 µl of sample buffer analyzed by Western blotting.

Preparation of recombinant Salmonella frozen stocks

To ensure reproducibility among the different immunization experiments, frozen stocks of recombinant *Salmonella* strains were prepared according to the Igwe method (25). A single colony of each recombinant *Salmonella* vaccine strain was inoculated in 5 ml of LB broth containing 60 µg/ml of ampicillin. Incubation at 27°C for 16 h with a shaking speed of 200 rpm was done for a range of 10-fold serial dilutions from 10^{-1} to 10^{-4}. Cultures with an OD_{600} of 0.5 were diluted to 0.1 at OD_{600}, followed by incubation to reach an OD_{600} of 0.8 to 1.0. Then, the recombinant *Salmonella* cells harboring RSV G and F proteins, were harvested separately, added to LB broth containing 10% glycerol and stored at -80°C until further use. To ensure the quality and quantity of stocks, a tube of each batch of recombinant *Salmonella* was counted for viable cells before and after freezing. The cell count was determined to be more than 90% each time.

Vaccine preparation

Prior to immunization, recombinant *Salmonella* stocks were thawed and washed twice with sterile PBS, then dilutions of 1 x 10^9 to 5 x 10^9 CFU/ml were prepared in PBS supplemented with 2% sucrose and 3% sodium bicarbonate. Subsequently, the cells were plated on standard plate count agar to determine the number of viable cell counts, which was adjusted spectrophotometrically (18).

Animal immunization and sampling

The Universiti Putra Malaysia (UPM) Animal Care and Use Committee approved all procedures used in this work (UPM/FPSK/PADS/BR-UUH/00234). Six- to eight-week-old Specific Pathogen Free (SPF) BALB/c mice were housed under pathogen-free conditions with a 12-h light-and-dark cycle, and fed with autoclaved rodent feed and acid-free water. The mice, in three different groups (Ten per group), were immunized orally with *Salmonella* harboring pKMSInak-G, *Salmonella* harboring pKMSInak-F and PBS (as control), separately. Prior to oral immunization, the mice were left for 4-6 h without food and water, then were fed 100 µl of either PBS, *Salmonella* or vaccine strains (1 x 10^9 to 5 x 10^9 CFU) by intragastric gavage with a 20/25-mm feeding needle attached to a 1-ml insulin syringe. Water and food were returned 2 h after immunization. Oral inoculation was repeated once per week for a total of 4 weeks. Twenty-one days after the last immunization, blood samples were collected from the heart of each mouse after it was anesthetized. The samples were allowed to stand at RT for 2 h followed by 30 min in a water bath at 37°C. Serum was collected by centrifugation at 1700 × g for 10 min and stored at -20°C until further use.

Stability of recombinant Salmonella in vivo

Five days after the last immunization, the mice were sacrificed (five per group). Their spleens were removed and homogenized in nutrient broth using a homogenizer. Then 200 µl of this homogenate was added on XLD

and MacConkey agar. After 24-h incubation at 37°C, the colonies of *Salmonella Ty21a* were confirmed using biochemical tests. Also, the number of viable bacteria was calculated using the standard plate count agar method with and without ampicillin (60 µg/ml).

Challenge and sampling

The other group of five mice were intranasally challenged with 10^6 pfu of RSV, 10 days after the last immunization and sacrificed (the mice were euthanized by anesthetic overdosing with 0.5 ml of freshly prepared filter-sterilized ketamine and xylazine injected i.p.) 5 days post challenge. Blood samples were taken as mentioned above. The left lungs were harvested, weighed and placed in sterile Hank's buffer (1 ml/g of lung) and homogenized with a glass tissue grinder. The homogenates were centrifuged (10,000 × g for 1 min) and the viral loads and presence of RSV were assayed immediately. Viral load was measured using the standard plaque assay as described by Cann (26). The right lungs were removed for histopathological examination.

Virus neutralization assay

Vero cells were cultured in 6-well microplates to achieve 100% confluency. Then, 250 µl of two-fold serial dilutions of heat-inactivated sera were mixed with 250 µl of 400 PFU RSV and incubated at room temperature for 60 min. The serum-virus mixture was added to wells containing Vero cells, then incubated for 1:30 h before adding 2 ml of 0.5% (W/V) agarose into the culture medium. After 6 days of incubation at 37°C, 5% CO_2, the plaques were calculated under a microscope. Neutralization titers were expressed as the reciprocal of the highest dilution that reduced plaque formation by at least 60%.

Lymphocyte Proliferation Test (LPT)

Lymphocyte proliferation test was carried out using the BrdU cell proliferation assay kit (Merck, Germany). A suspension (in RPMI-1640) was prepared from the pooled spleens of five mice from each group. Cell suspensions were passed through a 40-µm cell strainer. Erythrocytes were lysed using RBC lysis buffer, pH7.2. The resulting lysate was laid on Ficoll-paque plus 1:1 (density 1.077) and centrifuged at 1000 ×g for 20 min in a swing-bucket rotor centrifuge. Lymphocytes were cultured in 96-well microplates, with 5 x 10^4 cells/100 µl in each well. PHA, at a concentration of 5µg/ml, and RSV, at a concentration of 10µg/ml were added as the positive control and stimulator, respectively. The experiment was carried out based on the manufacturer's protocol. Briefly, cells were labeled with 20 µl/well of BrdU at 37°C, 5% CO_2 for 24 h. To remove the supernatant, the microplate was centrifuged at 240 ×g for 10 min. The cells were fixed using 200 µl/well of fixative/denaturing solution at RT or 30 min. The microplate was tapped on paper towels, then 100 µl/well of anti-BrdU was added at RT for 1 h. Then 100 µl/well of peroxidase Goat anti-Mouse IgG HRP conjugate was added at RT for 30 min and the washing step was carried out as mentioned above. Then, 100 µl of substrate was added in the dark at RT for 15 min, followed by the addition of 100 µl of stop solution to each well in the same order. The absorbance was read at 450 nm, with 540 nm as the reference wavelength, using an ELISA reader (Tecan, Austria). Lymphocyte proliferative responses were presented as Stimulation Indexes (SI). SI was calculated using the following formula: SI = OD of stimulated culture (BrdU uptake in the presence of the RSV antigen) / OD of unstimulated culture (BrdU uptake in the absence of RSV antigen).

Cytokine assay

To measure the serum levels of 11 different types of cytokines and chemokines simultaneously, the Bio-Plex Pro Mouse Cytokine (BioRad, USA) was performed according to the manufacturer's guidelines. Briefly, the microplate was pre-wetted with 100 µl of assay buffer. After vacuum-drying, 50 µl of beads prepared in the medium was added to each well. Then, washing was carried out twice by adding 100 µl of wash buffer followed by a second vacuum-drying. Standards and samples were prepared and added to the specific wells and incubated at RT for 30 min. After 3 times of washing, detection antibodies (30 µl) were added to each well and incubated with shaking (300 rpm) at RT for 30 min. Then 50 µl of Streptavidin-PE was added to each well. At this stage, the incubation time was 10 min in the same manner. The washing step was repeated and 125 µl of assay buffer was added to each well. The plate was read using a Bioplex machine (BioRad, USA). Data analyses of all assays were performed using Bio-Plex manager software (BioRad).

Immunoglobulin ELISA

ELISA was carried out to quantify the serum levels of total IgG, IgG1, IgG2a, IgG2b and IgA, using the Mouse immunoglobulin kits (ICL, USA). Briefly, 100 µl of each serum sample was added in triplicate. The microplate was incubated at RT for 30 min. After washing, 100 µl of appropriately diluted Enzyme-Antibody conjugate was added to each well and was incubated in the dark at RT for 30 min. Then, 100 µl of TMB substrate solution was added to each well and incubated in the dark at RT for 10 min, and then 100 µl of stop solution was added to each well to stop the reaction. Finally, the absorbance was read at 450 nm.

Histopathology and viral titration

The right lung was fixed by inflation with 10% phosphate-buffered formalin and stored at RT for 3 days until histology sectioning was performed. Five micron thick sections from paraffin embedded tissue were stained with hematoxylin and eosin (H & E) staining using slide stainer (Sakura DRS 2000, USA) to evaluate the pulmonary alveolar wall thickness and infiltration of inflammatory cells around bronchioles and blood vessels. The thickness of the pulmonary alveolar wall and also the number of inflammatory cells were randomly assessed in each slide, at a magnification of 400x. The degree of congestion was evaluated according to the following histologic scoring system: 0= absence of inflammatory cells, 1= a few inflammatory cell infiltrations, 2= moderate infiltration of inflammatory cells, 3= high degree of inflammatory cells infiltration. Viral titration was done using the plaque assay method as described earlier. Briefly, 1 g of lung tissue was homogenized in sterile PBS and passed through a 0.45-µm syringe filter. The homogenized filtrate was serially diluted to be used in the plaque assay.

RESULTS

Plasmid stability

To determine the stability of pKMSInak-G and pKMSInak-F plasmids in the recombinant *Salmonella*, the stability test was carried out. The result showed that almost all recombinant *Salmonella*

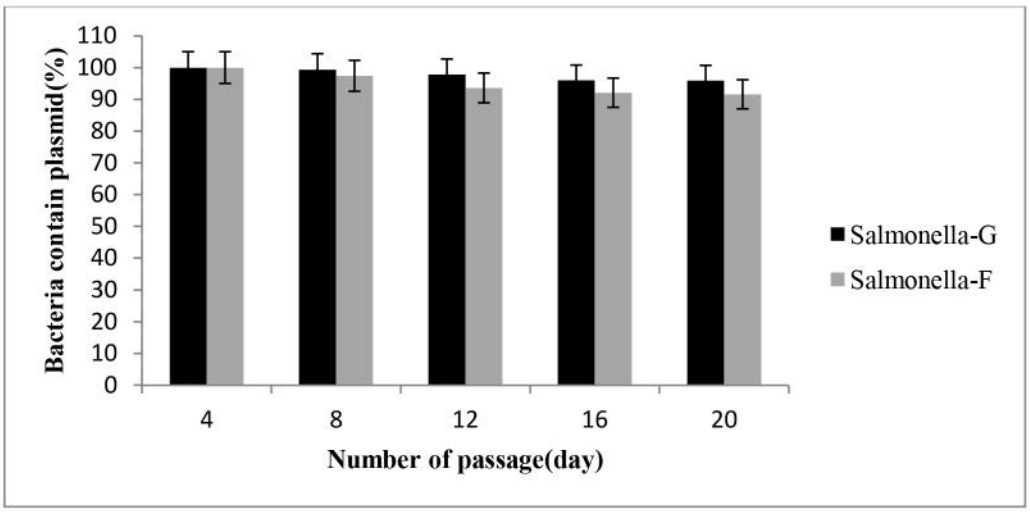

Fig. 1. *Plasmid stability. The recombinant Salmonella cells were grown in LB broth without antibiotics at 37°C, then the overnight cultures were diluted 1:1000 in fresh media and serial passages were performed daily. Plasmid stability test was calculated at each time point by dividing of bacteria containing plasmids to bacteria without plasmids multiplied by 100.*

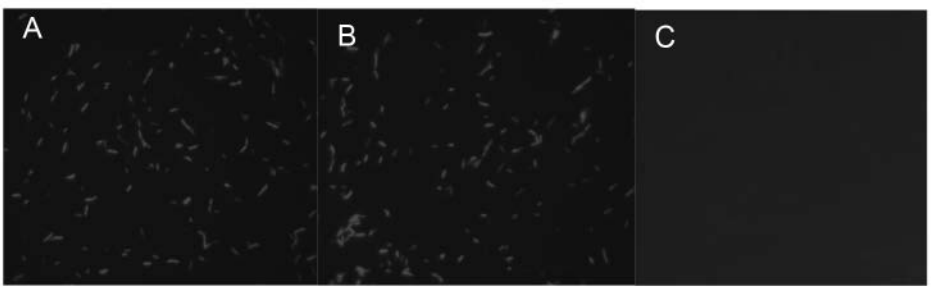

Fig. 2. *Surface display of RSV G and F domains on the recombinant Salmonella typhi Ty21a. Salmonella cells expressing G and F proteins were grown separately. IFA was carried out using anti-RSV polyclonal antibodies as the primary antibody and goat FITC-conjugated anti-mouse as the secondary antibody and labeled bacteria were observed under an IF-Microscope.* ***A)*** *Salmonella carrying pKMSInak-G.* ***B)*** *Salmonella carrying pKMSInak-F.* ***C)*** *Salmonella without plasmid as the negative control.*

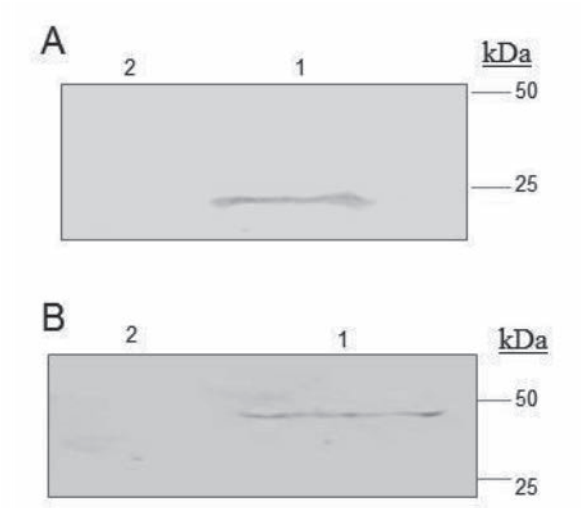

Fig. 3. *Outer membrane protein separation. Recombinant salmonella cells were grown to OD 10. The suspension was mixed with L-laurylsarcosinate and ultracentrifugated, followed by Western blotting.* ***A)*** *Surface displayed G domain protein. Lane 1: 25 µl; Lane 2: negative control (Salmonella).* ***B)*** *Surface displayed F domain protein. Lane 1: 15 µl; Lane 2: negative control (Salmonella). The presence of G (≈25 kDa) and F (≈48 kDa) bands at the appropriate sizes indicated the proper surface expression of these two proteins.*

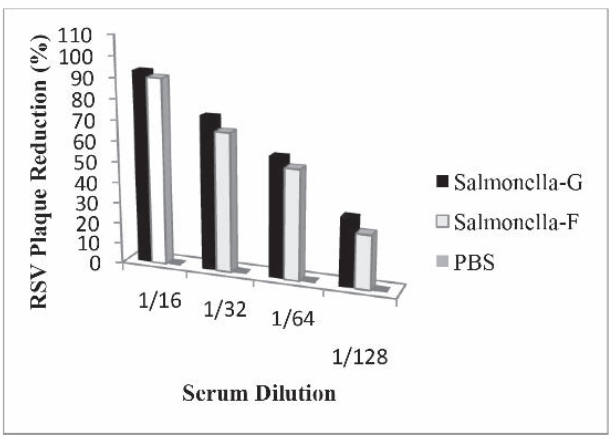

Fig. 4. *Virus neutralization assay. RSV neutralization activity was assessed by plaque assay. Results are reported as the percentage of plaque reduction (Y-axis) observed at the each serum dilution (X-axis).*

cells were stable (Fig. 1).

Detection of surface displayed RSV G and F proteins on Salmonella typhi Ty21a

Indirect immunofluorescence assay (IFA) was used to ensure the expression of RSV G and F domains on the surface of *Salmonella*. Both vaccine strains abundantly expressed G and F domains (Fig. 2).

To determine the localization of RSV G and F domains on the outer membrane of *Salmonella*, Western blot was carried out. The presence of G domain (25 kDa) F domain and (48 kDa) bands on the blotted membranes confirmed that the G and F domains were expressed on the surface of *Salmonella* cells (Fig. 3 A and B).

Neutralizing antibody response

Serum samples were collected 21 days after the last immunization. Different dilutions were assessed to determine the RSV neutralizing antibodies. The results indicated considerable RSV neutralizing activity for the *Salmonella*-G vaccine (>93% plaque reduction at dilution 1/16; >58% plaque reduction at dilution 1/64) and also the *Salmonella*--F vaccine (>90% plaque reduction at dilution 1/16; >53% plaque reduction at dilution 1/64), compared to the control which was inoculated with PBS ($p<0.05$) (Fig. 4). Results for neutralizing antibodies were consistent across repeated, independent immunization trials.

Lymphocyte proliferation

In response to RSV antigen, *in vitro* proliferation of lymphocytes isolated from the mice immunized with *Salmonella*-G and *Salmonella*-F were significantly ($p<0.05$) higher than that of PBS-immunized mice ($p<0.05$) (Table I).

Vaccine strains induce systemic antibody responses

The level of total IgG in the serum of immunized mice with *Salmoella*-G and *Salmonella*-F were significantly higher than PBS control group, both before and after challenge (Table II). We also determined the specific antibody isotypes that are prototypes for Th1 (IgG2a), Th2 (IgG1and IgG2b). The results showed that the levels of IgG1, IgG2a and IgG2b in the serum of immunized mice were significantly higher than the control group immunized with PBS, both before and after challenge. To evaluate mucosal immunity, the serum level of IgA was assessed. Both vaccine strains induced significantly ($p<0.05$) higher IgA responses in the immunized mice before and after virus challenge.

Table I. *Proliferation of lymphocyte isolated form the immunized mice in response to RSV.*

Lymphocyte proliferation	*Salmonella*-G	*Salmonella*-F	PBS control
Before challenge	1.83±0.06	2.21±0.04	0.64±0.15
After challenge	4.67±0.83	6.38±0.2	1.65±0.1

Results are expressed as mean ± SEM.

Table II. *Systemic antibody response in the immunized mice before and after virus challenge.*

Systemic antibody response(pg/mol)	PBS control		*Salmonella*-G		*Salmonella*-F	
	Before	After	Before	After	Before	After
IgG total	18..43±0.98	26.25±1.45	34.54±0.67	42.21±1.75	39.11±1.24	45.71±3.83
IgG1	5.21±0.08	6.65±0.23	13.99±0.23	25.88±0.96	25.92±0.35	22.73±1.56
IgG2a	11.88±0.15	12.91±0.22	19.85±0.06	20±0.06	20.64±0.77	21.18±0.32
IgG2b	6.86±0.07	7.07±0.15	14.93±0.75	24.75±0.66	26.64±3.3	23.25±0.51
IgA	3.69±0.01	3.78±0.01	5.9±0.78	7.71±1.14	6.7±1.27	7.78±0.38

Results are expressed as mean ± SEM.

Table III. *IgG1/IgG2a and IgG2b/IgG2a ratios.*

Vaccine strain	Immunized before challenge		Immunized after challenge	
	IgG1/IgG2a	IgG2b/IgG2a	IgG1/IgG2a	IgG2b/IgG2a
Salmonella-G	0.704 ± 0.016	0.751 ± 0.039	1.294 ± 0.025	1.238 ± 0.036
Salmonella-F	1.255 ± 0.044	1.290 ± 0.158	1.073 ± 0.045	1.097 ± 0.001

Results are expressed as mean ± SEM.

Table IV. *Serum level of Th1-associated cytokines in the immunized mice before and after RSV challenge.*

Th1-type cytokines	PBS control		*Salmonella*-G		*Salmonella*-F	
	Before	After	Before	After	Before	After
IL2	19.43±1.73	27±0.98	33±1.15	76±1.16	44.38±1.1	89.9±1.18
IFN-ɣ	90.01±4.38	172.39±1.44	144.12±4.18	287.45±4.38	246.15±2.4	374..42±8.34
TNF-α	91.03±2.45	159.62±1.44	123.99±4.71	185.82±1.73	175.22±0.55	199.54±3.08

Results are expressed as mean ± SEM.

Table V. *Serum level of Th2-associated cytokines in the immunized mice before and after RSV challenge.*

Th2- type cytokines	PBS control		*Salmonella*-G		*Salmonella*-F	
	Before	After	Before	After	Before	After
IL4	11.52±0.28	18±1.15	12.79±0.58[2]	29.1±1.15	14.5±0.86	18.83±1.45[2]
IL5	21.82±0.59	41.68±0.5	36.64±0.46	60±2.17	40.7±1.16	48.13±0.55
IL9	369.11±3.46	729.17±0.58	695.34±2.22	812.11±1.25	746.19±3.19	834.21±1.73
IL10	7.58±0.22	33.01±1.53	17.66±3.16	32.12±2.99[2]	39.08±3.08	41.28±2.99
IL13	508.64±1.31	831.99±1.15	568.44±1.67	905.57±1.73	602.88±1.58	905.25±2.87

[1]*Results are expressed as mean ± SEM.*
[2]*Not significant.*

Table VI. *The level of IL-17 in the serum of immunized mice before and after RSV challenge.*

Level of IL17	PBS control		*Salmonella*-G		*Salmonella*-F	
	Before	After	Before	After	Before	After
	107.53±7.15	138.86±10.4	151.46±2.74	164.08±15.01	165.96±10.29	197.34±5.38

Results are expressed as mean ± SEM.

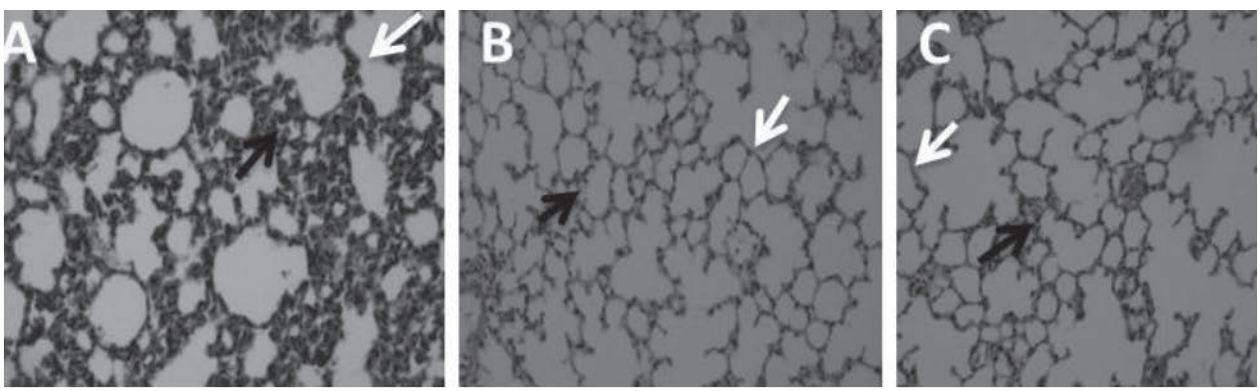

Fig. 5. *Histopathology of the mice lung following RSV challenge. Lung sections of the mice immunized with Salmonella-G, Salmonella-F and PBS, sacrificed on day 5 post-challenge.* ***A)*** *Immunized with PBS.* ***B)*** *Immunized with Salmonella-G.* ***C)*** *Immunized with Salmonella-F. All sections were stained with hematoxylin and eosin. Microscopic examination of lung tissue demonstrated a noticeable difference in pulmonary alveolar wall thickness (white arrows) and infiltration of inflammatory cells (black arrows).*

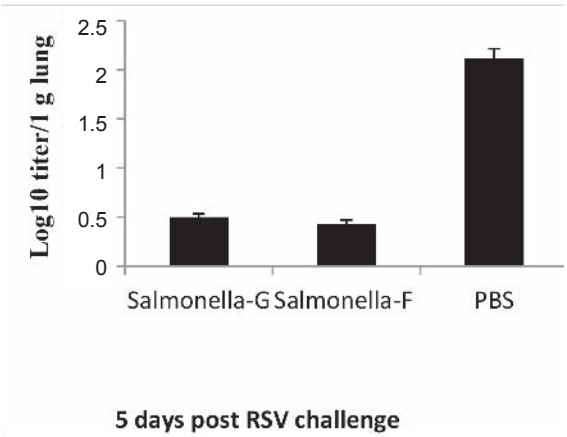

Fig. 6. *The titers of RSV in the lung of immunized mice with Salmonella-G and Salmonella-F vaccines after RSV challenge. The plaque assay results revealed a significant decrease ($p<0.05$) of viral titer in the vaccinated mice after RSV challenge.*

To determine the capabilities of developed vaccines for generating a balanced immune response, IgG1/IgG2a and IgG2b/IgG2a ratios were calculated (Table III).

Salmonella-G and Salmonella-F vaccines induce Th1- and Th2- associated cytokine secretion

Both vaccine strains significantly (p <0.05) increased the levels of Th1-related cytokines including IL-2, IFN-ϒ and TNF-α before and after virus challenge compared to PBS-immunized mice (Table IV).

The levels of all Th2-related cytokines including IL-5, IL-9, IL-10 and IL-13 (except IL-4) were significantly higher ($p<0.05$) in the serum of *Salmonella*-G immunized mice before challenge, in comparison with the PBS control group, After challenge however, all cytokines except IL-10 were significantly ($p<0.05$) higher in the immunized group (Table V).

Th2-related cytokines including IL-4, IL-5, IL-9, IL-10 and IL-13 in the serum of *Salmonella*–F immunized mice were significantly ($p<0.05$) higher than that of the control group. The same result was obtained for all cytokines after challenge except for IL-4 (Table V).

We also showed that the serum levels of IL-17 in both immunized groups were significantly ($p<0.05$) higher either before or after challenge compared to the control group (Table VI).

Histopathology

The inflammatory cell numbers, thickness of pulmonary alveolar and the level of congestion in mice immunized with *Salmonella*-G and *Salmonella*-F were significantly lower than the negative control after challenging with RSV (Table VII and Fig. 5).

Virus clearance after challenge

The *Salmonella*-G and *Salmonella*-F vaccine strains could significantly reduce the titer of RSV in the lungs of immunized mice after challenge with RSV compared with PBS–immunized group (Fig. 6).

DISCUSSION

The development of an effective vaccine against RSV has not been successful due to stringent characteristics of any RSV vaccine candidate (13). An effective vaccine should be able to induce a

Table VII. *Histopathological examination of mice lung tissue.*

Histopathology Parameters	Control PBS	*Salmonella*-G	*Salmonella*-F
Level of Congestion	3	1	1
Number of inflammatory cells	236±6.17	97±2.646	87.67 ±1.76
Pulmonary alveolar wall thickness (μm)	8.933±0.5	4.4±0.057	3.5±0.338

Infiltration of inflammatory cells was determined by scoring the level of congestion and number of inflammatory cells. The thickness of the pulmonary alveolar wall was measured at a magnification of × 400.

strong Th1 immune response as a high level of Th2 immune response exacerbates the disease after exposure to RSV and has an undesirable role in protection against re-infection (11, 27, 28). In this study, we developed two recombinant vectors which carry the RSV G or F immunogenic domains on their surfaces, without using any adjuvant.

It is believed that an ideal RSV vaccine candidate must induce Th1 and Th2–associated cytokine secretion (29-34). In this regard, our results revealed that the developed vaccines significantly elevated the serum level of Th1-type cytokines including IFN-ϒ, IL-2 and TNF-α as well as Th2-type cytokines such as IL5, IL13. To assess the effectiveness and safety of the recombinant *Salmonella*-G and *Salmonella*-F vaccines, we used indirect evidence including IgG2a as Th1 as well as IgG1 and IgG2b as Th2 markers. The results were analyzed using the ratio of IgG1/IgG2a or IgG2b/IgG2a (9, 17, 29). Our data analyses showed that the *Salmonella*-F vaccine increased the Th2/Th1 ratio in immunized mice before challenge (slightly higher than 1) but after virus exposure the Th2/Th1 ratio reached the maximum expected balance (~ 1). Conversely, *Salmonella*-G induced a strong Th1 immune response in the immunized mice before RSV challenge, where the ratios of Th2/Th1 were constantly lower than 1. After virus challenge however, the Th2/Th1 ratio slightly increased. Nonetheless, pathological examination of lung tissues and significant virus clearance from the lungs of immunized mice showed that neither of the vaccines caused any damage to the lungs after virus challenge. This suggests the developed vaccines generated a balanced immune response which modulated the adverse effects of Th2-related response.

Recently, it has been shown that an efficient RSV vaccine increased IL-17 production by CD4(+) T cells and natural killer cells and recruited regulatory cells and neutrophils which contributed to virus clearance after challenge (35). In this study, both vaccines also induced a significant increase of IL-17 in the serum of immunized mice before and after RSV challenge which might have been crucial to RSV clearance.

The developed vaccines in this study were able to induce robust mucosal and humoral immune responses. Previously, we reported that neutralizing antibodies against the G domain reduced 69.3% of plaques (8). Whereas, in this study the neutralizing antibodies induced by *Salmonella*-G decreased the plaques by 93% at the same dilution. The significant increase in the plaque reduction might be due to the use of a permissive host (mouse) and the nature of the vaccine strain. It seems that the synergism between *Salmonella* and RSV F or G domains could elicit stronger systemic and mucosal antibody responses. Interestingly, in contrast with other studies which reported that RSV F vaccine induced a considerable level of IgA when administered along with adjuvant (9, 36), the *Salmonella*-G and *Salmonella*-F vaccine strains could induce strong systemic as well as mucosal immune responses without any adjuvant.

In conclusion, we developed two recombinant *Salmonella*-based oral vaccines against RSV which induced a balanced immune response without Th2-mediated immunopathology. These findings suggest that the designed vaccines may have preventive potential against RSV.

ACKNOWLEDGEMENTS

This research was supported by the Malaysian Ministry of Science, Technology and Innovation (N0.02-01-04 SF0963). The funder had no role in study design, data collection and analysis or preparation of the manuscript.

Professor Zainul F. Zainuddin is gratefully acknowledged for donating pKMSInak plasmid.

REFERENCES

1. Simoes EA. Environmental and demographic risk factors for respiratory syncytial virus lower respiratory tract disease. J Pediatr 2003; 143:S118-26.
2. Mejias A, Chavez-Bueno S, Jafri HS, Ramilo O. Respiratory syncytial virus infections: old challenges and new opportunities. Pediatr Infect Dis J 2005; 24:S189-96
3. Shay DK, Holman RC, Newman RD, Liu LL, Stout JW, Anderson LJ. Bronchiolitis- associated hospitalizations among US children, 1980-1996. JAMA 1999; 282:1440-6.
4. Hacking D, Hull J. Respiratory syncytial virus--viral biology and the host response. J Infect 2002; 45:18-

24.
5. Harris J, Werling D. Binding and entry of respiratory syncytial virus into host cells and initiation of the innate immune response. Cell Microbiol 2003; 5**:**671-80.
6. Collins PL**.** Respiratory syncytial virus and metapneumovirus, fifth ed. Lippincott Williams & Wilkins, 2007 Philadelphia.
7. Huang Y, Anderson R. A single amino acid substitution in a recombinant G protein vaccine drastically curtails protective immunity against respiratory syncytial virus (RSV). Vaccine 2003; 21:2500-5.
8. Azizi Jalilian F, Jahanshiri F, Sekawi Z, Omar AR, Yusoff K. Dynamics of the bacterially expressed conserved immunogenicregion of the human respiratory syncytial virus G protein. Biotechnol Appl Biochem 2011; 58:97-102.
9. Singh SR, Dennis VA, Carter CL, Pillai SR, Jefferson A, Sahi SV, Moore EG. Immunogenicity and efficacy of recombinant RSV-F vaccine in a mouse model. Vaccine 2007; 25:6211-23.
10. Lim SH, Jahanshiri F, Jalilian FA, Rahim RA, Sekawi Z, Yusoff K. Glycosylation is not necessary for recognition of the fusion glycoprotein domain of the human respiratory syncytial virus by a polyclonal antibody. Acta Virol 2010; 54:181-7.
11. Hall CB, Walsh EE, Long CE, Schnabel KC. Immunity to and frequency of reinfection with respiratory syncytial virus. J Infect Dis 1991; 163:693-8
12. Collins PL, Graham BS. Viral and host factors in human respiratory syncytial virus pathogenesis. J Virol 2008; 82:2040-55.
13. Kapikian AZ, Mitchell RH, Chanock RM, Shvedoff RA, Stewart CE. An epidemiologic study of altered clinical reactivity to respiratory syncytial (RS) virus infection in children previously vaccinated with an inactivated RS virus vaccine. Am J Epidemiol 1969; 89:405-21.
14. van Drunen Littel-van den Hurk S, Mapletoft JW, Arsic N, Kovacs-Nolan J. Immunopathology of RSV infection: prospects for developing vaccines without this complication. Rev Med Virol 2007; 17:5-34.
15. Tang YW and Graham BS. T cell source of type 1 cytokines determines illness patterns in respiratory syncytial virus-infected mice. J Clin Invest 1997; 99:2183-91
16. Waris ME, Tsou C, Erdman DD, Zaki SR, Anderson LJ. Respiratory synctial virus infection in BALB/c mice previously immunized with formalin-inactivated virus induces enhanced pulmonary inflammatory response with a predominant Th2-like cytokine pattern. J Virol 1996; 70:2852-60.
17. Cano FH, Plotnicky-Gilquin TN, Nguyen S, Liljeqvist P, Samuelson Bonnefoy J, Stahl S, Robert A. Partial protection to respiratory syncytial virus (RSV) elicited in mice by intranasal immunization using live staphylococci with surface-displayed RSV-peptides. Vaccine 2000; 18:2743-52.
18. DiGiandomenico A, Rao J, Goldberg JB. Oral vaccination of BALB/c mice with *Salmonella enterica serovar Typhimurium* expressing *Pseudomonas aeruginosa* O antigen promotes increased survival in an acute fatal pneumonia model. Infect Immun 2004, 72:7012-21.
19. Li Y, Wang S, Scarpellini G, Gunn B, Xin W, Wanda SY, Roland KL, Curtiss R 3rd. Evaluation of new generation *Salmonella enterica serovar Typhimurium* vaccines with regulated delayed attenuation to induce immune responses against PspA. Proc Natl Acad Sci USA 2009; 106:593-8
20. Lee JS, Shin KS, Pan JG, Kim CJ. Surface-displayed viral antigens on *Salmonella* carrier vaccine. Nat Biotechnol 2000; 18:645-8.
21. Liljeqvist S, Stahl S. Production of recombinant subunit vaccines: protein immunogens, live delivery systems and nucleic acid vaccines. J Biotechnol 1999; 73:1-33.
22. Tacket CO, Kelly SM, Schodel F, Losonsky G, Nataro JP, Edelman R, Levine MM, Curtiss R 3rd. Safety and immunogenicity in humans of an attenuated *Salmonella typhi* vaccine vector strain expressing plasmid-encoded hepatitis B antigens stabilized by the Asd-balanced lethal vector system. Infect Immun 1997; 65:3381-5.
23. Jung HC, Lebeault JM, and Pan JG. Surface display of *Zymomonas mobilis levansucrase* by using the ice-nucleation protein of *Pseudomonas syringae*. Nat Biotechnol 1998; 16:576-80
24. Maurer J, Jose J, Meyer TF. Autodisplay: one-component system for efficient surface display

and release of soluble recombinant proteins from *Escherichia coli*. J Bacteriol 1997; 179:794-804.
25. Igwe EI, Russmann H, Roggenkamp A, Noll A, Autenrieth IB, Heesemann J. Rational live oral carrier vaccine design by mutating virulence-associated genes of *Yersinia enterocolitica*. Infect Immun 1999; 67:5500-7.
26. Cann TA (Ed.). Virus culture. A practical approach. New York: Oxford University Press,1999.
27. Hemming VG, Prince GA Immunoprophylaxis of infections with respiratory syncytial virus: observations and hypothesis. Rev Infect Dis 1990; 12(S):S470-4; discussion S474-5.
28. Piedra PA, Jewell AM, Cron SG, Atmar RL, Glezen WP. Correlates of immunity to respiratory syncytial virus (RSV) associated-hospitalization: establishment of minimum
29. Tripp RA, Oshansky C, Alvarez R. Cytokines and respiratory syncytial virus infection. Proc Am Thorac Soc 2005; 2:147-9.
30. Miller M, Cho JY, Baek KJ, et al. Plasmid DNA encoding the respiratory syncytial virus G protein protects against RSV-induced airway hyperresponsiveness. Vaccine 2002; 20:3023-33.
31. Xie C, He JS, Zhang M, et al. Oral respiratory syncytial virus (RSV) DNA vaccine expressing RSV F. Hum Gene Ther 2007; 18(8):746-52.
32. Joshi P, Shaw A, Kakakios A, Isaacs D. Interferon-gamma levels in nasopharyngeal secretions of infants with respiratory syncytial virus and other respiratory viral infections. Clin Exp Immunol 2003; 131:143-7
33. Bembridge G P, Rodriguez N, Garcia-Beato R, Nicolson C, Melero JA, Taylor G. DNA encoding the attachment (G) or fusion (F) protein of respiratory syncytial virus induces protection in the absence of pulmonary inflammation. J Gen Virol 2000; 81:2519-23.
34. Boelen A, Andeweg A, Kwakkel J, Lokhorst W, Bestebroer T, Dormans J, Kimman T. Both immunisation with a formalin-inactivated respiratory syncytial virus (RSV) vaccine and a mock antigen vaccine induce severe lung pathology and a Th2 cytokine profile in RSV-challenged mice. Vaccine 2000; 19:982-91.
35. Schnoeller C, Roux X, Sawant D, Raze D, Olszewska W, Locht C, Openshaw PJ. Attenuated *Bordetella pertussis* vaccine protects against respiratory syncytial virus disease via an IL-17-dependent mechanism. Am J Respir Crit Care Med 2014; 189(2).
36. Tebbey PW, Scheuer CA, Peek JA, et al. Effective mucosal immunization against respiratory syncytial virus using purified F protein and a genetically detoxified cholera holotoxin, CT-E29H. Vaccine 2000; 18:2723-34.

PROBING HEAD-TO-TOE DEFORMATION LAW ASSESSMENT FOR ABDOMINAL TUMOR THROUGH RESPIRATORY MOVEMENT SIMULATION AND CTVision RADIATION RESEARCH

EY. WANG[1,2], Y. WANG[1], ZH. QIAN[1], LY. ZHU[2] and RS. YU[1]

[1]Department of Radiology, Second Affiliated Hospital, Zhejiang University School of Medicine, Hangzhou, China; [2]Department of Radiology, Tumor Hospital of Taizhou, Wenling, China

Received November 22, 2014 – Accepted December 22, 2014

This paper aims to explore head-to-toe deformation law for abdominal tumor with CTVision and self-designed respiratory movement simulation mold and meanwhile verify the accuracy and correctness of the treatment. In experimental group, a self-designed respiratory movement mold was used. The image was scanned out by CT scanning based on the movement state and then sent to the planning system to compare the location variation of tumor and formulating the treatment plan accordingly, followed by verification and verified derivation values observation. A total of 21 cases of abdominal tumor were included in the case group. Their breathing movement was detected under a simulated locator and then the data was recorded. The image was scanned and sent to the planning system to compare the location variation of the tumor, the patients then underwent 3D conformal therapy (3D-CRT) and we performed verification and observed verified derivation values. Finally, the results of the case group and the experimental group were compared. The mean of the verified derivation values was smaller than respiratory motion values in experimental group (t=-10.78, P=0, P<0.05); the mean of verified derivation values of the patients was smaller than respiratory motion values in group f, g, h, i, j, l, n, o, p, q, r, s t, u in the case group (P<0.05); no remarkable difference was found between the two values in group a, b, c, k and m (P>0.05); group e was unable to undergo the statistical test since its standard deviation was 0; the mean of the verified derivation values was higher than respiratory motion values in group d (P>0.05). In conclusion, radiation therapy applied with CTVision proved to be accurate and convincing in the treatment of abdominal tumor.

In recent years, the incidence of abdominal tumors has gradually increased along with the mortality rate; in other words, it has become a sword threatening our health. Radiotherapy is one of the most important methods for treating abdominal tumor, however, respiratory movement affects the accuracy of abdominal tumor radiotherapy (1-2). Under the influence of respiratory movement the irradiation field expands, hence weakening the coincidence between radiation field and gross tumor volume (GTV) (3). Currently a wealth of experts and scholars are studying ways of stimulating respiratory movement as well as the influence of respiratory movement on tumor treatment and have achieved a lot. For those patients with a large margin of respiratory movement, respiratory gating can solve

Key words: abdominal tumor, 3D conformal radiotherapy, respiratory movement mold, deformation law, GTV, CTVision

Mailing address: Dr Risheng Yu,
The Department of Radiology,
Second Affiliated Hospital,
Zhejiang University School of Medicine,
No.88, Jiefang Road, Hangzhou, China
Tel.: +86-0371-67354312 Fax: +86-0371-67354312
E-mail: yrszjdx@163.com

0393-974X (2015)

the problem of the moving target in order to reduce the error of dose distribution (4). While developing and assessing respiratory movement compensation by SPECT/PET, phantom movement produced by GATE offers alternative means in the stimulation of respiratory movement which is characterized by a small amount of calculation and simple phantom set compared to the traditional method (5). Moreover, target region omission caused by respiratory movement can be effectively avoided if applying CT-CT image fusion prior to planned target region design (6).

In this paper, CTVision and self-designed respiratory movement simulation were applied to probe the deformation law of abdominal tumor, the way to measure the amplitude margin of the tumor by CT and to amend the plan without 4-Dimensional Computed Tomography (4D-CT), in order to achieve the desired therapeutic effect.

MATERIALS AND METHODS

Subjects

A total of 21 abdominal tumor patients aging between 18 and 80 years who had Karnofsky scores higher than 70 and had a history of radiotherapy treatment were included in this study. They underwent either 3-dimensional conformal radiotherapy or intensity modulated radiotherapy. All the patients have signed the informed consent and the therapeutic schedule was approved by the Medical Ethics Committee.

Respiratory movement stimulation mold

A respiratory movement stimulation mold was designed to study the influence of respiratory movement in the treatment of abdominal tumor, composed of support, control box, stepping motor, synchronous belt and tray. The support and tray were both made of organic glass which has low absorptivity to radial and therefore hardly affected by the experiment. Vertebra is placed into the mold as a point of reference and fixed by foam. A rounded wooden ball of 40 mm diameter used for stimulating the tumor was divided in the middle and implanted with a steel ball of 3 mm diameter. After re-bounding, it was placed on the tray on the black synchronous belt motioned by the stepping motor in order to stimulate respiratory movement.

Respiratory movement simulation experiment

The ball was placed on the mold tray and fixed with a rubber band. The wooden ball acted as the tumor, with a "0" marking the center of it. We turned the mold on and the ball made back and forth movements with "0" as its center. We scanned the image of the wooden ball in movement with normal breathing at 18 times/min and to-and fro movement route of 2 cm for 4 times within the same range and the thickness of the scanning slice was 3 mm. The images were transmitted to the planning system to compare the variation of tumor location and formulate the treatment plan followed by verification and verified derivation value observation. We measured the edge dose value in the planning target volume (PTV) and the center dose value in GTV and then calculated the dose derivation value.

Clinical experiment

The patient was placed in horizontal position. We applied heat molding to fix the thorax and abdomen, and then measured and recorded the respiratory motion value in the directions of head-to-toe, left and right, front and back using a simulator machine. When we used the CT to position, the patient with lung cancer was scanned from the lower jaw to the upper pole of the kidney while the whole liver was scanned for the patient with liver cancer. The same range was randomly scanned for two times and the thickness of the scanning slice was 5 mm. After scanning, the images were transmitted to the planning system twice for observation. It was found that the location of the tumor changed during the scanning under the influence of respiratory movement. We then developed the treatment plan according to the characteristics of the lung cancer and liver cancer and performed 3-Dimensional conformal radiotherapy for treatment on the patients. During the treatment, the patients had to undergo verification at least three times to observe the deviation value. Finally, the results of the case group were compared to the experimental group.

Observation index

Respiratory motion value: we observed the patient's respiratory motion mainly in head-to-toe direction (Y direction) by a simulator machine and recorded the data. The offset image of Y direction is shown in Fig. 1.

The theoretical maximum deformation degree of tumor: tumor size + respiratory motion value.

Dose deviation: the differences between the center dose value of the GTV and the edge dose value of the PTV divides the center dose value of the gross tumor volume.

Deviation value: the error value between the CT images obtained before the treatment and the planning image.

Observation methods

Experimental group: observe the tumor location

variation in the planning system, and measure the dose value of the clinical target volume (CTV) and the GTV. After formulating the treatment plan, every plan needed to be verified at least 3 times. We recorded and preserved the screen shots of the deviation in three directions and mainly recorded the deviation in the Y direction. To obtain the dose deviation, treatment planning system was used to measure the center dose value of the GTV and the edge dose value of the PTV.

Case group: we measured and recorded the respiratory motion value in the simulator machine before the radiotherapy and observed the location variation of the tumor in the planning system. During the radiotherapy, we needed to verify the value once a week or 3 times in total, and screen shots of the deviation were recorded and preserved in the three directions, especially the deviation in the Y direction.

Statistical analysis

SPSS17.0 software was applied for relative data analysis, and *t*-test for mean analysis. $P<0.05$ was considered to have statistical significance.

RESULTS

The experimental results of the respiratory movement simulation

Data obtained from the experiment of respiratory stimulation is shown in Table I. In the random group, the measured deformation degree drawn from the four random scanned location images was 57 mm, in the movement state with normal breathing at 18 times/min and a to-and-fro movement route of 2 cm, within the same range.

In the extreme group, the measured deformation degree drawn from the scanned location image was 60 mm, in the movement state with normal breathing at 18 times/min and a to-and-fro movement route of 2 cm, within the same range. This group was scanned under limiting conditions and the measured deformation degree equaled the theoretical maximum deformation degree, i.e., the sum of tumor size and respiratory motion.

We collected the information from the above two groups of data. The measured deformation degree of the random group was close to the theoretical maximum deformation degree, in other words, the measured deformation degree was close to the sum of tumor size and respiratory motion value. The tumor moved with the respiratory motion, the determinants of the range of tumor deformation was the tumor size and the respiratory motion. The larger the tumor and the respiration are, the larger the tumor size is. Under the effect of the respiratory movement, the tumor could move to any position within the theoretical maximum deformation degree.

To validate the accurateness of the treatment, dose derivation experiment was performed in extreme group in the moment that the wooden ball reached central position. The experiment data is shown in Table II.

As shown in Table II, we could figure out the dose derivation 3.705% and 4.07% from the edge dose of PTV forming by 15 mm and 20 mm external

Table I. *The experimental data analysis of the respiratory movement simulation.*

Group	Respiratory motion (mm)	Tumor size (mm)	Measured deformation degree (mm)	The maximum deformation degree (mm)
Random	±10	40	57	60
Extreme	±10	40	60	60

Table II. *Dose derivation analysis.*

Extended range (mm)	Central dose (cG)	Extreme dose (cGy)	Dose deviation
15	200	192.59	3.705%
20	200	191.86	4.07%

Table III. *Analysis of case data collection.*

(mm)	Respiratory motion	Tumor size	Measured deformation degree	The maximum deformation degree
a	±3.5	35	35	42
b	±1.5	60	60	63
c	±6	80	85	92
d	±5.5	55	60	66
e	±6	30	40	42
f	±5.5	50	60	61
g	±5	30	35	40
h	±7.5	70	75	85
i	±4	50	55	58
j	±5	25	30	35
k	±3.5	60	65	67
l	±10	70	90	90
m	±9	70	80	88
n	±7.5	30	40	45
o	±8	30	35	46
p	±7	50	55	64
q	±7.5	100	110	115
r	±8.5	70	85	87
s	±8.5	80	90	97
t	±7.5	125	130	140
u	±6.5	90	100	103

expansion and the center dose of GTV, and both were less than 5%. The treatment plan could be considered accurate and needed no correction since the dose derivation was within the acceptable range.

The experimental results showed that some patients had significant respiratory movements, while some had weak movements; the measured deformation degree of patients with weak respiratory movement was lower than those with significant respiratory movement. The tumor moved along with the respiratory motion, and tumor deformation degree depended on tumor size and respiratory motion. Under the effect of the respiratory movement, tumor could move to any position within the theoretical maximum deformation degree.

In the experimental group, the mean of the verified deviation values was lower than the respiratory motion values ($t=-10.78$, $p=0$, $P<0.05$). The mean of the verified deviation values of case group f, g, h, i, j, l, n, o, p, q, r, s, t, and u were lower than the respiratory motion values ($P<0.05$), indicating the treatment was accurate; the mean of the verified derivation values of group a, b, c, k, m were within the respiratory movement ranges, and it could be considered that their verified derivation values were consistent with the respiratory movement, thus had no influence on the treatment plan; group e was unable to perform the statistical tests since its standard deviation was 0, but the mean of verified derivation values in group e was lower than the respiratory motion values, indicating the treatment was not influenced and its accuracy could also be ensured. The mean of the verified deviation values of group d was higher than the respiratory motion values ($P>0.05$), therefore, the treatment was not accurate and needed correction. (Tables III and IV).

Table IV. *Comparison between experimental group and case group.*

	Group	The respiratory movement of Y direction (mm)	The data of Y direction (mm) /time														Average value	t	p
Experimental group		±10	12	-1	3	2	1	-8	-13	6	-15	4	6	-5	-4		-0.92	-10.78	0.000
Case group	a	±3.5		0	-8		0										-2.67	-3.63	0.068
	b	±1.5	-1	-3	13		1										2	-0.27	0.804
	c	±6	-1	-10	5												-2	-3.21	0.085
	d	±5.5	18	13	11												14	1.44	0.286
	e	±6	2	2	2												2	/	/
	f	±5.5	-1	4	5												2.67	-4.49	0.046
	g	±5	-11	-5	1	0											-3.75	-5.00	0.015
	h	±7.5	-1	1	-6												-2	-8.17	0.015
	i	±4	-6	-7	-7												-6.67	-44	0.001
	j	±5	1	0	1	6											2	-5.91	0.010
	k	±3.5	2	-6	9	0	5	1									1.83	-2.51	0.054
	l	±10	0	1	1	0											0.5	-67.55	0.000
	m	±9	-1	-8	11												0.67	-3.12	0.089
	n	±7.5	6	6	1												4.3	-6.4	0.020
	o	±8	-3	-7	-5												5	-9.53	0.011
	p	±7	9	7	5	13											8.5	-3.22	0.049
	q	±7.5	2	1	9												4	-4.37	0.049
	r	±8.5	-12	3	-4												-4.3	-4.92	0.039
	s	±8.5	0	4	1	14											4.75	-3.83	0.031
	t	±7.5	3	3	2												2.67	-37	0.001
	u	±6.5	0	1	0												0.33	-38	0.001

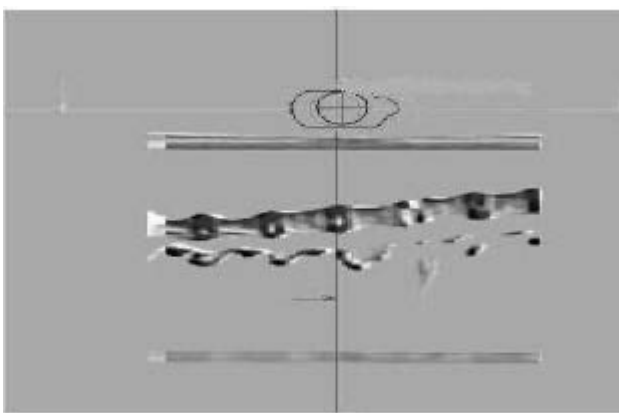

Fig. 1. *Offset image of Y direction.*

DISCUSSION

To date, surgery remains the main treatment method of liver cancer, and radiotherapy has not yet been recognized in evidence-based medicine. Nevertheless, treating liver cancer by radiotherapy was considered to be feasible by some experts and scholars. Professor F. Mornex (7) researched the feasibility and effectiveness of treating small hepatocellular carcinomas based on 3-Dimensional radiotherapy by performing clinical experiments on 27 patients with small hepatocellular carcinoma. Finally, 25 patients completed the treatment with the effective rate of 92%. Thus it can be seen that

treating liver cancer by radiotherapy is feasible and effective. At the same time, liver is one of the most important organs affected by the respiratory motion, therefore, patients with liver cancer are enrolled as clinical subjects in this research.

In the early stage of radiotherapy, i.e., within 90 days from the start of radiotherapy, there is a 30% risk of acute radiation pneumonitis which is a kind of spontaneous immune reaction mediated by inflammatory factor due to the large irradiation field, high dose and rapid irradiation. In the later stage, i.e., 6 to 18 months after radiotherapy ends, uncontrollable chronic pulmonary fibrosis is most likely to occur and advanced-stage esophageal injury usually occurs when the emission dose of esophagus is more than 70 Gy. Occurrence of the above side effects of radiotherapy is mostly due to the large irradiation field caused by the respiratory motion or the excessive high dose. To sum up, the excessive large irradiation caused by respiratory motion aggravates side effects of radiotherapy through damaging normal tissues and the surrounding organs while limiting the dosage ultimately weakens the radiotherapy effect of abdominal tumor and patients' living quality after the treatment.

Clinically, the main means used for controlling respiratory motion includes respiratory gating, deep inhalation breath holding (DIBH), active breathing control (ABC) and real-time tumor tracking, (8, 9) according to the research results of many experts and scholars. The above means are all able to control respiratory motion, but the respiratory gating has low ray utilization and working efficiency and requires high lung functions on behalf of the patients, although the irradiation scope can be reduced; therefore, this paper probed into the deformation law of abdominal tumor without controlling respiratory motion, and detected the margin of tumor amplitude applying CT without Four Dimensional Computed Tomography (4D-CT) to decide whether the treatment plan should be corrected.

In the location where the volume and shape of CTV changes due to motion is termed as internal target volume (ITV) by the 62nd report of Commission on Radiation Units and Measurements (ICRU), which is a concept that particularly focuses on respiratory motion. This study was carried out without controlling respiratory motion and 4D-CT, and mainly focused on the head-to-toe motion law of tumor. The experimental results of this paper suggested that tumor moved with respiratory motion and the motion degree depended on tumor size and breathing movement. Affected by the respiratory motion, tumor could move to the random location within the theoretical maximum movement degree. The results of the case group were consistent with the experimental group. Hence, the range of breathing movement should be considered when formulating treatment plan.

Dose derivation is one of the important indexes for measuring the accuracy of a treatment. In the article of Realization of 3D Evaluation Algorithm in Dose-guided Radiotherapy (10) published in 2012, Wang Yu, Li Gui et al. designed 3D evaluation algorithm in dose-guided radiotherapy through integrating the formulas and physics significance of assessment methods of dose derivation, positional derivation and g, in order to achieve 3D dose validation. Dose derivation refers to the ratio of the derivation between center dose value in gross tumor volume (GTV), edge dose value in planning target volume (PTV) and center dose value in GTV (11). A dose derivation of more than 5% can be considered as a derivation that exceeds the acceptable range in the irradiation target volume and PTV and therefore the treatment plan needs to be redesigned or corrected. In this experiment, PTV formed as GTV (head-to-toe) expanded outward for 15-20 mm and the radiotherapy plan was formulated. Through measuring the edge dose of PTV and the center dose of GTV it was established that dose derivation were 3.705% and 4.07% respectively, and both were less than 5%, indicating the treatment was accurate.

In conclusion, the means for respiratory motion control mentioned above are still effective although they are not so perfect in the clinical application. Through comparing experimental group and case group and validating the same plan for at least three times, we can conclude that the verified derivation value of patients in group d is higher than the respiratory motion value, thus the treatment plan needs to be corrected for retreatment, whereas the verified derivation values of patients from the other groups was less than the respiratory motion value, thus the correction is needed. All the findings above suggest that radiotherapy applying CTVision is

accurate, but validation is indispensable.

REFERENCES

1. Huang JL, Yan S, Wu SF, Xia YB. Differential Diagnosis of Respiratory Motion Artifact and Rib Fracture in 3D Reconstruction of Multi-slice Spiral CT. Chinese Medical Equipment Journal 2014; 35(1):85-6.
2. Gong GZ, Yin Y, Chen JH, Song JL, Ma CS, Shang DP, Lu J, Liu TH. The individual internal gross target volume for hepatocellular carcinoma: four-dimensional CT *vs* three-dimensional ct associated with active breathing control. Chinese J Radiation Oncology 2011; 20(6):517-20.
3. Fan H. A study on target mobility rule and dosimetry of primary middle and distal esophageal cancer during the radiotherapy. Luzhou Medical College 2013. http://cdmd.cnki.com.cn/Article/CDMD-10632-1014109075.htm
4. Xiao F, Tan LN, Sun XH, Ma K, Liu XL, Zhou B. Influence of respiratory motion on the dose distribution in dynamic intensity-modulated radiotherapy for lung cancer. Modern Oncol 2012; 20(3):608-11.
5. He JF. Respiratory motion simulation by digital geometrical phantom. J System Simulation 2010; 22(9):2227-34.
6. Liu KJ, Song R, Luo SX, et al. Impact of respiratory movement on the target volume for lung cancer therapy. biomedical engineering and clinical medicine 2013; 17(3):224-7.
7. Mornex F, Girard N, Beziat C, Kubas A, Khodri M, Trepo C. Feasibility and efficacy of high-dose three-dimensional-conformal radiotherapy in cirrhotic patients with small-size hepatocellular carcinoma non-eligible for curative therapies-mature results of the French Phase□RTF-1 trial. Int J Radiat Oncol Biol Phys 2006; 66(4):1152-8.
8. Zhang YJ, Li JB, Xing J, Li FX, Ma ZF, Ma CS, Liang CQ. Analysis of liver cancer target volume and tissue displacement based on 4-dimensional and 3-dimensional CT. Chin J of Radiat Oncol 2012; 21(3):261-2.
9. Zhang HM. Analysis on positioning of non-small cell lung cancer treated by continuous hyper fractionated accelerated conformal radiotherapy combined with deep inspiration breath-hold technique. Jilin Medi 2011; 32(26):5425-6.
10. Wang Y, Li G, Wang D, Wu YC, FDS Team. Realization of 3D evaluation algorithm in dose-guided radiotherapy. Nuclear Phy Review 2012; 29(3):305-9.
11. Forner A, Reig ME, de Lope CR, Bruix J. Current strategy for stagingand treatment: the BCLC update and future prospects. Semin Liver Dis 2010; 30(1):61-74.

THE INFLAMMATORY MILIEU AND THE INSULIN LIKE GROWTH FACTOR AXIS IN CHILDREN WITH INFLAMMATORY BOWEL DISEASE FOLLOWING RECOMBINANT HUMAN GROWTH HORMONE TREATMENT

S.C. WONG[1], A.M. DALZELL[2], P. MCGROGAN[3], M. DIDI[4], P. LAING[4] and S.F. AHMED[1]

[1]Developmental Endocrinology Research Group, Royal Hospital for Sick Children, Glasgow, United Kingdom; [2]Department of Gastroenterology, Royal Liverpool Children's Hospital, Liverpool, United Kingdom; [3]Department of Gastroenterology, Royal Hospital for Sick Children, Glasgow United Kingdom; [4]Department of Endocrinology, Royal Liverpool Children's Hospital, Liverpool, United Kingdom

Received July 14,2014 – Accepted January 27, 2015

It is unclear whether recombinant human growth hormone (rhGH) in inflammatory bowel disease (IBD) alters cytokine profile. The objective of this study is to evaluate changes in cytokines and systemic markers of the insulin growth factor axis following 6 months of rhGH treatment in children with IBD. In a six-month randomised control trial in children with IBD treated with rhGH at 0.067 mg/kg/day and controls (11 in each group), we measured pro-, anti-inflammatory cytokines and systemic markers of the IGF axis (total IGF-1, free IGF-1, total IGFBP-3, ALS, IGFBP-2) at baseline (T+0), and six months (T+6). Results expressed as median (range). In the rhGH group, TNFα was 3.1pg/ml (2.9, 100.6) and 3.6pg/ml (3.1, 5.3) at T+0 and T+6, respectively (p=0.85), whereas in the controls this was 3.3pg/ml (2.7, 4.0) and 3.1pg/m l (2.7, 4.7), respectively (p=0.79). In the rhGH group, IL1β was 18.0pg/ml (5.0,716.7) and 18.0pg/ml (1.7, 52.2) at T+0 and T+6 respectively(p=0.90), whereas in the controls this was 19.8pg/ml (4.1, 27.1) and 19.1pg/ml (2.4,77.3), respectively (p=0.65). None of the twenty-eight other cytokines analysed was different at T+6 in either group. Despite increase in total IGF1 in the rhGH group (p=0.03), free IGF1, IGFBP3, ALS and IGFBP2 did not change in either group at T+6. Percentage change in IGFBP3, was significantly associated with percentage change in IL2 (r=0.77, p=0.009) and IL4 (r=0.58, p=0.01). Percentage change in ALS was significantly associated with percentage change in IL2 (r=0.90, p<0.0001) and IL4 (r=0.63, p=0.04). Although changes in markers of the GH/IGF-1 axis do show an association with cytokines (IL-2, IL-4) in pediatric IBD, six months of rhGH treatment was not associated with any significant changes in levels of a range of pro and anti-inflammatory cytokine. Careful evaluation of disease process is required in future trials of rhGH in paediatric IBD.

Childhood inflammatory bowel disease (IBD), especially Crohn's disease (CD) is frequently complicated by growth retardation that may even lead to a reduction in final adult height in a small sub-set (1). Central to the underlying etiology of growth retardation are the modulatory effects of pro-

Key words: cytokines, growth hormone, insulin like growth factor, insulin growth factor binding protein, acid labile subunit, inflammatory bowel disease, inflammation, interleukin, tumour necrosis factor

Mailing address: Dr Sze Choong Wong,
Developmental Endocrinology Research Group,
School of Medicine, University of Glasgow,
Royal Hospital for Sick Children,
Glasgow, G3 8SJ, United Kingdom
Tel.: +44 141 201 0709
e-mail: jarod.wong@glasgow.ac.uk

0393-974X (2015)

inflammatory cytokines on systemic growth factors (2) and also directly at the level of the growth plate. Chronic inflammation is associated with functional growth hormone (GH) resistance, although a range of abnormalities in secretion and sensitivity of GH and insulin like growth factor-1 (IGF-1) is seen in children with IBD. Several clinical trials have demonstrated the efficacy of high dose recombinant human growth hormone (rhGH) for improving linear growth in juvenile idiopathic arthritis (JIA) (3) and IBD (4). Our recent randomised controlled trial of recombinant human growth hormone (rhGH) at 0.067 mg/kg/day, in a group of children with IBD and growth retardation demonstrated that treatment was associated with a median increase in height velocity of 140% in the treated group compared to 1.7% in the untreated, control group (4).

It is possible that rhGH treatment in IBD may also lead to an improvement in linear growth as a consequence of improvement in inflammatory status and reduction of inflammatory cytokine levels. Animal models of colitis suggest that there may be a beneficial role of rhGH in chronic inflammation (5, 6). One randomised trial in adults with CD (7) and another in children with CD (8) suggest that rhGH treatment may improve disease activity but the primary end-points in both studies were the CD activity index (CDAI) and paediatric CDAI (PCDAI). On the other hand, some studies in GH-sufficient children also suggest that rhGH therapy may up-regulate inflammatory cytokines (9). Given the close link between the GH axis and immune function, a comprehensive evaluation of inflammatory cytokines would be beneficial in those children with CD treated with rhGH.

We have recently reported that rhGH is effective in improving linear growth over a six-month period in paediatric IBD. The objective of the current study was to evaluate changes in a range of pro-, anti-inflammatory cytokines and markers of the IGF axis in a group of children with IBD undergoing rhGH therapy (4).

MATERIALS AND METHODS

Patients

Methodology and patient recruitment were previously described in detail. In brief, twenty-two children (11 in each group) were recruited from two UK tertiary pediatric hospitals (4). Inclusion criteria were a diagnosis of IBD confirmed endoscopically in children who were either very short (Ht SDS<-2.0) or relatively short but had been growing slowly (Ht SDS<-1.0 and HV SDS<-1.0) over the previous six months. Children were randomised by a computer-generated list to either receive rhGH (Norditropin Simplexx®, Novonordisk) administered at a dose of 0.067mg/kg/day as daily subcutaneous injections for six months or no treatment (control, Ctrl). The dose of rhGH was chosen as it has been shown to be effective for improving growth in children with JIA (3).

The study was not blinded and parents were informed of group assignment following randomisation at recruitment. Of the 22 children recruited, 11 (8M, 3F) with a median age 14.7yrs (9.1, 16.4) were randomised to the rhGH group, and 11 (8M, 3F) with a median age 13.7yrs (8.5, 15.5) were randomised to the Ctrl group. All children, except one, had CD and this single child who was in the Ctrl group had ulcerative colitis (UC).

The trial was approved by the UK multicentre research ethics committee, its conduct was approved by the Health Boards of both institutes and was audited by the UK Medicines and Healthcare products Regulatory Agency in 2009. Written informed consent was obtained from all parents and patients as appropriate.

Disease activity assessment

Paediatric Crohn's disease activity index (PCDAI) and abbreviated paediatric Crohn's disease activity index (APCDAI) were determined at each study visit. The PCDAI is a disease activity score with a maximum score of 100: subjective symptoms - 30 points, physical examination - 30 points, biochemical parameters - 20 points, growth data (including height velocity) -20 points. Clinical evaluations for calculation of the PCDAI were performed by the same researcher at baseline and six months. The APCDAI is a disease activity score with a maximum score of 60 and only includes subjective symptoms - 30 points and physical examination - 30 points components of the PCDAI. At each study visit, details of treatment and nutritional support were obtained. Oral prednisolone dose over the six-month period of the study were converted into mg/kg/day.

Laboratory data

All laboratory investigations were performed at 09.00 after an overnight fast. Research study blood samples were obtained for measurements of inflammatory cytokines and IGF axis of stored serum analysed at the end of the study. Blood samples were collected at baseline and 6 months in the rhGH and Ctrl group. Priority was given to measurement of total IGF-1 and inflammatory cytokines where sample volumes are limited. Inflammatory

cytokines were measured by a Luminex assay according to the manufacturer's protocol as previously described using the Multiplex system and Bio-Plex software (Biosource, Nivelles, Belgium) (10). All samples were assayed in triplicate and values determined by comparison to standard curves run in parallel. Levels of sensitivity for these assays vary between 5-15 pg/ml. Total IGF-1 was assayed using a two-site chemiluminescent immunoassay (Nichols Advantage®) with an intra-assay precision of less than 4% and an inter-assay precision of less than 7.8% over the assay range. Free IGF-1 and insulin growth factor binding protein (IGFBP)-3 were assayed using ELISA (Diagnostic Systems Laboratory INC, USA). The intra-assay and inter-assay precision of free IGF-1 was less than 5% and less than 11.1%, respectively. The intra-assay and inter-assay precision of IGFBP-3 was less than 9.6% and 11.4%, respectively. IGFBP-2 was assayed using ELISA (Mediagnost GmbH, Germany) with intra-assay and inter-assay precision of less than 6.5% and 7.5%, respectively. Acid labile subunit (ALS) was assayed using ELISA (Demeditech Diagnostic, Germany) with intra-assay and inter-assay precision of less than 6.8% and 9%, respectively.

Statistics

The clinical trial was powered based on the primary outcome measure which was the percentage difference in actual HV (cm/year) over six months between the two groups. Changes between parameters assessed at baseline and six months in the rhGH and Ctrl group respectively were analysed using the Wilcoxon signed rank test. Strengths of associations were analysed using Spearman's correlation. Data presented as median (range) were analysed using SPSS version 18.0. Statistical significance was assumed at $p<0.05$.

RESULTS

Disease characteristics

As previously reported, disease severity, duration of oral prednisolone treatment and changes in

Table I. *Pro- and anti-inflammatory cytokines before and after recombinant human growth hormone in paediatric inflammatory bowel disease.*

	rhGH T+0	rhGH T+6	P value (rhGH T+0 vs T+6)	Ctrl T+0	Ctrl T+6	P value (Ctrl T+0 vs T+6)
TNFβ (pg/ml)	3.1 (2.9, 100.6)	3.6 (3.1, 5.3)	0.85	3.3 (2.7, 4.0)	3.1 (2.7, 4.7)	0.79
IL1β (pg/ml)	18.0 (5.0, 716.7)	18.0 (1.7, 52.2)	0.90	19.8 (4.1, 27.1)	19.1 (2.4, 77.3)	0.65
IL6 (pg/ ml)	3.0 (3.0, 12.9)	3.0 (3.0, 17.3)	0.91	9.9 (3.0, 21.6)	7.2 (3.0, 49.5)	0.66
IL2 (pg/ml)	9.2 (2.8, 371.9)	5.6 (1.1, 18.5)	0.45	4.0 (0.5, 117.2)	2.1 (1.0, 21.9)	0.75
IL4 (pg/ml)	112.5 (97.6, 895.8)	112.0 (96.0, 128.5)	0.85	115.5 (94.6, 121.1)	112.4 (51.2, 130.2)	0.48
Il5 (pg/ml)	5.6(3.5,7)	5.1(3.5,7)	0.89	6.5 (3.7, 7.2)	6.4 (4.5, 6.9)	0.76
IL7 (pg/ml)	37.8(26.6,48.6)	38.1(29.1,66.5)	0.79	31.7 (16.3, 42.1)	34.9 (16.8, 49.5)	0.48
IL12 (pg/ml)	273.2(118.7,413.9)	294.8(187.5.412.7)	0.11	345.2 (237.1,435)	339.1 (251.6, 655.9)	0.93
IL15 (pg/ml)	116.3(78.6,133.8)	99.8(8.8,135.4)	0.44	100.1(75.6,119.9)	96.9(79.4,190.4)	0.93
1L17 (pg/ml)	33.1(2.9,323.4)	38.3(2.7,54.4)	0.67	46.7(9.5,317.1)	56(23.5,378.1)	0.89
IL8 (pg/ml)	36.2(9.9,158.5)	43.1(7.9,1571.4)	0.86	31.5(10.9,2093.2)	27.3(7.3,80)	0.72
MIP1α (pg/ml)	71.9(9.1,111.8)	105.6(12,125)	0.69	96.5(89,144.6)	97.2(30.3,146.3)	0.74
MIP1β (pg/ml)	98.5(37.5,1168.8)	104.4(20.8,163.2)	0.51	102.2(50.8,201.4)	110(49.5.378.9)	0.48
IFNα (pg/ml)	97.5 (25.1, 575.4)	97.9 (27.7, 894.6)	0.80	96.8 (53.6, 120.2)	100.5 (85.4, 145.6)	0.72
IFNγ (pg/ml)	25.0 (22.7, 894.6)	27.0 (4.7, 76.4)	0.77	26.7 (20.9. 34.5)	21.3 (18.3, 29.2)	0.64
IP10 (pg/ml)	50/9(29.3,196.5)	50.9(29.3,196.5)	0.11	46.4(15.8,252.8)	59.2(34.7,123.5)	0.13
Eotaxin (pg/ml)	101.3(70.8,303.5)	110(60.6,205.3)	0.59	169.4(67.5,273.2)	164.2(60.7.226.5)	0.59
RANTES (pg/ml)	4077.3(3034.8,19670.9)	3115.9(34,37594.2)	0.4	4212.8(2795.9,7209.5)	4995.1(2471,8668.7)	0.74
IL10 (pg/ml)	9.6(8.1,655.9)	9.9(3.5,864.4)	0.44	8.9(5.8,80)	9.3(5.1,51.5)	0.79
IL13 (pg/ml)	32.5 (19.7, 67.2)	30.4 (26.5, 58.4)	0.72	59.9 (46.9, 71.0)	31.2 (14.9, 63.6)	0.11
IL1RA (pg/ml)	1085.5(701,9307)	1256.8(715.3,1442.9)	0.51	1166(940.9,1450.3)	1083.7(768.9,1505.5)	0.66
IL2R (pg/ml)	542.4(378.1,4815.2)	562.3(412.6,668.8)	0.39	674.4(500.9,868.3)	521.2(472,1183.4)	0.31

rhGH: recombinant human growth hormone; Ctrl: control; pg/ml: pictogram per millilitre; TNF: tumour necrosis factor; IL: interleukin; MIP: macrophage inflammatory protein; IFN: interferon; IP interferon inducible protein; RANTES: regulated on activation normal T expressed and secreted; IL1RA: interleukin 1 receptor antagonist; IL2RA" interleukin 2 receptor; T+0: baseline; T+6: Six months

background medication did not differ between the two groups over the six-month period. (4). Of note, six of the 11 children in the rhGH group and two of the 11 in the control group were on oral Prednisolone at baseline. Two of the 11 children in the rhGH group and one of the 11 in the control group were on oral Prednisolone at six months. Two children in each group had acute relapse of their IBD during the study period. For the rhGH group, PCDAI was 12.5 (2.5, 37.5) and 5.0 (0.0, 40.0) at baseline and six months, respectively (p=0.04) whereas, in the control group, PCDAI was 12.5 (0.0, 30.0) and 23.8 (0.0, 35.0) at baseline and six months, respectively (p= 0.10). However, there was no difference in APCDAI at baseline and six months in the rhGH or control group. In the rhGH group, APCDAI was 0.0 (0.0, 20.0) and 0.0 (0.0, 35.0) at baseline and six months (p=0.50) and in the control group, APCDAI was 0.0 (0.0, 10.0) and 2.5 (0.0, 30.0), respectively (p=0.21).

Inflammatory cytokines

Table I shows the results for changes in pro- and anti-inflammatory cytokines in the rhGH and control groups. We had previously reported the lack of change in tumour necrosis factor (TNF)-α, interleukin (IL1)-β and IL-6 in the Ctrl and rhGH groups (4). None of any of the cytokines measured showed changes over the six months in either group. In addition, growth factors/inflammatory mediators: hepatocyte growth factor (HGF), fibroblast growth factor (FGF), granulocyte colony stimulating factor (GCSF), epidermal growth factor (EGF), monocyte chemoattractant protein 1 (MCP1), monocyte mRNA induced by interferon gamma (MIG), granulocyte monocyte colony stimulating factor (GMCSF), vascular endothelial growth factor (VEGF) did not change in either group over the six months (Data not shown). There were no statistical differences between any of the cytokines in the rhGH and Ctrl groups at baseline or at six months.

There were no significant associations between erythrocyte sedimentation rate (ESR) with IL1β (r= -0.01, p= 0.96), IL6 (r= 0.04, p= 0.96), TNFα (r= -0.12, p= 0.44), IL2 (r= 0.17, p= 0.39), IL2RA (r= 0.01, p= 0.94), IL4 (r= -0.11, p= 0.48) and IL10 (r= 0.07, p= 0.67) (Fig. 1). Similarly, there were no significant associations between C-reactive protein (CRP) with IL1β (r= -0.03, p= 0.86), IL2 (r= -0.03, p= 0.89), IL2RA (r= 0.13, p= 0.42), IL4 (r= 0.22, p= 0.16) and IL10 (r= 0.11, p= 0.48). There was a weak association between C-reactive protein (CRP) and IL6 although not statistically significant (r= 0.29, p= 0.06). There was a weak negative significant association between CRP and TNFα (r= -0.35, p= 0.03). When we excluded the one outlier, there was still no significant association between ESR with IL1β (r= 0.04, p= 0.81) and TNFα (r= -0.09, p= 0.59). Similarly when the outlier was excluded, there was no significant association between CRP and IL1β (r= -0.05, p= 0.77) but a weak negative association with TNFα (-0.37, p= 0.02).

IGF axis

Study samples were prioritised for measurement of total IGF-1 and as such some patients did not have sufficient samples for measurements of the other markers of IGF axis. Only patients with paired samples at baseline and six months were included for statistical analysis. Total IGF-1 increased significantly in the rhGH group, which was not paralleled by changes in IGFBP-3 and ALS. Free IGF1 did not change in either group (Figs. 2 and 3). The IGF-1/IGFBP-3 molar ratio showed a trend towards improvement in the rhGH group: 0.02 (0.01, 0.05) and 0.05 (0.02, 0.07) at baseline and six months, respectively (p=0.07). The IGF-1/IGFBP-3 molar ratio did not change in the control group: 0.02 (0.01, 0.04) and 0.03 (0.02, 0.05) at baseline and six months, respectively (p=0.88). The IGF-1/ALS molar ratio increased significantly in the rhGH group from 0.10 (0.06, 0.26) to 0.22 (0.10, 0.42) at baseline and six months, respectively (p=0.04). The IGF-1/ALS molar ratio did not change in the control group: 0.10 (0.05, 0.20) and 0.12 (0.07, 0.20) at baseline and six months, respectively (p=0.24). We evaluated the association of free IGF-1 of the ratio of total IGF-1 to binding proteins. Combining all the data of both groups at baseline, free IGF-1 was not associated with total IGF-1/IGFBP-3 (r=0.03, p=0.86), total IGF-1/ALS (r=0.29, p=0.08) and total IGF-1/ (IGFBP-3 + ALS) (r=0.10, p=0.56). There was, however, a significant positive association between free IGF-1 and total IGF-1: IGFBP-2 (r=0.55, p<0.0001).

Relationship of change in IGF axis and cytokines

As previous studies have reported significant

associations between IL-6 and markers of the GH-IGF axis in CD (11)and cystic fibrosis (12), we investigated the association of change in cytokines and the IGF axis in our cohort. Percentage change in total IGF-1 was not related to percentage change in any of the cytokines other than G-CSF (r=0.49, p=0.03). Percentage change in IGFBP-3 was significantly associated with a percentage change in IL-2 (r=0.77, p=0.009), IL-4 (r=0.58, p=0.01), IL-5 (r=0.50, p=0.03), and MCP (r=-0.53, p=0.02). Percentage change in ALS was significantly associated with percentage change in IL-2 (r=0.90, p<0.0001), IL-4 (r=0.63, p=0.004) and G-CSF (r=0.53, p=0.02). Percentage change in free IGF-1 was significantly associated with percentage change in IL-2 (r=0.83, p=0.003), IL-4 (r=0.53, p=0.02) and MCP (r=-0.53, p=0.02). Fig. 4 shows the association between percentage change in IGFBP3, ALS, free IGF1 with IL-2 and IL-4. Percentage change in IGFBP-2 was not related to percentage changes in any of the cytokines analysed. Age was not significantly associated with IL-2 (r= 0.21, p= 0.29), IL-4 (r= 0.17, p= 0.27), IL-5 (r= 0.20, p= 0.20 and G-CSF (r= -0.16, p= 0.36) but showed a modest significant association with MCP (r= 0.39, p= 0.01).

DISCUSSION

Recent studies on children with chronic disease like JIA (3)and IBD (4) have demonstrated the efficacy of rhGH as a growth promoting agent, despite a state of relative functional GH resistance in these children. This report is unique as it has comprehensively evaluated changes in a wide range of inflammatory cytokines and markers of the GH-IGF axis following rhGH therapy in children with chronic disease. The impact of rhGH therapy on the disease process is of interest given the link between the GH axis and the cytokine network (9, 13, 14). Detailed evaluation of markers of inflammation is also important to be certain that improvement in linear growth following rhGH therapy is not due to improvement in primary disease status given the remitting and relapsing nature of chronic inflammatory conditions and the possible role of rhGH on reduction of inflammation.

In children with GH deficiency, therapy with rhGH may be associated with an increase in inflammatory cytokines several hours after rhGH injection but levels return to normal within twenty-four hours (13, 15). Four days of rhGH injections in short non-GHD children has also been reported to be associated to an increase in TNFα, IL-1β, IL-2, IL-12 and IFNγ (9). The GH-IGF axis is known to have a bidirectional relationship with the cytokine network such that TNFα, IL-1β and IL-6 can affect the GH-IGF system (16). GH has also been reported to play a key role in priming macrophages for the production of TNFα, IL-1β and IL-6 (17) and induces interferon-γ production by lymphocytes (18).

In previous reports of rodent models with colitis, improvement in disease status following treatment with rhGH was associated with a reduction of mucosal apoptosis and reduced IL-6-dependent STAT3 activation (5, 6, 19). In a placebo-controlled study on adults with CD, rhGH therapy was associated with a reduction in CDAI after 4 months without changes in Hb, haematocrit, ESR, prealbumin, ferritin or iron levels (7). A recent study that explored the effect of rhGH on disease activity in paediatric CD, concluded that rhGH may be an adjunct for treatment of inflammatory disease based on an improvement in PCDAI (8). However, other markers of disease activity including endoscopic severity, faecal calprotectin and ESR did not show a significant difference. Given that growth velocity is used to calculate PCDAI, it is possible that the lower PCDAI in the rhGH group in that study may merely reflect the marked improvement in linear growth which was observed in the treated group.

Although the current study showed that rhGH therapy in paediatric IBD did not lead to a significant overall change from baseline to 6 months in a range of pro- and anti-inflammatory cytokines, significant positive associations were observed between IGF binding proteins with several cytokines, notably IL-2 and IL-4 which are cytokines released from activated T cells (20). It is also thought that GH interacts with the immune system via its effects on the T helper cells. Hypophysectomised rats treated with thirteen days of GH showed increased levels of IL-2 and IL-4 (21). GH treatment of irradiated human peripheral blood lymphocytes was able to restore the release of IL-2 (22). Other studies, on the other hand, suggest that IL-2 plays a role in the reduction of GH (23). Thus our data further confirm the tight link between the GH axis, the cytokine network and immune

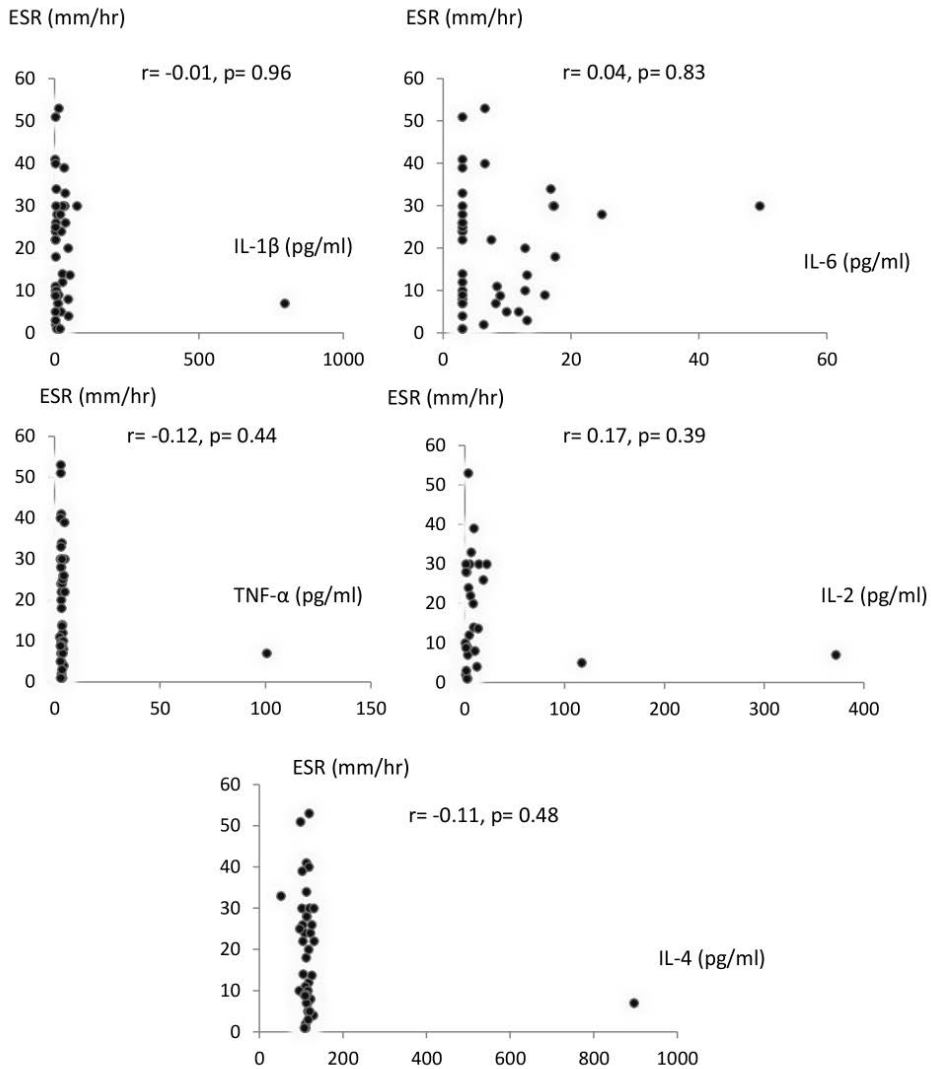

Fig. 1. *Relationship of ESR and cytokines. ESR: erythrocyte sedimentation rate; IL: interleukin; TNF-α: tumour necrosis factor alpha; mm/hr: millimetre per hour*

system.

In contrast to a few previous studies of rhGH treatment in JIA and IBD which have reported an increase in total IGF-1 and IGFBP-3 (24, 25), rhGH treatment on children with IBD in the current cohort only led to an improvement in total IGF-1. Molar ratios of IGF-1 to its binding proteins may provide a surrogate marker of free, bioavailable IGF-1 and IGF-1:IGFBP-3, and IGF-1:IGFBP-2 have been reported to increase significantly following introduction of a gluten-free diet in children with coeliac disease (26). In the current study, the molar ratio of IGF-1:ALS was significantly higher after six months of rhGH with a trend towards an increase in the molar ratios of IGF-1:IGFBP-3 and IGF-1:IGFBP-2 suggesting higher bioavailable IGF-1. However, on measuring free IGF-1, no significant change was detected in either group. Although, this may reflect the difficulty of measuring free IGF-1 (27), it is also possible that inflammation may lead to a greater clearance of free IGF-1 (28). The lack of association of free IGF-1 with molar ratios of total IGF-1 to binding proteins

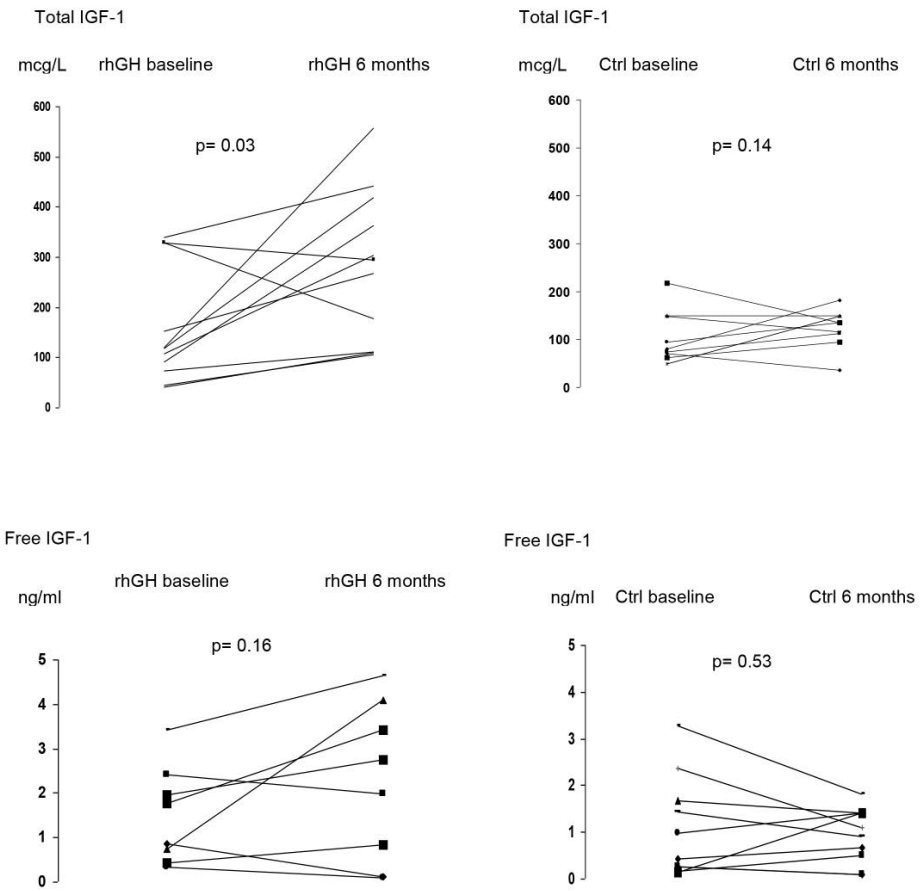

Fig. 2. *Total and free IGF-1 in paediatric inflammatory bowel disease. IGF-1: insulin like growth factor-1; rhGH: recombinant human growth hormone; Ctrl: control; mcg/L: microgram per litre; ng/ml: nanogram per millilitre*

assessed in this study lend support to that hypothesis. The limitations of our study include the small sample size, and not all of our patients had sufficient sample for measurement of all the binding proteins and free IGF-1.

Our observation of a positive association between free IGF-1 and the total IGF-1/IGFBP-2 molar ratio confirms a previous report of the raised IGFBP-2 during acute relapse in children with IBD (11). IGFBP-2 has shown to be inversely associated with short-term growth in children undergoing high-dose glucocorticoid therapy for remission of acute leukaemia (29). Percentage change in IGFBP-2 was positively associated with percentage change in IL-6 in a group of prepubertal children with cystic fibrosis (12). Similarly, IGFBP-2 was also positively associated with IL-6 in a group of young adults with cystic fibrosis (30). The precise role of IGFBP-2 in regulation of growth in chronic disease requires further exploration.

Inflammatory cytokines, especially TNFα, IL1β and IL6, are implicated in the pathogenesis of IBD, whereas in clinical practice ESR and CRP are measured to evaluate state of inflammation. It is unclear how individual cytokines are related to disease activity and clinical markers of inflammation in childhood IBD. Previous studies, howeve,r have found significant association between IL6 and CRP/ESR in children with IBD (11). We found a weak association between TNFα and CRP. However, as we have previously shown in a group of children with JIA, expression of a range of cytokines in serum and

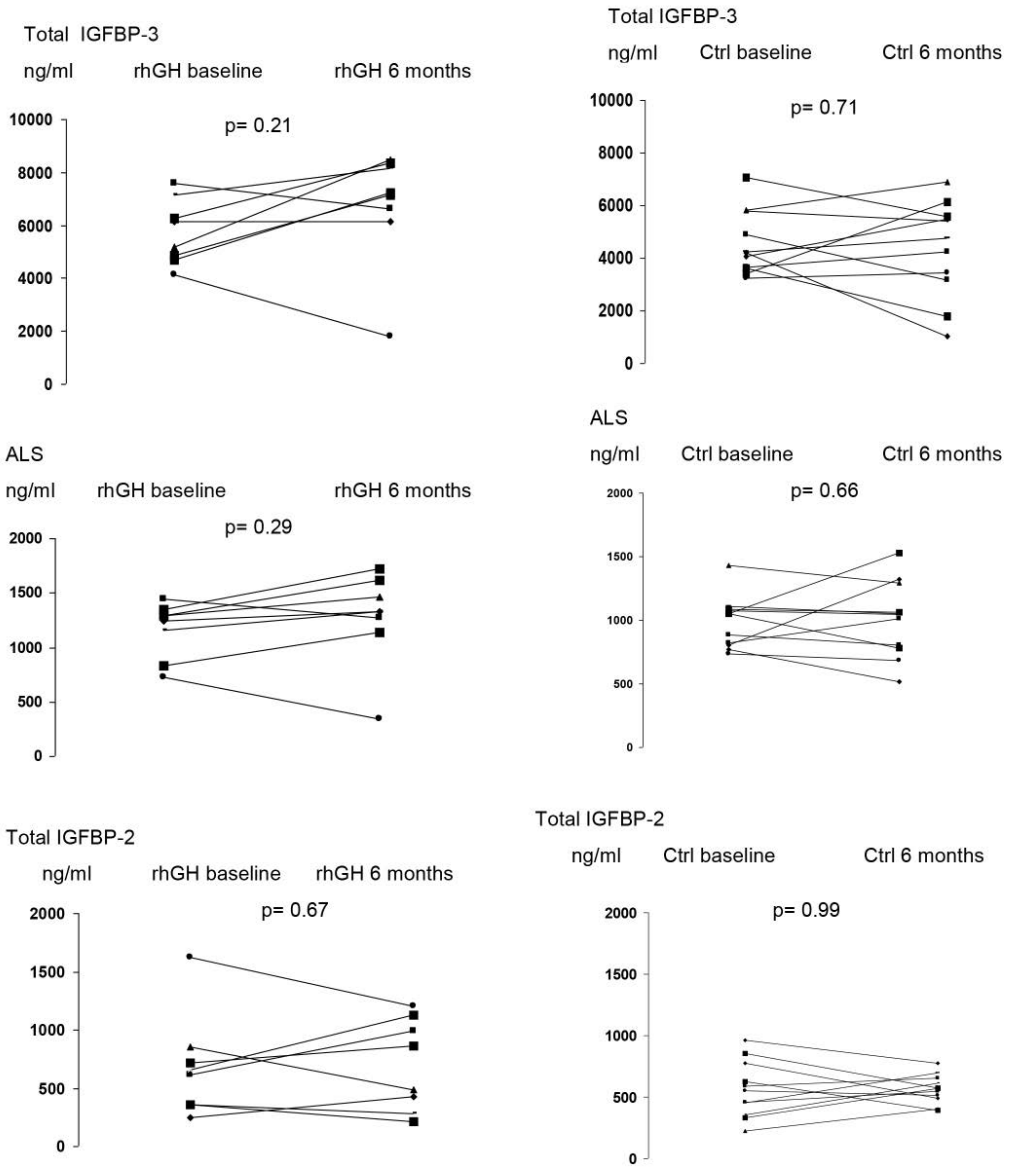

Fig. 3. *Insulin like growth factor binding proteins in paediatric inflammatory bowel disease. IGFBP-3: insulin like growth factor binding protein-3; ALS: acid labile subunit; IGFBP-2: insulin like growth factor binding protein-2; rhGH: recombinant human growth hormone; Ctrl: control; ng/ml: nanogram per millilitre*

synovial fluid can vary even within the same subtype of JIA (10) and a single cytokine measurement at one time point may not be very informative.

Our study is limited by the fact that this study was not powered to look at changes in markers of the GH-IGF axis and cytokines. In addition, we had no data on markers of the IGF axis and cytokines from healthy children from our population measured with the same assays. Finally, given the small numbers in our study, statistically significant associations could be due to chance.

To summarise, our preliminary study demonstrated for the first time that six months of rhGH treatment in paediatric IBD did not lead to significant increase

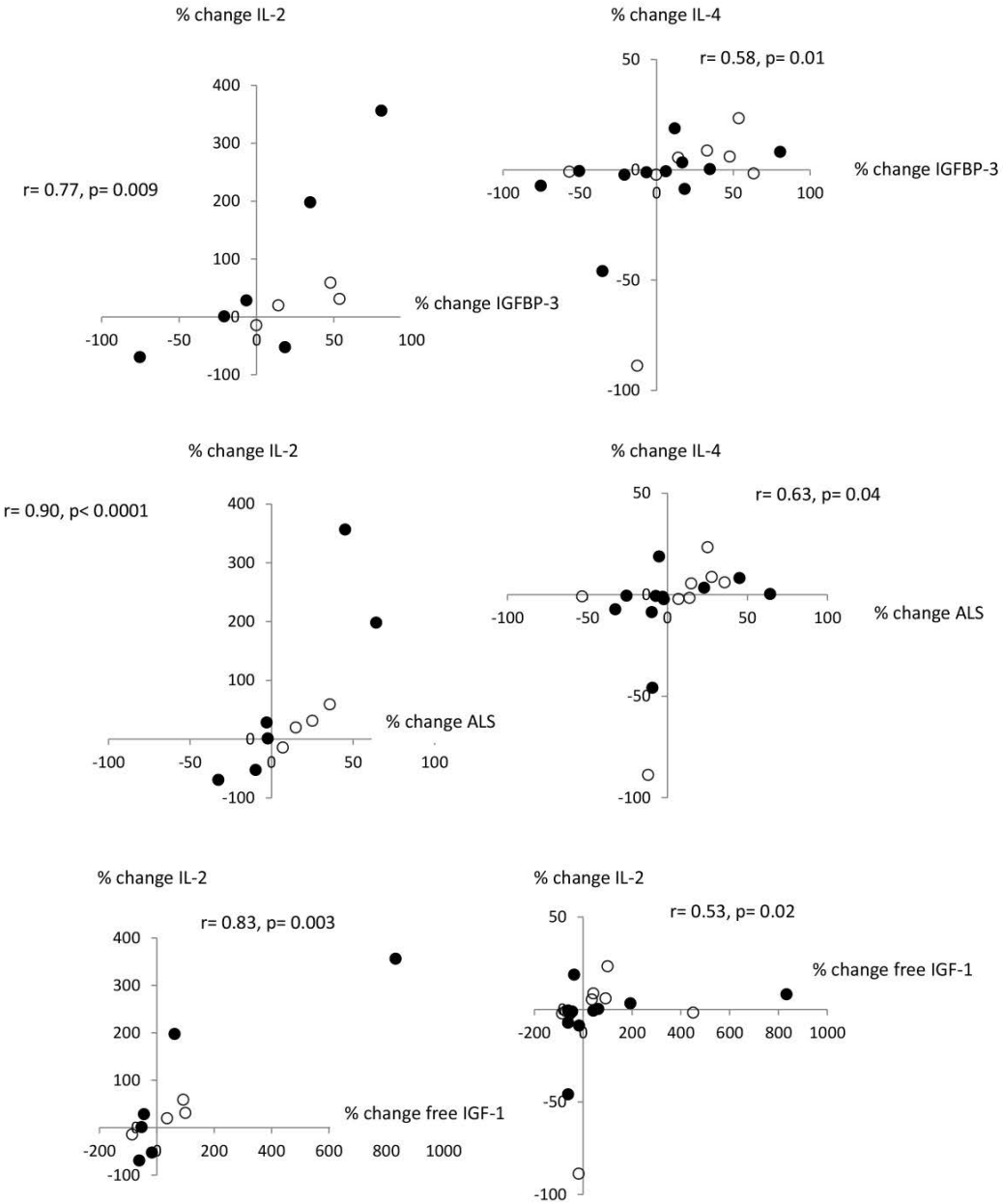

Fig. 4. *Relationship of percentage change of IGFBP-3, ALS, free IGF-1 and cytokines. %: percentage; IGFBP: insulin like growth factor binding protein; IGF: insulin like growth factor; IL: interleukin;* • *rhGH* ◦ *Control*

or reduction in a range of inflammatory cytokines. Changes in markers of the GH/IGF axis were associated with changes in circulating cytokines, confirming the link between the GH-IGF axis and the immune system/inflammatory network. Alterations in cytokines in inflammatory conditions may reflect the extent of GH resistance and this requires future study.

ACKNOWLEDGEMENTS

SCW was supported by the University of Glasgow and Novo Nordisk UK during the course of this clinical trial. We thank: the participating

children and their parents; E. McNeill and Z. Yung for patient education; A. Gracie, A.M. Wallace, J. Reilly, J. Jones, P. Newland and K. Padmore for technical assistance.

Conflict of interest: SCW has received clinical and research fellowship grants from Novo Nordisk UK, Novo Nordisk Australia and has received speaker's honorarium from Sandoz. MD is on advisory panels for Pfizer and Merck Serono. PL is on advisory panels for Novo Nordisk, Pfizer, Merck Serono, Ipsen, Sandoz and Ferring. SFA has received consultation fees and research grants from Ipsen and Novo Nordisk UK. The other authors have no conflict of interest to declare.

REFERENCES

1. Sawczenko A, Ballinger AB, Savage MO, Sanderson IR. Clinical features affecting final adult height in patients with pediatric-onset Crohn's disease. Pediatrics 2006; 118:124-29.
2. Wong SC, Smyth A, McNeill E, Galloway PJ, Hassan K, McGrogan P, Ahmed SF. The growth hormone insulin-like growth factor 1 axis in children and adolescents with inflammatory bowel disease and growth retardation. Clin Endocrinol (Oxf) 2010; 73:220-28.
3. Simon D, Bechtold S. Effects of growth hormone treatment on growth in children with juvenile idiopathic arthritis. Horm Res 2009; 72(S)1:55-59.
4. Wong SC, Kumar P, Galloway PJ, et al. A preliminary trial of the effect of recombinant human growth hormone on short-term linear growth and glucose homeostasis in children with Crohn's disease. Clin Endocrinol (Oxf) 2011; 74:599-607.
5. Han X, Sosnowska D, Bonkowski EL, Denson LA. Growth hormone inhibits signal transducer and activator of transcription 3 activation and reduces disease activity in murine colitis. Gastroenterology 2005; 129:185-203.
6. Kara E, Sungurtekin H, Sungurtekin U, Alkanat M, Ilkgul O. The effect of recombinant human growth hormone (rhGH) on trinitrobenzene sulfonic acid-induced colitis in rats: an experimental study. Inflamm Bowel Dis 2004; 10:112-15.
7. Slonim AE, Bulone L, Damore MB, Goldberg T, Wingertzahn MA, McKinley MJ. A preliminary study of growth hormone therapy for Crohn's disease. N Engl J Med 2000; 342:1633-37.
8. Denson LA, Kim M-O, Bezold R, et al. A randomized controlled trial of growth hormone in active pediatric Crohn disease. J Pediatr Gastroenterol Nutr 2010; 51:130-39.
9. Bozzola M, De Benedetti F, De Amici M, Jouret B, Travaglino P, Pagani S, Conte F, Tauber M. Stimulating effect of growth hormone on cytokine release in children. Eur J Endocrinol 2003; 149:397-401.
10. Wong SC, MacRae VE, Gracie JA, McInnes IB, Galea P, Gardner-Medwin J, Ahmed SF. Inflammatory cytokines in juvenile idiopathic arthritis: effects on physical growth and the insulin-like-growth factor axis. Growth Horm IGF Res 2008; 18:369-78.
11. Street ME, de'Angelis G, Camacho-Hubner et al. Relationships between serum IGF-1, IGFBP-2, interleukin-1beta and interleukin-6 in inflammatory bowel disease. Horm Res 2004; 61:159-64.
12. Street ME, Spaggiari C, Volta C, et al. The IGF system and cytokine interactions and relationships with longitudinal growth in prepubertal patients with cystic fibrosis. Clin Endocrinol (Oxf) 2009; 70:593-98.
13. Bozzola M, De Amici M, Zecca M, Schimpff RM, Rapaport R. Modulating effect of human growth hormone on tumour necrosis factor-alpha and interleukin-1beta. Eur J Endocrinol 1998; 138:640-43.
14. Bozzola M, Lorini R, Schimpff RM, Severi F, Job JC. Effects of human growth hormone administration on growth rate and growth-stimulating activity of serum, measured by lymphocyte bioassay in hypopituitary children. Horm Metab Res 1986; 18:264-67.
15. Pagani S, Meazza C, Travaglino P, De Benedetti F, Tinelli C, Bozzola M. Serum cytokine levels in GH-deficient children during substitutive GH therapy. Eur J Endocrinol 2005; 152:207-10.
16. Wolf M, Bohm S, Brand M, Kreymann G. Proinflammatory cytokines interleukin 1 beta and tumor necrosis factor alpha inhibit growth hormone stimulation of insulin-like growth factor I synthesis and growth hormone receptor mRNA levels in cultured rat liver cells. Eur J Endocrinol 1996; 135:729-37.
17. Edwards CK, 3rd, Lorence RM, Dunham DM, et al. Hypophysectomy inhibits the synthesis of tumor necrosis factor alpha by rat macrophages: partial restoration by exogenous growth hormone or interferon gamma. Endocrinology 1991; 128:989-

86.
18. Mustafa A, Nyberg F, Mustafa M, Bakhiet M, Mustafa E, Winblad B, Adem A. Growth hormone stimulates production of interferon-gamma by human peripheral mononuclear cells. Horm Res 1997; 48:11-15.
19. Williams KL, Fuller CR, Dieleman LA, DaCosta CM, Haldeman KM, Sartor RB, Lund PK. Enhanced survival and mucosal repair after dextran sodium sulfate-induced colitis in transgenic mice that overexpress growth hormone. Gastroenterology 2001; 120:925-37.
20. Cushley W, Harnett MM. Cellular signalling mechanisms in B lymphocytes. Biochem J 1993; 292(Pt 2):313-32.
21. Exon JH, Bussiere JL, Williams JR. Hypophysectomy and growth hormone replacement effects on multiple immune responses in rats. Brain Behav Immun 1990; 4:118-28.
22. Lempereur L, Brambilla D, Scoto GM, et al. Growth hormone protects human lymphocytes from irradiation-induced cell death. British J Pharmacol 2003; 138:1411-16.
23. Karanth S, McCann SM. Anterior pituitary hormone control by interleukin 2. Proc Natl Acad Sci U S A 1991; 88:2961-65.
24. Mauras N, George D, Evans J, et al. Growth hormone has anabolic effects in glucocorticosteroid dependent children with inflammatory bowel disease Metabolism 2002 51:127-35.
25. Davies UM, Jones J, Reeve J, Camacho-Hubner C, Charlett A, Ansell BM, Preece MA, Woo PM. Juvenile rheumatoid arthritis. Effects of disease activity and recombinant human growth hormone on insulin-like growth factor 1, insulin-like growth factor binding proteins 1 and 3, and osteocalcin. Arthritis Rheum 1997; 40:332-40.
26. Street ME, Volta C, Ziveri MA, et al. Changes and relationships of IGFS and IGFBPS and cytokines in coeliac disease at diagnosis and on gluten-free diet. Clin Endocrinol (Oxf) 2008; 68:22-28.
27. Bang P, Ahlsen M, Berg U, Carlsson-Skwirut C. Free insulin-like growth factor I: are we hunting a ghost? Horm Res 2001; 55 Suppl 2:84-93.
28. De Benedetti F, Meazza C, Oliveri M, et al. Effect of IL-6 on IGF binding protein-3: a study in IL-6 transgenic mice and in patients with systemic juvenile idiopathic arthritis. Endocrinology 2001; 142:4818-4826.
29. Crofton PM, Ahmed SF, Wade JC, Stephen R, Elmlinger MW, Ranke MB, Kelnar CJ, Wallace WH. Effects of intensive chemotherapy on bone and collagen turnover and the growth hormone axis in children with acute lymphoblastic leukemia. J Clin Endocrinol Metab 1998; 83:3121-29.
30. Street ME, Ziveri MA, Spaggiari C, Viani I, Volta C, Grzincich GL, Virdis R, Bernasconi S. Inflammation is a modulator of the insulin-like growth factor (IGF)/IGF-binding protein system inducing reduced bioactivity of IGFs in cystic fibrosis. Eur J Endocrinol 2006; 154:47-52

ASSOCIATION BETWEEN PROGESTERONE AND ESTRADIOL-17BETA TREATMENT AND PROTEIN EXPRESSION OF PGR AND PGRMC1 IN PORCINE LUMINAL EPITHELIAL CELLS: A REAL-TIME CELL PROLIFERATION APPROACH

B. KEMPISTY[1,2], K. WOJTANOWICZ-MARKIEWICZ[3], A. ZIÓŁKOWSKA[1], J. BUDNA[1], S. CIESIÓŁKA[1], H. PIOTROWSKA[4], A. BRYJA[1], P. ANTOSIK[3], D. BUKOWSKA[3], K. WOLLENHAUPT[5], M. BRUSKA[2], K.P. BRÜSSOW[5], M. NOWICKI[1] and M. ZABEL[1,6]

[1]Department of Histology and Embryology, Poznan University of Medical Science, Poznań, Poland; [2]Department of Anatomy, Poznan University of Medical Sciences, Poznań, Poland; [3]Institute of Veterinary Sciences, Poznan University of Life Science, Poznań, Poland; [4]Department of Toxicology, Poznan University of Medical Sciences, Poznań, Poland; [5]Institute of Reproductive Biology, Department of Experimental Reproductive Biology, Leibniz Institute for Farm Animal Biology, Dummerstorf, Germany; [6]Department of Histology and Embryology, Wroclaw Medical University, Wroclaw, Poland

Received July 23, 2013 – Accepted December 22, 2014

The first two authors contributed equally to the work

The correct functionality (sensitivity and receptivity) of endometrial tissue is regulated by paracrine and endocrine pathways that activate several mediators or metabolic pathways and gene cascades. This study aimed to investigate the influence of E2 and P4 on progesterone receptor (PGR) and progesterone receptor membrane component 1 (PGRMC1) protein expression in porcine luminal epithelial cells and their influence on the proliferation of these cells in real-time. Surface uterine luminal epithelial cells were removed using sterile surgical blades from uterine horns of ten crossbred anestrus gilts. Following treatment with collagenase I, cells were separated and transferred into 48-well E-Plates for use in a real-time cell analyzer (RTCA). The luminal epithelial cells were cultured *in vitro* (IVC) in standard DMEM cell culture medium and incubated with E2 (10 pg/ml, 40 pg/ml, 500 pg/ml) and P4 (10 ng/ml, 40 ng/ml, 500 ng/ml). The cell proliferation index was analyzed after 0-240 h, 0-120 h, 120-240 h. After using the RTCA analysis we found increased proliferation of luminal epithelial cells after treatment of low doses of P4 (10 and 40 ng/ml), (P<0.001). Higher doses of P4 led to decrease of proliferation (P<0.001). Conversely, higher doses of E2 (500 pg/ml) increased the proliferation index as compared to low doses (10 pg/ml) and control (P<0.001). Confocal microscopic observations revealed that higher concentrations of E2 upregulate the expression of both PGR and PGRMC1. Additionally, P4 used in lower concentrations stimulated the expression of these receptors, too. Our study presents a new influence of E2 and P4 on the expression of PGR and PGRMC1 and on the real-time proliferation of porcine luminal epithelial cells. The relationship between PGR or PGRMC1 expression and the proliferation of luminal epithelial cells may be influenced (up- or down regulated) by E2 or P4 in a steroid type- and dose-dependent manner.

Key words: steroids, progesterone receptors, luminal epithelial cells, pig

Mailing address: Bartosz Kempisty PhD., Department of Histology and Embryology, Poznan University of Medical Sciences, 6 Święcickiego St., 60-781 Poznań, Poland
Tel./Fax: (61) 8 546419/ (61) 8 546455
e-mail: bkempisty@ump.edu.pl

0393-974X (2015)

The endometrium is represented by mucosa that consists of two populations of cells: luminal and stromal. The proper functionality of these cells involves several morphological, biochemical and molecular changes that determine endometrium receptivity (1-4). It has been shown that the endometrium is an organ the functionality of which is associated with several paracrine and autocrine pathways that form the tissue and prepare it for decidualization and embryo attachment (5-9). Although the morphological changes during normal and abnormal reproductive cycles have been histologically well described, further biochemical metabolic pathways and gene and protein expression pattern analysis are still required.

It is also well recognized that endometrial cells undergo a cyclic proliferation process followed by tissue differentiation (10-12). These processes are regulated between others by the secretion of definite hormones that provide specific hormonal homeostasis during reproductive cycles in mammals. Steroids, which include estrogens and progesterone (P4), are hormones that are responsible for the regulation of endometrial cell growth and differentiation (13-15). It has been found that estrogens regulate the permeability of capillary endothelia and transudation, whereas P4 is the main regulator of endometrial cell secretory activity and cell apoptosis (16, 17). Furthermore, physicochemical assays have shown that estrogens down regulate endometrial viscosity, whereas P4 stimulates viscosity (18, 19).

There are numerous data indicating the role of steroids in the regulation of endometrial cell growth, proliferation and differentiation (12, 20, 21). However, differentiated progesterone receptor (PGR) gene expression and encoded protein distribution within luminal epithelial cells still require future investigation. Generally, PGR is a nuclear receptor and is responsible for transducing signals after binding agonists. PGR uses separated promoters that form two PGR isoforms, PRA and PRB, which differ by 165 amino acids present only in the N terminus of PRB. It has been clearly demonstrated that PGR plays a key role in the preparation of endometrial tissue for embryo attachment as well as in the maintenance of pregnancy in mammals (22, 23). Although PGR is a nuclear steroid receptor, after using the sequence of porcine PGR as a probe, Gerdes et al. (24) cloned progesterone receptor membrane component (PGRMC1), which is highly expressed in the liver and kidney.

It is well known that the postovulatory rise of P4 regulates the differentiation of endometrial cells to prepare this tissue for embryo attachment (25). Furthermore, in the absence of pregnancy, the decreasing levels of P4 lead to the induction of apoptosis. However, it is still unclear whether P4 or E2 regulates cell proliferation and/or apoptosis by activating the PGR-associated cascade. Therefore, in the present study, we investigated PGR and PGRMC1 protein expression in porcine luminal epithelial cells as well as real-time cell proliferation in relation to P4 and E2 treatment.

MATERIALS AND METHODS

Animals

In this study, crossbred gilts (n=10) aged approximately nine months and which displayed two regular estrous cycles were collected from a commercial herd. All the animals were checked daily for estrus behavior and were slaughtered after reaching the anestrus phase of the estrus cycle. The uteri were then transported to the laboratory within 30 min at 38°C.

Luminal epithelial cell selection and culture

After slaughter, the uterine horns were washed twice with PBS (137 mM NaCl, 27 mM KCl, 10 mM Na_2HPO_4, 2 mM KH_2PO_4, pH 7.4) and immediately cut into small pieces (25-35 mg). Surface uterine luminal epithelial cells were histologically, surgically removed using sterile surgical blades. The cell suspension obtained from this digestion was filtered through a mesh to remove non-dissociated fragments of tissue and then incubated with 0.05% collagenase I (Sigma Aldrich, Madison, USA) for 25 min at 38°C in a shaking water bath. Isolated cells were washed three times by centrifugation (10 min at 200 g) with Dulbecco's modified Eagle's medium (DMEM; Sigma Aldrich, Madison, USA) supplemented with gentamicin (20 μg/mL) and 0.1% BSA. The resulting luminal epithelial cells were filtered and washed three times by centrifugation (10 min at 200 g) with supplemented DMEM. The final pellet of luminal epithelial cells was resuspended in DMEM supplemented with 10% fetal calf serum (FCS; Sigma Aldrich, Madison, USA) and 10,000 U mL^{-1} penicillin G, 10 mg mL^{-1} streptomycin and 25 μg mL^{-1} amphotericin B (antibiotic antimycotic solution; Sigma Aldrich, Madison, USA). The viability of the cells was 90 to 95%, as judged by trypan blue staining (Sigma

Aldrich, Madison, USA). The cells were cultured at 38°C in a humidified atmosphere of 5% CO_2. The culture medium was changed every 2 to 3 days.

In vitro luminal epithelial cell cultivation using a real-time cell analyzer (RTCA)

During cultivation, the cells were transferred into 48-well E-Plates for use in a real-time cell analyzer (RTCA, Roche-Applied Science, GmbH, Penzberg, Germany) consisting of an RTCA analyzer, an RTCA SP station and RTCA software. The luminal epithelial cells were then cultured in 200 µl DMEM for 240 h and incubated with different doses of estradiol-17beta (E2) (10 pg/ml) and progesterone (P4) (10 ng/ml), respectively. The PGR and PGRMC1 protein expression after double treatment with E2 and P4 (P4-20 ng/ml+E2-10 pg/ml), was also evaluated. After 240 h of cultivation, the cells were treated with trypsin (0.25% trypsin in a balanced salt solution, Sigma-Aldrich, St. Louis, MO, USA), and the collected pool of proliferating cells was used for further confocal microscopy. After respective steps of cultivation (0-240 h, 0-126 h, 126-240 h), the cell index (CI) and the normalized cell index were measured and used to evaluate the relative and quantitative changes in electrical cell impedance. The status of cells was determined using RTCA software.

Confocal microscopy for PGR, PGRMC1, cytokeratin 8 and 18 expression and distribution in porcine luminal epithelial cells

After 240 h of proliferation, the luminal epithelial cells were collected, fixed using acetone-methanol (1:1) for 10 min at -20°C and washed three times in PBS/PVP (0.2%). To block nonspecific binding, samples were incubated in 3% BSA in PBS with 0.1% Tween20 for 30 min at RT. The luminal epithelial cells were incubated for 1 h at room temperature (RT) with rabbit polyclonal anti-PGR (C-20) antibody (Ab) and/or goat polyclonal anti-PGRCM1 (D-16) antibody (Ab), purchased from Santa Cruz Biotechnology (Santa Cruz, CA, USA), as well as mouse monoclonal anti-cytokeratin 8 antibody (SPM192) and mouse monoclonal anti-cytokeratin 18 antibody (DC10) (purchased from Abcam and Dako, respectively) diluted 1:500 in PBS/1.5% BSA/0.1% Tween 20. After several washes with PBS/0.1% Tween 20, samples with the primary antibodies mentioned above were incubated for 1 hour at RT with fluorescein isothiocyanate (FITC)-conjugated goat anti-rabbit IgG Ab and diluted 1:500 in PBS/0.1% Tween 20. Following washing in PBS/0.1% Tween 20, the luminal epithelial cells were stained with 0.1 µg/ml 4,6-diamino-2-phenylindole (DAPI; Santa Cruz Biotechnology, Santa Cruz, CA, USA) in mineral oil, mounted on glass slides in an antifade solution drop and examined under an LSN 510 confocal system in a Fluoview 10i microscope (Olympus). FITC was excited at 488 nm with an argon laser, and emissions were imaged through a 505-530 nm filter. All confocal microscopic images were analyzed using Imaris 7.2 software (BitPlane, Zurich, Switzerland). The cytokeratin 8 and 18 was used as positive control for epithelial cells.

Statistical analysis

One-way ANOVA followed by the Tukey post-test was used to compare the real-time (RTCA) quantification results. The experiments were carried out with at least two replicates. The cell proliferation index results were obtained using the RTCA system. The differences were considered to be significant at $*P < 0.05$, $**P < 0.01$ and $***P < 0.001$ for RTCA analyses. The statistical calculations were applied to compare the results in each investigated group to the highest normalized proliferation index at each time point. GraphPad Prism version 4.0 software (GraphPad Software, San Diego, CA, USA) was used for all statistical calculations.

RESULTS

Using RTCA assays, we analyzed the index of proliferation of isolated porcine luminal epithelial cells after 0-240 h, 0-120 h, 0-44 h and 120-240 h (Fig. 1 A, B, C and D, respectively), which were treated previously with 10 pg/ml of E2 and 10 of P4. We found the increased proliferation index after treatment of 10 ng/ml of P4 as compared to untreated control cells ($P<0.001$), (Fig. 1 A, B, C). Contrarily, low doses of E2 (10 pg/ml) led to inhibition of proliferation as compared to untreated control ($P<0.001$), (Fig. 2 A, B, C).

When PGR expression was analyzed after E2 treatment, we found no differences in expression of PGR after 10 pg/ml of E2 treatment as compared to control (Fig. 3 A-E). Confocal microscopy observation revealed an increased expression of PGR after cultivation of cells with 10 ng/ml of P4 compared to control ($P<0.001$), (Fig. 4 A-E). When analyzed double treatment (E2 and P4), we observed no differences in expression of PGR when treated with (P4-20 ng/ml, E2-10 pg/ml), (Fig. 5A-E).

The alterations in expression of PGRMC1 after 10 pg/ml of E2 and P4 (10 ng/ml) treatment were not significant (Fig. 6 A-E, Fig. 7 A-E). The expression profile of PGRMC1 was not changed with (P4-20 ng/ml, E2-10 pg/ml) (Fig. 8A-E). The epithelial cells markers, antibodies against cytokeratin 8 and

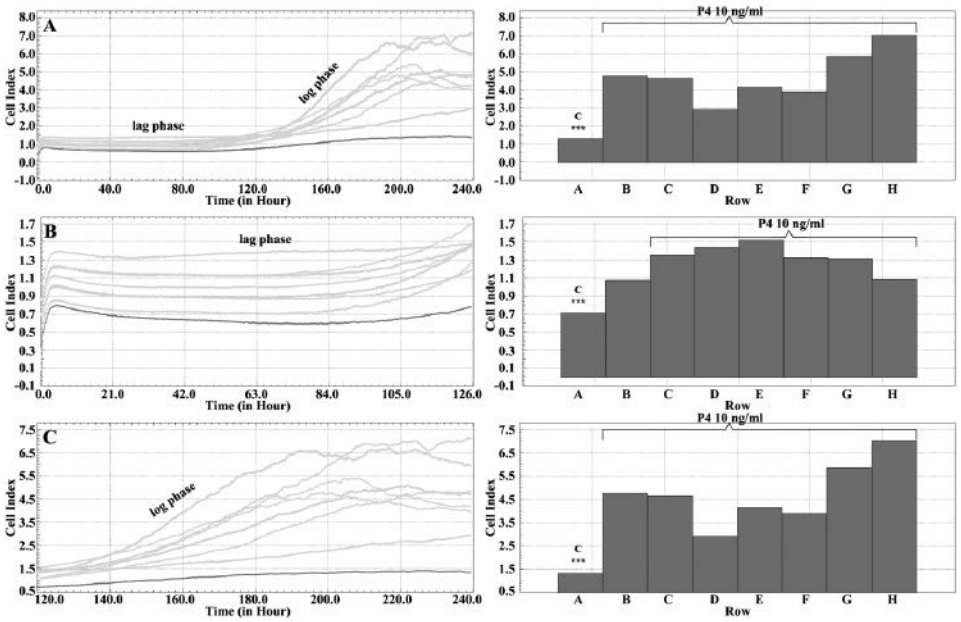

Fig. 1. *Proliferation index of luminal epithelial cells cultivated for 240 hours treated with P4. The luminal epithelial cells were recovered and treated with collagenase for 10 min at 38.5ºC. Then, the cells were immediately transferred into an E-Plate 48 of a real-time cell analyzer (RTCA, Roche-Applied Science, GmbH, Penzberg, Germany). The experiment consisted of four replicates involving cultivation of the same population of collected cells. At every step of the experiment, the cell proliferation index was assessed in real-time in vitro cultivation for the time periods of 0-240 h (**A**), 0-120 h (**B**), and 120-240 h (**C**). During cultivation cells were treated with doses of P4 (10 ng/ml). The differences were considered to be significant at the level of $^{*}P<0.05$, $^{**}P<0.01$ and $^{***}P<0.001$. c-control, P4-progesterone.*

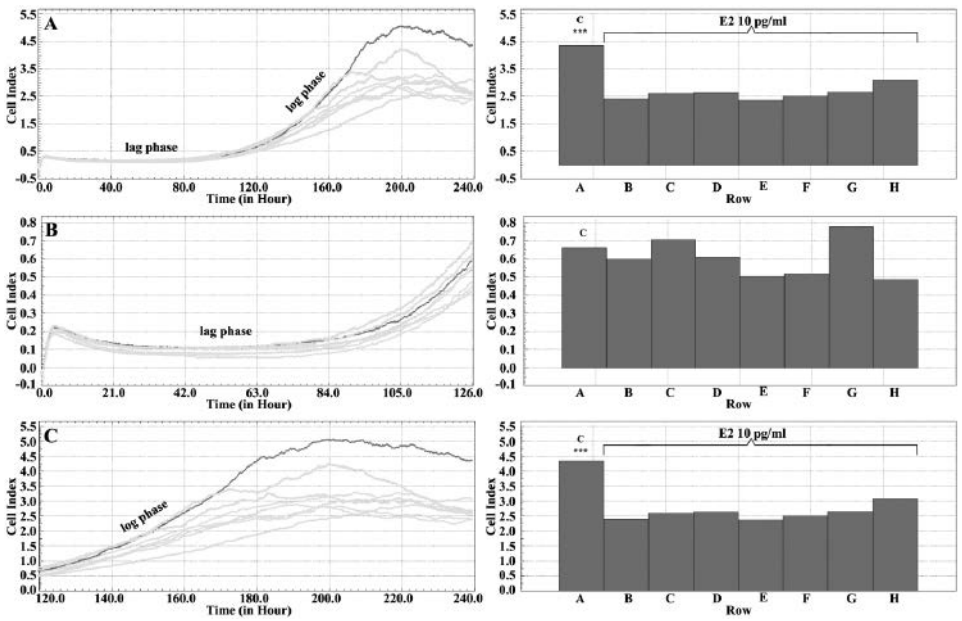

Fig. 2. *Proliferation index of luminal epithelial cells cultivated for 240 hours treated with E2. At every step of the experiment, the cell proliferation index was assessed in real-time in vitro cultivation for the time periods of 0-240 h (**A**), 0-120 h (**B**), and 120-240 h (**C**). During cultivation cells were treated with doses of E2 (10 pg/ml). The differences were considered to be significant at the level of $^{*}P<0.05$, $^{**}P<0.01$ and $^{***}P<0.001$. c-control, E2-etradiol-17beta.*

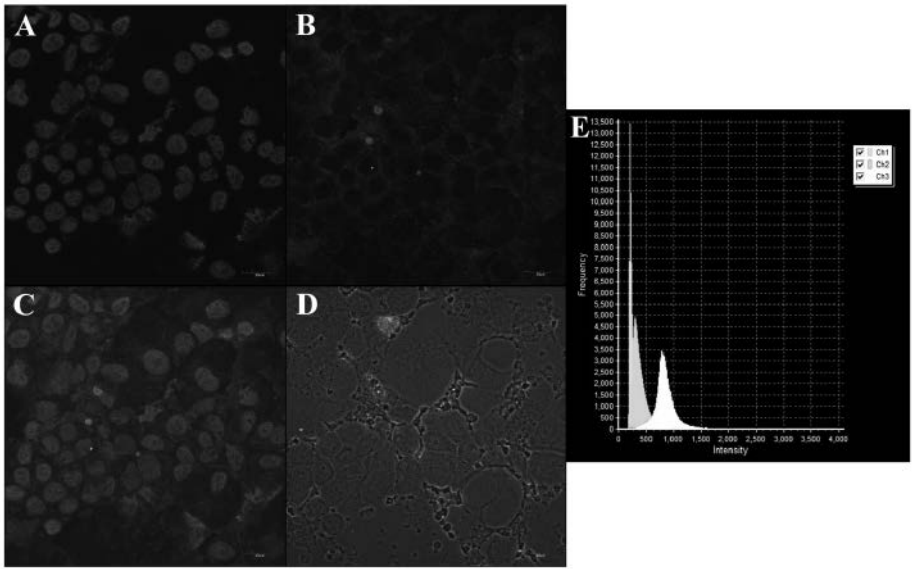

Fig. 3. *Confocal microscopic observation of PGR protein levels and cellular distribution in porcine luminal epithelial cells after treated with E2. The luminal epithelial cells were treated with E2 (10 pg/ml, **A-E**), and stained with 0.1 µg/ml 4,6-diamino-2-phenylindole (DAPI; Santa Cruz Biotechnology, Santa Cruz, CA, USA) in mineral oil following staining for porcine PGR (rabbit polyclonal anti-PGR Ab). Secondary antibodies were labeled with FITC (fluorescence isothiocyanate), which emits a green fluorescent signal after excitation at 488 nm. The fluorescence intensity of protein expression level is presented by histograms. The scale bars represent 20 µm.*

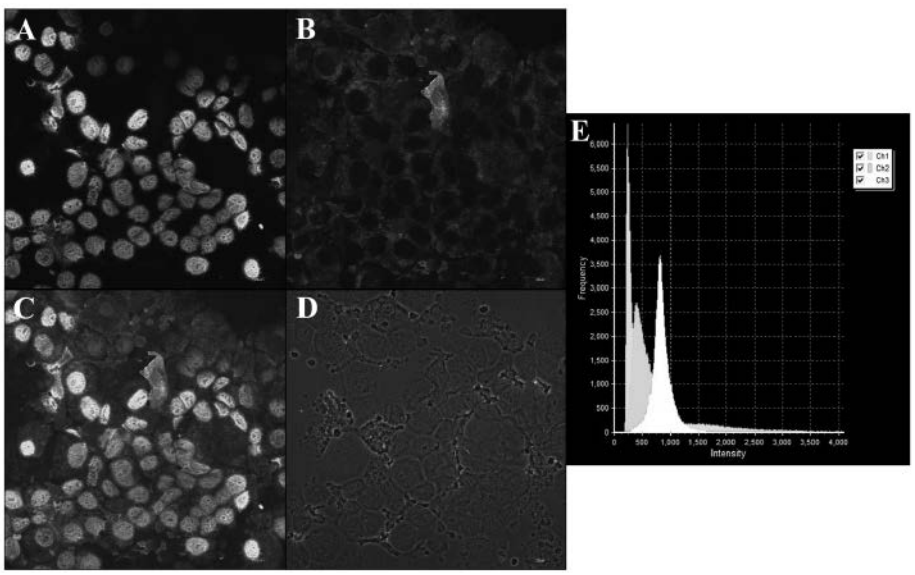

Fig. 4. *Confocal microscopic observation of PGR protein levels and cellular distribution in porcine luminal epithelial cells after treated with P4. The luminal epithelial cells were treated with and P4 (10 ng/ml, **A-E**), and stained with 0.1 µg/ml 4,6-diamino-2-phenylindole (DAPI; Santa Cruz Biotechnology, Santa Cruz, CA, USA) in mineral oil following staining for porcine PGR (rabbit polyclonal anti-PGR Ab). Secondary antibodies were labeled with FITC (fluorescence isothiocyanate), which emits a green fluorescent signal after excitation at 488 nm. The fluorescence intensity of protein expression level is presented by histograms. The scale bars represent 20 µm.*

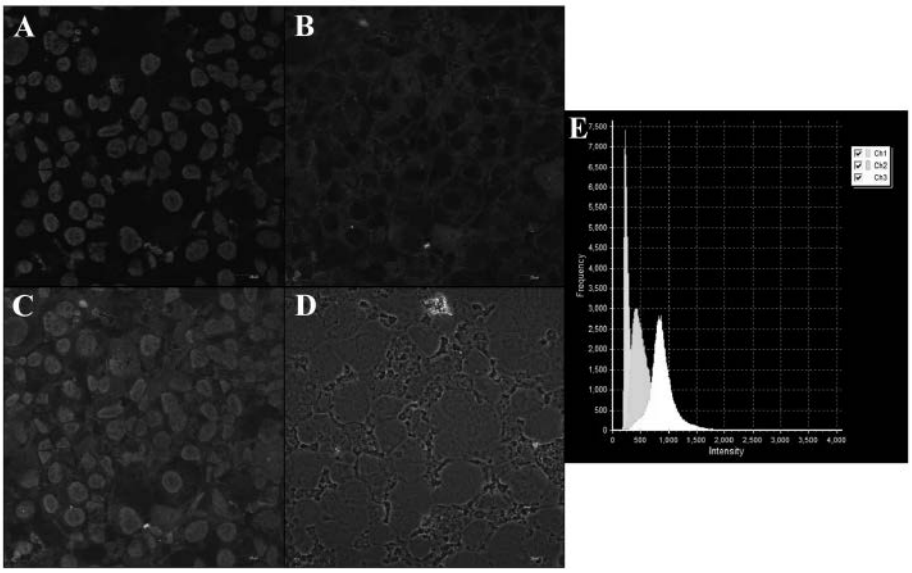

Fig. 5. *Confocal microscopic observation of PGR protein levels and cellular distribution in porcine luminal epithelial cells after double treated with E2 and P4. The luminal epithelial cells were treated with E2 and P4 (P4-20 ng/ml, E2-10 pg/ml), (**A-E**) and stained with 0.1 µg/ml 4,6-diamino-2-phenylindole (DAPI; Santa Cruz Biotechnology, Santa Cruz, CA, USA) in mineral oil following staining for porcine PGR (rabbit polyclonal anti-PGR Ab). Secondary antibodies were labeled with FITC (fluorescence isothiocyanate), which emits a green fluorescent signal after excitation at 488 nm. The fluorescence intensity of protein expression level is presented by histograms. The scale bars represent 20 µm.*

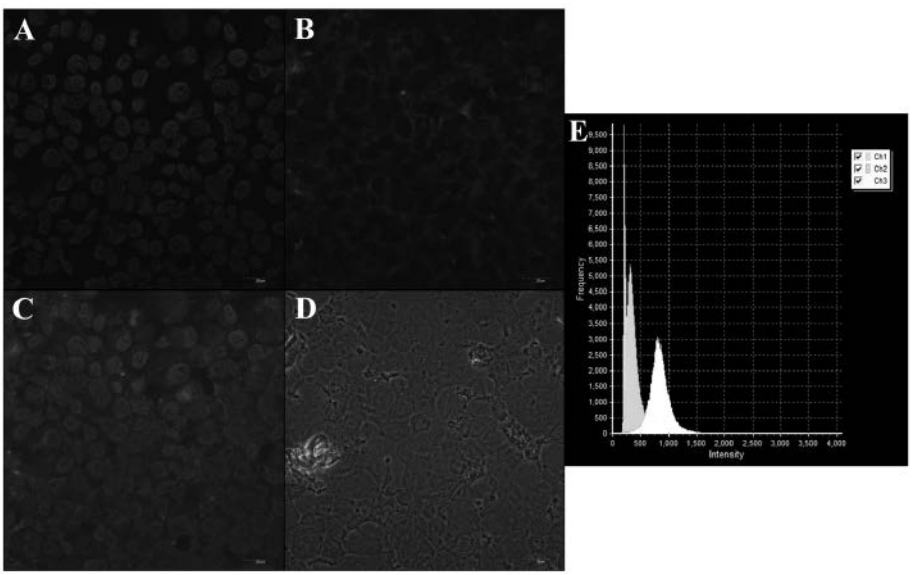

Fig. 6. *Confocal microscopic observation of PGRMC1 protein levels and cellular distribution in porcine luminal epithelial cells after treated with E2. The luminal epithelial cells were treated with E2 (10 pg/ml, **A-E**), and stained with 0.1 µg/ml 4,6-diamino-2-phenylindole (DAPI; Santa Cruz Biotechnology, Santa Cruz, CA, USA) in mineral oil following staining for porcine PGRMC1 (goat polyclonal anti-PGRMC1 Ab). Secondary antibodies were labeled with FITC (fluorescence isothiocyanate), which emits a green fluorescent signal after excitation at 488 nm. The fluorescence intensity of protein expression level is presented by histograms. The scale bars represent 20 µm.*

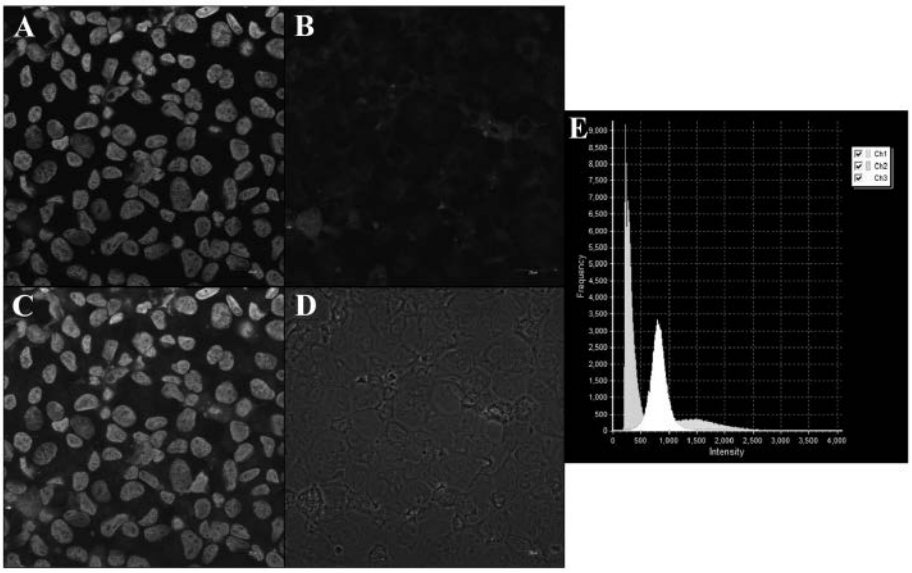

Fig. 7. *Confocal microscopic observation of PGRMC1 protein levels and cellular distribution in porcine luminal epithelial cells after treated with P4. The luminal epithelial cells were treated with and P4 (10 ng/ml, **A-E**), and stained with 0.1 µg/ml 4,6-diamino-2-phenylindole (DAPI; Santa Cruz Biotechnology, Santa Cruz, CA, USA) in mineral oil following staining for porcine PGRMC1 (goat polyclonal anti-PGRMC1 Ab). Secondary antibodies were labeled with FITC (fluorescence isothiocyanate), which emits a green fluorescent signal after excitation at 488 nm. The fluorescence intensity of protein expression level is presented by histograms. The scale bars represent 20 µm.*

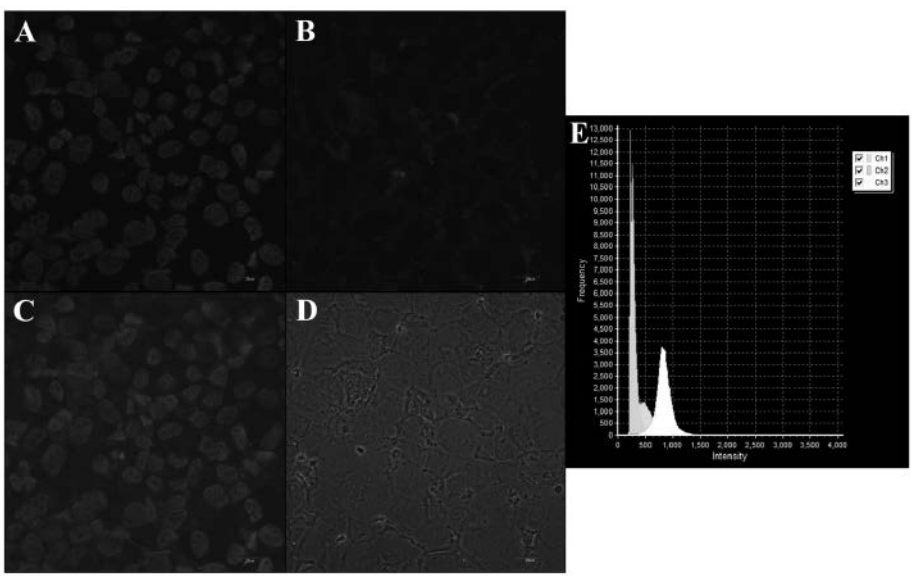

Fig. 8. *Confocal microscopic observation of PGRMC1 protein levels and cellular distribution in porcine luminal epithelial cells after treated with E2 and P4. The luminal epithelial cells were treated with E2 and P4 (P4-20 ng/ml, E2-10 pg/ml), (**A-E**, respectively) and stained with 0.1 µg/ml 4,6-diamino-2-phenylindole (DAPI; Santa Cruz Biotechnology, Santa Cruz, CA, USA) in mineral oil following staining for porcine PGRMC1 (goat polyclonal anti-PGRMC1 Ab). Secondary antibodies were labeled with FITC (fluorescence isothiocyanate), which emits a green fluorescent signal after excitation at 488 nm. The fluorescence intensity of protein expression level is presented by histograms. The scale bars represent 20 µm.*

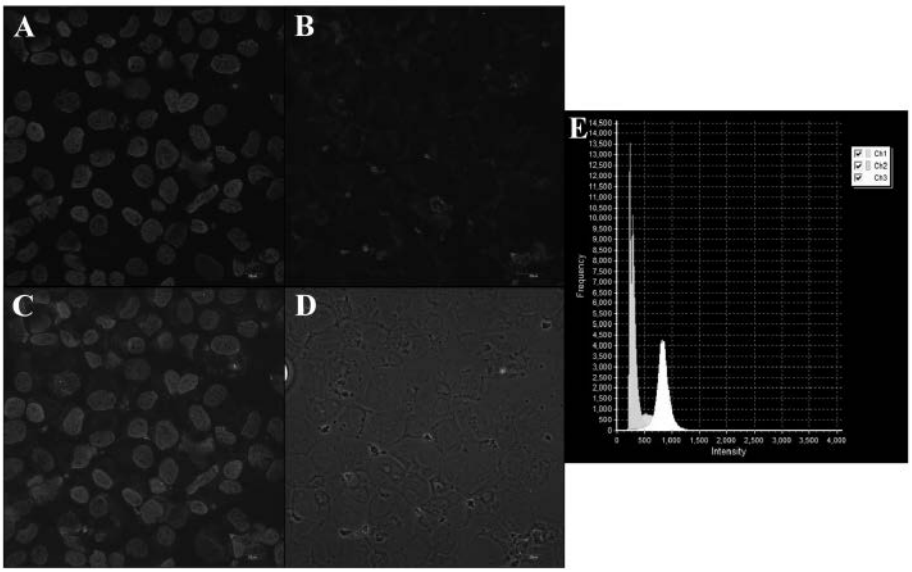

Fig. 9. *Confocal microscopic observation of cytokeratin 8 protein levels and cellular distribution in control cells. The untreated luminal epithelial cells were used as control to determine cytokeratin 8 (**A-E**) protein expression level and stained with 0.1 µg/ml 4,6-diamino-2-phenylindole (DAPI; Santa Cruz Biotechnology, Santa Cruz, CA, USA) in mineral oil following staining for cytokeratin 8 (mouse monoclonal anti-cytokeratin 8 Ab). Secondary antibodies were labeled with FITC (fluorescence isothiocyanate), which emits a green fluorescent signal after excitation at 488 nm. The fluorescence intensity of protein expression level is presented by histograms. The scale bars represent 20 µm.*

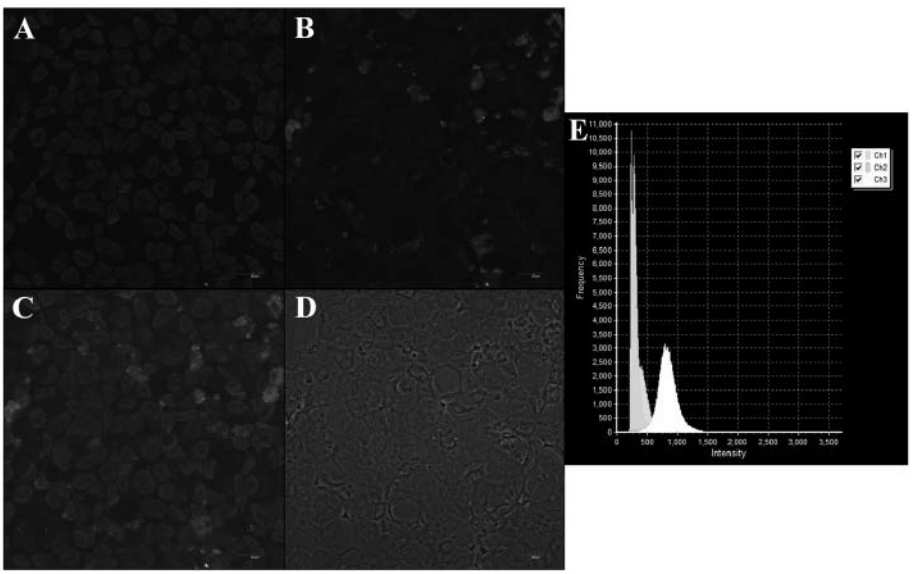

Fig. 10. *Confocal microscopic observation of cytokeratin 18 protein levels and cellular distribution in control cells. The untreated luminal epithelial cells were used as control to determine cytokeratin 18 (**A-E**) protein expression level and stained with 0.1 µg/ml 4,6-diamino-2-phenylindole (DAPI; Santa Cruz Biotechnology, Santa Cruz, CA, USA) in mineral oil following staining for cytokeratin 18 (mouse monoclonal anti-cytokeratin 18 Ab). Secondary antibodies were labeled with FITC (fluorescence isothiocyanate), which emits a green fluorescent signal after excitation at 488 nm. The fluorescence intensity of protein expression level is presented by histograms. The scale bars represent 20 µm.*

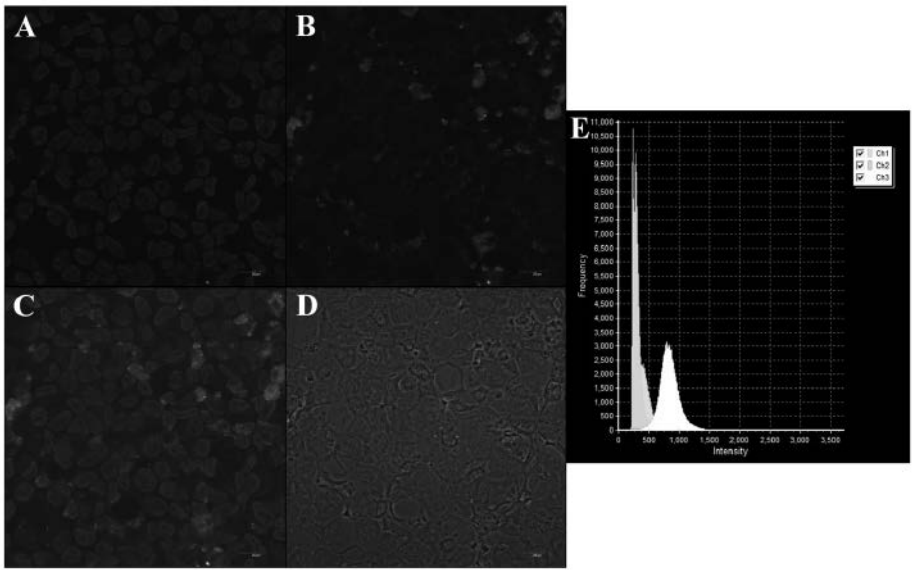

Fig. 11. *Confocal microscopic observation of PGR protein levels and cellular distribution in control cells. The untreated luminal epithelial cells were used as control to determine PGR (**A-E**) protein expression level and stained with 0.1 µg/ml 4,6-diamino-2-phenylindole (DAPI; Santa Cruz Biotechnology, Santa Cruz, CA, USA) in mineral oil following staining for porcine PGR (rabbit polyclonal anti-PGR Ab). Secondary antibodies were labeled with FITC (fluorescence isothiocyanate), which emits a green fluorescent signal after excitation at 488 nm. The fluorescence intensity of protein expression level is presented by histograms. The scale bars represent 20 µm.*

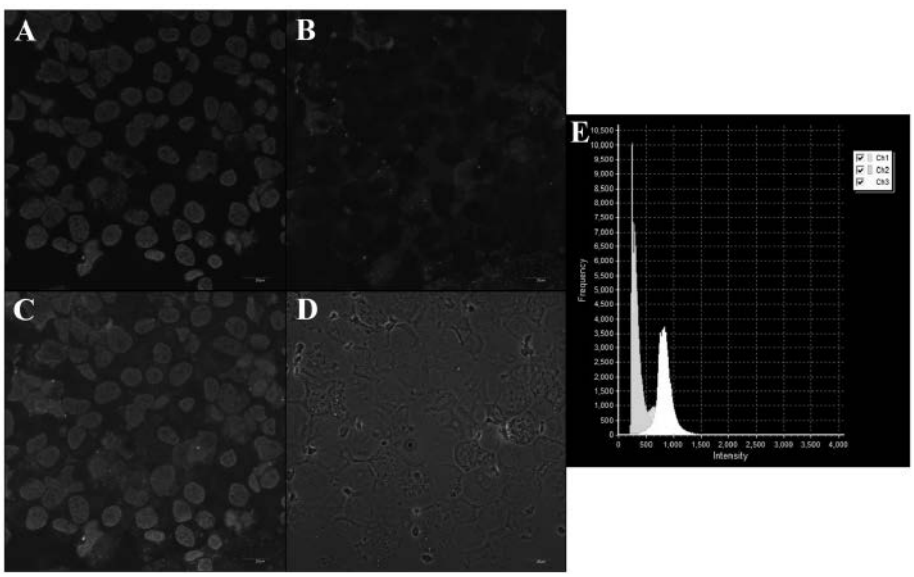

Fig. 12. *Confocal microscopic observation of PGRMC1 protein levels and cellular distribution in control cells. The untreated luminal epithelial cells were used as control to determine PGRMC1 (**A-E**) protein expression level and stained with 0.1 µg/ml 4,6-diamino-2-phenylindole (DAPI; Santa Cruz Biotechnology, Santa Cruz, CA, USA) in mineral oil following staining for porcine PGRMC1 (goat polyclonal anti-PGRMC1 Ab). Secondary antibodies were labeled with FITC (fluorescence isothiocyanate), which emits a green fluorescent signal after excitation at 488 nm. The fluorescence intensity of protein expression level is presented by histograms. The scale bars represent 20 µm.*

cytokeratin 18, were used, (Fig. 9 A-E, Fig. 10 A-E). As controls, the untreated luminal epithelial cells were used for PGR (Fig. 11 A-E) and PGRMC1 (Fig. 12 A-E).

DISCUSSION

It is well recognized that the proper physiological function of the endometrium is regulated by paracrine and autocrine pathways that involve the activation of several mediators and metabolic pathways. The main role of the endometrium is to prepare the related tissue parts for embryo attachment and implantation. However, the endometrium cannot function by itself and it is permanently morphologically and biochemically modified. This is closely linked to a hormonal pathway between the hypothalamus, the pituitary gland, the ovaries and the endometrium. It is also accepted that estrogens and progesterone play significant roles in several endometrium functions during the reproductive cycle. Currently, there are limited data indicating the role of both these hormones in the regulation of PGR and PGRMC1 expression in porcine endometrium or luminal epithelium. Makker et al. (26) revealed changes in nuclear and cytosolic estradiol (ER) and progesterone (PGR) receptor concentrations in the antimesometrial and mesometrial segments of the uterus of guinea pigs in relation to circulating hormone levels, as well as histological alterations. Since both nuclear and cytosolic ER and PGR were increased in the antimesometrial segment of the uterine horn, they considered a significant role of estradiol and progesterone in the induction of endometrial sensitivity, and growth and development of decidua in endometrial tissue. To our knowledge there are no data available indicating an influence of different E2 or P4 concentrations on PGR and PGRMC1 expression in porcine luminal epithelium. The results of our study lead to assume that both E2 and P4 are be involved in the regulation of endometrial proliferation, but in a dose-dependent manner. Tarleton et al. (27) studied the influence of E2 treatment on ER and PGR mRNA expression in neonatal porcine uteri as well as its role in adult uterine function. In their study, E2 treatment did not affect endometrial ER and PGR mRNA expression. They concluded that transient postnatal estrogen treatment affects porcine endometrial responsiveness to embryotrophic factors and that endometrium estrogen-sensitivity regulates postnatal uterine size and functionality. In agreement with these results, we observed that an increased concentration of E2 stimulated the protein expression of both PGR and its membrane component PGRMC1, whereas P4 treatment increased the expression of these proteins in lower doses. Furthermore, the expression of ERs and PGR in the sow uterus at different stages of the estrus cycle, in inseminated sows and during early pregnancy was recently investigated by Sukjumlong et al. (28). They showed an increased expression of PGR mRNA in the porcine myometrium at proestrus and estrus in cycling sows as well as at estrus in newly inseminated sows. In the endometrium, the expression of PGR mRNA was similar for cyclic and early pregnant females. Moreover, the expression of PGR mRNA was lowest at diestrus and late diestrus (d 11 and d 19). Thus, the expression of ERs and PGR differs significantly between the endometrium and the myometrium and is varying between the stages of the estrus cycle and pregnancy. Taking into account our results and these observations, it can be assumed that different stages of the estrus cycle and various estrus cycle-hormonal pathways, such as those influenced by different concentrations of E2 and P4 (probably as used in our experiment) alter PGR and PGRMC1 protein expression in a steroid type- and dose-dependent manner. However, our results cannot be directly compared to the results obtained by Sukjumlong et al. (28) because they did not use steroid treatment or endometrial tissue cultivation.

Regarding proliferation, Bazer et al. (29) determined that P4 activates a cascade of genes encoding mediators (e.g., interferon, IFN) or down regulates its receptor (PGR) to promote cell proliferation and migration. Our results obtained *in vitro* are partly in agreement with these observations. We found that proliferation increased with low doses of P4 after the first 120 h of IVC. Moreover, higher concentrations of E2 influence increased luminal epithelial cell proliferation. Here, we clearly demonstrate that low doses of P4 and higher doses of E2 lead to increase of luminal epithelial cells proliferation *in vitro*. These observation suggest a different role of both steroids in differentiation of porcine endometrial cells, which is also observed when analyzing the role of E2 and P4 in regulation of the oestrus cycle in pigs. Although the general

effect of steroids on the proliferative activity of endometrial tissues is well known, there is still a lack of data regarding the influence of E2 and P4 on porcine luminal epithelial cell proliferation during cultivation in real-time, and further investigations are still necessary.

Our *in vitro* study leads to presume that the expression of PGR and PGRMC1 may be up- or down regulated also *in vivo* by E2 and P4 in a steroid type- and dose-dependent manner. Additionally, real-time proliferation of porcine luminal epithelial cells *in vitro* is not always associated with progesterone receptor expression after steroid treatment, which implies an involvement of other factors or mediators in the regulation of these mechanisms.

ACKNOWLEDGEMENTS

This study was made possible by grant number 2014/13/D/NZ9/04798 “SONATA” from the Polish National Centre of Science.

REFERENCES

1. Banerjee P, Fazleabas AT. Endometrial responses to embryonic signals in the primate. Int J Dev Biol 2010; 54:295-302.
2. Fazleabas AT. Physiology and pathology of implantation in the human and nonhuman primate. Semin Reprod Med 2007; 25:405-9.
3. Martínez-Conejero JA, Simón C, Pellicer A, Horcajadas JA. Is ovarian stimulation detrimental to the endometrium? Reprod Biomed Online 2007; 15:45-50.
4. Nikas G, Makrigiannakis A. Endometrial pinopodes and uterine receptivity. Ann N Y Acad Sci 2003; 997:120-3.
5. Diedrich K, Fauser BC, Devroey P, Griesinger G. Evian Annual Reproduction (EVAR) Workshop Group. The role of the endometrium and embryo in human implantation. Hum Reprod Update 2007; 13:365-77.
6. Kim ST, Marquard K, Stephens S, Louden E, Allsworth J, Moley KH. Adiponectin and adiponectin receptors in the mouse preimplantation embryo and uterus. Hum Reprod 2011; 26:82-95.
7. Geisert R, Fazleabas A, Lucy M, Mathew D. Interaction of the conceptus and endometrium to establish pregnancy in mammals: role of interleukin 1β. Cell Tissue Res 2012; 349:825-38.
8. Lessey BA. Assessment of endometrial receptivity. Fertil Steril 2011; 96:522-9.
9. Bukowska D, Kempisty B, Jackowska M, Woźna M, Antosik P, Piotrowska H, Jaśkowski JM. Analysis of integrins and vascular endothelial growth factor isoforms mRNA expression in the canine uterus during perimplantation period. Pol J Vet Sci 2011; 14:253-8.
10. Miernik K, Karasinski J. Porcine uterus contains a population of mesenchymal stem cells. Reproduction 2012; 143:203-9.
11. Wollenhaupt K, Kettler A, Brüssow KP, Schneider F, Kanitz W, Einspanier R. Regulation of the expression and bioactivation of the epidermal growth factor receptor system by estradiol in pig oviduct and endometrium. Reprod Fertil Dev 2001; 13:167-76.
12. Ka H, Jaeger LA, Johnson GA, Spencer TE, Bazer FW. Keratinocyte growth factor is up-regulated by estrogen in the porcine uterine endometrium and functions in trophectoderm cell proliferation and differentiation. Endocrinology 2001; 142:2303-10.
13. Rosario G, Sachdeva G, Okulicz WC, Ace CI, Katkam RR, Puri CP. Role of progesterone in structural and biochemical remodeling of endometrium. Front Biosci 2003; 8:924-35.
14. Cooke PS, Borsdorf DC, Ekman GC, Doty KF, Clark SG, Dziuk PJ, Bartol FF. Uterine gland development begins postnatally and is accompanied by estrogen and progesterone receptor expression in the dog. Theriogenology 2012; 78:1787-95.
15. Al-Sabbagh M, Lam EW, Brosens JJ. Mechanisms of endometrial progesterone resistance. Mol Cell Endocrinol 2012; 358:208-15.
16. Qi XF, Nan ZC, Jin YP, Qu YY, Zhao XJ, Wang AH. Stromal-epithelial interactions modulate the effect of ovarian steroids on goat uterine epithelial cell interleukin-18 release. Domest Anim Endocrinol 2012; 42:210-9.
17. Keator CS, Mah K, Ohm L, Slayden OD. Estrogen and progesterone regulate expression of the endothelins in the rhesus macaque endometrium. Hum Reprod 2011; 26:1715-28.
18. Witte TS, Melkus E, Walter I, Senge B, Schwab S,

Aurich C, Heuwieser W. Effects of oral treatment with N-acetylcysteine on the viscosity of intrauterine mucus and endometrial function in estrous mares. Theriogenology 2012; 78:1199-208.
19. Jablonski EM, McConnell NA, Hughes FM Jr, Huet-Hudson YM. Estrogen regulation of aquaporins in the mouse uterus: potential roles in uterine water movement. Biol Reprod 2003; 69:1481-7.
20. Welter H, Wollenhaupt K, Einspanier R. Developmental and hormonal regulated gene expression of fibroblast growth factor 2 (FGF-2) and its receptors in porcine endometrium. J Steroid Biochem Mol Biol 2004; 88:295-304.
21. Gray CA, Bartol FF, Tarleton BJ, Wiley AA, Johnson GA, Bazer FW, Spencer TE. Developmental biology of uterine glands. Biol Reprod 2001; 65:1311-23.
22. Bazer FW, Wu G, Spencer TE, Johnson GA, Burghardt RC, Bayless K. Novel pathways for implantation and establishment and maintenance of pregnancy in mammals. Mol Hum Reprod 2010; 16:135-52.
23. Ross JW, Ashworth MD, Mathew D, Reagan P, Ritchey JW, Hayashi K, Spencer TE, Lucy M, Geisert RD. Activation of the transcription factor, nuclear factor kappa-B, during the estrous cycle and early pregnancy in the pig. Reprod Biol Endocrinol 2010; 8:39.
24. Gerdes D, Wehling M, Leube B, Falkenstein E. Cloning and tissue expression of two putative steroid membrane receptors. Biol Chem 1998; 379:907-11.
25. Glasier MA, Wiebe JP, Hobkirk R. Progesterone metabolism by guinea pig intrauterine tissues. J Steroid Biochem Mol Biol 1994; 51:199-207.
26. Makker A, Singh MM, Chowdhury SR, Maitra SC, Kamboj VP. Uterine estradiol and progesterone receptor concentration in relation to circulating hormone levels and histoarchitecture during high endometrial sensitivity and induced decidualization in guinea pigs. J Steroid Biochem Mol Biol 1994; 48(5-6):535-43.
27. Tarleton BJ, Braden TD, Wiley AA, Bartol FF. Estrogen-induced disruption of neonatal porcine uterine development alters adult uterine function. Biol Reprod 2003; 68(4):1387-93.
28. Sukjumlong S, Persson E, Dalin AM, Janson V, Sahlin L. Messenger RNA levels of estrogen receptors alpha and beta and progesterone receptors in the cyclic and inseminated/early pregnant sow uterus. Anim Reprod Sci 2009; 112(3-4):215-28.
29. Bazer FW, Spencer TE, Johnson GA, Burghardt RC, Wu G. Comparative aspects of implantation. Reproduction 2009; 138:195-209.

BIOMARKERS FOR THE EVALUATION OF IMMUNOLOGICAL PROPERTIES DURING THE SHIKOKU WALKING PILGRIMAGE

K. YOSHINO[1], A. UMENO[2], M. SHICHIRI[1], H. WATANABE[1], N. ISHIDA[1], M. KOJIMA[1], S. IWAKI[1], Y. HAGIHARA[1], M. NAKAMURA[2] and Y. YOSHIDA[2]

[1]Health Research Institute, National Institute of Advanced Industrial Science and Technology (AIST), Midorigaoka, Ikeda, Osaka, Japan; [2]Health Research Institute, National Institute of Advanced Industrial Science and Technology (AIST), Hayashi-cho, Takamatsu, Kagawa, Japan

Received September 1, 2014 – Accepted January 7, 2015

The first three authors contributed equally to the manuscript

It is important to determine the immunological properties for the maintenance of health. We chose the Shikoku Walking Pilgrimage to assess the proper biomarkers for the evaluation of immunological properties. We examined whether the Shikoku Walking Pilgrimage could have a positive effect on the mental and physical health of walking participants by using several biomarkers proposed by our laboratory. Twelve non-randomized healthy male volunteers including 3 twice attendees walked the Shikoku Walking Pilgrimage distance of 58.9 km over 3 days. Plasma, serum, urine, and saliva were collected from the volunteers during the pilgrimage and at 1 week before and after it. Immunological biomarkers, including lipid metabolism, oxidative stress, immune function, and catecholamines, were measured. Additionally, mood state scores, alertness, autonomic nervous system activity, and body motion levels during sleep were assessed. A significant decrease was observed in the subjective tension-anxiety levels and in the concentrations of serum low-density lipoprotein cholesterol, plasma hydroxyoctadecadienoic acid (HODE), and urine adrenaline during the pilgrimage as compared to the values of these parameters before the participants embarked on the pilgrimage. The serum levels of brain-derived neurotrophic factor (BDNF) were significantly increased 1 week after the pilgrimage relative to those assessed previously. No significant differences in subjective fatigue and the flicker perception threshold were observed. These results suggest that the Shikoku Walking Pilgrimage can exert a positive effect on mental and physical health as particularly shown in the reduction of tension-anxiety and oxidative stress without the accompaniment of fatigue. HODE correlated significantly with typical immunological marker natural killer cell activity and immunoglobulin G. This suggests that there are promising biomarkers such as HODE, NK activity, BDNF, LDL-c, and IgG for assessing the immunological properties.

Key words: mental health, physical health, oxidative stress, brain-derived neurotrophic factor, mood, tension-anxiety, walking pilgrimage, ohenro

Mailing address: Mototada Shichiri, M.D., Ph.D.
Health Research Institute, National Institute of Advanced Industrial Science and Technology (AIST),
1-8-31 Midorigaoka, Ikeda,
Osaka, 563-8577, Japan
Tel.: +81 72 751 8734 Fax: +81 72 751 9517
e-mail: mototada-shichiri@aist.go.jp

0393-974X (2015)

DISCLOSURE: ALL AUTHORS REPORT NO CONFLICTS OF INTEREST RELEVANT TO THIS ARTICLE.

In order to determine the proper biomarkers for the assessment of both physical and mental effects of daily life from the viewpoint of the immunological aspect, we chose the Shikoku Walking Pilgrimage "Ohenro". The "Ohenro" is a Buddhist circuit pilgrimage of 88 temples in the Shikoku region of Japan. Approximately 300,000 people participate each year. It was traditionally performed by walking; however, an increasing number of pilgrims have used buses and other vehicles to complete the circuit in recent years. About 40 days in total is required to visit all 88 temples of the Shikoku Pilgrimage if the participants walk approximately 30 km per day. The reasons for embarking on this pilgrimage include the fulfillment of prayers; however, aims such as the advancement of health and hobbies have become common recently, and the age of the pilgrims varies widely.

In a questionnaire survey on the motive for embarking on the pilgrimage, over 40% of respondents answered that they aimed to improve their health (1). However, to date, no comprehensive investigation has been conducted on the effect of walking pilgrimages on both the mental and physical health. To investigate the impact of a walking pilgrimage on vascular function and metabolic parameters, Bemelmans et al. (2-3) measured the body weight, waist circumference, blood pressure, serum glucose levels, pulse rate, insulin, and lipids during the Santiago de Compostela pilgrimage, which involves a similar long-distance walk like the Shikoku Walking Pilgrimage. The results showed a reduction in low-density lipoprotein (LDL), an increase in high-density lipoprotein (HDL), and a reduction in body weight. Accordingly, walking pilgrimage affects mental and physical conditions which may result in affecting immunological properties.

We have previously reported that appropriate biomarkers for oxidative stress are reflected on the central nerve system by cell (4-5) and human (6) studies. These biomarkers include hydroxyoctadecadienoic acids (HODEs) and 7β-hydroxycholesterol (7β-OHCh) which are determined by Liquid Chromatography tandem Mass Spectrometry (LC-MS/MS) and Gas Chromatograph Mass Spectrometer (GC-MS), respectively, after reduction and saponification. HODE induces adaptive response against after-coming stress (4-5) and 7β-OHCh reflects human fatigue (6). Thus these biomarkers are considered to be good biomarkers for immunological responses.

In this study, we comprehensively investigated the promising biomarkers for immunological properties by clarifying the effect of the Shikoku Walking Pilgrimage on both the mental and physical health of the participants in addition to examining metabolic parameters. This study was the preliminary one for determining the appropriate biomarkers toward clarifying the immunological properties by choosing the Shikoku Walking Pilgrimage.

MATERIALS AND METHODS

Study design

This study was approved by the Committee for Ergonomic Experiments and the Committee for Ethics on Experiments with Human Derivative Samples at the National Institute of Advanced Industrial Science and Technology.

Nine healthy men (age: 36–48 years, non-athletes) applied for participation, and all of them passed a medical interview. All volunteers provided informed written consent. They walked 58.9 km of the Shikoku Walking Pilgrimage distance from Ichinomiya Temple to Ookubo Temple over 3 days (17.7 km on day 1, 22.7 km on day 2, and 18.5 km on day 3), worshipping at 6 pilgrimage temples. The experiment was divided into 2 parts performed in December 2011 and July 2012. Five volunteers participated in 2011 and 7 volunteers participated in 2012. Three of them participated twice for clarifying the reproducibility of this study. All the subjects were non-athletes, walked the pilgrimage route at nearly the same speed, and were fed the same typical Japanese food during the pilgrimage.

Sample processing

Blood and urine samples were obtained from the volunteers upon awakening on 4 different occasions: days 1, 2, and 3 of the Shikoku Walking Pilgrimage, and the day after the pilgrimage (day 4). Volunteers were instructed to fast for 10 hours prior to blood and urine collection in order to reduce the effects of food intake. From days 1 to 3, saliva was collected 3 times in total before the evening meal (which took place after the completion of the pilgrimage for that particular day), using a Salivette saliva collection device (Salimetrics Oral Swab, SAL-5001-20, State College, PA, USA).

Psychophysiological measurement

Before breakfast, lunch, and dinner, the volunteers

answered a simple Japanese version of the Profile of Mood States (POMS) (7). Based on the answers to the simplified POMS, the scores for 6 indicators of mood state (tension-anxiety, depression-dejection, fatigue, vigor, anger, confusion) were calculated. Before breakfast and dinner, a critical flicker perception threshold test was performed using an FHM mobile computer (Flicker Health Management Co., Ltd., Japan). In this assessment, the frequency or luminance contrast of a flashing light on the screen is changed until the volunteer can discern the flickering. The critical measurement obtained during the test is the threshold at which the flickering is perceived (i.e., the flicker perception threshold), which has been found to decrease during reduced alertness (8). To measure the balance of the volunteer's autonomic nervous system activity, a portable heart rate variability sensor was attached to the volunteer's chest during the experiment. To measure body motion during sleep, actigraph body motion sensors (AMI, USA) were attached to the wrist of the volunteer's non-dominant arm; the actigraph records the number of times the acceleration data crosses the 0 level in 1 minute.

The above measurements were obtained 1 week before and after the Shikoku Walking Pilgrimage. Hereafter, these are referred to as the pre-experiment and post-experiment, respectively. The pre- and post-experiments were each performed over the course of 1 day in the 2011 experiment (Fig. 1 A) and 3 days in the 2012 experiment (Fig. 1 B). The subjects were fed meals of typical Japanese food during the pre- and post-experiments.

We measured the physiological variables and blood and urine variables at the same time (upon awaking and before the breakfast) during the pre-, and post-experiments and the pilgrimage.

Biomarker analysis

Biomarker concentrations were measured as described in Table I. using the collected blood samples. These included typical immunological markers natural killer (NK) cell activity and Immunoglobulin G (IgG). Serum samples collected from the volunteers were stored at −80°C until assay. The serum concentration of brain-derived neurotrophic factor (BDNF) was determined according to previous reports (9-10) using the BDNF Emax Immunoassay System kit (Promega, Madison, WI, USA).

Oxidative stress markers were measured as follows. The plasma (200 μL) was mixed with 300 μL of saline. Subsequently, 500 μL of methanol containing the internal standards 8-iso-prostaglandinF2α-d4 (50 ng), 13-(S)-hydroxyoctadecadienoic acid (13-HODE-d4; 50 ng), 7β-hydroxycholesterol (7β-OHCh-d7; 19 ng), 16-hydroxyhexadecanoic acid (70 ng), and 100 μM butylated hydroxytoluene were added to the samples.

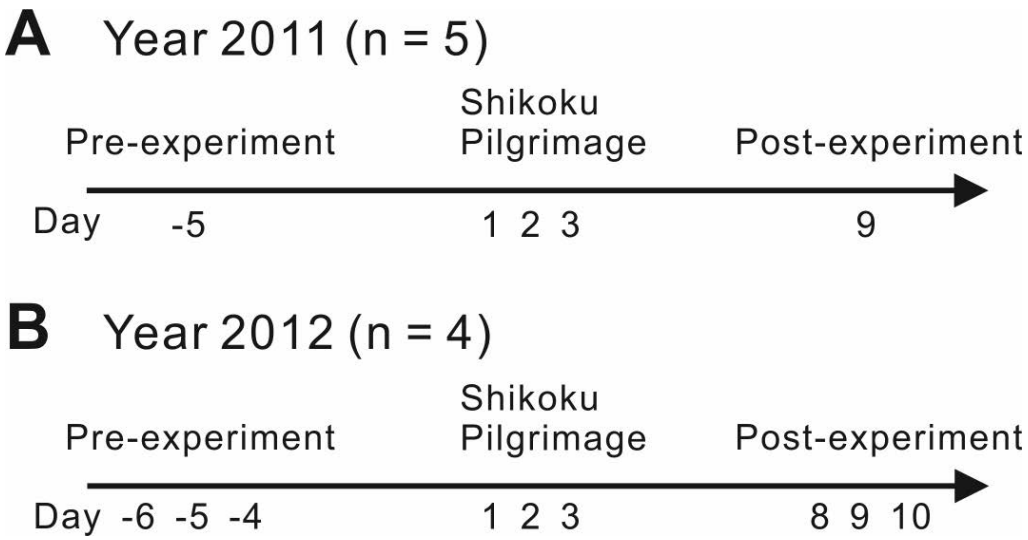

Fig. 1. *Experimental schedule of the Shikoku Walking Pilgrimage. The experiments were conducted 1 week before (pre-experiment), during, and 1 week after (post-experiment) the 3-days Shikoku Walking Pilgrimage. The pre- and post-experiments were each performed over the course of 1 day in the (A) 2011 experiment and 3 days in the (B) 2012 experiment.*

Table I. *Analyzed blood biomarkers and measurement methods*.

Classification	Biomarker name	Measurement method and kit
Immunological system	Immunoglobulin G (IgG)/total protein	Immunoturbidimetric method. N-assay TIA IgG-SH1
	Immunoglobulin A (IgA)/total protein	Immunoturbidimetric method. N-assay TIA IgA-SH1
	Immunoglobulin M (IgM)/total protein	Immunoturbidimetric method. N-assay TIA IgM-SH1
	Natural Killer (NK) cell activity	51Cr liberation method. (11)
Lipid metabolism	Low-density lipoprotein (LDL) cholesterol	Direct method. Cholestetest LDL2
	High-density lipoprotein (HDL) cholesterol	Direct method. Cholestetest HDL2
Lipid oxidation	total hydroxyoctadecadienoic acid (tHODE)/linoleates	LC-MS/MS and GC-MS
	Isoprostane	LC-MS/MS
	7β-hydroxycholesterol (7β-OHCh)/total cholesterol	GC-MS
Neurotrophin	Serum Brain-derived neurotrophic factor (BDNF)	ELISA
Liver	Alanine aminotransferase (ALT)	JSCC4 consensus method. Cicaliquid ALT5
	Aspartate aminotransferase (AST)	JSCC4 consensus method. Cicaliquid AST5
	γ-glutamyl transpeptidase (γ-GTP)	JSCC4 consensus method. Cicaliquid γ-GT5
	Total bilirubin acid	Chemical oxidation method. Total Bilirubin E-HR6
	Cholinesterase	JSCC* consensus method. Cicafit ChE5
Endocrine system	Creatine kinase (CK)	JSCC* consensus method. Cicaliquid γ-GT5
	Glucose	Hexokinase UV method. Cicaliquid GLU5
	Amylase	Enzymatic method (Gal-G2-CNP substrate method). Cicaliquid AMY5
	Cortisol	Solid-phase RIA (radio immunological assay). Cortisol kit TFB7
Kidney	Urea nitrogen	Urease, LED, UV methods. Cicaliquid UN5
	Uric acid	Enzymatic method (uricase POD method). Pureauto S UA3

1Nittobo Medical Co. Ltd., 2Fujirebio Inc., 3Sekisui Medical Co. Ltd., 4Japan Society of Clinical Chemistry, 5Kanto Chemical Co. Ltd., 6Wako Pure Chemical Industries Ltd., 7TFB Inc..

This was followed by the reduction of hydroperoxides by using an excess amount of triphenylphosphine (final concentration; 1 mM) at room temperature for 30 minutes. Next, the reduced sample was mixed with 1 M KOH in methanol (500 μL) under nitrogen and incubated in a shaker for 30 min in the dark at 40°C. The mixture was cooled on ice, acidified with 10% acetic acid in water (2 mL), and extracted with chloroform and ethyl acetate (chloroform/ethyl acetate = 4/1, v/v, 5 mL). The sample was mixed using a vortex mixer for 1 min and centrifuged at 1500 x g for 10 min at 4°C. The chloroform and ethyl acetate layer was concentrated to about 1 mL

after the removal of the water layer and divided equally into 2 portions. The divided chloroform and ethyl acetate solution was evaporated to dryness under nitrogen. The derivatized sample was reconstituted with methanol and water (methanol/water = 70/30, v/v, 200 μL), and a portion of the sample (10 μL) was subjected to LC-MS/MS (Thermo Finnigan TSQ Quantum Discovery Max, a triple-quadrupole mass spectrometer; Thermo Fisher Scientific, CA, USA). With the use of this protocol, hydroperoxides and hydroxides of both free and esterified forms of linoleic acid were assessed as the total hydroxyoctadecadienoic acid (tHODE), which includes enzymatic and non-enzymatic products; 9- and 13-(Z, E)-HODE, non-enzymatic free radical-mediated products; and 9- and 13-(E, E)-HODE. Totally assessed 7β-OHCh was measured by a gas chromatograph (GC 6890 N, Agilent Technologies, Palo Alto, CA, USA) equipped with a quadrupole mass spectrometer (5973 Network, Agilent Technologies). The tHODE concentration was divided by the totally assessed linoleic acids (linoleates) in order to reduce the effects of food intake.

Catecholamine (adrenaline, noradrenaline, and dopamine) concentrations in the urine samples were determined using high-performance liquid chromatography. Urine creatinine concentrations were measured using enzymatic detection (Pure Auto S CRE-L; Sekisui Medical, Tokyo, Japan). Adrenaline, noradrenaline, and dopamine concentrations were divided by the creatinine concentration to produce a normalized value. The average catecholamine levels for each volunteer's urine sample were calculated on each day of the pre-experiment, the Shikoku Walking Pilgrimage, and the post-experiment.

Cortisol concentrations in the collected saliva samples were measured by using an enzyme-linked immunosorbent assay (Enzaplate cortisol kit, Daiichikishimoto-rinshokensa-center, Sapporo, Japan). Saliva immunoglobulin A (sIgA) concentrations were also measured by using an enzyme-linked immunosorbent assay (EIA sIgA test, MBL, Aichi, Japan).

Physiological data analysis

From the R-wave to R-wave (RR) interval data calculated using the heart rate variability meter, the balance of the autonomic nervous system was evaluated as follows: the 6-hour RR interval data obtained from the response time following each morning flicker test was demarcated into windows of 256-second intervals. Windows in which the ratio of the RR intervals in the range of 0.3 seconds to 1.5 seconds was less than 60% were excluded from the analysis. After the removal of these windows and the RR intervals outside the range of 0.3 seconds to 1.5 seconds from the analysis set, the heart rate (as derived from the number of heartbeats) and the high frequency power of heart rate variability in normalized units (HFnu) was calculated from each window of the RR interval data (12). Finally, the heart rate and the average HFnu of each volunteer were calculated for each day of the pre-experiment, the Shikoku Walking Pilgrimage (day 4 was removed because of readings only being obtained in the morning), and the post-experiment. The average body motion level during sleep was calculated for each night, as measured using the actigraph body accelerometers.

Statistical analysis

For the indices measured in the 2012 experiment (n = 4), an average of 3 days was used for both the pre-experiment and post-experiment. For the 2011 experiment (n = 5), the measurements were obtained as is (since they were obtained over just 1 day) and were used in the subsequent analysis. The data for the first attendance were used after the confirmation of the reproducibility in the two experiments.

The following statistical tests were conducted to investigate whether there was a significant difference in the value of each index at the 6 different data collection points (or the 5 different data collection points, as pertains to the heartbeat assessments) corresponding to the pre-experiment, the first, second, third, and fourth days of the pilgrimage, and the post-experiment. A one-factor repeated measures analysis of variance (ANOVA) was performed for measurements involving the 6 different data collection points. A multiple comparison test (Bonferroni correction) was performed where the main effects were found at the 5% level, and was conducted to identify parameters with values that differed significantly between the pre-experiment, the pilgrimage, and the post-experiment. However, the ratio data outside the range of ±5 standard deviations from the average of all volunteers were removed.

Correlations of representative indices found to have a main effect from the results of the ANOVA were analyzed. A Pearson's correlation coefficient was calculated for each pair of indices after conversion to a normalized value for each volunteer. All data were analyzed using MATLAB.

RESULTS

Psychological indices

The morning subjective tension-anxiety scores of the simplified version of POMS for the third and fourth days of the Shikoku Walking Pilgrimage were significantly lower than those of the pre-experiment (Fig. 2 A). Furthermore, it is interesting and striking that the score of post-experiments was not higher

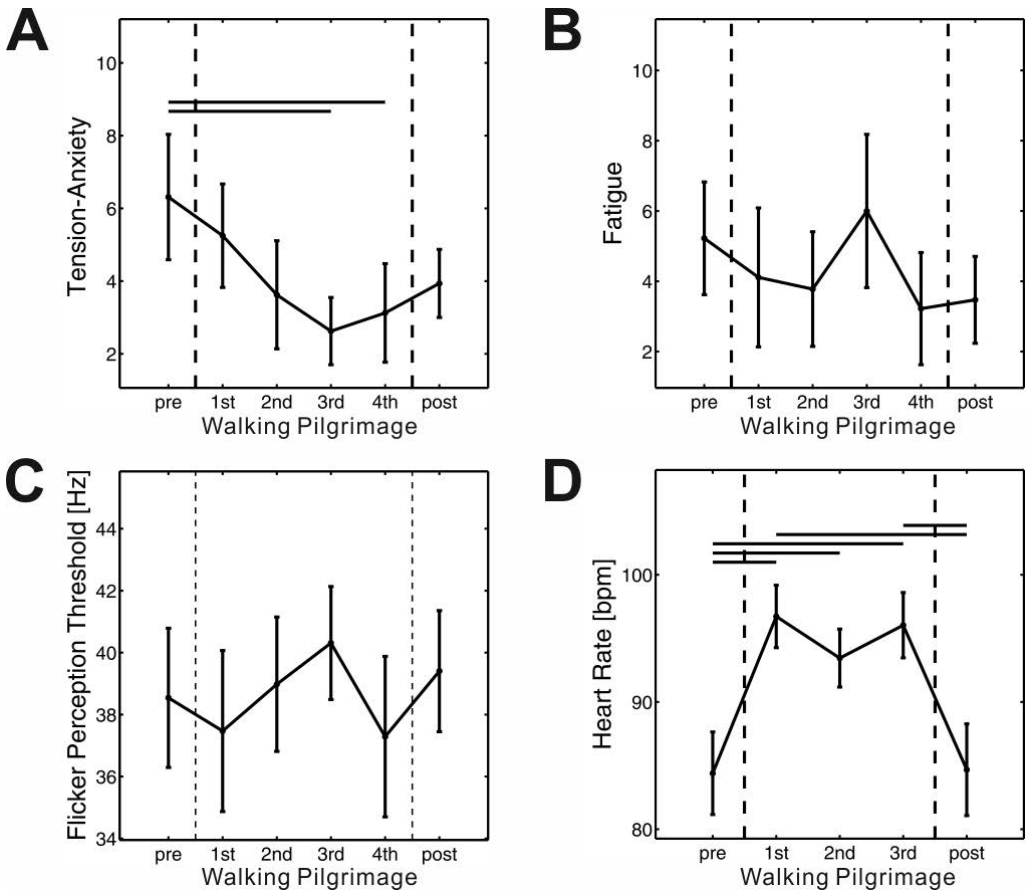

Fig. 2. *Effects of Shikoku Walking Pilgrimage on psychophysiological indices. Average (A) tension-anxiety POMS scores, (B) fatigue POMS scores, (C) flicker perception threshold in the morning, and (D) heart rate across all subjects ± standard error for the pre-experiment, each day of the pilgrimage, and the post-experiment. Horizontal bars indicate significant ($p < 0.05$) differences.*

than that of pre-experiment in all subjects. No main effects were found in the other 5 mood state scores, including fatigue (Fig. 2 B), during the Shikoku Walking Pilgrimage.

Physiological indices

No main effects were found in either the morning or evening score of the critical flicker perception threshold test (Fig. 2 C). During the pilgrimage experiment, the heart rate was significantly higher than that during the pre-experiment (Fig. 2 D). Additionally, on the morning of the first and third days of the pilgrimage, this value was significantly higher than that of the post-experiment. However, the high frequency power of heart rate variability in normalized units (HFnu) of the heart rate variability was not found to be a main effect of the Shikoku Walking Pilgrimage. The average amount of body motion during sleep was not found to be a main effect of the Shikoku Walking Pilgrimage.

Typical immunological markers

Compared to the days from the second to fourth day of the Shikoku Walking Pilgrimage, the day of the post-experiment revealed significantly increased NK cell activity (Fig. 3 A). On the fourth day of the Shikoku Walking Pilgrimage, the serum IgG concentration (divided by total protein, TP) was

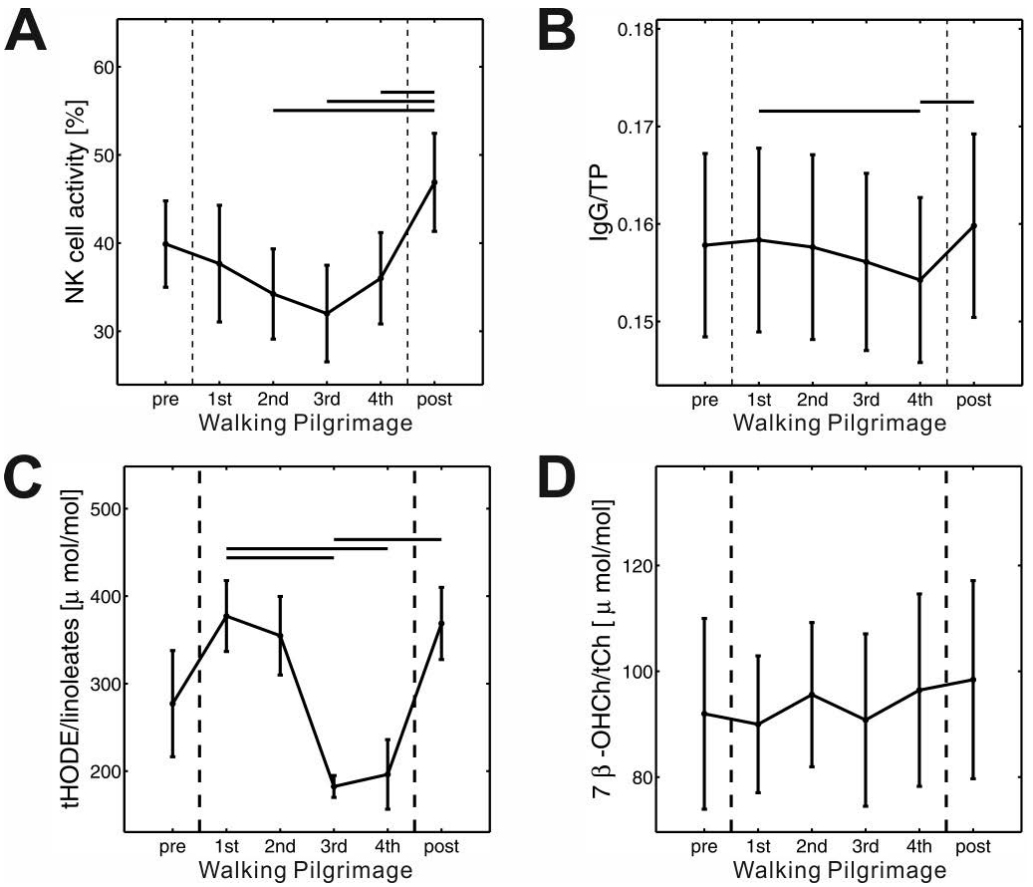

Fig. 3. Effects of Shikoku Walking Pilgrimage on lipid metabolism and oxidation indices. Average fasting (A) natural killer (NK) cell activity, (B) serum immunoglobulin G (IgG) concentration divided by total protein (TP), (C) plasma tHODE concentration divided by linoleate values, and (D) plasma 7β-OHCh concentration divided by total cholesterol across all subjects ± standard error for the pre-experiment, each day of the pilgrimage, and the post-experiment. Horizontal bars indicate significant ($p < 0.05$) differences.

significantly lower when compared to the first day of the pilgrimage and the post-experiment (Fig. 3 B). Similar trends were found for serum IgA and IgM. However, it is striking that the post levels of NK activity and IgG/TP increased compared to pre levels in 7 subjects out of 9, suggesting that immunological properties would be affected later than this event.

Other immunological biomarkers

To evaluate the changes of lipid oxidation stress markers, the concentration of tHODE and 7β-hydroxycholesterol (7β-OHCh), generated from linoleate and total cholesterol, respectively, were measured. Compared to the first day of the Shikoku Walking Pilgrimage, the third and fourth days showed a significantly reduced fasting tHODE concentration (divided by the totally assessed linoleates) (Fig. 3 C). Additionally, on the morning of the third day of the pilgrimage, this value was significantly lower than that of the post-experiment. No variation was found in the concentration of plasma isoprostane, oxidation product generated from arachidonate or the 7β-OHCh concentration divided by the total cholesterol value (Fig. 3 D) during the pilgrimage.

The urine adrenaline concentration (divided by creatinine for normalization) upon the subject awakening on the second day of the Shikoku Walking Pilgrimage was significantly lower than that of the

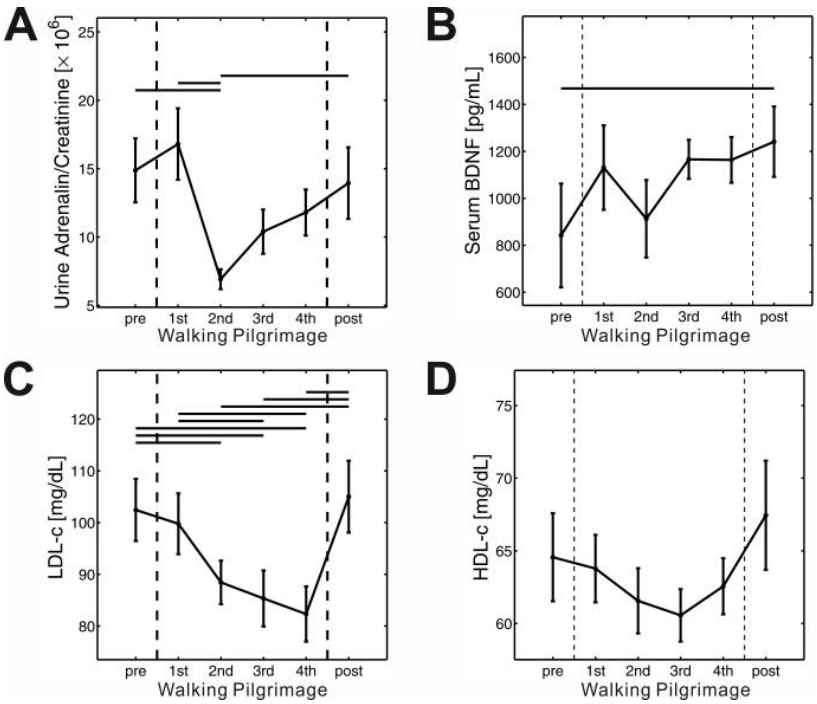

Fig. 4. *Effects of Shikoku Walking Pilgrimage on biochemical indices. Average fasting (A) urine adrenaline concentration (creatinine-normalized), (B) serum brain-derived neurotrophic factor (BDNF) concentration, (C) serum low-density lipoprotein (LDL) cholesterol concentration, and (D) serum high-density lipoprotein (HDL) cholesterol concentration across all subjects ± standard error for the pre-experiment, each day of the pilgrimage, and the post-experiment. Horizontal bars indicate significant ($p < 0.05$) differences.*

mornings of the pre-experiment, the first day of the pilgrimage, and the post-experiment (Fig. 4 A). There was no main effect for urine noradrenaline and dopamine (both creatinine-normalized) in relation to the pilgrimage. No main effects were found in the serum and saliva cortisol concentrations and saliva immunoglobulin A (sIgA) concentration, which were measured to evaluate stress.

The serum brain-derived neurotrophic factor (BDNF) concentration, which is used as a depression marker, tended to increase in the post-experiment compared to the pre-experiment (Fig. 4. B). In fact, 8 subjects out of 9 showed the same results.

Other biomarkers

Between the second and fourth days of the Shikoku Walking Pilgrimage, the fasting serum low-density lipoprotein LDL cholesterol concentrations were significantly lower as compared to those of the pre-experiment and post-experiment (Fig. 4. C). There was no main effect in relation to the pilgrimage for the fasting serum HDL cholesterol (Fig. 4 D).

The serum γ glutamyl transpeptidase (γ-GTP) concentration was significantly lower on the second day of the Shikoku Walking Pilgrimage in comparison to those of the pre-experiment and post-experiment and on the third day in comparison to that of the post-experiment. Between the second and fourth days of the pilgrimage, the fasting cholinesterase concentration was significantly lower than that in the pre-experiment and post-experiment. However, these reductions were within normal range. Main effect was found in serum alanine aminotransferase (ALT). There was no change in serum aspartate aminotransferase (AST) and total bilirubin concentrations.

On the third and fourth days of the pilgrimage, the serum creatine kinase concentration was significantly higher in comparison to the pre-experiment. On the second and third days of the pilgrimage, the fasting

Table II. *Correlation coefficients between each pair of variables.*

	TEN	LDL	NKA	IGG	GTP	HOD	GLU	BDN	CK	ADR
TEN	---	+0.31	-0.06	+0.16	+0.22	+0.15	-0.24	-0.19	-0.15	+0.26
LDL	---	---	+0.47*	+0.41*	+0.64*	+0.43*	-0.26	-0.09	-0.35	+0.15
NKA	---	---	---	+0.36*	+0.58*	+0.45*	-0.30	+0.16	-0.25	+0.04
IGG	---	---	---	---	+0.12	+0.40*	+0.04	-0.13	-0.40*	+0.00
GTP	---	---	---	---	---	+0.36	-0.43*	+0.10	-0.19	+0.16
HOD	---	---	---	---	---	---	-0.30	-0.03	-0.44*	+0.07
GLU	---	---	---	---	---	---	---	+0.10	+0.28	-0.06
BDN	---	---	---	---	---	---	---	---	+0.25	-0.03
CK	---	---	---	---	---	---	---	---	---	-0.21
ADR	---	---	---	---	---	---	---	---	---	---

*TEN: Tension-Anxiety, LDL: LDL-cholesterol, NKA: Natural killer cell activity, IgG: IgG/total protein, GTP: γGTP, HOD: tHODE/linoleates, GLU: Glucose, BDN: serum BDNF, CK: Creatine kinase, ADR: urine adrenaline, +: positive correlation, -: negative correlation. *:p<0.01*

serum glucose concentration was significantly higher than in the pre-experiment. Additionally, on the morning of the third day of the pilgrimage, this value was significantly higher than that of the post-experiment. The serum levels of uric acid, blood urea nitrogen, and amylase were not influenced by the Shikoku Walking Pilgrimage.

Analysis of the correlations between each marker

Table II shows the Pearson's correlation coefficients calculated for each pair of the ten representative indices for which a main effect was found in the above results. A significant correlation was observed between LDL cholesterol, NK activity, IgG/TP, γ-GTP, and tHODE/linoleates and a comparatively large number of other indices. In contrast, tension-anxiety, BDNF, and urine adrenaline did not show significant correlations with the other indices.

DISCUSSION

In the present study, we investigated the effect of walking in a 3-day Shikoku Walking Pilgrimage on mental and physical health to determine the appropriate biomarkers for the assessment of immunological properties toward maintaining the human health. We chose and measured immunological biomarkers such as NK cell activity, IgG, IgA, IgM, BDNF, and our original HODE and 7β-OHCh in comparison with the psychological and physiological indices. The main factors in considering the impact of the pilgrimage on the health of the participants seem to be the exercise from the long-distance walking, the mental tranquility from worshipping, and a respite from daily life. There was a significant reduction in subjective tension-anxiety during the pilgrimage, serum LDL cholesterol concentrations, tHODE, and serum γ-GTP and morning urine adrenaline concentrations. Interestingly, the NK cell activity and IgG/TP concentration tended to increase 1 week after the pilgrimage as compared to the week preceding the pilgrimage. These results suggest that the walking pilgrimage reduced oxidative stress instantly by affecting the mental and physical health positively and then enhanced immunological properties later.

The morning tension-anxiety levels on the third and fourth days were significantly lower when compared to that before the pilgrimage (Fig. 2 A). Conversely, there was no increase in subjective fatigue according to the POMS data (Fig. 2 B). In addition, neither the flicker perception threshold nor 7β-OHCh, an indicator of alertness related to fatigue, was observed to be a main effect of the pilgrimage (Figs. 2 C and 3 D). We previously demonstrated that the flicker perception threshold and the ratio of 7β-OHCh to total cholesterol related

with fatigue induced by overnight deskwork (6). Accordingly, the Shikoku Walking Pilgrimage did not induce central fatigue. Acute moderate exercise has been reported to have an elevating effect on the positive mood (vigor) and a reducing effect on the negative mood (tension, anxiety, dejection) of healthy individuals (13-14). Song et al. reported that tension-anxiety level score was significantly lower after walking in the urban park than after walking in the city area (15). Thus, the reduction in tension-anxiety obtained in the present study is in agreement with these previous findings. The mental effects of worship may have also reduced tension-anxiety. Indeed, Kawauchi et al. (1) reported that more than 70% of people have the impression that a pilgrimage confers a feeling of enrichment. Other than physical exercise and effects on mental condition, additional factors such as climatological effects and holidays might reduce the tension-anxiety level.

A typical immunological biomarker NK cell activity has been reported to increase during long-duration, relatively high-intensity treadmill running; however, the activity then decreases to a level far below that at exercise commencement, requiring 1–7 days to return to normal (16-17). The present study revealed a transient reduction of NK cell activity and IgG concentration during the pilgrimage (Figs. 3. A and B). It is reported that the Ig and NK cell activity response to exercise was due to the state of the autonomic nervous system rather than to the change in immunological response (18-19). Thus, the transient reduction in NK cell activity and serum IgG concentration in the present study were not necessarily due to a decline in the immune system. In the present study, NK cell activity and IgG concentration during the post-experiment tended to increase (Fig. 3, A and B). There have been reports of NK cell activity being enhanced by a mental healing effect (20).

The relationship between acute exercise and oxidative stress has been studied recently (21). Further, we previously reported that the plasma levels of the lipid oxidation product tHODE increased in such diseases as Alzheimer's disease and lifestyle diseases (22-23). In particular, its increase was observed in patients with diabetes and early stage Alzheimer's disease (23-24). However, the effect of exercise on plasma tHODE concentrations has not been reported to date. In the present study, plasma tHODE concentrations (divided by those of linoleates) were reduced during the Shikoku Walking Pilgrimage (Fig. 3 C).

Catecholamine (adrenaline, noradrenaline) concentrations have been reported to increase during moderate to high-intensity exercise and long-term exercise, and then return to normal after 1 hour (25-26). The present study showed a reduction in urine adrenaline upon concentration waking on the second day of the pilgrimage (Fig. 4. A). This result cannot be explained by the physical exercise, suggesting other causes such as psychological effects.

It has been reported that for healthy individuals participating in anything more than moderate and acute exercise over short periods, serum BDNF increases immediately after exercise and then returns to its previous level within 30 minutes (27-30). There has also been a report of BDNF decreasing to below the resting level 2–3 hours after the completion of exercise (31). In the present study, it is noteworthy that the serum BDNF concentration increased 1 week after completion of the Shikoku Walking Pilgrimage (Fig. 4 B), suggesting that the changes in the BDNF concentration may have been due to psychological or other factors, rather than exercise, in the Shikoku Walking Pilgrimage.

Morning serum LDL cholesterol concentrations were significantly reduced on the second to fourth days compared to those before the Shikoku Walking Pilgrimage was undertaken (Fig. 4 C). This is in agreement with the results from the Spanish pilgrimage study by Bemelmans et al. (2-3). Moreover, LDL cholesterol has been reported to be reduced by an acute, long-duration exercise of over 3 hours (32-33). Accordingly, the observed reduction in LDL cholesterol concentrations during the Shikoku Walking Pilgrimage was due to the long-duration nature of the exercise.

Acute reduction of oxidative stress shown in tHODE/linoleates may lead to enhancement of immunological properties one week after the walking pilgrimage. The tHODE/linoleates can be an appropriate measure for assessing immunological properties.

This study is a preliminary evaluation of the Shikoku Pilgrimage to identify proper immunological biomarkers. Although the present study was limited in

number and period, we comprehensively investigated various types of biomarkers. The findings suggest that the Shikoku Walking Pilgrimage can exert a reductive effect of tension-anxiety and a positive effect on physical health (as particularly shown in the reduction of oxidative stress) without the accompaniment of fatigue (as shown in POMS and 7β-OHCh). Furthermore, this study provided several promising measures including tHODE/linoleates, NK activity, BDNF, LDL-c, and IgG for clarifying immunological properties. It is valuable to examine these promising biomarkers in the future large-scale study.

ACKNOWLEDGEMENTS

The authors acknowledge Ms. Noriko Umeno for her technical support in collecting blood sample during the Shikoku Walking pilgrimage. We also acknowledge Ms. Naomi Anzai for serving as guide for the pilgrimage.

We acknowledge Mr. Yuichiro Tanima for his technical support.

Trial Registration: UMIN Clinical Trials Registry UMIN000012182.

REFERENCES

1. Kawauchi T, Saitoh M, Akao Y, Gotoh M, Nishiyama K. A study of mental well being and the Shikoku pilgrimage. Bull Shikoku Univ 1999; 11:1-7 (in Japanese).
2. Bemelmans RH, Coll B, Faber DR, Westerink J, Blommaert PP, Spiering W, Visseren FL. Vascular and metabolic effects of 12 days intensive walking to Santiago de Compostela. Atherosclerosis 2010; 212:621-27.
3. Bemelmans RH, Blommaert PP, Wassink AM, Coll B, Spiering W, Graaf YV, Visseren FL. The relationship between walking speed and changes in cardiovascular risk factors during a 12-day walking tour to Santiago de Compostela: a cohort study. BMJ open 2012; 2:e000875.
4. Chen ZH, Yoshida Y, Saito Y, Sekine A, Noguchi N, Niki E. Induction of adaptive response and enhancement of PC12 cell tolerance by 7-hydroxycholesterol and 15-deoxy-delta12,14-prostaglandin J2 through up-regulation of cellular glutathione via different mechanisms. J. Biol Chem 2006; 281:14440-45.
5. Chen ZH, Yoshida Y, Saito Y, Noguchi N, Niki E. Adaptive response induced by lipid peroxidation products in cell cultures. FEBS Lett 2006; 580:479-83.
6. Shichiri M, Harada N, Ishida N, Komaba LK, Iwaki S, Hagihara Y, Niki E, Yoshida Y. Oxidative stress is involved in fatigue induced by overnight deskwork as assessed by increase in plasma tocopherylhydroqinone and hydroxycholesterol. Biolog Psychol 2013; 94:527-33.
7. McNair DM, Lorr M, Droppleman LF. Profile of Mood States. Educational and Industrial Testing Service. San Diego, 1992.
8. Niepel G, Bibani RH, Vilisaar J, Langley RW, Bradshaw CM, Szabadi E, Constantinescu CS. Association of a deficit of arousal with fatigue in multiple sclerosis: effect of modafinil. Neuropharmacology 2013; 64:380-88.
9. Nakazato M, Hashimoto K, Shimizu E, et al. Decreased levels of serum brain-derived neurotrophic factor in female patients with eating disorders. Biol Psychiatry 2003; 54:485-90.
10. Egan MF, Kojima M, Callicott JH, et al. The BDNF val66met polymorphism affects activity-dependent secretion of BDNF and human memory and hippocampal function. Cell 2003; 112:257-69.
11. Brunner KT, Mauel J, Cerottini JC, Chapuis B. Quantitative assay of the lytic action of immune lymphoid cells on 51-Cr-labelled allogeneic target cells in vitro; inhibition by isoantibody and by drugs. Immunology 1968; 14:181-96.
12. Akselrod S, Gordon D, Ubel FA, Shannon DC, Berger AC, Cohen RJ. Power spectrum analysis of heart rate fluctuation: a quantitative probe of beat-to-beat cardiovascular control. Science 1981; 213:220-22.
13. Maroulakis E, Zervas Y. Effects of aerobic exercise on mood of adult women. Percept Mot Skills 1993; 76:795-801.
14. Landers DM, Arent SM. Physical activity and mental health. In Handbook of sports psychology. 2nd edition. Singer RN, Hausenblas HA, Janelle CM, ed. Willey. New York, 2001; p. 740-765.

15. Song C, Ikei H, Igarashi M, Miwa M, Takagaki M, Miyazaki Y. Physiological and psychological responses of young males during spring-time walks in urban parks. J Physiol Anthropol 2014; 33:8.
16. Pedersen BK, Ullum H. NK cell response to physical activity: possible mechanisms of action. Med Sci Sports Exerc 1994; 26:140-46.
17. Shek PN, Sabiston BH, Buguet A, Radomski MW. Strenuous exercise and immunological changes: a multiple-time-point analysis of leukocyte subsets, CD4/CD8 ratio, immunoglobulin production and NK cell response. Int J Sports Med 1995; 16:466-74.
18. Nagatomi R. The implication of alterations in leukocyte subset counts on immune function. Exerc Immunol Rev 2006; 12:54-71.
19. Gleeson M. Mucosal immune responses and risk of respiratory illness in elite athletes. Exerc Immunol Rev 2000; 6:5-42.
20. Li Q, Morimoto K, Kobayashi M, et al. Visiting a forest, but not a city, increases human natural killer activity and expression of anti-cancer proteins. Int J Immunopathol Pharmacol 2008; 21:117-27.
21. Fisher-Wellman K, Bloomer RJ. Acute exercise and oxidative stress: a 30 year history. Dynamic Med 2009; 8:1.
22. Umeno A, Shichiri M, Ishida N, et al. Singlet oxygen induced products of linoleates, 10- and 12-(Z,E)-hydroxyoctadecadienoic acids (HODE), can be potential biomarkers for early detection of type 2 diabetes. PLoS One 2013; 8:e63542.
23. Yoshida Y, Umeno A, Shichiri M. Lipid peroxidation biomarkers for evaluating oxidative stress and assessing antioxidant capacity in vivo. J Clin Biochem Nutr 2013; 52:9-16.
24. Yoshida Y, Yoshikawa T, Kinumi Y, Ogawa Y, Saito K, Ohara K, Yamamoto H, Imai Y, Niki E. Hydroxyoctadecadienoic acid and oxidatively modified peroxiredoxins in the blood of Alzheimer's disease patients and their potential as biomarkers. Neurobiol Aging 2009; 30:174-85.
25. Galbo H, Holst JJ, Christensen NJ. Glucagon and plasma catecholamine response to graded and prolonged exercise in man. J Appl Physiol 1975; 38:70-76.
26. Kanaya S, Fujino T, Komiya S, et al. The responses of plasma catecholamines, serum potassium, lipids, and blood glucose levels during graded exercise and recovery. J Health Sci 1985; 7:51-59 (in Japanese).
27. Gold SM, Schulz KH, Hartmann S, et al. Basal serum levels and reactivity of nerve growth factor and brain-derived neurotrophic factor to standardized actute exercise in multiple sclerosis and controls. J Neuroimmunol 2003; 138:99-105.
28. Rojas Vega S, Strüder HK, Vera Wahrmann B, Schmidt A, Bloch W, Hollmann W. Acute BDNF and cortisol response to low intensity exercise and following ramp incremental exercise to exhaustion in humans. Brain Res 2006; 1121:59-65.
29. Ferris LT, Williams JS, Shen CL. The effect of acute exercise on serum brain-derived neurotrophic factor levels and cognitive function. Med Sci Sports Exerc 2007; 39:728-34.
30. Tang SW, Chu E, Hui T, Helmeste D, Law C. Influence of exercise on serum brain-derived neurotrophic factor concentrations in healthy human subjects. Neurosci Lett 2008; 431:62-65.
31. Castellano V, White LJ. Serum brain-derived neurotrophic factor response to aerobic exercise in multiple sclerosis. J Neurol Sci 2008; 269:85-91.
32. Goodyear LJ, Van Houten DR, Fronsoe MS, Rocchio ML, Dover EV, Durstine JL. Immediate and delayed effects of marathon running on lipids and lipoproteins in women. Med Sci Sports Exerc 1990; 22:588-92.
33. Föger B, Wohlfarter T, Ritsch A, Lechleitner M, Miller CH, Dienstl A, Patsch JR. Kinetics of lipids, apolipoproteins, and cholesteryl ester transfer protein in plasma after a bicycle marathon. Metabolism 1994; 43:633-39.

EFFECT OF TRIMETAZIDINE ON SERUM INTERLEUKIN-6 AND C-REACTIVE PROTEIN CONCENTRATIONS IN PATIENTS WITH STABLE CORONARY ARTERY DISEASE

J. SZKODZINSKI[1], A. DANIKIEWICZ[2], B. HUDZIK[1], M. SZEWCZYK[3], M. GĄSIOR[1] and B. ZUBELEWICZ-SZKODZINSKA[2]

[1]Third Department of Cardiology, Silesian Center for Heart Disease, Zabrze, Poland;
[2]Department of Food-related Disease Prevention, Medical University of Silesia, Bytom, Poland;
[3]Cardiology Ward, County Hospital, Piekary Slaskie, Poland

Received September 18, 2014 – Accepted January 12, 2015

The first two authors contributed equally to the manuscript

Trimetazidine is widely used in the treatment of stable coronary artery disease (CAD) and its cytoprotective effect has been confirmed in animal studies and in many clinical trials. Given the inflammatory milieu of CAD and trimetazidine effect on the inflow of neutrophilis to the ischemic area, it is interesting to consider whether trimetazidine actions could be also explained through the inhibition of inflammatory mediators, including cytokines. The aim of this study was to (i) examine the influence of treadmill exercise test (TET) on serum C-reactive protein (CRP) and interleukin-6 (IL-6), and (ii) the influence of three-month trimetazidine therapy on serum CRP and IL-6 concentrations. One hundred and fifty-six patients with stable CAD were included. TET was performed (according to the standard Bruce protocol) twice for all subjects – at baseline and after the three-month trimetazidine treatment. Serum IL-6 and CRP concentrations were determined prior to and after performing each TET. Exercise led to the increase of CRP (2.35 *vs* 2.81 mg/L, p<0.05) and IL-6 concentrations (1.64 *vs* 1.92 pg/ml, p=0.0318) in patients without trimetazidine. Three-month treatment resulted in the increase in the TET duration (378.0s *vs* 410.9s, p<0.05) and decrease in serum CRP concentration, both before (2.35 *vs* 1.51 mg/L, p<0.05) and after TET (2.81 *vs* 1.69 mg/L, p<0.05). There was no significant increase of CRP after the second TET (1.51 *vs* 1.69 mg/l, p=NS). Three-month trimetazidine treatment increased IL-6 concentrations (1.64 *vs* 2.23 pg/mL, p<0.05). TET was not associated with further changes in IL-6 concentrations (2.23 *vs* 2.18 pg/mL, p=NS). Serum IL-6 and CRP concentrations increase during exercise in patients without trimetazidine. Three-month trimetazidine prolonged the duration of TET. Moreover, it resulted in the reduction of CRP concentration The increase of IL-6 concentration after three-month trimetazidine treatment and the lack of changes of its concentration after TET is associated with yet another mechanism of trimetazidine.

Currently, a greater role is assigned to the significance of the inflammatory process in the development of atherosclerosis. Endothelial damage leads to the activation of inflammatory

Key words: trimetazidine, interleukin-6 , CRP, coronary heart disease, cardiac stress test

Mailing address: Dr. Janusz Szkodzinski, MD PhD
Third Department of Cardiology,
Silesian Center for Heart Disease,
M. Curie-Skłodowskiej 9, 41-800 Zabrze, Poland
Tel.: +48 32 3733788
e-mail: bartekh@mp.pl

0393-974X (2015)

DISCLOSURE: ALL AUTHORS REPORT NO CONFLICTS OF INTEREST RELEVANT TO THIS ARTICLE.

processes, the formation of atherosclerotic plaque, and subsequently to arterial stenosis. Clinically, all of these processes result in symptoms produced by myocardial ischemia (1-4).

It has been proposed that etiopathology of stable CAD and acute coronary syndromes differ substantially. In stable CAD, the symptoms are produced by the progression of atherosclerotic plaque (increasing arterial stenosis), thus decreasing the coronary blood flow and oxygen supply. Conversely, acute coronary syndromes are caused by the formation of thrombus upon a ruptured atherosclerotic plaque which often does not cause a significant coronary artery stenosis.

Inflammation is said to be at the core of endothelial activation. Also other factors (immune reactions, infections) can trigger the inflammatory process within coronary artery walls leading to the formation of atherosclerosis and producing clinical symptoms.

Thrombus formation upon ruptured atherosclerotic plaque is the cornerstone of acute coronary syndromes. Albeit, other important contributors are involved in that process. Inflammatory markers seem to make a major contribution (5, 6).

Particular attention should be given to the potential IL-6 modifying action of the atherosclerotic plaque. It is a cytokine produced by activated smooth muscle cells, coronary vessels, endothelium and macrophages and lymphocytes. Its pivotal role in the pathogenesis of CAD has also been reported. It acts as a substance participating in the acute phase response (systemic effect) and as a factor produced by the majority of cell types within the atherosclerotic plaque (local effect). High IL-6 concentrations have been implicated with an increased risk of cardiovascular adverse events.

In patients with acute coronary syndromes (unstable angina or myocardial infarction alike), serum IL-6 concentrations are elevated. IL-6 was found to be in high concentrations within unstable atherosclerotic plaques, in comparison to stable plaques. Hence, IL-6 is assumed as a possible marker of plaque instability.

The acute phase response is a non-specific reaction of the organism to every disturbance of homeostasis triggered by various factors. It varies widely from activation of the complement system, escalation of chemotaxis, increased secretion of factors destabilizing the atherosclerotic plaque, to the reduction of the bioavailability of endothelial nitric oxide synthases, all of which are responsible for the changes within the plaque (7-10).

Recent evidence suggests that a strong association between cytokines and cardiovascular disease exists. It has been demonstrated that they play a pivotal role in the pathogenesis of atherosclerosis, stable CAD, acute coronary syndromes, remodeling, and angiogenesis.

Numerous data on the role of CRP as the marker of CAD have been presented. It has been shown that high CRP concentrations – especially highly sensitive CRP – predict incident myocardial infarctions, both in patients with stable CAD and acute coronary syndromes (9-11). Moreover, inflammatory activation and atherosclerotic plaque rupture is responsible for increased circulating cytokine levels at an early stage. The extension of the disease is associated with the impairment of coronary circulation and inflammatory actions.

When talking about myocardial ischemia, it is important to note that there are cardioprotective mechanisms that counteract myocardial injury. Various cytokines with anti-inflammatory properties take part in that process (12, 13). A considerable amount of literature has been published on the cardioprotective actions of various pharmacologic agents. In that aspect, trimetazidine is one of the most widely used groups of anti-ischemic agents. It is the only anti-ischemic metabolic modulator recommended by the European Society of Cardiology in the management of stable CAD (14).

The cytoprotective actions of trimetazidine have been reported in animal studies and in many clinical trials. Its anti-ischemic properties have been demonstrated in clinical trials, both in monotherapy, compared to other anti-anginal agents, and in addition to β-blockers and calcium channel antagonists (15, 16).

Given the inflammatory milieu of CAD and trimetazidine effect on the inflow of neutrophilis to the ischemic area, it is interesting to consider whether trimetazidine actions could be also explained through the inhibition of inflammatory mediators, including cytokines secreted by peripheral blood cells and endothelial cells.

The effect of trimetazidine on cytokine synthesis and secretion has not yet been established. No previous study has investigated this subject which is pivotal, given the fact that trimetazidine is used in patients with stable CAD. The aim of this research project has therefore been to try and establish the cardioprotective properties of trimetazidine through the modulation of cytokine release. This paper will examine: i) the influence of treadmill exercise test (TET) on serum C-reactive protein (CRP) and interleukin-6 (IL-6) in patients with stable CAD; and ii) the influence of three-month trimetazidine therapy on serum CRP and IL-6 concentrations before and after TET.

MATERIALS AND METHODS

One hundred and fifty-six patients aged 47–65 years were enrolled in the study: 51 women and 105 men. One hundred and forty patients were included in the final analysis. The remaining patients were excluded from the study because of acute infections (12 patients), surgical treatment during follow-up (2 patients) and lack of informed consent (2 patients). One hundred and thirty-eight patients had hypertension. All patients received acetylsalicylic acid, 135 (96%) patients received β-blockers, 134 patients (95%) received angiotensin converting enzyme inhibitors, 84 patients (60%) received sustained-release nitrates, 60 patients (43%) received calcium channel antagonists, and 39 patients (28%) received diuretics.

Inclusion criteria were: age 40–65 years, prior CAD, rest electrocardiogram without ischemic changes, absence of moderate/severe angina – Canadian Cardiovascular Society functional class 1 or 2.

Exclusion criteria were: acute coronary syndromes, very positive result of the TET, history of stroke (ischemic and hemorrhagic) within 12 months prior to the study, unsteady body weight (≥10kg gain/loss within 6 months prior to the study), other comorbidities including autoimmune disease, metabolic disease (diabetes, hyperthyroidism and hypothyroidism), liver disease (viral hepatitis, congestive jaundice) acute infectious disease, chronic inflammatory conditions (i.e., AIDS, tuberculosis, colitis ulcerosa), chronic kidney disease (eGFR <60 mL/kg per 1.73 m2), severe congestive heart failure (functional NYHA class 3 and 4), neoplasms, mental disorders, addictions: tobacco and drugs, treatment with glucocorticoids, androgens, non-steroidal anti-inflammatory drugs (within a month prior to the study), lack of informed consent.

The study was approved by the local Bioethics Committee. All subjects were informed of the study design and gave their written consent.

Peripheral blood samples were obtained at the following time points:

i. prior to performing the initial TET,

ii. after performing the initial TET,

iii. before the follow-up TET performed three months after trimetazidine therapy,

iv. after the follow-up TET performed three months after trimetazidine therapy.

Methods

Serum IL-6 and CRP concentrations were evaluated for all patients. IL-6 concentration was determined with enzyme immunoassay test (ELISA) using R&D Systems kits (USA). CRP concentration was determined with latex immunoturbidimetric test using the BIO-BAS kits. Blood samples were drawn from the cubital vein. Prior to the study, the subjects were not administered drugs described in inclusion and exclusion criteria. All tests were performed concurrently in duplicates in order to avoid interkit variability.

IL-6 concentration was determined with enzyme immunoassay test (ELISA) using R&D Systems kits (USA): sensitivity of the method < 0.039 pg/mL, the within-run variation at 7.8% and between-run variation at 9.6%. CRP concentration was determined with latex immunoturbidimetric test using the BIO - BAS kits, the sensitivity of the method < 4.2 mg/L, the within-run variation at 6.52% and between-run variation at 7.7%.

Statistical analysis

The statistical analysis was carried out using StatSoft STATISTICA 6.0 software. Quantitative data are presented as means ± standard deviations or medians and interquartile ranges (lower and upper quartiles). Qualitative data are presented as frequencies. The Shapiro-Wilk test was used to determine whether a random sample was normally-distributed. Unpaired *t*-test (for normal distributions) or Mann-Whitney U test (for distributions other than normal) were used to detect intergroup differences. Paired t test (for normal distributions) or Wilcoxon signed-rank test (for distributions other than normal) were used to detect differences between baseline and follow-up values. A value of two-tailed $P < 0.05$ was considered significant.

RESULTS

Fig. 1 presents mean time of the TET duration described in reference to sex and trimetazidine treatment.

Significant extension of TET duration was observed after the three-month trimetazidine

treatment in men with stable CAD (447.1±37.7s *vs* 497.3±37.2s p<0.05). No extension of TET duration was observed after the three-month trimetazidine treatment in women with stable CAD (274.4±27.4s *vs* 281.0±32.9s p = 0.45) (Table I).

Fig. 2 presents a mean of the number of METs obtained during TET depending on the patient sex and trimetazidine treatment status.

A significant increase in the number of METs was observed after three-month trimetazidine treatment in men with stable CAD (8.3±0.55 *vs* 9.2±0.58 p<0.05). No increase in the number of METs was observed after three-month trimetazidine treatment in women with stable CAD (5.9±0.33 *vs* 6.0±0.38 p=NS) (Table II).

Fig. 3 presents IL–6 concentration changes before and after the TET depending on trimetazidine treatment.

Baseline IL–6 concentration before the TET significantly increased after the TET (1.64±0.12 pg/mL *vs* 1.92±0.17 pg/mL p<0.05). After three-month trimetazidine treatment IL-6 concentrations before the second TET were higher (2.23±0.20 pg/ml p= 0.013). The concentration did not change significantly after the TET (2.18±0.2371 pg/mL p=NS) (Table III).

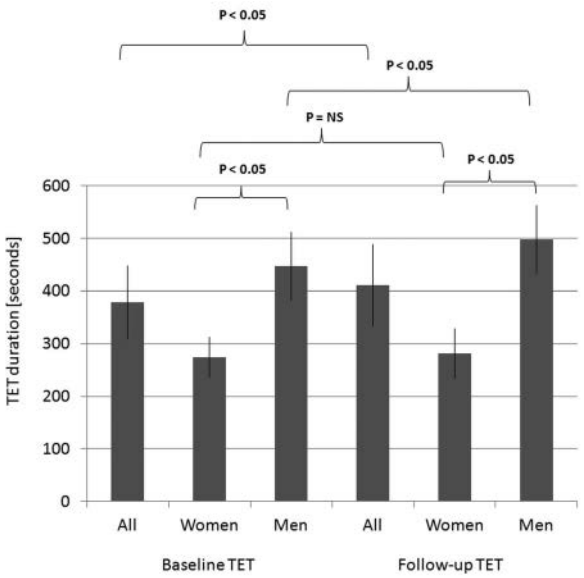

Fig. 1. *Time of duration of treadmill exercise test (TET) before and after trimetazidine treatment.*

Table I. *Duration (in seconds) of treadmill exercise test by sex.*

	Baseline before trimetazidine treatment			Follow-up after three-month trimetazidine treatment		
	All	Women	Men	All	Women	Men
Mean	378.0	274.4	447.1	410.9	281.3	497.3
Median	370.0	277.5	442.5	411.0	257.5	515.0
Standard deviation	140.0	77.4	130.5	156.8	93.2	128.7

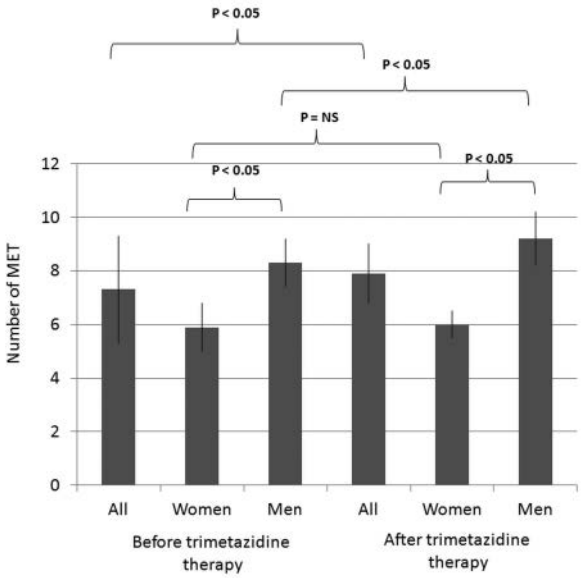

Fig. 2. *Number of metabolic equivalent of task obtained before and after trimetazidine treatment.*

Table II. *Number of metabolic equivalent of task (METs) obtained during treadmill exercise depending on sex and trimetazidine treatment status.*

	Baseline before trimetazidine treatment			Follow-up after three-month trimetazidine treatment		
	All	Women	Men	All	Women	Men
Mean	7.3	5.9	8.3	7.9	6.0	9.2
Median	7.1	5.9	8.2	7.7	5.7	9.3
Standard deviation	1.99	0.95	1.91	2.30	1.07	1.99
MET – metabolic equivalent of task						

Fig. 4 and Table IV present the effect of trimetazidine therapy on the concentration of CRP before and after TET. Baseline CRP concentration before the TET were significantly increased after the TET (2.35±0.40 mg/L vs 2.81±0.48 mg/L $p<0.05$). After three-month trimetazidine treatment CRP concentrations before the second TET were lower (1.51±0.22 mg/L $p<0.05$). The concentration did not change significantly after the TET (1.69±0.31 mg/L p=NS).

DISCUSSION

CAD, in most cases, is caused by the progression of atherosclerotic plaque which leads to coronary artery stenosis (1-4). Atherosclerosis is a chronic inflammatory response within the artery wall (17). In the process of its development the crucial role is triggered by factors inducing vascular endothelial damage. These factors include, among others: cholesterol, arterial hypertension, infections, metabolic disorders (namely diabetes), and tobacco use (17, 18). The key element of the inflammatory process is the modification of the proteins and lipid components of the LDL lipoprotein, namely their oxidation, proteolysis, and glycosylation (19). Activated endothelial cells, through the production of specific proteins and chemotactic agents lead to

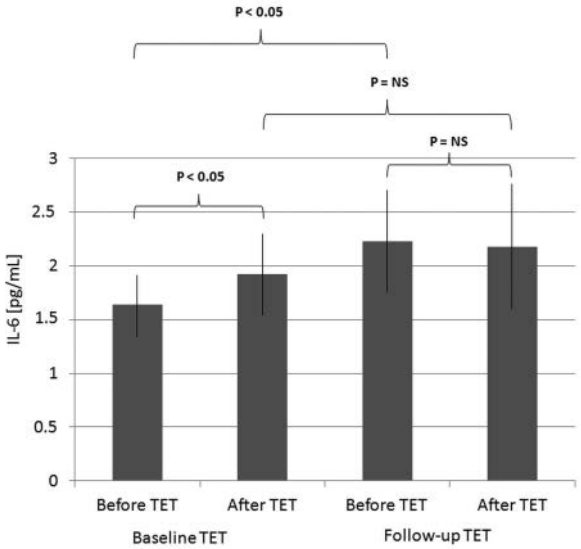

Fig. 3. *Interleukin-6 (IL-6) concentrations in the studied groups. TET - treadmill exercise test.*

Table III. *IL-6 concentrations (pg/ml) before and after treadmill exercise test (TET) depending on trimetazidine treatment status.*

IL-6	Baseline before trimetazidine treatment		Follow-up after three-month trimetazidine treatment	
	Before TET	After TET	Before TET	After TET
Mean	1.64	1.92	2.23	2.18
Median	1.5	2.0	2.1	2.0
Standard deviation	0.54	0.76	0.93	1.06
TET – treadmill exercise test, IL-6 – interleukin-6				

the accumulation of monocytes in the intima which are next converted into macrophages (17, 20). Macrophages are the source of chemokins, cytokines, growth factors and proteolytic enzymes. Their permanent stimulation, constituting the foundation of atherosclerotic process, is also the essence of the inflammatory reaction of the vascular endothelium.

When the plaque ruptures the tissue factor induced by the inflammatory signaling triggers the thrombus that causes most acute complications of atherosclerosis. An increased inflammatory process in surrounding tissues is responsible for the destabilization of the plaque. IL-1 and IL-6 stimulate the synthesis of the intercellular matrix and adhesion molecules which increase the permeability of the endothelium and enhance its procoagulant activity (21).

In light of the aforementioned information, many authors have set out to measure the concentration of various cytokines in different clinical settings (from stable CAD, unstable angina, to myocardial infarction), hoping it will facilitate noninvasive diagnosis of CAD.

IL-6 is a multipotential cytokine. Apart from mechanisms described earlier, it also stimulates the transcription of CRP gene in the liver and the production of serum amyloid A protein (SAA) in the liver. Thus, it promotes SAA embedding into the serum HDL-cholesterol particles. This, in turn, results in HDL-cholesterol molecules acquiring new, pro-

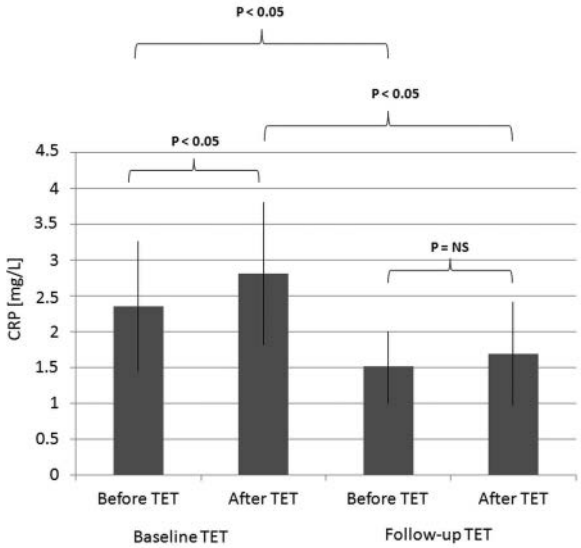

Fig. 4. *C-reactive protein concentrations in the studied group. TET - treadmill exercise test.*

Table IV. *CRP concentrations (mg/l) before and after treadmill exercise test (TET) depending on trimetazidine treatment status.*

	Baseline before trimetazidine treatment		Follow-up after three-month trimetazidine treatmer	
	Before TET	After TET	Before TET	After TET
Mean	2.35	2.81	1.51	1.69
Median	1.9	2.2	1.4	1.4
Standard deviation	1.82	2.01	0.99	1.44
TET – treadmill exercise test, CRP – C-reactive protein				

inflammatory properties. Rus et al. and van Leten et al. demonstrated that elevated IL-6 concentrations in patients with stable CAD are associated with the risk of clinical symptom progression and exacerbation (18, 22).

Mazurow et al. assessed the concentration of interleukins both in serum and in the wall of the atherosclerotic lesions. Increased serum concentrations of IL-1 β, IL-2, IL-6, IL-8, and TNFα were observed in comparison to the control group (healthy volunteers). Concentration of the studied cytokines within atherosclerotic lesion was heterogeneous. IL-2 mRNA expression was significantly higher in the aorta, whereas IL-1β and IL-6 mRNA expression was increased in peripheral arteries (19, 23).

Lee et al. assessed the concentration of inflammatory markers in patients with different types of CAD (stable CAD, unstable angina) in comparison to healthy volunteers. Elevated CRP concentrations were found in patients with unstable angina. Moreover, it was identified as a prognostic marker for incident cardiovascular adverse events during six-month follow-up (21). Similarly, Lubrano et al. showed that IL-6 and CRP concentrations were higher in patients with unstable angina in comparison to healthy volunteers (24). Moreover, cut-off levels for IL-6 and high-sensitivity CRP were established. This will enable better risk stratification of CAD patients (25). Bossowska et al. reported

similar results in regard to IL-6, IL-6R, and IL-10 concentrations (23).

The increase of the concentrations of IL-6 and other cytokines secreted by activated monocytes was shown in many studies concerning unstable angina (12, 13) and silent myocardial ischemia (14, 26). Similarly, it was demonstrated that IL-6 and CRP increase significantly in patients with stable CAD after TET. Among cytokines for which the link was established, the strongest was identified for IL-6.

Trimetazidine shares versatile properties. These include, among others, optimization of energy processes, limitation of intracellular acidosis and cellular overload with calcium and sodium, upholding the ATP synthesis, as well as protection cell membrane from damage by free radicals. It diminishes cellular apoptosis and improves the function of the endothelium. Potential anti-inflammatory action, however, is most probably demonstrated by the reduction of cellular damage induced by reactive forms of oxygen and the inhibition of myocardial fibrosis and the inflammatory process (12-14). Its potential therapeutic values have been described in numerous studies. A significant benefit from trimetazidine use in reference to the inflammatory process assessed with the concentration of CRP in plasma was shown (14, 27).

Our paper examined the significance of the possible anti-inflammatory action of trimetazidine by assessing serum CRP and IL-6 concentrations before and after TET in patients with stable CAD. Anti-inflammatory trimetazidine properties were also reported by Ruixing et al. (6) and Di Napoli et al (7). These studies indicated its potential anti-inflammatory properties by regulating the apoptosis and improving the function of endothelium. Williams et al. also reported a significant limitation of leukocyte infiltration in the area of ischemia. Additionally, the concentration of pro-inflammatory cytokines did not change (12). Also other authors demonstrated similar observations, showing a significant reduction of neutrophil accumulation in the area of the ischemia (13).

Pudil et al. also examined the effect of trimetazidine on the concentration of pro-inflammatory cytokines in patients following myocardial infarction treated with intravenous trimetazidine. A significant CRP reduction was observed, while the IL-6 concentration increased. Concentration of other cytokines (IL-8, TNFα) was similar to the control group (28).

Our results agree with those of Pudil et al. (28). Three-month trimetazidine treatment resulted in lower CRP concentration before the follow-up TET compared to baseline CRP before the initial TET. Moreover, follow-up TET did not affect CRP concentrations. However, the results obtained differ from those published by Zhang et al., who did not confirm the effect of trimetazidine hsCRP concentration (14). This discrepancy might arise from the difference in the sensitivity of the assays used to measure CRP. Perhaps it also comes from the fact that the cited paper is a meta-analysis, rather than the description of a single study.

We examined whether TET has any effect on serum CRP and IL-6 concentrations in patients with stable CAD. Furthermore, we sought to determine whether three-month trimetazidine treatment influences the change in IL-6 and CRP concentrations.

We found that IL-6 concentration after three-month trimetazidine treatment increased significantly in comparison to baseline values and did not change after follow-up TET. However, at baseline before trimetazidine addition, TET resulted in a substantial increase of IL-6 concentration. Hence, it seems that trimetazidine has a protective action against IL-6 elevation during the following exercise. It is difficult to explain the increase of IL-6 with simultaneous CRP decline observed after three-month trimetazidine treatment. Perhaps it results from the IL-6 dual nature, which can share both pro-inflammatory and anti-inflammatory properties in different concentrations.

All cytokines have numerous pleiotropic effects in a network of very complicated interdependence, and it cannot be ruled out that the observed increase in IL-6 concentration is a summary effect of trimetazidine effect on specific inflammatory markers.

Most recently, Yenicerioglu et al. presented even more data pointing to anti-inflammatory actions of trimetazidine (29). They observed a significant decrease of TNFα, IL-6 and IL-1β concentrations in patients with acute pancreatitis induced by L-arginine.

The following conclusions can be drawn from the conducted study: a prolongation of TET duration

can be achieved with a three-month trimetazidine treatment (increase in the number of METs); without trimetazidine therapy, serum concentrations of inflammatory markers, IL-6 and CRP in patients with stable CAD increase during TET; a three-month trimetazidine treatment causes reduction of CRP concentration, showing anti-inflammatory potential and hepatoprotective action. Observed increase in the IL-6 concentration after three months of trimetazidine treatment and the lack of changes in its concentration after the TET is connected to another mechanism of trimetazidine which still needs to be explained.

In summary, the results of the current study indicate the beneficial effect of trimetazidine on clinical manifestation of the disease in patients with stable CAD. Trimetazidine-treated patients demonstrated a significant improvement in the TET tolerance. When duration of TET was prolonged an increase in the number of METs was observed.

The anti-inflammatory effects of trimetazidine, per se, has long been reported. However, for the first time, to our knowledge, we present novel findings regarding the effect of trimetazidine on IL-6. Following a three-month trimetazidine treatment, reduction of CRP concentration might suggest its anti-inflammatory action. Notwithstanding, these results must be interpreted with caution. Perhaps, this is the way that anti-inflammatory IL-6 properties come to light. It is also important to note the lack of increase of IL-6 concentration after TET following trimetazidine treatment. Numerous mechanisms are possible, although the underlying ones are probably cardio- and cytoprotective properties.

REFERENCES

1. Ross R. Atherosclerosis - an inflammatory disease. N Engl J Med 1999; 340:115-26.
2. Libby P. Current concepts of the pathogenesis of the acute coronary syndromes. Circulation 2001; 104:365-72
3. Libby P, Ridker PM. Inflammation and atherosclerosis: role of C-reactive protein in risk assessment. Am J Med 2004; 116(S):9S-16S.
4. Ridker PM, Buring JE, Cook NR, Rifai N. C-reactive protein, the metabolic syndrome, and risk of incident cardiovascular events: an 8-year follow-up of 14 719 initially healthy American women. Circulation 2003; 107:391-97
5. Orford JL, Selwyn AP, Ganz P, Popma JJ, Rogers C. The comparative pathobiology of atherosclerosis and restenosis. Am J Cardiol 2000; 86:6H-11H.
6. Ruixing Y, Wenwu L, Al-Ghazali R. Trimetazidine inhibits cardiomyocyte apoptosis in a rabbit model of ischemia-reperfusion. Transl Res 2007; 149:152-60.
7. Di Napoli P, Chierchia S, Taccardi AA, Grilli A, Felaco M, De Caterina R, Barsotti A. Trimetazidine improves post-ischemic recovery by preserving endothelial nitric oxide synthase expression in isolated working rat hearts. Nitric Oxide 2007; 16:228-36.
8. Asano S, Okano A, Ozawa K, et al. In vivo effects of recombinant human interleukin-6 in primates: stimulated production of platelets. Blood 1990; 75:1602-5
9. Avanzas P, Arroyo-Espliguero R, Cosin-Sales J, Quiles J, Zouridakis E, Kaski JC. Multiple complex stenoses, high neutrophil count and C-reactive protein levels in patients with chronic stable angina. Atherosclerosis 2004; 175:151-57.
10. Arroyo-Espliguero R, Avanzas P, Cosin-Sales J, Aldama G, Pizzi C, Kaski JC. C-reactive protein elevation and disease activity in patients with coronary artery disease. Eur Heart J 2004; 25: 401-8.
11. Kralisz P, Kemona H, Dobrzycki S, Bachorzewska-Gajewska H, Nowak K, Sawicki Z. Changes in C-reactive protein levels following coronary stent implantation depend on the extent of periprocedural arterial injury. Kardiol Pol 2006; 64:364-71
12. Williams FM, Tanda K, Kus M, Williams TJ. Trimetazidine inhibits neutrophil accumulation after myocardial ischaemia and reperfusion in rabbits. J Cardiovasc Pharmacol 1993; 22: 828-33
13. Kiyosue T, Nakamura S, Arita M. Effects of trimetazidine on action potentials and membrane currents of guinea-pig ventricular myocytes. J Mol Cell Cardiol 1986; 18:1301-11.
14. Zhang L, Lu Y, Jiang H, Sun A, Zou Y, Ge J. Additional use of trimetazidine in patients with chronic heart failure: a meta-analysis. J Am Coll Cardiol 2012; 59:913-22.
15. Detry JM, Leclercq PJ. Trimetazidine European Multicenter Study versus propranolol in stable angina

pectoris: contribution of Holter electrocardiographic ambulatory monitoring. Am J Cardiol 1995; 76:8B-11B
16. Levy S. Combination therapy of trimetazidine with diltiazem in patients with coronary artery disease. Group of South of France Investigators. Am J Cardiol 1995; 76:12B-16B
17. Garrido-Urbani S, Meguenani M, Montecucco F, Imhof BA. Immunological aspects of atherosclerosis. Semin Immunopathol 2014; 36:73-91.
18. Rus HG, Vlaicu R, Niculescu F. Interleukin-6 and interleukin-8 protein and gene expression in human arterial atherosclerotic wall. Atherosclerosis 1996; 127:263-71.
19. Mazurov VI, Veber VV, Stolov SV, Zaraiskii MI. Immunological interactions in different forms of coronary heart disease. Vestn Ross Akad Med Nauk 2005; 7:9-14
20. Osterud B, Bjorklid E. Role of monocytes in atherogenesis. Physiol Rev 2003; 83:1069-112.
21. Lee WH, Lee Y, Kim JR, et al. Activation of monocytes, T-lymphocytes and plasma inflammatory markers in angina patients. Exp Mol Med 1999; 31:159-64
22. Van Lenten BJ, Hama SY, de Beer FC, et al. Anti-inflammatory HDL becomes pro-inflammatory during the acute phase response. Loss of protective effect of HDL against LDL oxidation in aortic wall cell cocultures. J Clin Invest 1995; 96:2758-67.
23. Bossowska A, Kiersnowska-Rogowska B, Bossowski A, Galar B, Sowinski P. Cytokines in patients with ischaemic heart disease or myocardial infarction. Kardiol Pol 2003; 59:105-14
24. Lubrano V, Cocci F, Battaglia D, Papa A, Marraccini P, Zucchelli GC. Usefulness of high-sensitivity IL-6 measurement for clinical characterization of patients with coronary artery disease. J Clin Lab Anal 2005; 19:110-14.
25. Rajappa M, Sen SK, Sharma A. Role of pro-/anti-inflammatory cytokines and their correlation with established risk factors in South Indians with coronary artery disease. Angiology 2009; 60:419-26.
26. Formato M, Farina M, Spirito R, et al. Evidence for a proinflammatory and proteolytic environment in plaques from endarterectomy segments of human carotid arteries. Arterioscler Thromb Vasc Biol 2004; 24:129-35.
27. Banasiak W, Wilkins A, Pociupany R, Ponikowski P. Pharmacotherapy in patients with stable coronary artery disease treated on an outpatient basis in Poland. Results of the multicentre RECENT study. Kardiol Pol 2008; 66:642-49;
28. Pudil R, Pidrman V, Krejsek J, Gregor J, Tichy M, Andrys C, Drahosova M, Blaha V. The effect of trimetazidine on C-reactive protein, cytokines and adhesion molecules in the course of acute myocardial infarction. Acta Medica (Hradec Kralove) 2001; 44:135-40
29. Yenicerioglu A, Cetinkaya Z, Girgin M, Ustundag B, Ozercan IH, Ayten R, Kanat BH. Effects of trimetazidine in acute pancreatitis induced by L-arginine. Can J Surg 2013; 56:175-79.

METHYL MERCAPTAN AND HYDROGEN SULFIDE PRODUCTS STIMULATE PROINFLAMMATORY CYTOKINES IN PATIENTS WITH NECROTIC PULP TISSUE AND ENDODONTICALLY TREATED TEETH

E. JACOBI-GRESSER[1], S. SCHÜTT[2], K. HUESKER[2] and V. VON BAEHR[2]

[1]Private Practice of Oral Surgery and Implantology, Mainz, Germany; [2]Department of Immunology, Laboratory Center Berlin, Berlin, Germany

Received September 29, 2014 – Accepted January 8, 2015

Bacterial infections of the residual dentin or infected pulp tissue are responsible for most cases of endodontic treatment failures. Persisting microorganisms in necrotic pulp tissue produce sulphur components such as methyl mercaptan and hydrogen sulfide as well as thioether derivatives. Although there is emerging evidence that these sulphur compounds stimulate immune cells and induce the inflammatory cascade, the immunological mechanisms of local and systemic inflammation have not been described. In this retrospective study we evaluated the *ex-vivo* immune response of peripheral blood mononuclear cells to sulphur compounds in 53 patients with clinical or radiologic endodontic treatment failure, 20 patients with clinical discomfort or radiological findings without previous endodontic treatment and a control group of 31 patients who had received successful endodontic treatment at least five years previously. Patients with endodontic abnormalities showed significantly higher *ex-vivo* sulphur compound-stimulated interferon-gamma (IFN-γ) and interleukin-10 (IL-10) levels as compared to the control group. The association between *ex-vivo*-stimulated cytokines and endodontically derived sulphur compounds was further substantiated by the fact that the number of IFN-γ and/or IL-10-positive patients decreased significantly 3-8 months after re-treatment of the root canal or tooth extraction. Furthermore, serum tumor necrosis factor-alpha (TNF-α) levels were higher in patients than in controls, and at the same time, the TNFA -308 G/A polymorphism was associated with endodontic treatment failure in our study population. We conclude that a cellular immune response to sulphur compounds contributes to the inflammatory process observed in relation to endodontic treatment failures.

According to recent studies, state-of-the-art endodontic treatments are successful in up to 90% of cases. In cases of recurrent inflammation revisions by endodontic specialists can achieve success rates of about 80%, which is significantly better than the success rates of dentists without respective specialization (1). Despite these achievements, even today 12% of patients suffer from persisting low-to-moderate grade adverse effects post-endodontic surgery, despite adherence to the approved protocol (2). The re-treatment success rate for primarily unfound and untreated canals is approximately 80% (3, 4). A recently published meta-analysis comparing the literature published between 1922 and 2002

Key words: pulp inflammation, methyl mercaptan, hydrogen sulfide, thioether, interferon-γ, interleukin-10, tumor-necrosis-factor-α

Mailing address: Volker von Baehr, M.D.
Department of Immunology,
Laboratory Center Berlin,
Nicolaistr. 22,
12247 Berlin, Germany
Tel.: +49 30 77001220 Fax: +49 30 77001236
e-mail: v.baehr@imd-berlin.de

0393-974X (2015)

DISCLOSURE: ALL AUTHORS REPORT NO CONFLICTS OF INTEREST RELEVANT TO THIS ARTICLE.

yielded an average success rate of 75% for re-treated root canals with apical periodontitis (5). According to the statements of the German Society of Dental, Oral and Craniomandibular Sciences (DGZMK) and the German Society for Conservative Medicine (DGZ), the available data, however sparse, support a full recovery rate of 90% within 3 to 4 years. At the same time, the frequency of post-endodontic apical periodontitis may have been underestimated due to inadequate radiological imaging (6).

It is generally accepted that persisting bacterial infections in dentin or pulp tissue account for most cases of treatment failure (7). Complete elimination of bacterial infections is limited by currently available techniques, and persisting microorganisms located in necrotic pulp tissue produce a wide range of metabolites. Sulphur compounds, including methyl mercaptan and hydrogen sulfide as well as thioether derivatives, such as dimethyl sulfide and diethyl sulfide, are metabolic products mainly generated by anaerobic bacteria through desulfuration of cysteine-rich glutathione, L-methionine and L-methionyl-containing peptides. The main producers of hydrogen sulfide products are *Porphyromonas gingivalis*, *Prevotella intermedia*, *Fusobacterium nucleatum*, *Treponema denticola* and *Veillonella alcalescens*. Methyl mercaptan is predominantly produced by *Porphyromonas gingivalis*, *Porphyromonas intermedia* and *Fusobacterium nucleatum* (8).

Sulfate-reducing bacteria are etiologically involved in destructive periodontal diseases and promote disease progression (9). Sulfide compounds are detectable in gingival fluid of periodontal pockets (8). It has been described that these sulphur compounds can exert toxic effects with the central nervous system as primary target. Hydrogen sulfide can severely alter the neural architecture and growth characteristics, as shown for Purkinje cells (10). In the oral cavity hydrogen sulfide damages epithelial cells and increases mucosal permeability (11). Methyl mercaptan decreases collagen synthesis by human fibroblasts inhibiting cell migration to periodontal ligament cells, potentially contributing to the pathogenesis of periodontal disease (12).

Sulphur compounds can also exert activating or modulating effects on immune cells, contributing to inflammatory tissue degradation. Methyl mercaptan has been shown to promote the production of interleukin 1 (IL-1) by human mononuclear cells. Similarly, the production of interleukin 6 (IL-6) stimulated by lipopolysaccharides (LPS) is increased in the presence of methyl mercaptan (13). Furthermore, methyl mercaptan alone or in combination with IL-1 or LPS, can significantly enhance the secretion of PGE2 and cAMP, which are required for the synthesis of matrix metalloproteinases and other procollagenases in human gingival fibroblasts and polymorphonuclear leucocytes (14). These effects may promote production of collagenase and subsequent tissue destruction in human periodontal disease. Methyl mercaptan also enhances the activity of aspartate protease cathepsin B in gingival infiltrated leucocytes, increasing the rate of collagen degradation (14).

The majority of data on sulphur compounds in tissue degradation have been derived from studies on periodontal diseases. Conversely, a putative role of methyl mercaptan and thioethers in necrotic pulp tissue and chronic pulpitis has not been substantiated, even if several studies have shown that anaerobic bacteria in the root canal are the predominant cause for endodontic treatment failures. Lin and coll. demonstrated the presence of stainable bacteria in root canals in 69% of patients suffering from endodontic treatment failures. Furthermore, the severity of periradicular inflammation correlates to presence of bacteria in the root canal (15). Non-vital teeth are less resistant to bacterial invasion into dentinal tubules than vital teeth (16). Anaerobes most frequently isolated from primarily and secondarily infected root canals are sulfate-reducing bacteria similar to those found in periodontal disease, including *Porphyromonas gingivalis* and *Fusobacterium nucleatum*, the main producers of methyl mercaptan, dimethylsulfide und diethylsulfide (17). Notwithstanding this evidence, apical periodontitis can reportedly affect even radiologically impeccable endodontic treatments without correlation to any residual microbiological load. This observation suggests a contribution of host factors, such as a generally increased inflammatory predisposition or individual differences in the immune response to vital bacteria, persisting bacterial antigens or sulphur compounds.

The aims of this retrospective study were firstly to investigate the relation of the *ex-vivo*

immune response to sulphur compounds to clinical and radiologic findings, and secondly to identify predisposing factors for endodontic treatment failure. Data were obtained from a group of patients with clinical or radiologic endodontic treatment failure and from a control group of individuals who had received successful endodontic treatment more than five years previously, as defined by sufficiently filled canals and the absence of radiologic abnormalities or clinical symptoms.

MATERIALS AND METHODS

Study population

One hundred and four patients presenting only one single- or multi-rooted avital tooth in the upper or lower jaw were examined in a dental practice with endodontic specialization between March 2010 and October 2012. Patients with periodontitis or several affected teeth were excluded. All patients received dental treatments and laboratory diagnostics in the course of routine medical care. For retrospective evaluation of the data, patients were grouped into a patient group (n=73) and a control group (n=31) based on presence or absence of clinical symptoms and radiological findings, respectively. 20 out of 73 patients showed clinical discomfort or radiological findings without previous endodontic treatment measures. Fifty-three out of 73 patients had undergone previous endodontic treatment that proved to be insufficient by radiological imaging (inhomogeneous filling, fully or partially unfilled root canals) or had developed apical periodontitis. Scoring of clinical symptoms was based on the sensitivity to percussion or occlusal load, local pain or signs of periodontal inflammation such as mucosal redness and swelling. Anamnestic data were collected at the first consultation for pain sensation or at the time of endodontic treatment. Available imaging data (dental x-ray, panoramic x-ray, 3D –cone beam) were taken into consideration.

The control group of 31 symptom-free patients had undergone successful endodontic treatment of one tooth at least 5 years previously (>5 - 24 years). By means of radiological imaging the treated teeth showed sufficiently filled root canals and an intact periodontal space.

According to the Declaration of Helsinki, all patients gave written informed consent for the scientific evaluation of their data. The local IRB waived the demand of an approval as all diagnostic tests and treatment protocols were part of routine care.

Dental treatment and laboratory diagnostics

Out of 73 patients, 45 and 28 patients underwent re-treatment of the existing root canal filling and tooth extraction, respectively. Tooth extraction was performed in the presence of severe endodontic and/or periodontal lesions, inadequate removal of filling material and unfeasible tooth restoration.

Routine laboratory diagnostics were conducted for the entire study population and comprised genotyping of IL1A, IL1B, IL1RN and TNFA genes, ex-vivo lymphocyte stimulation assays in the presence of sulphur compounds and the determination of TNF-α, IP-10 and MBL levels in serum. Except for genotyping, all diagnostic tests were performed when the patient presented to the dentist for the first time and 3-8 months after initial treatment when follow-up samples were taken.

Revision

Upon generation of an access cavity using rubber dam and microscopic imaging (Kaps Typ SOM 32, Asslar), probing and preparation of the coronal third of the canal was performed, as well as probing of the glide path and preparation of canals up to the apical constriction to minimum ISO 30. Endometrical length measurement was controlled using an electronical apexfinder (ROOT-ZX, J. Morita Corporation, Tokyo, Japan The rinse protocol comprised of 5% sodium hypochlorite, EDTA-solution and Chlorhexidin. Irrigation was performed using ultrasonic procedure (30 THz). Shaping and cleaning of the root canal were finalized by applying Ca(OH)2 and a bacteria tight seal using cement or composite. After 1-2 weeks, obturation was carried out by vertical condensation of gutta-percha cones (Roeko-Coltene/ Whaledent, Switzerland) sealed with AH plus (Dentsply DeTrey, Konstanz, Germany). In case of immunological sensitizations, standard materials were replaced by individually tolerated alternative materials such as Epiphany (Pentron Clinical Technologies, Wallingford USA) and MTA (Dentsply DeTrey, Konstanz, Germany). A bacteria tight composite filling was applied to prevent microbial recontamination. Treatment outcome was controlled by dental X-ray or 3D-cone beam.

Extraction

All tooth extractions were performed under local anesthesia. To minimize the risk of contamination, alveoles were gently reamed out by a surgical ball cutter and irrigation was performed by sterile sodium chloride-solution to facilitate uncontaminated bone regeneration. Extraction sites were never stabilized by augmentation.

Genotyping

For genetic analyses, genomic DNA was extracted from 2 ml EDTA-whole blood using the QIAamp DNA Mini Kit (Qiagen, Hilden, Germany). Genotyping of

polymorphisms rs1800587 (IL1A), rs1143634 (IL1B) and rs419598 (IL1RN) was performed by multiplex PCR and subsequent reverse hybridization, according to the manufacturer's protocol (GenoType IL-1; VER 1.0, HAIN Lifescience, Nehren, Germany). Genotyping of rs1800629 (TNFA) was carried out by real-time PCR and melting curve analysis using a Light Cycler 1.5 (Roche Diagnostics, Mannheim, Germany) as published elsewhere (18).

Cytokine analyses

Serum samples were obtained by centrifugation of coagulated whole blood and stored at -80°C for further analysis. Cytokine concentrations were determined by commercially available enzyme-linked immunosorbent assays (ELISA), including TNF-α Immulite (DPC Biermann, Bad Nauheim, Germany), IP-10 (MERCK/ Millipore, Darmstadt, Germany) and MBL (AntibodyShop, Gentofte, Denmark). Analyses were performed according to the manufacturer's instructions. The MBL assay detects functional MBL oligomers, excluding the measurement of inactive MBL monomers.

Sulphur compound ex-vivo stimulation assay

Peripheral blood mononuclear cells (PBMC) were isolated from 10 ml venous heparinized whole blood by Ficoll-Paque (Pharmacia, Uppsala, Sweden) density gradient centrifugation. PBMC were resuspended in RPMI 1640 (Biochrom KH, Berlin, Germany), supplemented with 2 mM L-glutamine (Sigma) and 10% heat-inactivated autologous serum. PBMC at the concentration of 1 x 10^6 / ml were seeded in flat-bottom 24-well microtiter plates (Nunclon, Wiesbaden, Germany) and stimulated with 500 ng/ml methanethiol (CH3SH, methyl mercaptan, Sigma, Germany) and dimethyl sulphide each (CH3SCH3, Dimethylthioether, Sigma, Germany). For comparison to baseline cytokine levels, PBMCs cultured in the absence of sulphur compounds served as control. Cells were cultured in a humidified incubator with 5% CO2 at 37°C for 24 hours. After collection of cell supernatants by centrifugation, secreted IFN-γ and IL-10 were determined using Human Cytokine Panel I (MPXHCYTO-60K; Merck, Darmstadt, Germany), according to the manufacturer's instructions. The Luminex® 200™ with xPonent® Software (Luminex, Austin, USA) was used for detection. Final IFN-γ and IL-10 values were obtained by subtracting unstimulated control values from sulphur compound stimulated values. In addition, Trypan blue staining was performed to confirm that applied doses of sulphur compounds were not cytotoxic after 24-h stimulation.

Statistics

The *Chi*-squared test was used to compare anamnestic and clinical parameters, as well as genotype frequencies between patient and control groups. Patients' ages, *ex-vivo* stimulation test results and cytokine levels were analyzed by Mann Whitney U-Test. Comparison of positive or negative scores of the *ex vivo* stimulation test was done by *Chi*- squared test. A positive score was defined as IFN-γ > 0.3 IU/ml or IL-10 >10 pg/ml (upon subtraction of basal values). P-values <0.05 were considered as statistically significant. Outcomes of primary and follow-up testings were compared by Mc-Nemar test. Statistical analyses were performed using IBM SSP Statistics, version 19.

RESULTS

Endodontic abnormalities were associated with IFN-γ and IL-10 stimulation by sulphur compounds

In order to assess potential differences in the immune responses to sulphur compounds in patient and control groups, the production of cytokines in isolated PBMC was analyzed after 24 h stimulation with and without sulphur compounds. Whereas IFN-γ served as marker for TH1 based immune responses, IL-10 was used to detect TH2 responses. PBMCs in the patient group produced significantly higher levels of IFN-γ and IL-10 after stimulation with sulphur compounds as compared to control group (IFN-γ 1.53 IU/ml *vs* 0.1 IU/ml, p<0.0001; IL-10: 46.09 pg/ml *vs* 27.41 pg/ml; p<0.0001; Fig. 1). Detailed evaluation of the data revealed that out of 73 patients, 9 showed increased IFN-γ levels, 19 increased IL-10, and 11 both increased IFN-γ and IL-10 concentrations. In 34 patients neither increased IFN-γ nor IL-10 levels could be detected. In contrast to the patient group, increased IL-10 levels were only observed in 1 patient of the control group. In addition, IFN-γ levels were not altered in PBMCs isolated from the control group upon stimulation with sulphur compounds. Defining a positive result of the *ex-vivo* stimulation assay as IFN-γ > 0.3 IU/ml and or IL-10 < 10 pg/ml, 39/73 patients (53.4%) scored positive, as compared to 1/31 controls (3.2%). The difference proved to be statistically significant by Mann-Whitney U-test (p<0.001).

The outcome of ex-vivo sulphur compound stimulation test was independent on age and gender as well as smoking and medical preconditions of patients

We tested potential confounders of the correlation

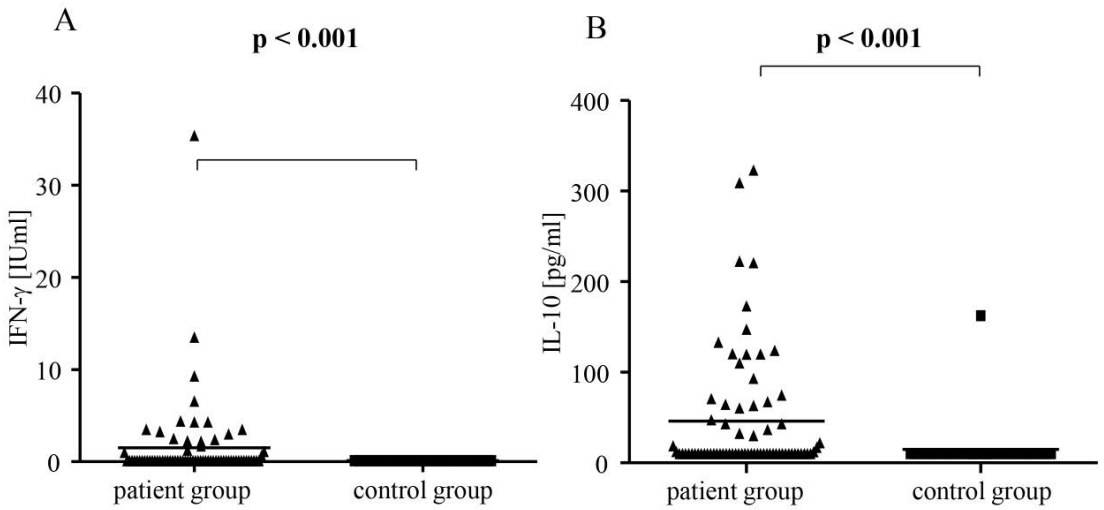

Fig. 1. *Levels of ex-vivo-stimulated IFN-γ (**A**) and IL-10 (**B**) in patients (n=73) and controls (n=31). Values were obtained by subtraction of baseline cytokine levels from stimulated cytokine levels. Patients display significantly higher values for both cytokines (Mann-Whitney U-Test).*

Table I. *Evaluation of potential confounders.*

	patient group (n = 73)		**control group (n = 31)**		**p-value**
Average age (years)	50.6		53.0		0.221
Range (years)	22-76		33-73		
Gender (F/M)	57/16		25/6		1.000
	n	**%**	**n**	**%**	
Smokers	13	17.8	3	9.7	0.382
General medical conditions					
hypertension	16	21.9	7	22.6	1.000
Sensitizations	38	52.8	12	38.7	0.205
Allergic rhinitis	16	21.9	9	29.0	0.459
autoimmune diseases	14	19.7	4	12.9	0.574
cancer history	8	11.3	2	6.5	0.719
Daily oral hygiene					
good	72	98.6	31	100	1.000
poor	1	1.4	0	0	
Bruxism					
yes	25	34.2	9	29.0	0.654
no	48	65.8	22	71.0	
Alcohol					
yes	5	6.8	2	6.5	1.000
no	68	93.2	29	93.5	

Age, gender, smoking habits and medical preconditions of patients (n=73) and controls (n=31). Statistics were evaluated by Mann Whitney U-Test with exception of patients' ages (Chi-squared test).

Table II. *TNFA -308 G/A is associated with endodontic treatment failure.*

Genotype	patient group n=73 n (%)	control group n=31 n (%)	p-value
IL1A -889 C/T			
CC	42 (57.5)	19 (61.3)	
CT or TT	31 (42.5)	12 (38.7)	0.829
IL1B +3953 CT			
CC	45 (61.6)	20 (64.5)	
CT or TT	28 (38.4)	11 (35.5)	0.828
IL1RA +2018 T/C			
TT	37 (50.7)	19 (61.3)	
CT or CC	36 (49.3)	12 (38.7)	0.392
TNFA -308 G/A			
GG	41 (56.2)	26 (83.9)	
GA or AA	32 (43.8)	5 (16.1)	**0.007**

Allele frequencies of IL1A rs1800587 (-889 C/T), IL1B rs1143634 (+3954 C/T), IL1RN rs419598 (+2018 T/C) and TNFA rs1800629 (-308 G/A). Only TNFA rs1800629 (-308 G/A) shows a significant association (Chi-squared test, p=0.007).

between endodontic treatment failure and positive sulphur compound stimulation test outcome. Logistic regression analysis showed however, that the association was independent on age, gender and smoking habits (Table I). Similarly, there was no significant correlation with medical conditions such as hypertension, pollen and other allergies, autoimmune disease and cancer, as well as the status of personal oral care, bruxism and alcohol consumption (Table I).

TNFA -308 G/A polymorphism predisposes for endodontic treatment failure

IL-1, interleukin 1 receptor antagonist (IL-1RN) and tumour necrosis factor alpha (TNF-α) represent key cytokines of the innate immune responses. In order to analyze the potential contribution of functional polymorphisms in these cytokine genes to the outcome of endodontic treatment, the polymorphisms IL1A rs1800587 (-889 C/T), IL1B rs1143634 (+3954 C/T), IL1RN rs419598 (+2018 T/C) and TNFA rs1800629 (-308 G/A) were genotyped in patients and controls (Table II).

For interpretation of data, the presence of at least one minor allele was defined as the "risk genotype" for the respective polymorphism. The comparison of TNFA genotypes in the different groups revealed a significant increase in the prevalence of the TNFA risk genotype among patients as compared to controls (43.8% *vs* 16.1%, p= 0.007). Conversely, IL1A -889 C/T- , IL1B +2953 C/T and IL1RA +2018 T/C risk genotypes showed no significant differences between either group (Table II).

Endodontic treatment failure was associated with increased TNF-α levels

In order to examine levels of systemic inflammation, we measured TNF-α concentrations in serum samples obtained from the patient and control groups. The patient group displayed increased TNF-α concentrations in serum as compared to the control group (14.51pg/ml *vs* 11.90pg/ml, $p < 0.05$, Fig. 2). Mannose binding lectin (MBL) involved in mucosal immune defence and Interferon-inducible protein-10 (IP-10), a chemokine promoting the

Table III. *Stimulation test outcome before and after treatment, extraction group.*

	time point 1			time point 2		
patient ID	IFN-γ	IL-10	result	IFN-γ	IL-10	result
61	35.4	74.7	**positive**	<0.1	<10	negative
45	9.3	<10	**positive**	<0.1	54	**positive**
53	4.4	<10	**positive**	<0.1	<10	negative
69	4.3	124.2	**positive**	<0.1	<10	negative
46	3.5	22.3	**positive**	<0.1	<10	negative
52	3	<10	**positive**	<0.1	<10	negative
65	2.2	12.4	**positive**	<0.1	<10	negative
48	1	<10	**positive**	<0.1	<10	negative
43	<0.1	<10	negative	<0.1	<10	negative
44	<0.1	<10	negative	<0.1	<10	negative
47	<0.1	173.3	**positive**	<0.1	<10	negative
49	<0.1	<10	negative	<0.1	<10	negative
50	<0.1	309	**positive**	<0.1	<10	negative
51	<0.1	18.8	**positive**	<0.1	<10	negative
54	<0.1	120.5	**positive**	<0.1	<10	negative
55	<0.1	<10	negative	<0.1	<10	negative
56	<0.1	43	**positive**	<0.1	<10	negative
57	<0.1	<10	negative	<0.1	99	**positive**
58	<0.1	32.6	**positive**	<0.1	<10	negative
59	<0.1	<10	negative	<0.1	<10	negative
60	<0.1	<10	negative	<0.1	<10	negative
62	<0.1	120.3	**positive**	<0.1	<10	negative
63	<0.1	<10	negative	<0.1	<10	negative
64	<0.1	<10	negative	<0.1	<10	negative
66	<0.1	<10	negative	<0.1	<10	negative
67	<0.1	60.6	**positive**	<0.1	240	**positive**
68	<0.1	<10	negative	<0.1	26.6	**positive**

migration of activated T cells, did not show any statistically significant difference between patients and controls, albeit a tendency to higher IP-10 values in patients (MBL: 1438pg/ml *vs* 1541pg/ml; IP-10: 733.3pg/ml *vs* 661.7pg/ml; Mann-Whitney U-Test).

Stimulation test results normalize upon revision or extraction

We hypothesized that removal of the source of sulphur compounds may reduce cytokine production in the sulphur compound *ex-vivo* stimulation test. Therefore, we repeated the test 3-8 months after tooth extraction or re-treatment of the root canal at two time points. Sixty-nine of the initial 73 patients were available for follow-up testing (extraction group: 27/69 patients; re-treatment group: 42/69 patients). Patients who showed a negative outcome (IFN-γ < 0.3 IU/ml and IL-10 < 10 pg/ml) at either time point were scored as negative. As shown in Tables III and IV, both re-treatment and extraction are followed by a significantly reduced frequency of positive stimulation test outcomes.

In the extraction group, 16/27 patients (59.3%) scored positive before treatment, while only 4/27 (14.8%) scored positive after extraction (p= 0.004; Table III). Detailed evaluation showed that out of 16 patients who had been positive before treatment, 14 turned negative upon extraction. Two patients remained positive, one of which (ID 45) normalized IFN-γ secretion from 9.3 to 0.1 pg/ml but remained IL-10 positive. The other persistently positive patient (ID 67) remained IFN-γ negative but increased IL-10

Table IV. *Stimulation test outcome before and after treatment, revision group.*

	time point 1			time point 2		
patient ID	IFN-γ	IL-10	result	IFN-γ	IL-10	result
1	13.5	<10	**positive**	<0.1	<10	negative
15	6.6	43	**positive**	3.4	<10	**positive**
16	4.3	323	**positive**	<0.1	<10	negative
22	3.5	222.4	**positive**	<0.1	<10	negative
12	3.3	110	**positive**	<0.1	<10	negative
8	2.5	<10	**positive**	<0.1	<10	negative
5	2.4	<10	**positive**	<0.1	<10	negative
21	2.3	<10	**positive**	<0.1	<10	negative
7	1.7	36.7	**positive**	<0.1	<10	negative
3	1.1	<10	**positive**	<0.1	10.1	**positive**
9	0.7	147.4	**positive**	<0.1	87.3	**positive**
2	<0.1	17.2	**positive**	<0.1	<10	negative
4	<0.1	93.2	**positive**	<0.1	<10	negative
6	<0.1	<10	negative	<0.1	<10	negative
10	<0.1	63.3	**positive**	<0.1	<10	negative
11	<0.1	<10	negative	<0.1	<10	negative
13	<0.1	<10	negative	<0.1	14.4	**positive**
14	<0.1	<10	negative	<0.1	<10	negative
17	<0.1	<10	negative	<0.1	<10	negative
18	<0.1	47.4	**positive**	<0.1	<10	negative
19	<0.1	64.6	**positive**	<0.1	<10	negative
20	<0.1	<10	negative	<0.1	<10	negative
23	<0.1	<10	negative	<0.1	<10	negative
24	<0.1	<10	negative	<0.1	14.1	**positive**
25	<0.1	220.8	**positive**	<0.1	<10	negative
26	<0.1	<10	negative	12.3	<10	**positive**
27	<0.1	<10	negative	<0.1	<10	negative
28	<0.1	67.5	**positive**	<0.1	<10	negative
29	<0.1	30.1	**positive**	1	<10	**positive**
30	<0.1	<10	negative	<0.1	<10	negative
31	<0.1	<10	negative	<0.1	<10	negative
32	<0.1	<10	negative	<0.1	<10	negative
33	<0.1	<10	negative	<0.1	<10	negative
34	<0.1	<10	negative	<0.1	14.4	**positive**
35	<0.1	<10	negative	<0.1	<10	negative
36	<0.1	<10	negative	<0.1	11.5	**positive**
37	<0.1	12.3	**positive**	<0.1	<10	negative
38	<0.1	<10	negative	<0.1	<10	negative
39	<0.1	<10	negative	<0.1	<10	negative
40	<0.1	<10	negative	<0.1	<10	negative
41	<0.1	119.9	**positive**	<0.1	<10	negative
42	<0.1	70.9	**positive**	3.7	36.5	**positive**

secretion. Two patients scored negative in the initial testing but turned IL-10 positive during follow-up (ID 57 and ID 68). No IFN-γ negative patient turned IFN-γ positive.

In the revision group, 22/42 patients (52.4%) were positive for at least one cytokine in the sulphur compound stimulation test before treatment, while 10/42 scored positive during follow-up after re-

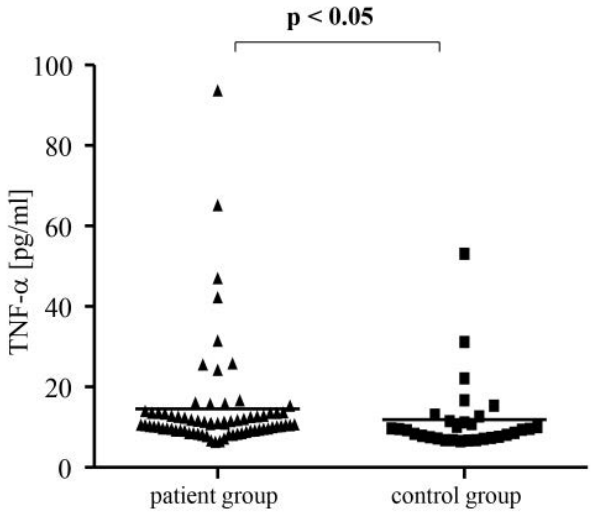

Fig. 2. *Distribution of TNF-α serum levels in patients and controls. Each symbol represents an individual. The horizontal lines represent the mean TNF-α serum value of the group. Mann-Whitney U-Test shows a significant group difference (p < 0.05).*

treatment (23.8%, p=0.023; Table IV). Detailed evaluation shows that 17 of the initially 22 positive patients had turned negative. Five patients maintained positive test results (IDs 3, 9, 15, 29, 42) and five initially negative patients turned positive during follow-up (IDs 13, 24, 26, 34, 36). Of these five however, four showed only marginal elevation of IL-10 (up to 14.4 pg/ml). Only one initially negative case showed strong cytokine induction (ID 26: IFN-γ 12.3 IU/ml, IL-10 negative).

Stimulation test results remain unchanged in controls

To test both the biological variability and the inter-assay reproducibility we repeated the sulphur compound stimulation test also for 28 of the initial 31 controls, who had not received any endodontic treatment in the meantime. Testing was performed in the same time window as for the patient group. Twenty-five out of 28 patients did not score positive at any time point, indicating high inter assay stability. The only initially positive patient scored negative six months later. However, two initially negative patients showed marginally increased IL-10 secretion at the follow-up time point (13.1 pg/ml and 27.7 pg/ml).

DISCUSSION

The present study demonstrates that immunological sensitization to methyl mercaptan and thioethers is associated with endodontic treatment failure. *Ex-vivo* stimulation of patient lymphocytes with sulphur compounds showed significantly increased cytokine release for patients with clinical complaints or radiological abnormalities. The fact that analyses were performed with systemically circulating mononuclear blood cells argues for a type IV immune sensitization to sulphur compounds. As T-lymphocytes produce both IFN-γ and IL-10, they likely account for the observed increase in cytokine levels. Still, other cellular components of PBMCs represent potential sources, such as natural killer cells, which have been shown to secrete IFN-γ (19) as well as blood monocytes and B-lymphocytes, which reportedly both release IL-10 (20). However, these cells lack antigen specific recognition sites and are therefore activated only by unspecific activation signals. Unspecific activation by methyl mercaptan and/or dimethyl sulfide is in fact highly unlikely due to the consistently negative cytokine scores in the control group.

The observation that sulphur compounds can stimulate immune cells to produce proinflammatory cytokines is well documented in the literature. Methyl mercaptan has been shown to induce the production of IL-1 by human mononuclear cells (14) and LPS-stimulated IL-6 production is augmented when methyl mercaptan is present (13). Furthermore, methyl mercaptan alone or in combination with IL-1 or lipopolysaccharide can significantly enhance the secretion of PGE2 and cAMP, which are required for induction of local inflammatory processes (14). Proinflammatory cytokines like IL-1, interleukin-8 (21), TNF-α (22) or even the T-cell mediator interleukin-2 (23) are increased in inflamed pulp tissue specimens of patients with irreversible pulpitis. Even if none of our patients suffered from irreversible pulpitis but had clinical signs of an avital tooth, it is tempting to speculate that the proinflammatory pathomechanism may be comparable.

A putative causal link between immunological sensitization to methyl mercaptan and apical inflammation is supported by the observation that elimination of methyl mercaptan/thioether exposition by re-treatment of the root canal or tooth extraction leads to a significant reduction of sulphur compound-induced cytokine production. It is well known that removal of a stimulating antigen reduces the number of the respective antigen specific precursor T cells in the blood. The fact that both in the re-treated and in the extraction group a minority of primarily negative patients turned IL-10 positive during follow-up may be explained by regulatory mechanisms. These patients are exposed to sulphur compounds and may develop immune tolerance based on the action of regulatory T-lymphocytes. In *ex-vivo* stimulation set-ups IL-10 is considered a marker for regulatory T-cells and IFN-γ indicates the TH1 mediated effector cell response that is associated with local and/or systemic inflammation. As we focused the study on sensitization to sulphur compounds, we limited our analysis to these cytokines. Subsequent endodontic surgery may reactivate a latent tolerance reaction against sulphur compounds. It is important to note that this study was not designed to examine the influence of re-treatment *vs* extraction on the long-term success rate based on sulphur compounds associated immune phenomena.

While IL-10 upregulation typically occurs along with INF-γ production in T-cell mediated immune activation, the fact that three control individuals without signs of clinical findings scored IL-10 positive is in line with published data showing that isolated IL-10 does occur in absence of manifest inflammation or allergic response. This has been reported for allergens, especially for drug sensitized patients (24). Whether positive IL-10 scores designate the beginning of immune processes or, alternatively, demarcate stable immune tolerance cannot be determined on the basis of the present data but will require extended studies with strengthened clinical focus. Accordingly, further studies will be required to elucidate the clinical significance of isolated IL-10 positive scores.

Conversely, the re-treatment group patient who showed strong upregulation of IFN-γ during follow-up testing reflects a different situation. A likely explanation is that in this case revision may have triggered the release of sulphur compounds from the canal. Alternatively, these patients may have developed another independent endodontic lesion in the meantime.

The present data show that an immunological laboratory test may serve as a diagnostic tool for patients with chronic necrotic dental pulp tissue conditions. Follow-up testing may yield objective criteria for the success of endodontic treatment. As expected from its well-described proinflammatory action, positive IFN-γ confers a higher predictive value. Still, the predictive significance of positive IL-10 is underscored by its higher frequency in the patient group and by the fact that root canal re-treatment and extraction lead to IL-10 reduction in most cases. The data reveal that the novel laboratory tests presented here may provide additional criteria for the prognosis of endodontic treatment, supporting clinical judgement and well-established imaging techniques.

In addition to our data implicating the TNFA -308 G/A polymorphism as a predisposing factor for failure of endodontic treatment or apical periodontitis, earlier studies have shown a contribution of this polymorphism to a wide range of chronic inflammatory disorders, such as diabetes mellitus (25), inflammatory bowel disease (26), atherosclerosis and stroke (27) as well as periodontitis (28) and periimplantitis (29). Other studies show a significant association of TNFA -308 G/A with local inflammatory processes, activating osteoclasts and synovial fibroblasts through induction of RANKL expression, which in turn increases bone resorption (30). At the same time, TNF-α increases periodontal tissue destruction by inducing matrix metalloproteinases (31). It seems likely that patients with increased inflammatory predisposition respond to sulphur compounds as potentially immunogenic stimuli with increased local inflammation. Importantly however, TNFA -308 G/A occurs also in the control group, albeit less frequently, making clear that this polymorphism does not represent the only relevant risk factor.

Increased serum TNF-α levels in our patient group further support the clinical significance of this cytokine. Intriguingly, TNFA -308 G/A is reportedly associated with increased TNF-α transcription (32). Considering the relatively small average differences

in serum levels between patients and controls however, serum TNF-α does not represent a valid marker to identify endodontic patients. Also serum MBL and IP-10 proved unsuitable for endodontic diagnostic discrimination, even though the latter showed a trend to higher levels in our patient group. It is important to note that normal serum IP-10 does not preclude systemic immune activation based on a local T-cell mediated immune process. IP-10 is significantly elevated in systemic infectious TH1-mediated diseases such as chronic active hepatitis or concurrent HIV/tuberculosis infection (33) but not in other inflammatory diseases, such as acute peptic ulcer (34), atopic dermatitis or Parkinson's disease (35). The fact that TH1 lymphocytes contribute to organ pathologies and systemic inflammation in these IP-10 negative diseases emphasizes that normal serum IP-10 does not exclude activation of TH1 lymphocytes. Diagnostic sensitivity of serum IP-10 is most likely not sufficient to reliably detect local inflammatory processes.

Taken together, this retrospective study shows that sulphur compound specific T cells are significantly increased in patients with clinical or radiologic signs of endodontic treatment failure. The data argue that endodontic re-treatment following a standardized protocol effectively normalizes immune parameters, presumably by reducing sulphur compounds in the root canal system. Our novel *ex-vivo* sulphur compound stimulation assay may therefore serve as a tool to complement established clinical and radiological diagnostic measures for monitoring endodontic treatment outcome. Furthermore, TNFA -308 G/A is associated with a higher risk for endodontic treatment failure, predisposing for local inflammatory processes.

This study points out systemic and prognostic immune parameters that are relevant for endodontic proinflammatory processes. Further studies will be necessary to confirm the reported association between sulphur compounds and systemic inflammatory processes and to verify the diagnostic value of our novel laboratory parameters.

REFERENCES

1. Weiger R, Geurtsen W, Heidemann D, Löst C, Petschelt A, Raab W, Schäfer E, Hicke R. Stellungnahme der DGZMK und der DGZ: Zur Prognose von Wurzelkanalbehandlungen. Dtsch Zahnärztl Z 2001; 56:206.
2. Polycarpou N, Ng YL, Canavan D, Moles DR, Gulabivala K. Prevalence of persistent pain after endodontic treatment and factors affecting its occurrence in cases with complete radiographic healing. Int Endod J 2005; 38:169-78.
3. Allen RK, Newton RW, Brown CE. A statistical analysis of surgical and non-surgical endodontic retreatment cases. J Endod 1989;15:261-66.
4. Gorni FG, Gagliani MM. The outcome of endodontic retreatment: a 2-yr follow up. J Endod 2004; 30:1-4.
5. Ng YL, Mann V, Rahbaran S, Lewsey J, Gulabivala K. Outcome of primary root canal treatment: systematic review of the literature - part 1. Effects of study characteristics on probability of success. Int Endod J 2007; 40:921-39.
6. Huumonen S, Kvist T, Gröndahl K, Molander A. Diagnostic value of computed tomography in re-treatment of root fillings in maxillary molars. Int Endod J 2006; 39:827-33.
7. Figdor D, Microbial aetiology of endodontic treatment failure & pathogenic properties of selected species. Dissertation Umea, Sweden: Umea University 2002.
8. Persson S, Edlund MB, Claesson R, Carlsson J. The formation of hydrogen sulfide and methyl mercaptan by oral bacteria. Oral Microbiol Immunol 1990; 5:195-201.
9. Langendijk PS, Hanssen JT, Van der Hoeven JS. Sulfate-reducing bacteria in association with human periodontitis. J Clin Periodontol 2000; 27:943-50.
10. Hannah RS, Roth SH. Chronic exposure to low concentrations of hydrogen sulfide produces abnormal growth in developing cerebellar Purkinje cells. Neurosci Lett 1991; 122:225-28.
11. Ng YL, Tonzetich J. Effect of hydrogen sulfide and methyl mercaptan on the permeability of oral mucosa. J Dent Res 1984; 63:994-7.
12. Johnson PW, Yaegaki K, Tonzetich J. Effect of methyl mercaptan on synthesis and degradation of collagen. J Periodontal Res 1996; 31:323-9.
13. Coil J, Tam E, Waterfield JD. Proinflammatory cytokine profiles in pulp fibroblasts stimulated with lipopolysaccharide and methyl mercaptan. J Endod

2004; 30:88-91.
14. Ratkay LG, Waterfield JD, Tonzetich J. Stimulation of enzyme and cytokine production by methyl mercaptan in human gingival fibroblast and monocyte cell cultures. Arch Oral Biol 1995; 40:337-44.
15. Lin LM, Pascon EA, Skribner J, Gängler P, Langeland K. Clinical, radiographic, and histologic study of endodontic treatment failures. Oral Surg Oral Med Oral Pathol Oral Radiol Endod 1991; 71:603-11.
16. Nagaoka S, Miyazaki Y, Liu HJ, Iwamoto Y, Kitano M, Kawagoe M. Bacterial invasion into dentinal tubules of human vital and nonvital teeth. J Endod 1995; 21:70-73.
17. Jung IY, Choi BK, Kum KY, Roh BD, Lee SJ, Lee CY, Park DS. Molecular epidemiology and association of putative pathogens in root canal infection. J Endod 2000; 26:599-604.
18. Guis S, Balandraud N, Bouvenot J, et al. Influence of -308 A/G polymorphism in the tumor necrosis factor alpha gene on etanercept treatment in rheumatoid arthritis. Arthritis Rheum 2007; 57:1426-30.
19. Bonmort M, Ullrich E, Mignot G, Jacobs B, Chaput N, Zitvogel L. Interferon-gamma is produced by another player of innate immune responses: the interferon-producing killer dendritic cell (IKDC) Biochimie 2007; 89:872-7.
20. Moore KW, O'Garra A, de Waal Malefyt R, Vieira P, Mosmann TR. Interleukin-10. Annu Rev Immunol 1993; 11:165-90.
21. Silva AC, Faria MR, Fontes A, Campos MS, Cavalcanti BN. Interleukin-1 beta and interleukin-8 in healthy and inflamed dental pulps. J Appl Oral Sci 2009; 17:527-32.
22. Pezelj-Ribaric S, Anic I, Brekalo I, Miletic I, Hasan M, Simunovic-Soskic M. Detection of tumor necrosis factor alpha in normal and inflamed human dental pulps. Arch Med Res 2002; 33:482-4.
23. Rauschenberger CR, Bailey JC, Cootauco CJ. Detection of human IL-2 in normal and inflamed dental pulps. J Endod 1997; 23:366-70.
24. Sachs B, Erdmann S, Malte Baron J et al. Determination of interleukin-5 secretion from drug-specific activated ex vivo peripheral blood mononuclear cells as a test system for the in vitro detection of drug sensitization. Clin Exp Allergy 2002; 32:736–744.
25. Feng RN, Li Y, Sun CH. TNF 308 G/A polymorphism and type 1 diabetes: a meta-analysis. Diabetes Res Clin Pract 2009; 85:4-7.
26. Bouma G, Xia B, Crusius JB, Bioque G, Koutroubakis I, Von Blomberg BM, Meuwissen SG, Peña AS. Distribution of four polymorphisms in the tumour necrosis factor (TNF) genes in patients with inflammatory bowel disease (IBD). Clin Exp Immunol 1996; 103:391-6.
27. Szabó GV, Acsády G. Tumornecrosis-Factor-α 308 GA Polymorphism in Atherosclerotic Patients. Pathol Oncol Res 2011; 17:853-7.
28. Erciyas K, Pehlivan S, Sever T, Igci M, Arslan A, Orbak R. Association between TNF-alpha, TGF-beta1, IL-10, IL-6 and IFN-gamma gene polymorphisms and generalized aggressive periodontitis. Clin Invest Med 2010; 33:85.
29. Jacobi-Gresser E, Huesker K, Schütt S. Genetic and immunological markers predict titanium implant failure: a retrospective study. Int J Oral Maxillofac Surg 2013; 42:537-43.
30. Boyce BF, Li P, Yao Z, Zhang Q, Badell IR, Schwarz EM, O'Keefe RJ, Xing L. TNF-alpha and pathologic bone resorption. Keio J Med 2005; 54:127-31.
31. Birkedal-Hansen H. Role of cytokines and inflammatory mediators in tissue destruction. J Periodontal Res 1993; 28:500-10.
32. Wilson AG, Symons JA, McDowell TL, McDevitt HO, Duff GW. Effects of a polymorphism in the human tumor necrosis factor alpha promoter on transcriptional activation. Proc Natl Acad Sci U S A 1997; 94:3195-9.
33. Djoba Siawaya JF, Ruhwald M, Eugen-Olsen J, Walzl G. Correlates for disease progression and prognosis during concurrent HIV/TB infection. Int J Infect Dis 2007; 11:289-99.
34. Jafarzadeh A, Nemati M, Rezayati MT, Khoramdel H, Nabizadeh M, Hassanshahi G, Abdollahi H. Lower circulating levels of chemokine CXCL10 in Helicobacter pylori-infected patients with peptic ulcer: Influence of the bacterial virulence factor CagA. Iran J Microbiol 2013; 5:28-35.
35. Scalzo P, de Miranda AS, Guerra Amaral DC, de Carvalho Vilela M, Cardoso F, Teixeira AL. Serum levels of chemokines in Parkinson's disease. Neuroimmunomodulation 2011; 18:240-4.

SILENCING OF STAT4 GENE INHIBITS CELL PROLIFERATION AND INVASION OF COLORECTAL CANCER CELLS

J-M. CHENG, M-R. YAO, Q. ZHU, X-Y. WU, J. ZHOU, W-L. TAN and S-H. ZHAN

Department of Radiology, Shu Guang Hospital, Shanghai University of Traditional Chinese Medicine, Shanghai, China

Received December 16, 2014 – Accepted February 3, 2015

Signal transducers and activators of transcription (STAT) play critical roles in development, proliferation, and immune defense. However the consequences of STAT hyperactivity can predispose to diseases, including colorectal cancer. In the present study, we aimed to evaluate the function of STAT4 in human colorectal cancer (CRC). The expression of STAT4 was examined by immunohistochemical assay using a tissue microarray procedure. A loss-of-function experiment was carried out to investigate the effects of lentivirus-mediated STAT4 shRNA (Lv-shSTAT4) on cell proliferation and invasive potential indicated by MTT and Transwell assays in CRC cell lines (SW480 and Caco2). As a consequence, it was found that the expression of STAT4 protein was significantly increased in CRC tissues compared with that in adjacent non-cancerous tissues (ANCT) (71.1% *vs* 44.4%, *P*=0.015), and was related with the Duke's staging and depth of invasion in CRC patients (*P*=0.022; *P*=0.001). Silencing of STAT4 gene suppressed cell proliferation and invasion of CRC cells. Taken together, these findings demonstrate that increased expression of STAT4 is positively correlated with the depth of invasion in CRC patients, and inhibition of STAT4 expression represses the growth and invasion of CRC cells, suggesting that STAT4 may be a promising therapeutic target for the treatment of CRC.

Colorectal cancer (CRC) is one of the most common tumors worldwide. Though surgical treatment is available for CRC, it has high risk and high mortality for functional considerations, rectal anatomic features and surgical technical issues (1). In terms of the benefit from targeted therapy for specific anti-VEGF or anti-EGFR treatment (2), molecular biology and medical genetics research efforts have been made to understand the cellular and molecular mechanisms of oncogene and tumor-suppressor in CRC. Thus, developing direct and effective targets for cancer therapy has revolved around a family of transcription factors known as signal transducers and activators of transcription (STATs).

STATs are cytoplasmic transcription factors involved biological responses, including cell proliferation and differentiation (3). It is reported that STATs act as signaling components located in the plasma membrane and the nucleus or as transcription factors binding specific DNA in the nucleus (4). STATs are found to be important mediators of phosphortyrosine-regulated signaling in metazoan cells and the components of JAK/STAT signal pathway involved in immune responses, cell fate, proliferation, migration and programmed cell death in multicellular organisms (5).

Key words: STAT4, colorectal cancer, proliferation, invasion

Mailing address: Dr Song-Hua Zhan,
Department of Radiology, Shu Guang Hospital,
Shanghai University of Traditional Chinese Medicine,
No. 185, Pu An Road, Huang Pu District,
Shanghai 200021, China
Tel.: +86 21 20256568 Fax: +86 21 20256568
e-mail: zhansonghua1412@163.com

0393-974X (2015)

STAT4, one member of the STAT family as cytoplasmic transcription factors, is a central mediator in generating inflammation during protective immune responses and immune-mediated diseases (6). It confers protection against endotoxin-induced death and regulates systemic inflammation (7). Some reports show that the members of the STAT family including STAT4 are highly expressed in CRC tissues and are associated with the survival of CRC patients (8). In addition, STAT4 has a function in inflammation and immunity in liver disease (9), and decreased expression of STAT4 is an independent prognostic factor for hepatocellular carcinoma (HCC) (10). On the other hand, STAT4 has no significant link with clinical parameters of HCC (11). To elucidate the function of STAT4 in cancer, we hypothesized that inhibition of STAT4 expression represses the growth and invasion of CRC cells, suggesting that STAT4 may be a promising therapeutic target for the treatment of CRC.

MATERIALS AND METHODS

Materials

The CRC cell lines (SW480 and Caco2) used for these experiments were from the Institute of Biochemistry and Cell Biology (Shanghai, China). Lv-shSTAT4, negative control vector and virion-packaging elements were from Genechem (Shanghai, China). The primer of STAT4 was synthesized by Applied Biosystems (ABI, USA). STAT4 antibody was from Santa Cruz Biotechnology (USA).

Drugs and reagents

Dulbecco's Modified Eagle medium (DMEM) and fetal bovine serum (FBS) were from Thermo Fisher Scientific Inc (Waltham, MA, USA); TRIzol Reagent and Lipofectamine 2000 were from Invitrogen (Carlsbad, CA, USA); M-MLV Reverse Transcriptase was from Promega (Madison, WI, USA); SYBR Green Master Mixture was from Takara (Otsu, Japan). ECL-PLUS/Kit was from GE Healthcare (Piscataway, NJ, USA).

Clinical data

Tissue microarray was prepared for the IHC test. Human CRC tissues and the corresponding ANCT were obtained from biopsy prior to chemotherapy from a total of 45 consecutive patients with CRC admitted to our hospital. The study was approved by the Medical Ethics Committee of Shanghai University of Traditional Chinese Medicine, and written informed consent was obtained from the patients or their parents before sample collection. Two pathologists respectively reviewed all of the cases.

IHC staining

Anti-STAT4 antibody was used for IHC detection of the expression of STAT4 protein in tissue microarrays. Tissue microarray sections were processed for IHC analysis of STAT4 protein as follows. IHC examinations were carried out on 3-mm thick sections. For anti-STAT4 IHC, unmasking was performed with 10 mM sodium citrate buffer, pH 6.0, at 90°C for 30 min. For anti-STAT4 IHC, antigen unmasking was not necessary. Sections were incubated in 0.03% hydrogen peroxide for 10 min at room temperature, to remove endogenous peroxidase activity, and then in blocking serum for 30 min at room temperature. Anti-STAT4 antibody was used at a dilution of 1:200. The antibody was incubated overnight at 4°C. Sections were then washed three times for 5 min in PBS. Non-specific staining was blocked with 0.5% casein and 5% normal serum for 30 min at room temperature. Finally, staining was developed with diaminobenzidine substrate and sections were counterstained with hematoxylin. PBS replaced STAT4 antibody in negative controls.

Quantification of protein expression

The expression of STAT4 was semiquantitatively estimated as the total immunostaining scores, which were calculated as the product of a proportion score and an intensity score. The proportion and intensity of the staining was evaluated independently by two observers. The proportion score reflected the fraction of positive staining cells (score 0, <5%; score 1, 5%-10%; score 2, 10%-50%; score 3, 50%-75%; score 4, >75%), and the intensity score represented the staining intensity (score 0, no staining; score 1, weak positive; score 2, moderate positive; score 3, strong positive). Finally, a total expression score was given ranging from 0 to 12. Based on prior analysis, STAT4 was regarded as negative expression in CRC tissues if the score <2, and positive expression if the score ≥2.

Cell culture and infection

CRC cells were cultured in DMEM medium supplemented with 10% heat-inactivated FBS, 100 U/ml of penicillin and 100 μg/ml of streptomycin. They were all placed in a humidified atmosphere containing 5% CO_2 at 37°C. On the day of transduction, CRC cells were replated at 5×10^4 cells/well in 24-well plates containing serum-free growth medium with polybrene (5 mg/ml). When 50% confluence was reached, cells were transfected with recombinant Lv-shSTAT4 or control virus at the optimal MOI (multiplicity of infection) of 50, and cultured at 37°C and 5% CO_2 for 4 h. Then the supernatant was discarded and serum containing growth

medium was added. At 4 days of post-transduction, transduction efficiency was measured by the frequency of green fluorescent protein (GFP)-positive cells. Positive stable transfectants were selected and expanded for further study. The clone in which the Lv-shSTAT4 transfected was named as Lv-shSTAT4 group and the negative control vectors transfected was named as NC group.

Quantitative Real-time PCR

To quantitatively determine the mRNA expression level of STAT4 in CRC cells, Real-time PCR was used. Total RNA of each clone was extracted with TRIzol according to the manufacturer's protocol. Reverse-transcription was carried out using M-MLV and cDNA amplification was carried out using SYBR Green Master Mix kit according to the manufacturer's protocol. Target genes were amplified using specific oligonucleotide primer and β-actin gene was used as an endogenous control. Data were analyzed using the comparative Ct method ($2^{-\Delta\Delta Ct}$). Three separate experiments were performed for each clone.

Western blot assay

CRC cells were harvested and extracted using lysis buffer (Tris-HCl, SDS, Mercaptoethanol, Glycerol). Cell extracts were boiled for 5 min in loading buffer and then equal amount of cell extracts were separated on 15% SDS-PAGE gels. Separated protein bands were transferred into polyvinylidene fluoride (PVDF) membranes and the membranes were blocked in 5% skim milk powder. The primary antibody against STAT4 was diluted according to the instructions of antibodies and incubated overnight at 4°C. Then, horseradish peroxidase-linked secondary antibodies were added at a dilution ratio of 1:1000, and incubated at room temperature for 2 h. The membranes were washed with PBS for three times and the immunoreactive bands were visualized using ECL-PLUS/Kit according to the kit's instructions. The relative protein level in different groups was normalized to GAPDH concentration. Three separate experiments were performed for each clone.

Cell proliferation assay

Cell proliferation was analyzed with the MTT assay. Briefly, cells infected with Lv-shSTAT4 were incubated in 96-well-plates at a density of 1×10^5 cells per well with DEME medium supplemented with 10% FBS. Cells were treated with 20 µl MTT dye, and then incubated with 150 µl of DMSO for 5 min. The color reaction was measured at 570 nm with enzyme immunoassay analyzer (Bio-Rad, American). The proliferation activity was calculated for each clone.

Transwell invasion assay

Transwell filters were coated with matrigel (3.9 mg/ml, 60-80 ml) on the upper surface of a polycarbonic membrane (diameter 6.5 mm, pore size 8 mm). After incubating at 37°C for 30 min, the matrigel solidified and served as the extracellular matrix for analysis of tumor cell invasion. Harvested cells (1×10^5) in 100 ml of serum free DMEM were added into the upper compartment of the chamber. A total of 200 ml conditioned medium derived from NIH3T3 cells was used as a source of chemoattractant, and was placed in the bottom compartment of the chamber. After 24 h incubation at 37°C with 5% CO_2, the medium was removed from the upper chamber. The non-invaded cells on the upper side of the chamber were scraped off with a cotton swab. The cells that had migrated from the matrigel into the pores of the inserted filter were fixed with 100% methanol, stained with Hematoxylin, and mounted and dried at 80°C for 30 min. The number of cells invading through the matrigel was counted in three randomly selected visual fields from the central and peripheral portion of the filter using an inverted microscope (200×magnification). Each assay was repeated three times.

Statistical analysis

SPSS 20.0 was used for the statistical analysis. Kruskal-Wallis H test and *Chi*-squared test were used to analyze the expression rate in all groups. One-way analysis of variance (ANOVA) was used to analyze the differences between groups. The LSD method of multiple comparisons was used when the probability for ANOVA was statistically significant. Statistical significance was set at $P < 0.05$.

RESULTS

Expression of STAT4 protein in CRC tissues

The expression of STAT4 protein in CRC tissues was examined by IHC staining. The positive expression of STAT4 protein was detected in the nucleus of CRC tissues and ANCT (Fig. 1). The positive rates of STAT4 expression were found in 71.1% (32/45) of the CRC tissues and 44.4% (20/45) in the ANCT (P=0.015, Table I).

Correlation of STAT4 expression with clinicopathologic characteristics

The correlation of STAT4 expression with various clinicopathologic characteristics was analyzed. As shown in Table II, STAT4 expression did not associate with the age, gender and CEA level of the CRC patients (each P>0.05). Upregulation of STAT4 expression was not associated with

Table I. *Expression of STAT4 protein in CRC.*

Variables	Group	Cases (N)	Expression levels (n)				Positive rate(%)	χ^2	*P*
			-	+	++	+++			
STAT4	CRC	45	13	17	10	5	71.1		
	ANCT	45	25	11	7	2	44.4	5.897	0.015

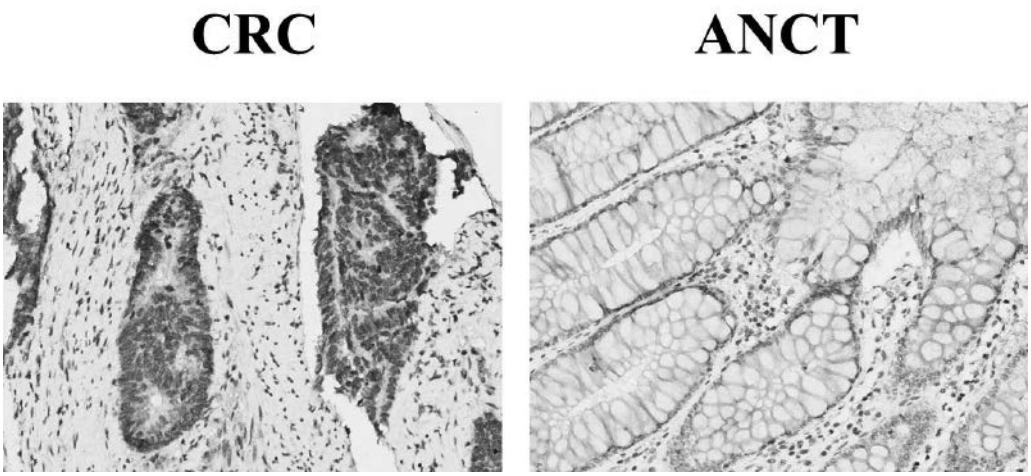

Fig. 1. *The expression of STAT4 protein in human CRC (× 200). The expression of STAT4 protein was examined by IHC assay. High expression of STAT4 was found in the CRC tissues, but low expression of STAT4 in ANCT tissues.*

tumor size and degree of differentiation (*P*=0.107; *P*=0.673). However, positive expression of STAT4 was correlated with Duke's staging the depth of invasion (*P*=0.022; *P*=0.001).

Silencing of STAT4 gene in CRC cells

After CRC cells (SW480 and Caco2) were transfected with Lv-shSTAT4 for 24 h, the expression level of STAT4 was detected by Real-time PCR and Western blotting, indicating that the mRNA (Fig. 2A, B) and protein level (Fig. 2C, D) of STAT4 were significantly silenced in the Lv-shSTAT4 group compared with the NC group (each $^{**}P<0.01$).

The effect of STAT4 silencing on cell proliferation

To examine the effect of STAT4 silencing on cell growth, we investigated the proliferative activities of CRC cells by MTT assay. As a result, silencing of the STAT4 gene significantly decreased cell proliferative activities of CRC cells in a time-dependent manner (each $^{**}P<0.01$, Fig. 3A, B).

Effect of STAT4 silencing on cell invasion

To determine the effect of STAT4 silencing on cell invasion, Transwell assay was performed. The invasive potential was determined on the basis of the ability of cells to invade a matrix barrier containing laminin and type IV collagen, the major components of the basement membrane. Representative micrographs of Transwell filters can be seen in Fig. 4A, B. The invasive potential of CRC cells was lowered in Lv-shSTAT4 group compared to the NC

Table II. *Correlation of STAT4 expression with clinicopathologic characteristics.*

Variables	Cases (n)	STAT4 (n)		*P*
	45	(-)	(+)	
Age		13	32	
≤60	26	7	19	
>60	19	6	13	0.736
Gender				
Male	18	4	14	
Female	27	9	18	0.426
Tumor size (cm)				
≤.5	13	6	7	
>5	32	7	25	0.107
Duke's staging				
A+B	16	8	8	
C+D	29	5	24	**0.022**
Depth of invasion				
Within serosa	18	10	8	
Beyond serosa	27	3	24	**0.001**
Degree of differentiation				
Well	22	5	17	
Moderate	14	5	9	
Poor	9	3	6	0.673
CEA(ng/ml)				
≥5	27	8	19	
>5	18	5	13	0.894

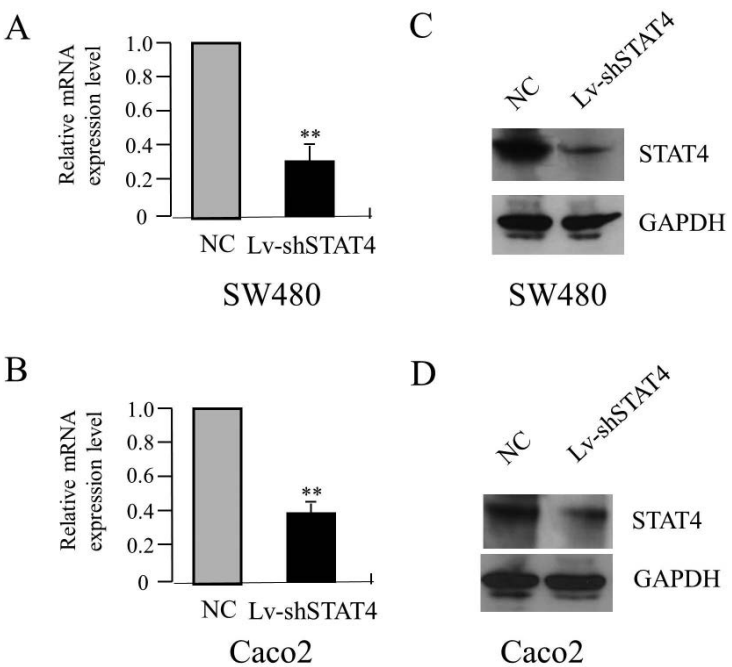

Fig. 2. *Silencing of STAT4 gene in CRC cells. The target gene for STAT4 was identified by Real-time PCR (A, B) and Western blot assays (C, D) in CRC cells, indicating that the expression level of STAT4 was significantly decreased in the Lv-shSTAT4 group compared with the NC group (each **P<0.01).*

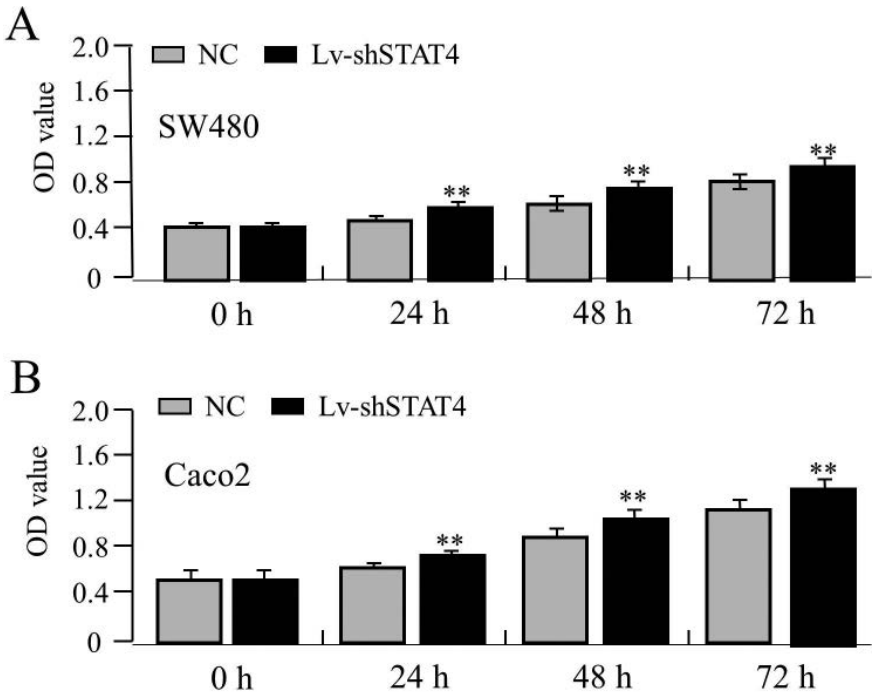

Fig. 3. *Effect of STAT4 silencing on cell proliferation. A, B) The proliferative activities of CRC cells were assessed by MTT assay, indicating that silencing of STAT4 gene reduced the proliferative activities of CRC cells in a time-dependent manner.*

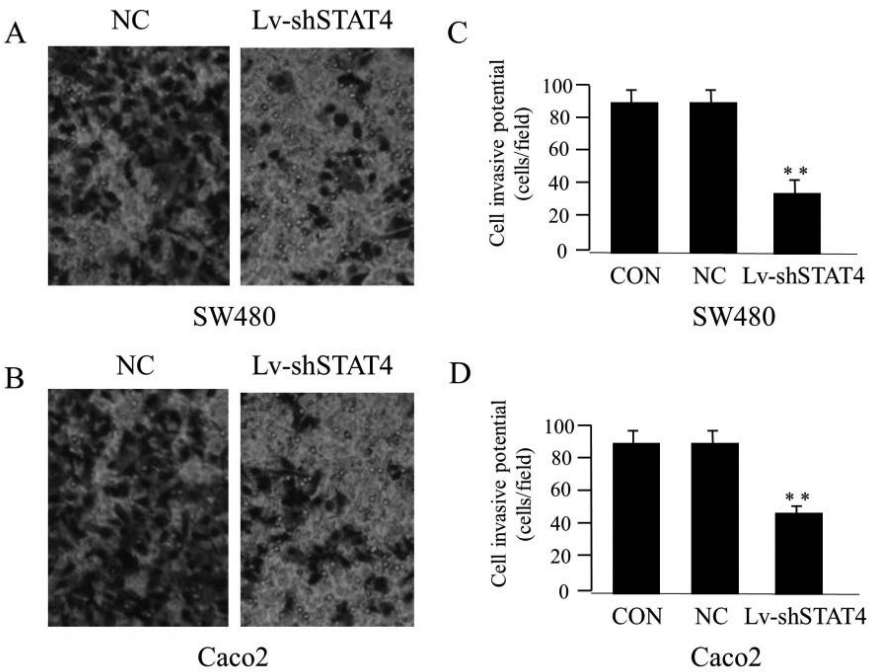

Fig. 4. *Effect of STAT4 silencing on cell invasion. A, B) The effect of STAT4 silencing on cell invasion was observed by Transwell assay. (C, D) The invasive potential of CRC cells was significantly weakened in the Lv-shSTAT4 group compared with the NC group (**P<0.01).*

and CON groups (**$P < 0.01$) (Fig. 4C, D).

DISCUSSION

STAT proteins are cytoplasmic transcription factors that have been discovered in the context of cytokine and growth factor signaling (12). STAT4 is expressed in several tissues including spleen, heart, brain, peripheral blood cells, and testis (13). Compared with normal cells and tissues, STAT4 is detected in a wide variety of human cancer cell lines, such as childhood acute lymphoblastic leukemia (14), CRC (8), breast tumor (15), and gastric cancer (16), but no differential expression is found between prostate cancer and the non-cancer tissues (17). Moreover, STAT4 expression is closely associated with the survival and prognosis of cancer patients (8,15). But, the clinical significance of STAT4 in CRC is not comprehensively understood. We found that STAT4 was highly expressed in the nucleus of CRC tissues compared to the ANCT, and was closely correlated with the Duke's staging and invasive depth of CRC patients, suggesting that STAT4 might be related with the tumorigenesis of CRC.

Functionally, inhibition of STAT4 suppresses the growth and invasion in breast cancer (15) and gastric cancer cells (16), and STAT4 phosphorylation can be activated in prostate tumor (18). But, the loss of STAT4 predisposes mice to tumor induction and demonstrates crucial roles of STAT4 in the prevention of tumors (19). Few reports show that anti-tumor immunity is regulated via the STAT6-dependent pathway, rather than STAT4 (20). STAT4 exerts a critical role in modulating the function of natural killer cells (NK) via interleukin-12 (21, 22), and engenders greater clonal expansion of the Ag-activated CD8 cells (23), suggesting STAT4 has an effective function in immunotherapy of cancer (24). Reciprocally, NKT increases expression of STAT4 to mediate anti-tumor activity, holding promise as a novel mode of immune therapy for HCC (25, 26). Therefore, further study should be carried out. In the present study, we found that knockdown of STAT4 could inhibit the proliferation and invasion of CRC cells, suggesting a tumor-promoting role of STAT4 in CRC.

In conclusion, our findings demonstrate that increased expression of STAT4 is positively correlated with the depth of invasion in CRC patients, and inhibition of STAT4 expression represses the growth and invasion of CRC cells, suggesting that STAT4 may be a promising therapeutic target for the treatment of CRC.

ACKNOWLEDGEMENTS

This study was supported by a grant from the Science and Technology Commission Foundation of Shanghai Municipality (No. 10411952300) and a grant from Leading Academic Discipline of Hepatology of State Administration of TCM China (NO: 2010sh).

REFERENCES

1. Kosinski L, Habr-Gama A, Ludwig K, Perez R. Shifting concepts in rectal cancer management: a review of contemporary primary rectal ancertreatment strategies. CA Cancer J Clin 2012; 62:173-202.
2. Kirstein MM, Lange A, Prenzler A, Manns MP, Kubicka S, Vogel A. Targeted Therapies in metastatic colorectal cancer: A systematic review and assessment of currently available data. Oncologist 2014; 19:1156-1168.
3. Pfeifer AC, Timmer J, Klingmüller U. Systems biology of JAK/STAT signalling. Essays Biochem 2008; 45:109-20.
4. Wittig I, Groner B. Signal transducer and activator of transcription 5 (STAT5), a crucial regulator of immune and cancer cells. Curr Drug Targets Immune Endocr Metabol Disord 2005; 5:449-63.
5. Kawata T. STAT signaling in Dictyostelium development. Dev Growth Differ 2011; 53:548-57.
6. Kaplan MH. STAT4: a critical regulator of inflammation *in vivo*. Immunol Res 2005; 31:231-42.
7. Lentsch AB, Kato A, Davis B, Wang W, Chao C, Edwards MJ. STAT4 and STAT6 regulate systemic inflammation and protect against lethal endotoxemia. J Clin Invest 2001; 108:1475-82.
8. Slattery ML, Lundgreen A, Kadlubar SA, Bondurant KL, Wolff RK. JAK/STAT/ SOCS-signaling pathway and colon and rectal cancer. Mol Carcinog 2013; 52: 155-66.
9. Chambers JC, Zhang W, Sehmi J, et al. Genome-

wide association study identifies loci influencing concentrations of liver enzymes in plasma. Nat Genet 2011; 43:1131-8.
10. Jiang DK, Sun J, Cao G, et al. Genetic variants in STAT4 and HLA-DQ genes confer risk of hepatitis B virus-related hepatocellular carcinoma. Nat Genet 2013; 45:72-5.
11. Clark A, Gerlach F, Tong Hv, et al. A trivial role of STAT4 variant in chronic hepatitis B induced hepatocellular carcinoma. Infect Genet Evol 2013; 18:257-61.
12. Turkson J. STAT proteins as novel targets for cancer drug discovery. Expert Opin Ther Targets 2004; 8:409-22.
13. Yamamoto K, Kobayashi H, Arai A, Miura O, Hirosawa S, Miyasaka N. cDNA cloning, expression and chromosome mapping of the human STAT4 gene: both STAT4and STAT1 genes are mapped to 2q32.2-->q32.3. Cytogenet Cell Genet 1997; 77:207-10.
14. Chang JS, Wiemels JL, Chokkalingam AP, et al. Genetic polymorphisms in adaptive immunity genes and childhood acute lymphoblastic leukemia. Cancer Epidemiol Biomarkers Prev 2010; 19:2152-63.
15. Zhou J, Xu XZ, Hu YR, Hu AR, Zhu CL, Gao GS. Cryptotanshinone induces inhibition of breast tumor growth by cytotoxic CD4+ T cells through the JAK2/ STAT4/ perforin pathway. Asian Pac J Cancer Prev 2014; 15:2439-45.
16. Zhou X, Xia Y, Su J, Zhang G. Down-regulation of miR-141 induced by helicobacter pylori promotes the invasion of gastric cancer by targeting STAT4. Cell Physiol Biochem 2014; 33:1003-12.
17. Ni Z, Lou W, Lee SO, Dhir R, DeMiguel F, Grandis JR, Gao AC. Selective activation of members of the signal transducers and activators of transcription family in prostate carcinoma. J Urol 2002; 167:1859-62.
18. Nowak M, Arredouani MS, Tun-Kyi A, Schmidt-Wolf I, Sanda MG, Balk SP, Exley MA. Defective NKT cell activation by CD1d+ TRAMP prostate tumor cells is corrected by interleukin-12 with α-galactosylceramide. PLoS One 2010; 5:e11311.
19. Zhang SS, Welte T, Fu XY. Dysfunction of Stat4 leads to accelerated incidence of chemical-induced thymic lymphomas in mice. Exp Mol Pathol 2001; 70:231-8.
20. Zhang S, Bernard D, Khan WI, Kaplan MH, Bramson JL, Wan Y. CD4+ T-cell-mediated anti-tumor immunity can be uncoupled from autoimmunity via theSTAT4/STAT6 signaling axis. Eur J Immunol 2009; 39:1252-9.
21. Wang KS, Zorn E, Ritz J. Specific down-regulation of interleukin-12 signaling through induction of phospho-STAT4protein degradation. Blood 2001; 97:3860-6.
22. Athié-M V, Flotow H, Hilyard KL, Cantrell DA. IL-12 selectively regulates STAT4 via phosphatidylinositol 3-kinase and Ras-independent signal transduction pathways. Eur J Immunol 2000; 30:1425-34.D
23. Li Q, Eppolito C, Odunsi K, Shrikant PA. IL-12-programmed long-term CD8+ T cell responses require STAT4. J Immunol 2006; 177:7618-25.
24. Wang KS, Frank DA, Ritz J. Interleukin-2 enhances the response of natural killer cells to interleukin-12 through up-regulation of the interleukin-12 receptor and STAT4. Blood 2000; 95:3183-90.
25. Uemura A, Takehara T, Miyagi T, et al. Natural killer cell is a major producer of interferon gamma that is critical for the IL-12-induced anti-tumor effect in mice. Cancer Immunol Immunother 2010; 59:453-63.
26. Margalit M, Shibolet O, Klein A, et al. Suppression of hepatocellular carcinoma by transplantation of *ex-vivo* immune-modulated NKT lymphocytes. Int J Cancer 2005; 115:443-9.

EFFICACY OF A FOOD SUPPLEMENT IN PATIENTS WITH HASHIMOTO THYROIDITIS

M. NORDIO and S. BASCIANI

Department of Experimental Medicine, University "Sapienza", Rome, Italy

Received September 17, 2014 – Accepted February 3, 2015

Thyroid inflammation has been commonly seen in recent decades, due to a series of factors and is considered as the most frequent thyroid illness. It is characterized by some distinctive traits, which include morphological and hormonal modifications, often in association with an elevated anti-thyroid autoantibody title. The aim of the therapy is to improve symptoms as fast as possible, treating inflammation and subsequent hypothyroidism, when present. Therefore, we evaluated the efficacy of a Food Supplement (FS) containing enzymes which is commonly used in various inflammatory processes and is able to modulate immune reactions during inflammation in a very rapid and efficacious way. An open, controlled study was then designed and 45 patients with Hashimoto thyroiditis were enrolled and divided into 3 groups (FS alone; thyroid hormones alone; FS plus thyroid hormones). Blood, morphological and subjective parameters were considered. The results obtained indicate that the FS used in our study is efficacious and safe when used alone and/or in combination with thyroid hormones in the treatment of autoimmune thyroiditis, as documented by the improvement of the majority of the parameters considered. The efficacy was considered faster than thyroid hormones alone as far as subjective symptomatology is considered. In conclusion, the use of the food supplement evaluated herein during inflammation may be considered an additional tool in clinicians' hands, when facing patients with autoimmune thyroiditis, especially in presence of subjective symptomatology, in order to rapidly alleviate it.

It is well known that the frequency of thyroidal illnesses has progressively grown throughout the last decades (1). This seems to be due at least to three main factors. First of all, genes play an important role, since an individual with a family history positive for thyroid pathology has a significantly higher possibility of developing a thyroid problem. Secondly, environment factors may contribute to the development of such pathologies (namely pollution, radioactive accidents, other illnesses, iatrogenic, etc.), especially those associated to autoimmunity. Thirdly, the so called "constitutional factors", such as age and sex, may influence and facilitate the appearance of thyroidal illnesses (2-6).

Among the various pathologies, thyroiditis is the most frequent (roughly about 20% of all thyroidal illnesses) and is classified as acute, subacute or chronic. The presence of a variable amount of auto-antibodies against thyroid is a distinctive trait during their evolution. The autoimmune process seems to be initiated by a downregulation of suppressor T-lymphocytes and a consequent activity against thyroglobulin (a protein that is fundamental to the production and storage of thyroid hormones)

Key words: thyroid, Hashimoto thyroiditis, therapy, nutraceuticals, hormones

Mailing address:
Maurizio Nordio,
Via Flaminia, 29
00196 Rome, Italy
Tel.: +39 3331285693
Fax: +39 0636005188
e-mail: maurizionordio1@gmail.com

0393-974X (2015)

DISCLOSURE: ALL AUTHORS REPORT NO CONFLICTS OF INTEREST RELEVANT TO THIS ARTICLE.

and thyroid-peroxidase (involved in hormone synthesis). Once the mechanism has been activated, T-lymphocytes may stimulate B-lymphocytes to produce specific antibodies (7). In addition, recent data documented that oxidative stress has a role in favoring auto-immunity disorders. Therefore, an increase in both antibody concentrations - against thyroglobulin: TGAb, and thyroid peroxidase: TPOAb - is very frequently seen. Their concentrations may vary during life, as do thyroid morphology and the ability of follicular cells to produce thyroid hormones. Their presence may lead to a progressive damage of thyroid tissue, in terms of hormone production. In fact, patients with thyroiditis demonstrate a decline towards hypothyroidism, during long-term follow-up (2, 8).

As far as the therapeutical approach is concerned, two main aspects should be taken into account. The presence of a thyroid hormone defect (or excess) and, secondly, the presence of signs of flogosis, since the latter may influence hormone synthesis. To this purpose, the correct therapy should include the use of preparations containing thyroid hormones (alone or in combination, when appropriate) and the use of anti-inflammatory preparations that have the advantage to directly improve the subjective symptoms, the flogosis parameters and indirectly contribute to equilibrate hormonal production and secretion by the thyroid.

On these bases, the purpose of the present study was to evaluate the efficacy of a preparation containing appropriate enzymes (proteases) and bioflavonoids (Wobenzym Vital, Named) in a population of patients with autoimmune thyroiditis. The choice of that preparation derived by the fact that it exploits the so called "Systemic Enzyme Therapy" (SET), which is commonly used in various inflammatory diseases, and is able to modulate immune reactions during the inflammatory process in a very rapid and efficacious way (9, 10). In addition, the presence of bioflavonoids, with their antioxidative effects, constitutes an additional benefit. The mechanism of action of proteases, in terms of anti-inflammatory potential, is driven through their reaction with the α-2-macroglobulins. Their binding is necessary to acquire the ability of the complex to neutralize inflammatory cytokines (i.e., TNF-α, IL-1β, IL-6) (11).

MATERIALS AND METHODS

Study design

The study was carried out according to the principles stated by the Declaration of Helsinki and the Good Clinical Practice expressed by the guidelines CPMP/135/95 defined by the International Conference of Harmonization. Each subject was informed about the aspects of participating in the study, including the risks and benefits. In particular, it was explained that participation was completely free of any possible charge; the patient's decision to drop out of the study was devoid of any consequence, especially in terms of patient care; the therapy was given completely free. All patients gave their informed signed consent.

Inclusion criteria

A patient was considered adequate to be included if: the age was between 18 and 80; the presence of an autoimmune thyreopathy, with or without hypothyroidism, was previously documented; the absence of important illnesses such as renal or liver insufficiency, immunopathies, blood clotting problems was documented; the availability and possibility to participate was confirmed; the explicit consent, given through the sign on the appropriate form.

Exclusion criteria

A patient was not included if: the use of cortisone, NSAID or other antiinflammation agents, anticoagulants was documented; smoke addiction or alcohol or drug abuse was documented; pregnancy was documented or even presumed, or lactating.

Since this was an open study, the inclusion of a patient in a group or another was discretional, on the basis of clinical, laboratory and technical findings, in order to obtain three homogeneous groups, in terms of thyroid status. In addition, patients already treated for chronic illnesses, such as diabetes and mild cardiovascular pathologies, were allowed to continue their therapies. Besides that, other therapies, as long as not interfering with the protocol, were also permitted.

The study was designed as a controlled open-label study, with a group of 45 patients in whom an autoimmune thyroiditis had been previously diagnosed. In particular, the enrolled patients were divided into three groups (n=15) and given the following treatments: group 1 = Wobenzym vital alone; group 2 = Wobenzym vital plus appropriate thyroid hormone therapy; group 3 = thyroid hormones alone, for a period of 6 months. The length of the treatment period was chosen on the basis of the literature data. The primary endpoint of the study was the evaluation of the efficacy, in terms of improvement of systemic and local inflammation parameters, and tolerability of a preparation for systemic enzyme therapy

in a group of patients with autoimmune thyroiditis, with or without hypothyroidism. The secondary endpoint was the evaluation of any reduction in thyroid antibody levels.

At enrolment (T=0), each patient underwent a complete anamnesis followed by physical examination in order to ascertain inclusion and exclusion criteria and define the clinical status by weight, height, BMI, neck circumference, thyroid and neck palpation. In addition, 2 questionnaires to evaluate the level of quality of life of the patient (General Health Questionnaire: GHQ-28) (12) and the level of subjective symptomatology due to the thyroid inflammation process were compiled, and a series of specific exams, in order to qualify and quantify thyroid condition were also prescribed. These were blood determinations (FreeT3, FreeT4, TSH, HTG, TGAb, TPOAb, blood count, triglycerides, PCR, Homocysteine, ANA) and high resolution ultrasound scan of the thyroidal area, in order to provide additional information concerning thyroid tissue texture and echogenicity, with a particular attention to the evaluation of the so called Systolic Peak Velocity (SPV) of the lower thyroid artery, blood flux of which is known to be altered during the inflammatory process, using Doppler sonography (13).

At the end of the evaluation process, each patient received an amount of Wobenzym vital or/and the prescription for thyroid hormones sufficient for 6 months, according to the protocol. Wobenzym vital administration was as follows: 4 tablets twice daily (total of 8) for 1 week and 2 tablets twice daily (total of 4) for the rest of the 6-month period. After 1 month (T=+1) patients were evaluated for their compliance to the treatment and were asked to orally indicate any problem presumably connected to the treatment. After 3 months (T=+3) patients were evaluated as in T=0, also with blood samples, but without ultrasound. By the end of the study period (T=+6) patients underwent the final evaluation, as in T=0, blood evaluation and ultrasound scan included.

Statistics

Data obtained are expressed as mean values ±SD and were finally processed to ascertain whether statistical differences among them could be demonstrated by Graph Pad Prism, version 6.0f (Mac, San Diego, CA,USA). In particular, the significance of differences between the pre- and post-treatment measures was analyzed using one-way ANOVA. In addition, the paired t-test was also used where indicated. p values less than 0.05 were considered to be statistically significant.

RESULTS

A total of 56 patients were enrolled, aged between 26 and 63 years (mean±SD= 44.3±6.8 yrs), 38 females and 18 males. Eleven patients of the 56 (4 females and 7 males, 19.64%) decided to drop out of the study (n=10: 8 due to poor compliance and 2 due to mild discomfort, nausea and flatus, one in the L-Thyr group and another in the Wob+L-Thyr group) or were excluded by the medical staff (n=1 in

Table I. *Anthropometric and blood pressure data at: 0, +3 e +6 months.*

		T 0	T +3	T +6
NECK CIRCUMFERENCE (cm)	Wob	38.5±4.1	35.4±5.1	34.4±4.3
	L-Thyr	40.2±3.9	34.6±4.3	34.9±5.1
	Wob + L-Thyr	37.9±4.4	34.1±3.7	33.1±4.6
BMI (kg/cm-2)	Wob	25.6±8.4	25.3±7.9	25.4±6.8
	L-Thyr	24.7±6.1	23.1±4.2	23.0±3.4
	Wob + L-Thyr	27.1±9.9	26.6±3.5	26.1±4.7
WEIGHT (kg)	Wob	68.9±11.4	69.3±10.7	68.6±9.7
	L-Thyr	63.2±8.3	61.4±6.2	61.2±5.9
	Wob + L-Thyr	70.1±8.7	67.3±8.9	66.4±7.4
BLOOD PRESSURE (mmHg)	Wob	135/85	130/80	125/85
	L-Thyr	130/80	125/85	130/85
	Wob + L-Thyr	130/80	130/80	130/85

Data are expressed as Mean ± SD. Statistical analysis of the parameters did not demonstrate any significant variation ($p>0.05$).

the L-Thyr group, due to side effects depending upon L-Thyroxine administration). None of the 10 patients decided to quit the study because of side effects presumably connected with the use of Wobenzym vital. Therefore, 45 patients completed the study, 34 females and 11 males, giving three numerically equivalent groups of 15 individuals each. Those groups were homogeneous as far as anthropometric data are considered (Table I).

Questionnaire evaluation

At time points: 0, +3 and +6 months patients were asked to answer 2 questionnaires to evalute their subjective response to treatments. The GHQ28 questionnaire which consisted of 28 items concerning the level of general wellbeing, indicated an increase in the general feeling of wellness by the patients in all 3 groups, without particular differences among the groups (data not shown). However, when the second questionnaire, regarding the level of subjective symptomatology (7 items, ranging from the level of pain to the degree of discomfort during swallowing, with an arbitrary scale between 0=no symptoms and 4=very important symptoms), was considered, the results were quite different. In fact, the analysis of the data obtained documented that the groups of patients treated with Wobenzym vital alone or in combination with thyroid hormones demonstrated a significant decrease of symptomatology discomfort three months after the beginning of the treatment that was maintained thereafter, until the end of the study. On the contrary, in the group treated with thyroid hormones alone, the decrease became significant only by the end of the 6-month period (Fig. 1). In particular, when the answers to each of the 7 items were considered, the question regarding pain reported the sharpest improvement in both groups of patients treated with Wobenzym vital.

Ultrasound scans

In order to minimize the variability of data collected in the study, all the assays and the ultrasound scans were performed by the same laboratory, the same specialist, using the same machine (MyLab, Esaote, Genova, Italy) equipped with a 12MHz linear probe. For the same reason, as far as the ultrasound morphology of the thyroid tissue is concerned, all the photos were evaluated by the same specialist that performed ultrasound evaluation. He was unaware of the treatment of the patient and was instructed to give an arbitrary score (between 0 and 4) as follows: 0= homogeneous;

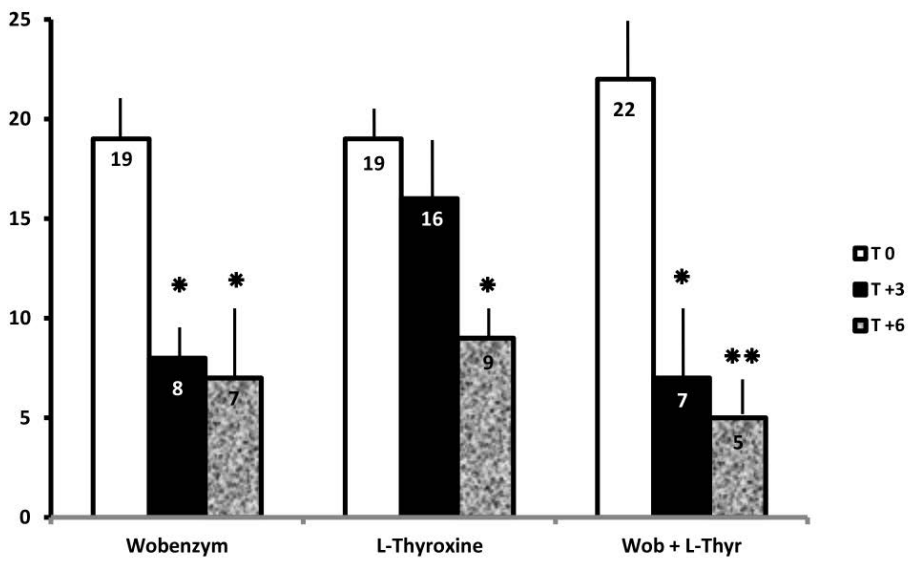

Fig. 1. *Schematic diagram of changes in subjective symptomatology levels in the 3 groups. The arbitrary scale indicates the sum of the score derived by the answer to the 7 items questionnaire (data expressed as Mean ± SD of 15 determinations). *= p<0.05 vs T 0; **= p<0.001 vs T0.*

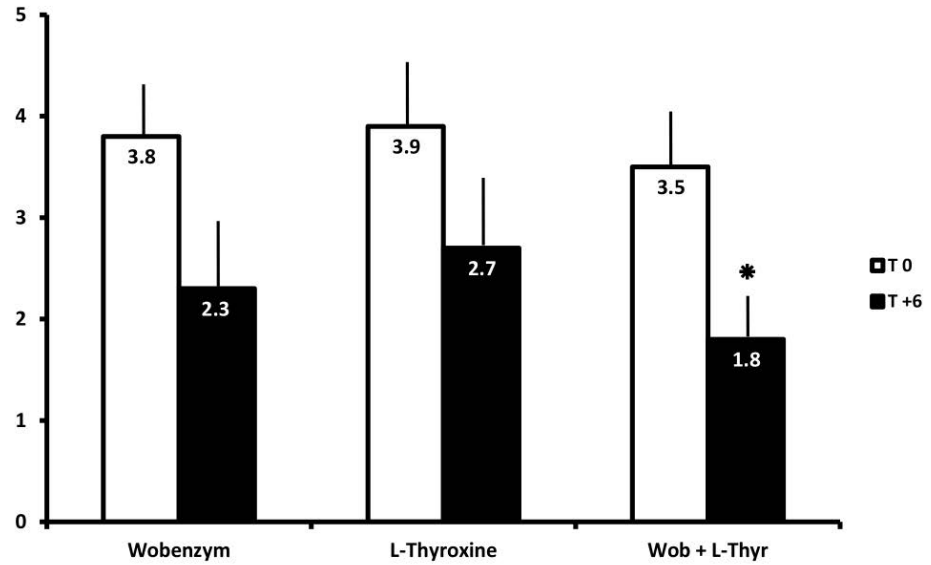

Fig. 2. *Schematic diagram of the inhomogeneity degree of thyroidal tissue, as seen at ultrasound scan, before and after the treatments, in the 3 groups considered (n = 15 each). The arbitrary scale indicates a score that was chosen to quantify the level of inhomogeneity (see text). Data are expressed as Mean ± SD. *= p<0.05 vs T 0.*

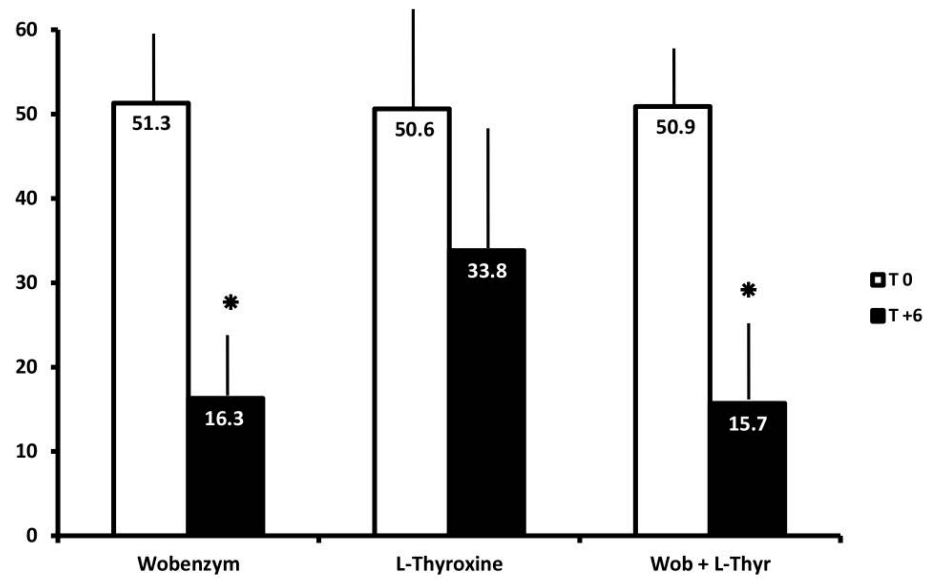

Fig. 3. *Schematic diagram of the inferior thyroid artery systolic speed velocity (cm/sec), before and after the treatments with Wobenzym vital and L-Thyroxine, alone or in combination. Data as Mean ±SD. *= p<0.05.*

1= slightly inhomogeneous; 2= inhomogeneous; 3= very inhomogeneous; 4= pseudonodular. Data obtained documented a significant reduction in the level of inhomogeneity in the Wobenzym vital plus L-Thyroxine group only (Fig. 2). In addition, data concerning inferior thyroid artery SPV demonstrated a reduction in all the groups considered that reached the level of significance only in the groups treated

with Wobenzym vital (Fig. 3).

Blood parameters

As expected, the analysis of the results obtained herein documented a reduction in TSH concentrations (mcIU/ml) in all 3 groups (TSH normal values 0.4-4.0 mcIU/ml) (14). However, it was considered statistically significant in the 2 groups where thyroid hormones were used. In particular, in the group treated with the combination Wob + L-Thyr the significance level reached the highest value (Wob: T=0 3.3±1.4, T=+6 2.6±1.2; L-Thyr: T=0 3.6±1.1, T=+6 1.2±0.4, $p<0.05$; Wob+L-Thyr: T=0 3.8±1.0, T=+6 0.7±0.3, $p<0.05$) (Fig. 4). Furthermore, as a consequence a slight reduction in FreeT3 levels was noted in the 3 groups, whilst not significant, probably indicating a better hormonal balance (data not shown). As far as HTG (ng/ml), HTGAb (IU/ml) and TPOAb (IU/ml) concentrations are concerned, the data obtained indicate a significant reduction in the Wob+L-Thyr only (HTG, Wob: T=0 37.6±16.1, T=+6 16.4±9.3, $p<0.05$; L-Thyr: T=0 41.1±11.7, T=+6 36.6±12.3; Wob+L-Thyr: T=0 38.8±13.9, T=+6 14.5±10.7, $p<0.05$)(TGAb, Wob: T=0 896±312, T=+6 435±323; L-Thyr: T=0 787±298, T=+6 662±304; Wob+L-Thyr: T=0 814±242, T=+6 387±168, $p<0.05$) (TPOAb, Wob: T=0 1017±674, T=+6 619±473; L-Thyr: T=0 971±574, T0±6 818±379; Wob+L-Thyr: T=0 937±518, T=+6 475±327)(Figs. 5, 6).

Finally, when PCR data (mg/l) as inflammation marker were considered, a reduction in all 3 groups was noted. However, the level of significance was reached in the Wob and Wob+L-Thyr groups only (PCR, Wob: T=0 6.3±1.9, T=+6 2.9±1.3, $p<0.05$; L-Thyr: T=0 5.8±2.8, T=+6 3.1±1.8; Wob+L-Thyr: T=0 6.7±1.4, T=+6 2.2±1.2, $p<0.05$)(Fig. 7). Data concerning blood parameters at T +3 demonstrated a smaller variation, but well in accordance with the T +6 time point. For this reason, data of T +3 blood parameters are not shown.

Side effects and compliance

The identification and evaluation of possible side effects and data concerning the compliance during the treatment period were recorded through appropriate forms that patients filled in during periodical interviews. Data obtained indicate that most frequent side effects were gastrointestinal

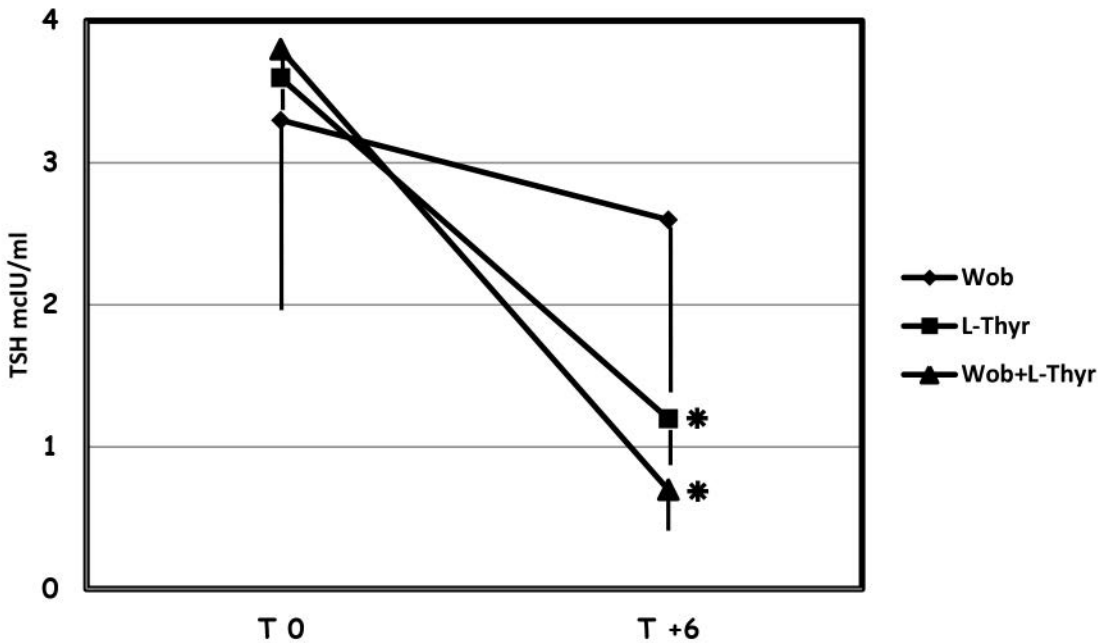

Fig. 4. *TSH variations (mcIU/ml) before and after Wobenzym vital and/or L-Thyroxine treatment in the 3 groups considered (n = 15). Results are expressed as Mean±SD. *= $p<0.05$ vs T 0.*

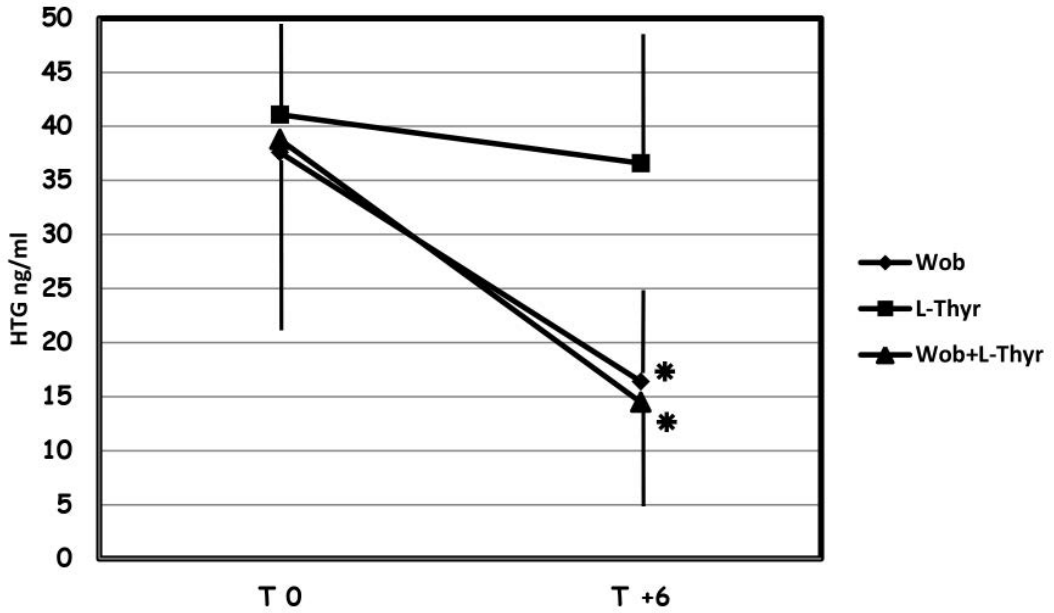

Fig. 5. *HTG variations (ng/ml) before and after Wobenzym vital and/or L-Thyroxine treatment in the 3 groups considered (n = 15). Results are expressed as Mean ± SD. *= p<0.05 vs T 0.*

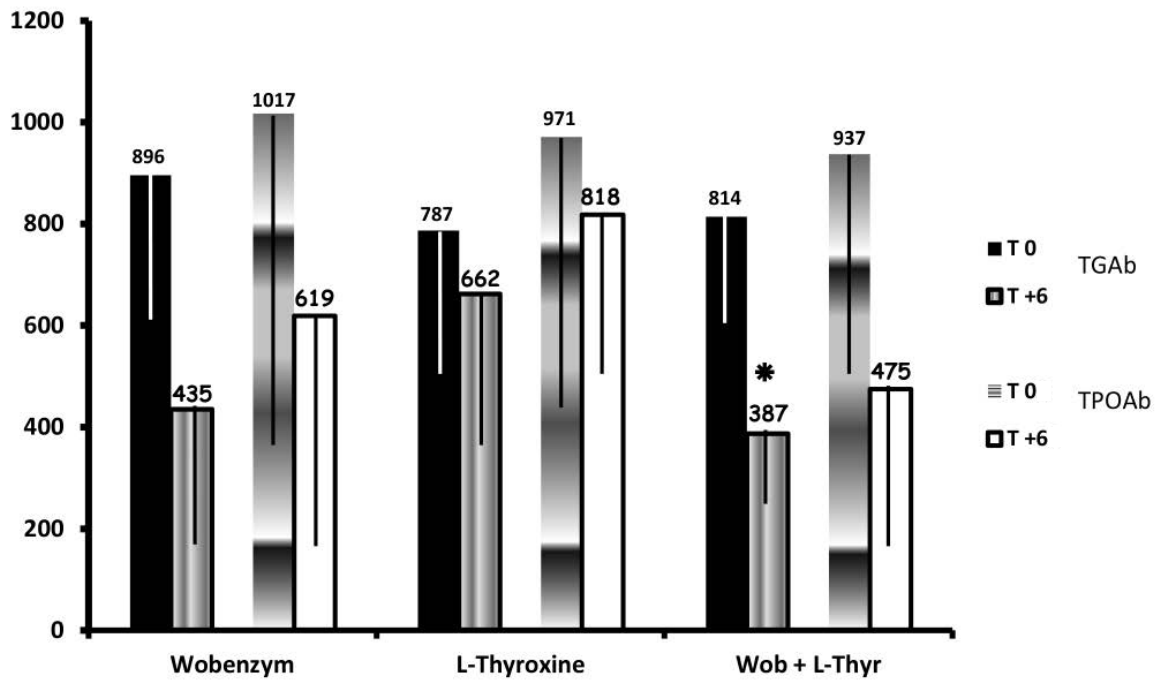

Fig. 6. *Schematic diagram of TGAb and TPOAb concentrations (IU/ml) before and after Wobenzym vital and/or L-Thyroxine treatment in the 3 groups considered (n = 15). Results are expressed as Mean ± SD. *= p<0.05 vs T 0.*

(nausea, bloated bowel) and cardiovascular (occasional tachycardia in the groups treated with thyroid hormones only). However, the symptoms disappeared during the treatment (especially after L-Thyroxine dose reduction). In 3 patients only, of 56 (5.35%) it was decided to suspend the treatment and quit the study (2 cases for personal decision of the patients, 1 Wob and 1 Wob+L-Thyr, and 1 case due to medical staff decision, L-Thyr).

The compliance evaluation indicated that 8 patients of 56 (14.28%) spontaneously decided to quit the study, giving different motivations, but mainly related either to the presumed difficulties in respecting the strict administration rules (Wobenzym vital must be taken on an empty stomach, at least 3 hours after a meal and not earlier than 2 hours before the following meal), or to the considered high number of tablets to be taken during the day (4 tablets together twice a day for the first week and 2 tablets twice a day for the rest of the study).

DISCUSSION

On the basis of the results obtained herein it is possible to focalize some important aspects and some limitations raised during and after the conclusion of the present study. First of all, the administration of Wobenzym vital and thyroid hormones, alone or in combination, was able to improve the specific symptomatology and the outcome of patients with autoimmune thyroiditis in a significant number of cases. The improvement was evident either from a subjective point of view (better score after questionnaire administration) as well as from an objective one (better results in blood and ultrasound scans parameters), in both Wob and Wob+L-Thyr groups. L-Thyroxine administration alone was able to obtain similar results, in terms of general health increase and local symptomatology decrease, as expected; however, when specific and non-specific inflammatory parameters are considered (PCR, HTG, TGAb, TPOAb, thyroid tissue modifications, blood flow in the inferior thyroid artery), Wobenzym vital administration, alone or in combination resulted in a faster reduction of symptomatology than thyroid hormones alone. In fact, whilst administration of L-Thyroxine alone was able to significantly improve subjective symptomatology at T=+6 only, Wobenzym vital alone and (even better) in association with L-Thyroxine was able to obtain significant results immediately after 3 months of treatment. In addition, a substantial number of patients indicated the improvement of their subjective symptomatology immediately after 1 month only (data not shown because no questionnaires were administered at that timepoint).

As far as thyroid tissue inhomogeneity degree before and after the end of the study is concerned, data obtained indicate a reduction in all the considered groups, whilst statistically significant in the Wob+L-Thyr group only. On the other hand, data concerning the inferior thyroid artery blood flux (which, when increased, is considered an index of thyroid inflammation)(13) demonstrate that Wobenzym vital, alone or in combination with thyroid hormones was sufficient to determine a decrease of blood flux, thus indicating a decrease in the level of inflammation. In the group treated with thyroid hormones alone, the reduction of blood flux was also apparent whilst not significant, probably due to the small size of the population considered in the study.

The evaluation of the data concerning TGAb and TPOAb responses to the treatments is far more complex. In fact, the analysis of the results indicates the enormous variability of both considered antibodies in our patients, therefore complicating the possibility to point out significant differences, especially in a relatively small number of patients as in our study. In this view, our results of a significant reduction of antibody levels obtained in the combined group should only be considered as expected, since it is well known to clinicians how difficult it is to obtain an important and stable reduction of such antibodies. Nonetheless, their presence, sometimes at very high concentrations, indicates a thyroid inflammatory process and their reduction may be considered a parameter of process improvement, especially when associated to subjective and objective data (15-18).

Hormonal data indicate that the therapy with thyroid hormones, alone or in combination with Wobenzym vital, obviously significantly decreased TSH levels, while Wobenzym vital treatment alone did not. It is interesting to note that TSH values decreased in a higher degree when the combined therapy (Wob+L-Thyr) is considered (whilst not

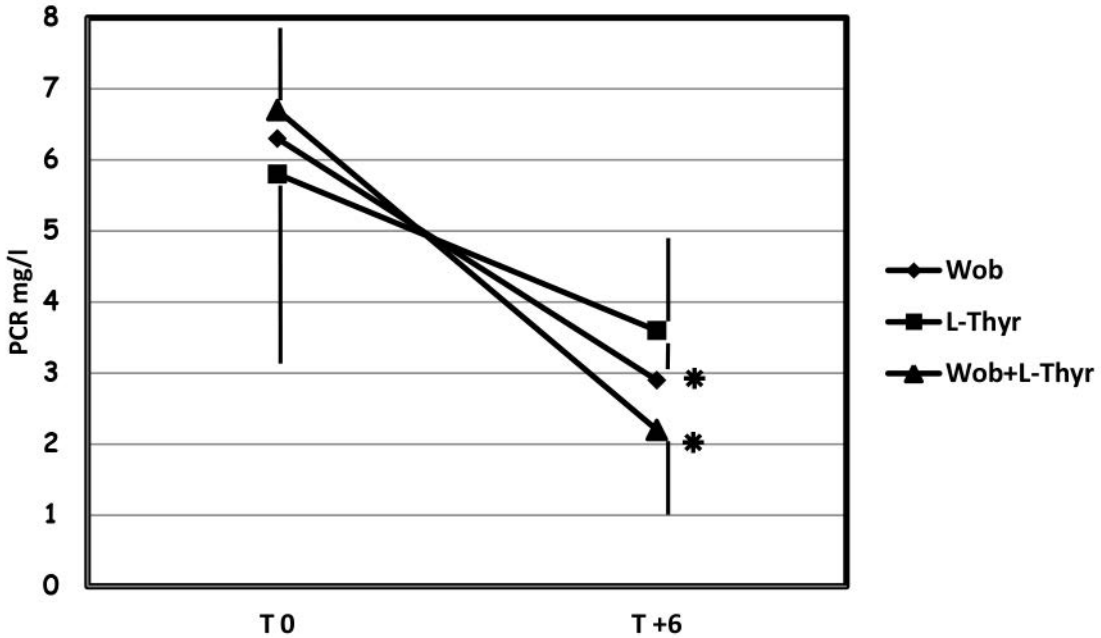

Fig. 7. *PCR variations (mg/l) before (T 0) and after (T +6) Wobenzym vital and/or L-Thyroxine treatment in the 3 groups considered (n = 15). Results are expressed as Mean ± SD. *= p<0.05 vs T 0.*

significant), in respect to L-Thyr alone treatment, suggesting that the Wobenzym vital treatment could positively affect thyroid function, therefore rebalancing hormonal status. For that reason, it may be possible to speculate that in those conditions a lesser amount of thyroid hormones could be used to obtain euthyroidism, when needed. Accordingly, FT3 and FT4 concentrations slightly decreased in all the 3 considered groups, indicating a better hormonal balance after therapy. It is important to note that the same decrease was present in the group treated with Wobenzym vital alone.

As far as side effects and compliance data are considered, the results obtained indicate their percentage is more than acceptable. However, when the compliance is considered it is noteworthy to underline that it was impossible to ascertain whether the patients took their daily therapy in line with the instructions received and the role of this in final outcome measures is impossible to be quantified.

Therefore, on the bases of data obtained and expressed herein it is possible to summarize our results as follows: treatment with Wobenzym vital, alone or in combination with thyroid hormones seems to be efficacious in autoimmune thyroiditis; Wobenzym vital effects are mainly upon inflammation, the improvement of which is beneficial to thyroid morphology and function; subjective symptoms downgrade quite rapidly when Wobenzym vital, alone or in combination, is used, while during administration of thyroid hormones alone the symptomatology decrease was slower; the effects on antibody concentrations were unexpectedly insufficient, but probably due to the size of the population considered in our study; obviously the effect of Wobenzym vital on TSH levels is definitely much lower than thyroid hormones, thus confirming that its activity is not on TSH, but on inflammation, the improvement of which induces a better thyroid functionality.

In conclusion, the use of Wobenzym vital during inflammation may be considered an additional tool in clinicians' hands when facing patients with autoimmune thyroiditis, with or without concomitant thyroid hormone therapy, especially in the presence of subjective symptomatology, in order to rapidly alleviate it. In addition, Wobenzym vital therapy may be prolonged in the attempt to favor the maintenance

of a correct thyroid function as long as possible.

REFERENCES

1. McLeod DS, Cooper DS. The incidence and prevalence of thyroid autoimmunity. Endocrine 2012; 42:252-65.
2. Orgiazzi J. Thyroid autoimmunity. Presse Med 2012; 41(12 P 2):e611-25.
3. Menconi F, Hasham A, Tomer Y. Environmental triggers of thyroiditis: hepatitis C and interferon-α. J Endocrinol Invest 2011; 34:78-84.
4. Tomer Y. Genetic susceptibility to autoimmune thyroid disease: past, present, and future. Thyroid 2010; 20:715-25.
5. Ron E, Brenner A. Non-malignant thyroid diseases after a wide range of radiation exposures. Radiat Res 2010; 174:877-88.
6. Somers EC, Thomas SL, Smeeth L, Hall AJ. Autoimmune diseases co-occurring within individuals and within families: a systematic review. Epidemiology 2006; 17:202-17.
7. Nada AM, Hammouda M. Immunoregulatory T cells, LFA-3 and HLA-DR in autoimmune thyroid diseases. Indian J Endocrinol Metab 2014; 18:574-81.
8. Cooper DS, Biondi B. Subclinical thyroid disease. Lancet 2012; 379:1142-54.
9. Heyll U, Münnich U, Senger V. Proteolytic enzymes as an alternative in comparison with nonsteroidal anti-inflammatory drugs (NSAID) in the treatment of degenerative and inflammatory rheumatic disease: systematic review. Med Klin 2003; 98:609-15.
10. Steffen C, Menzel J. Basic studies on enzyme therapy of immune complex diseases. Wien Klin Wochenschr 1985; 97:376-85.
11. Armstrong PB. Proteases and proteases inhibitors: a balance of activities in host-pathogen interaction. Immunobiology 2006; 211:263-81.
12. Sterling M. General Health Questionnaire - 28 (GHQ-28). J Physiother 2011; 57:259.
13. Banaka I, Thomas D, Kaltsas G. Value of the left inferior thyroid artery peak systolic velocity in diagnosing autoimmune thyroid disease. J Ultrasound Med 2013; 32:1969-78.
14. Jonklaas J, Bianco AC, Bauer AJ, et al. Guidelines for the treatment of hypothyroidism: prepared by the American Thyroid Association task force on thyroid hormone replacement. Thyroid 2014; 24:1670-751.
15. Delshad H, Mehran L, Tohidi M, Assadi M, Azizi F. The incidence of thyroid function abnormalities and natural course of subclinical thyroid disorders, Tehran, I.R. Iran. J Endocrinol Invest 2012; 35:516-21.
16. Radetti G, Maselli M, Buzi F, et al. The natural history of the normal/mild elevated TSH serum levels in children and adolescents with Hashimoto's thyroiditis and isolated hyperthyrotropinaemia: a 3-year follow-up. Clin Endocrinol 2012; 76:394-8.
17. Rho MH, Kim DW, Hong HP, Park YM, Kwon MJ, Jung SJ, Kim YW, Kang T. Diagnostic value of antithyroid peroxidase antibody for incidental autoimmune thyroiditis based on histopathologic results. Endocrine 2012; 42:647-52.
18. Caturegli P, De Remigis A, Rose NR. Hashimoto thyroiditis: clinical and diagnostic criteria. Autoimmun Rev 2014; 13:391-7.

A CYTOTOXIC ANALYSIS OF A SARDINIAN PLANT EXTRACT CREAM ON HUMAN ORAL PRIMARY CELL CULTURES: AN *IN VITRO* STUDY

B. SINJARI, F. DIOMEDE, G. MURMURA, T. TRAINI, I. MERCIARO, O. TRUBIANI and S. CAPUTI

Department of Medical, Oral and Biotechnological Sciences, University "G. D'Annunzio", Chieti-Pescara, Italy

Received September 4, 2014 – Accepted January 14, 2015

Wound healing agents support the natural healing process, reduce trauma and likelihood of secondary infections and hasten wound closure. The aim of this work was to evaluate the effect of different concentration of a new Sardinian plant cream (RD7) on two human primary cultures: Periodontal Ligament Stem Cells (hPDLSCs) and Gingival Fibroblasts (hGFs) derived from oral tissues in terms of morphological changes, cell proliferation and wound healing properties. RD7, is an interactive dressing containing phytocomplex derived from Sardinian endemic or not, medicinal plant extracts, with an important anti-radical, anti-inflammatory and antiseptic activity finalized to rapidly promote tissue regeneration and the formation of granulation tissue. hPDLSCs and hGFs were seeded at different concentrations (0.5, 1, 2.5 and 5 mg/ml) of RD7. The cell proliferation and viability was evaluated using colorimetric assays (MTT assay) and trypan blue exclusion test. Meanwhile, the morphological cell changes were evaluated by means of optic (OM) and scanning electronic microscopes (SEM). The induction of the migratory properties was evaluated by means of wound healing assay. *In vitro* results, using hPDLSCs and hGFs, showed a decrease of cell growth starting at 24 h of incubation, at high concentrations (2.5 mg/ml and 5 mg/ml). This cell growth reduction was associated to evident morphological changes, whilst, at low concentrations (0.5 and 1 mg/ml) a typical unchanged morphology of both hPDLSCs and hGFs was shown. Wound healing assay showed a complete wound full closure occurring after 24 h of treatment in samples treated with low concentration of RD7. The results of the present work indicate that low concentrations of RD7 have no cytotoxicity effect, stimulate cell proliferation and contribute to induce the migratory properties in hPDLSCs and hGFs, therefore it could be considered a new product for use in clinical practice.

Wound healing is a complex system where well-organised cascade of biochemical and cellular events involving tissue repair and regeneration occurs (1, 2). It is a connective tissue feedback and involves the activity of an intricate network of cytokines, growth factors and blood cells, which ultimately leads to the restoration of the injured tissue to normal condition (3, 4). The aim of wound care, which must occur in a physiologic environment conducive to tissue repair and regeneration, is to promote healing in the shortest time possible, exclude secondary infections and minimize pain, discomfort and scarring (5). The

Key words: anti-inflammatory cream, human periodontal ligament stem cells, human gingival fibroblasts

Mailing address: Dr. Bruna Sinjari,
Department of Medical,
Oral and Biotechnological Sciences,
University "G. D'Annunzio", Chieti-Pescara,
Via dei Vestini, 29 66100 Chieti, Italy
Tel.: +39 08713554125
e-mail: b.sinjari@unich.it

0393-974X (2015)

wound healing process, which begins at the moment of tissue injury and may continue for a prolonged period, includes the Inflammatory, Proliferative and Remodelling phases, each of which is characterised by a series of events (6). The above-mentioned healing processes are influenced by several factors such as type and sites of wound, certain disease conditions, individual nutrition, infections, drugs and hormones (7). Agents with wound healing potential, which are obtained from natural and synthetic bioactive materials have the propensity for antioxidant, chelation and antimicrobial activities, and may act through one or more of these phases. There are many topical pharmaceutical products comprised of semisolid formulations, which include ointments, creams, lotions, gels, and dressings, available to the clinician for use in treating skin wounds. Numerous agents are valued for their antimicrobial activity, which can prevent colonized wounds from becoming infected, thereby assisting the wound to heal. However, it is evident that agents which can be toxic to bacterial cells may also be toxic to the skin cells themselves and delay healing.

Different authors and several papers in the literature describe the cytotoxicity of wound dressings. In particular, a number of investigations have been carried out by researchers worldwide on the potential toxic effect to the patient of for e.g. silver-containing products and dressings which, on the other hand is balanced by their efficacious antimicrobial activity and their cost effectiveness (7-10).

To examine cytotoxicity worldwide, researchers have applied different techniques which include: the evaluation of cell morphology under an inverted microscope (11); proliferation assays with Brd U to measure DNA synthesis (12); cell viability testing using MTT dye (13); and apoptosis detection with analysis on a FAC Scan (14).

In this study we examined the cytotoxic effect of a new Sardinian plant extract cream (RD7) on two different primary cell cultures by using MTT dye, cell morphology on optic and scanning electronic microscope and the migratory capacity through wound healing assay

MATERIALS AND METHODS

RD7 (RP-Farmadin srl, Cagliari-Italy) is an interactive skin-regeneratin soothing cream containing phytocomplex derived from medicinal Sardinian endemic or not plant extracts, with an important anti-radical, anti-inflammatory and antiseptic activity finalized to promote tissue regeneration and the rapid formation of granulation tissue. Its composition is shown on Table I.

Periodontal ligament stem cell culture

Human periodontal ligament stem cell (hPDL) biopsies were carried out after informed consent on ten patients (range age 20-35 years). All volunteers were free from systemic and oral diseases. Biopsies were obtained from alveolar crestal and horizontal fibers of the PDL by scraping the roots of non-carious third molar teeth with a Gracey's curette. hPDLSCs were obtained and cultured in Mesenchymal Stem Cell Growth Medium (MSCGM) (Lonza Walkersville Inc, Walkersville, MD, USA) according to Trubiani et al. 2013 (15). Cells migrated from the explants, and on day 7 adherent cells which were 80–90% confluent, as determined by phase contrast microscopy, were isolated using 0.1% trypsin solution and plated in tissue culture polystyrene flasks at $5x10^3$ cells/ cm^2. Primary cultures of hPDLSCs were constituted of colonies of fibroblast-like cells which, after subcultivation, proliferated with a population-doubling time of 48 h reaching a confluent growth-arrested condition. Single-cell suspensions of the developing adherent layer were prepared by trypsin/ ethylenediaminetetraacetic acid

Table I. *Chemical composition of tested solution.*

Ingredients
Aqua, Glycerin, Carbomer, Propylene Glycol, PEG-40 hydrogenated castor oil, Sedum Telephium Extract*, Chamomilla Recutita Extract*, RD7*, Hyaluronic acid, Phenoxyethanol, Thymus vulgaris oil, Alkyl acrylate crosspolymer, Acrylates/ C10-30, Benzyl Alcohol, Ethyl-paraben, Methylparaben, Triethanolamine, Butylparaben, Propylparaben, Limonene, Linalool.

** Phytocomplexes developed by RP-Farmadin srl –Via Tramontana,11-09126 Cagliari, Italy*

(EDTA) and cell viability was evaluated by the trypan blue dye exclusion test.

Gingival fibroblast cell cultures

Human gingival fibroblasts (hGFs) were obtained from fragments of healthy marginal gingival tissue from the retromolar area taken during surgical extraction of impacted third molars. Signed informed consent was obtained from the donors according to a protocol approved by the University of Chieti. The tissue fragments were immediately placed in Dulbecco's modified Eagle's medium (DMEM)/F12 (Lonza) for at least 1 h, rinsed three times in phosphate-buffered saline solution (PBS) (Lonza), minced into small tissue pieces, and cultured in DMEM/F12 containing 10% fetal bovine serum (Lonza), 1% penicillin and streptomycin, 1% fungizone. Cells were maintained at 37°C in a humidified atmosphere of 5% (v/v) CO2. Cultured hGFs of passages 4–8 were used for these studies (16).

Cellular proliferation

Cell viability seeded with progressively increasing concentrations of RD7 (0.5, 1, 2.5 and 5 mg/ml) eluted in basal medium was evaluated by MTT assay. In brief, the cells were seeded into flat-bottom 96-well plates ($2x10^3$/ well) in 200 µL medium, containing increasing concentrations of RD7, for different time points (24 h, 48 h, 72 h up to 1 week). At the designated time, 20 µL MTT was added to each well and incubated for 3 h. Absorbance at 570 nm was measured with a reference wavelength of 630 nm. The cytotoxicity experiment was conducted independently in duplicate with six replicates for each experiment. Moreover, the doubling-time of the trypan blue harvested cells, at 24, 48, 72 h and 1 week of culture, was calculated by using an algorithm available online (http://www.doubling-time.com). Cells were analyzed by an inverted light microscope (Leica DMIL; Leica Microsystems S.p.A, Milan, Italy).

Light microscopy evaluations

The morphological aspect of hPDLSCs and hGFs were observed by a light microscope (Leica Microsystem, Milan, Italy) and documented photographically.

Scanning electron microscopy analysis

Glass-adherent hPDLSCs and hGFs at P2 cultured with different RD7 concentration (0.5, 1, 2.5 and 5 mg/ml) and cells seeded without the above-mentioned cream were used as the control group. The samples were fixed with 2.5% glutaraldehyde in 0.1M cacodylate buffer pH 7.4 for 1 h.. After fixation the samples were postfixed with 1% osmium tetroxide, dehydrated increasing ethanol concentrations and then critical point dried. Then all the samples were mounted on alluminium stubs and gold-coated in an Emitech K550 (Emitech Ltd. Ashford, UK) sputter-coater before imaging by means of a SEM (Karl Zeiss, EVO 50, Germany).

In vitro wound healing assay

To perform this assay, 8-9 x 10^4 hPDLSCs and hGFs were seeded in six-well plates with markings on the outer bottom of the well to be used as reference points during image acquisition. Cells were grown in basal medium until monolayers reached 80-90% confluence. Wounds were created by manually scraping the cell monolayer with a yellow pipette tip and the plates were then vigorously rinsed with PBS to remove pieces of cellular debris that can reattach randomly to the cell layer. After wound creation, serum-free medium containing increasing concentrations of RD7 (0.5, 1, 2.5 and 5 mg/ml), was added to each well, and plates were incubated at 37°C, in a humidified atmosphere of 5% CO_2. hPDLSCs and hGFs grown in the presence of basal medium were used as negative control. The wound was observed at 6 and 24 hours using an optical microscope at 10X magnification. Each wound was photographed at two locations along the original wound boundary. Duplicate wells of each condition were examined for three independent experiments (17).

Statistical analysis

The Statistical Package for Social Science (SPSS, v 21.0, Inc. Chicago, IL, USA) was used for data analysis. Parametrical methods were used after having verified the existence of the required assumptions. In particular, the normality of the distribution and the equality of variances were assessed by the Shapiro-Wilk test.

The significance of the differences of viability among the time within each group Ctrl, 0.5, 1, 2.5 and 5 mg/ml were assessed by an ANOVA repeated measures test. The significance of the differences among the groups within each time point was assessed by a one-way ANOVA test. When significant interactions were seen, *post hoc* analyses were carried out according to proper Bonferroni corrections with the Tukey's test. A p value less than 0.05 was considered statistically significant.

RESULTS

In vitro cell culture provides an ideal tool to investigate the cytocompatibility and cytotoxicity of many different biomaterials, and in the current study we assessed the cellular response to four different concentrations of RD7. hPDLSCs and hGFs primary cultures were used. The cells displayed typical fibroblastic and morphological features with

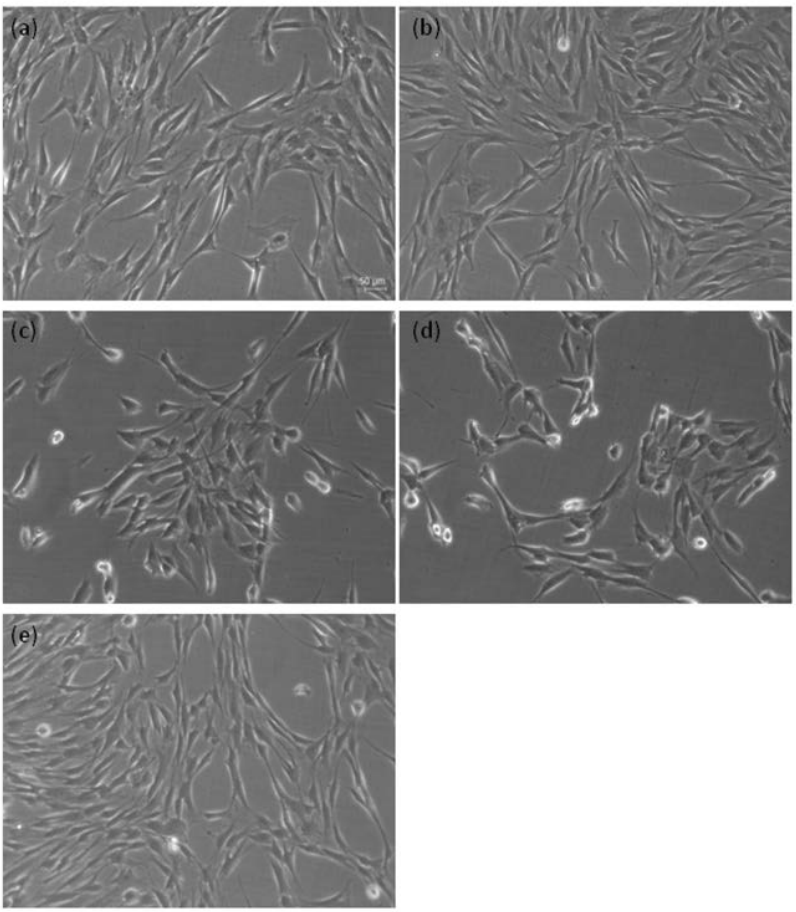

Fig. 1. *Micrograph at light microscopy after 24h of incubation at different concentration of RD7 solution of the hPDLSCs.* ***a****) 0.5 mg/ml,* ***(b)*** *1 mg/ml,* ***(c)*** *2.5 mg/ml,* ***(d)*** *5 mg/ml and* ***(e)*** *control cells. (Mag: 10X)*

roundish or elliptical nucleus containing one or more nucleoli (Fig. 1 e; Fig. 2 e).

Moreover, at light and scanning microscopy, proliferating spindle-shaped cells with extended cellular processes as filopodia and lamellipodia at low concentrations (0.5 and 1 mg/ml) were detectable (Fig. 1 a, b; Fig. 2 a, b). On the contrary, at high concentrations (2.5 and 5 mg/ml) morphological changes were present; the cells were smaller, retracted and the greater part of them was roundish, and uneven changes of the cytoskeleton structure were evident; the presence of cells detached from the bottom well was suggestive of cell death (Fig. 1 c, d; Fig. 2 c, d).

At scanning microscopy the characteristic cell features were detectable without evident damage of cell structure when hPDLSC exposed to 0.5 mg/ml of RD7 solution was compared to control cells (Fig. 3 a, b). SEM imaging showed few cells placed with high concentration (2.5 and 5 mg/ml) of RD7 cream (Fig. 3 c, d)

By MTT assay, we evaluated the proliferation rate and viability of hPDLSCs and hGFs incubated for 24 h, 48 h, 74 h and 1 week with the above-mentioned concentrations. The obtained results showed a decrease of the cell growth after 24 h of incubation at high concentration of tested solution (2.5 and 5 mg/ml). After 1 week of culture the cell growth

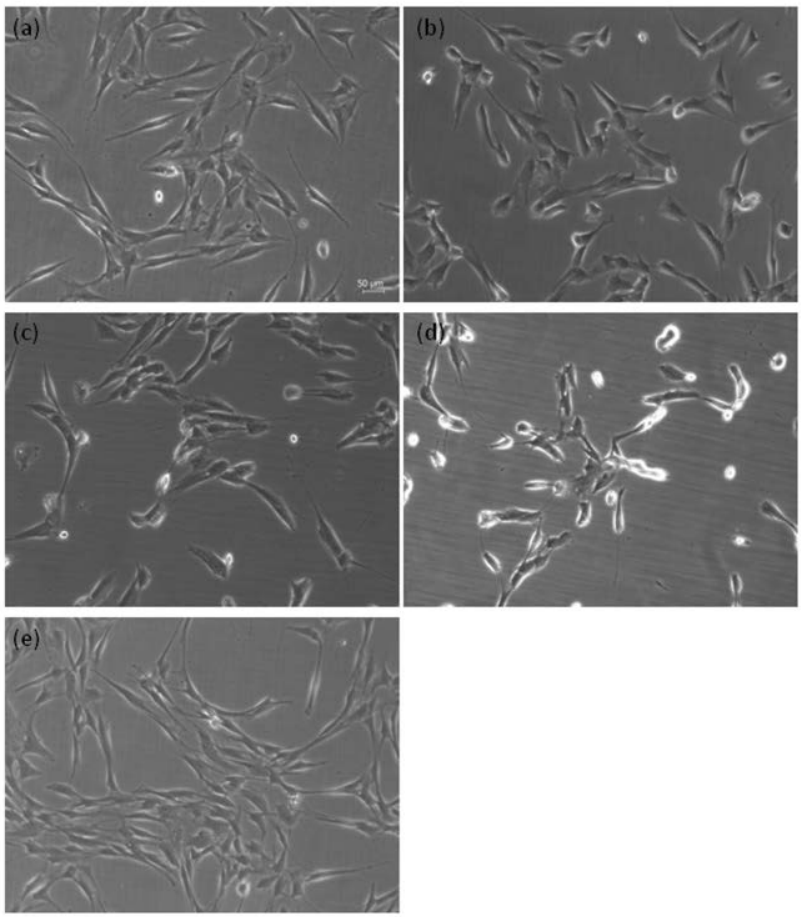

Fig. 2. *Micrograph at light microscopy after 24 h of incubation at different concentration of RD7 cream of the hGFs.* ***a****) 0.5 mg/ml,* ***(b)*** *1 mg/ml,* ***(c)*** *2.5 mg/ml,* ***(d)*** *5 mg/ml, and* ***(e)*** *control cells. (Mag: 10X)*

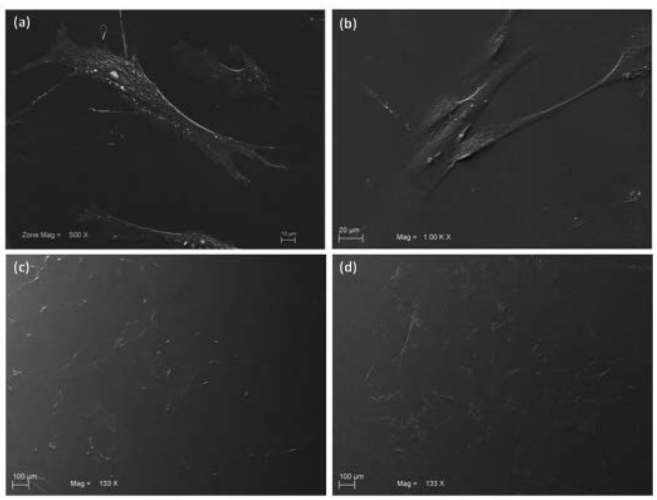

Fig. 3. *SEM representative micrograph of hPDLSCs. The ultrastructural analysis indicated that after 24h of culture with 0.5 mg/ml of RD7 cream cells showed the characteristic fibroblast-like morphology.* ***(a)*** *control cell,* ***(b)*** *cell seeded with low concentration (0.5 mg/ml) of cream solution,* ***(c)*** *cells seeded with high concentration of RD7 cream 2.5 mg/ml, and* ***(d)*** *5 mg/ml.(Mag: 133X, 500X and 1000X)*

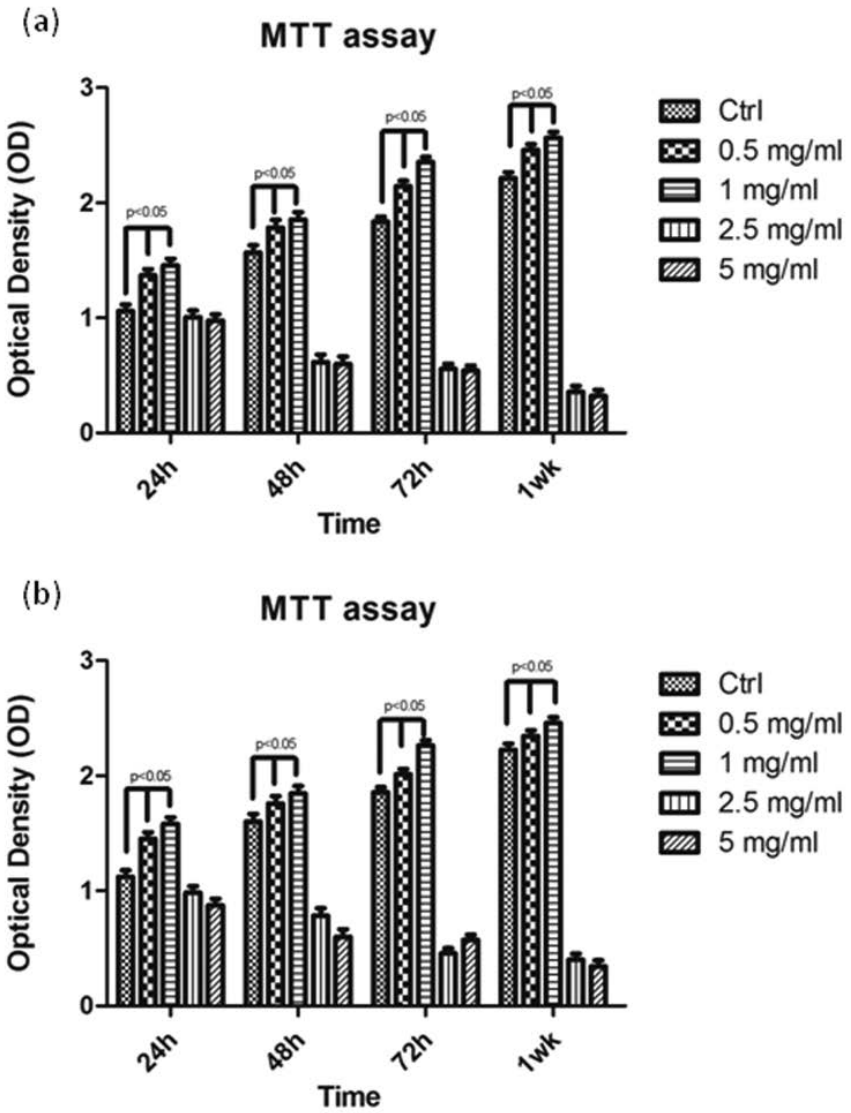

Fig. 4. *MTT assay. Cellular viability of hPDLSCs (**a**) and hGFs (**b**) exposed to different concentration of RD7 cream . Cytotoxicity was evaluated at different time points: 24, 48, 72 h and 1 week. Error bars indicate ± SEM ($p<0.05$ was considered statistically significant).*

increased in all examined samples, but it was lower in high concentration compared to the exposure to low concentration (0.5 and 1 mg/ml) (Fig. 4).

The studies carried out at light microscopy and scanning electron microscopy level confirmed the results obtained by MTT assay. *In vitro* wound healing assay showed that RD7 was able to stimulate cell migratory properties. Full closure of the wound occurred after 24 h of treatment at in hPDLSCs and hGFs cultured with 0.5 and 1 mg/ml of RD7 solution (Fig. 5 a, b; Fig. 6 a, b). Cells seeded with high concentration (2.5 and 5 mg/ml) of RD7 solution did not show migratory ability and regeneration properties (Fig. 7 c, d; Fig. 8 c, d).

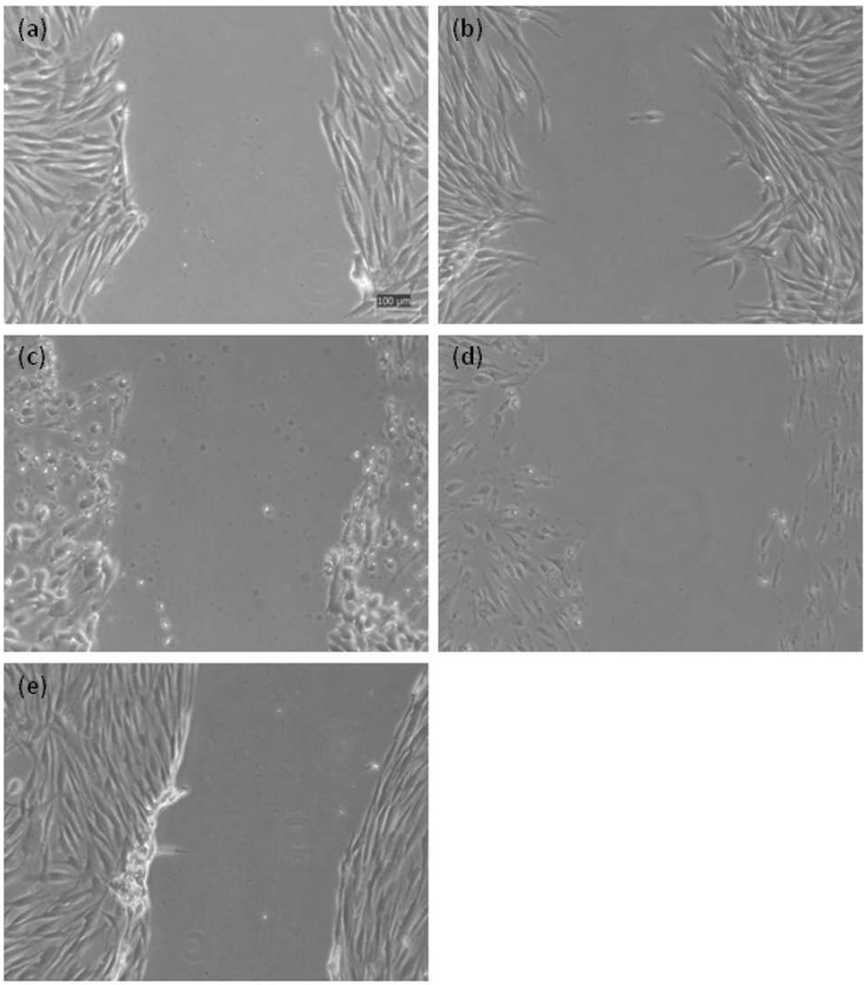

Fig. 5. *Micrograph at light microscopy after 6 h to wound hPDLSCs monolayer and treated with increasing concentration of RD7 cream.* ***a****) 0.5 mg/ml, (****b****) 1 mg/ml, (****c****) 2.5 mg/ml, (****d****) 5 mg/ml and (****e****) control cells. (Mag: 10X)*

DISCUSSION

In the present study, it was demonstrated that low concentrations (0.5 and 1 mg/ml) of RD7 stimulate hPDLS and hGF cell proliferation. Meanwhile, at high concentrations (2.5 and 5 mg/ml) a decrease in cell viability was demonstrated. Moreover, at the optical and scanning microscopy the cells displayed typical fibroblastic and morphological features with roundish or elliptical nucleus containing one or more nucleoli. On the contrary, at high concentrations (2.5 and 5 mg/ml) morphological changes were present.

Tissue healing depends predominantly on proliferation and migration of specific cells to the wound site. Wound healing assay, despite not being an exact duplication of cell migration *in vivo*, is a simple and inexpensive method to study *in vitro* cell migration and the its underlying biology. The basic steps involve creation of a "wound" on monolayer cells, capture of images at the beginning

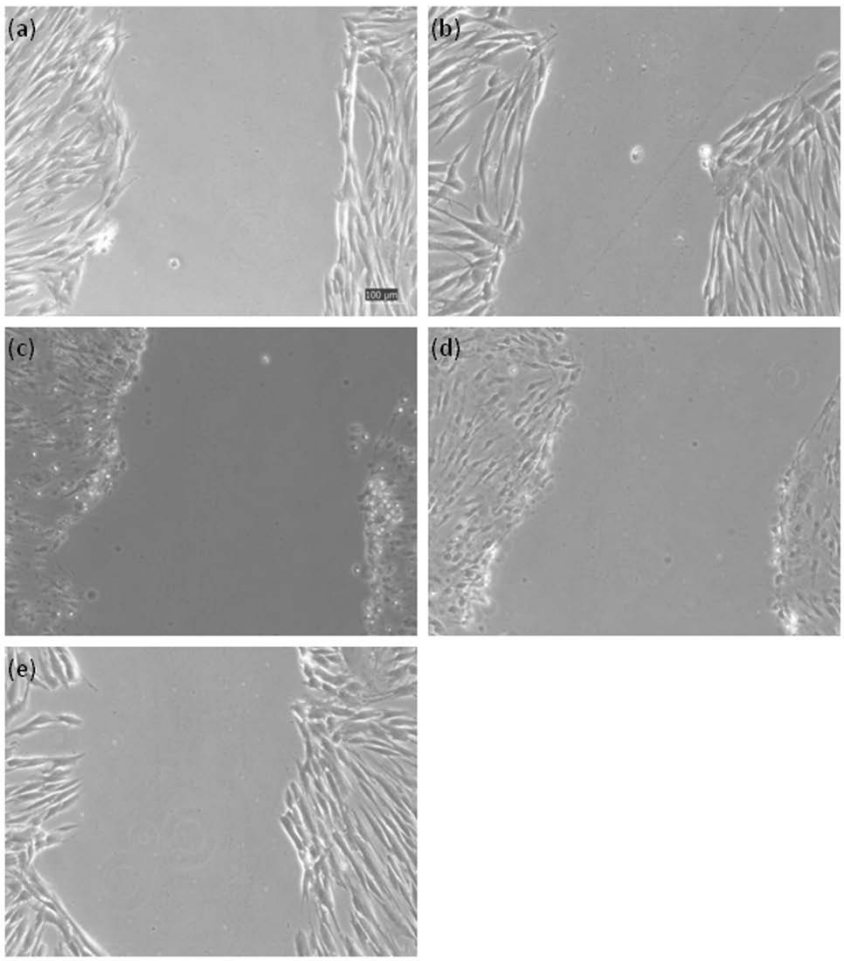

Fig. 6. *Micrograph at light microscopy after 6 h to wound hGFs monolayer and treated with increasing concentration of RD7 cream.* ***a****) 0.5 mg/ml, (****b****) 1 mg/ml, (****c****) 2.5 mg/ml, (****d****) 5 mg/ml, and (****e****) control cells. (Mag: 10X)*

and at regular intervals during wound closure, and comparison of the images to determine the rate of cell migration (17). Low concentrations of RD7 stimulate cell migration during wound healing assay. In fact, in the present study a complete healing closure of wound was evident after 24 h of treatment.

As most wound beds are prone to colonization of pathogens such as bacteria and fungi, wounds treatment also require antiseptics. Ulcers and large burns, in the majority of cases, contain aerobic Gram-negative (*Pseudomonas aeruginosa* and anaerobic cocci) and Gram-positive bacteria (*Staphylococcus aureus*) (18, 19). The bacteria colonization in a wound can impair optimal wound healing. If left untreated their colonization can lead to morbidity and even mortality of the patient. For this reason it is crucial that the wound healing agents must have the capacity not only to accelerate the healing process but also to inhibit bacteria colonization. Current studies of our laboratory are evaluating the anti-inflammatory and antimicrobial activity of this cream and of the its single components. Moreover, several polysaccharides of RD7, both with the plant juice, promote tissue repair by a mechanism not yet

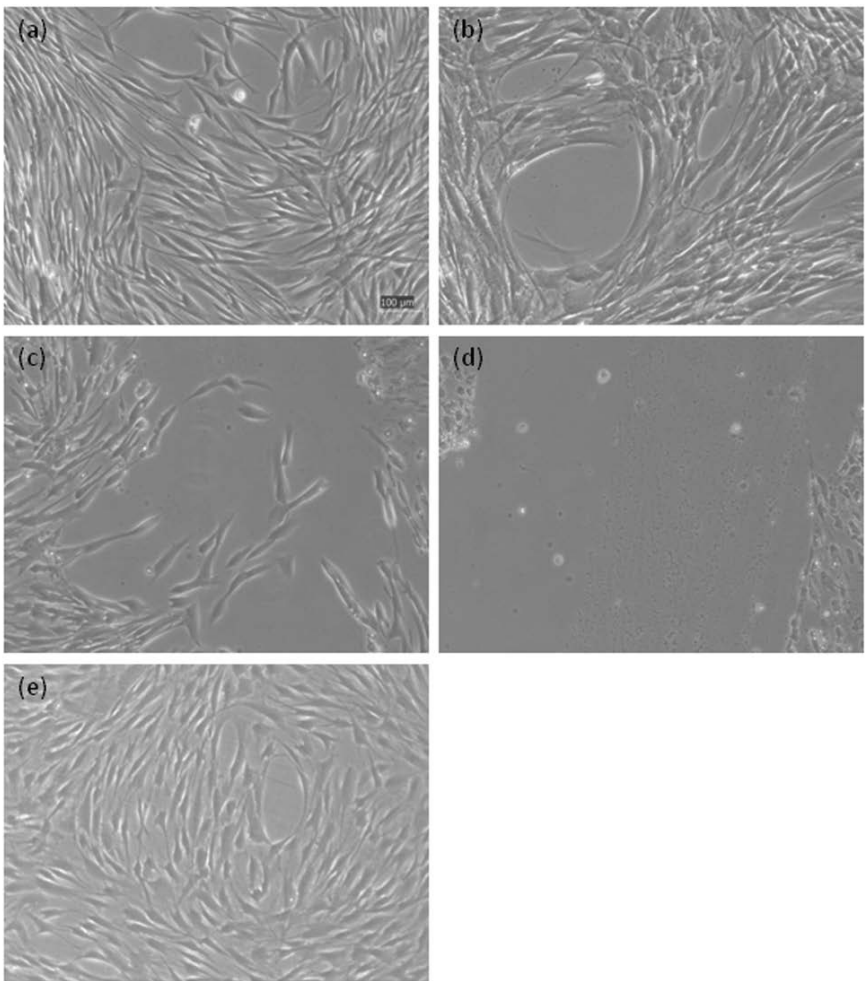

Fig. 7. *Micrograph at light microscopy after 24 h to wound hPDLSCs monolayer and treated with increasing concentration of RD7 cream.* ***a****) 0.5 mg/ml, (****b****) 1 mg/ml, (****c****) 2.5 mg/ml, (****d****) 5 mg/ml, and (****e****) control cells. (Mag: 10X)*

fully clarified that seems to predict the induction of collagen synthesis and fibroblast proliferation. A further object of the present invention is therefore a use in the treatment of skin wounds. Another feature is to act on a large group of skin diseases that cause an alteration of corneum stratum. Phenytoin may promote wound healing through multiple mechanisms, including stimulation of fibroblast proliferation, facilitation of collagen deposition, glucocorticoid antagonism, and antibacterial activity.

Previous data (yet unpublished) of RD7 cytotoxicity on human epithelial corneum cells seeded in different concentrations, showed that low concentration of RD7 do not inhibit the cell proliferation over 72 hours of incubation, confirming the results of the present study.

To the author's best knowledge, no studies in the literature have referred to the cytotoxicity of RD7 on different human cell cultures, thus there is a lack of information on this product that might lead to anecdotal and non-scientifically driven clinical procedures

In conclusion, the present *in vitro* study on the cytotoxicity of RD7 revealed that at low

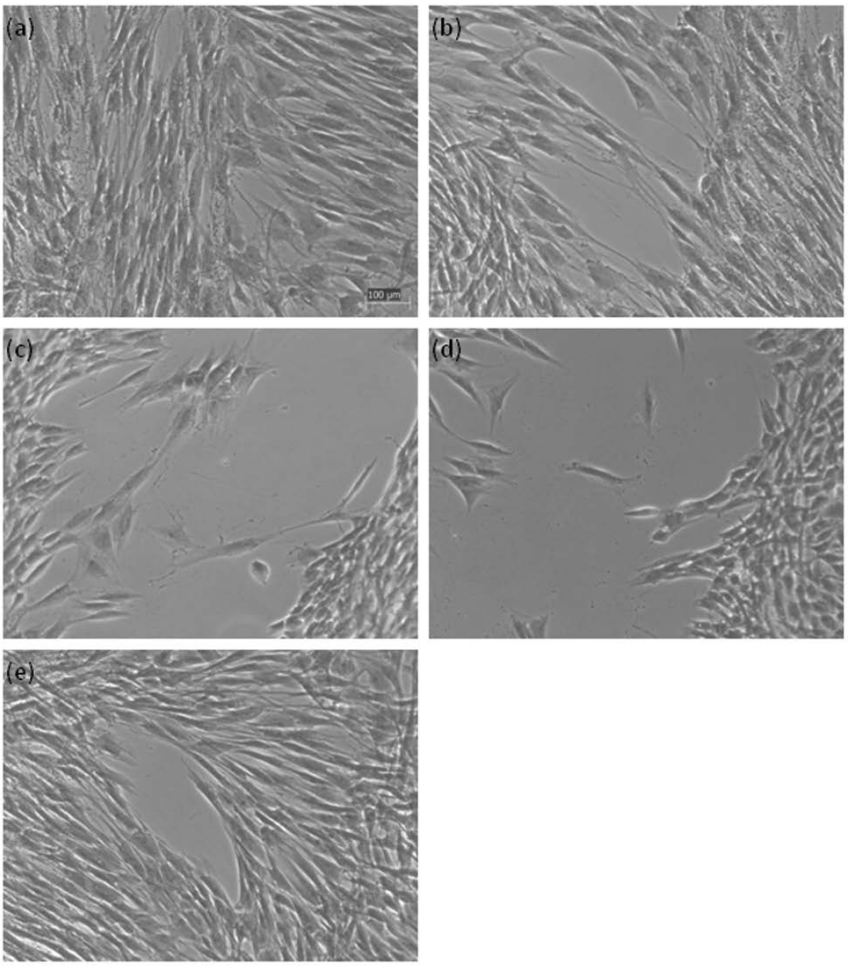

Fig. 8. *Micrograph at light microscopy after 24 h to wound hGFs monolayer and treated with increasing concentration of RD7 cream.* ***a****) 0.5 mg/ml, (****b****) 1 mg/ml, (****c****) 2.5 mg/ml, (****d****) 5 mg/ml and (****e****) control cells. (Mag: 10X)*

concentrations (0.5 and 1 mg/ml), RD7 stimulates cellular growth and proliferation of hPDLS and hGF cell cultures, while at a higher concentration it decreases the cell growth.

Although there is still a lack of information and there are no studies on the effects of RD7, it shows the ability to stimulate cell proliferation and migration at low concentrations (0.5 and 1 mg/ml), and may be effective in wound healing therapy.

Further studies will appreciate the optimal concentration to be used *in vivo*, by conducting clinical trials to appreciate the efficacy and safety of topical RD7 applications in treatment of different kinds of wounds.

ACKNOWLEDGEMENTS

This work was supported by OT ex-60% University of Chieti fund, and partly by PRIN 20102ZLNJ5 “Stem cells and 3D scaffolds: a novel construct in bone regeneration” financed by the Ministry of Education, University and Research

(M.I.U.R.), Rome, Italy.

REFERENCES

1. Esimone CO, Eck G, Duong TN, Uberla K, Proksch P, Grunwald T. Potential anti-respiratory syncytial virus lead compounds from Aglaia species. Pharmazie 2008; 63:768-73.
2. Diegelmann RF, Evans MC. Wound healing: an overview of acute, fibrotic and delayed healing. Front Biosci 2004; 9:283-89.
3. Clark RA. The commonality of cutaneous wound repair and lung injury. Chest 1991; 99:57S-60S.
4. Shetty S, Udupa S, Udupa L. Evaluation of antioxidant and wound healing effects of alcoholic and aqueous extract of ocimum sanctum linn in rats. Evid Based Complement Alternat Med 2008; 5:95-101.
5. Bowler PG, Duerden BI, Armstrong DG. Wound microbiology and associated approaches to wound management. Clin Microbiol Rev 2001; 14:244-69.
6. Thomas JC, Desrosiers M, St-Pierre Y, Lirette P, Bisaillon JG, Beaudet R, Villemur R. Quantitative flow cytometric detection of specific microorganisms in soil samples using rRNA targeted fluorescent probes and ethidium bromide. Cytometry 1997; 27:224-32.
7. Jeffery SL. Advanced wound therapies in the management of severe military lower limb trauma: a new perspective. Eplasty 2009; 9:e28.
8. Atiyeh BS. Nonsurgical management of hypertrophic scars: evidence-based therapies, standard practices, and emerging methods. Aesthetic Plast Surg 2007; 31:468-92.
9. Cuttle L, Naidu S, Mill J, Hoskins W, Das K, Kimble RM. A retrospective cohort study of Acticoat versus Silvazine in a paediatric population. Burns 2007; 33:701-7.
10. Cuttle L, Kempf M, Kravchuk O, et al. The efficacy of Aloe vera, tea tree oil and saliva as first aid treatment for partial thickness burn injuries. Burns 2008; 34:1176-82.
11. Rosdy M, Clauss LC. Cytotoxicity testing of wound dressings using normal human keratinocytes in culture. J Biomed Mater Res 1990; 24:363-77.
12. Paddle-Ledinek JE, Nasa Z, Cleland HJ. Effect of different wound dressings on cell viability and proliferation. Plast Reconstr Surg 2006; 117:110S-8S.
13. Burd A, Kwok CH, Hung SC, Chan HS, Gu H, Lam WK, Huang L. A comparative study of the cytotoxicity of silver-based dressings in monolayer cell, tissue explant, and animal models. Wound Repair Regen 2007; 15:94-104.
14. Van Den Plas D, De Smet K, Lens D, Sollie P. Differential cell death programmes induced by silver dressings in vitro. Eur J Dermatol 2008; 18:416-21.
15. Eleuterio E, Trubiani O, Sulpizio M, et al. Proteome of human stem cells from periodontal ligament and dental pulp. PLoS One 2013; 8:e71101.
16. Trubiani O, Toniato E, Di Iorio D, Diomede F, Merciaro I, D'Arcangelo C, Caputi S. Morphological analysis and interleukin release in human gingival fibroblasts seeded on different denture base acrylic resins. Int J Immunopathol Pharmacol 2012; 25:637-43.
17. Rodriguez LG, Wu X, Guan JL. Wound-healing assay. Methods Mol Biol 2005; 294:23-9.
18. Pruitt BA, McManus AT, Kim SH, Goodwin CW. Burn wound infections: current status. World J Surg 1998; 22:135-45.
19. Jones SG, Edwards R, Thomas DW. Inflammation and wound healing: the role of bacteria in the immuno-regulation of wound healing. Int J Low Extrem Wounds 2004; 3:201-8.

BORTEZOMIB-INDUCED PERIPHERAL NEUROTOXICITY IN HUMAN MULTIPLE MYELOMA-BEARING MICE

C. MEREGALLI[1], V.A. CAROZZI[1], B. SALA[1], A. CHIORAZZI[1], A. CANTA[1], N. OGGIONI[1], V. RODRIGUEZ-MENENDEZ[1], E. BALLARINI[1], C. CERESA[1], G. NICOLINI[1], L. CRIPPA[2], M. ORCIANI[3], G. CAVALETTI[1] and P. MARMIROLI[1]

[1]Experimental Neurology Unit and Milan Center for Neuroscience, Department of Surgery and Translational Medicine, University of Milan Bicocca, Monza (MB), Italy; [2]Veterinary Pathology Labs, ISTOVET, Monza, Italy; [3]Department of Clinical and Molecular Sciences—Histology, Marche Polytechnic University, Ancona, Italy

Received September 25, 2014 – Accepted December 19, 2014

The proteasome inhibitor bortezomib is an antineoplastic drug mainly used for the treatment of multiple myeloma (MM). Despite its effectiveness, bortezomib clinical use is often limited by the onset of peripheral neuropathy (BiPN). To better understand the mechanisms of BiPN several rat and mice models have been proposed, but no studies in MM-bearing animals allowing to test the antitumor activity of the selected schedules and the role of MM by itself in peripheral nervous system damage have been reported to date. Here, we carried out a study using immunodeficient C.B-17/Prkdcscid (SCID) mice injected with RPMI8266 human MM cells and treated with bortezomib 1 mg/kg once a week for five weeks. Animals were assessed with neurophysiological, behavioral and pathological methods and tumor volume measurement was performed along the study. At the end of the study BiPN was evident in bortezomib-treated animals, and this neurotoxic effect was evident using a schedule able to effectively prevent tumor growth. However, neurophysiological and pathological evidence of MM-induced peripheral nervous system damage was also reported. This model based on MM-bearing animals is more reliable in the reproduction of the clinical setting and it is, therefore, more suitable than the previously reported models of BiPN to study its pathogenesis. Moreover, it represents an optimal model to test the efficacy of neuroprotective agents and at the same time their non-interference with bortezomib antineoplastic activity.

Multiple myeloma (MM) is caused by uncontrolled growth of clonal B cell within the bone marrow (1). Treatment with corticosteroids and autologous stem cell transplantation in combination with chemotherapeutic drugs such as the proteasome inhibitor bortezomib (BTZ) and immunomodulatory agents such as thalidomide or lenalidomide has greatly improved survival in MM patients (2, 3). Unfortunately, bortezomib-induced peripheral neuropathy (BiPN) is a severe, potentially dose-limiting side effect of treatment in 10-37% of MM patients (4, 5), while nerve damage severity is lower

Key words: bortezomib, peripheral neuropathy, allodynia, multiple myeloma, antitumor activity, mice

Mailing address: Dr. Meregalli Cristina, PhD
Department of Surgery and Translational Medicine,
University of Milan-Bicocca,
Via Cadore 48,
20900, Monza (MB), Italy
Tel.: +3902 6448 8122 Fax: +3902 6448 8250
e-mail: cristina.meregalli@unimib.it

0393-974X (2015)

in patients treated with thalidomide or lenalidomide (6). BiPN is characterized by sensory neuropathy and neuropathic pain, reflecting damage of small myelinated and unmyelinated nerve fibers (7). Recent studies suggested that subcutaneous BTZ administration reduces the incidence and severity of BiPN, but the number of observations is still relatively low and follow-up quite limited (8).

A remarkable feature of BiPN is that its frequency is much higher in MM patients than in those with solid tumors, and this might reflect important aspects of its pathogenesis (9). Neuropathy in patients with MM before chemotherapy treatment involves individual and disease-related causes (10). The mechanism of BiPN and the interplay existing between drug administration and possible MM-related nerve damage are still unclear, but a multifactorial pathogenesis seems likely (5, 11).

To investigate this complex issue we first characterized the cytotoxicity of BTZ on human MM cells (12) and, based on our already established mice immunocompetent model reproducing BiPN (13), we set up a new human MM xenograft murine model, where the effect of MM on the peripheral nervous system with or without BTZ administration was investigated.

MATERIALS AND METHODS

Experiments were performed using immunodeficient C.B-17/Prkdcscid (SCID) mice (17-20g, Harlan Italy, Correzzana, Italy). Animals were handled and housed according to national (Italian Legislative Decree 26/2014, Gazzetta Ufficiale della Repubblica Italiana, No 40, February 18, 1992 and subsequent modifications) and international laws (EEC Council Directive 86/609; Italian, 1992; Guide for the Use of Laboratory Animals, U.S. National Research Council, 8th ed. 2011). The experimental plan was approved by the Ethics Committee for Animal Studies of the University of Milan Bicocca (approval ID: 0015349/12), and the guidelines for investigation of pain in animals from the International Association for the Study of Pain (IASP) were followed (14). Animals were housed at the University of Milan Bicocca U8 limited access animal facility in environmentally enriched ventilated cages with a 12-h light/dark cycle and food and water access *ad libitum*.

Drug

Bortezomib (LC Laboratories, Woburn, MA, USA) was solubilized in a vehicle solution composed by absolute ethanol/tween80/saline (5/5/90%) before each drug injection and it was intravenously administered attaining to a treatment schedule adapted from Carozzi et al. (13).

Experimental design

The study was designed to characterize the BiPN in SCID mice, and to describe antitumor activity and neurotoxicity of BTZ in the same MM-bearing murine model. The animals were randomized in 4 groups: untreated control animals (CTRL, n=8), BTZ-treated mice (BTZ, n=8); animals treated intravenously with BTZ 1 mg/kg once a week for 5 weeks), untreated MM mice (myeloma, n=8) and BTZ-treated MM-bearing mice (myeloma+BTZ, n=8). Human RPMI8226 MM cells were grown in floating culture in RPMI medium (EuroClone SpA, Pero, Italy) containing 10% fetal bovine serum (Hyclone Laboratories, Inc., Logan, UT), penicillin and streptomycin (EuroClone SpA, Pero, Italy). At the beginning of the study the animals in the myeloma and in the myeloma+BTZ groups were subcutaneously injected in the flank with $1x10^7$ RPMI8266 cells, and BTZ treatment was started when the tumor was measurable. Caliper measurement of the tumor diameters was performed once a week to estimate the tumor volume according to the following formula: ½ [(length (mm) x width (mm)]^2. Animals were sacrificed if the tumor was $\geq$ 2 cm^3 or if ulceration/necrosis occurred. During all the experiment the outcome parameters described in the following sections were assessed.

General toxicity

The general toxicity was assessed daily in mice by examinations for clinical signs. Moreover, body weight changes were measured weekly for the assessment of mice general health and BTZ dose adjustment.

Nerve conduction studies

At baseline and at the end of the treatment period, caudal and digital nerve conduction velocity (NCV) was determined using an electromyography apparatus (Myto2 ABN Neuro, Firenze, Italy) as previously described in the immunocompetent model (13). Briefly, caudal NCV was assessed by placing two recording electrodes proximally on the tail and simultaneously two stimulating needle electrodes were placed 3.5 cm distal to the recording electrodes. Moreover, the digital NCV was evaluated in the hind paw by placing the recording electrodes near the ankle and the stimulating electrodes in the fourth toe near the digital nerve.

Mechanical nociceptive threshold

At the end of experiment, the mechanical detection

threshold was measured by Dynamic Aesthesiometer test (model 37450, Ugo Basile Biological Instruments, Comerio, Italy) to assess the occurrence of neuropathic pain (allodynia) as previously described (15). Briefly, the mice were positioned in a plexiglas chamber on a wire platform, and a metallic filament was placed under the plantar surface of the hind paw of the animals. The filament induced a progressively increasing pressure with a gram force ramp of 1g/sec under the paw of the mice. The latency of paw-withdrawal of the mice was recorded as the mechanical nociceptive threshold index. The filament was applied three times to each paw and an average of measures indicated the value for each animal.

Histological methods

At the end of the study, the animals were sacrificed and sciatic nerve and dorsal root ganglia (DRG) samples were harvested and processed according to previously reported protocols (13, 16). Briefly, nerves and DRG were fixed in 3% glutaraldehyde and 4% paraformaldehyde/2% glutaraldehyde, respectively, and embedded in epoxy resin. Light microscopy observation was carried out on 1 µm-semi-thin sections stained with toluidine blue using a Nikon Eclipse E200 light microscope (Nikon, Firenze, Italia). Morphometric analysis was performed on DRG sensory neurons obtained from mice belonging to all experimental groups (13, 17) and, similarly, the size of axons and entire myelinated fiber was measured in sciatic nerve specimens in order to calculate the *g-ratio,* expressed as axonal diameter/entire fiber diameter (17).

To validate the MM xenograft model, at the time of sacrifice tumors were excised, fixed in 10% buffered formalin and embedded in paraffin according to standard histological techniques. Sections were stained with rabbit monoclonal anti-human protein IRF4 antibody (MUM1p) (1:1000, Dako, Carpinteria, CA, USA) directed against the product of the homologous gene involved in the myeloma-associated t(6;14) (p25;q32) (18).

Statistical analysis

Body weight changes, electrophysiological analysis, behavioral test and morphometric analysis of DRG and sciatic nerves were statistically analyzed by One-way ANOVA, Tukey–Kramer post hoc-test, using the GraphPad 3.0 software (GraphPad Software, La Jolla, CA, USA; significance level was set at $p<0.05$).

RESULTS

General toxicity of BTZ treatment

BTZ-treatment was well tolerated by the animals and no distress signs or mortality were observed. No significant decrease of BTZ-treated animals' body weight was detected in comparison with the control group at each time point till the end of BTZ-treatment. Moreover, no significant weight change was observed in the myeloma or in the myeloma+BTZ groups (data not shown).

BTZ effect on tumor growth

The inoculation of $1x10^7$ RPMI 8226 MM cells raised the onset of a measurable tumor in 80% of the exposed animals after 3 weeks. The average tumor volume was 128 mm^3 ± SD 70.9 at the beginning of treatment. As shown in Fig. 1, the neurotoxic schedule of BTZ treatment was able to effectively inhibit tumor growth ($p<0.05$ *vs* CTRL at day 7, 21; $p<0.01$ *vs* CTRL at day 14, 28).

Neurophysiological assessment

No difference between the groups was observed in the caudal or digital NCV at baseline (data not shown). BTZ-administration induced a significant reduction in both caudal and digital NCV (Fig. 2A-B) and a significant decrease was also observed in myeloma+BTZ mice (Fig. 2A-B). However, it is remarkable that in the untreated animals belonging to the myeloma group a significant decrease in digital NCV *vs* CTRL animals was also recorded (Fig. 2B;

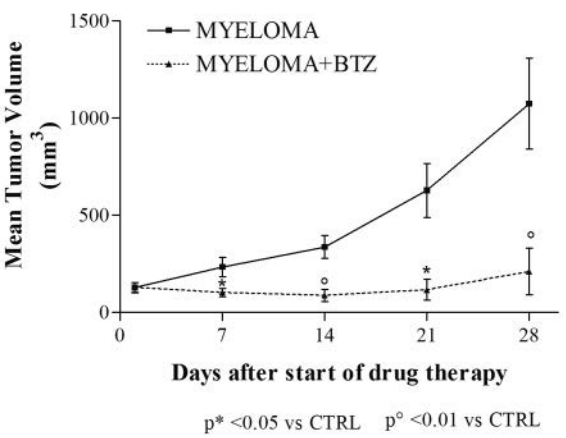

Fig. 1. *Evaluation of antitumor activity of bortezomib on myeloma growth in vivo. Groups: untreated myeloma mice (myeloma), BTZ-treated myeloma mice groups (myeloma+BTZ) (mean values ± SEM).*

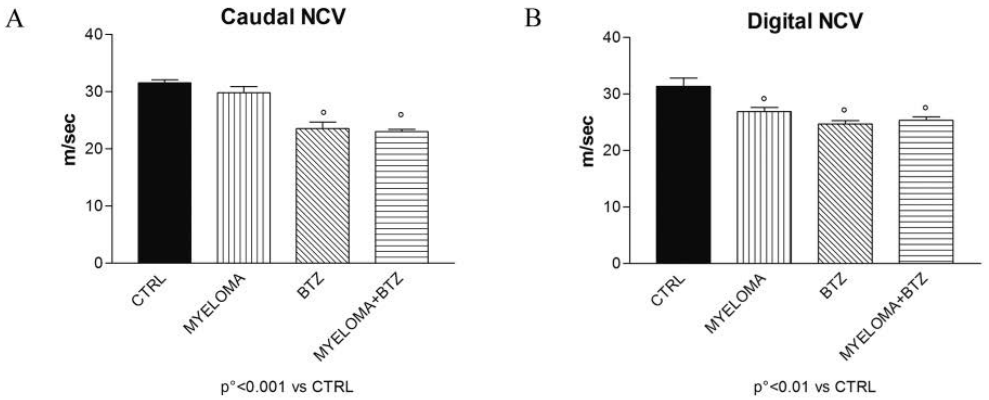

Fig. 2. *Study of neurotoxicity by caudal (**A**) and digital (**B**) nerve conduction velocity. Groups: untreated controls (CTRL), untreated myeloma mice (myeloma), BTZ-treated mice (BTZ) and BTZ-treated myeloma mice (myeloma+BTZ) (mean values ± SEM).*

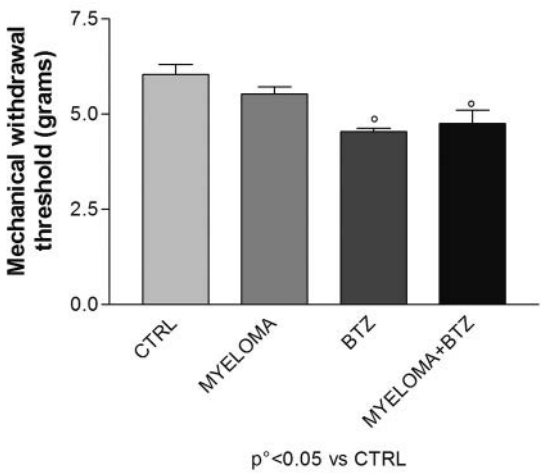

Fig. 3. *Analysis of mechanical allodynia by dynamic test. Groups: untreated controls (CTRL), untreated myeloma mice (myeloma), BTZ-treated mice (BTZ) and BTZ-treated myeloma mice groups (myeloma+BTZ) (mean values ± SEM).*

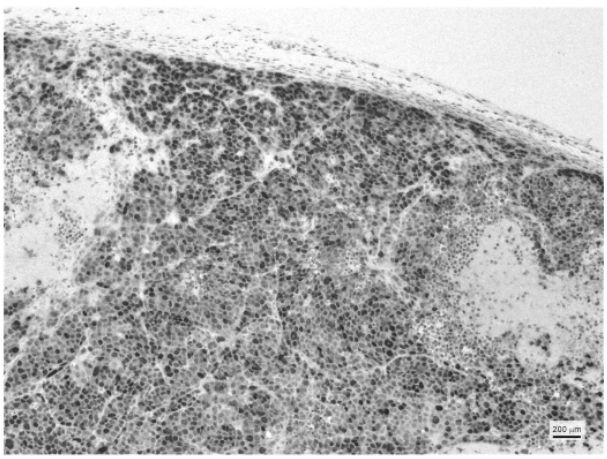

Fig. 4. *Histopathological characterization of inoculated plasmacytoma. A monoclonal antibody (MUM1p) was used to detect the expression of MUM1/IRF4 protein in the plasmacytoma.*

p<0.01).

Pain sensibility

At the end of BTZ-treatment, the BTZ-treated mice showed a significant decrease of mechanical threshold in respect to the control animals (Fig.3; p<0.05 *vs* CTRL), while the presence of MM in untreated mice did not alter their mechanical threshold.

Histopathology

Immunocytological staining of specimens from MM-bearing mice confirmed the growth of

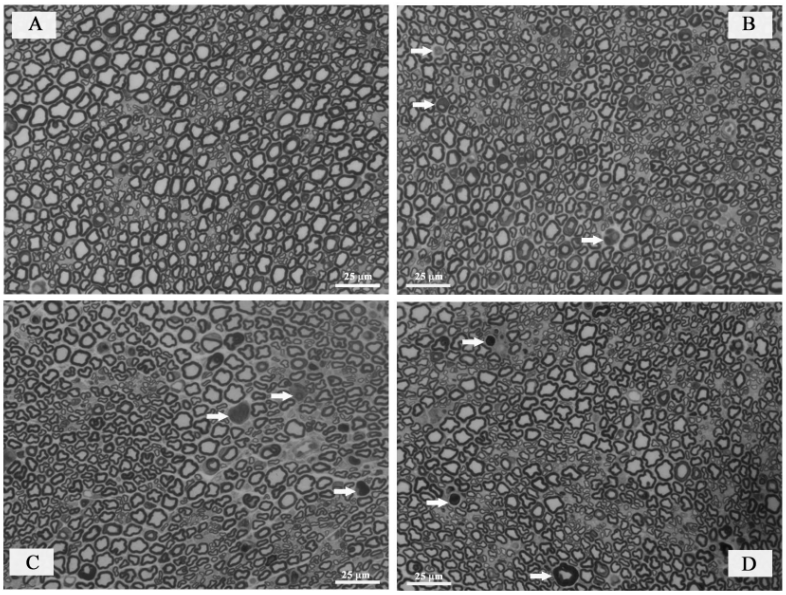

Fig. 5. *Morphological evaluation of sciatic nerve. The degeneration of fibers in the BTZ-treated animals (C, D) and in the myeloma-bearing mice (B) was indicated by arrows. Groups: (**A**) control mice; (**B**) myeloma-bearing mice; (**C**) BTZ-treated mice; (**D**) BTZ-treated myeloma-bearing mice.*

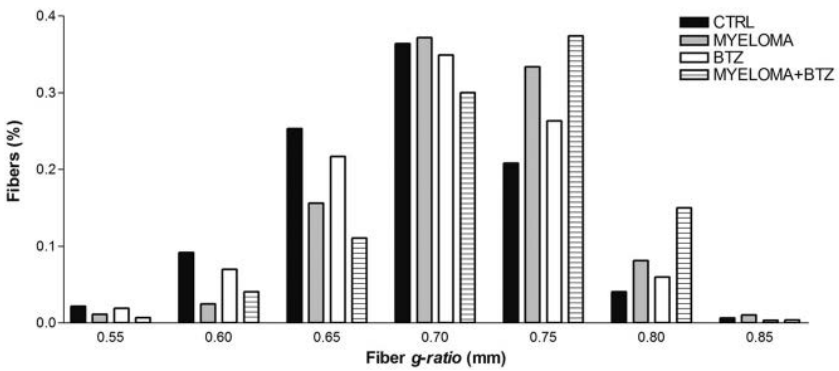

Fig. 6. *Evaluation of frequency distribution of the fiber g-ratio by morphometric assessment. Groups: control (CTRL), untreated myeloma mice (myeloma), BTZ-treated (BTZ) and BTZ-treated myeloma-bearing mice groups (myeloma+BTZ).*

inoculated tumor cells, with MUM1p expressed in the nuclei and cytoplasm of plasma cells and a small percentage of germinal center B cells (Fig. 4).

At the end of treatment period sciatic nerve examination of the BTZ-treated animals showed the occurrence of axonal degeneration of myelinated fibers intermingled with fibers with a normal axon but an apparent reduction of myelin thickness (Fig. 5C,D). Remarkably, these pathological aspects were present also in the specimens collected from the MM-bearing animals, but not treated with BTZ, although the severity of the pathological changes was less marked (Fig. 5B).

The morphometric analysis of sciatic nerve fibers which did not undergo axonal degeneration evidenced a shift to the right of fiber *g-ratio* distribution in

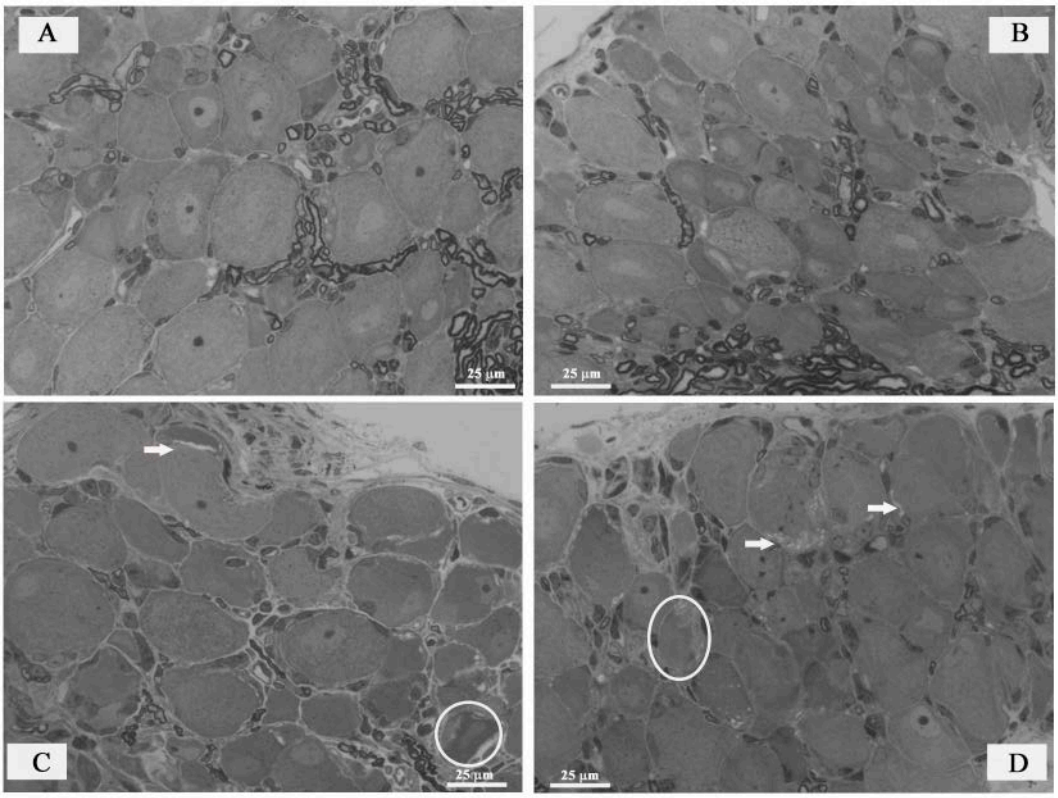

Fig. 7. *DRG morphological observation. Intracytoplasmatic vacuolization of satellite cells was indicated by arrows and neuronal degeneration was shown by circle in BTZ-treated and myeloma-bearing mice. Groups: (**A**) control mice; (**B**) myeloma-bearing mice; (**C**) BTZ-treated mice; (**D**) BTZ-treated myeloma-bearing mice.*

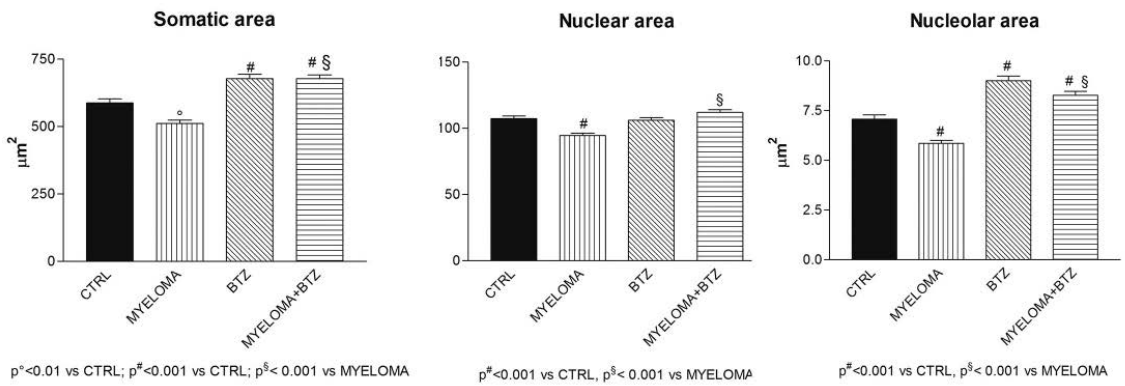

Fig. 8. *Morphometrical analysis of soma (**A**), nucleus (**B**) and nucleolus (**C**) of DRG. Groups: untreated controls (CTRL), untreated myeloma-bearing mice (Myeloma), BTZ-treated mice (BTZ), and BTZ-treated myeloma-bearing mice (myeloma+BTZ) (mean values ± SEM).*

BTZ, myeloma and myeloma+BTZ groups (Fig. 6). This shift reflected a significant increase of *g-ratio* value in BTZ ($p<0.01$ *vs* CTRL), myeloma ($p<0.001$ *vs* CTRL) and myeloma+BTZ ($p<0.001$ *vs* CTRL) mice groups and it was in agreement with the morphological observations suggesting the reduction of myelin thickness in non-degenerating myelinated fibers.

Light microscopic examination of DRG collected from BTZ mice at the end of the experiment showed cytoplasmic vacuolization in satellite cells and, more rarely, degeneration of sensory neurons (Fig. 7C); moreover, similar pathological changes were confirmed in the myeloma+BTZ mice (Fig. 7D), while DRG obtained from the myeloma animals had a normal appearance.

The morphometric evaluations of BTZ-treated DRG sensory neurons showed a statistically significant increase in somatic ($p<0.001$) and nucleolar ($p<0.001$) size compared to their controls (Fig. 8A,C). By contrast, a significant decrease of somatic, nuclear and nucleolar size in myeloma mice compared to CTRL was evidenced (Fig. 8A-C), while a significant increase in both somatic and nucleolar size in myeloma+BTZ mice was observed ($p<0.001$ *vs* CTRL). A significant increase of somatic, nuclear and nucleolar sizes was reported in myeloma+BTZ mice compared to myeloma ($p<0.001$).

DISCUSSION

BTZ has remarkably improved MM patient survival, but BiPN is still a serious and potentially dose-limiting side effect despite the lower neurotoxicity of subcutaneous administration (19). The mechanisms underlying BiPN are still unknown, although it was demonstrated that they include direct DRG toxicity and nerve fiber damage (20), and that the severity of BiPN is remarkably different when the drug is used to treat MM than solid tumors. This incomplete knowledge coupled with the evident clinical need indicate the importance of a deeper understanding of BiPN pathogenesis, also using innovative animal models encompassing both MM and BTZ effects (21). The reason for the use of the more complex model described in this study relies on the possible "paraneoplastic" effect of cancer, i.e. neurological damage in the absence of direct nerve invasion. Several animal studies evaluated the effects of BTZ on the peripheral nervous system. For instance, recent studies in immunocompetent BALB/c and Swiss OF1 mice (13, 22) extensively examined the features of animal BiPN using electrophysiological, behavioral and pathological methods. However, no animal studies were performed on MM-bearing animals, thus overlooking the complex nervous impairments typical of BTZ-treated MM patients.

The aim of this work was to move a substantial step forward in animal models of BiPN through the characterization of its neurophysiological, behavioral and neuropathological features in MM-bearing SCID mice to perform studies on the neurotoxicity of BTZ and on its antineoplastic activity against cancers of human origin. The selected dose of BTZ and the treatment schedule were based on our previous study on immunocompetent mice (13).

In the present work a significant inhibition of tumor growth was achieved in BTZ-treated mice, as reported in several murine xenograft models (23, 24) and this occurred at neurotoxic doses. In fact, in agreement with previous preclinical studies on immunocompetent mice (13, 22, 15, 25), BTZ-treatment induced evident neurophysiological changes consistent with the development of a sensory, painful neuropathy with axonal and myelin damage. All these experimental features are in substantial agreement with the results observed in clinical practice (4, 26). Moreover, it is a well accepted concept in clinical neurology that patients affected by MM frequently show a length-dependent peripheral neuropathy (27), and also this feature was reproduced in our model. In particular, recent clinical study demonstrated the development of subclinical neuropathy in treatment-naïve patients with MM, associated with peripheral innervation involvement (10).

Remarkable pathological changes were also observed in the DRG of BTZ-treated mice, and the morphological observations were supported by the morphometric demonstration of a significant enlargement of the neuronal cell body and of the nucleolus in comparison with healthy untreated controls. Moreover, similar increase in somatic and nuclear size was observed in other immunocompetent and immunodeficient strains such as Balb/c, CD1 and Hola Hsd Nu nu mice examined in our

laboratory (Meregalli C, personal observation), possibly representing the effect of a secondary compensatory up-regulation of proteasome subunit expression (28) induced by BTZ administration. In fact, Palanca et al. (29) reported in an acute model of BiPN a nucleolar hypertrophy as a compensatory activation of the nucleolar transcription in response to proteasome inhibition in DRG. Furthermore, Bruna and collaborators in a similar animal model demonstrated an increased proportion of medium to large size peptidergic DRG neurons, interpreted as a dynamic adaptive response of damaged neurons to BTZ exposure (22). Casafont et al. (30) demonstrated in DRG neurons of BTZ-treated animals an accumulation of ubiquitylated proteins and retention of poly(A) RNAs in nuclear granules, with a relevant dysfunction of transcription and RNA processing in the neuronal population. These events occurring at the intracellular level have already been reported also in non-neuronal cells treated with proteasome inhibitors (31).

It is remarkable that our results show that not only peripheral nerves, but also DRG neurons harvested from MM-bearing mice were significantly different from those obtained from control animals, showing generalized atrophy. While nerve damage in MM patients is well known, this effect of MM on DRG neurons has never been demonstrated at the morphometric level, although it is was reported as early as in 1958 that post-mortem DRG neurons obtained from MM patients were altered (32). The neurotoxic mechanisms of the different response of DRG cells to damage induced by BTZ and/or MM itself remain unclear and will require further studies, although it should be noted that BTZ administration is able to overcome the effect on DRG neurons when the drug is administered in MM-bearing mice.

In conclusion, our study demonstrates that BTZ has significant *in vivo* antitumor activity at doses that are tolerated by mice and are neurotoxic. Therefore, this model represents a new *in vivo* tool to study the pathogenesis of BiPN in a clinically-relevant setting, extending the information actually available in literature. Thus, this model might be exploited to perform a realistic and reliable assessment of the effectiveness and non-interference of neuroprotective agents during BTZ treatment. Finally, even if BTZ neurotoxicity is now more easily manageable, since BiPN might well represent a class-effect of proteasome inhibitors and side effects similar to BiPN might hamper the development and use of new effective drugs, the knowledge achievable through this model might also benefit new therapeutic developments.

ACKNOWLEDGEMENTS

Human RPMI8226 MM cells used in this study were donated by Dr. Maurizio D'Incalci ("Mario Negri" Institute for Pharmacological Research, Milan, Italy). Financial support: this work was supported in part by a research grant from Fondazione Banca del Monte di Lombardia to PM. The funders had no role in study design, data collection and analysis, decision to publish, or preparation of the manuscript.

REFERENCES

1. Kuiper R, Broyl A, de Knegt Y, et al. A gene expression signature for high-risk multiple myeloma. Leukemia 2012; 26:2406-13.
2. Brenner H, Gondos A, Pulte D. Recent major improvement in long-term survival of younger patients with multiple myeloma. Blood 2008; 111:2521-26.
3. Delforge M, Bladé J, Dimopoulos MA, et al. Treatment-related peripheral neuropathy in multiple myeloma: the challenge continues. Lancet Oncol 2010; 11:1086-95.
4. Argyriou AA, Bruna J, Marmiroli P, Cavaletti G. Chemotherapy-induced peripheral neurotoxicity (CIPN): an update. Crit Rev Oncol Hematol 2012; 82:51-77.
5. Richardson PG, Mitsiades C, Schlossman R, Ghobrial I, Hideshima T, Munshi N, Anderson KC. Bortezomib in the front-line treatment of multiple myeloma. Expert Rev Anticancer Ther 2008; 8:1053-72.
6. Cundari S, Cavaletti G. Thalidomide chemotherapy-induced peripheral neuropathy: actual status and new perspectives with thalidomide analogues derivatives. Mini Rev Med Chem 2009; 9:760-68.
7. Cata JP, Weng HR, Burton AW, Villareal H, Giralt S, Dougherty PM. Quantitative sensory findings in

patients with bortezomib-induced pain. J Pain 2007; 84:296-306.
8. Rajkumar SV. Multiple myeloma: 2013 update on diagnosis, risk-stratification, and management. Am J Hematol 2013; 88:226-35.
9. Roccaro AM, Vacca A, Ribatti D. Bortezomib in the treatment of cancer. Recent Pat Anticancer Drug Discov 2006; 1:397-403.
10. Kosturakis AK, He Z, Li Y, et al. Subclinical peripheral neuropathy in patients with multiple myeloma before chemotherapy is correlated with decreased fingertip innervations density. J Clin Oncol 2014; pii: JCO.2013.54.5418.
11. Broyl A, Corthals SL, Jongen JL, et al. Mechanisms of peripheral neuropathy associated with bortezomib and vincristine in patients with newly diagnosed multiple myeloma: a prospective analysis of data from the HOVON-65/GMMG-HD4 trial. Lancet Oncol 2010; 11:1057-65.
12. Meregalli C, Ceresa C, Canta A, et al. CR4056, a new analgesic I2 ligand, is highly effective against bortezomib-induced painful neuropathy in rats. J Pain Res 2012; 5:151-67.
13. Carozzi VA, Canta A, Oggioni N, et al. Neurophysiological and neuropathological characterization of new murine models of chemotherapy-induced chronic peripheral neuropathies. Exp Neurol 2010; 226:301-9.
14. Zimmermann M. Ethical considerations in relation to pain in animal experimentation. Acta Physiol Scand Suppl. 1986; 554:221-33.
15. Carozzi VA, Renn CL, Bardini M, et al. Bortezomib-induced painful peripheral neuropathy: an electrophysiological, behavioral, morphological and mechanistic study in the mouse. PLoS One 2013; 12e72995.
16. Persohn E, Canta A, Schoepfer S, et al. Morphological and morphometric analysis of paclitaxel and docetaxel-induced peripheral neuropathy in rats. Eur J Cancer 2005; 41:1460-6.
17. Cavaletti G, Tredici G, Marmiroli P, Petruccioli MG, Barajon I, Fabbrica D. Morphometric study of the sensory neuron and peripheral nerve changes induced by chronic cisplatin (DDP) administration in rats. Acta Neuropathol 1992; 84:364-71.
18. Falini B, Fizzotti M, Pucciarini A, et al. A monoclonal antibody (MUM1p) detects expression of the MUM1/IRF4 protein in a subset of germinal center B cells, plasma cells, and activated T cells. Blood 2000; 95:2084-92.
19. Richardson PG, Briemberg H, Jagannath S, et al. Frequency, characteristics, and reversibility of peripheral neuropathy during treatment of advanced multiple myeloma with bortezomib. J Clin Oncol 2006; 24:3113-20.
20. Broyl A, Jongen JL, Sonneveld P. General aspects and mechanisms of peripheral neuropathy associated with bortezomib in patients with newly diagnosed multiple myeloma. Semin Hematol 2012; 49:249-57.
21. Kyle RA, Rajkumar SV. Treatment of multiple myeloma: a comprehensive review. Clin Lymphoma Myeloma 2009; 9:278-88.
22. Bruna J, Udina E, Alé A, Vilches JJ, Vynckier A, Monbaliu J, Silverman L, Navarro X. Neurophysiological, histological and immunohistochemical characterization of bortezomib-induced neuropathy in mice. Exp Neurol 2010; 223:599-608.
23. Amiri KI, Horton LW, LaFleur BJ, Sosman JA, Richmond A. Augmenting chemosensitivity of malignant melanoma tumors via proteasome inhibition: implication for bortezomib (VELCADE, PS-341) as a therapeutic agent for malignant melanoma. Cancer Res 2004; 64:4912-8.
24. Cusack JC Jr, Liu R, Houston M, Abendroth K, Elliott PJ, Adams J, Baldwin AS Jr. Enhanced chemosensitivity to CPT-11 with proteasome inhibitor PS-341: implications for systemic nuclear factor-kappaB inhibition. Cancer Res 2001; 61:3535-40.
25. Bruna J, Alé A, Velasco R, Jaramillo J, Navarro X, Udina E. Evaluation of pre-existing neuropathy and bortezomib retreatment as risk factors to develop severe neuropathy in a mouse model. J Peripher Nerv Syst 2011; 16:199-212.
26. Badros A, Goloubeva O, Dalal JS, Can I, Thompson J, Rapoport AP, Heyman M, Akpek G, Fenton RG. Neurotoxicity of bortezomib therapy in multiple myeloma: a single-center experience and review of the literature. Cancer 2007; 110:1042-9.
27. Kelly JJ Jr, Kyle RA, Miles JM, O'Brien PC, Dyck PJ. The spectrum of peripheral neuropathy in myeloma. Neurology 1981; 31:24-31.
28. Lee CS, Tee LY, Warmke T, Vinjamoori A, Cai

A, Fagan AM, Snider BJ. A proteasomal stress response: pre-treatment with proteasome inhibitors increases proteasome activity and reduces neuronal vulnerability to oxidative injury. J Neurochem 2004; 91:996-1006.

29. Palanca A, Casafont I, Berciano MT, Lafarga M. Reactive nucleolar and Cajal body response to proteasome inhibition in sensory ganglion neurons. Bioch et Bioph Acta 2014; 848-859.
30. Casafont I, Berciano MT, Lafarga M. Bortezomib induces the formation of nuclear poly(A) RNA granules enriched in Sam68 and PABPN1 in sensory ganglia neurons. Neurotox Res 2010; 17:167-78.
31. Zimmermann J, Erdmann D, Lalande I, Grossenbacher R, Noorani M, Fürst P. Proteasome inhibitor induced gene expression profiles reveal overexpression of transcriptional regulators ATF3, GADD153 and MAD1. Oncogene 2000; 8:2913-20.
32. Dickenman RC, Chason JL. Alterations in the dorsal root ganglia and adjacent nerves in the leukemias, the lymphomas and multiple myeloma. Am J Pathol 1958; 34:349-61.

TRANSCRIPTIONAL ACTIVITY OF NEUTROPHILS EXPOSED TO HIGH DOSES OF COLCHICINE: SHORT COMMUNICATION

G. MANUKYAN[1,2], M. PETREK[1], Z. NAVRATILOVA[1], S. MARGARYAN[2] and A. BOYAJYAN[3]

[1]Department of Pathological Physiology, Faculty of Medicine and Dentistry, Palacky University, Olomouc, Czech Republic; [2]Group of Molecular and Cellular Immunology, Institute of Molecular Biology, National Academy of Sciences, Yerevan, Armenia; [3]Laboratory of Macromolecular Complexes, Institute of Molecular Biology, National Academy of Sciences, Yerevan, Armenia

Received October 22, 2014 – Accepted December 3, 2014

Colchicine is an antimitotic drug which binds to tubulin and at high doses results in cytoskeleton disruption. Colchicine is believed to be an anti-inflammatory agent, though its modulatory effects on the level and transcriptional activity of genes is still a matter of debate. There is growing evidence that alterations in the cytoskeleton exert specific effects on the expression of various genes. This study was undertaken to analyze whether disrupting the microtubule cytoskeleton by colchicine modulates transcriptional levels of MEFV, NF-κB p65, NLRP3, HMGB1, and caspase-3 in neutrophils from patients with familial Mediterranean fever (FMF) and healthy subjects. In the present study, colchicine caused increased expression of NLRP3 (p=0.007) and MEFV (p=0.03), but had no effect on caspase-3, NF-κB p65 and HMGB1 genes in healthy neutrophils. FMF neutrophils were less responsive to the drug treatment. This study supports the hypothesis that, being an anti-inflammatory agent, colchicine at relatively high concentrations might lead to the activation of pro-inflammatory signalling pathways in neutrophils.

Cellular activity is partly regulated by the internal organization of the cytoskeletal network (tubulin, actin, filaments) (1), and many intracellular signalling pathways require the correct working of this network to become specific and efficient (2). Disruption of the cytoskeleton results in signal impairment. The antimitotic agent colchicine (COL) is an alkaloid which acts intracellularly to alter microtubule dynamics. Colchicine binds specifically to tubulin, inhibiting its polymerization into microtubules (3), and at high concentrations causes microtubule depolymerization (4). It is a well-known drug for treatment and prophylaxis of inflammatory disorders such as acute gout, pseudogout or Behçet's disease (5). COL is not the first-line treatment for these diseases because of its serious side effects (6); for familial Mediterranean fever (FMF), however, it is the drug of choice, allowing extended periods of remission as well as preventing amyloidosis, the main and potentially lethal complication of the disease (7).

FMF is a hereditary autoinflammatory syndrome characterized by seemingly unprovoked acute attacks of polyserositis and fever followed by attack-free periods. FMF is caused by mutations in the *MEFV* gene encoding the protein pyrin (8, 9) which

Key words: colchicine, neutrophils, familial Mediterranean fever, mRNA

Mailing address: Dr. Gayane Manukyan,
Group of Molecular and Cellular Immunology,
Institute of Molecular Biology,
National Academy of Sciences,
7 Hasratyan St., 0014 Yerevan, Armenia
Tel.: +37410231499 Fax: +37410282061
e-mail: g_manukyan@mb.sci.am

0393-974X (2015)

is expressed primarily by cells of myeloid lineage, mainly polymorphonuclear neutrophils (PMNs), eosinophils, and monocytes (8). Through cognate pyrin domain association, pyrin interacts with ASC (apoptosis-associated speck-like protein with a caspase recruitment domain) and thus participates in the regulation of apoptosis, inflammation, and cytokine processing (10). Evidence of pyrin association with microtubules and actin filaments has led to the suggestion that pyrin can regulate inflammation also at the level of the leukocyte cytoskeleton (11).

COL is thought to inhibit various functions of neutrophils, including mitosis, adhesion, migration, and phagocytosis (12). Another mechanism by which COL exerts its anti-inflammatory properties is inhibition of monosodium urate (MSU) crystal-induced NALP3 inflammasome-driven caspase-1 activation (13). While other, i.e. antimitotic, properties of colchicine are well known, its effect on gene expression is still a matter of debate (14, 15). Our recent study was concerned with the *in vivo* effects of high doses of COL on late transcriptional activity of several target genes. The obtained data showed selective increase of IL-1β and IL-8 mRNAs in healthy and FMF PMNs, and decreased expression of caspase-1 in FMF PMNs (16). In the present study, we continued our ongoing investigation of modulatory effects of COL on mRNA transcripts of *MEFV*, nuclear factor kappa B subunit *NF-κB* p65 (*RELA*), NLR family, pyrin-containing domain 3 *(NLRP3*), high-mobility group box 1 (*HMGB1*), and caspase-3 (*CASP3*) were evaluated in colchicine-treated peripheral PMNs *in vitro.*

MATERIALS AND METHODS

Study subjects

Sixteen FMF patients in remission (12 males, 4 females; age 14-41 years, mean age 24.2 years) were enrolled in the study. Clinical diagnosis and definition of the disease period were based on the Tel-Hashomer criteria. Genetic confirmation of the *MEFV* mutations was performed at the Centre of Medical Genetics, Yerevan, Armenia. All patients were treated with colchicine (1.0-1.5 mg per day). The control group included 11 sex- and age-matched healthy individuals without a family history of FMF (7 males, 4 females; age 22-39 years, mean age 27.3 years). The study was approved by the Ethics Committee of the Institute of Molecular Biology of the NAS RA (IRB IORG0003427) and written informed consent was obtained from all subjects.

Preparation and culture of neutrophils

Neutrophils were isolated from blood by density gradient centrifugation using Histopaque-1077 (Sigma, St. Louis, USA). Neutrophils ($5x10^6$ cells/mL) were cultured at 37°C in RPMI 1640 supplemented with 10% foetal calf serum, 2 mmol/L L-glutamine, 1 mM sodium pyruvate, 5 mM HEPES, 100 units of penicillin, and 100 μg of streptomycin in the absence or presence of 1 μg/mL Colchicine (Sigma) in a total volume of 1 mL for 24 hours. After stimulation, neutrophils were washed once with cold PBS and stored in 150 μL of RNAlater (Qiagen, Hilden, Germany) at -20°C until RNA extraction.

RNA extraction and RT-qPCR

Isolation of total RNA, cDNA synthesis, and real-time RT-qPCR were conducted as previously described (17). PCR assays were conducted with predeveloped TaqMan assay primers and probes (NLRP3: Hs00918082_m1, RELA: Hs00153294_m1; Applied Biosystems) and (CASP3: Hs.PT.47.2840197, HMGB1: Hs.PT.47.1940089; Integrated DNA Technologies) or were self-developed with the following oligonucleotide sequences: PSMB2 (forward) –5'-AGA GGG CAG TGG AAC TCC TT-3', PSMB2 (reverse) –5'-AGG TTG GCA GAT TCA GGA TG-3', PSMB2 LNA probe #50; RPL32 (forward) - 5'-GAA GTT CCT GGT CCA CAA CG-3', RPL32 (reverse) - 5'-GCG ATC TCG GCA CAG TAA G-3', RPL32 LNA probe #17; MEFV (4-5 exons) (forward) –5'-GGA GAA GGC AGT GAG CTT TC-3', MEFV (reverse) –5'-TGC TGC TCC AGG AAG TAG TAC A -3', MEFV LNA probe #78. The RPL32 gene was used as a reference gene for normalization of targeted mRNA quantification data in circulating neutrophils; a human universal reference RNA (Stratagene, La Jolla, USA) was used as the calibrator at a concentration of 1.25 ng of RNA/reaction in quadruplicates. Relative expression was calculated using the second derivative method (Rotor Gene software 6.1.71, Corbett Research).

Statistical analysis

Statistical analyses were performed using the statistical software Graph Pad Prism 5.01 (Graph Pad Software, San Diego, USA). The results are expressed as the mean ± SEM. Data were compared using paired (unstimulated versus stimulated) and unpaired (all other comparisons) Student's *t*-tests. P-values <0.05 were considered as significant.

RESULTS

Effect of colchicine on the expression of RELA, MEFV, CASP3, NLRP3 and HMGB1 mRNAs

To evaluate the effects of COL on gene expression known to be involved in inflammation and apoptosis,

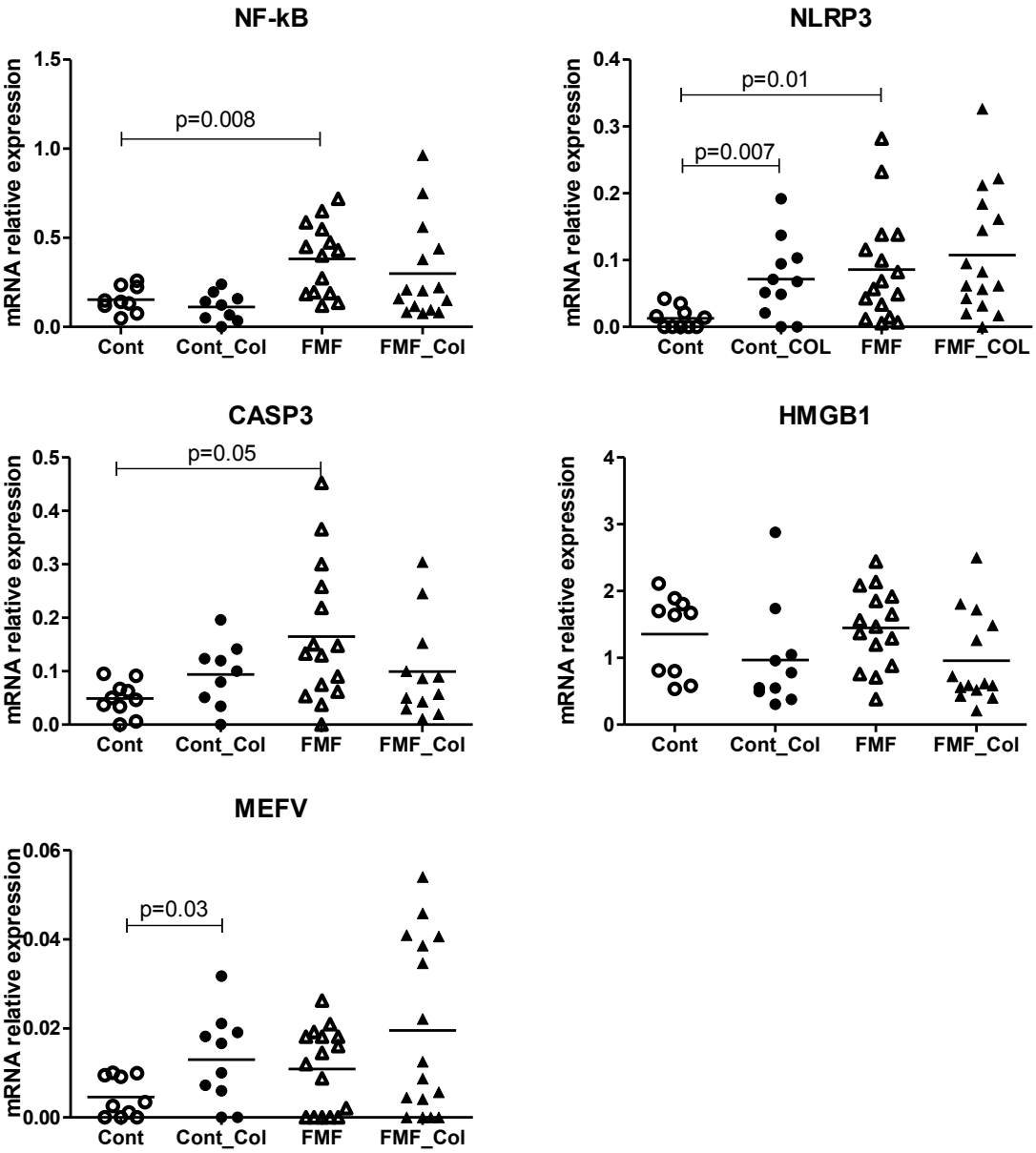

Fig. 1. *Scatterplots showing effects of COL on gene expression by PMNs isolated from FMF patients and healthy subjects as assessed by RT-qPCR. Isolated blood neutrophils from 16 patients with FMF in remission and 11 healthy controls (Cont) were cultured for 24 h in the presence and absence of COL (1μg/mL). The expression of genes of interest was normalized to that of RPL32. Horizontal bars represent the mean values for each group*

neutrophils from FMF patients and healthy controls were treated with 1 μg/mL of colchicine for 24 hours. COL significantly up-regulated expression of NLRP3 (untreated *vs* treated; 0.013±0.005 *vs* 0.072±0.017, p=0.007) and MEFV (0.004±0.001 *vs* 0.013±0.003, p=0.03) genes in the cells from healthy subjects; by contrast, NF-κB p65, caspase-3 and HMGB1 transcripts did not show any modulation (p>0.05). In patient cells, COL had no significant effect on the studied target genes (Fig. 1).

Genes expressed differentially between FMF patients and control subjects

When comparing samples from healthy and diseased cells cultured with COL, differences in gene expression between the two groups were observed.

However, the differences were not robust enough to generate an acceptable p-value. Expression of three genes was altered in the cells cultured only with media with a predominant up-regulation in patients. The genes differentially expressed between patients and controls cultured only in media (control culture) were NF-κB p65 (controls *vs* patients; 0.144±0.029 *vs* 0.396±0.069, p=0.009), NLRP3 (0.013±0.005 *vs* 0.086±0.020, p=0.01) and CASP3 (0.052±0.012 *vs* 0.160±0.037, p=0.05) which were up-regulated in the patient group (Fig. 1).

DISCUSSION

Colchicine has a range of biologic and pharmacologic effects, mostly in preventing FMF attacks and a serious complication called systemic amyloidosis AA (7, 18). COL exerts various anti-inflammatory effects mostly related to microtubule disruption and depolymerization in a dose-dependent manner (3, 4, 12). Having observed the capacity of COL to induce the expression of a number of pro-inflammatory genes (16), we intended to analyze the influence of this drug on expression of MEFV, NF-κB p65, NLRP3, HMGB1, and caspase-3 genes.

In a study by Martinon et al., administration of COL produced anti-inflammatory effects by suppressing the production of IL-1β in MSU crystal-induced model, along with unchanged levels of pro-IL-1β (13). Similar results were reported in our previous study with regard to decreased mRNA transcripts of caspase-1 (16), which might be an important downstream mechanism to control inflammation through the reduced IL-1β maturation. However, up-regulated expression of NLRP3 in the present study does not completely support this concept. Increased expression of pro-inflammatory mediators exposed by COL can be explained by reorganization of the microtubule network. There is growing evidence that IL-1β expression and cytoskeletal associations are interrelated (19). Furthermore, cytoskeleton disruptors may directly alter mitochondrial functions and thereby lead to mitochondrial destabilization and damage which was found to be required for NLRP3 inflammasome activation (20). At first glance, the activation of certain pro-inflammatory mediators *in vitro* seems rather contradictory to the conventional view that COL is an anti-inflammatory agent. However, a number of isolated reports have already suggested additional effects of Col on leukocytes and showed activation of pro-inflammatory signalling pathways in neutrophils (16, 21).

FMF is caused by abnormal activation of leukocytes, and unprovoked trafficking of these cells into the affected sites (9, 18). Whether efficacy of COL in FMF is limited by its antimitotic activity is still unclear. It is accepted that this protein is a part of colchicine-sensitive inflammatory pathway. There is a possibility that microtubule dynamic changes have specific effects on *MEFV* gene expression. Indeed, we demonstrated increased mRNA levels of MEFV after COL treatment in healthy PMNs, which is in contrast with data showing no enhanced effect of this drug in these cells (8). The discrepancy may arise in part from differences in the COL concentrations used. Furthermore, the expression patterns of the MEFV gene are dependent on the cellular source. For example, MEFV is up-regulated upon COL exposure in monocytes (8) and peritoneal fibroblasts (22). Compared to healthy cells, FMF neutrophils were less responsive towards the drug. Among the possible reasons that could account for the observed 'hyporesponsiveness' of FMF cells to COL is drug accumulation in these cells due to colchicine treatment received by all the studied FMF patients.

Need to note here that FMF neutrophils, when cultured alone in RPMI media, displayed elevated mRNA levels of NF-κB p65, NLRP3, and caspase-3 compared to healthy PMNs. These results are consistent with our previous data (16, 17) showing high sensitivity of FMF neutrophils towards stress conditions, thus suggesting that increased activation of FMF neutrophils might be due to the host-derived ligands.

Although the importance of the actin cytoskeleton in the execution phase of apoptosis (i.e. release/retraction; blebbing; fragmentation) is well established (23), the significance of microtubules in the executive phase of apoptosis is still a matter of debate. Recent studies have revealed that microtubules have important contributions in late apoptosis, and caspases are important in coordinating apoptotic microtubule dynamics (24). It has been shown that colchicine at micromolar doses can induce apoptosis in a number of cells (25, 26), mainly through intrinsic pathway (26). Altered mitochondrial functions caused by cytoskeleton

disruption contribute to the release of pro-apoptotic signals and caspase-3 activation (27). In our study, however, the microtubule disrupting agent had no effect on caspase-3 levels, which is in consistence with the results demonstrating the absence of COL-induced alteration of the apoptotic rate of neutrophils (data not shown).

In conclusion, COL-mediated cytoskeleton stress may play a modulatory role on the expression of inflammatory genes and exert specific and opposite effects in a dose-dependent manner, being dependent on the cellular source and experimental conditions; the mechanisms of its action are more complex than initially thought. Further understanding of the molecular mechanisms by which COL interferes with inflammatory pathways should be sought.

ACKNOWLEDGEMENTS

This study was supported by Palacky University Olomouc grant no. IGA_PU_LF_2014_012, CZ.1.07/2.3.00/30.0004 and State Committee Science MES RA, in frame of the research project no. SCS 13-1F236.

REFERENCES

1. Fuchs E, Karakesisoglou I. Bridging cytoskeletal intersections. Genes Dev 2001; 15:1-14.
2. Willard FS, Crouch MF. Nuclear and cytoskeletal translocation and localization of heterotrimeric G-proteins. Immunol Cell Biol 2000; 78:387-94.
3. Sackett DL, Varma JK. Molecular mechanism of colchicine action: induced local unfolding of beta-tubulin. Biochemistry 1993; 32:13560-5.
4. Margolis RL, Wilson L. Addition of colchicine–tubulin complex to microtubule ends: the mechanism of substoichiometric colchicine poisoning. Proc Natl Acad Sci U S A 1977; 74:3466-70.
5. Terkeltaub RA. Colchicine update: 2008. Semin Arthritis Rheum 2009; 38:411-19.
6. Jordan KM, Cameron JS, Snaith M, Zhang W, Doherty M, Seckl J, Hingorani A, Jaques R, Nuki G; British Society for Rheumatology and British Health Professionals in Rheumatology Standards, Guidelines and Audit Working Group (SGAWG). British Society for Rheumatology and British Health Professionals in Rheumatology guideline for the management of gout. Rheumatology 2007; 46:1372-4.
7. Goldfinger SE. Colchicine for familial Mediterranean fever. N Engl J Med 1972; 287:1302.
8. Centola M, Wood G, Frucht DM, et al. The gene for familial Mediterranean fever, MEFV, is expressed in early leukocyte development and is regulated in response to inflammatory mediators. Blood 2000; 95:3223-31.
9. Stojanov S1, Kastner DL. Familial autoinflammatory diseases: genetics, pathogenesis and treatment. Curr Opin Rheumatol 2005; 17:586-99.
10. Gumucio DL, Diaz A, Schaner P, Richards N, Babcock C, Schaller M, Cesena T. Fire and ICE: the role of pyrin domain-containing proteins in inflammation and apoptosis. Clin Exp Rheumatol 2002; 20 (S):S45-S53.
11. Mansfield E, Chae JJ, Komarow HD, Brotz TM, Frucht DM, Aksentijevich I, Kastner DL. The familial Mediterranean fever protein, pyrin, associates with microtubules and colocalizes with actin filaments. Blood 2001; 98:851-9.
12. Dalbeth N, Lauterio TJ, Wolfe HR. Mechanism of action of colchicine in the treatment of gout. Clin Ther 2014: S0149-2918(14)00457-3.
13. Martinon F, Pétrilli V, Mayor A, Tardivel A, Tschopp J. Gout-associated uric acid crystals activate the NALP3 inflammasome. Nature 2006; 440:237-41.
14. Santell L, Marotti K, Bartfeld NS, Baynham P, Levin EG. Disruption of microtubules inhibits the stimulation of tissue plasminogen activator expression and promotes plasminogen activator inhibitor type 1 expression in human endothelial cells. Exp Cell Res 1992; 201:358-65.
15. Nair RR, Rodgers JR, Schwarz LA. Enhancement of transgene expression by combining glucocorticoids and anti-mitotic agents during transient transfection using DNA-cationic liposomes. Mol Ther 2002; 5:455-62.
16. Manukyan G, Petrek M, Tomankova T, Martirosyan A, Tatyan M, Navratilova Z, Paulu D, Kriegova E. Colchicine modulates expression of pro-inflammatory genes in neutrophils from patients with familial Mediterranean fever and healthy subjects. J Biol Regul Homeost Agents 2013; 27:329-36.
17. Manukyan G, Petrek M, Kriegova E, Ghazaryan K, Fillerova R, Boyajyan A. Activated phenotype

of circulating neutrophils in familial Mediterranean fever. Immunobiology 2013; 218:892-8.
18. Ben-Chetrit E, Levy M. Familial Mediterranean fever. Lancet 1998; 351:659-64.
19. Böcker U, Sirenko OI, Morris JS, Sartor RB, Singer MV, Haskill JS, Watson JM. Expression and localization of IL-1beta mRNA is interrelated with cytoskeletal rearrangement in monocytes stimulated by adherence: a light microscopy in situ hybridization study. Immunol Cell Biol 2001; 79:444-53.
20. Misawa T, Takahama M, Kozaki T, Lee H, Zou J, Saitoh T, Akira S. Microtubule-driven spatial arrangement of mitochondria promotes activation of the NLRP3 inflammasome. Nat Immunol 2013; 14:454-60.
21. Tsai MA, Waugh RE, Keng PC. Passive mechanical behavior of human neutrophils: effects of colchicine and paclitaxel. Biophys J 1998; 74:3282-91.
22. Abedat S, Urieli-Shoval S, Shapira E, Calko S, Ben-Chetrit E, Matzner Y. Effect of colchicine and cytokines on MEFV expression and C5a inhibitor activity in human primary fibroblast cultures. Isr Med Assoc J 2002; 4:7-12.
23. Franklin-Tong VE, Gourlay CW. A role for actin in regulating apoptosis/programmed cell death: evidence spanning yeast, plants and animals. Biochem J 2008; 413:389-404.
24. Moss DK, Betin VM, Malesinski SD, Lane JD. A novel role for microtubules in apoptotic chromatin dynamics and cellular fragmentation. J Cell Sci 2006; 119:2362-74.
25. Bonfoco E, Ceccatelli S, Manzo L, Nicotera P. Colchicine induces apoptosis in cerebellar granule cells. Exp Cell Res 1995; 218:189-200.
26. Chen XM, Liu J, Wang T, Shang J. Colchicine-induced apoptosis in human normal liver L-02 cells by mitochondrial mediated pathways. Toxicol In Vitro 2012; 26:649-55.
27. Marks N, Berg MJ, Guidotti A, Saito M. Activation of caspase-3 and apoptosis in cerebellar granule cells. J Neurosci Res 1998; 52:334-41.

LETTER TO THE EDITOR

CLINICAL RESEARCH ON NEUROBLASTOMA BASED ON SERUM LACTATE DEHYDROGENASE

QM. PANG[1,2], K. LI[3,4], LJ. MA and RP. SUN[1]

[1]Pediatric Department, Qilu Hospital of Shandong University, Jinan, China; [2]Pediatric Department, Zibo Central Hospital, Zibo, China; [3]Department of Gynaecology and Obstetrics, Affiliated Hospital of Shandong Academy of Medical Sciences, Jinan, China; [4]Shandong Academy of Medical Sciences, Jinan, China

Received November 22, 2014 – Accepted December 19, 2014

In recent years, more and more scholars tend to study neuroblastoma (NB) since it possesses increasing morbidity, but lack of effective treatment. This paper aims to investigate variation and clinical significance of the neuron-specific enolase (NSE) and lactic dehydrogenase (LDH) level in serum of children with NB before and after Auto Peripheral Blood Stem Cell Transplantation (APBSCT). A total of 90 children with NB from various hospitals were included in this research, and we analyzed the relationship between levels of NSE and LDH and the change of disease by comparing the two levels before and after APBSCT treatment. The results indicated that the positive rate of NSE in serum was high before treatment, and the levels of NSE and LDH were remarkably higher than those when the treatment was valid; after comprehensive treatment of chemotherapy, excision and radiotherapy, there was a significant difference of NSE and LDH levels in serum between children with complete remission (CR) and those with partial remission (PR); however, no significant differences of NSE and LDH levels were found among children in progressive stage compared to before treatment. It is believed that NSE and LDH levels are associated to the recurrence and treatment effect of NB, proving that both can reflect tumor load, therefore they can be taken as the auxiliary indicators for monitoring curative effects of NB treatment.

Neuroblastoma (NB) mostly occurs in childhood, originates from primitive neural crest cells, composed of undifferentiated sympathetic nerve cells (1-3). Usually, NB is discovered in the advanced stage since it is prone to transfer in the early stage. Few children can be partially remitted, and the disease is more likely to recur even when the children are completely remitted after comprehensive treatment such as conventional chemotherapy. It is reported that NB patients show high positive rates of NSE in serum. Moreover, other studies have found that LDH is related to the stages of NB and tumor load (the ratio of tumor volume and body surface area) (4, 5), to date, few researchers have studied the relationship between NSE in serum and the curative effect of APBSCT treatment of children with advanced-stage NB, therefore, we undertook this research. This study, based on the analysis of clinical data of 90 children with advanced stage NB after being treated by high dose chemotherapy (HDCT) combined with APBSCT, discusses the influence of NSE and LDH levels in serum together with the change of NB.

Key words: neuroblastoma, NSE level, LDH level, treatment of APBSCT

Mailing address: Dr Ruopeng Sun,
Pediatrics Department,
Qilu Hospital of Shandong University,
44 Wenhuaxi Road,
Lixia District, Jinan,
Shandong, China
e-mail: srpqlyy@163.com

0393-974X (2015)

MATERIALS AND METHODS

Study subjects

A total of 90 children [45 males and 45; ages ranging from 1.4 to 14.2 years (mean 6.5±3.4 years)] from various hospitals who had been diagnosed as advanced-stage NB were included in this study; onset to transplant ranged from 4 to 72 months (mean 11.0±2.3 months). With regard to primary sites, 35 cases were in the retroperitoneum, 40 cases in the paranephros, 14 cases in the breast, and 1 case in the chest and abdomen.

Clinical data

All children were treated by powerful induction, consolidation chemotherapy, surgery and local radiotherapy for 4~18 months (mean 9±4 months) before transplant. Before transplant, 41 cases were in complete remission (CR) stage, 33 cases in partial remission (PR) stage, and 16 cases in tumor progressive stage. Of the 41 cases in CR stage, 35 cases remained in continuous CR; another 6 cases recurred one year after the operation but were still sensitive to the chemotherapy and they survived with tumor. Of the 33 cases in the PR stage, 25 cases recovered after attaining CR, and another 8 cases remained PR (5 cases out of these 8 cases died 8 months later because of metastasis in the brain, and the remaining 3 cases survived with tumor). Of the 16 cases in the progressive stage, 1 patient died 5 days after the bone marrow transplant suppression period because of cardio-pulmonary failure; the remaining 15 cases temporarily remitted, but then died at different times due to metastasis of the cytoma.

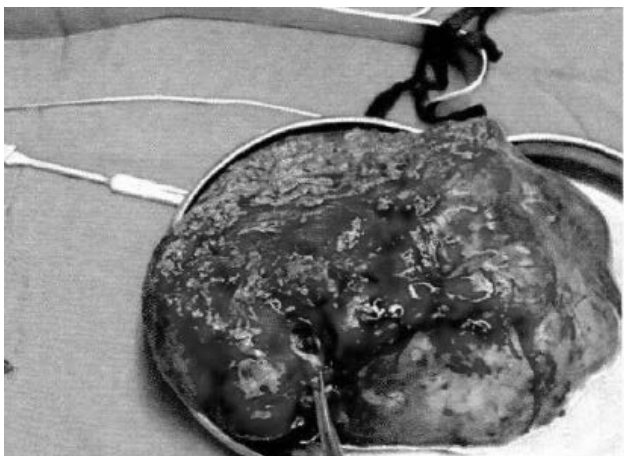

Fig. 1. S*pecimen of neuroblastoma after operation.*

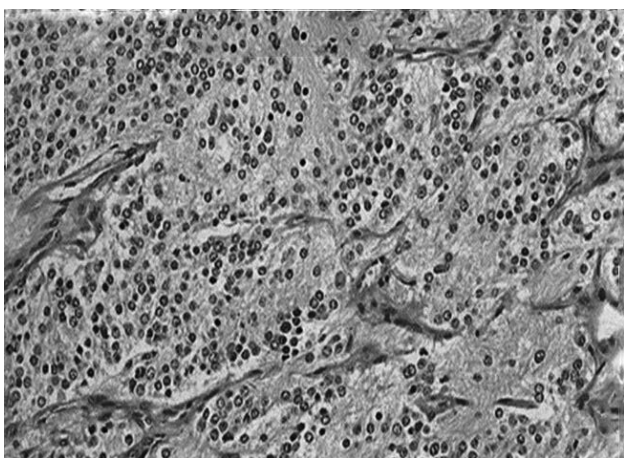

Fig. 2. *Specimen of neuroblastoma before treatment.*

Research methods

Clinical materials of the recruited children was collected. We aimed to analyze the variation of NSE level in serum of the peripheral blood before and after APBSCT, and discuss the relationship between NSE and LDH. NSE was detected by ECLIA, and its normal reference value is 0 ~ 15.2μg/L, and LDH by automatic biochemistry analyzer based on velocity method.

Statistical analysis

Data analysis was performed by SPSS 19.0 software. Mean of the three groups of samples was compared by *t*-test. $p<0.05$ was considered to have statistical significance. Spearman rank correlation analysis was used in correlation analysis.

RESULTS

Figs. 1, 2 and 3 show two cell samples from children with NB, reflecting the variation of NB

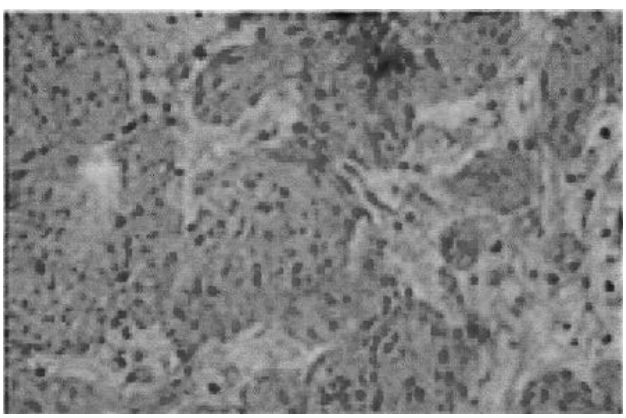

Fig. 3. *Specimen of neuroblastoma after treatment.*

before and after APBSCT. This comparison is beneficial to the following analysis of the results and disease discussion.

Analysis of the condition of the children before treatment

NSE in serum of children with advanced-stage NB exhibited high positive rate (82/90), (NSE is positive when >15.2μg/L). NSE and LDH levels were remarkably higher than those when the treatment was valid (P<0.01).

After the comprehensive treatments of chemotherapy, excision and radiotherapy, the NSE level of NB in different stages (CR stage, PR stage and progressive stage) before APBSCT treatment was analyzed as follows: (1) NSE and LDH levels of children in CR stage had significant difference compared to those in PR stage (P<0.05); (2) NSE and LDH levels in the progressive stage of tumor had no significant difference compared to before treatment (P>0.05) (Table I).

Conditions of children after treatment

After treatment with APBSCT, 1 child in the progressive stage died 5 days after transplant because of cardio-pulmonary failure, and the other 89 cases were detected with NSE and LDH levels two weeks after surgery (Table II).

The relationship between NSE and LDH level in serum

NSE levels of 90 children were 10.2~576 μg/L at the first visit, and the Spearman rank correlation analysis showed that NSE was positively correlated with LDH levels (r=0.05, P<0.01).

DISCUSSION

NB, as a malignant tumor, has high incidence among children, together with leukemia and lymphoma. NB tends to lead to multiple metastasis in the early stage, and what is worse, children who receive treatment in the advanced stage are less likely to recover, most of them having recurrence even when the disease has stablilised (6, 7). Worldwide reports show that, for children in CR stage, the disease-free survival of 5 years could only improve 30% ~ 50% after treatment of SCT, sensitizing antibody combined cell factors GM-CSF and IL-2. Similarly, it has also been reported in China that, for children in NB later period, the disease-free survival of 4 years could only improve 29.2% by high dose of pretreatment of chemotherapy and HSCT based on excision and local radiotherapy (8). Therefore, early diagnosis, early treatment and recidivation monitoring of NB are all helpful to improve curative effects and prognosis.

Table I. *Age distribution and comparison of NSE and LDH level in serum of children in different clinical stages before transplant.*

Clinical stages	Case number	Age	NSE(μg/L)	LDH(U/L)
CR stage	41	6.28±2.26	14.04±3.02a	226.71±1.19a
PR stage	33	6.70±2.75	23.40±2.69a	329.00±0.55a
Progressive stage	16	6.49±5.64	48.19±5.28b	391.94±1.53b

a:(P<0.05); b (P>0.05)

Table II. *Comparison of NSE and LDH level in serum before and after transplant of 17 cases (*$\bar{x}$±s).

Stages before transplant	Case number	Index	Before transplant	After transplant	P
CR stage	41	NSE	14.04±3.02	13.47±4.15	>0.05
		LDH	226.71±1.19	140±3.52	<0.05
PR stage	33	NSE	23.40±2.69	17.40±3.55	<0.05
		LDH	329±0.55	235.83±4.45	<0.05
Progressive stage	15	NSE	48.19±5.28	30.44±5.28	>0.05
		LDH	391.94±1.53	333.75±6.39	>0.05

NSE belonging to the glycolytic enzyme normally disperses in neurons, peripheral nerve tissue and neurosecretory tissues, and has a high sensitivity and specificity to NB, the increase of which often denotes the later stage and bad prognosis (9). In this study 90 children with later stage of NB were divided into CR stage, PR stage and progressive stage on the basis of the reaction to conventional chemotherapy before transplant. A statistical significance of NSE levels was found in children in CR stage, PR stage and progressive stage through observing the volatility of NSE numerical value before and after APBSCT treatment. After the treatment, the NSE levels decreased and tended to be normal when entering the CR stage, and the NSE levels in serum of patients with no remission had no obvious decrease, revealing that it could reflect tumor load and apostasis accurately as tumor marker. LDH, one of the important enzymes in the glycolytic pathway existing in tumor tissue, can be used to evaluate the size and situation of tumor load in the whole body; therefore, detecting the LDH level in serum is of great significance to estimate prognosis of NB and guide treatment (10).

NB is most likely to occur in children under 5 years of age, with no specificity in early-stage clinical manifestation. Usually, it presents as fever, anemia and lump of unknown origin, early-stage metastasis and difficult diagnosis. The simplest way to confirm NB children is to detect urinary anillylmandelic acid (VMA) and NSE in serum or by B ultrasound. Patients with confirmed NB are seldom cured completely by current medical means since the curative effect and prognosis of NB is poor; hence, early detection, diagnosis and treatment are of great importance.

This paper observed the value of LDH of 90 children before and after treatment, finding that LDH levels in serum were in the normal range or slightly higher than when the treatment is valid, and the LDH levels in the serum of children in the CR stage and progressive stage were significantly higher than normal. Our study demonstrates the positive correlation of NSE and LDH levels, showing that NSE and LDH level can jointly act as the auxiliary index to monitor the curative effect of NB treatment, so as to coordinate the treatment of NB patients and finally enhance the chance of recovery.

ACKNOWLEDGEMENTS

The project number of Shandong Province Natural Science Fund: ZR2009CL027. The star fund project of Jinan City science and Technology Bureau: 20100118. The medical fund item number of Shandong Provincial Academy of Medical Sciences: 201023.

REFERENCES

1. Xiong XL, Li Y. The progress of treatment of recidivity and refractory neuroblastoma. China Pediatric Blood and Cancer 2011; 6(1):44.
2. Yu M, Zhu YY, Yang CM, et al. Screening and identification of candidate GeNSE associated with progression of neuroblastoma. China Medical University 2012; 41(2):148-157.
3. Zhong L, Chen CX, Zou J, et al. Pulmonary metastases at diagnosis of neuroblastoma in pediatric patients: radiographic and clinical characteristics. Radiologic Practice 2011; 26(8):883-85.
4. Parodi F, Passonli L, Massimo L, et al. Identification of novel prognostic markers inrelapsing localized referable neuroblastoma. OMICS 2011; 15(3):113-21.
5. Baker DL, Schmidt M, Cohn S, et al. Outcome after reduced chemotherapy forintermediate-risk neuroblastoma. N Engl J Med 2012; 363(14):1313-23.
6. Kubota M. The role of surgery in the treatment of neuroblastoma. Surg Today 2010; 40(6): 526-32.
7. Chen YX, Zou J, Chen LY, et al. Pancreatic metastasis in a child with neuroblastoma: report of one case. J China Clin Med Imaging 2011; 22(7):527-28.
8. Tang SQ. The targeted therapy of neuroblastoma. Chinese J Pediatric Surg 2010; 15(6):252-53.
9. Gao XW. Clinical analysis of 38 cases of children with neuroblastoma. Zhengzhou, Zhengzhou University 2012.
10. Zhang CX, Du XJ, Liu YF. Clinical analysis of 34 cases of children with neuroblastoma. Basic Clin Oncol 2010; 26(3):233-35.

LETTER TO THE EDITOR

OBSERVATION OF THE CLINICAL EFFECTS OF IONTOPHORESIS OF A CHINESE DRUG IN THE TREATMENT OF DEGENERATIVE OSTEOARTHROPATHY

XL. GENG, XH. SUN, J. ZHANG, LB. YANG and QD. LIANG

Department of Orthopedic Surgery, the First Affiliated Hospital of Xinxiang Medical University, Weihui, China

Received November 22, 2014 – Accepted January 9, 2015

Degenerative osteoarthropathy, a kind of arthrosis induced by various factors, mainly affects articular cartilage and causes syndesmophyte formation. Its morbidity increases year by year, tending to occur more among young people than previously. This paper mainly discusses the clinical effects of iontophoresis of the Chinese drug in treating degenerative osteoarthropathy. A total of 296 cases of degenerative osteoarthropathy were randomly divided into two groups (of both genders): the iontophoresis group: the joint was treated with iontophoresis of the Chinese drug and a medium frequency electrotherapy instrument; the frequency electrotherapy group: the joint was treated only by medium frequency electrotherapy. The two groups were both treated for 30min once a day, for a total of 4 weeks. The results of the study showed that, the total effective rate in the medium frequency electrotherapy group was 74.3%, the iontophoresis group was 93.2%, indicating the curative effect of iontophoresis of the Chinese medicine. The above finding indicates that, iontophoresis has a good clinical effect in the treatment of osteoarthropathy and deserves to be promoted and applied.

Degenerative osteoarthropathy that is also called osteoarthropathy, retrograde osteoarthritis and senile osteoarthritis is a common chronic joint disease, mostly occurring in middle aged and elderly people. It results from the degeneration, hyperplasia of cartilago articularis and osteophyte formation caused by cartilago articularis degeneration and chronic damage of joints and is characterized by arthralgia, degeneration and restrained activity. Research data indicates that, the prevalence rate is from 10% to 17% in 40 year-olds, 50% in over 60 year-olds, and in over 75 year-olds it is 80%; the disease can be permanently disabling (1). Therefore, the treatment of degenerative osteoarthropathy arouses great concern.

Christian et al (2) studied the mechanism of load variation of lower limb weight-bearing joints and found that, increasing mechanical motion and changing biomechanics are the important factors for the occurrence and development of osteoarthritis; moreover, trauma such as intra-articular fracture often induces articular cartilage injury and even deep injury, thereby affecting subchondral bone and blood supplies, presenting as hematoma, formation and fibrosis of granulation tissue and new bone; moreover, the complex function between intra-articular tissue and mechanical stress could lead to meniscus crush injury. There is also a study indicating that meniscus crush injury might be related to meniscus tear, bad knee force line and cartilage

Key words: degenerative osteoarthropathy, iontophoresis of the Chinese drug, middle frequency electrotherapy

Mailing address: Dr Qiudong Liang,
Department of Orthopedic Surgery,
the First Affiliated Hospital
of Xinxiang Medical University,
No.88 Healthy Road, Weihui, China
Tel./Fax: +86 13938555760
e-mail: lqdxxdy@163.com

0393-974X (2015)

injury (3). Shi Xiaoming (4) et al made a summary on the pathogenesis of osteoarthritis in relation to the structure of cartilago articularis, the theory of cytokines, the free radical theory, and concluded that, its pathogenesis was complex and multifactorial. Western medicine focuses on symptomatic and pain relief in the treatment of osteoarthritis, and uses nonsteroidal anti-inflammatory drugs, non NSAIDS liniment (capsaicin) (5). Some also adopt surgery such as joint replacement, but this causes a heavy economical burden and considerable pain for patients. Chinese medicine usually adopts the Chinese drug endotherapy, external treatment, acupuncture and the manipulation in the treatment of osteoarthritis, which are more convenient with fewer side effects and is more economical. At present, iontophoresis of the Chinese medicine (6, 7), combined with traditional Chinese medicine and local symptomatic treatment, is widely accepted and recognized by patients, proving to have a good curative effect. Research indicates that, iontophoresis can stimulate the expression of basic fibroblast growth factor (BFGF), inhibit or improve the pathological change of cartilage in patients with osteoarthritis through promoting collagen matrix metabolism, and accelerate the repair of cartilage, thereby effectively treating osteoarthritis (4). All in all, Chinese medicine and western medicine can both, to some extent, relieve the pain of patients in the treatment of degenerative osteoarthritis. but considering the patients with degenerative osteoarthritis are mostly middle aged and elderly people, Chinese medicine merits more consideration

This paper observes the curative effect of iontophoresis by treating 296 cases of degenerative osteoarthritis with iontophoresis and medium frequency electrotherapy, specifically analyzing its curative effect in the perspective of statistics.

MATERIALS AND METHODS

General materials

A total of 296 cases of chronic degenerative osteoarthritis received and treated clinically between Oct. 2010 and Sep. 2012. Random numeric representation was used for grouping. There were 148 cases in the iontophoresis group and 148 cases in the medium frequency electrotherapy group, with no significant differences in gender, age or medical history. Patients with pathogenic sites on neck, waist and knee accounted for 91.6%. (1) There were 70 cases of lumbocrural pain, including protrusion of lumbar intervertebral disc, lumbar intervertebral disk prominence, lumbar retrogression, vertebral compression fractures, lumbar spondylolisthesis, etc.; patients mainly presented with lumbago, lower limb radiation pain, pressure pain on the ischiadic nerve; in some cases both lower extremities had intermittent or alternating pain. Examined by CT or CR, patients were found with lumbar intervertebral space or foraminal stenosis, protrusion or bulging of intervertebral disc, vertebral arch fracture, compression fracture (2). There were 75 cases of cervical spondylosis, including herniated cervical disc, cervical facet disorder and dislocation, degenerative cervical lesion; patients mainly presented with neck and shoulder pain, pain or numbness in the upper limb, aching and limp neck, dizziness and headache, giddiness, nausea, chest distress or pain Also when examined by CR or CT, patients were found with vertebral artery blood-supply schemia, protrusion or bulging of cervical intervertebral disc, cervical degenerative lesion (3). There were 126 cases of knee osteoarthritis, including meniscus injury, bone degeneration; patients presented with knee pain, pain increasing when loading or going up and down, joint swelling and stiffness, friction or crepitation when moving joints; Also on CR or MRI examination, patients were found with meniscus injury, hyperostosis, uneven articular surface, synovial hypertrophy or episome formation. (4) There were 25 cases with pathogenic sites on other parts, including thoracic vertebra, shoulder, elbow, wrist, etc.

Therapeutic method

The iontophoresis group: local joint was treated by iontophoresis with liquid drug+medium frequency electrotherapy, with 30 min/time, 1 time/ day, for a total of 4 weeks The medium frequency electrotherapy group: the electro-therapeutic apparatus used in medium frequency eletrotherapy group was the same as for the iontophoresis group; this group was treated with medium frequency electrotherapy, for 30 min, 1 time/day, for a total of 4 weeks. Neither group received any other type of treatment during this period.

The formula of the liquid used for iontophoresis is: fructus psoraleae 30 g, angelica sinensis 20 g, ligusticum wallichii 15 g, radix achyranthis bidentatae 15 g, flowers carthami 10 g, frankincense 10 g, myrrh 10 g, notopterygium root 15 g, radix angelicae pubescentis 15 g, radix sileris 15 g, spina gleditsiae 10 g, woodlouse 10 g, teasel 20 g, rhizoma cibotii 20 g, garden balsam stem 30 g, liquorice 10 g. These herbs were soaked in water for 30 min, boiled and then decocted for 1 h. Finally, the concoction was filtered. These herbs were heated again for 30 min according to the above method. The liquid obtained was

mixed and applied externally on the joints. Electrode slice was connected with iontophoresis apparatus. The higher the frequency, the deeper the stimulus. Medium frequency electrotherapy was performed 1 ~ 2 times/ day for 30 min. Tolerance value of the frequency was determined based on the patient's condition and personal tolerance degree. Generally, on the body it ranged from 40 to 60 MA, and on the four limbs from 35 to 50 MA.

Response evaluation criteria

The effects of the treatments are shown in Table I. Final effective rate= (clinical cure+marked effect+ effective) / n ×100%. Visual analogue scale (VAS) was applied for pain score (8). A 10 cm-long line was labelled 0 to 10: 0 refers to no pain and 10 refers to the severest pain. Patients were asked to mark the location of the current pain, and then the length of the distance was measured to express pain degree (Table I).

Assessment of motion range

Motion range of joints of patients was compared before and after treatment and divided into grades of excellent, good or poor.

Statistical analysis

SPSS 17.0 statistical software was used to process data, compare joint mobility and clinical evaluation. P value < 0.05 was considered as statistically significant.

Statistical analysis was carried out on the two groups after the 4th week of treatment.

RESULTS

Comparisons of VAS before and after the treatment

After one-way analysis of variance on results, it was found that, VAS of the iontophoresis group before treatment was close to the control group, and there was no statistical significance (P>0.05), whereas after treatment, the two groups had statistical significance (P<0.01). It can be seen from Table I that, VAS difference of the iontophoresis group was greater than in the medium frequency electrotherapy group, indicating that the treatment for the iontophoresis group had a better curative effect than that for the medium frequency electrotherapy group (Table II).

Comparison of effectiveness after treatment

As shown in Table III, of 147 patients in the iontophoresis group, 47 patients were cured, no longer suffering from pain and their joint motion ranges returned to normal. Examined by CT or CR, most patients were found to have improved joint distortion, thereby guaranteeing their return to normal daily life. As to 60 patients with marked effects, the swelling and pain in the pathogenic sites decreased: patients with arthritis in their legs no longer felt severe heaviness when going up and down; as to patients with periarthritis of shoulder, snapping sound was not heard between joints any more and the pain disappeared during daily movement. Thirty one patients with effective treatment had slight pain when the pathogenic sites were pressed, but the motion range was enhanced compared to before treatment. Different curative effects of the medium frequency electrotherapy group were close to the iontophoresis group, but overall, the well-healed patients of the iontopheresis group were more than in the medium frequency electrotherapy group. The total effective rate was 93.2% in the iontophoresis group and 74.3% in the medium frequency electrotherapy group, indicating that the curative effect of patients in the iontopheresis group was better than in the medium frequency electrotherapy group.

Comparison of motion range of joints

Assessment of motion range of joints, mainly focusing on the maximum movement arc of patients, that is, the normal motion range of joints. At the 2nd and 4th weeks after treatment, patients in the iontopheresis group significantly improved compared to before treatment; and after 4 weeks, the curative effect for the iontopheresis group was much better than in the medium frequency electrotherapy group, as shown in Table IV. Of 148 patients in the iontopheresis group, 50 patients could move freely with the greatest movement arc after the pathogenic sites were treated; 89 patients could fulfill the basic actions such as leg flexion and extension, but failed to do large amplitude movements; the remaining 9 patients had severe pain when doing basic actions after treatment and could not fulfill the specified actions smoothly. Curative effect assessment was also performed on the medium frequency electrotherapy group based on the same assessment indexes, but its total effective rate (76.4%) was lower than in the iontopheresis group (93.9%).

Treating degenerative osteoarthropathy with iontopheresis had few toxic and side effects which could be ignored, and worse joint pain and severe

Table I. *Response evaluation criteria.*

Effect	Determination criteria	Improvement rate
Clinical cure	Joint motion recovery to normal and swelling and pain completely disappearing	≥95%
Marked effect	Swelling and pain of joint relief and no spontanous pain	70%~95%
Effective	Locally slightly painful or painful when pressed and improvement in motion range.	< 70%
Invalid	Symptoms and physical sign have no improvement.	< 30%

Table II. *Comparison of VAS before and after treatment (mean ± SD, cm).*

Group	Case	Before treatment	After treatment	Difference	t value	P value
Chinese drug iontophoresis group	148	6.50±0.58	1.99±1.78	4.51±1.20	30.51	< 0.01
Medium frequency electrotherapy group	148	6.44±0.76	3.15±2.28	3.29±1.51	28.22	< 0.01

Table III. *Comparison of the two groups after treatment.*

Group	Total case number	Cure	Marked effect	Effective	Invalid	Total effective rate (%)
Chinese drug iontophoresis group	148	47	60	31	10	93.2%
Medium frequency electrotherapy group	148	28	35	47	38	74.3%

Table IV. *Comparison of motion range of joint at 4 weeks after treatment.*

Groups	Total case number	Excellent	Good	Poor	Total effective rate (%)
Chinese drug iontophoresis group	148	50	89	9	93.9
Medium frequency electrotherapy group	148	28	85	35	76.4

allergic reactions did not occur, since the Chinese drugs applied were safe (Table IV).

DISCUSSION

Degenerative osteoarthosis presents as a degenerative change of joint surface and secondary hyperostosis (9), mostly occurring among the middle aged and elderly population. Under the conditions of overload working of the spine and joints or long-term exposure to wind, cold and dampness, arterial blood perfusion and insufficient oxygen supply, metabolins

tend to deposit, thereby leading to dystrophia of the cartilago articularis, and finally induce degenerative osteoarthosis.

Osteoarthritis can be divided into primary osteoarthritis and secondary osteoarthritis. The former (10) is senile osteoarthritis related to aging but in no correlation with other diseases; its pathogenesis is not clear, and is supposed to be related to advanced age, gender, occupation. The latter is caused by systemic disease, acute trauma or chronic strain, such as trauma, rheumatoid arthritis, nerve and endocrine diseases (11-12). Clinical manifestation of osteoarthritis includes arthralgia, arthrocele, limited movement and joint deformity. Under X ray, it presents as narrowing joint space, subchondral bone densification, bone trabecula fracture, sclerosis, cystic degeneration, hyperplasia at the edge of joints, deformation of extremities in the later stage and uneven articular surfaces.

Traditional treatment includes conservative treatment and operative treatment. Conservative treatment includes physical therapy, nonsteroidal anti-inflammatory drugs, cortisone injection into joint; operative treatment includes joint clear operation, osteotomy, joint replacement, joint fusion, etc. (13). However, conservative treatment for osteoarthritis has disadvantages of slow effect, long treatment course, and often reoccurs after stopping drugs; moreover, it is costly and painful. Iontophoresis of the Chinese drug is being widely considered since it can relieve local joint pain, thereby treating an internal illness by external treatment. Effective biological iontophoresis of the Chinese drug can ease pain through blocking pain impulse and releasing endogenous opioid peptides, and expel toxicant through improving blood circulation, eliminating tissue edema and reducing muscle spasm caused by ischemia.

Iontophoresis of this Chinese drug is a unique therapy that integrates traditional Chinese medicine, acupoint, meridians and voltaic physics action together. A drug that can promote circulation, remove stasis, and relieve swelling and pain is directed into the lesion site. During local therapy, the effective components of the drug have direct pharmacological effects after being absorbed through tissues and organs. A high concentration of the drug on the local site leads to long-term accumulation and performance, thereby prolonging the effect of the treatment, reducing side effects, and avoiding toxicity. Iontophoresis of the Chinese drug has been clinically researched in many subjects. Yang Min (14) et al. attempted to treat fatty liver accompanied by metabolic syndrome by rhizoma alismatis and salvia combined with iontophoresis of the Chinese drug. The total effective rate in the treatment group was 83.93% while in the control group it was 59.52%, proving that the curative effect of the treatment group was significantly higher than for the control group, and with less negative effects. Wang Xihong (15) et al. applied angelica, salvia, safflower, peach kernel, uncaria, Chinese starjasmine and notopterygium with iontophoresis of the Chinese drug to treat 120 cases of angina pectoris. After 15 days of treatment, the total improvement rate of the treatment group was 91.67% while in the control group it was 66.67%; electrocardiograms showed a total improvement rate in the treatment group of 90.0% while in the control group it was 65.0%. The experiment demonstrated that, iontophoresis of the Chinese drug is a safe and effective therapy for angina pectoris. In iontophoresis of the liquid Chinese drug, angelica has functions of enriching and activating the blood, dispelling dampness and relieving pain, which can improve microcirculation of lesioned parts and decrease platelet aggregation; safflower, frankincense, myrrh, ligusticum wallichii, radix achyranthis bidentatae and peach kernel can activate blood and remove stasis; garden balsam stem, radix angelicae pubescentis and radix puerariae have functions of expelling wind-damp and cold, removing numbness, relaxing tendons and relieving pain. Iontophoresis of the liquid Chinese drug can also effectively inhibit exudation of inflammatory substance in the joint and reduce subchondral bone edema while delaying joint cartilage degeneration. Middle frequency electrotherapy applies an electric field of direct current and poles with the aim of driving drugs into the human body by electrodes. In addition, medium frequency electrotherapy alone can effectively improve local blood circulation in joints, warm meridian and dredge stasis, lower pressure within bone, promote metastasis, diminish inflammation and relieve pain.

Treating degenerative osteoarthritis by iontophoresis of the Chinese drug proved to be

reliable and have no significant toxic and side effects. Comparing the iontophoresis group to the medium frequency electrotherapy group, we found that, patients in the iontophoresis group greatly improved in regard to pain and degree of joint motion after treatment, proving the curative effect of the Chinese drug.

In conclusion, the experimental research in this paper demonstrated that, during the treatment for osteoarthritis patients, medium frequency electrotherapy and iontophoresis of the Chinese drug together can mitigate the disease. The total effective rate in the iontophoresis group in treating osteoarthritis was 93.2% and the cure rate was 31.8%, showing that its curative effect was superior than that obtained in the medium frequency electrotherapy group. As to VAS and range of motion, the results after treatment with iontophoresis were positve with a significant difference in improvement. All these findings suggest that iontophoresis of the Chinese drug is remarkably effective in the treatment of osteoarthritis and highlights its unique effects for easing pain and improving joint functions. Considering the characteristics of joint structure, iontophoresis of the Chinese drug is beneficial for the absorption of effective components of the drug; meanwhile, it can avoid drug stimulation of the digestive system and reduce toxin and side effects. All in all, the use of iontophoresis of the Chinese drug deserves to be promoted. Lastly, through follow-up on patients, we find that iontophoresis of the Chinese drug has fewer side effects in the treatment of degenerative osteoarthropathy and the patients are highly satisfied with the treatment. Compared to medium frequency electrotherapy, iontophoresis of the Chinese drug is more easily accepted by middle aged and elderly people. In practical clinical treatment, the method used should be comprehensively considered according to age, gender, physical condition and disease stage. No matter whether it is Chinese medicine, western medicine or a combination of both, doctors should consider the needs of the patient and formulate the best individual plan of treatment.

REFERENCES

1. Wei L. Pathogenesis and clinical research progress of osteoarthritis. Hebei Med J 2010; 32(5):611-14.
2. Christian E, Thomas H, Victor V. Biomechanics and pathomechanisms of osteoarthritis. Swiss Med Wkly 2012; 142:w13583.
3. Michel DC, Frank WR, David TF, Martin E, Wang K, Mohamed Jarraya. Factors associated with meniscal extrusion in knees with or at risk for osteoarthritis: the multicenter osteoarthritis study. Radiology 2012; 264:494-503.
4. Shi XM, Yu ZG. The research progress of osteoarthritis pathogenesis. Chin J of Clinicians (Electronic Version) 2013; 7(24):11607-10.
5. Sawitzke AD, Shi HFinco MF, Dunlop DD, et al. Clinical efficacy and safety of glucosamine, chondroitin sulphate, their combination, celecoxib or placebo taken to treat osteoarthritis of the knee: 2-year results from GAIT. Ann Rheum Dis 2010; 69(8):1459-64.
6. Li SZ, Bai L. Treatment research progress of knee osteoarthritis treated by iontophoresis of Chinese medicine. Chin Archives of Tradit Chin Med 2013; 31(3):481-482.
7. Fan ZC. Curative observation of acupotomy combined with iontophoresis of Chinese medicine in treatment of knee osteoarthritis. Shanghai J of Acup and Moxibustion 2010; 29(9):604-5.
8. Zhang T, Wang RT, Hu YJ, Song JF, Ma CZ. The visual analogue scale in the knee arthroplasty after analgesia. Progress in Modern Biome 2011; 11(22):4362-63.
9. Zhang JH, Li L, Liu JZ. Correlative factors of degenerative gonarthritis. Mod Clin Nursing 2010; 9(2):10-11.
10. Jin FY. Non-operation treatment of primary knee osteoarthritis. J Clin Rehabilit Tissue Engin Researc 2013; 17(30):5531-38.
11. Li KC, Yu Q. CT Evaluation of osteoarthritis secondary to adults with severe developmental dysplasia of hip. Chin Comput Med Imagin 2010; 16(2):139-41.
12. Huang J, Huang CB. Improvement in diagnosis and treatment of rheumatoid arthritis. Clin Med J 2010; 8(1):1-5.
13. Zhang CL, Lu JH, Zhang XG. The minimally invasive operation of arthroscope for knee osteoarthritis. Sichuan J Anato 2012; 20(2):44-45.
14. Yang M, Yang DP, Xu LP. Iontophoresis of Chinese medicine in treatment of fatty liver accompanied by

metabolic syndrome. Practical Clin J Integr Tradit Chin and West Med 2010; 10(1):82.
15. Wang CH, Yang GF. Observation of 120 cases of angina pectoris treated by iontophoresis of Chinese medicine. Chin J Mod Drug Appl 2014; 4(15):111-12.

LETTER TO THE EDITOR

THE EXPRESSION OF P53, MGMT AND EGFR IN BRAIN GLIOMA AND CLINICAL SIGNIFICANCE

T. LIN[1], M. WANG[2], HS. LIANG[1] and EZ. LIU[1]

[1]Key Laboratory of Neurosurgery, College of Heilongjiang Province, First Affiliated Hospital of Harbin Medical University, Harbin, China
[2]Department of Oncology, the Tumour Hospital of Harbin Medical University, Harbin, China

Received November 22, 2014 – Accepted 9 January, 2015

In order to discuss the expression of P53, MGMT (O^6-methylguanine-DNA methyltransferase) and EGFR (epidermal growth factor receptor) in brain glioma and their clinical significance, this paper collected clinical features of 40 patients. We observed the expression of P53, MGMT and EGFR in samples using immuohistochemistry assay and analyzed their interaction, as well as their relationship to brain glioma. It was found that among 40 cases of brain glioma samples, cases with positive P53 expression accounted for 47.5%, and its expression in high-grade brain glioma was higher than in low-grade brain glioma (P<0.05); cases with positive MGMT expression accounted for 37.5%, and its expression in high-grade glioma and low-grade brain glioma had no statistical significance (P>0.05); cases with positive EGFR expression accounted for 55%, and its expression in high-grade brain glioma was higher than in low-grade brain glioma (P<0.05); the expression of P53, MGMT and EGFT were not correlated to age, gender or size of tumor; P53 expression was negatively correlated to MGMT expression (P<0.05) but positively correlated to EGFR expression (P< 0.05) demonstration that P53, EGFR and MGMT play important roles in the occurrence and development of brain glioma.

Recurrent, hard to cure brain glioma characterized by high malignancy and mortality is a commonly observed intracranial primary tumor in the central nervous system. P53, a type of cancer suppressor gene, can promote malignant cell transformation; however, it loses its function as a cancer inhibitor when transforming from wild to mutant. O^6-methylguanine-DNA methyltransferase (MGMT), a type of DNA repairer, is related not only to brain glioma's drug resistance to alkylating agents, but also to the malignant transformation of brain glioma. Epidermal growth factor receptor (EGFR) is a kind of transmembrane glycoprotein with tyrosine kinase activity, involved in the growth, repair and survival of tumor cells, as well as the generating of new vessels, invasion and metastasis.

Detection of P53 signifies that its inactivation increases as pathological grade rises; mutant P53 is related to grading degree, metastasis and recurrence, therefore can be considered as an index of tumor grading; inactivation of P53 may lead to overexpression of CyclineE/CDK2 through P21CIP1, while expression of P27kip1 decreases due to phosphorylation; common inactivation of cancer suppressor genes is able to promote the malignant evolution of glioma cells (1).

Keywords: brain glioma, P53, MGMT, EGFR

Mailing address: Dr Enzhong Liu,
Department of neurosurgery, The First Affiliated Hospital,
of Harbin Medical University,
23 Youzheng St, Nangang District,
150001, Harbin, Heilongjiang, P.R. China
Tel.: +451 85555109 Fax: +451 85555109
e-mail: lezenzhong@163.com

0393-974X (2015)

DISCLOSURE: ALL AUTHORS REPORT NO CONFLICTS OF INTEREST RELEVANT TO THIS ARTICLE.

Research on glioma cells from molecular biology and molecular genetics demonstrate that closing or down-regulating tumor genes within tumor cells or introducing cancer suppressor genes and pro-apoptotic genes is the basic method for gene therapy based on molecular mechanism of tumor progression. For instance, signal transduction interference therapy with MGMT and the EGFR as a target is likely to be specific and effective for malignant glioma, especially for the primary malignant kind. Gene therapy for malignant glioma could be a successful breakthrough by adopting multi-gene combined therapy or a combination of conventional treatment and gene therapy (2).

High EGFR expression usually indicates a poor differentiation of glioma, as it expresses remarkably high in poorly differentiated glioma (high level), which is closely correlated to pathological grading (3). There is a large number of researchers that are proving that EGFR signal pathway performs an important role in regulating radio-resistance for human brain glioma. For instance, Li et al. (4) found that gamma knife combined with antisense EGFR therapy (mainly down-regulating the expression of EGFR in brain glioma) in the treatment of *in vitro* test of malignant glioma can effectively inhibit cell proliferation and induce cell apoptosis. By means of the same method it was found that growth of orthotopic transplantation tumor (C6 glioma) is also effectively restrained. Hence, many researchers sustain that combining antisense EGFR and gramma knife radiotherapy is a potentially feasible strategy for treating malignant glioma.

This study explored the effects of P53, MGMT and EGFR on the occurrence and development of brain glioma through detecting and analyzing their expressions in 40 cases of paraffin specimens of brain glioma.

MATERIALS AND METHODS

We collected 40 cases of paraffin specimens of brain glioma which had completed clinical data and which were extracted from March 2009 to September 2011 in various hospitals; of the 40 cases, 26 cases were male and14 were female, ranging in age from 10-74 years (mean 44.5 years). All of the brain glioma specimens were pathologically diagnosed. According to the 2000 WHO classification of tumors of the central nervous system, all the tumors were classified into low-grade malignancy group (grade I/ II) (18 cases) and high-grade malignancy group (grade III/IV) (22 cases). All the patients had detailed clinical materials and operation notes but had not undergone radiotherapy and chemotherapy before surgery. Experts from the pathology department studied the films of all the samples which had undergone normal and HE staining in the examination.

Main reagents and methods

The main reagents included mouse anti-human P53 (monoclonal antibody), mouse anti-human MGMT (monoclonal antibody), mouse anti-human EGFR (monoclonal antibody), S-P kit and DAB enzyme substrates chromogenic kit. All the reagents were purchased from Beijing Zhong Shan - Golden Bridge Biological Technology Co., Ltd. We performed immunohistochemical staining with SP method. Paraffin specimens were cut into sections of 4 um, followed by dewaxing using xylene and hydration using ethanol. The sections were then incubated for 5 to 10 min in 3% H_2O_2 deionized water to block endogenous peroxidase. After washing by PBS for 5 to 10 min, primary antibodies were added the sections and incubated at room temperature for 1 to 2h; after washing with PBS for 2min × 3 times, a second antibody was added and incubated at room temperature for 30 min; after washing with PBS for 2 min × 3 times, DBA color agent was added. Five to 10 min later, the developing color was controlled under an illuminated microscope. After washing with distilled water, the sections were redyed using hematoxylin and normally dehydrated. Finally, the sections were mounted with neutral resins. Normal PBS was regarded as negative, taking the place of primary antibody. Breast cancer tissue section was considered positive for P53; liver tissue section was considered positive for MGMT; colorectal cancer tissue section was regarded positive for EGFR.

Criteria for assessment

Mark staining intensity: 0 point indicates colorless, 1 point indicates faint yellow, 3 points indicate sepia. Mark percentage of positive cells: 0 point indicates negative, 1 point indicates positive cells ≤10%, 2 points indicate 11%-50%, 3 points indicate 51%-75%, 4 points indicate >75%. The result of staining intensity and the percentage of positive cells >3 points is considered to be positive immunoreaction. We randomly selected 5 high power fields with mean staining (10×40 times) and calculated the proportion of positive staining cells (6). Yellow or tan particles in cell nucleus are considered as positive staining of P53 protein, as shown in Fig. 1; yellow or tan particles in cell nucleus is considered as positive staining of MGMT, as shown in Fig. 2. Yellow or tan particles in

cytomembrane or cytoplasm are considered as positive staining of EGFR, as shown in Fig. 3.

Statistical analysis

SPSS19.0 software was used for statistical processing. In addition, Spearman's correlation analysis was applied. $P<0.05$ was considered to have statistical significance. We analyzed the difference between expression of P53, MGMT and EGFR in brain glioma with different malignancy, different sizes of tumor, age and gender, as well as the correlations between indexes.

RESULTS

The positive expression rate of P52, MGMT and EGFR was 47.5%, 37.5% and 55%, respectively. The positive expression rate of P53 was 63.6% in high-grade (grade III/ IV) brain glioma tissue (63.6%) was higher than that in low-grade (grade I/II) brain glioma tissue (27.8%) ($P<0.05$). The positive rate of MGMT in low-grade (grade I/II) brain glioma was 44.4%, and in high-grade (grade III/ IV) brain glioma was 31.8%. Through a statistical test, it was found that the positive expression of high/low grade brain glioma did not vary ($P<0.05$). The positive expression rate of EGFR was 63.6% in high-grade (grade III/IV), brain glioma tissue and higher than that in low-grade (grade I/II), brain glioma tissue (27.8%) ($P<0.05$) (Table I).

Among 26 cases of male brain glioma, cases with positively expressed P53 accounted for 46.2%, MGMT for 38.5% and EGFR for 57.7%; among 14 female patients, those with positively expressed P53 accounted for 50%, MGMT for 35.7% and EGFR for 57.7%. Among 28 patients younger than 50

Table I. E*xpression of P53, MGMT and EGFR in brain glioma.*

Grade	P53					MGMT					EGFR				
	+/n	-/n	Positive rate /%	x^2	P	+/n	-/n	Positive rate /%	x^2	P	+/n	-/n	Positive rate /%	x^2	P
I/II	5	13	27.8	5.105	0.024	8	10	44.4	0.673	0.412	6	12	33.3	6.208	0.013
III/IV	14	8	63.6				15	31.8			16	6	72.7		
Total	19	21	47.5			15	25	37.5			22	18	55.0		

+: positive; -: negative.

Table II. *Expression of P53, MGMT and EGFR in brain glioma with different clinical features (%).*

	Grouping	n	P53				MGMT				EGFR			
			+/n	Positive rate /%	x^2	P	+/n	Positive rate /%	x^2	P	+/n	Positive rate /%	x^2	P
Gender	Male	26	12	46.2	1	0.539	10	38.5	0.029	0.864	15	57.7	0.218	0.641
	Female	14	7	50.0			5	35.7			7	50.0		
Age	>50	28	13	46.4	0.143	0.836	8	28.6	3.175	0.075	14	50.0	0.590	0.533
	≥50	12	6	50.0			7	58.3			2	66.7		
Size of tumor /cm	>5	14	4	28.6	2.037	0.154	6	42.9	0.264	0.608	5	35.7	3.327	0.072
	≥5	26	15	57.7			9	34.6			17	65.4		

+: positive; -: negative.

Table III. *Pairwise correlations among P53, MGMT and EGFR.*

		MGMT		r	P	EGFR		r	P
		+/n	-/n			+/n	-/n		
P53	+/n	4	15	-0.323	0.042	16	3	0.558	0.000
	-/n	11	10			6	15		
EGFR	+/n	6	16	-0.234	0.147				

+: positive; -: negative.

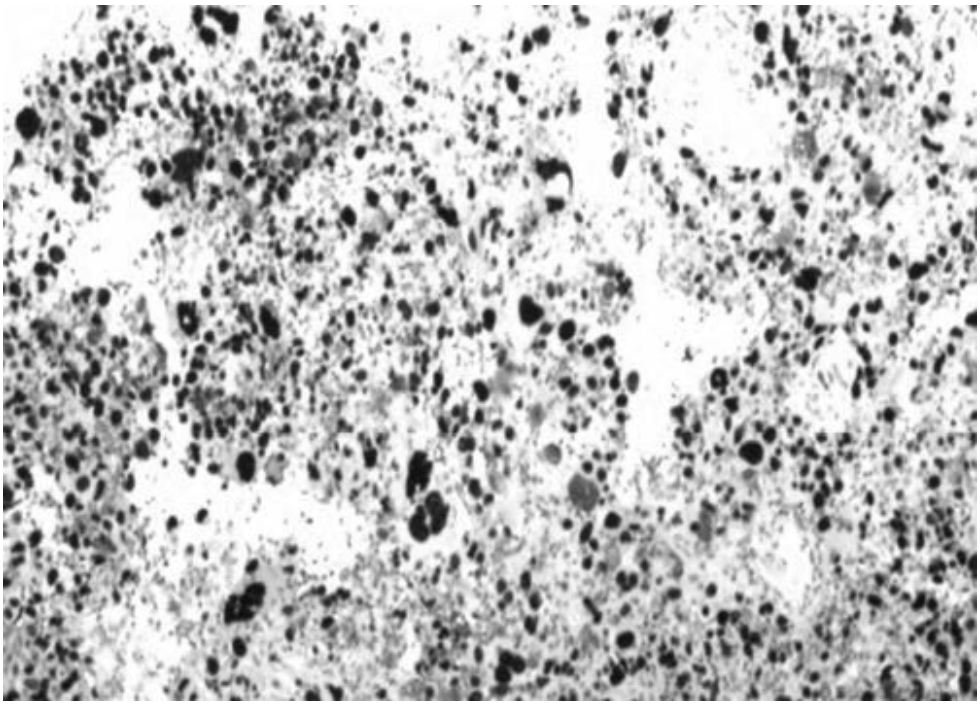

Fig. 1. E*xpression of P53 in brain glioma.*

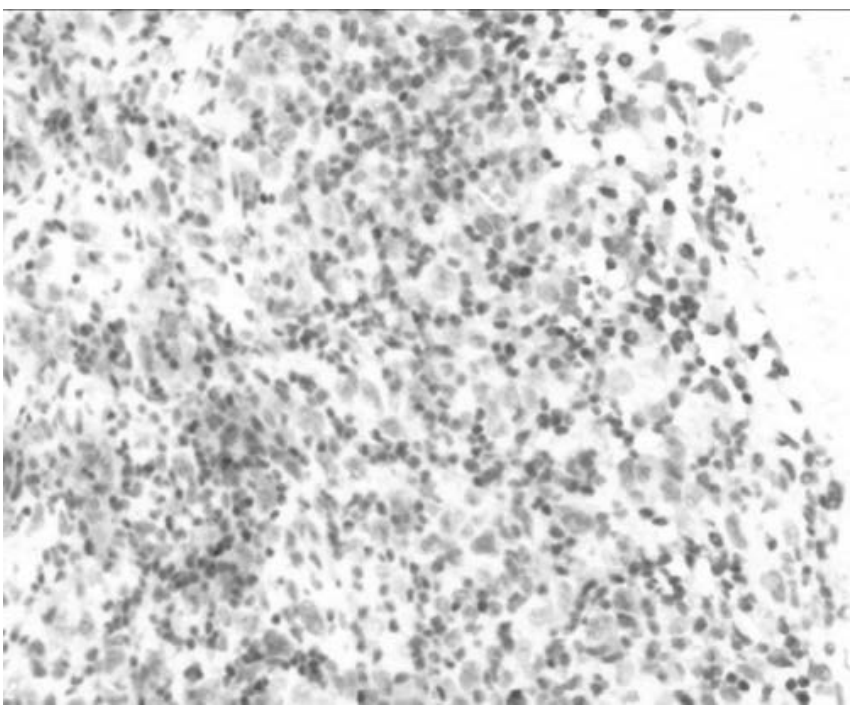

Fig. 2. E*xpression of MGMT in brain glioma.*

years, those with positively expressed P53 accounted for 46.4%, MGMT for 28.6% and EGFR for 50%; among12 patients older than 50 years, those with positively expressed P53 accounted for 50%, MGMT for 58.3% and EGFR for 66.7%; among 14 patients with maximum parameter of tumor less than 5 cm,

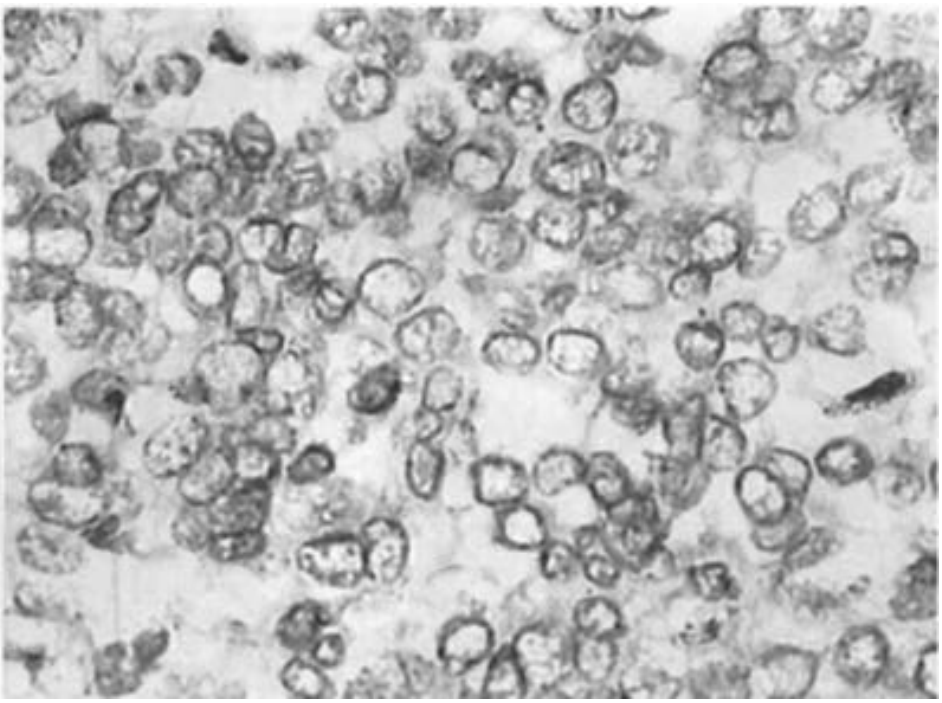

Fig. 3. *Expression of EGFR in brain glioma.*

patients with positively expressed P53 accounted for 28.6%, MGMT for 42.9% and EGFR for 35.75; among 26 patients with a maximum parameter of tumor no less than 5cm, patients with positively expressed P53 accounted for 57.7%, MGMT for 34.6% and EGFR for 65.4%. Through statistical test, the expression of P53, MGMT and EGFR had no statistical difference ($P<0.05$) where patients with brain glioma were of different genders, age (< or ≥50 years) and sizes of tumor (< or ≥5cm), as shown in Table II.

In regards to brain glioma tissue, the positive expression of P53 was negatively correlated to the positive expression of MGMT ($r=-0.323$, $P<0.05$); the positive expression of P53 was positive correlated to the positive expression of EGFR ($r=0.558$, $P<0.05$); the positive expression of MGMT was in not correlated to the positive expression of EGFR ($r=-0.234$, $P>0.05$), as shown in Table III.

DISCUSSION

P53 functions as DNA bonding and repairing, controlling cell cyclic process and cell apoptosis involved in cell differentiation and plasticity regulation of genes. P53 mainly induces cell suicide through programmed cell death, thereby inhibiting cancer (5). Mutational P53 gene has no cancer inhibition function but has the activity to promote cell malignant transformation which can lead to the spread of malignant tumor.

Mutational P53 featured by changed protein conformation, increased stability and longer half-life period accumulates to 100 times in cancer cells and can be detected by immunohistochemistry. Therefore, it was generally believed that immunohistochemistry for detecting P53 was consistent with mutational P53. The detection results of this study was that the expression of P53 in low-grade (grade I/II) brain glioma was 27.8% and in high grade (grade III/ IV) was 63.6%; the expression of P53 in high-grade brain glioma was significantly higher than low-grade brain glioma. It suggested that the inactivation of wild type p53 involved in the occurrence and development of brain glioma might be one of the indexes for poor prognosis.

MGMT, a sort of DNA repair protein, is able to remove mutagenic alkyl adduct of guanine on DNA, repair injured guanine, protecting cells against damage from alkylating agent. Therefore, the highly

expressed MGMT can affect the curative effect of alkylating agents and is also the molecular basis for cells resisting to them. It has been proved that the expression of MGMT in brain glioma significantly affect the curative effects of alkylating agents, thus influencing the patient prognosis (6). This study showed that the expression of MGMT was not correlated with the age and gender of patients, which suggested that the expression of MGMT might be related to the endocrine hormone levels of the body. The fact that the results showed that there was no difference in the positive expression rate of MGMT in brain glioma of different malignancies was in line with Ji Lie, et al. (7). As to the expression of MGMT in brain glioma, different research facilities have acquired different research results. Some sustain that the positive expression rate of MGMT in high-grade brain glioma was significantly lower than low-grade brain glioma (8-9), while some other scholars obtained different research results (10-11). For instance, Sun Yanhui, et al. stated that the expression of MGMT in high-grade brain glioma was significantly higher than low-grade brain glioma; with the increase of tumor malignancy degree and positive expression, it was believed that MGMT was related to tumor malignancy; moreover the lifespan of patients with positive MGMT expression was significantly shorter than patients with negative expression. The two different test results might be connected to non-uniformity of distribution and expression of MGMT in tumor tissue. We also found that in the same section, the cells with positive staining of MGMT had nonhomogeneous coloring and distribution. We analyzed functioning on different target cells in the perspective of MGMT: MGMT can repair injured DNA, but the result varies when it acts on different cells. Repairing tumor cell DNA can lead to tumor cell drug resistance to alkylating agent. Currently there is a study (12) proving that application of an alkylating agent such as temozolomide in the treatment of brain glioma with negatively expressed MGMT, can achieve good curative effect, however, MGMT can prevent damage of cells from carcinogenic factors such as alkylating agents while acting on non-tumor cells. However, further studied need to be carried out in order.to establish when and by which means the two aspects above dominate.

EGFR is the expression result of protooncogene cerbB-1. Its over-expression and mutation in tissue cells can lead to excessive DNA duplication and cell division, thus provoking out of control cell growth and malignant transformation and finally result in cell canceration. Studies (13-15) indicated high EGFR expression in various malignant tumor tissues such as lung cancer, gastric cancer, nasopharynx cancer, etc., suggesting that the occurrence mechanism of the above tumors might be related to the out of control expression of EGFR. The result of this study indicated that the positive expression rate of EGFR in high-grade brain glioma was significantly higher than in low-grade brain glioma, which is similar to the research results of Dong Lun, et al, from neurosurgery of Clinical Medicine College of Yangzhou University (16). It suggested that the positive expression of EGFR might be related to the malignant progression of brain glioma. Moreover, tumor with positive expression of EGFR has a stronger activity of division and proliferation, which plays avery important role in malignant progression of brain glioma.

This study revealed that the expression of P53 was in negative correlation to the expression of MGMT, which might be due to the protection function produced by the high expression of MGMT on the DNA of P53. Blough (17) found through mice test that the expression of MGMT in star brain glioma cells with mutational P53 significantly decreased. It was inferred that P53 played an important regulation function in expression and transcription of MGMT. More mutual function relationship and mechanism between P53 and MGMT need to be researched.

This study found that the expression of P53 and EGFR improved with the increase of tumor malignancy degree, and that the two were in positive correlation. It indicated that P53 and EGFR might be involved in the malignant transformation and development of brain glioma or that the mutation of P53 might induce the over-expression of EGFR. However, the detailed functions of P53, MGMT and EGFR that play in the occurrence and development of brain glioma as well as whether P53 can promote the expression of MGMT and EGFR need to be further studied, so as to clear their clinical significance.

REFERENCES

1. Hu T, Tian XH, Ji HM, Zhao ZL. Expression of

P27kip1 and P53 in brain glioma and relative pathological significance. J of Inner Mongolia University for Nationalities 2009; 15(5):8-10.
2. Zhou HJ, Qin XL, Wang HW, Liu CQ. Progress of EGFR and Ki-67 expression in glioma. Biotechnol Bulletin 2011; (1):56-9.
3. Pore N, Jiang Z, Gupta A. EGFR tyrosine kinase inhibitors decrease VEGF expression by both hypoxia-inducible factor(HIF)-1-independent HIF-1-dependent mechanisms. Cancer Res 2006; 66(6):3197-204.
4. Li Y, Jia Q, Zhang J, et al. Combination therapy with Gamma Knife radosurgery and antisence EGFG for malignant glioma in vitro and orthotopic xenografts. Oncol Rep 2010; 23(6):1585-91.
5. Hu X, Miao W, Zou Y, Zhang W, Zhang Y, Liu H. Expression of p53, epidermal growth factor receptor, Ki-67 and O-methylguanine-DNA methyltransferase in human gliomas. Oncol Lett 2013; 6(1):130-4.
6. Hegi ME, Diserens A-C, Gorlia T, et al. MGMT gene silencing and benefit from temozolomide in glioblastoma. N Engl J Med 2005; 325(10):997-1003.
7. Ji L, Zhou FM. The correlation of the expression of MGMT and P53 in Human Brain Gliomas with Tumor Grade or Prognosis. Chinese J of Clinical Neurosciences 2011; 19(6):588-93.
8. Ma R, de Pennington N, Hofer M, Blesing C, Stacey R. Diagnostic and prognostic markers in gliomas-an update. Br J Neurosurg 2013; 27(3):311-5.
9. Lin Y, Hao ZF, Huang SZ, et al. Experssion of DNA repair enzyme MGMT and Ki-67 antigen in human brain gliomas. Guangdong Med J 2005; 26 (8):1063-5.
10. Zheng CQ, Ji SP, Gong F, Li AM, Tai JL, Zhang YP. Detection of O6-methylguanine-DNA methyltransferase promoter methylation in chemotherapy for qlioma. Chinese J Cancer 2009; 06:75-80.
11. Wei XT, Du W, Zheng J, et al. Expression and clinical value of DNA repair enzyme MGMT and NF-kB in human brain gliomas. Chinese J of Practical Neruous Diseases 2008; 11(10):8-10.
12. Roger S, Monika EH, Warren PM, et al. Effects of radiotherapy with concom itant and adjuvant temozolomide versus radiotherepy alone on survival in glioblastoma in randomized phase III study 5-year analysis of the EORTC-NCIC trial. Lancet Oncol 2009; 10(11):459-66.
13. Meert A P, Martin B, Delmotte P, et al. The role of EGFR expression on patient survival in lung cancer: a systematic review with meta-analysis. Eur Respir J 2002; 20(4):975-81.
14. Yu GZ, Chen Y, Pan J, et al. Expression of ANXA1 and EGFR in gastric carcinoma and its relationship with prognosis. Chinese Clinical Oncology 2008; 13(8):691-4.
15. Wang SS, Guan ZZ, Xiang YQ, et al. Significance of EGFR and p-ERK expression in nasopharyngeal carcinoma. Chinese J of Oncology 2006; 28(1):28-31.
16. Dong L, Pu PY, Wang H, et al. The expression of EGFR, p53 and Ki-67 in Glioma. Chinese J of Neurosurgery 2006; 22(7):442-4.
17. Blough MD, zlatescu MC, Cairncross JG, et al. O6 - methylguanine-DNA methyltransferase regulation by p53 in astrocytic cell. Cancer Res 2007; 67:580-4.

LETTER TO THE EDITOR

CLINICAL RESEARCH OF PERSIMMON LEAF EXTRACT AND GINKGO BILOBA EXTRACT IN THE TREATMENT OF VERTEBROBASILAR INSUFFICIENCY

SG. GUO[1], SH. GUAN[2], GM. WANG[3], GY. LIU[1], H. SUN[1], BJ. WANG[1] and F. XU[4]

[1]Department of Neurology, Shandong Provincial Hospital Affiliated to Shandong University, Jinan, China; [2]Department of Anesthesiology, Taian Central Hospital, Taian, China; [3]Department of Anesthesiology, Shandong Provincial Hospital Affiliated to Shandong University, Jinan, China; [4]Department of Neurology, Tongji Hospital, Tongji Medical College, Huazhong University of Science and Technology, Wuhan, China

Received November 22, 2014 – Accepted January 9, 2015

This paper aims to compare the curative effects of persimmon leaf extract and ginkgo biloba extract in the treatment of headache and dizziness caused by vertebrobasilar insufficiency. Sixty patients were observed, who underwent therapy with persimmon leaf extract and ginkgo biloba extract based on the treatment of nimodipine and aspirin. After 30 days, 30 patients treated with persimmon leaf extract and 30 patients with ginkgo biloba extract were examined for changes in hemodynamic indexes and symptoms, such as headache and dizziness. The results showed statistically significant differences of 88.3% for the persimmon leaf extract and 73.1% for the ginkgo biloba extract, P<0.05. Compared to the group of ginkgo biloba extract, the group of persimmon leaf extract had more apparent improvement in the whole blood viscosity, plasma viscosity, fibrinogen, hematokrit, and platelet adhesion rate, and the difference was statistically significant (P<0.05 or P<0.01). Based on these analyses, it can be concluded that persimmon leaf extract is better than ginkgo biloba extract in many aspects, such as cerebral circulation improvement, cerebral vascular expansion, hypercoagulable state lowering and vertebrobasilar insufficiency-induced headache and dizziness relief.

In modern society dietary habits are changing, and with the increase of unhealthy eating the occurrence of cerebrovascular diseases increases accordingly and constantly; for example, vertebrobasilar insufficient vertigo (VBIV) which is an ischemic cerebrovascular disease of the vertebrobasilar system. Common in emergency internal medicine, vertebrobasilar insufficiency itself is an ischemic cerebrovascular disease, which mainly causes headache and dizziness (1-2). VBIV is part of traditional Chinese medical science, but it is caused by specific cerebrovascular factors, i.e. it is an independent disease differing from the "dizziness" in general Chinese medicine. As a common disease with frequent occurrence, vertebrobasilar insufficiency is highlighted by its recurrent attacks and lingering after effects, which cause great pain. Thus, clinical intervention of vertebrobasilar insufficiency has become a hot topic.

With high occurrence in the elderly, some cases of vertebrobasilar insufficiency are due to organic brain changes and some are not. Various medicines are used to treat vertebrobasilar insufficiency but

Key words: persimmon leaf extract, ginkgo biloba extract, vertebrobasilar insufficiency

Mailing address:
Prof. Gongming Wang,
Department of Anesthesiology,
Provincial Hospital Affiliated to Shandong University,
Jingwuweiqi Road,
Jinan 250021, China
e-mail: wqllzjl@163.com

0393-974X (2015)

seldom lead to assured curative effects. Besides Western medicines, commonly used medicines in clinics include Chinese herb preparations, such as persimmon leaf extract (Naoxinqing tablets) and ginkgo biloba extract (ginkgo biloba tablets) (3), which promote circulation and dissipate stasis.

Ginkgo biloba possesses a neutral nature, has a bitter-sweet and astringent taste, and mainly functions on the heart and lungs; for instance, its extracts are effective in lung astringency, asthma relief, blood circulation activation, stasis dissipation and pain relief. In addition, blood vessel expansion and micro-circulation enhancement are also due to ginkgo biloba extracts, an effective medicine in treating VBIV (4).

Persimmon leaf contains abundant nutritional substances and functional components, whose products are safe for consumption without poisonous factors, leading to promising prospects in health food development. To date, persimmon leaf is mainly used to process and make multi-functional health foods, such as persimmon leaf tea, persimmon leaf beverage and persimmon leaf crystal. While clinically speaking, persimmon leaf has been made into persimmon leaf injection, blood purifying tablets, and styptic powder for therapy. Persimmon leaf extract and ginkgo biloba extract still remain to be researched in detail for their curative effects in treating vertebrobasilar insufficiency

Based on the application of nimodipine and aspirin, this paper treated in-hospital vertebrobasilar insufficiency patients with persimmon leaf extract and ginkgo biloba extract and observed the curative effects of the two extracts.

MATERIALS AND METHODS

A total of 60 in-hospital patients, 38 male and 22 female aged from 41 to 79 years (mean age: 60.2 years), were studied in this research. Of these 60 subjects, 41 had high blood pressure, 29 hyperlipidemia, 36 diabetes and 49 cervical spondylosis. With disease course varying from 14 days to 22 years, the patients suffered from continuous or repeated headaches and dizziness accompanied by cervical pain and limb numbness. In the worst cases, 20 patients had also once suffered from cataplexy and fainting. The examination by Transcranial Cerebral Doppler (TCD) showed that vertebrobasilars in all cases had different degrees of insufficient blood supply, such as slow blood flow, which conformed to the diagnosis of vertebrobasilar insufficiency according to Practical Neurology criteria.

Methods

The patients were randomly divided into two groups of 30: one group to be treated with persimmon leaf extract and one group with ginkgo biloba extract. The differences in age, gender, symptoms, disease course and test indexes between the two groups were compared with $P>0.05$. Both groups regularly took nimodipine orally (Bayer medicine, 30 mg 3 times/day) and aspirin (Bayer medicine, 100 mg 3 times/day), aiming to expand blood vessels, lower blood viscosity and improve cerebral blood flow. On this basis, the patients in the persimmon leaf extract group took 2 Naoxinqing tablets orally (Guangzhou Baiyun Mountain Hutchison Whampoa) 3 times a day, while patients in the ginkgo biloba extract group took 1 ginkgo biloba tablet orally (Jiangsu Yangtze Medicine) 3 times a day. After a course of 20 days, several aspects were observed, such as clinical signs and hemodynamic indexes, and TCD was carried out to observe other indexes, such as blood flow velocity mean (Vm), systolic blood flow velocity (Vs) and diastolic blood flow velocity (Vd) in the middle cerebral artery (MCA), anterior cerebral artery (ACA), posterior cerebral artery (PCA), basilar artery (BA) and vertebral artery (VA).

Therapeutic criteria

The following criteria was used to categorize the results. Remarkably effective: disappearance of simultaneous phenomenona like dizziness, blurred vision or unstable feeling, while the results of hemorheology and TCD proved to be normal and regular. Effective: simultaneous phenomenon such as dizziness were obviously relieved, and compared to pre-treatment, blood flow in vertebrobasilar artery checked by TCD was improved over 50% while hemorheology indexes were apparently lowered. Invalid: besides the relief of dizziness, the indexes detected by hemorheology and TCD did not meet the requirements mentioned above.

Statistical analysis

χ^2 test was used for statistical analysis, and SPSS17.0 software was used for processing.

RESULTS

Comparison of improvement of clinical symptoms between the two groups

Comparison of clinical symptom improvement between the two groups: of the 30 cases in the group of persimmon leaf extract, 20 resulted remarkably effective (66.7%), 6 effective (20%), and 4 invalid (13.3%), thus a total of 86.7% with effective rate.

Table I. *Comparison of improvement of clinical symptoms between the two groups.*

	Persimmon leaf extract group	Ginkgo biloba extract group
Remarkably effective	20	16
Effective	6	7
Total effective rate	26	23
Invalid	4	7

Table II. *Changes of hemorheology indexes before and after treatment in the two groups.*

Indexes	Persimmon leaf extract		Ginkgo biloba extract	
	Before treatment	After treatment	Before treatment	After treatment
High cut of whole blood viscocity (mPa.s)	5.87±2.38	4.11±1.21▲	5.81±2.84	4.98±1.34
Low cut of whole blood viscocity (mPa.s)	12.79±3.02	8.36±1.68▲	12.54±3.22	9.85±1.92
Plasma viscosity (mPa.s)	1.94±0.25	1.43±0.52▲	1.92±0.23	1.76±0.54
Fibrous protein (g/L)	4.91±0.84	3.47±0.48▲	4.88±0.74	4.37±0.81
Hematokrit (%)	43.45±6.35	35.06±4.53▲	42.77±6.38	39.31±4.92
Platelet adhesion rate (%)	42.55±4.29	31.09±2.17■	42.44±4.78	39.88±2.72

(1) (Mean ± SD)
Note: compared to the group of ginkgo biloba extract after treatment: ▲P<0.05, and ■P<0.01.

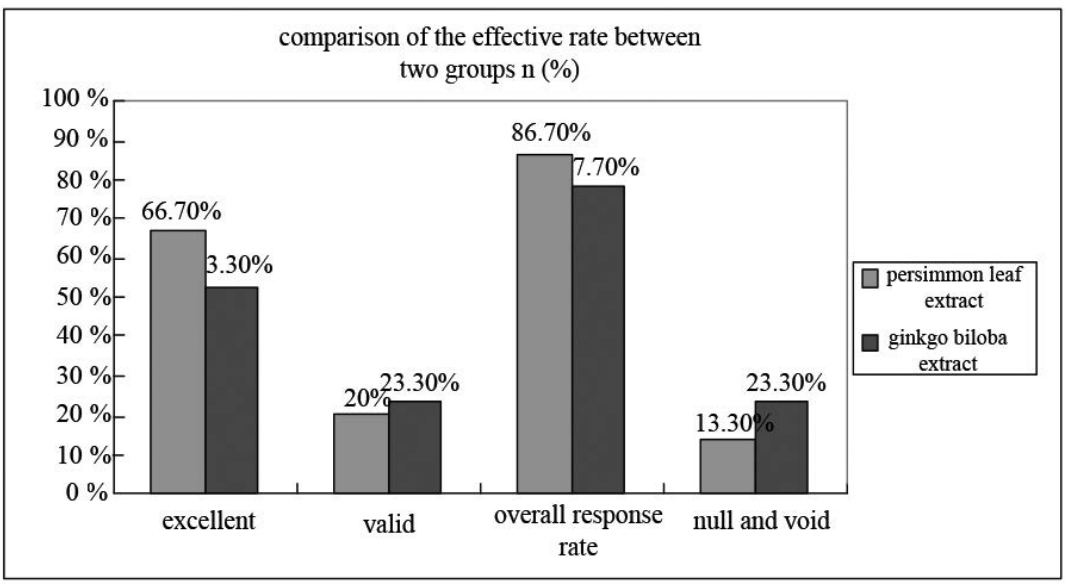

Fig. 1. *Comparison of effective rate between the two groups n (%).*

Of the 30 cases in the group of ginkgo biloba extract, 16 were remarkably effective (53.3%), 7 effective (23.3%), and 7 invalid (23.3%), with a total of 77.7% effective rate. With these comparisons, it was noted that persimmon leaf extract obtained a higher improvement rate with statistically significant differences (P<0.05). Results of the improvements are shown in Table I, and comparison of effective rate between the two groups is demonstrated in Fig. I.

Changes of hemorheology indexes before and after treatment are shown in Table II.

Changes of blood flow velocity through TCD before and after treatment

As shown in Table III, both ginkgo biloba extract and persimmon leaf extract improved blood flow to

Table III. *Relationship of the expression of E-cad and Bcl-2 protein with the clinicopathologic feature of breast cancer.*

		MCA		ACA		PCA		BA		VA	
		Before treatment	After treatment	Before treatment	After treatment	Before treatment	After treatment	Before treatment	After treatment	Before treatment	After treatment
Persimmon leaf extract group	Vm	37±14	55±3■	41±8	49±7▲	31±9	39±6■	27±8	42±7▲	26±9■	38±3
	Vs	64±26	93±7■	61±16	79±13▲	30±13	49±12■	42±10	63±9▲		
	Vd	32±7	47±6■	21±5	37±5■	22±5	32±5▲	20±7	32±5■		
Ginkgo biloba extract groups	Vm	38±17	46±8▲	43±9	47±2	33±4	36±8	29±7	38±5▲	27±8▲	34±3
	Vs	68±14	82±11▲	62±11	68±16	31±2	38±7▲	41±8	55±13▲		
	Vd	32±12	40±9▲	23±2	30±8▲	22±7	27±5	22±6	27±7▲		

Note: comparison between persimmon leaf extract group and ginkgo biloba extract group after treatment was with ▲$P<0.05$ and ■$P<0.01$.

treat vertebrobasilar insufficiency, but the latter was more effective in the enhancement of blood flow velocity mean, which was seen in the remarkable improvement of the arteries. Furthermore, persimmon leaf extract was more efficient in improving both systolic blood flow velocity and diastolic blood flow velocity.

DISCUSSION

Hemodynamic abnormality is one of the factors that cause vertebrobasilar insufficiency. Hyperostosis and cervical hypertrophy narrow the vascular lumina of the vertebral artery and basilar artery, leading to lower blood flow; and vertebral basilar artery spasm results from stimulation on the cervical sympathetic nerve. Moreover, in the elderly, blood flow velocity is decreased by the arteriosclerosis of heart and cerebral vessels, dysfunction of blood flow, and the increase of blood viscosity and coherence. In addition, the deposition of immune complexes on the vascular wall from autoimmune reaction causes poor cerebral blood flow, which leads to local ischemia and hypoxia of brain tissue of the vertebrobasilar system. Clinically, the corresponding outcomes are cerebral dysfunction, dizziness, etc. (5-6).

Ginkgo biloba injection is the extract of dry ginkgo leaves (Fig. 2), with the effect of restraining lung inflammation, promoting blood circulation and removing meridian problems. The injection is able to improve vascular functions of the heart and brain, expand blood vessels, increase brain blood flow, lower vertebral artery obstruction, and increase mean vertebrobasilar artery blood flow velocity. Moreover, when the injection eliminates oxygen free radicals and inhibits lipid peroxidation of cell membrane to stabilize the cell membrane, it also enhances brain functions by reducing angiotensin permeation, regulating blood lipids, and promoting brain tissue metabolism, finally relieving clinical symptoms (7). Active ingredients of ginkgo biloba extract mainly contain ginkgetin and terpenoid, such as ginkgolide and bilobalide. Various functions of persimmon leaf have been proved in pharmacological studies (3-4). Firstly, ginkgetin, a trapper and scavenger of oxygen free radicals, protects brain cells through free radical removal and lipid peroxidation resistance. Secondly, terpenoid is a natural antagonist of platelet-activating factor (PAF), which is able to reduce PAF-induced platelet aggregation, microthrombus and lipid metabolism disordes. Thirdly, ginkgo biloba extract can expand blood vessels of the brain and increase cerebral blood volume. Fourthly, with ginkgo biloba, blood viscosity degree is decreased, erythrocyte is improved in plastic deformation and blood circulation is enhanced. Finally, while ischemic tissues effectively apply oxygen and glucose, brain circulation and metabolism are improved to enhance memory and increase some neurotransmitters.

Lu Minming et al. (8) carried out a study on 96 patients who were divided into a treatment group and a control group. For the treatment group, patients took betahistine 6 mg orally 3 times a day

Fig. 2. *Extract of dried ginkgo biloba.*

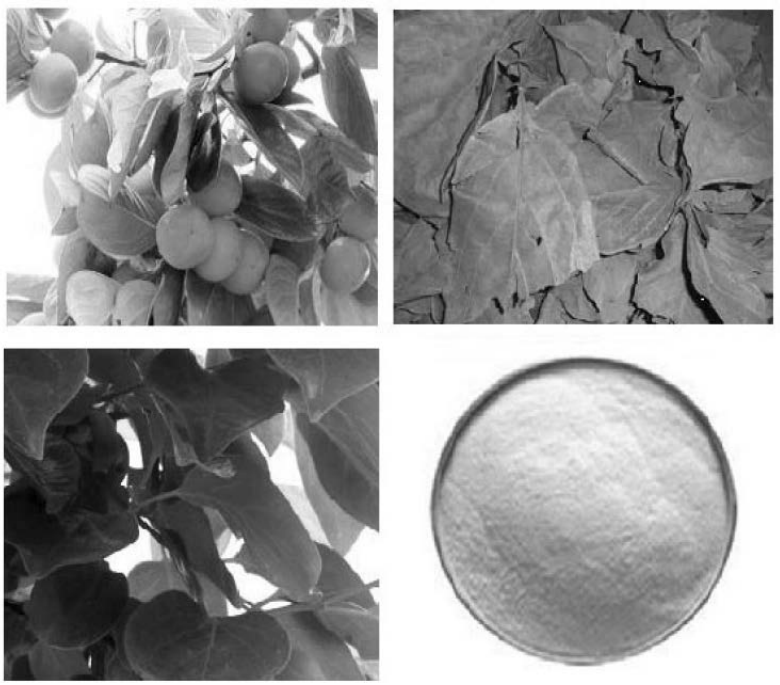

Fig. 3. *Extract of dried persimmon leaf.*

for 14 days; meanwhile, they were intravenously infused with 30 ml dipyridamole injection of ginkgo biloba extract combined with 250 ml 5% glucose injection 4 times a day. The patients in the control group underwent intravenous infusion of compound injection of red sage root. After observing the clinical curative effects before and after treatment and measuring mean velocity by TCD, the overall effectiveness of the treatment group was determined to be 94.2% and the control group 67.9%.

In an 8-week treatment, Zhu Min et al. (9) gave 80 patients in the treatment group ginkgo biloba (each containing 19.2 mg flavonol and 4.8 mg terpene inner fat) which was taken orally, 1 pill 3 times a day; at the same time, flunarizine was taken orally 5 mg each night. For reference, 80 patients in the control group took flunarizine 5 mg orally each night, after which clinical curative effects were rechecked by TCD and compared to those before treatment. Overall effectiveness of the treatment group of 92.5% and the control group of 80.0% indicated that the former group had more notable brain blood velocity improvement.

Naoxinqing tablet is a pure traditional Chinese medicine made from active extracts of natural persimmon leaf (Fig. 3), whose three effective constituents are suggested and discussed in research. The first is flavonoid which can improve blood-supply, protect nerves, reduce myocardial infarction and regulate blood lipids. The second is organic acid which functions on inflammation resistance, pain relief, blood vessel softening and thrombus dissolution. The third are coumarins with the role of having effects in resisting freezing and improving hemorheology. The above constituents enable Naoxinqing tablets to have multiple mechanisms of action. On the one hand, Naoxinqing tablets have obvious therapeutic effects on enhancing coronary artery and cerebral blood flow, and improving blood and oxygen supplement for heart and brain tissues. On the other hand, they cooperate with medicines for anti-platelet and vascular dilation to enhance their effects (10-11).

Persimmon leaf extract is a histamine-like medicine, significantly expanding cerebral blood vessels, and the cardiovascular and vertebrobasilar artery systems (12). The extract can remarkably increase circulating blood flow in the heart and brain and their surroundings, and reduce high agglutination conditions. Via the blood-brain barrier, the pharmaceutical and biological effects act directly on smooth muscle of the cerebral blood vessels to substantially increase blood flow of internal cervical arterial circulation and dredge cerebral blood circulation, which rapidly relieves vertebrobasilar insufficiency. Compared with ginkgo biloba extract, persimmon leaf extract is more effective in improving vertebrobasilar insufficiency. With remarkable effects of lowering blood pressure and easing anxiety, persimmon leaf extract can relieve dizziness and spinning sensation, and eliminate tension, irritation and anxiety in a shorter time. Therefore, persimmon leaf extract has a promising future in the treatment of vertebrobasilar insufficiency.

The results of this research show that both persimmon leaf extract and ginkgo biloba extract could effectively improve vertebrobasilar insufficiency; but based on index changes of hemorheology, the improvement of blood circulation by the persimmon leaf extract was more significant. To be specific, although ginkgo biloba extract did relieve vertebrobasilar insufficiency, its curative effect was less comprehensive than the persimmon leaf extract in improving the symptoms mentioned above. Furthermore, Naoxinqing tablets improved cerebral circulation in an effective way, expanding cerebral blood vessels and reducing high agglutination conditions.

In conclusion, the formation and development mechanism of cerebral arteriosclerosis is complicated with multi-aspect involvement, which determines its comprehensive treatment with various factors rather than single-medicine treatment (13-16). It can not be denied that ginkgo biloba maintains satisfying curative effects in treating vertebrobasilar insufficiency; but compared to persimmon leaf, ginkgo biloba functions in a single way without comprehensive effects.

Naoxinqing tablets and their active constituents can reduce blood pressure and blood lipid fat, improve hemorheology and inhibit platelet aggregation. Moreover, they regulate immunologic functions, decrease adhesion between lymphocyte and nerve cells and control inflammation. For the relief of radical damage in ischemic brain tissues, the tablets improve oxidation-reduction of nerve cells, increase antioxidant gene expression, remove free radicals,

and inhibit lipid peroxidation. In addition, they can regulate the stability of calcium ion, and resist toxicity of excited glutamic acid to control cell apoptosis and cerebral edema, which protects ischemia brain tissues. While promoting the recovery of nerve cell functions, they cut off the genesis and development of cerebral arteriosclerosis at different levels with various targets to prevent cerebral ischemia injury and protect nervous tissue, aiming to prevent and treat cerebral arteriosclerosis more efficiently.

ACKNOWLEDGEMENTS

This study was funded by the National Nature Science Foundation of China (No. 81171171, 30970991, 30872433), and the Science and Technology Development Foundation of Shandong Province (No. 2014GSF118117).

REFERENCES

1. Wang H. Clinical curative effect of ginkgo biloba extract in the treatment of cerebral insufficiency. Seek Med and Ask the Med 2012; 15(9):512-13.
2. Liu SP, Liu HJ. Clinical observation of ginkgo biloba extract in the treatment of 50 patients with cerebral insufficiency. Seek Med and Ask the Med 2011; 9(11):601-2.
3. Qu Y. Therapeutic effect of ginkgo biloba extract in the treatment of ischemic encephalopathy. Chongqing Med 2010; 89(18):423-56.
4. Chen FH, Xu L. Clinical effect of ginkgo biloba extract in the treatment of cerebral insufficiency. Shanxi Med J 2009; 38(12):1669-70.
5. Li S. Observation of the curative effect of treating cerebral insufficiency with ginkgo biloba leaf extract injection. Chin and Foreign Med Res 2010; 51(7):237-38.
6. Deng YK, Wei F, Zhang DG. erythrocyte protective effects of ginaton in patients undergoing hypothermic cardiopulmonary bypass. HSRI Res Rev 2010; 30(4):365.
7. Zhang YH. Discussion of treating vertebrobasilar insufficiency with betahistine combined ginkgo-damole. China Practic Med 2012; 7(8):162-63.
8. Lu CM, Zhou CQ. Effect observation of betahistine combined with ginkgo leaf extract and dipyridamole Injection (GLEDI) in the treatment of 52 patients with vertigo caused by vertebrobasilar insufficiency. West China J of Pharm Sci 2010; 25(6):766-67.
9. Zhu M, Hu Y, Ye M. The treatment of 60 patients with vertebrobasilar insufficiency by ginkgo tablet combined with flunarizine. Chin J of Integr Med on Cardio-/Cerebrovas Dis 2009; 7(12):1488-89.
10. Gu XL. Observation of the curative effect of treating cerebral insufficiency with silver educational brain capsule combined betahistine hydrochloride. Chin J of Integr Med on Cardio/Cerebrovas Dis 2011; 9(11):1335-36.
11. Yu WY, Guo JL, Shi H. Curative effect observation of treating cerebral insufficiency with yangxueqingnao granule combined betahistine methanesulfonate. Hebei J of Tradit Chin Med 2008; 30(11):1205-06.
12. Yue HB, Yang HL. Research on the combined application of betahistine and ginkgo-damole in the treatment of cerebral insufficiency. Med Innov of China 2013; 10(2):129-30.
13. Wang GH. Effect of ginkgo biloba leaf extract injection on vertebrobasilar insufficiency. J of Changchun Univ of Tradit Chin Med 2008; 24(6):677-78.
14. Li L. Curative effect observation of treating vertebrobasilar insufficiency with shuxuening combined sibelium. Chin J of Clin Rational Drug Use 2010; 22(3):50-51.
15. Gan YX, Zhang SL. Meta analysis on curative effect of ginkgo biloba leaf extract injection in treating vertebrobasilar insufficiency. Chin J of Hospital Pharm 2012; 32(20):1667-71.
16. Li JQ, Zhang XJ, Li B. Research progress of diagnosis and treatment of vertebrobasilar insufficiency. Chin and Foreign Med Researc 2010; 9(30):154-56.

LETTER TO THE EDITOR

CHANGES OF SERUM VASCULAR ENDOTHELIAL GROWTH FACTOR OF PATIENTS WITH RECTAL CANCER BEFORE AND AFTER NEOADJUVANT CHEMOTHERAPY AND TUMOR PROGRESS

L. WANG, G. SHAN, X. LIU and X. SUN

Department of Radiation Oncology, Zhengzhou People's Hospital, Zhengzhou, China

Received November 22, 2014 – Accepted December 19, 2014

In the rapid development of armamentarium, neoadjuvant chemotherapy has become an important part of a multi-instrument comprehensive treatment of malignant tumor, which presents promising application prospects. This paper researches changes of Vascular Endothelial Growth Factor (VEGF) and Vascular Endothelial Growth Factor-2 (VEGF-2) in serum of patients with rectal cancer before and after neoadjuvant chemotherapy and discusses how tumor progression rules relate to curative effect and prognosis. Enzyme linked immunosorbent serologic assay (ELISA) was applied for the detection of VEGF expression and VEGF-2 expression of 45 patients with rectal cancer (treatment group) before and after neoadjuvant chemotherapy, which was compared to the expressions of 45 healthy people (control group). After 8 weeks of continuous neoadjuvant chemotherapy, the results did not present obvious differences of VEGF and VEGF-2 expression in patients with different curative effects between pre-chemotherapy and post-chemotherapy. However, VEGF and VEGF-2 expression of patients with CR+PR and NC significantly decreased. This proved the excellent curative effect of neoadjuvant chemotherapy, with which the expressions of VEGF and VEGF-2 of rectal cancer patients decreased. The above experiment provides new ideas for the application of neoadjuvant chemotherapy in treating rectal cancer.

Rectal cancer, a very common malignant tumor, has frequent occurrence in Europe and America. In recent years, since the pace of living has increased, rectal cancer has tended to occur more frequently in China (1). Operations are able to treat rectal cancer radically, and pure radical operation in stage I of rectal cancer can obtain satisfying long term survival rates. Compared with post-operative chemotherapy or radiotherapy, synchronous radiotherapy and chemotherapy before an operation proves advantageous in degrading the tumor, increasing the resection rate and protecting the anus, etc (2).

Vascular endothelial growth factor (VEGF), discovered in recent years, belongs to the factor that can promote the growth of vascular endothelial cells with high specificity (3). It mainly functions in inducing the proliferation and migration of vascular endothelial cells and increasing the permeability of vessels. Through double antibody sandwich enzyme-linked-immunosorbent serologic assay (DAS-ELISA), Yang Kai et al. carried out studies on serum MMP-9 in female primary and invasive breast ductal carcinoma before and after neoadjuvant chemotherapy. Based on research, it was discussed

Key words: neoadjuvant chemotherapy, rectal cancer, vascular endothelial growth factor

Mailing address: Dr Lin Wang,
Department of Radiation Oncology,
Zhengzhou People's Hospital,
NO.33, Huanghe Road,
Jinshui District,
Zhengzhou, China
e-mail: wlzzrmyy@163.com

0393-974X (2015)

how serum MMP-9 correlated to chemotherapy curative effect and pre-chemotherapy clinical staging. Pre-chemotherapy MMP-9 was found correlated to pre-chemotherapy clinical staging, and changed with the implement of neoadjuvant chemotherapy, having an impact on the chemotherapeutic effect. All the above findings have certain clinical significance for the prediction of the effect of neoadjuvant chemotherapy (4).

Gu Jinhua et al. tested the level of VEGF, CEA, CA19-9 and SF of advanced gastric cancer patients prior to chemotherapy and one week after chemotherapy, and evaluated the curative effect two weeks after chemotherapy. Meanwhile, the analysis of serum VEGF indicated that the change of CEA, VEGF and CA19-9 was correlated with gastric cancer chemotherapeutic effect. Therefore the detection of CEA, VEGF and CA19-9 was helpful in predicting the chemotherapeutic effect (5). To explore the clinical curative effect of neoadjuvant chemotherapy combined with laparoscopic surgery in the treatment of colorectal cancer, Yang Chunhong treated patients in two different ways. One was laparoscopic surgery only and another was neoadjuvant chemotherapy combined with laparoscopic surgery. After surgery, Yang observed the patients' physical conditions and functions and calculated their survival rates in the following 3 years. Neoadjuvant chemotherapy combined operative treatment proved to have more remarkable clinical effects, so it deserved clinical promotion and application for its effectiveness in enhancing patient's physical condition and improving functions (6). Most researches indicated that anti-VEGF treatment could effectively inhibit tumor progress with good outcome (7).

For this study 45 patients with rectal cancer and 45 healthy persons as controls were selected. Firstly, ELISA was applied in detecting the expression of VEGF and VEGFR-2 of 45 rectal cancer patients before and after neoadjuvant chemotherapy; then the results were compared with the expressions of the control group. Selecting VEGF and VEGF-2 as research indexes, this paper discusses the changes of the above-mentioned indexes before and after neoadjuvant chemotherapy and the relationship between the indexes and prognoses. As a result, this paper provides a theoretical basis for the biological mechanism of neoadjuvant chemotherapy on rectal cancer.

MATERIALS AND METHODS

Materials

A total of 45 patients (30 male and 25 female) with rectal cancer, of which 26 cases were in stage III and 19 stage IV, hospitalized in the period between January 2013 and June 2013 were selected. Patients were all pathologically identified as rectal cancer patients by colonoscopic biopsy prior to chemotherapy and their ages ranged from 23 to 80 years (mean age 52.36±15.66 years). Based on multi-subject researches, optionality, clinical staging and treatment strategy were determined. All patients gave their informed consent. Karnofsky Performance Status (KPS) before treatment was higher than 60 points, which predicted over 3-month life-span of those patients without allergic constitution. Heart, liver and kidney functions of the patients before chemotherapy were all normally healthy, and those patients undergoing their first treatment of rectal cancer had not undergone other anti-tumor therapies in the previous month. The control group was formed of 45 healthy persons after qualified physical examinations between January and June 2013. The age of the 28 males and 17 females was between 25 and 75 years. Diseases in vital organs like liver, heart, cerebrum, kidney and internal secretion were excluded in patients from both groups whose hepatorenal function examinations were normal and regular. The differences of gender and age were not considered to be statistically significant.

Neoadjuvant chemotherapy

Patients were treated with FolFox-6 with their consent. In details, patients were intravenously infused with oxaliplatin 135mg/m2 for 3 h and with calcuim folinate (CF) 200mg/m2 for 2 h; then intravenously injected with 5-fluorouracil (5-Fu) 400mg/m2 and finally intravenously infused 5-Fu 2400~3600mg/m2 in a Baxter pump for 48 h. Some drugs were used to relieve the chemotherapy after-effects, such as those for central antemetic, liver protection, and body immunity strengthening. After chemotherapy, routine blood and liver and kidney functions were examined and found to be normal without apparent adverse reactions. Each case had chemotherapy for more than two courses, and each course lasted three weeks.

Specimen collection

A 5 ml sample of venous blood of the treatment group was taken twice in the morning on an empty stomach, before chemotherapy and after two courses of chemotherapy. In the control group, a venous blood sample was taken only once. These specimens were anti-frozen with 2% edetic

acid. Specimens were immediately centrifuged at 3000 r/min for 10 min to separate serum. The remaining serum was maintained at -80°C for later tests. The instructions on the ELISA kit were strictly followed for each step and the results were tested by ELISA at 450 nm wavelength.

Surgery

Depending on particular situations, the patients undergoing neoadjuvant chemotherapy rested for 3 to 6 weeks before preoperative assessment which decided on the type of surgical operation. The same method was suitable for patients in both groups, which was adopted with the assistance of laparoscopy according to total mesorectal excision (TME). First, under direct vision, sharp dissection of the fascia and the wall of the inter-layer of the presacral space; second, maintain the fascia without any damage; third, if excision occurred, the excision extension of tumor distal mesorectum had to be more than 5 cm. To clean regional lymph nodes, mesorectal excision, including the root of arteriae mesenterica inferior was necessary. If possible, the anterior resection was implemented on the condition that the resection margin of distal rectal was over 2 cm from the lower margin of the tumor. Otherwise, Miles or Hartmann surgery was carried out and frozen sections of suspected positive margins were rapidly examined to confirm complete resection.

Evaluation criteria

Routine blood and hepatorenal functions were all examined before and after chemotherapy. According to the chemotherapy evaluation criteria set by World Health Organization (WHO) on solid tumor, the curative effect was divided into four parts, complete remission (CR), partial remission (PR), Stable (NC) and Progress (PD) (8). Clinically effective treatment referred to complete remission and partial remission (CR+PR), while invalidity included stable and progress (NC+PD). The lesion processes before and after chemotherapy were evaluated by two clinically experienced oncologists.

Response evaluation criteria

Standard curve was drawn-up as a standard graph: the X-axis giving standard concentration, and Y-axis OD value with standard concentrations linked by a smooth curve. The concentration of specimens were assessed through the OD450 value from the standard curve, the result of which, multiplied by dilution ratio, was presented as Mean±SD.

Statistical analysis

The data obtained from the patients in the two groups were analyzed by SPSS17.0 software. Measurement data was expressed by Mean±SD deviation and analyzed by *t*-test and *q*-test, variance analysis and rank correlation.

RESULTS

Expression of VEGF and VEGFR-2 of the two groups before chemotherapy

Before neoadjuvant chemotherapy, the expressions of VEGF and VEGFR-2 in the treatment group were 243.59±30.53 and 248.33±53.44, respectively; while the expressions of VEGF and VEGFR-2 in the control group were 27.12±4.56 and 24.03±8.73, respectively (Table I).

Therapeutic effect after chemotherapy

In the treatment group, two courses of treatment resulted in 3 cases of CR, 25 PR, 12 NC and 5 PD. Thus the 28 cases of clinical effectiveness were 62% and 17 cases of clinical invalid accounted for 38%.

Therapeutic effect of VEGF and VEGFR-2 expression before and after chemotherapy

The levels of VEGF and VEGFR-2 in the treatment group did not have remarkable differences in pre-chemotherapy patients with different curative effects. But after chemotherapy, VEGF and VEGFR-2 levels in cases of effectiveness were 87.23±45.78 and 80.27±58.67, respectively; and in cases of NC were respectively 144.96±12.35 and 125.66±13.78. As for VEGF and VEGFR-2 in PD, significant improvement was witnessed after chemotherapy, as shown in Table II and Fig. 1.

Post-surgery treatment of patients with rectal cancer in both groups

In the group undergoing neoadjuvant chemotherapy, tumors were not reduced for iconography; but some post-surgery pathological necrosis or fibrosis tumor cells were found. Anastomotic leakage did not occur, but one case of abdominal incision infection in the group of neoadjuvant chemotherapy was successfully treated. Table III presents the patient conditions in both groups, such as gas relief time, meal time, in-hospital period after surgery and incision infection. It could be noticed that the differences between the two groups were not statistically significant (Figs. 2-4).

DISCUSSION

With the advancement of comprehensive

Table I. *Comparison of VEGF and VEGFR-2 levels between treatment group and control group before chemotherapy (Mean±SD, ng/L).*

Group	n	VEGF	VEGFR-2
Treatment group	45	243.59±30.53	248.33 ± 53.44
Control group	45	27.12 ± 4.56	24.03 ± 8.73

Table II. *Comparison of VEGF and VEGFR-2 levels of patients with different curative effects in the chemotherapy group (Mean±SD, ng/L).*

Curative effect	n	VEGF		VEGFR-2	
		Before chemotherapy	After chemotherapy	Before chemotherapy	After chemotherapy
CR+ PR	28	238.47±30.45	87.23±45.78	232.41±32.78	80.27±58.67
NC	12	235.11±17.27	144.96±12.35	270.32±77.34	125.66±13.78
PD	5	268.39 ±35.07	312.45±23.45	298.87±50.33	345.88±19.75

Table III. *Post-surgery recovery of patients in both groups.*

	Gas relief time (day)	Meal time (day)	In-hospital period (day)	Incision infection
Chemotherapy	3.18±0.810	6.12±1.219	13.67±1.560	0.03±0.174
Control	2.97±0.882	6.03±1.649	13.61±1.898	0.00±0.000

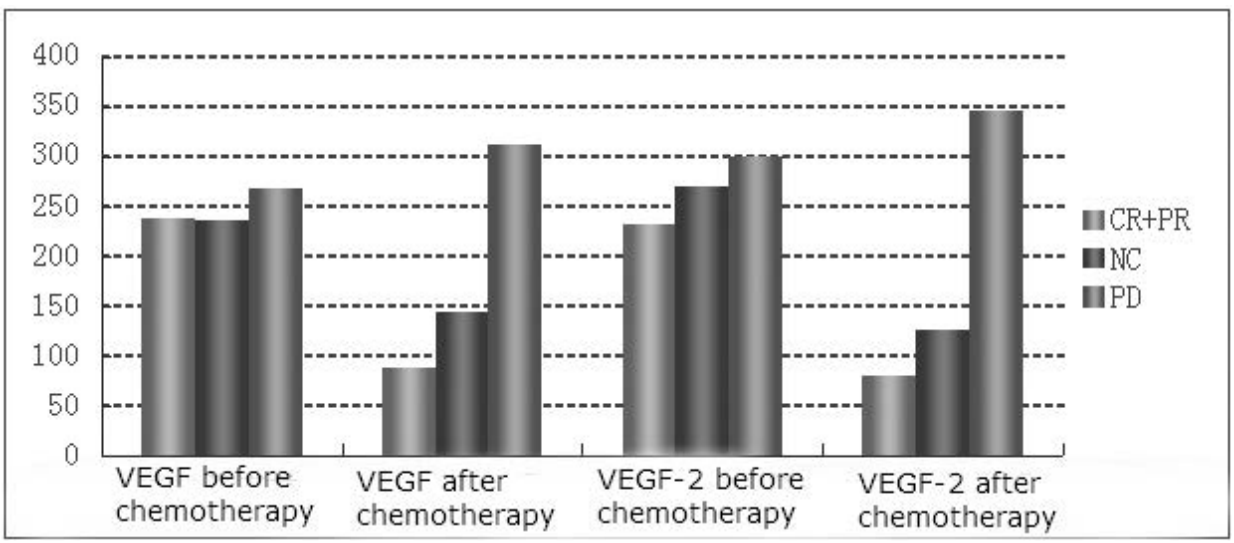

Fig. 1. *Comparison of VEGF and VEGFR-2 levels of patients with different curative effects in the chemotherapy group.*

treatment, neoadjuvant chemotherapy has been highlighted for its enhancement on resection rates. Neoadjuvant chemotherapy, namely pre-surgery chemotherapy, refers to systematic chemotherapy or local chemotherapy for malignant tumors before local treatment (surgery or radiotherapy) with the purpose of enhancing tumor radical resection rates. Neoadjuvant chemotherapy is regarded as the decrement therapy of tumor cells, and its significance is to enhance resection rates through lessening tumor size and degrading clinical staging. In addition, it aims to decrease tumor micro-metastasis to reduce tumor metastasis and recurrence; it also determines the sensitivity of patients to chemotherapeutics to

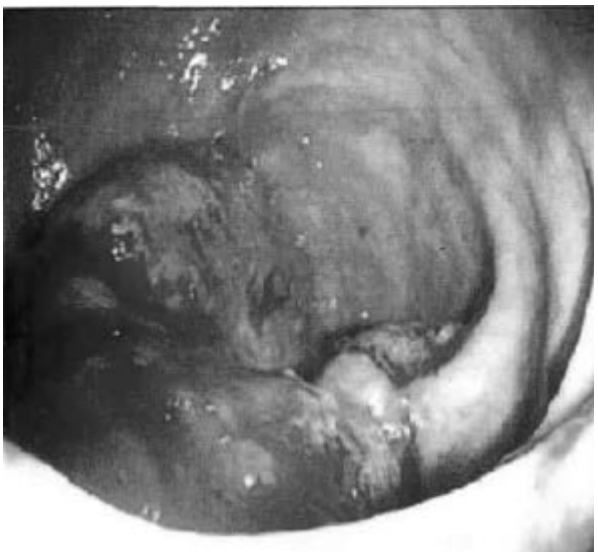

Fig. 2. *Before neoadjuvant chemotherapy (enteroscopy).*

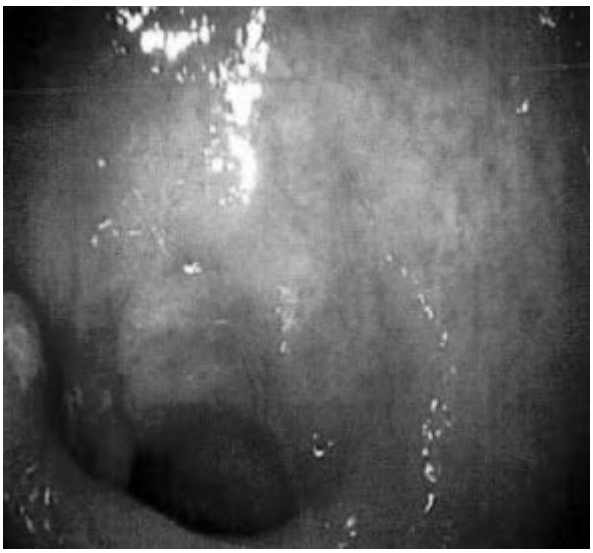

Fig. 3. *Before neoadjuvant chemotherapy (enteroscopy).*

guide postoperative chemotherapy and improve prognosis (9).

Although neoadjuvant chemotherapy has been applied for quite a long time, only a few indexes can be used to judge the curative effects of neoadjuvant chemotherapy, commonly including: remission of clinical symptoms and remission of blood biochemical index and iconography. For blood biochemical indexes, traditional tumor markers with low sensitivity are still regarded as the main references, such as carcino-embryonic antigen (CEA), carbohydrate antigen125 (CA125) and carbohydrate antigen199 (CA199) (10). In recent years, VEGF and VEGFR-2 have been the major target sites in various anti-tumor vascular targeted therapies, and studies on anti-tumor vessel taking VEGF and VEGFR-2 as target sites have been carried out in the field of oncology fundamental research.

The "Tumor angiogenesis theory" holds that tumor growth depends on angiogenesis. The formation of numerous microvessels is the basis of tumor occurrence and development, closely connected with tumor formation, invasion, metastasis and relapse. "Angiogenic switch theory" divides tumor growth into prevascular stage and vascular stage. In the prevascular stage, tumor cells remain in a dormant state if new vessels are not formed; while in the vascular stage, tumor cells constantly split and produce to cause invasion and further metastasis because the generation of new vessels satisfies the tumor tissues' demand of further growth and metabolism (11).

Among angiogenic growth factors involved in tumor vessel growth, VEGF is currently the most powerful and concentrated factor promoting the proliferation of vascular endothelial cells (12). VEGF is a type of exocrine dimer glycoproyein, and plays an important role in regulating cascular

Fig. 4. *Post-surgery pathology.*

development. The proliferation of vascular endothelial cells with special activation is the idiocratic mitosis of endothelial cells, which regulate vascular permeability and the inhibition of cell apoptosis. New vessels are generated in the stages of the proliferation and diffusion of a malignant tumor. To form new tumor blood-supply vasoganglion, VEGF is able to prevent the degeneration of lumen net structure of vascular endothelial cells and cell apoptosis. Besides, VEGF promotes the degeneration, migration and proliferation of vascular endothelial cells and enhances vascular permeability. Therefore, regarded as the index of tumor growth, invasion and metastasis, VEGF induces the formation of new-born tumor vessels and increases vascular permeability. In addition, it also assists cancer tumors to enter into vascular tissue and promotes the invasion and metastasis of a malignant tumor. VEGFR-2, a receptor type tyrosine kinase, is one of the vascular endothelial cell growth factors whose main function is regulating the permeability of vascular endothelium and promoting cellular mitosis and chemotaxis, to promote the formation of new vessels. Moreover, it also can resist the apoptosis of endothelial cells and maintain the survival of endothelial cells (13).

It has been reported that VEGFR-2 plays a leading role in the signal transduction of VEGF and the generation of vascular endothelium. The combination of VEGF and VEGFR-2 causes a series of changes in vascular endothelial cells, which regulates their survival and promotes the formation of new vessels with integrity through anti-apoptosis. In addition, VEGF can continuously stimulate VEGFR-2 to mediate the DNA synthesis of tumor vascular endothelial cells to induce the migration and proliferation of endothelial cells. It also changes the vascular permeability, increasing plasma leakage. Research (14) showed that rectal cancer invades the adjacent normal tissues firstly through generating new vessels. In the early stage, a continuous increase of the VEGF receptor of colonic mucosa results in rectal cancer occurrence.

This research shows that the expression of VEGF and VEGFR-2 in the serum of rectal cancer patients was evidently higher than that in healthy persons. Compared to pre-chemotherapy expression, the expression of VEGF and VEGFR-2 in serum after chemotherapy declined, but was still higher than the control group. Therefore, it is believed that the levels of VEGF and VEGFR-2 in serum are related to the occurrence of rectal cancer, which suggests that VEGF and VEGFR-2 are reliable tumor markers. VEGF and VEGFR-2 of patients with CR+PR and NC all remarkably decreased after chemotherapy, and the decrease in the former was more significant than the decrease in the latter. This indicates that chemotherapy effectively inhibits the birth of new vessels and induces tumor cell apoptosis to reduce the expression of VEGF and VEGFR-2, which leads to anti-tumor effects. Otherwise, the level of VEGF and VEGFR-2 in serum would not decline, which can be deducted from the PD group. Furthermore, VEGF and VEGFR-2 were expressed highly before chemotherapy and they presented positive correlation. After chemotherapy, VEGF and VEGFR-2 was reduced in a greater degree in the CR+PR group than in the NC group, indicating that VEGF and VEGFR-2 contributes to the occurrence and development of rectal cancer. Thus the supposition that the detection of VEGF and VEGFR-2 contributes to the assessment and evaluation of the curative effects of chemotherapy and prognosis.

To sum up, VEGF and VEGFR-2 are two effective indexes for tumor progression and migration, while neoadjuvant chemotherapy helps to improve the expression of VEGF and VEGFR-2 in the blood of patients with rectal cancer, to degrade tumor staging. Besides, neoadjuvant chemotherapy lessens tumor size and decreases the probability of local relapse, which has positive significance in middle and advanced rectal cancer. During the administration of neoadjuvant chemotherapy, tumor changes should be closely observed and monitored to adjust therapeutic planning, so that patients can be treated with an optimal curative effect. In addition, changes of VEGF expression and VEGFR-2 expression after chemotherapy can reflect the short-term effects of chemotherapy. Besides, biological functions of VEGF and VEGFR-2 and their roles in tumor angiogenesis offer new concepts in various aspects, such as rectal cancer treatment, assessing prognosis and targeted drug development. It is believed that the curative effects of rectal cancer will be enhanced in the near future if patients undergo individual neoadjuvant chemotherapy in an effective and safe way according to their conditions.

REFERENCES

1. Zhu J, Chen JG, Zhang YH, Chen YS, Ding LL. An analysis of incidence trend of colorectal cancer in Qidong, 1972-2011. China Cancer 2014; (8):648-55.
2. Chen XJ, Liu YQ, Ji SQ, Wang JH, Liu HL. Neoadjuvant concurrent chemoradiotherapy combined withsurgery in patients with locally advanced middle and lower rectal cancer. Henan Med Res 2013; 22(2):173-75.
3. Ravikumar G, Crasta JA. Vascular endothelial growth factor expression in ovarian serous carcinomas and its effect on tumor proliferation. South Asian J Cancer 2013; 2(2):87-90.
4. Yang K, Yang Y, Cao Y, Wang ZH. The correlation of matrix metalloproteinase 9 expression and neoadjuvant chemotherapy efficacy in breast cancer. J Mod Oncol 2014; 22(5):1058-61.
5. Gu JH, Gu T, Zhou LN, Wang LQ, Chen L. Values of serum VEGF, CEA, CA19-9 and SF for predicting the efficacy to chemotherapy in advanced gastric cancer. Int J Lab Med 2014; (18):19.
6. Yang CH. The analysis of therapeutic effect of neo-adjuvant chemotherapy combined with laparoscopic colorectal surgery for colorectal cancer. For All Health 2014; 8(7):89.
7. Deng LC, Shen WS, Zhang Y. Influence of chemotherapy on VEGF level in serum of patients with advanced colorectal cancer. J Clin Med Pract 2010; 14(3):90-91.
8. Bachmann A, Muir GH, Collins EJ, et al. 180-W XPS GreenLight laser therapy for benign prostate hyperplasia: early safety, efficacy, and perioperative outcome after 201 procedures. Eur Urol 2012; (3):600-607.
9. Shibuya M. Tyrosine kinase receptor Flt /VEGFR family: its characterization related to angiogenesis and cancer. Genes Cancer 2010; 1(11):1119-23.
10. Zhu SL, Wang H. Value of CA724, CA125, CA199, CEA in the diagnosis of colorectal cancer. J Hainan Med Coll 2014; 20(001):87-89.
11. Li XL, Ma J. Clinical research progress of treating colorectal cancer with combined treatment of traditional Chinese medicine and Western medicine. Mod J Integr Trad Chin Med West Med 2013; 22(3):323-25.
12. Lan YP, Zhao Y, Qiu MY, Chen XQ, Chen LF, Zeng LF. Preliminary discussion of relationship between the expression of colorectal cancer IL-8 and tumor angiogenesis factor. Lab Med Clin 2014; 11(11):1537-38.
13. Ye YZ, Shi ZH, Lu T. Advanced in research on VEGFR-2 tyrosine kinase Inhibitors. Progr Pharm Sci 2014; 1:5.
14. Lian W, Chen ZP, Yang P, Liao SW, Sun Z, Zhang WJ, Zeng SQ, Cao J. Changes of VEGF and VEGFR-2 of rectal cancer before and after neoadjuvant chemotherapy and its clinical significance. Mod J Integr Trad Chin Med West Med 2014; 3(3):235-37.

LETTER TO THE EDITOR

EFFECT OF INTEGRIN COMBINED LAMININ ON PERIPHERAL BLOOD VESSEL OF CEREBRAL INFARCTION AND ENDOGENOUS NERVE REGENERATION

R. DU, Y. WANG, JF. TENG, H. LU, R. LU and Z. SHI

The First Affiliated Hospital of Zhengzhou University, Zhengzhou, China

Received November 22, 2014 – Accepted January 9, 2015

The third Chinese nationwide survey on causes of death states that cerebrovascular disease, accounting for 22.45% of total deaths, ranks as the first cause of death among rural and urban residents. It has become a serious public health problem since it has the highest disability and fatality rate among single diseases. Cerebral infarction is the most common cerebrovascular disease. In order to enhance the treatment response of cerebral infarction, this paper established male Sprague Dawley (SD) rat reperfusion model with 2 h of cerebral artery embolism by suture method. Neurological function deficit was scored according to rat improvement 24 h after model establishment, and 50 rats with scores between 10 and 13 were included in an ultimate experiment and were randomly divided into 5 groups: undisturbed control group, vascular endothelial growth factor (VEGF) up-regulated vessel group, endostatin down-regulated vessel group, ventricle injected Cxc Chemokin Receptor 4 (CXCR4) antibody group, ventricle injected α6β1 antagonist (GoH3 antibody) group, respectively. The experiment was initiated after grouping and measurement of the relative data. The obtained results showed that the behavioral recovery of the VEGF group was more obvious compared with the control group, and the differences were statistically significant. The research was carried out using decreased modified neurological severity scores (mNSS), and the time a rat took to remove a pasted object. However, the behavioral recovery in the endostatin group, anti-CXCR4 group and GoH3 group was slow, and the difference was statistically significant, which showed as slowly decreased mNSS scoring and inconspicuous improved time of a rat removing a sticker. Compared with the control group, the number of peripheral BrdU+/ vWF+ cells of rat cerebral infarction in the VEGF group increased, and the peripheral VEGF expression quantity of cerebral infarction increased, thus the difference was statistically significant. However, cells in the endostatin group, anti-CXCR4 group, and GoH3 group were fewer and VEGF expression was reduced, and the difference was statistically significant. All these findings suggest that the promotion of angiogenesis after cerebral infarction can better provide the vascular niche for the proliferation, migration and differentiation of neural stem/progenitor cells (NSPCs), thereby further promoting endogenous nerve regeneration. NSPCs can always closely connect with vessels through the interaction of integrin α6β1 and laminin; furthermore, under the support provided by the vascular niche and the chemotaxis of stromal cellderived factor (SDF-1), NSPCs can migrate from the subventricular zone (SVZ) to the periphery of infarction.

Cerebral apoplexy is one of the most common and frequently occurring diseases, characterized by high

Key words: integrin, cerebral infarction behavioristics, angiogenesis

Mailing address: Dr Ran Du,
The First Affiliated Hospital
of Zhengzhou University,
No.1, Jianshe E Road, Erqi District, Zhengzhou,
Henan, China
Tel./Fax: +86 13938555760
e-mail: drhnzz@163.com

0393-974X (2015)

morbidity, and high fatality, disability and recurrence rates. Cerebral apoplexy includes cerebral arterial thrombosis and hemorrhagic apoplexy, of which the morbidity of cerebral arterial thrombosis accounts for 70%-80% of cerebral apoplexy, causing severe harm to humans (1). Its poor prognosis is mainly because of the difficult repair of scathing brain tissue after ischemia reperfusion. However, to date, there are no effective means to completely repair the damaged tissues. Moreover, neurological function impairment after cerebral infarction lasts for a lifetime, leading to a low quality of life for the patient himself, his family and society. As a result, a means to enhance the treatment response of cerebral infarction is the core problem to be solved by researchers. The article of Liu Chunhon, et al. (2) discussed the influence factors for cognitive disorder after cerebral infarction and analyzed the relationship between prognosis of cerebral infarction and cognitive disorder, to help speed up the recovery of patients in the later stage of rehabilitation. The manuscript by Duan and Zou (3) summarized the risk factors of cerebral infarction in order to correctly improve the health of patients with the influencing factors of cerebral infarction, and provide reference for the prevention of cerebral infarction. Zhang et al. (4) discussed the value of susceptibility weighted imaging (SWI) to assess reperfusion injury after cerebral infarction and its correlation with clinical state. It proved that SWI technology could sensitively and objectively evaluate the bleeding and collateral circulation of reperfusion injury after cerebral infarction. Therefore, SWI is expected to be an effective method for disease prediction and therapy evaluation for cerebral infarction patients.

In recent years, many studies have been carried out concerning cerebral infarction, especially the phenomena of angiogenesis after cerebral infarction and endogenous nerve regeneration. Research has found that the promotion of angiogenesis around the infarction after cerebral infarction can notably activate endogenous nerve regeneration, thereby achieving better neural function recovery (5). However, whether angiogenesis directly leads to endogenous nerve regeneration should be further studied, as well as the involved molecular mechanism. By up-regulating and down-regulating the angiogenesis surrounding infarction, this paper discusses the relationship between angiogenesis and endogenous nerve regeneration after cerebral infarction on the basis of previous research. Also, this manuscript further discusses the molecular mechanism of laminin and its receptor integrin α6β1 in regulating vascular nerve regeneration after cerebral infarction.

MATERIALS AND METHODS

Experimental materials and objects

A total of 50 healthy male SD rats were selected, and the main reagents and their functions are shown in Table I.

Main experimental instruments and their functions are shown in Table II.

Experimental methods

This paper established male SD rat reperfusion model with 2 h of cerebral artery embolism with suture method. Neurological function deficit was scored according to rat improvement 24 h after the model establishment, and 50 rats with scores between 10 and 13 were incorporated into an ultimate experiment. The rats were randomly divided into 5 groups: 10 in each group: A: undisturbed control group; B: VEGF up-regulated vessel group, in which an osmotic micro pump (alzet 1007D/kit2,100ul/lw) was implanted in infarction periphery 3 days after the model establishment, and VEGF accumulated to 4 ug; C: endostatin down-regulated vessel group, in which an osmotic micro pump (alzet 1007D/kit2,100ul/lw) was implanted in infarction periphery 3 days after the model establishment, and endostatin accumulated to 20 ug; D: ventricle injected CXCR4 antibody group, in which an osmotic micro pump (alzet 1007D/kit2,100ul/lw) was implanted in infarction periphery when the model was stabilized 3 days after model establishment, and anti-CXCR4 accumulated to 4 ug; E: ventricle injected a6pi antagonist (GoH3 antibody) group, in which an osmotic micro pump (alzet 1007D/kit2,100ul/lw) was implanted in infarction periphery when the model was stabilized 3 days after model establishment, and GoH3 accumulated to 4 ug. After model establishment, the rats were intraperitoneally injected with 5- bromodeoxyuridine (BrdU) in the first day, and were marked with the proliferated endogenous NSPCs (1). Neural functional recovery condition was assessed with modified neurological severity scores (mNSS) and a sticky object removing experiment (2). The change of peripheral metabolism of cerebral infarction after injecting VEGF and endostatin was analyzed by 18F-FDGmicro-PET (3). The proliferation, migration and differentiation of NSPCs in SVZ, infarction periphery and corpus striatum were marked by fluorescence double

dyeing with BrdU, nestin, doublecortin (DCX), glial fibrillary acidic protein (GFAP), neuron-specific nuclear protein (NeuN) and von Willebrand factor (vWF) (4). SVZ whole amount: SVZ was dissected and isolated in the infarction side. Through BrdU marking proliferated stem cells, laminin marking vascular and a6pi antibody marking NSPCs, the relationships were studied between NSPCs, laminin and vessel, the distance was measured between NSPCs and the closest vessel and the vascular microenvironment of SVZ.

Data acquisition

Photographs of immunofluorescence were carried out under laser scanning confocal microscope or common fluorescence microscope. The excitation and emission wavelength of FITC were 492 nm and 520 nm, respectively; the excitation and emission wavelength of Cy3 were 550 nm and 570 nm, respectively; the excitation and emission wavelength of DAPI were 350 nm and 450 nm, respectively. Aimed at the same index, 5 groups of brain slices of the same position were taken and 6 brain slices of each rat were analyzed, with the interval of 120 mm; the main viewing zones were SVZ, subgranular zone (SGZ) or infarcted border zone (IBZ). The analysis and count of positive cells were calculated by ImageProPlus software, and then the average value of six brain slices was taken.

mNSS score

mNSS (6) scores were givento the rats 1 day before modeling and 1 day, 1 week, 2 week, and 4 week after modeling.

Experiment of feeling and removing sticker

Before the experiment, the animals familiarized with the experimental environment, and urine and faeces were promptly removed. A sticky circular patch, 8 mm diameter, was stuck on the first joint of bilateral forepaws of rats. Normal rats would attempt to remove the sticker under the stimulation of stickiness. A specifically assigned person recorded the time taken to remove the sticker. Rats which could remove the sticker in 10 s on bilateral sides were included for modeling. This experiment was performed 1 day before modeling and 1 day, 1 week, 2 weeks and 4 weeks after modeling. The test was repeated 3 times for each experiment, with a time interval of more than 10 min. The order and times of sticker removal were recorded for the right side and left side and then the average value of the results of 3 tests was calculated. Specific criteria are shown in Table 3.

Statistical analysis

SPSS 19.0 data analysis software was applied and metrical data was expressed by Mean ± SD. The survival rates of the groups were compared by *chi*-square test; behavioral score of the groups were compared by variance analysis of repeatedly measured data; immunoflurescence measured data, comparative infarction volume, blood perfusion data, and Western blot results of the groups were detected by sample *t*-test.

RESULTS

Behavioral comparison

Behavioral score of MCAO model one day before, one day after, and three days after modeling in the VEGF group, endostatin group, CXCR4 group, GoH3 antibody group and control group were compared, and the difference was of no statistical significance.

On the 7th day, the results of the sticker removing test of the VEGF group was statistically significant compared to the control group, with a shorter time for sticker removal; behavioral score of the GoH3 group was statistically significant compared to the control group, as mNSS decreased slowly and the time of sticker removal was longer. However, the other groups had no statistical significance compared to the control group.

Micro-PET

Four days after establishing MCAO model, rats were examined under micro-PET. The results of the undisturbed control group, VEGF group, and endostatin group showed that infarction was located on the artery blood supply area on the right side of the brain (cerebral cortex and basal ganglia lateral infarcts) (Fig. 1). Differences of metabolism defects in the side of cerebral infarction between groups were not able to be statistically analyzed since the sample size was too small. Fourteen days after establishing MCAO model, cortex and corpus striatum in the side of cerebral infarction took more 18F-FDG compared to four days after establishing the model (Fig. 1B, see point indicated by arrow), but had remarkably decreased metabolism defects and the decline range was larger than the in control group. In the endostatin group, cortex and corpus striatum on the side of cerebral infarction had no remarkable change compared to 4 days after establishing the model, nor was there improvement of metabolism. Statistical analysis could not be carried out due to the small size of the sample.

Table I. *Main reagents and their functions*

Main reagent	Function	Usage Stage
10% chloral hydrate	Anesthesia	Modeling stage
4% paraformaldehyde solution	Cardiac perfusion and brain fixation	Dying stage
20% sucrose solutions	Dehydration	Dying stage
(Tris Buffered Saline) TBS	Rinse section	Dying stage
Confining liquid	Incubate brain tissue	Dying stage

Table II. *Main experimental instruments and their functions*

Main experimental instruments	Usage	Stage
Electronic balance	Weigh	Modeling stage
Low temperature and high speed centrifuge	Collect brain cells	Modeling stage
Nylon thread	Placing into the brain of mice to form blood flow	Modeling stage
Operating microscope	Zoom in the picture of mouse brain for observation	Modeling stage
Abrasive drilling	Drill skull	Modeling stage
Freezing microtome	Slice brain tissue	Dying stage
Confocal laser scanning microscope	Take photo	Dying stage

Influence of different interventions on angiogenesis

BrdU and vWF fluorescence double dyeing were used to mark the proliferated vascular endothelial cells after cerebral infarction. Results showed that BrdU+/vWF+ cell count around cerebral infarction in the VEGF group comparatively increased compared to the control group, and the difference was statistically significant (Fig. 2). The number of BrdU+/vWF+cells around cerebral infarction in the Endostatin group comparatively decreased compared to the control group (Fig. 3). However, BrdU+/vWF+ cell count in the CXCR4 group and the GoH3 group had no statistical difference compared to the control group. Fig. 4 shows the difference more directly of BrdU/vWF+ cell count in the different groups.

Influence of down-regulating or up-regulating angiogenesis on the proliferation and migration of endogenous NSPCs

Endogenous NSPCs in SVZ in the side of cerebral infarction was marked by nestin dyeing. Nestin+ cell count in SVZ in the VEGF group obviously increased when compared with the control group, while the positive cells mentioned above in the endostatin group comparatively decreased compared to the control group.

Neuronal-restricted precursor cells were marked by DCX dyeing and the migration situation of endogenous NSPCs after differentiating to neuronal-restricted precursor cells was traced. BrdU and DCX double dyeing results showed that DCX+ cell count in SVZ in the side of cerebral infarction in the VEGF group increased compared to the control group.

Influence after anti-CXCIU or anti-α6β1 on the proliferation and migration of endogenous NSPCs

Endogenous NSPCs in SVZ in the side of cerebral infarction was marked by nestin dyeing. The number of nestin+cells in SVZ of the CXCR4 group had no significant difference when compared with the control group, while positive cells in the GoH3 group mentioned above comparatively decreased when compared with the control group.

Neuronal-restricted precursor cells were marked by DCX dyeing and the migration situation of endogenous NSPCs after differentiating to neuronal-

Table III. *mNSS of rats.*

Content of function test	Scores
Movement test (lift rat tail)	
Foreleg shrinkage	1
Hind leg shrinkage	1
Head movement and deviate perpendicular line for more than 10 degrees	1
Place rats on the floor	
Normal walking	0
Not able to walk normally	1
Rotate towards paresis side	1
Leans towards paresis side	1
Feeling test	
Topognosis test: move animal towards lateral side but the animal can not move	1
Proprioception test: put the affected limb at the edge of table and the animal has no shrinkage response	1
Cross bar balance test	
Balance	0
Grab one side of cross bar	1
Clasp cross bar and one limb falls down	2
Clasp cross bar and two limbs fall down; or clasp cross bar for rotating for more than 60 degrees	3
Attempt to balance; but fails and falls down (>40 s)	4
Attempt to balance; but fails and falls down (> 20 s)	5
Fall down (< 20 s)	6
Areflexia and abnormal movement	
Auricle reflex (shakes head after stimulating ear canals)	1
Cornea reflex (blinks after stimulating cornea with cotton)	1
Scare reflex (moves or screams while hearing sound)	1
Tic, myoclonus and dystonia	1

restricted precursor cells was traced. BrdU and DCX double dyeing results showed that DCX+ cell count in SVZ in the side of cerebral infarction in the CXCR4 group had no significant difference when compared with the control group. The number of DCX+ cells in SVZ in the GoH3 group decreased compared to the control group.

Endogenous NSPCs in SVZ in the side of cerebral infarction was marked by BrdU dyeing. The number of DCX+ cells in SVZ in CXCR4 had no significant difference when compared with the control group; the number of BrdU+cells in the corpus striatum area and around infarction comparatively decreased more than the control group; however, BrdU positive cells in SVZ, corpus striatum and peripheral infarction in GoH3 group decreased more than in the control group.

DISCUSSION

Angiogenesis refers to the growth and development of new vessels. Research has found that most neuronal-restricted precursor cells gather near the vascular endothelial cells in mitosis. These endothelial cells can secrete some soluble factors for inducing the proliferation of neuronal-restricted

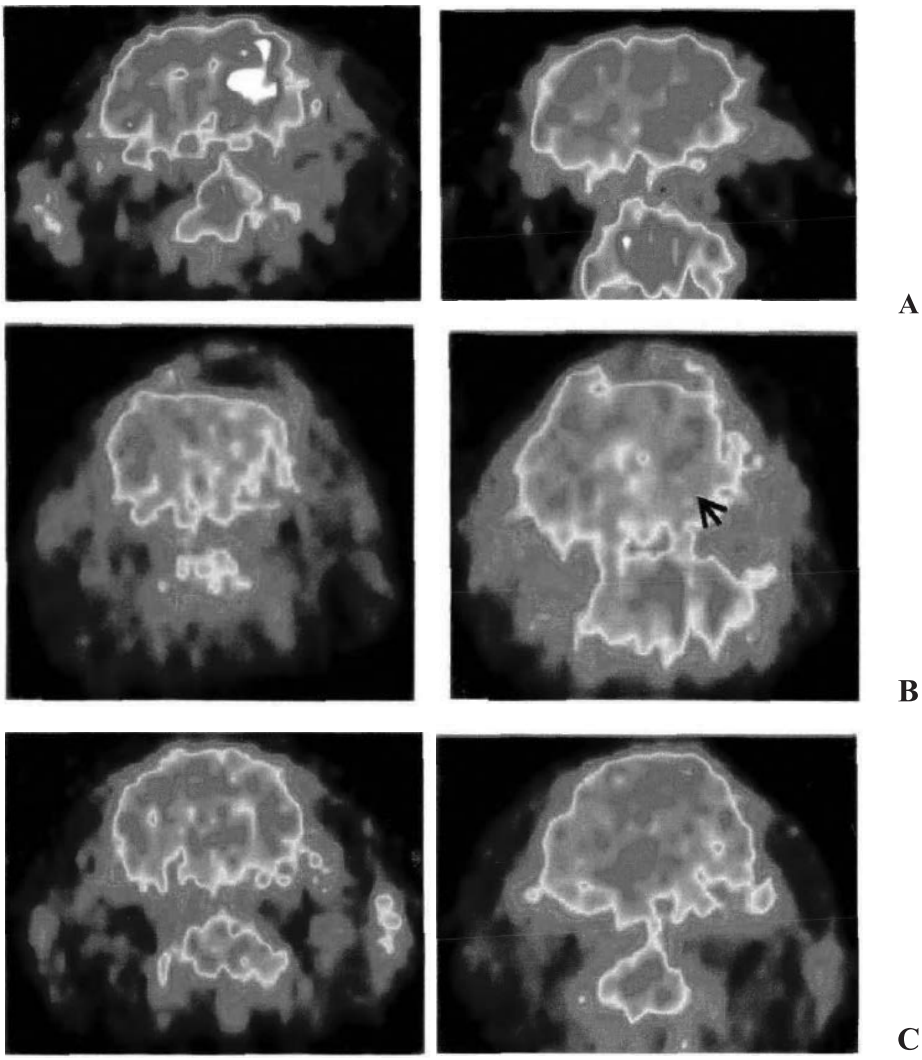

Fig. 1. ***A****) Micro-PET examination results of undisturbed control group at 4th day and 14th day.* ***B****) Micro-PET examination results of VEGF group at 4th day and 14th day.* ***C****) Micro-PET examination results of endostatin group at 4th day and 14th day.*

precursor cells, which is also called nerve regenerative vascular niche. The close relationship between angiogenesis and nerve regeneration indicates that multiple factors in the vascular system can promote nerve regeneration. In the literature, many studies (7, 8) focused on the effect of VEGF on angiogenesis, and an increasing number of researchers believe that VEGF is a multi-functional growth factor that can affect nerve cells by multiple approaches. In addition, there are also other research results suggesting that many other cytokines, such as BDNF, IGF-1, BFGF and TGF, can promote angiogenesis, but they all depend on the up-regulation of VEGF expression. In this experiment, the neuro proliferation, migration and differentiation in SVZ in the VEGF group comparatively increased compared to the control group, indicating that nerve regeneration also significantly strengthened after angiogenesis was promoted. However, the endostatin group which inhibited angiogenesis acquired opposite results. All the above findings demonstrate that the promotion of angiogenesis after cerebral infarction can better provide the vascular niche for the proliferation, migration and differentiation of NSPCs, thereby

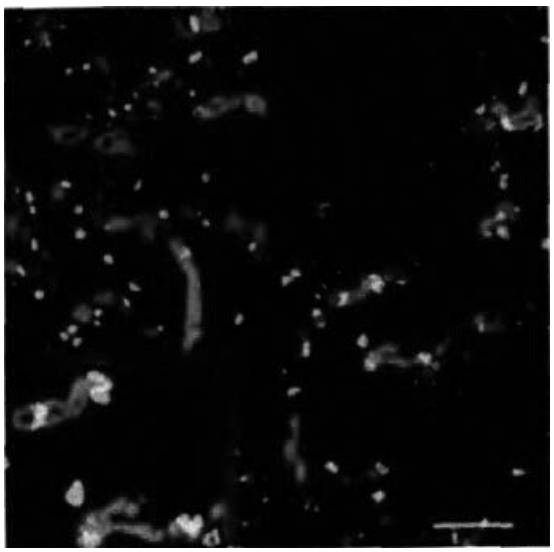

Fig. 2. *BrdU+/vWF+ cell count around cerebral infarction in VEGF group.*

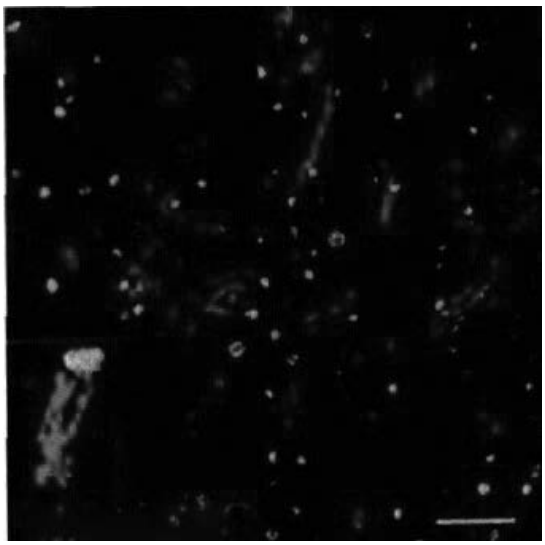

Fig. 3. *BrdU+/vWF+ cell count around cerebral infarction in Endostatin group.*

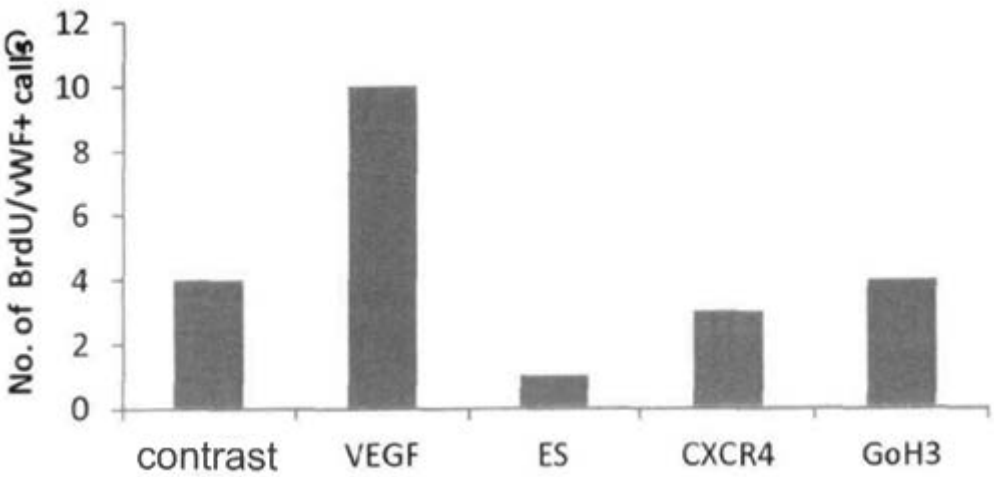

Fig. 4. *BrdU+/vWF+ cell count in different groups.*

further promoting endogenous nerve regeneration.

Previous studies (9, 10) have shown that vascular endothelia cells can compound mass of laminin released to the peripheral matrix in vessels. Therefore, the laminin is highly expressed around vessels and the receptor of laminin is integrin α6β1. Recently, it was also found that the expression of integrin α6β1 was the common feature of multiple stem cells, including embryonic stem cell, neural stem cell of embryonic period, hematopoietic stem cell, etc., and NSPCs in SVZ of adults also expressed integrin α6β (11). This experimental result showed that the proliferation of NSPCs in SVZ had no remarkable change after injecting CXCR4 antibody into the ventricle, but

its migration and differentiation ability decreased. After injecting GoH3 antibody into the ventricle, cell proliferation, migration and differentiation in SVZ were all inhibited. Therefore, we deduced that the reason NSPCs can always keep close connection with the vessel is because of the interaction between integrin α6β1 and laminin. Under the support provided by the vascular niche and the chemotaxis of SDF-1/CXCR, NSPCs could migrate from "healthy" SVZ to peripheral infarction.

Recent decades have seen a rapid development in basic research and preclinical research. To date, besides hematopoietic stem cell transplantation, other stem cells are still in an early stage of research. Undoubtedly, the achievements of this experiment provide a new idea for the treatment of cerebral infarction, focusing on endogenous nerve regeneration. Promoting endogenous nerve regeneration upon actions of exogenous cytokines can offer a theoretical basis for stem cell transplantation, and is also a treatment that can avoid rejection because of ethics and immunology.

REFERENCES

1. Qian J, Liu L, Wang Y. Risk factors and prevention of stroke in the Chinese population. J Stroke Cerebrovas Dis 2010; 2(8):1-6.
2. Liu CH, Liang HF, Feng LN, Sun K, Tang J, Xu SZ, Wang H. After cerebral infarction cognitive dysfunction of correlation analysis. Chin J of Gerontol 2012; 32:456-59.
3. Duan CM, Zou SF. Progress in research of the risk factor of cerebral infraction. Chin J of Practic Nervous Dis 2012; 15(3):93-95.
4. Zhang Q, Yang ZH, Wu LJ, Zhang JW, Miao YW. susceptibility weighted imaging of reperfusion injury after mass cerebral infarction and correlation to clinical measures. Chin J of Magnetic Resonance Imaging 2010; 1(1):23-27.
5. Bao XJ, Feng M, Wei JJ, et al. Transplantation of Flk-1+ human bone marrow-derived mesenchymal stem cells promotes angiogenesis and neurogenesis after cerebral ischemia in rats. Euro J Neurosci 2011; 34:87-98.
6. Shen L, Li Y, Chen J, et al. One-year follow-up after bone marrow stromal cell treatment in middle-aged female rats with stroke. Stroke 2007; 38:2150-56.
7. Zhao H, Bao XJ, Wang RZ, et al. Postacute ischemia vascular endothelial growth factor transfer by transferrin-targeted liposomes attenuates ischemic brain injury after experimental stroke in rats. Human Gene Therap 2011; 22:207-15.
8. Huang XS. Blood pressure and cerebravascular disease. Chin J of Geriatric Heart Brain and Vessel Dis 2010; 12(3):287-88.
9. Duan LJ, Zhu HY, Li HP. The influence of TNF-α and IL-1β by different electroacupuncture intensity on acute cerebral ischemia reperfusion in rats. J of Xinjiang Med Univ 2012; 35(5):604-7.
10. A. Rosell, V. Agin, M. Rahman, et al. Distal occlusion of the middle cerebral artery in mice: are we ready to assess long-term functional outcome? Transl Stroke Res 2013; 4(3):297-307.
11. Zhang JK, Qiu XF, Zhang LT. Theoretical basis of EBSPTR therapy on promoting angiogenesis. J of Hubei Univ of Chin Med 2010; 12(5):47-48.

LETTER TO THE EDITOR

EXPRESSION OF PLEIOTROPHIN IN SMALL CELL LUNG CANCER

HQ. WANG and J. WANG

Department of Respiratory Medicine, the First Affiliated Hospital, Zhengzhou University, Zhengzhou, China

Received November 22, 2014 – Accepted January 29, 2015

Pleiotrophin (PTN) is a kind of heparin binding growth factor closely related to tumor progression. This study aimed to discuss the significance of the expression of PTN in benign and malignant lung cancer tissues, especially small cell lung cancer. Lung cancer samples were collected for study and lung tissue samples with benign lesions were taken as controls. The expression of PTN was detected using tissue chip combined with the immunohistochemical method, and the differences of small cell lung cancer with non-small cell lung cancer and benign lesion tissue were compared. It was found that PTN expression was mainly located in the cytoplasm and membrane of cells; PTN expression in the lung cancer group was higher than that in the control group ($p<0.01$), and PTN expression in the small cell cancer group was higher than that in the squamous carcinoma group and glandular cancer group ($p<0.05$). In addition, PTN expression quantity in patients with lung cancer were in close correlation with TNM staging, pathological type and tumor differentiation degree ($p<0.05$). PTN was found to express abnormally high in lung cancer, especially small cell lung cancer tissue. PTN is most likely to be a new tumor marker for diagnosis and prognosis of lung cancer.

Lung cancer with increasingly higher incidence and mortality has become one of the most common malignant tumors and ranks the primary cause of deaths induced by various tumors (1). Recently, increasing importance has been given to a new method of target gene therapy for treatment of tumours. Pleiotrophin (PTN), a protooncogene with high affinity, plays an important role in the growth and metastasis of tumor cells. Some studies have found that PTN is highly expressed in multiple tumor cells and tumor tissues. Other studies (2-5) have reported that PTN also expresses in lung cancer, and its expression in small cell lung cancer is higher than that in non-small cell lung cancer. Harris, et al. (6) found that compared with lung squamous carcinoma and adenocarcinoma, small cell lung cancer has the shortest multiplication time, which might be related to the growth promoting effect of PTN. Yao, et al. (7) found that PTN protein expressed highly in pancreatic cancer, and that it was thought to be correlated to TNM staging, lymph node metastasis and prognosis. On this basis, PTN is speculated to play a role in promoting tumor growth and inducing proliferation and differentiation of lung cancer cell. This study was based on the expression of PTN in benign and malignant lung cancer, especially small cell lung cancer.

MATERIALS AND METHODS

A total of 83 cases of lung cancer patients who provided complete clinical data and who underwent

Key words: pleiotrophin, small cell lung cancer, expression research, tumor marker

Mailing address: Dr Jing Wang,
Department of Respiratory Medicine,
the First Affiliated Hospital,
Zhengzhou University,
No.1, Jianshe East Road,
Zhengzhou, Henan, 450052, China
e-mail: huanqinwhq@163.com

0393-974X (2015)

DISCLOSURE: ALL AUTHORS REPORT NO CONFLICTS OF INTEREST RELEVANT TO THIS ARTICLE.

operation between September 2006 and March 2011 in our hospital were enrolled in this study. Of the 83 lung cancer specimens, 59 were from men and 24 women, with age ranging from 39 to 86 years (mean 62.8±9.0 years). None of the subjects had undergone radiotherapy or chemotherapy before operating, and the samples were confirmed by pathological examination after operation. There were 12 cases of squamous carcinoma (squamous carcinoma group), 30 cases of adenocarcinoma (adenocarcinoma group) and 41 cases of small cell carcinoma (small cell carcinoma group). Based on TNM staging, 10 cases were in stages I and II and 31 were in stages III and IV. Of 12 cases of squamous carcinoma, 11 were high-differentiated and medium differentiated squamous carcinoma and 1 was low-differentiated squamous carcinoma; 4 cases had not suffered from lymphatic metastasis while 8 cases had. Of 30 cases of adenocarcinoma, 11 cases were high-differentiated and medium-differentiated, and the remaining 19 cases were low-differentiated; 5 cases had not suffered from lymphatic metastasis while 25 cases had. Of 41 cases of small cell carcinoma, 34 cases were high-differentiated and medium-differentiated and the remaining 7 cases were low-differentiated. In addition, lung tissue samples from 13 patients [5 male and 8 female, with age ranging from 29 to 74 years (mean 55.9 ±11.5 years)] who were confirmed as benign were taken as controls.

The main reagents used were mouse anti-human PTN monoclonal antibody (British Abcam Company), goat anti-mouse IgG secondary antibody, diaminobenzidine (DAB) chromogenic reagent kit (Fujian Maixin Biotechnology Co., Ltd.).

Immunohistochemical SP

The tissues were embedded with paraffin, sliced and then heated for 20 min at 68°C. The sections were then dewaxed by dimethylbenzene and dehydrated by alcohol gradient; moreover, the endogenous peroxidase content was blocked. After repairing by antigen, the lung cancer tissue was sealed by goat serum and added with PTN monoclonal antibody in a ratio of 1:250. The next day it was rinsed with 0.01 mol/L PBS and then added with biotin (second antibody). Streptomycin ovalbumin working solution labelled by horseradish peroxidase was added, and the tissue was rinsed by 0.01 mol/L PBS; the liquid was developed by DAB, redyed and dehydrated gradually. After mounting with neutral balsam, the result was observed under light microscope. 0.01 mol/L PBS was used as the negative control taking the place of second antibody.

Assessment criteria

Cells with yellow or claybank dyeing inside cytomembrane or cytoplasm were considered as positive cells. Photos were taken at five non-overlapping views with even dying for every dot matrix under 400x light microscope. Absorbance value of positive dying in every picture was measured using Image-proplus 6.0 and then the average value was calculated as the average absorbance value of that section. Because the average absorbance value was positively correlated to the expression of protein in positive cells, the value was taken as the semi-quantitative value of PTN expression of that sample.

Statistical analysis

GraphPad Prism 5.0 statistical software was used for data analysis. Measurement data were expressed by median and carried out by non-parametric Mann-Whitney μ test. Enumeration data were expressed by rate and c^2 test. $P< 0.05$ was considered statistically significant.

RESULTS

Cytoplasm and cytomembrane were the main locations for positive expression of PTN as yellow, claybank or brown particles could be observed in lung cancer tissue. But there was no positive expression of PTN in benign lung tissue (Fig. 1).

The average absorbance value of PTN positive protein was 0.2134 (0.0226-0.3737) in the lung cancer group, higher than that in the control group [0.0460 (0-0.1943)] ($p<0.01$); the average absorbance value of PTN protein in small cell cancer group was higher than that in squamous carcinoma group and glandular cancer group, and the specific values are shown in Table I. The cases were divided into a high and medium differentiation group and a low differentiation group based on the different cell differentiation of lung cancer. The average optical density of two groups was 0.2065 (0.0226-0.2853) and 0.2214 (0.0443-0.3736), respectively, and a statistical significance was found in the difference ($P<0.05$) (Table II).

The cases were divided into a high expressed PTN group and a low expressed PTN group according to the average absorbance value. The average absorbance value of the high expression group was more than 0.2134, while that of the low expression group was less than 0.2134. It was found that PTN expression of patients with lung cancer was correlated to TNM staging (except for the small cell cancer group), pathological type and tumor differentiation degree, but with no correlation

Table I. *Average absorbance value of PTN protein in different lung cancer groups.*

Lung cancer group	Average absorbance value of PTN protein
Small cell carcinoma group	0.2330(0.1919-0.3737)
Squamous carcinoma group	0.2134(0.0292-0.2977)
Glandular cancer group	0.2005(0.0226-0.2854)

Table II. *Expression of PTN in lung cancer tissues with different differentiation.*

Group	Case number	Median and average optical density	P value
High differentiation group	56	0.2065 (0.0226-0.2853)	< 0.05
Low differentiation group	27	0.2214 (0.0443-0.3736)	

Table III. *Correlation between PTN expression level and clinical index of patients.*

Clinical index	Case number	Percentage (%)	High expression	Low expression	P value
Age					
≥60years	55	66	28	27	> 0.05
< 60years	28	34	13	15	
Gender					
Male	59	71	32	27	> 0.05
Female	24	29	9	15	
Smoking habit					
Yes	56	67	30	26	> 0.05
No	27	33	11	16	
Tumor size					
≥3cm	66	80	27	39	> 0.05
< 3cm	17	20	14	3	
Lymph node metastasis					
Yes	56	68	26	30	> 0.05
No	27	32	15	12	
Distant metastasis					
Yes	12	14	5	7	> 0.05
No	71	86	36	35	
TNM staging					
I–II	10	24	2	8	< 0.05
III–IV	32	76	20	12	
Differentiation degree					
High and medium differentiation	56	67	24	32	< 0.05
Low differentiation	27	33	17	10	
Pathological types					
Squamous carcinoma	12	14	6	6	< 0.05
Glandular cancer	30	36	14	16	
Small cell cancer	41	49	21	20	

Note: TNM staging except for small cell cancer group

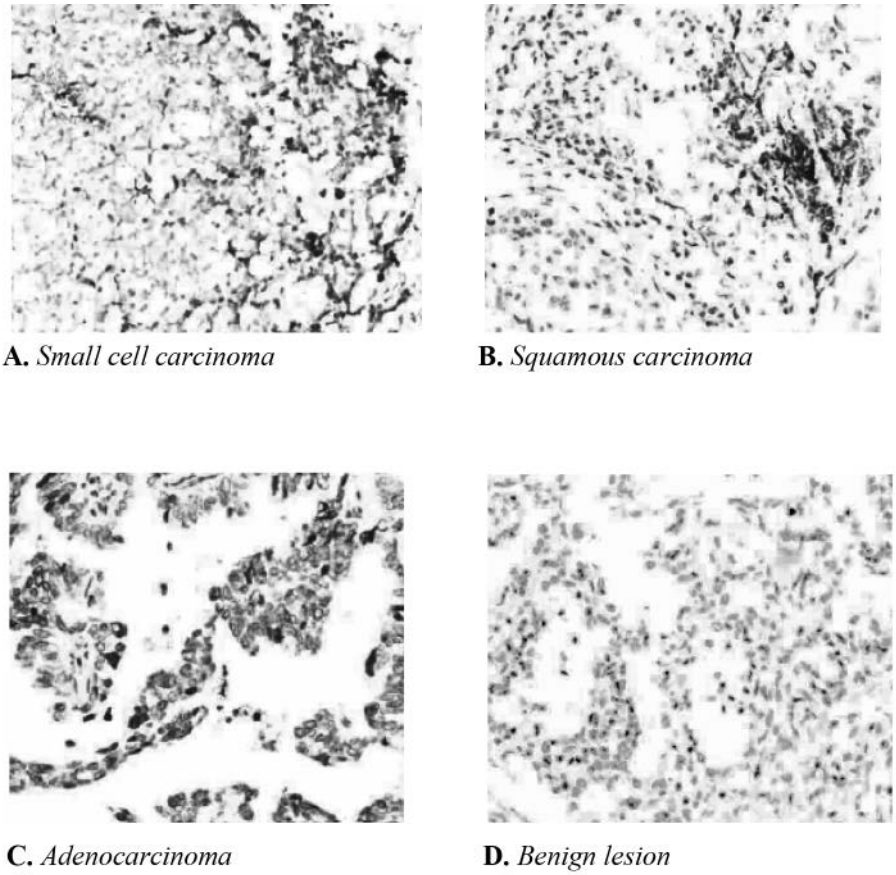

Fig. 1. *PTN expression in malignant and benign lung cancer (SP method, ×400).*

regarding age, gender, smoking or not, tumor size and lymph node metastasis. The correlation between PTN expression level and clinical index of patients is shown in Table III.

DISCUSSION

PTN is also called heparin affinity regulatory peptide, the mRNA and protein expression of which can be found in different types of tumor cell lines and tumor specimens of different sources. PTN, a kind of growth promoting protooncogene, expresses highly in multiple tumors, like breast cancer, pancreatic cancer, colorectal cancer, etc.. Small cell cancer is one of the neuroendocrine neoplasms with the highest degree of malignancy. It has been proved that the content of PTN mRNA in small cell lung cancer is much higher than that in non-small cell lung cancer at gene level (5). In the present study, the average absorbance value of PTN positive protein in the lung cancer group was higher than that in the control group, and the average absorbance value of PTN positive protein in the small cell lung cancer group was higher than that in both the squamous carcinoma group and glandular cancer group. It showed that PTN expression was related to the pathological type of lung cancer. In addition, Harris, et al. (5) once found that compared with squamous lung cell carcinoma and adenocarcinoma of lung, small cell lung cancer had the shortest multiplication time. In their *in vitro* study, Jägar, et al. (8) found that the positive expression rate of PTN mRNA in small

cell lung cancer lines was distinctly higher than that in non-small cell lung cancer lines; and PTN in small cell lung cancer was more likely to express higher than in non-small cell lung cancer, which is consistent with the finding in the present study that the expression of PTN was more highly expressed in the small cell lung cancer group than in the squamous carcinoma group and the adenocarcinoma group. These clinical findings lay a certain basis for PTN to become the tumor marker of small cell lung cancer diagnosis.

These studies showed that the expression of PTN in lung cancer was obviously higher than that in benign lesion tissues, and the expression of PTN in lung cancer was in positive correlation with TNM staging and differentiated degree. The study of Tsirmoula, et al. (9) implied that the highly expressed PTN could lead to malignant phenotype of cancer cell, and at the same time, the down-regulated expression of PTN was able to inhibit the proliferation, metastasis and invasion of tumor cell. Jägar, et al. (8) through experimental research verified that PTN expression in serum from patients with lung cancer increased and presented a correlation with TNM staging, which is evidence for the research results of this paper. However, age, gender, smoking or not, tumor size, lymph node metastasis and distant metastasis were not found to be correlated with the expression level of PTN. In order to prove these results, further study on a larger number of specimens is necessary.

The above studies demonstrate that PTN expresses highly in lung cancer, especially small cell lung cancer; furthermore, PTN may play an important role in the occurrence, development and metastasis of tumor. Future studies are suggested to concentrate on PTN as the target of drug action or synthesize PTN inhibitor *in vitro*, so as to down regulate PTN or achieve complete inhibition, thereby blocking the further growth and metastasis of tumor. However, the mechanism of the role of PTN in the occurrence and development of tumor is still not confirmed, therefore, more research and discussions are needed.

REFERENCES

1. Siegel R, Naishadham D, Jemal A. Cancer Statistics, 2012. CA Cancer J Clin 2012; 62(1):10-29.
2. Yang LX, Li M, Li XN, Li JH. Expression and significance of PTN in lung adenocarcinoma patients. Chinese J of Histochemistry and Cytochemistry 2011; 20(3):275-80.
3. Jiang JP, Yu Y, Du ZY, Shi MH. Expression and significance of pleiotrophin in lung cancer. Jiangsu Medical J 2014; 40(1):24-26.
4. Yu Y. Gene therapy experimental study of recombined ientivirus-mediatal sirna technology targeting pleiotrophin in small cell lung cancer. Jiangsu: Suzhou University 2010. http://cdmd.cnki.com.cn/Article/CDMD-10285-1011032852.htm
5. Yu Y, Shi MH, Xu X, Zhang ZL, Hu HC. Analysis of expression profiles of some tumor growth-related genes after silencing of pleiotrophin in human small cell lung cancer H446 cells. Chinese J of Oncology 2010; 32(6): 405-9.
6. Harris K, Khachaturova I, Azab B, et al. Small cell lung cancer doubling time and its effect on clinical presentation: a concise review. Clin Med Insights Oncol 2012; (6):199-203.
7. Yao J, Ma Q, Wang L, Zhang L. pleiotrophin expression in human pancreatic cancer and its correlation with clinicopathological features, perineural invasion and prognosis. Dig Dis Sci 2009; 54(4):895-901.
8. Jägar R, List B, Knabbe C, et al. Serum levels of the angiogenic factor pleiotrophin in relation to disease stage in lung cancer patients. Br J Cancer 2002; 86(6):858-63.
9. Tsirmoula S, Dimas K, Hatziapostolou M, Lamprou M, Ravazoula P, Papadimitriou E. Implications of pleiotrophin in human pc3 prostate cancer cell growth in vivo. Cancer Sci 2012; 103(10):1826-32.

JOURNAL OF BIOLOGICAL REGULATORS & HOMEOSTATIC AGENTS Vol. 29, no. 1, 181-186 (2015)

LETTER TO THE EDITOR

βig-h3 CORRELATES WITH RELATED FACTORS OF PERITONEAL METASTASIS OF GASTRIC CANCER

F. WANG, XW. LI, WB. LU and JH. JIN

Department of Oncology, Wujin People's Hospital The Affiliated Hospital of Jiangsu University, Jiangsu, China

Received November 22, 2014 – Accepted January 29, 2015

βig-h3 is an extracellular matrix protein induced by transforming growth factor-β1 (TGF-β1) and involved in adhesion between cell and cell, cell and matrix. It has been proved that βig-h3 is highly expressed in human lung cancer and colorectal cancer cells, and thus it is considered to have the same effect on gastric cancer cells. This research applied histochemical staining and RT-PCR to detect the content of βig-h3 in peritoneal mesothelial cells and the content of carcino embryonic antigen (CEA) mRNA in abdominal dropsy or peritoneal washing liquid, in order to explore the relationship between the factors of peritoneal metastasis of gastric cancer and βig-h3. It was found that the positive ratio of βig-h3 in the gastric cancer group was higher than that in the benign disease group, and the positive rate of immunohistochemistry was closely related to the relative factors of peritoneal metastasis such as tumor infiltration depth, serosal types, macroscopic peritoneal metastasis, CEA mRNA, results of pleural lavage cytology (PLC) examination, etc. Research found that βig-h3 expressed distinctly in gastric cancer peritoneal metastasis, therefore, it is useful for monitoring biological behavior of gastric cancer.

Gastric cancer originating from canceration of gastric mucosa epithelial cells is one of the most common malignant tumors with high incidence and mortality (1, 2). Complete resection is its main treatment method. However, patients still die due to the spread of the tumor cells even after surgery, with a percentage of 40% to 50%. The reason is considered to be that cancer cells penetrate gastric serosa or that the metastatic lymph gland capsule has gone into enterocoelia before operation, and after a certain period metastasis nodules form (3-5).

Currently, the "seed and soil" theory aiming at the gastric cancer peritoneal metastasis has been recognized and supported by most scholars. Form, structure, function and influence factors of soil-peritoneal mesothelium cells in the process of metastasis are becoming the main focus points of studies on gastric cancer peritoneal metastasis. Cast-off cells, activated cancer cells or the cytokines they secretes can change the form of peritoneum, thereby turning it into a state suitable for tumor cells to plant, adhere and grow and during the process TGF-β1 plays an important role (6-9). In 1992, Skonier et al. found that TGF-β1, that is induced and synthetised from TGF-β, is involved in the adhesion between cell and cell, cell and matrix in human lung adenocarcinoma cancer cell line A549. In addition, there is research proving that highly expressed βig-h3 in human lung

Key words: gastric cancer peritoneal metastasis, βig-h3, peritoneal fibrosis

Mailing address:
Dr Jianhua Jin,
Department of Oncology,
Wujin People's Hospital The Affiliated Hospital of Jiangsu University, No. 2, Yongning North Street,
Changzhou, Jiangsu 213002, China
e-mail: goldjhua@163.com

0393-974X (2015)

cancer carcinoma cells and colorectal cancer cells strengthened the ability of invasion and metastasis of tumor (9, 10). Based on that, it is speculated that βig-h3 plays a function in the process of TGF-β1 inducing peritoneal metastasis of gastric cancer. Therefore, Li Zhen et al. (9) stimulated peritoneal mesothelial cells by gastric cancer cells SGC-7901 cultured with TGF-β1 at different concentrations and found a remarkably increased concentration of βig-h3, proving that culture supernatant fluid of gastric cancer cells SGC-7901 and TGF- β1 can promote HMrSV5 expression and βig-h3 secretion.

This paper aims to further explore the relationship between the expression of βig-h3 in peritoneal mesothelial cells from patients with gastric cancer and the biological behavior of gastric cancer, as well as its relationship with related factors of peritoneal metastasis. Differing from previous researches on gastric cancer peritoneal metastasis that are mostly based on cast-off cells of gastric cancer, this paper emphatically studies the relationship between the related factors of peritoneal metastasis of gastric cancer and βig-h3 through detecting the expression of βig-h3 based on the form and function of peritoneal mesothelial cells, applying immunohistochemical methods and detecting the content of CEA mRNA in abdominal dropsy or peritoneal washing liquid by RT-PCR method.

MATERIALS AND METHODS

Materials

The research subjects were 75 cases of gastric cancer undergoing surgical oncology in the First Hospital of China Medical University from May 2011 to September 2011. Of the 75 patients, 51 were male and 24 were female, with age ranging from 32 to 81 years (mean 61 years). Also, samples were taken from 14 patients with gastric benign lesions in the same period as controls. All the patients had not undergone radiotherapy or chemotherapy, and gave informed consent.

Rat anti-human βig-h3 monoclonal antibody (Protein Tech Co., USA), SP immunohistochemical knit (Maixin Biological Technology Development Co., Ltd, Fuzhou).

Sample collection and PLC examination

During operation, a catheter was placed in the Douglas cavity after laparotomy and then 100 ml of normal saline was injected. The liquid was absorbed out of the cavity after ot had been lightly stirred. If the patient already had abdominal dropsy, then the abdominal dropsy was absorbed directly. The abdominal cavity washing liquid sample was centrifuged at 2000 r/min for 20 min. Cytologic examination was performed on partial sediment. Afterwards, RNA was extracted from other washing liquid sediment, and stored in the cryogenic refrigerator. Peritoneal tissue was took from the lower part of the front abdominal wall and immediately fixed with 10% formaldehyde solution. Then the tissue was embedded by paraffin wax and sliced (5 μm). Immunohistochemical staining was carried out later.

Immunohistochemistry

The major procedures of SP staining method are: 1. slice paraffin wax, followed by dewaxing and hydration; 2. antigen retrieval: put the sections into 0.01 mol/L sodium citrate buffer solution with pH 6.0 and repair the antigen using microwave hot (high fire for 3 min and low fire for 16 min); 3. after adding peroxidase, the liquid was incubated at room temperature for 20 min; 4. after washing by phosphate buffered saline (PBS), add non-immune animal serum and incubate it at room temperature for 15 min; 5. add primary antibody for dilution at the ratio of 1:10, and place it at 4°C overnight; 6. After washing by PBS, add biotin to mark second antibody and leave at room temperature for 20 min; 7. After washing by PBS, add biotin to mark third antibody and incubate it at room temperature for 20 min; 8. develop the color by DAB (3,3′-diaminobenzidine) and mount the slice with neutral balsam. Primary antibody was replaced by PBS as the negative contrast.

RT-PCR

Dalian TaKaRa Co., Ltd synthesized primer sequences. PCR primer A of CEA mRNA was: 5' -CATCATGATTG-GAGTGCTGGTTG-3'; primer B was: 5'-CACGATGTTGGC-TAGGATGGTC-3', product 199 bp; according to the illustration of RT-PCR knit (BioEev-Tech. Scientific & Technical Co., Ltd), add 2 μg RNA into reaction system and place it at 42°C for incubation for 120 min. Then perform 95°C thermal denaturation for 5 min afterwards, mRNA was reverse transcribed into cDNA. PCR reaction conditions (94°C for 50 s, 55°C for 50 s, 72°C for 60 s) which were repeated for 32 times. Finally, it was placed at 72°C for 8 min.

Analysis criteria

Japanese Gastric Cancer Pathology Statute was taken as the standard to determine lesion differentiation degree, growth pattern, serosal type and whether macroscopic peritoneum was present or not. Depth of invasion was based on Stage T in the 7th edition of TNM staging system formulated by UICC. The PLC examination results of gastric cancer peritoneal washing liquid was divided into

PLC (-) group and PLC (+) group. Under the premise of excluding nonspecific staining, peritoneal mesothelium cytoplasm was yellow, claybank and sandy beige particle inside were considered as the positive markers. After PCR was augmented, the product was electrophoresed in 2% sepharose gel containing EB coloring agent. If positive strip was found at 199 bp, then CEA mRNA was considered as positive.

Statistical analysis

SPSS16.0 was applied for data analysis. The indexes between groups were compared by c^2 test. $P < 0.05$ was considered to have statistical significance.

RESULTS

Immunohistochemical staining of βig-h3 in peritoneal tissue in gastric cancer group and benign disease control group

The positive ratio of the gastric cancer group was much higher than the benign disease group ($p<0.05$), and a statistical significance was found between them. Amount of positive and negative cases are as shown in Table I.

The pattern of peritoneal mesothelium cell cytoplasm after immunohistochemical staining is shown in Figs. 1 and 2.

Relationship between Big-H3 in peritoneal tissue and the biological behavior of gastric cancer pathology

Of 75 cases of gastric cancer, βig-h3 from 29 cases showed positive immunohistochemical staining results. The positive rate of the peritoneal tissue increased in undifferentiated gastric cancer with a diffused growth and positive lymphatic metastasis but the difference had no statistical significance; it significantly increased in soakage serosa (T4) and serosa with tendinous and colorfully diffused pattern. The difference had statistical significance ($p < 0.05$) (Table II).

Relationship between βig-h3 in peritoneal tissue with macroscopic peritoneal metastasis, PLC examination and CEA mRNA expression

Of 75 cases of gastric cancer, 13 cases had macroscopic peritoneal metastasis, and exfoliated cancer cells which in 20 cases were positive. The PLC (+) results are as shown in Fig. 3.

In addition, CEA mRNA in 32 cases was found positive. The positive rate of βig-h3 expression significantly increased in the positive macroscopic peritoneal metastasis group, the positive exfoliated cancer cell group and the positive CEA mRNA group; besides, the P value of the macroscopic peritoneal metastasis, the PLC and the CEA mRNA group were all distinctly lower than 0.05; the difference had statistical significance ($P<0.05$) (Table III).

DISCUSSION

βig-h3, the extra cellular matrix protein, plays a regulation function in the growth, differentiation, injury repair and formation of cells. Using immunohistochemical methods, Ma et al. (11) proved that βig-h3 in colon cancer tissue expressed significantly high compared to normal intestinal mucosal tissue; if the expression was inhibited, then the invasion and metastasis of colon significantly decreased. It was speculated that βig-h3 played an important role in gastric cancer peritoneal metastasis. Through detecting the expression of βig-h3 in patients with gastric cancer and gastric benign disease, it was found that the positive rate in patients with gastric cancer was significantly higher than that in patients with gastric benign disease.

Implantation metastasis is the major approach of gastric cancer peritoneal metastasis (12). In clinical practice, we found that intraperitoneal exfoliated cancer cells did not always cause peritoneal

Table I. *Cases of patients with gastric cancer and gastric benign disease.*

Condition of patients	Gastric cancer patients		Gastric benign Disease patients	
	Positive	Negative	Positive	Negative
Case number	29	46	1	13
Positive rate	38.7%		7.1%	
P value	0.030			

Table II. *Relationship between the expression of βig-h3 in peritoneal mesothelial cell and pathological biological factors of gastric caner.*

Pathological biological factor	Immunohistochemical staining of βig-h3 (n)		P value
	-	+	
Differentiation situation			0.555
Differentiation	19	10	
Undifferentiation	27	19	
Growth pattern			0.362
Type with block mass and nest pattern	22	17	
Diffuse type	24	12	
Invasion depth			0.016
T1, T2, T3	32	12	
T4	14	17	
Lymphatic metastasis			0.338
Negative	21	16	
Positive	25	12	
Serosal type			0.037
Normal reaction type	13	3	
Nodular type	19	9	
Type with tendinous and colorfully diffused pattern	14	17	

Table III. *Relationship between βig-h3 expression in peritoneal mesothelial cell and relative factors of gastric cancer peritoneal metastasis.*

Related factor of peritoneal metastasis	Immunohistochemical staining of βig-h3 (n)		P value
	-	+	
Macroscopic peritoneal metastasis			0.002
Negative	43	19	
Positive	3	10	
PLC			0.005
Negative	39	16	
Positive	7	13	
CEA mRNA		20	0.027
Negative	31	12	
Positive	15	17	

metastasis. This is because the adhesion of cancer cells and peritoneum determine whether the metastasis occurs or not (13, 14). As to the content of TGF-β1 in peritoneal fluid, previous tests have demonstrated that it was higher in the gastric cancer patients than in the gastric benign disease patients; in addition, the content of TGF-β1 increased as the gastric cancer staging progressed. The progression of gastric cancer also affects the degree of peritoneal fibrosis. The effect mechanism of TGF-β1 promoting

Fig. 1. *Immunohistochemical staining of peritoneal mesothelium cell cytoplasm: negative.*

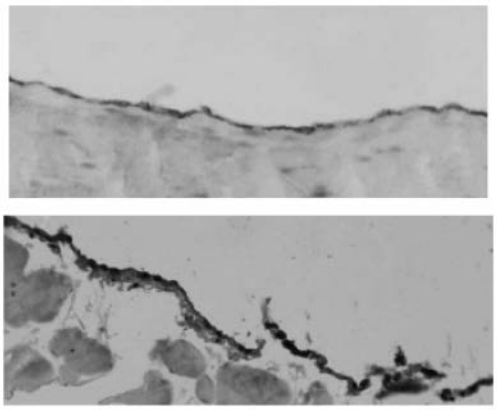

Fig. 2. *Immunohistochemical staining of peritoneal mesothelium cell cytoplasm: positive.*

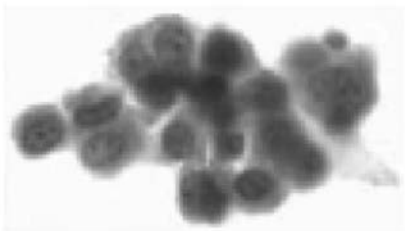

Fig. 3. *Positive results in PLC examination.*

peritoneal metastasis is: first, TGF-β1 stimulates the expression of peritoneal mesothelium cell type III collagen and fibronectin, thereby promoting peritoneal fibrosis; then type III collagen and fibronectin selectively adhere to the glycoprotein on cell membrane and finally promote peritoneal fibrosis (6, 9, 13, 15). *In vitro* experiments proved that TGF-β1 could promote the expression of βig-h3 in peritoneal mesothelial cells. However, whether βig-h3 is involved in peritoneal fibrosis, gastric cancer cell adhesion and its mutual action with gastric cancer metastasis needs to be further verified by experiments (9). The traditional method for detecting peritoneal subclinical metastasis is by PLC, however it is not effective enough due to the false negative rate and low sensitivity. In view of this, detecting the expression of CEA mRNA in enterocoelia by RT-PCR is gradually becoming the more used method (13). The experimental results show that 10 out of 13 cases of macroscopic peritoneal metastasis was immunohistochemically positive. This study also shows that the P values of tumor invasion depth, serosal type, microscopic peritoneal metastasis, PLC and CEA mRNA were 0.016, 0.037, 0.005 and 0.002 respectively and the differences had statistical significance. The expression of βig-h3 increased as the stages of gastric cancer progressed, indicating that positive rate in immunohistochemistry was closely related to the relative factors of peritoneal metastasis. The expression of βig-h3 is considered to be in a correlation with the peritoneal metastasis of gastric cancer; therefore, it can be regarded as one of the indexes for predicting gastric cancer peritoneal metastasis (13).

In conclusion, the expression of βig-h3 in peritoneal mesothelial cells increases as the gastric cancer progresses and that it is related to the relative factors of peritoneal metastasis of gastric cancer such as tumor invasion depth, macroscopic peritoneal metastasis, PLC examination result, CEA mRNA, etc.. However, the functions played by the mechanism of increased expression of βig-h3 in the process of induction of exfoliated cell adhesion and proliferation is still not thoroughly studied and need to be further verified.

REFERENCES

1. Deng L, Huang H, Lu ML, Zheng MY, Chang J, Liu LM. Risk factors and prognosis for peritoneal seeding metastasis in gastric cancer. Chinese J General Surgery 2012; 21(10):1191-5.
2. A jani JA, Barthel JS, Bekaii-Saab T, et al. Gastric cancer. J Natl Compr Canc Netw 2010; 8(4):378-409.
3. Li P. Risk factors of peritoneal recurrence after curative resection of advanced gastric cancer. J

Chongqing Med Uni 2011; 36(1):95-7.
4. Li FX, Zhang RP, Liu H, et al. Risk factors for early recurrence after radical resection of proximal gastric cancer. Chinese J Gastrointest Surg 2012; 15(2):129-32.
5. Choi JY, Ha TK, Kwon SJ. Clinicopathologic characteristics of gastric cancer patients according to the timing of the recurrence after curative surgery. J Gastric Cancer 2011; 11(1):46-54.
6. Yagi Y, Fushida S, Harada S, et al. Biodistribution of humanized anti-VEGF monoclonal antibody/ bevacizumab on peritoneal metastatic models with subcutaneous xenograft of gastric cancer in mice. Cancer Chemother Pharmacol 2010; 66:745-53.
7. Mino K, Ozaki M, Nakanishi K, et al. Inhibition of nuclear factor-kappaB suppresses peritoneal dissemination of gastric cancer by blocking cancer cell adhesion. Cancer Sci 2011; 102:1052-8.
8. Zhao L, Zhao AG. Advances in the treatment of peritoneal metastasis of gastric cancer. World Chinese J Digestol 2011; 19(26):2746-51.
9. Li Z, Miao ZF, Sun GP, Shen MY, Xu HM. Culture supernatants of human gastric cancer cell and transforming growth Factor-β1 stimulate the expression of pig-β3 protein in human peritoneal mesothelial cell. Chinese J Bases Clinics in Gen Surg 2012; 19(7):768-70.
10. Wang N, Zhang H, Yao Q, et al. TGFBI promoter hypermethylation correlating with paclitaxel chemoresistance in ovarian cancer. J Exp Clin Cancer Res 2010; 31(1):6.
11. Ma C, Rong Y, Radiloff DR, et al. Extracellular matrix protein Betaig-h3/TGFBI promotes metastasis of colon cancer by enhancing cell extravasation. Genes Dev 2008; 22:308-21.
12. Liu Z, Han X, Liu H, et al. Comparative study on detection of peritoneal free cancer cells of gastric surgery. Chin J Bases Clinics Gen Surg 2010; 17(8):803-7.
13. Li Z, Miao ZF, Xu YX, Xu M, Xu HM. Correlation of βig-h3 expression in peritoneal mesothelial cells with pathological parameters and peritoneal metastasis in gastric cancer. World Chin J Digestol 2012; 20(16):1402-6.
14. Deng J, Liang H, Wang D, Sun D, Pan Y, Liu Y. Investigation of the recurrence patterns of gastric cancer following a curative resection. Surg Today 2011; 41:210-15.
15. Imaizumi T, Aoyagi K, Miyagi M, Shirouzu K. Suppressive effect of bevacizumab on peritoneal dissemination from gastric cancer in a peritonel metastasis model. Surg Today 2010; 40:851-57.

LETTER TO THE EDITOR

META-ANALYSIS ON POSTOPERATIVE COMPLICATIONS OF WRISTBAND ACUPOINT PRESSURE THERAPY

GL. ZHANG, SY. YANG, ZL. ZHU and PX. MU

Department of General Surgery, Xinxiang Central Hospital, Xinxiang, China

Received November 22, 2014 – Accepted January 23, 2014

Through searching database such as MEDLINE, CNKI, etc., this paper assesses the effect of wristband acupoint pressure, acting on the neiguan acupoint, to relieve postoperative complications of adults (mainly nausea and vomiting) using nine randomized controlled trials (RCT) and RevMan5.0. In the experimental group, acupoint pressure wristband effectively reduced the incidence rate of postoperative vomiting by acting on the neiguan point, compared to the placebo control group (RR=0.50, 95%CI: 0.37~0.66, P<0.01). As to the incidence rate of postoperative nausea, there was no statistical significance between the experimental group and the placebo control group (RR=0.85, 95%CI: 0.72~1.00, P>0.05). It was revealed that the application of acupoint pressure wristband on neiguan point in postoperative care could effectively relieve postoperative vomiting; while postoperative vomiting was not relieved distinctly. Therefore, researchers are required to carry out more reliable RCT test for further study and discussion, and nurses can bring in acupoint pressure wristband for researches on its effectiveness and adaptability.

Postoperative Nausea and Vomiting (PONV) is one of common postoperative complications, accounting for 20%~30% of total incidence rate (1). Possibility of PONV occurring in gynecological operations, laparoscopic cholecystectomy and craniotomy can be as high as 70% (1, 2). Acupoint pressure can be an effective controlling measure without any adverse reaction for patients during the period of postoperative recovery. It was found that acupoint pressure was effective for recovery of intestinal function after gynecological abdominal surgery (3). Ji Ling, et al. (4) adopted neiguan point massage for preventing nausea and vomiting after cheolecystetomy, since the neiguan point is the specific acupoint to relieve nausea and vomiting. Following the principle and theory of acupuncture and moxibustion, acupoint pressure substitutes acupuncture with pressure massage (shiatsu or instrumental pressure) (5). It draws increasing attention from medical workers, especially foreign nursing specialists, for its advantages of simple and non-invasive use. Diversified wristband products with pressure effect on the neiguan point have emerged on the world market. There is a raised button inside the wristband. The button aims at the neiguan point and produces pressure and massage effect when the wristband is correctly adorned. Some researchers have studied the effect of acupoint pressure in postoperative care with this kind of wristband by establishing a placebo control group. It is not only simple to operate but also saves manpower compared to manual

Key words: acupoint pressure wristband, postoperative nausea and vomiting, neiguan point, postoperative care, meta-analysis

Mailing address: Dr. Suyu Yang,
Jinsui Road No. 56,
Xinxiang Central Hospital,
Xinxiang, Henan,
453000, China
Tel.: +8613939061358
e-mail: glz@ibhsedu.com

0393-974X (2015)

DISCLOSURE: ALL AUTHORS REPORT NO CONFLICTS OF INTEREST RELEVANT TO THIS ARTICLE.

shiatsu. Moreover, the randomized controlled trials (RCT) successively applied have provided high-level evidence in verifying the effectiveness of acupoint pressure. This meta-analysis is a comprehensive, systematic and quantitative analysis of the results of multiple independent researches on this topic. It is the quantitative review of the literature, based on strict design, proper statistical method as applied for systematical, objective and quantitative analysis on multiple research results. Its advantage lies in increasing the reliability and solving the inconsistency with a larger sample size (6). This paper collected RCT literature on relieving PONV by acupoint pressure and testing its effectiveness.

MATERIALS AND METHODS

Criteria for incorporating literature

Study type: the eligible literature is that on RCT. Study object: patients of over 28 years old, without limitation of gender, disease condition and race. Intervening measure: patients in the treatment group wore wristbands with acupoint pressure effect, acting on the neiguan point. Contrast measure: placebo control. Patients in the control group also wore the wristbands, but with the point not on the neiguan point. Outcome index: the incidence of postoperative nausea and vomiting. This study acquired approval from the medical ethics committee and all the patients gave informed consent.

Exclusion criteria was if other therapeutic methods were also applied, such as drug therapy besides the wristband therapy.

Search strategy

Acupressure and postoperative nausea and vomiting were the keywords to retrieve MEDLINE and CINAHL database. Acupoint pressure, acupoint massage, acupuncture and postoperative nausea were the keywords to retrieve CNKI, VIP, CBM and Wanfang database. Retrieval date was up to August 2010.

Research screening and data extraction

With reference to the selection methods mentioned in Cochrane Collaboration Network System Assessor Handbook (Edition 5.0): import retrieval results into reference management software; put forward the repeated and obviously not relevant research reports by reading headline and abstract; obtain the full text of research report which may be related; merge the multiple references that report the same research, and delete the repeated references; contact the main researchers to obtain the lost data; check research report according inclusive criteria specified above; make the final decision for selection. The extracted data include: basic information of research (such as the author, the year), sample size, characteristics of research object, intervening and control measures, outcome index, Jadad score.

Evaluation criteria

Jadad scoring method was applied for blind, random quality assessment, lack of follow-up of 9 studies on RCT, with score from 0 to 5 points. 0 to 2 points stands for low quality research, and 3 to 5 points stands for high quality research.

Data analytical methods

Data was statistically analyzed using RevMan 5.0.24 provided by Cochrane Collaboration Network. Therapeutic effect was expressed by relative risk (RR), and 95% Confidence Intervals (CI) for therapeutic effect was calculated. When the results of meta-analysis was of heterogeneity ($p<0.10$), Random Effects Model (REM) was used to express that, otherwise, Fixed Effects Model (FEM) was used. Publication bias was determined using funnel plot.

RESULTS

Information retrieval and screening result

We obtained altogether 50 non-repeated articles, of which 33 were excluded through reading headline and abstract. The remaining 17 articles were further assessed after the full texts were acquired. Nine article on RCTwere chosen, 4 were from Asia, 4 from Europe and 1 from North America.

Basic characteristics of the selected literature

The nine studies on RCT selected involved altogether 1,117 surgical patients. The type of operation involved included laparoscopic cholecystectomy or gynecological operation, cardiac surgery, cesarean delivery and urological surgery. Of the nine articles, five carried out two groups of tests and the other 4 carried out three groups of tests. Of the 4 articles with three groups of tests, 2 established antemetic (metoclopramide or ondansetron) control groups and another 2 blank control groups. The specific characteristics and methodology quality of the studies is shown in Table I.

Effectiveness of acupoint pressure wristband in relieving post operative nausea

Among all the groups of the selected researches,

Table I. *Specific characteristics and methodology quality of the studies.*

Literature	Sample size (man/woman)	Intervening measures	Contrast measures	Outcome index	Measuring time	Jadad score
Harmon 1999 (7)	104(-)	wristband presses neiguan point	wristband placebo	nausea degree (no, light, medium, heavy), vomiting frequency (no, light, medium, heavy), cases of nausea and vomiting	2h to 24h after operation in post anesthesia care unit	4
Alkaissi 1999 (8)	60(0/60)	wristband presses neiguan point	wristband placebo; blank control	the nausea and vomiting degree is evaluated by VAS, and cases of nausea and vomiting	30min, 60min, 120min, 24h after operation	4
Harmon 2000 (9)	94(0/94)	wristband presses neiguan point	wristband placebo	VAS evaluates the incidence of nausea and vomiting	6h, 24h after operation	3
Agarwal 2000 (10)	200(97/103)	wristband presses neiguan point	wristband placebo	nausea degree (non, light, medium, heavy), cases of nausea and vomiting	6h, 24h after operation in post anesthesia care unit	4
Alkaissi 2002 (11)	410(0/410)	wristband presses neiguan point	wristband placebo; blank control	nausea is evaluated using 7-point scale, and cases of nausea and vomiting	20:00, 8:00, 20:00	4
Agarwal 2002 (12)	150(49/101)	wristband presses neiguan point	wristband placebo; ondansetron	degree and incidence rate of nausea and vomiting	After operation 6h, 24h after operation	4
Samad 2003 (13)	50(-)	wristband presses neiguan point	wristband placebo	incidence rate of nausea and vomiting	assess once per hour for 6h after operation	4
Andrew 2004 (14)	152(129/23)	wristband presses neiguan point	wristband placebo	nausea degree and incidence rate of nausea and vomiting	1 h, 2 h, 4 h, 6 h, 8 h, 12 h, 16 h, 20 h, 24 h after operation	4
Sadighha 2008 (15)	156(132/24)	wristband presses neiguan point	wristband placebo; metoclopramide	degree and incidence rate of nausea and vomiting	2h, 6h, 24h after operation in post anesthesia care unit	2

only the research results of the wristband groups and placebo groups were considered. The results of the meta-analysis is shown in Fig.1. The heterogeneity test was P=0.29, indicating that the 9 researches were valid, thus we adopted the statistical methods FEM and Mantel-Haenszel. RR of incidence rate of postoperative nausea was 0.85, and 95% CI was between 0.72 and 1.00, and the difference was of no statistical significance (p=0.06). Therefore, the statistical results could not support the speculation that the effect of wristband acupoint pressure on the neiguan point could effectively decrease the incidence rate of postoperative nausea.

Effectiveness of acupoint presses wristband on relieving postoperative vomiting

Among all the groups of the selected researches, only the research results in the wristband group and the placebo group were taken. The results of the meta-analysis is shown in Figure 2. The heterogeneity

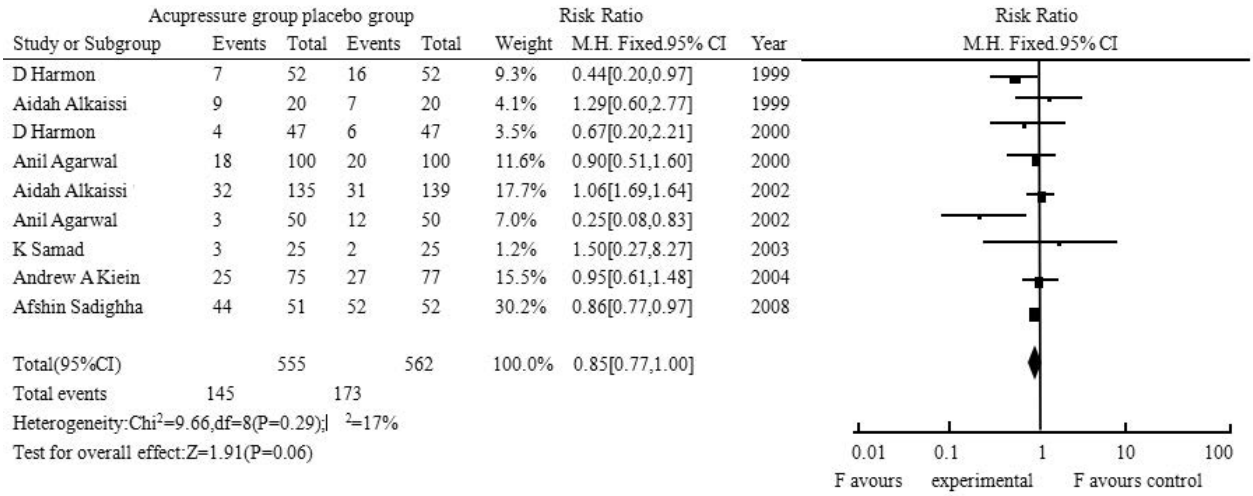

Fig. 1. *Comparison of incidence rate of postoperative nausea between experimental group and placebo group (FEM).*

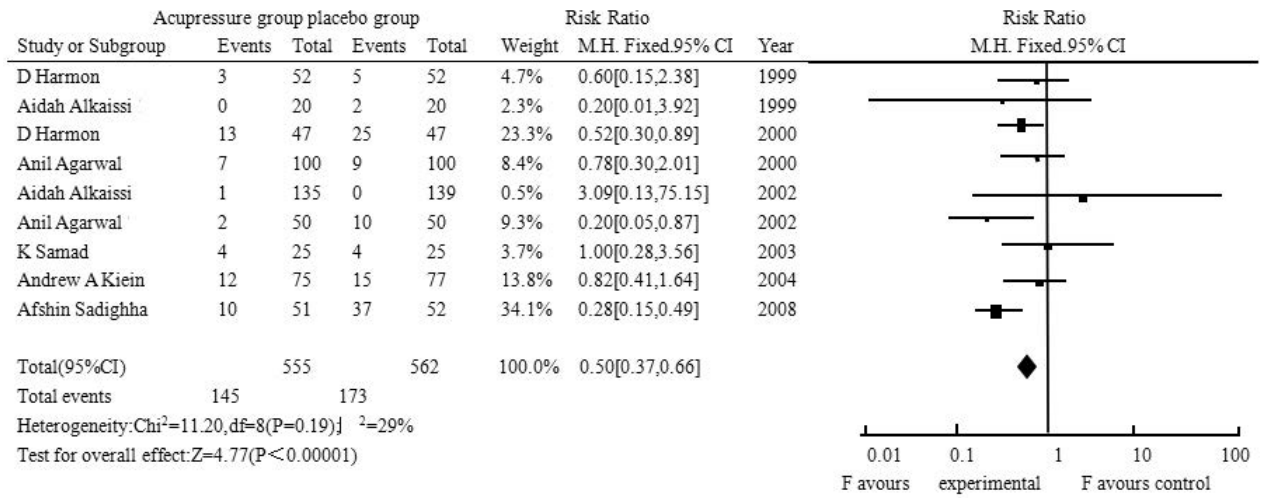

Fig. 2. *Comparison of incidence rate of postoperative vomiting between experimental group and placebo group (FEM).*

test was P=0.19, indicating that the 9 researches were valid, thus we adopted FEM. RR of incidence rate of postoperative nausea was 0.50, and 95%. CI was between 0.37 and 0.66, and the difference was statistically significant (p<0.01). The statistical results suggest that the effect of acupoint pressure wristband on neiguan point can effectively decrease the incidence rate of postoperative vomiting.

Sensitivity analysis

Statistical analysis was performed using REM, and the result obtained was fundamentally unchanged. RR of incidence rate of postoperative nausea was 0.87, and 95% CI was between 0.73 and 1.04, and the difference was of no statistical significance (p=0.12). RR of incidence rate of postoperative vomiting was 0.52, and 95% CI was between 0.35 and 0.77, and the difference was statistically significant (p<0.01). These findings suggest that the results of this assessment were stable.

DISCUSSION

Curative effect analysis

Based on quantitative and comprehensive analysis, it was found that the application of wristband acupoint

pressure on the neiguan point in postoperative care can effectively relieve postoperative vomiting. As to postoperative nausea, there was no statistically significant difference between experimental group and control group. Thus we cannot ensure the application of wristband acupoint pressure on the neiguan point in postoperative care has a relaxating effect.

Comparison with the former literature

Stimulating the neiguan point (including acupuncture, electric acupuncture, laser stmulation, percutaneous nerve stimulation, acupoint pressure, etc.) can not only reduce the incidence rate of postoperative nausea, but also can effectively reduce the incidence rate of postoperative vomiting (16). A work on meta-analysis published by Shiao, et al (17) in 2006 also drew the same conclusion, that stimulating the neiguan point can reduce the incidence rate of post operative nausea and vomiting. The conclusion drawn by this paper is different from the above two because of the different criteria and number of articles included. The above two reports selected various therapeutic methods related to acupuncture, including acupuncture, electric acupuncture, acupoint pressure, etc.. The former one included 40 experimental researches and the latter 9 experimental researches. This paper focuses on the effect of wrist acupoint pressure acting on the neiguan point, selecting nine researches. In addition, the influence of chance factors cannot be excluded because of the small number of articles considered.

Analysis of the evaluation methods of nausea symptoms

Nausea is very difficult to accurately and uniformly evaluate because it is a subjective symptom. The nine researches selected in this paper applied three kinds of evaluation methods, that is, VAS, patient self evaluation questionnaire (4 grades), 7-point scale. The way to evaluate nausea has been argued by researchers for decades. However, as for the problem studied in this paper, the evaluation of nausea and vomiting is indispensable. In the experimental research on nausea evaluation methods, Del et al. reported that the results of the nausea evaluation methods mentioned above were consistent for those not including measures to stop vomiting. Thus, researchers in the future are required to pay more attention to the evaluation methods for nausea and vomiting when they evaluate the effectiveness of measures to stop vomiting (18). Del et al. also stated that there was a sound correlation between nausea and vomiting of those who accepted measures to stop vomiting, but after taking these, some people only felt nausea but without vomiting. Therefore, nausea and vomiting should be evaluated separately when evaluating the effectiveness of any kind of measure to stop vomiting. This paper also explained the different effects of wristband acupoint pressure on the neiguan point in relieving nausea and vomiting.

Analysis of placebo effect

Though there was no statistical difference between the experimental group and the placebo control group in relieving postoperative nausea, two researches which established a blank control group showed that stimulating the neiguan point by acupoint could reduce the incidence rate of nausea 24 h after operation. It indicated that the relief of postoperative nausea may be due to the effect of a placebo rather than the effect from wrist acupoint pressure. However, only 2 researches established a blank control. Thus, more blank controls are suggested in future experimental researches so as to better evaluate the effect of a placebo. Today, the mechanism is still not clear and the approach of acupuncture and the placebo design may have a certain degree of effect (19). Complex therapeutic measures may have a larger placebo effect than a single drug therapy. In addition, some features of acupuncture therapy are correlated with placebo effect, such as the secret theoretical framework, the stress on personal specificity, the frequent communication between patients and doctors, etc. (20).

The possible deviations

Patients who have a history of nausea and vomiting are more likely to feel these symptoms when stimulated by the vision, hearing and smell of vomiting. However, in most of the relative researches, there were no relative steps to cope with the bias brought by sensory perception stimulation due to multiple times of nausea and vomiting evaluation. Therefore, methodology

(more evaluation/less evaluation) should be added to the design of future experiments, so as to study whether multiple times of nausea and vomiting can produce psychological effects which makes patients feel nausea and vomiting. Multi-factor analysis may be used to discuss whether nausea and vomiting is related to the history of nausea and vomiting (17), so as to ensure the accuracy and authenticity of research results.

Currently, such studies are very common, and there are also clinical reports about relieving postoperative nausea and vomiting using shiatsu acupoint. Ma Chunyan (20) pointed out that neiguan point pressure combined with deep breath could effectively relieve PONV. Tang Ying, et al. (21) pointed out that, the total effective rate of nausea and vomiting improvement reached more than 90% after pressing the neiguan point by shiatsu for 10sec, and within certain time limit (3-10sec). Nausea and vomiting symptoms improved more as the time for pressing shiatsu increased. Compared with pressing acupoint by shiatsu, the use of the wristband is a more convenient application, easy to control and saves manpower. Therefore, wristband acupoint pressure should be used and promoted in clinical care. Researchers should study the difference of the effectiveness of pressing acupoint by shiatsu or by wristband and explore application value of this therapy in postoperative or chemotherapy nursing.

Results of meta-analysis demonstrate that, wristband acupoint pressure could effectively relieve postoperative vomiting by acting on the neiguan point, but its effect on relieving postoperative nausea was not obvious. Researchers are required to make further studies through carrying out more reliable tests. More importantly, the design of the placebo and assessment of it on nausea and vomiting should be more strict and accurate. Moreover, researchers should explore the feasibility of this kind of wristband for medical use in nursing.

REFERENCES

1. Liu Y, Zhu WS. The grading and control strategy on influence factors of postoperative nausea and vomiting. Modern Practic Med 2010; 22(2):232-34.
2. Lu B, Li J. Discussion on the relation of nausea and vomiting with anesthesia after gynecological laparoscopic surgery. Chin Primary Health Care 2010; 24(12):56-57.
3. Shi LJ, Fang KQ, Zhou P, Du NN, Yu HY. Influence of ear acupoint seeds burying and acupressure on intestinal functional rehabilitation of patients after accepting gynecological abdominal operation. Chin Nursing Res 2011; 25(4):863-65.
4. Ji L, Ye BL, Tu JF, Zhang JW, Zheng XF, Jiang FZ. Neiguan massaged to prevent ache and nausea and vomit after laparoscopic cholecystectomy-a randomized controlled clinical trial. J Zhejiang Chin Med Uni 2010; 34(5):745-46.
5. Wang YM, Wang QY, Zhang J, Guo YL. Comparative study on acupoint pressing and medication for angina pectoris due to coronary heart disease. Chin Acupunc Moxibust 2011; 31(7):595-98.
6. Zeng XT, Leng WD, Guo Y, Liu JY. One of meta analysis series: types of meta analysis. Chin J Evidence-based Cardiovasc Med 2012; 4(1):3-5.
7. Harmon D, Gardiner J, Harrison R, et al. Acupressure and the prevention of nausea and vomiting after laparoscopy.Br J Anaesth 1999; 82 (3):387-90.
8. Alkaissi A, Stalnert M, Kalman S. Effect and placeboeffect of acupressure (P6) on nausea and vomiting after outpatient gynaecological surgery .Acta Anaesthesiol Scand 1999; 43(3):270-74.
9. Harmon D, Ryan M, Kelly A, et al. Acupressure andprevention of nausea and vomiting during and after spinalanaesthesia for Caesarean section .Br J Anaesth 2000; 84(4):463-67.
10. Agarwal A, Pathak K, Gaur A. Acupressure wristbands do not prevent postoperative nausea and vomiting after urological endoscopic surgery .Can J Anaesth 2000; 47 (4):319-24.
11. Alkaissi A, Evertsson K, Johnsson V A, et al. P6 acupressure may relieve nausea and vomiting after gynecological surgery: an effectiveness study in 410 women. Can J Anesth 2002; 49(10):1034-1039.
12. Agarwal A, Bose N, Gaur A, et al. Acupressure and ondansetron for postoperative nausea and vomiting after laparoscopic cholecystectomy. Can J Anaesth 2002; 49(6):554-60.
13. Samad K, Afshan G, Kamal R. Effect of acupressure on postoperative nausea and vomiting in laparoscopic cholecystectomy .J Pak Med Assoc 2003; 53 (2):68-72.
14. Andrew A K, George D, Jacek K, et al. Acupressure

wristbands for the prevention of postoperative nausea and vomiting in adults undergoing cardiac surgery. J Cardiothorac Vasc Anesth 2004; 18(1):68-71.

15. Sadighha A, Nural N. Acupressure wristbands versus metoclopramide for the prevention of postoperative nausea and Vomiting. Ann Saudi Med 2008; 28(4):287-291.
16. Lv H. Clinical observation of acupuncture of neiguan point to prevent the nausea and vomiting of 50 patients with general anesthesia. Nei Mongol J Trad Chin Med 2011; 30(21):86-87.
17. Shiao SY, Dune LS. Meta-analyses of acu-stimulations: effects on nausea and vomiting in postoperative adult patients. Explore (NY) 2006; 2(3):202-15.
18. Tang RJ. Clinical analysis on nausea and vomiting of 78 patients of digestive system department. Chin Pract Med 2013; 18:138-39.
19. Wang JJ, Wu ZC. Thinking about the conclusion of no difference between the acupuncture and sham-acupuncture in the clinically therapeutic effects on migraine abroad. Chin Acupunct Moxibust2009; 29(4):315-18.
20. Ma YC. Intervention of acupoint pressure on nausea and vomiting after gynecological operation. Tianjin J Nurs 2006; 14(1):35.
21. Tang Y, Zeng YF. Research on the reason of nausea and vomiting after gynecological operation and the nursing treatment of Shiatsu acupoint. Med Inform 2010; 23(3):165-66.

LETTER TO THE EDITOR

RESEARCH ON THE INFLUENCE OF α-GalCer ACTIVATING EXPERIMENTAL AUTOIMMUNE MYASTHENIA GRAVIS MICE NKT CELLS AT DIFFERENT TIMES ON MYASTHENIA GRAVIS

YH. WANG[1], JC. JIA[1], G. LIU[2] and YF. WANG[3]

[1]Emergency Clinical Department, the First Affiliated Hospital, Henan Science and Technology University, Luoyang, China; [2]Molecular Biology Laboratory, the First Affiliated Hospital, Henan Science and Technology University, Luoyang, China; [3]Basic Medical, Henan Science and Technology University, Luoyang, China

Received November 22, 2014 – Accepted December 19, 2014

This study aims to observe the effect of natural killer T (NKT) cell activation on experimental autoimmune myasthenia gravis (EAMG) model by injecting mice with α-GalCer in enterocoelia at different times, thus to provide a new therapy for EAMG. EAMG animal model of C57BL/6 mice was established and the mice were injected with α-GalCer irritant in enterocoelia. Vα14 NKT cells were then activated through the transfer of CD1d. This paper discusses the effect of NKT cell activation on EAMG at different times by observing the variation of weight, clinical performance and relevant immunity indexes of mice. In C57BL/6 mice, the EAMG incidence rate of the Vehicle Group was 90%, the average onset duration was 37±6 days; The incidence rate of α-GalCer prevention group was 30%, the average onset duration was 51±9 days. The forward immunization of α-GalCer activates NKT and protects C57BL/6 mice from the occurrence of EAMG, which provides basis for prevention and treatment of EAMG and other autoimmune diseases.

Myasthenia gravis (MG) is a chronic autoimmune neuromuscular disease characterized by varying degrees of weakness of the skeletal (voluntary) muscles of the body (1). MG, of which the main clinical expression is myasthenia in the eyes or the whole body, is a common, difficult and complicated neurological disease. Normally there is no radical cure. The present treatment aims at minimizing the untoward effects while rebuilding or optimizing the joint function of the neuro and muscle. To date, clinical double-blind randomized control experiments have rarely been reported, for the treatment of MG involves many factors, such as the range lesion involved, the course of the disease, the severity, the degree of functional damages and the relative risk of treatment linked to age, gender, compliance of the patient and untoward effects during the monitoring of the drug. At present, there are but few clinical therapies for MG which include cholinesterase inhibitors that improve messaging function at the joint of neuro and muscle, plasma exchange or specific immunity, eliminating acetylcholine receptor (AchR) (2) in blood, nonspecific immune inhibitors or regulators that treat the immunoreaction of antiacetyl-choline

Key words: myasthenia gravis, NKT cells, α-GalCer

Mailing address: Dr Yuhua Wang,
Emergency Clinical Department,
the First Affiliated Hospital,
Henan Science and Technology University,
N. 636 Guanlin Street, Luolong District, Luoyang, China
Tel.: +86-379-69823119 Fax: +86-379-69823699
e-mail: wyhhnkj@163.com

0393-974X (2015)

receptor and thymusectomy. Though specific treatment that targets the autoimmunity deficiency of MG is still insufficient, with knowledge of the new immunological mechanism of MG, we can treat the disease by eliminating the specific reaction of the acetylcholine receptor.

EAMG is an animal model which simulates human MG (3-5). As they are quite alike in many aspects, such as clinical performance, electrophysiology, immunology and pharmacology, the animal model is reliable for MG research.

Recent studies show that as a new kind of immunoregulation cell, NKT plays a crucial role in resisting tumor immunity, overcoming immune injection of transplant and inhibiting autoimmune disease (6). NKT cells can recognize the lipid material of some bacteria and meanwhile express T Cell Receptor (TCR) with little or no variability. The receptor restricts NKT cells to react to limited kinds of lipid or carbohydrate antigen (7). At present, the material which can activate NKT cells through these receptors is α-galactosylceramide (α-GalCer is galactose sphingosine), a glycosphingolipid deriving from sponge and a natural-occurring substance capable of activating NKT cells (8). This study aims to discuss the effect of NKT cells on the clinical performance and the relevant immunity indexes of EAMG after injecting irritant α-GalCer, therefore providing a new method of prevention and cure of EAMG.

MATERIALS AND METHODS

Major reagents

Immunogen: AchR is extracted and purified from the electronic organ (Pacific biomarine, Venice, CA) of torpedo California.

Irritant: α-galactosylceramide(α-GalCer is galactose sphingosine), the vehicle for the control reagent.

Experimental animals

We prepared 30 healthy female C57BL/6 mice (B6) ranging in age from 8 to 12 months, weighting from 14 to 16 g.

Method

The mice were randomly divided into 3 groups with 10 in each. Forward immunization group (group A): each mouse was injected with 6 μg α-GalCer in enterocoelia during the last week before immunization (-7d), on the day of immunization (0d) and on the first week after immunization (7d) respectively, for a total of 3 injections; combined immunization team (group B): each mouse was injected, in enterocoelia, with 6μg α-GalCer on the day of immunization (0d), during the first week after the immunization (7d) and during the second week after the immunization (14d) respectively, for a total of 3 injections; control group (group C): the mice were injected with Vehicle (control reagent), the drug dose and drug-delivery method were the same as group A.

Test index

Each index test records the morbidity of each mouse, measures the weight every two days after AchR sensitization, scores EAMG clinically and measures the IgG of AchR antibody of mice serum 35 days after the first sensitization of AchR. EAMG clinical scoring methods are as follows: two observers clinically assess the EAMG severity degree of the mice applying blind method every day; 0 points: no clear sign of myasthenia; 1 point: myodynamia is normal when at rest but unable to rise after 20 continuous climbs; 2 points: incapable of rising even at rest; 3 points: paralyzed, dying or dead.

Statistical analysis

All the data was expressed by $c^2 \pm s$. Data comparison between groups was tested using one-way ANOVA: Post Hoc Multiple Comparisons with SPSS19.0 software. All results were considered statistically significant as $P<0.05$.

RESULTS

The morbidity of each group was recorded, as shown in Table I. Clean B6 mice of the same age and weight were randomly divided; there was no significant difference in weight before the sensitization; they were then weighed every two days after the sensitization, and the weight is shown in Fig. 1. The weight of the mice in the forward immunization group, compared with the control group, at 45, 60, 75, 90 and 105 d, is distinctly higher than the control group ($p<0.001$); there is no significant difference between the weight of the mice of the combined immunization group and control group at 45, 60, 75, 90 and 105 d ($p>0.05$).

Result of EAMG clinical scoring is shown in Fig. 2. The scores of the forward immunization group compared with the control group at 45, 60, 75, 90 and 105 d are much lower than control group ($p<0.001$); there is no significant difference between the combined immunization group and control group

Table I. *Morbidity state of the mice.*

Group	Number	Morbidity	Onset duration (d)
Forward immunization group	10	30%	51±9
Combined immunization team	10	100%	33±5
Control group	10	90%	37±6

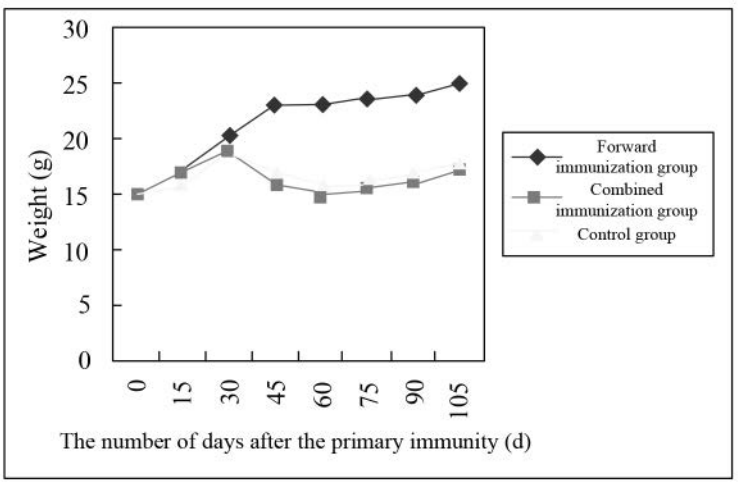

Fig. 1. *Measurement of mice weight.*

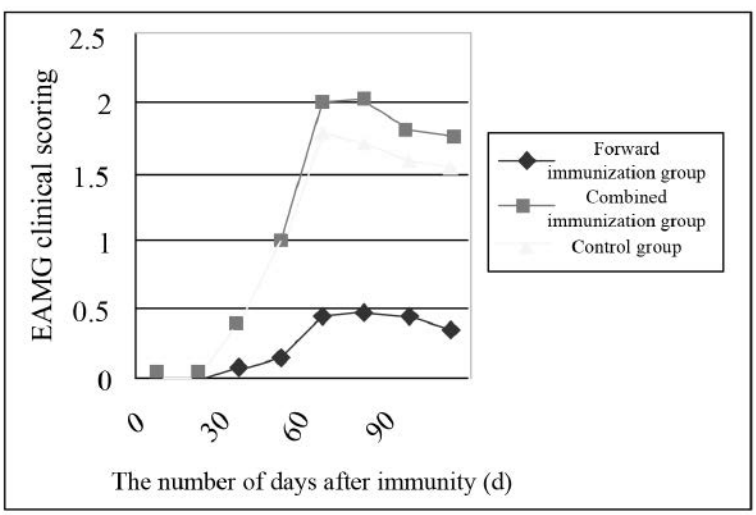

Fig. 2. *Clinical scoring of EAMG mice.*

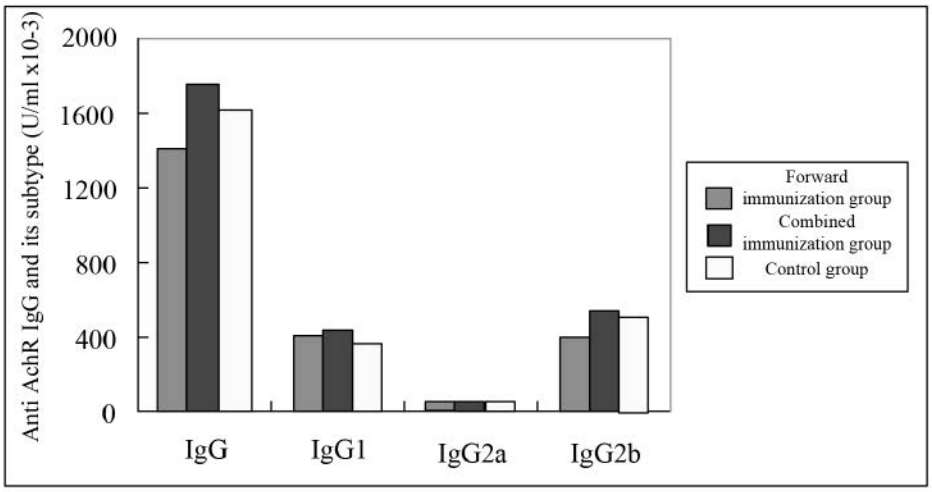

Fig. 3. *Anti-AchR IgG and its subtype.*

in assessment at 45, 60, 75, 90 and 105 d ($p>0.05$).

The specific results of the determination of anti AchR antibody IgG and its subtype is shown in Fig. 3. IgG and IgG2b of the forward immunization group compared with the control group are obviously lower ($p<0.05$, respectively 0.004 and 0.003), there is no significant difference in IgG1 and IgG2a, $p>0.05$; IgG and IgG2b of the forward group compared with the combined immunization group are distinctly lower, $p<0.05$ (0.001 and 0.004 respectively), there is no significant difference in IgG1 and IgG2a, $p>0.05$.

DISCUSSION

MG is an autoimmune disease in which anti acetycholine-receptor mediates (9-10). For now, the treatment of autoimmune disease most applied both locally and abroad is immunosuppressor which probably inhibits the immune system of the patients causing infection and yielding tumor, however is not able to prevent or treat the palindromia effectively. Therefore it is of great importance to find a new therapy. Recent studies show NKT cell as a new immunoregulation cell. It is irreplaceable in antitumor immunity, preventing transplant rejection and inhibiting the occurrence of autoimmune disease. The dysfunction of NKT cell relates to the occurrence of several diseases, such as: tumor metastasis, autoimmune diseases (diabetes, systematic lupus erythematosus and multiple sclerosis, etc) (11). NKT cell is the first T cell subset found in mice with TCRαβand and as it has NK 1.1, the surface marker of NK cell; it is considered a natural killer of T cells (NKT cells). At present, EAMG model is formed mostly of rats and mice. Among the rats, Lewis is the most susceptible while in mice, B6 has the highest susceptibility. As NKT cells mainly exist in mice, our experiment chose B6 mice as an EAMG model and observed the effect of MKT cell on clinical symptoms and immunity indexes after activation.

Another feature of NKT cells is that the cells of the same species have only one TCRα chain encoding genes (for mice it's Vα14-Jα281) and extremely limited TCRβ chain encoding genes (12). In respect to other T cells, NKT cell recognizes only the lipid antigen submitted by CD1d molecule on cell surface and the natural ligand is not clear. A-GalCer is a seaweed ramification which is isolated from sponge and modified to its final form. It functions in CD1d restriction of NKT cells, expresses constant Vα14TCR, activates NKT cells and regulates immune and autoimmune response through secreting cytokines.

Based on the features above, this experiment treated the mice with α-GalCer intraperitoneal injection at different times and observed the effect of activated NKT cell on EAMG model. Through the study results we found that the EAMG morbidity

of forward immunization group (0d, 7d, 14d, ip α-GalCer) was much lower than the control group; not only hadn't the weight reduced, on the contrary it gradually increased; the clinical scoring was distinctly lower than the control group (0d, 7d, 14d, ip α-GalCer) which confirmed that α-GalCer forward immunization could induce the mice to resist AchR sensitization and prevent the occurrence of EAMG. As for the combined immunization group, the EAMG morbidity did not vary distinctly from the control group although it was slightly higher. The weight reduced after invasion and reached its peak at 60 d, then slightly increased again; the clinical scoring was slightly higher than the control group but there was no statistical significance. It suggested that α-GalCe combination immunization can't induce mice to resist AchR sensitization or prevent EAMG occurrence. The conclusion of the experiment was that the forward immunization group represented the prevention group which could distinctly inhibit EAMG, however, the combined immunization group was equivalent to the treatment group. This suggested that when α-GalCer NKT cell is activated it varied the natural lesion process of MG, which agrees with the research results of Wang ML et al. (13).

The experiment detected the anti AchR antibody IgG and its subtype of the mice which received its primary immunization 35 days prior. We found that compared with control group, the IgG AND IgG2b of the forward immunization group was much lower (P was 0.004 and 0.003 respectively), while there was no significant difference between them in IgG1 and IgG2a; there was no obvious difference in anti AchR antibody and its subtype between the combined immunization group and the control group. The results suggested that the main lethal factor of EAMG was IgG antibody and among all the subtypes IgG2b it was the most pathogenic.

The study of the effect of the activation of NKT cell on autoimmune disease now focused on diabetes, systematic lupus erythematosus and multiple sclerosis. Previous studies have proved that tmice (NOD mice) with spontaneous insulin dependent diabetes mellitus (DDM) have the problem of NKT cell quantity reduction and function deficiency. DDM is prevented if we import the NOD mice with NKT cells of normal mice, increase NKT cell quantity using Vα14-Jβ281 transgenosis treatment or activated NKT cells with repeated rejection of α-GalCer (13-16). But, for now, there are very few reports on the effect of activating NKT cells with α-GalCer, which may, to some degree, result from the purification difficulty of AchR.

This study found that forward immunization to α-GalCer could obviously remit the clinical symptom of EAMG, however combined immunization of α-GalCer (treatment group) might worsen the situation. Therefore, the new immunization regulation cell (BKT cell) is only suitable for the forward prevention of MG for the high risk population. However, it provides a pathway for MG treatment and has a bright prospect.

REFERENCES

1. Wen YJ. The Research on treatment of myasthenia gravis with the root of kudzu vine and other herbs. J of Shaanxi College of Trad Chinese Medi 2012; 35(2):64-6.
2. Wu W, Shi S, Ljunggren HG, Cava AL, Van Kaer L, Shi FD, Liu R. NK Cells Inhibit T-bet-deficient, Autoreactive Th17 Cells. Scandinavian J of Immu 2012; 76(6):559-66.
3. Chang T, Li ZY. Research development of myasthenia gravis immunology pathogenesis. Chin J of Neuroi and Neur 2011; 18(5):357-60.
4. Liu LH, Wang LH, Li J, Zhang HX. Establishment and application of myasthenia gravis animal model. J of Brain and Nervous Diseases 2013; 21(2):155-8.
5. Wang HF, Li S, Dong L, Wang YF. Influence of "Warming Yang and Nourishing Qi" acupuncture treatment in serum IL-12 and IL-18 expression levels in experimental autoimmune myasthenia gravis rats and its mechanism. Chin J of Immu 2014; 30(7):909-12.
6. Wu ZY, Zhu YM. The activating mechanism and significance of NKT cells in the treatment of sepsis. Chin J of Emer Medi 2013; 22(3):321-4.
7. Wei XL, Huang Z, Li X, Liu W. Role of Foxp3 and regulatory T cells in pathogenesis of passive transferred myasthenia gravis in young mice. Acta Acade Medi Mili Tert 2010; 32(4):353-6.
8. Zheng QH, Zhang AH, Zheng AH, Yao WB, Gao JM, Zhang QB, Li J. MiR-150 Deletion increases IFN-γ

production of NKT cell and inhibits lung metastasis of mice melanoma cells. Progress in Bio and Bio 2013; 40(5):454-60.
9. Meriggioli MN, Sanders DB. Autoimmune myasthenia gravis: emerging clinical and biological heterogeneity. The Lancet Neu 2009; 8(5):475-90.
10. Qiu SB, Liang Y, Liu P. Research development on relevant antibody of myasthenia gravis and interleukin. Chin J of Immu 2011; 27:1205-7.
11. Long YM, Hu XQ. Research development on autoimmune disease pathogenesis of nervous system and the treatment. Chin J of Cont Neu and Neuro 2010; 10(1):49-63.
12. Li LY, Cui JW. Research development on antitumor immunity of NKT cells. Chin J of Clin (Elect Version) 2013; 7(20):9278-81.
13. Wang ML, Mei YW. Research progress on relevant cell factor of myasthenia gravis. Internal Medicine of China 2010; 5(6):621-4.
14. Skeie GO, Apostolski S, Evoli A, et al. Guidelines for treatment of autoimmune neuromuscular transmission disorders. Euro J of Neuro 2010; 17(7):893-902.
15. Chen B, Hou JT, Yang XJ, Liu FB. Multivariate analysis of risk factors for myasthenic Crisis-A 252 cases analysis study. Chin J of Ner and Mental Dis 2011; 17(7):893-902.
16. Sathasivam S. Current and emerging treatments for the management of myasthenia gravis. Thera and Clini Risk Mana 2011; 7:313-23.

LETTER TO THE EDITOR

ANALYSIS OF IMMUNITY INDEX AND IMMUNOPATHOGENESIS PATTERN OF LUPUS NEPHRITIS PATIENTS

J.X. GAO[1], H.L. DIAO[2], Y.Q. LIU[1], M. LV[1], H. DONG[1], X.M. ZHANG[1] and Y.N. WANG[1]

[1]Department of Nephrology, Binzhou Medical University Hospital, Binzhou, China; [2]Department of Physiology, Binzhou Medical University, Binzhou, China

Received December 22, 2014 – Accepted January 29, 2015

Joint detection of anti-dsDNA antibodies, anti-U1RNP, anti-SM antibodies, anti-SSA antibodies, anti-ribosomal P protein antibodies, anti-nucleosome antivodies (Anua), anti-histone antibodies (AHA) and antinuclear antibodies brings to the early diagnosis of systemic lupus erythematosus (SLE) and speculation of renal lesion degree of lupus nephritis patients in order to choose a specific therapeutic schedule. This paper analyzed the abnormal immunology features and connections of each pathological pattern of LN renal biopsy and probed into the essence in order to provide basis for diagnosis, treatment, pathological pattern speculation and forward assessment of LN. We chose 97 cases, treated them with renal biopsy and pathological pattern classification, analyzed pathological pattern distribution, different pathological patterns and the correlation of immunity index with anti-dsDNAantibodies, anti-U1RNP, anti-Sm antibodies, anti-SSA antibodies, anti-ribosomal P protein antibodies, Anua, AHA and ANA of the first renal biopsy were taken as the experiment index. The results showed that the morbidity of the male was distinctly lower than the female and the age of onset was much lower (P<0.05); pattern I, pattern II, pattern III, pattern IV, pattern V, and pattern VI accounted for 1.0%, 3.1%, 12.4%, 47.4%,16.5%, 15.5%, 4.1%, 0%, respectively; among all the LN patients, there were respectively 59, 43, 28, 52, 51, 48, 36 and 93 cases in which anti-dsDNA antibody, anti-U1RNP antibody, anti-Sm antibody, anti-SSA antibody, anti-ribosomal P protein antibodies, Anua, AHA and ANA had increased and the positive rate was 60.8%, 44.3%, 28.9%, 53.6%, 52.6%, 49.5%, 37.1% and 95.9%, respectively. In conclusion, pattern IV is the most common of all pathological patterns of LN. Among the immunity index, anti-U1RNP antibodies and anti-SSA antibodies are positively correlated with anti-dsDNA antibodies; Anua is positively correlated with anti-dsDNA antibodies and AHA; anti-dsDNA antibodies, anti U1RNP antibodies, anti-Sm antibodies, anti SSA antibodies, AHA, anti-ribosomal P protein antibodies and ANA have no obvious correlation with LN renal lesions degree; Anua level of serum is positively correlated with LN renal lesions degree.

Lupus nephritis (LN) is an immune complex nephritis which is the common complication of SLE and involves several pathogenic mechanisms. During the last decade, interdisciplinary study has researched the pathogenesis of LN from lymphocyte (1), cytokines (2, 3), interleukin (4), tumor necrosis factor

Key words: lupus nephritis, renal biopsy, pathological patterns, immunity index

Mailing address: Dr Jinxiang Gao,
Department of Nephrology,
Binzhou Medical University,
Hospital, No.661,
Huanghe Second Road,
of Binzhou China
e-mail: gjxbzyy@163.com

0393-974X (2015)

(5), high-mobility group protein (6), metalloprotease (7), anti-dsDNA antibodies (8, 9) and apotosis (5). The correlation between them has been verified. Research shows that the autoimmunity antibodies such as anti-dsDNAantibodies, anti SSA antibodies, anti-ribosomal P protein antibodies, Anua, AHA and ANA were involved in the morbidity of LN, and many antibodies correlate with the activity of LN.

Anti-dsDNAantibodies are a recognized index that correlate with SLE state and activity and an auto-antibody involved in LN pathogenesis of which the importance of antibody degrades while the activity and remission of the disease become negative (8). It was found that anti-dsDNA antibodies exist in the serum of almost all the 117 patients and are closely related to clinical performance (Fang et al.) (10). Yang et al. (11) researched ANA, anti SSA, anti SSB, anti-Sm and anti-dsDNA and verified the correlation with the state of LN and its activity and pathological pattern. The research of Liu et al. (12) also showed that the positive rate of AnuA increased as the activity of the state of the disease increased. Through their research, Mai et al. (13) verified that the SLE patients whose anti SSA antibodies are positive are more likely to suffer pulmonary hypertension, neuropsychiatric disease and other severe diseases, almost at the active stage of lupus.

On the basis of the above, this study examined the pathological patterns of LN, analyzed the pathological distribution of patterns of the different patients and the correlation of immunity indexes with anti-dsDNA antibodies, anti U1RNP, anti-Sm antibodies, anti SSA antibodies, anti-ribosomal P protein antibodies, Anua, AHA and ANA as experimental indexes and served as reference for the diagnosis, treatment and pathological pattern deduction of LN.

MATERIALS AND METHODS

Clinical data

Ninety-seven SLE patients received pathological examination of renal puncture and were diagnosed in our department from January 2010 to December 2013. Among them were 88 females (90.7%) and the age of onset ranged from 13 to 76 (mean 38.5±14.1 years). Nine males (9.3%) that ranged from 17 to 57 years (mean 30.1±13.0 years). The ratio of male to female was 1:9.7 which showed that the morbidity of males is much lower than females. Compared to females, the onset age of male patients was comparatively low ($P<0.05$). Exclusion criteria: all the patients conformed to the 4 diagnosis standards for SLE by American College of Rheumatology revised in 1997. All of them had a clinical performance of renal lesion (such as proteinuria, hematuresis or renal insufficiency) and had received pathological examination of renal puncture biopsy with a complete medical history and laboratory examination record. All the patients or their relatives had signed the informed consent.

Laboratory index

The laboratory examination results all came from renal biopsies. ds-DNA antibodies, anti-Sm antibodies, anti SSA antibodies, anti-ribosomal P protein antibodies, Anua, AHA and ANA were detected by the clinical laboratory of our hospital using Euroline.

Pathology of renal biopsy

Percutaneous renal biopsy was carried out with guided color Doppler flow imaging. Each renal puncture sample was divide into three parts for light microscope and immunofluorescence examination. Some exceptional cases were examined by electronic speculum. In light microscope the sample contained more than 10 glomerulus that was embedded with paraffin, sliced up to sections of about 1-2μm thickness and processed with HE, PAS, PASM, MASSON staining, respectively. In immunofluorescence we considered the frozen section applied the direct immunofluoresence method to goat anti-human IgG, IgA, IgM, C3, C4, C1q and fibrinogen (Fib) marked with fluorescein isothiocyannate. In the electronic speculum we referred to the demand of clinical diagnosis, and renal puncture samples were examined by electronic microscopy.

PAS, Masson, PASM, immunofluorescent staining

The staining method and the reagent preparation were carried out according to the method of Gao (14).

Pathological type

According to the results of nephridial tissue light microscopic and immune-fluorescence examination that refer to the LN pathological scheme of ISN/RPS in 2003, we divided LN pathological type into slight membranous lupus nephritis (type 1), membranous proliferative lupus nephritis (type 2), focal segmental proliferative lupus nephritis (type 3), diffuse proliferative lupus nephritis (type 4), membranous lupus nephritis (type 5) and severe hard lupus nephritis (type 6). Type 4, with diffuse membranous lesion (LM shows wide fuchsinophilic deposits and rete ridges outside the basement membrane, immunofluorescence displays the immune globulin and additive deposit along

with the basement membrane of glomerulus or electronic microscope shows the electron dense granules deposit or rete ridges outside the membrane) is named type 3+4. Type 5, with segmental proliferation lesion in glomerulus such as loop necrosis, crescent or segmental proliferative lesion within loops and glomerulus of less than 50% of normal is considered type 3+5.

Statistical analysis

Statistical analysis was performed using SPSS17.0 software. Count data was expressed by rate and comparison between groups was calculated with c^2 test or correction method of c^2 test. Measurement data was expressed with Mean±SD. Comparison between groups was calculated with *t*-test. All results were considered statistically significant as $P<0.05$.

RESULTS

Pathological-type distribution

In the analysis of pathological type distribution of renal biopsy there was one case of slight membranous lupus nephritis (type 1) (1%), 3 cases of membranous proliferative lupus nephritis (type 2) (3.1%), 12 cases of focal segmental proliferative lupus nephritis (type 3) (12.4%), 46 cases of diffuse proliferative lupus nephritis (type 4) (47.4%), 16 cases of membranous lupus nephritis (type 5) (16.5%), 15 cases of type 4 +5(15.5%), 4 cases of type 3 +5 (4.1%) and no severe hard lupus nephritis (type VI6) occurred. Type 4 LN accounted for the highest proportion (47.4%), as shown in Fig. 1.

We divided the patients into groups of children (≤14 years), young and middle-aged (15-49 years) and the aged (≥50 years). The results showed that children accounted for 2.1% with 2 cases of females and no males involved; young and midldle-aged accounted for 74.2% with 64 cases of females and 8 cases of males; the aged accounted for 23.7% with 2 cases of females and 1 case of males. LN gender distribution is shown in Table I, age distribution of each type LN IS shown in Table II.

Table I. *LN gender distribution cases (%).*

	Children group (n=2)	Young and middle-aged group (n=72)	Elderly group (n=23)
Male	0 (0)	8 (88.9)	1 (11.1)
Female	2 (2.3)	64 (72.7)	22 (25.0)

Table II. *Age distribution of different pathological types cases (%).*

	Pathological types						
	I (n=1)	II (n=3)	III (n=12)	IV (n=46)	V (n=16)	III + V (n=4)	IV + V (n=15)
Child group	0(0)	0(0)	0(0)	2(100)	0(0)	0(0)	0(0)
Young and middle-aged group	1(1.4)	2(2.8)	9(12.5)	35(48.6)	11(15.3)	3(4.1)	11(15.3)
Elderly group	0(0)	1(4.4)	3(13.0)	9(39.1)	5(21.7)	1(4.4)	4(17.4)

Table III. *Correlation between pathological type and immunology index cases (%).*

	I (n=1)	II (n=3)	III (n=12)	IV (n=46)	V (n=16)	IV + V (n=15)	III + V (n=4)	Total
Anti ds-DNA antibodies	1(100)	1(33.3)	2(16.7)	31(48.4)	6(37.5)	15(100)	3(75)	59
Anti U1RNP antibodies	1(100)	1(33.3)	2(16.7)	21(45.7)	9(56.2)	7(46.7)	2(50)	43
Anti sm antibodies	0(0)	1(33.3)	2(16.7)	17(37.0)	4(25)	2(13.3)	2(50)	28
Anti SSA antibodies	1(100)	1(33.3)	5(41.7)	26(56.5)	10(62.5)	5(33.3)	4(100)	52
Anti-nucleosome antibodies	1(100)	2(66.7)	5(41.7)	23(50)	11(68.8)	6(40)	3(75)	51
Anti-histone antibodies	0(0)	1(33.3)	5(41.7)	24(52.2)	4(25)	11(73.3)	3(75)	48
Ribosome P	1(100)	0(0)	4(33.3)	14(30.4)	6(37.5)	8(53.3)	3(75)	36
Antinuclear antibodies titer positive	1(100)	3(100)	12(100)	44(95.7)	16(100)	14(93.3)	4(100)	94

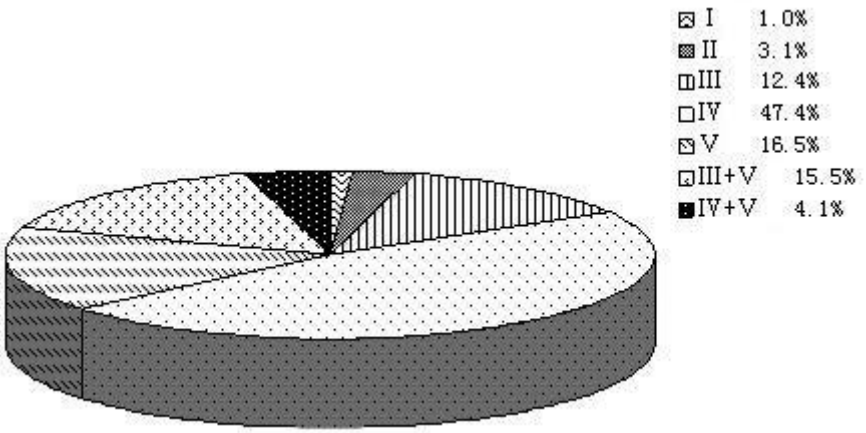

Fig. 1. *Distribution of different pathological types of LN.*

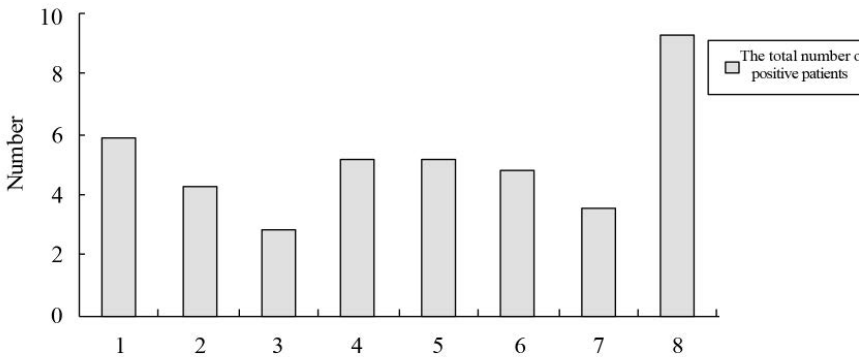

Fig. 2. *Positive cases of different immunology index.*

Immunology index of LN of different pathological types

Among the 97 cases of LN patients, the number of patients with increased ds-DNA antibpdies, anti-U1RNP antibodies, anti-Sm antibodies, anti-SSA antibodies, anti-ribosomal P protein antibodies, Anua, AHA, AMA titer were 59 cases, 43 cases, 28 cases, 52 cases, 51 cases, 48 cases, 36 cases and 93 cases, respectively. The positive rates were 60.8%, 44.3%, 28.9%, 53.6%, 52.6%, 49.5%, 37.1% and 95.9% respectively, as shown in Fig. 2.

Analysis of the positive rate of the immunology index of each pathological type that showed anti-U1RNP antibodies, anti-Sm antibodies and anti-SSA antibodies were positively correlated with anti-dsDNA antibodies ($P<0.05$). Anti-Sm antibodies were positively correlated with anti-SSA antibodies and anti-ribosomal P protein antibodies ($P<0.05$). Anua was positively correlated with anti-dsDNA antibodies and AHA ($P<0.05$) as shown in Table III:

DISCUSSION

SLE, which is featured by several abnormal immunoreactions, is an autoimmunity disease which involves several systems and organs of the whole body. The prominent expressions are several autoantibodies that through immune complex jeopardize almost all the organs and systems of the body including the kidney. The renal biopsy light microscope examination combined with immunofluorescence and electronic microscope showed that 100% SLE patients have a renal lesion of a different degree (12, 15). Morbidity of LN is

an important cause of the death rate of SLE and medium and end-stage renal disease is one of the most lethal factors of SLE death. This study shows that the ratio of male to female patients was 1:9.7; the morbidity of male patients is distinctly lower than females, and compared with female patients, the onset age of males is much lower. Among the different pathological types, type 4 accounted for the highest proportion (47.4%) followed by type 5, with a proportion of 16.5%. The data is consistent with the majority of Chinese studies (16, 17).

This study analyzed the pathological type distribution, the correlation between different pathological types and immunity index, taking into account anti ds-DNA antibodies, anti-U1RNP, anti-Sm antibodies, anti-SSA antibodies, anti-ribosomal P protein antibodies, Anua, AHA and ANA of the first renal biopsy as the experiment index. Anti-dsDNA antibodies of SLE already have a history of more than 50 years and have been regarded as an important serology landmark in diagnosis and assessment of disease state activity. Anti-Sm antibodies are also a symbolic antibody and like anti-dsDNA antibodies, have high specificity and low positive rate. Studies showed that the positive rate of anti-dsDNA antibodies and anti-Sm antibodies are respectively 60.8% and 28.9%, which is not significantly related with pathological types of LN and is consistent with former reports (8, 12). Anti-U1RNP antibody is normally seen in mixed connective tissue disease and the positive rate of anti-U1RNP antibodies of SLE patients can reach 30% to 40%, which is correlated with myositis, Raynaud's phenomenon and nephritis (18). In this study the positive rate of anti-U1RNP antibodies of LN was 44.3%, and had no significant correlation with LN pathological type. Anti-SSA antibody is a common antibody. The study of Jin et al. (19) suggested that the positive rate of anti-SSA antibody is 64% and positive anti-SSA antibody has a certain clinical value for SLE diagnosis. Another study proposed that the patient whose anti-SSA antibody is positive is more likely to suffer from pulmonary hypertension, nervous system disease and other severe diseases (13). This study shows the positive rate of anti-SSA antibody is 53.6% and it has no obvious correlation with LN renal lesion degree. Anua comes from the apoptotic cells within the body. Xu et al. (20), in their study, suggested that the occurrence of Anua is closely related with LN and the serum standard reflects the renal lesion degree. Other reports have suggested that Anua is positively correlated with SLEDAI assessment and the positive rate of Anua increases as the disease state activity increases. In this study there were 51 Anua patients and the positive rate was 52.6% which is obviously correlated with the morbidity of LN ($P<0.05$). Anua positive rate reflected the renal lesion degree. Therefore, we believe that Anua can be used in SLE diagnosis. Meanwhile, it conduces to the clinical speculation of pathological type of LN and provides guidelines for the clinical treatment. Anti-ribosomal P protein antibodies have no correlation with SLE (12). In this data group, there were 36 patients whose anti-ribosomal P protein antibodies were positive which accounted for about 37.1%. Among them, the positive rate of type 5 LN patients was 37.5% which was higher than the other pathological types, but there was no statistical significance between anti-ribosomal P protein antibodies and LN pathological types. This study also showed that the positive rate of AHA was about 50%, which has no correlation with renal pathology of LN patients. However, though it has no significant correlation with anti-dsDNAantibodies, it was positively correlated with antinuclear antibodies. Studies on AHA are insufficient at this time, its diagnostic significance to SLE and the speculation of the renal lesion degree of LN patients require further research. ANA is very sensitive to SLE. In the present study the positive LN rate of 97 patients was 95.7% and the positive rate of type 1 patients was 100%, probably because the patients who had no history of renal lesion had not received renal puncture biopsy and the sample size was small. But this research suggested ANA had no significant correlation with pathological type of LN, which is consistent with the majority of reports at present. In short, there is still no simple laboratory examination which is 100% sensitive and specific to SLE diagnosis. Joint detection benefits the early diagnosis of SLE and can hypothesize the renal lesion degree of LN patients through the clinical performance and the Anua standard of serum, therefore a particular therapeutic schedule can be selected.

In conclusion, type 4 (accounted for 47.4%) is the most common pathological type of LN, the

morbidity of males is much lower than females and the onset age of males is lower than females. Anti-U1RNP antibodies and anti-SSA antibodies are correlated with anti-Ds DNA; Anua is positively correlated with anti-dsDNA antibodies and AHA; anti-dsDNA antibodies, anti-SSA antibodies, anti-ribosomal P protein antibodies, Anua, AHA, ANA are not statistically correlated with renal lesion degree of LN; Anua standard of serum is positively correlated with lesion degree of LN renal disease.

REFERENCES

1. Chen DY, Chen YM, Wen MC. T-Y Hsieh, W-T Hung, J-L Lan. The potential role of Th17 cells and Th17-related cytokines in the pathogenesis of lupus nephritis. Lupus 2012; 21(13):1385-96.
2. Brugos B, Vincze Z Sipka S Szegedi G, Zeher M. Serum and urinary cytokine levels of SLE patients. Die Pharmazie-An International Journal of Pharmaceutical Sciences 2012; 67(5):411-3.
3. Xu XL, Yu XH, Li YN. Levels and clinical significance of B cell activating factor and interferon-α in systemic lupus erythematosus. Clin Focus 2013; (5):522-4.
4. Li SQ, Huang XB, Feng LC. Association of serum interleukin-6 level with active lupus nephritis. International Med & Health Guidance News 2013; (11):1007-245
5. Lech M, Anders HJ. The pathogenesis of lupus nephritis. J Am Soc Nephrol 2013; 24(9):1357-66.
6. Sun LP, Wu YM, Yang LL. The expression of TLR2 and high mobility group protein 1 in systemic lupus erythematosus. Chin J of Rheumatol 2012; (10):688-91.
7. Jiang ZX, Sui T, Wang B. Relationships between MMP-2, MMP-9, TIMP-1 and TIMP-2 levels and their pathogenesis in patients with lupus nephritis. Rheumatol international 2010; 30(9):1219-26.
8. Liu YH, Wu LJ, Li CP. Research development of anti-dsDNAantibodies, anti-nuclear antibodies and anti dsDNA-NcX in Systemic lupus erythmatosus. Xinjiang Medl J 2013; 43(2):1219-26.
9. Wang ZQ, Gong CX, Li ZB. Research development on lupus nephritis immunizing pathogenesis. J of Difficult and Complicated Cases 2011; 10(5):1219-26.
10. Fang XX, Fang M, Liao HJ, Rong YL, Chen LS, Wu JR. ANA, anti ENA antibodies and anti-dsDNAantibodies detection of 117 SLE patients. The J of Practic Med 2008; 15(1):46.
11. Yang JF, Du JL, Wang HM, Xiao P, Sun SR, Ren Yan, He XJ. Discussion of the correlation of ANA anti SSA, anti SSB, anti-Ds DNA, anti Sm and the pathology of lupus nephritis. J of Yanan Univer (Med Sci) 2011; 9(3):6-7.
12. Liu KM. Research on the correlation of SLE activity, addiment and autoantibody level. International J of Lab Med 2012; 2(4):494-5.
13. Mai Y, Shou T, Lin J. Clinical features of SLE patients whose anti SSA antibodies are positive. Chin J of Misdiagnostics 2010; 10(15):3596-7.
14. Gao WH. Analysis of immunity index and pathological type of 97 lupus nephritis patients. Jilin: JilinUniversity2014. http://cdmd.cnki.com.cn/Article/CDMD-10183-1014271066.htm
15. Wei H, Lv ZQ, Ru JL, Li XF, Xu K, Weng HY. The detection of DNA-associated autoantibodies to cell membrane and its combination with other autoantibodies in the diagnosis of systemic lupus erythematosus. Chin J of Rheumatol 2010; 14(3):185-7.
16. Jin OY, Sun LY. Development of pathological typing of lupus nephritis. Chin J of Rheumatol 2007; 11(3):185-8.
17. Liu JC, Cheng JZ, Hu SL. Development on immunosuppression therapy of lupus nephritis. The J of Practic Med 2011; 27(9):1704-95.
18. Huang JM, Li XD, Tang HY, Ni XY. Clinical significance of anti U1RNP antibodies detection of SLE patients. J of Clin Pulmonary Med 2010; 15(5):734-5.
19. Jin YP, Lin GG, Yan C. Significance of anti-Ro-52 kDa and SSA antibodies in patients with autoimmune diseases. J of Modern Lab Med 2011; (5):137-8.
20. Xu WH, Zou YF, Guan XD, Liang X, Chen KQ. Clinical significance of antinucleosome antibody in patients with lupus nephritis. Chin J of Postgraduates of Med 2012; 5(4):26-8.

LETTER TO THE EDITOR

THE COMPARISON BETWEEN VITAMIN D CONCENTRATION IN UPPER SILESIA PATIENTS WITH PROSTATE CANCER AND WITH BENIGN PROSTATIC HYPERPLASIA

K. WIECZOREK[1], R.S. BRACZKOWSKI[2], M. SKRZYPEK[3], P.J. STRYJEWSKI[4], A. KUCZAJ[5] and G. AL-SRORY[6]

[1]Urology Department, E. Michalowski Specialist Hospital, Katowice, Poland; [2]Department of Public Health, School of Public Health, Silesian Medical University, Poland; [3]Department of Epidemiology, School of Public Health, Biostatistics, Silesian Medical University, Bytom, Poland; [4]Department of Cardiology, City Hospital, Chrzanow, Poland; [5]2nd Department of Cardiology, Zabrze, Medical University of Silesia, Katowice, Poland; [6]Health Center, Jastrzębie Zdrój, Poland

Received September 24, 2014 – Accepted December 22, 2014

A number of studies have shown that vitamin D has a protective effect against the development of cancer, which may also be related to prostate cancer. Low serum vitamin D concentration has also been demonstrated in benign prostate hyperplasia. We compared serum vitamin D concentration in two groups of Polish men with prostate cancer and benign prostate hyperplasia. Each group comprised 30 patients. The concentration was determined by ELISA. To assess the difference between the study population, non-parametric Mann Whitney U test was used. The results revealed that patients with prostate cancer are deficient in vitamin D (median =25.3, quartiles q1 - q3: 13.4 -33.4). The concentration of vitamin D in the group of patients with prostate cancer was lower than in the group of benign prostatic hyperplasia with vitamin D deficiency (median =34.8, quartiles q1 - q3: 17.9 – 44.3). Vitamin D concentration in Polish men with prostate cancer is lower compared to patients with benign prostatic hyperplasia.

Vitamin D is usually associated with the regulation of calcium-phosphate metabolism. However, for more than two decades a number of (epidemiological, experimental, and clinical) studies have indicated many other features of this vitamin. The most frequently reported include the impact on the immune system and the prevention of cardiovascular and mental diseases (1-6). In 1941 Apperly was the first to indicate a correlation between low solar radiation and cancer-related mortality (7). Since that time many studies have shown that vitamin D has a protective effect against the development of cancer. This protective effect has been demonstrated, for instance, in breast, pancreatic and colorectal cancers (8-10). It was highlighted that such a relationship may also be observed in prostate cancer. Prostate cancer was also on the list presented by Apperly. Since that time a number of studies have confirmed this relationship (11, 12). On the other hand, some reports did not show such a clear relationship (13-15). Moreover, within the last few years a number of studies have demonstrated that low vitamin D concentration is also found in benign prostatic hyperplasia (BPH) (16, 17).

Key words: benign prostatic hypertrophy, p cancer, vitamin D

Mailing address: Piotr Jozef Stryjewski MD, PhD
Department of Cardiology,
City Hospital Topolowa 16 st.,
32-500 Chrzanow, Poland
Tel.: +48 509 59 89 59
Fax: +48 32 624 72 58
e-mail: pstryjewski@o2.pl

0393-974X (2015)

DISCLOSURE: ALL AUTHORS REPORT NO CONFLICTS OF INTEREST RELEVANT TO THIS ARTICLE.

However, it is estimated that approximately one billion people worldwide are deficient in vitamin D (18-21). It is related to persons with vitamin D deficiency i.e. 25(OH)D3 concentration below 25 nmol/L (10ng/ml) as well as with vitamin D insufficiency (25 - 75 nmol/L; 10 – 30 ng/ml). Therefore many researchers recommend additional vitamin D supplementation (22-24). However, some reports suggest that there are too little data regarding cancer prevention in the form of vitamin D supplementation (25). Bearing in mind the above, we decided to investigate serum vitamin D concentration in patients with prostate cancer and to compare it with the group of patients with BPH. Both groups were treated in The E. Michalowski Specialist Hospital in Katowice, Poland.

MATERIALS AND METHODS

This study was approved by the Research Ethics Committee of the Silesian Medical University in Poland. A total of sixty patients (aged 35-70 years) were enrolled in the study i.e. 30 consecutive patients with prostate cancer up to T3aN0M0 stage (group 1) and 30 consecutive patients with BPH – stages 3 and 4 (group 2). The patients were admitted to The E. Michalowski Specialist Hospital in Katowice between 2011 and 2012 for prostatic electroresection or biopsy.

The group enrollment started after obtaining the histological findings. Patients with hypercalcemia, sarcoidosis, systemic connective tissue diseases and other types of cancer were excluded from the study. Patients with prostate-specific antigen (PSA) above 4 ng/ml in whom histological findings did not confirm cancer and patients who had been staying within the last 3 months in countries with high sun exposure were also excluded from the study. Serum concentration of 25(OH) D3 was determined by ELISA method, with the use of 25(OH) –Vitamin D Xpress ELISA Kit produced by Immundiagnostik AG. delivered by IMMUNIQ (Żory, Poland). The concentration assessment was performed with the use of INFINITE M200 PRO reader produced by TECAN Austria (Magellan software) at wavelengths 450 nm and 620 nm (reference wavelength).

Statistical analysis

For all statistical analyses the adopted level of significance was $\alpha = 0.05$. The test was performed using SAS v9.4 (SAS Institute Inc., Cary NC). Since the assumption of a normally distributed random variable was not proven by the Shapiro-Wilk test, a nonparametric Mann Whitney U test was used to assess the difference

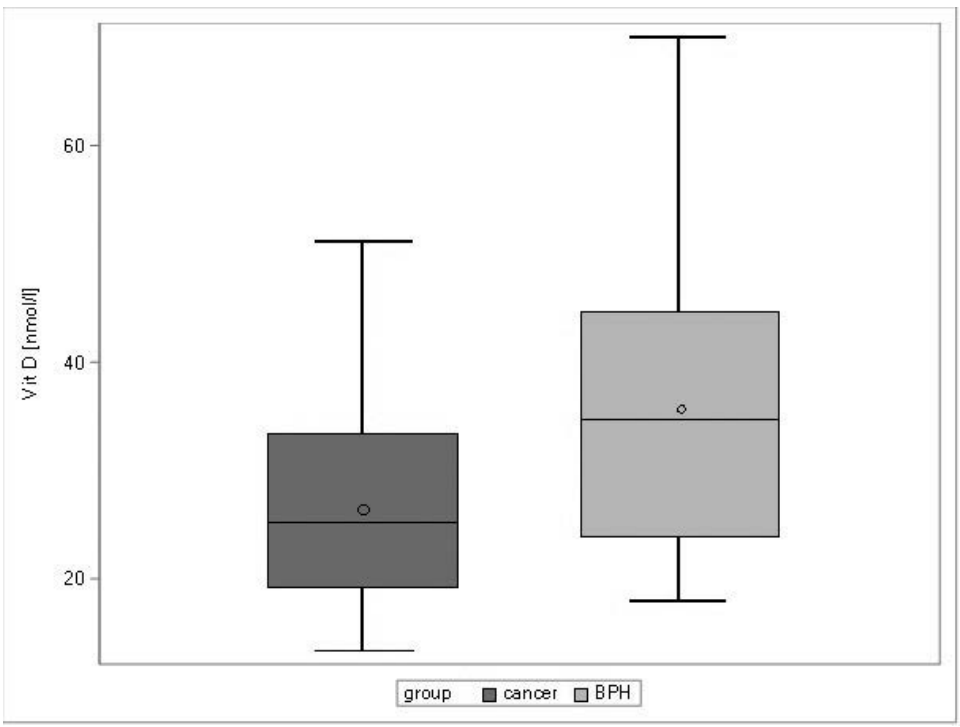

Fig. 1. *Concentration of vitamin D in patients with prostate cancer and with BPH (Mann-Whitney U test).*

Table I. *Concentration of vitamin D (nmol/l) in patients with prostate cancer and BPH.*

Group	Number of patients (N)	Average ± SD	Minimum	Lower quartile	Median ± SD	Upper quartile	Maximum
Prostate cancer	30	27.76 ±10.52	13.40	19.30	25.26	33.40	70.10
BPH	30	35.82 ±13.68	17.90	24.50	34.80	44.30	51.20

between the study population.

The study was approved by the Bioethics Committee of Silesian University and written informed consent was obtained from all patients.

RESULTS

Patients with prostate cancer were insufficient in vitamin D (median =25.3, quartiles q1 - q3: 13.4 -33.4. The Mann-Whitney U test (p = 0.02) showed that vitamin D concentration in the group of patients with prostate cancer was statistically significantly lower than in the group of BPH (median =34.8, quartiles q1 - q3: 17.9 – 44.3). In this group serum vitamin D concentration was also low and the patients were also classified as having vitamin D insufficiency (Table I, Fig. 1).

DISCUSSION

We selected two groups of patients scheduled for prostate biopsy or electrocautery due to prostate cancer or BPH. These patients had been living in similar conditions for a few weeks prior to the determination of serum vitamin D concentration.

Similar environmental factors have an influence on the results of vitamin D concentration. The fact that all the subjects who were treated in one hospital came from the same region of Poland increased group homogeneity.

In light of the results, patients with prostate cancer were insufficient in vitamin D. Vitamin D concentration in this group was lower than in the group of patients with BPH. However, in the group of BPH patients, vitamin D concentration was only slightly higher than the tolerable lower limit defining insufficiency. As yet, no studies have been conducted on vitamin D concentration in the population of patients with prostate cancer or BPH in Upper Silesia, the south-central part of Poland. The lowered vitamin D concentration in this group is similar to the concentration in the population in an urban area in northern Poland as presented by Kmieć et al. (21).

It is also consistent with study results obtained by other authors investigating the central European population. In the group of 129 healthy men (mean age 44 y, range 20-59 y) living in Ukraine, vitamin D insufficiency was established based on a year-round assessment (vitamin D concentration:37.5±25 nmol/L) (26).

In the Hungarian population comprising 36 healthy men aged over 43 years, vitamin D assessment between March and May showed that the mean concentration was 67.5 nmol/L (range: 55-85), which also corresponded to vitamin D insufficiency (27).

Therefore we do not suggest that vitamin D concentration in our group is lower than in the general population as this requires further research. Due to the fact that only a small number of cases were surveyed, it is difficult to determine whether the reduced vitamin D concentration increases the risk of the development of prostate cancer. Lifestyle and dietary habits that affect low vitamin D concentration may also affect the risk of developing prostate cancer. It cannot be excluded that in the case of a significantly reduced vitamin D concentration signaling pathways leading to cell proliferation are different than in the case when vitamin D concentration is only slightly reduced. Analyzing the results between the groups in the present study, large differences in vitamin D concentration were visible between the groups.

Human prostate cells contain receptors for 1α,25-dihydroxyvitamin D. Some scientists suggest that prostate cancer cells may respond to vitamin

D3 with increases in differentiation and apoptosis, and decreases in proliferation, invasiveness and metastasis (28). Based on in vitro studies, a causative relationship between vitamin D3 concentration and prostate cancer was demonstrated. However, in vivo mechanisms are much more complex than the mechanisms observed in vitro. Participation of other factors and mechanisms which may have a pivotal role in cancerogenesis may be reason of a non-causative correlation between vitamin D3 concentration and prostate cancer.

At present, when so much attention is paid to an individual approach to the incidence of cancer and individualized therapy, we could suspect that the protective effect of vitamin D on the development of prostate cancer is also individual. It may for instance result from the polymorphism of vitamin D receptor and the activity of vitamin D metabolizing enzymes. We cannot exclude that also other factors which are still poorly understood may interfere with this phenomenon. Our patients remain in the follow-up. It would be useful to check whether vitamin D supplementation is beneficial for patients from both groups. Further studies in this area are planned.

In conclusion, the results of the present study showed that vitamin D concentration was statistically significantly lower in a group of patients with prostate cancer as compared to a group with BPH. The results, although performed on a small group of patients, may indicate the potential role of vitamin D in the pathogenesis of prostate cancer.

ACKNOWLEDGEMENTS

The authors thank Dr. Małgorzata Huzarska from the Department of Clinical Pharmacology for performing laboratory tests.

The study was sponsored by the Grant KNW 2-127/10 of Silesian Medical University.

REFERENCES

1. Munger KL, Levin LI, Hollis BW, Howard NS, Ascherio A. Serum 25-hydroxyvitamin D levels and risk of multiple sclerosis. JAMA 2006; 296:2832-83.
2. Welles CC, Whooley MA, Karumanchi SA, Hod T, Thadhani R, Berg AH, Ix JH, Mukamal KJ. Vitamin D deficiency and cardiovascular events in patients with coronary heart disease: data from the heart and soul study. Am J Epidemiol 2014; 179:1279-87.
3. Melamed ML, Muntner P, Michos ED, Uribarri J, Weber C, Sharma J, Raggi P. Serum 25-hydroxyvitamin D levels and the prevalence of peripheral arterial disease: results from NHANES 2001 to 2004. Arterioscler Thromb Vasc Biol 2008; 28:117985.
4. Itzhaky D, Amital D, Gorden K, Bogomolni A, Arnson Y, Amital H, et al. Low serum vitamin D concentrations in patients with schizophrenia. Isr Med Assoc J 2012; 14:88-92.
5. Balion C, Griffith LE, Strifler L, et al. Vitamin D, cognition, and dementia: a systematic review and meta-analysis. Neurology 2012; 25:1397-40.
6. Brouwer-Brolsma EM, van de Rest O, Tieland M, et al. Serum 25-hydroxyvitamin D is associated with cognitive executive function in Dutch prefrail and frail elderly: a cross-sectional study exploring the associations of 25-hydroxyvitamin D with glucose metabolism, cognitive performance and depression J Am Med Dir Assoc 2013; 14:852e9-852e17.
7. Apperly FL. The relation of solar radiation to cancer mortality in North America. Cancer Res 1941; 1:191-95.
8. Bulathsinghala P, Syrigos KN, Saif MW. Role of vitamin D in the prevention of pancreatic cancer. J Nutr Metab 2010; 2010:721365.
9. Kang W, Lee S, Jeon E, Yun YR, Kim KH, Jang JH. Emerging role of vitamin D in colorectal cancer World J Gastrointest Oncol 2011; 3:123-27.
10. Rollison DE, Cole AL, Tung KH, Slattery ML, Baumgartner KB, Byers T, Wolff RK, Giuliano AR. Vitamin D intake, vitamin D receptor polymorphisms, and breast cancer risk among women living in the southwestern U.S. Breast Cancer Res Treat 2012; 132:683-91.
11. Loke TW, Sevfi D, Khadra M. Prostate cancer incidence in Australia correlates inversely with solar radiation BJU Int 2011; 108(2):66-70.
12. Gloth FM, Gundberg C, Hollis B, Haddad JG jr, Tobin J. Vitamin D deficiency and insufficiency among patients with prostate cancer. BJU Int 2009; 104:909-14.
13. Gilbert R, Metcalfe C, Fraser WD, Donovan J, Hamdy F, Neal DE, Lane JA, Martin RM. Associations

of circulating 25-hydroxyvitamin D with prostate cancer diagnosis, stage and grade. Int J Cancer 2012; 23:1865-73.

14. Trump DL, Chadha MK, Sunga AY, et al. Vitamin D deficiency and insufficiency among patients with prostate cancer. BJU Int 2009;104:909-14
15. Corder EH, Guess HA, Hulka BS, et al. Vitamin D and prostate cancer: a prediagnostic study with stored sera. Cancer Epidemiol Biomarkers Prev 1993; 2:467-72.
16. Haghsheno MA, Mellström D, Behre CJ, Damber JE, Johansson H, Karlsson M. Low 25-OH vitamin D is associated with benign prostatic hyperplasia. J Urol 2013; 190:608-14.
17. Manchanda PK, Kibler AJ,Zhang M, Ravi J, Bid HK. Vitamin D receptor as a therapeutic target for benign prostatic hyperplasia. Indian J Urol 2012; 28:377-81.
18. Holick MF. Vitamin D deficiency. N Engl J Med 2007; 357:266-281.
19. Harinarayan CV, Ramalakshmi T, Venkataprasad U. High prevalence of low dietary calcium and low vitamin D status in healthy south Indians. Asia Pac J Clin Nutr 2004; 13:359-64.
20. Pellicane AJ, Wysocki NM, Schnitzer TJ. Prevalence of 25-hydroxyvitamin D deficiency in the outpatient rehabilitation population. Am J Phys Med Rehabil 2010; 89:899-904.
21. Kmieć P, Zmijewski M, Waszak P, Sworczak K, Lizakowska-Kmieć M. Vitamin D deficiency during winter months among an adult, predominantly urban, population in northern Poland. Endokrynol Pol 2014; 65:105-13.
22. Bischoff-Ferrari HA, Shao A, Dawson-Hughes B, Hathcock J, Giovannucci E, Willett WC. Benefit-risk assessment of vitamin D supplementation. Osteoporos Int 2010; 21:1121-32.
23. Vashi PG, Trukova K, Lammersfeld CA, Braun DP, Gupta D. Impact of oral vitamin D supplementation on serum 25-hydroxyvitamin D levels in oncology. Nutr J 2010; 9:60.
24. LaCroix AZ, Kotchen J, Anderson G, et al. Calcium plus vitamin D supplementation and mortality in postmenopausal women: the Women's Health Initiative calcium-vitamin D randomized controlled trial. J Gerontol A Biol Sci Med Sci 2009; 64:559-67.
25. Manson JE, Mayne ST, Clinton SK. Vitamin D and prevention of cancer-ready for prime time? N Engl J Med 2011; 3(64):1385-87.
26. Povoroznyuk VV, Balatska NI, Muts V, Solonenko T, Vayda V. Vitamin D deficiency and insufficiency in Ukrainian population. Bone 2011; 48:202-3.
27. Virágh E, Horváth D, Lőcsei Z, Kovács L, Jáger R, Varga B, Kovács L G, Salamonné Toldy E. Vitamin D supply among healthy blood donors in County Vas, Hungary. Orvosi Hetilap 2012; 153(41):1629-37.
28. Chen TC, Holick MF. Vitamin D and prostate cancer prevention and treatment. Trends Endocrinol Metab 2003; 14(9):423-30.

LETTER TO THE EDITOR

EFFECT OF PROLONGED DUAL ANTI-PLATELET THERAPY ON REDUCING MYOCARDIAL INFARCTION RATE AFTER PERCUTANEOUS CORONARY INTERVENTION

HQ. DUAN, PS. DONG, HL. WANG, ZJ. LI, LJ. DU and YW. ZHAO

The First Affiliated Hospital of Henan University of Science & Technology, Henan, China

Received November 21, 2014 – Accepted February 10, 2015

This paper aimed to review the interferential effect of prolonged dual anti-platelet therapy after Percutaneous Coronary Intervention (PCI), and the influence on reducing the myocardial infarction rate. A computer search was carried out in the relevant libraries and databases, regarding all the short-term (≤ 6 months) and long-term (> 6 months) dual anti-platelet therapies, and the curative and observational studies on the effects and safety of interventional therapy. RevMan5.1 software was used to meta-analyze the standard research. A total of 8 papers were finally selected. In the randomized controlled research, meta-analysis showed that the myocardial infarction rate of a long-term dual anti-platelet treatment group was lower than the short-term treatment group [OR=0.74, 95%CI (0.56, 0.98), P<0.0001]. The meta-analysis of observational research showed that the myocardial infarction rate of the long-term treatment group was lower than the short-term treatment group [OR=0.7, 95%CI (0.45, 1.08), P=0.11]; the incidence rate of late stent thrombosis in the long-term treatment group was lower than in the short-term treatment group [OR=0.40, 95%CI (0.15, 1.07), P=0.07]. It can be concluded that in the long-term group (>6 months) dual anti-platelet therapy after PCI can reduce the incidence rate of myocardial infarction or death. In addition, long-term treatment can reduce the occurrence tendency of late stent thrombosis. Furthermore, in the long-term treatment group, serious bleeding events did not increase.

Acute myocardial infarction is a myocardial necrosis disease caused by persistent and severe myocardial ischemia and hypoxia, which are part of coronary heart disease. The clinical symptoms include shock, chest pain, heart failure and arrhythmia (1). At present it is important for us to promote the research of acute myocardial infarction, to provide accurate scientific information for better therapeutic treatment. Acute myocardial infarction is a disease caused by platelet aggregation and coronary artery spasm which leads to thrombosis, on the precondition of atherosclerosis of coronary artery (2, 3). At present, the main methods of treating coronary atherosclerotic heart disease are drug treatment, Percutaneous Coronary Intervention (PCI) and Coronary artery bypass graft operation (CABG).

PCI has become an effective treatment in coronary revascularization, but we should pay attention to its safety after the operation, as the appearance of

Key words: Percutaneous Coronary Intervention (PCI), dual anti-platelet therapy, randomized controlled research, observational research, meta-analysis

Mailing address: Dr Pingshuan Dong,
The First Affiliated Hospital
of Henan University of
Science & Technology,
Guanlin Street, Luolong
District, Luoyang, 471000, China
e-mail: dhqduan@163.com

0393-974X (2015)

DISCLOSURE: ALL AUTHORS REPORT NO CONFLICTS OF INTEREST RELEVANT TO THIS ARTICLE.

postoperative adverse cardiovascular events has aroused wide concern as has anti-platelet therapy after PCI (4, 5). Especially for patients with coronary drug-eluting stent (DES), many clinical studies show that, after the operation, dual anti-platelet therapy using aspirin and thienopyridine (6) can effectively prevent acute large cardiovascular events such as sub-acute intravascular thrombosis and late stent thrombosis, and can reduce the occurrence of major adverse cardiovascular events (MACE). However, premature discontinuation of anti-platelet therapy can significantly increase the risk of MACE occurrence (7), and prolonged anti-platelet therapy may increase the risk of hemorrhage.

Malignant cardiovascular events of PCI therapy mainly related with mechanical injury of coronary plaque, hypercoagulable state of the body and excessive activation of platelets. During PCI treatment, the imbedding of stents leads to local artery injury, plaque rupture of atherosclerotic plaque near the injured artery, even tunica media vasorum injury. Endothelium exposure and release of fibronectin, such as vascular von Willebrand factor (vWF), leads to platelet adhesiveness, aggregation and activation; activated platelet release thromboxane A2 (TXA2), 5-hydroxytryptamine, adenosine diphosphate (ADP) and platelet factor, which promotes platelet aggregation and forms thrombus. On the other hand, the activation of platelets obviously accelerates the formation of thrombin and activates coagulation. Meanwhile, tunica intima vasorum injury and the release of tissue factor activates endogenous and exogenous blood coagulation pathway. In addition, the stent itself is a metal foreign matter; the electric charge of positive ion on the surface of a metal stent is one of the important causes leading to thrombus formation. Moreover, drug eluting stent applies drugs which inhibit cell hyperplasia of vascular endothelial cells, inhibiting platelet aggregation and cellulose sediment, which is a natural barrier against the formation of thrombus. Insufficient coverage of vascular endothelium weakens or eliminates the natural barrier function of endothelium against thrombus formation, and exposes the metal stent to blood coagulation factor, leading to increased platelet adhesiveness and aggregation, and eventually results in the formation of thrombus. To date, dual anti-platelet therapy has been verified as the most likely to induce an adverse cardiovascular complication of PCI therapy.

At present, in China and other countriess research on the duration of anti-platelet therapy after PCI has gradually increased, however the study results are not completely consistent. Meta-analysis is used to analyze several research results, to improve the reliability of conclusions. Thus, we can use meta-analysis to evaluate the effect of dual anti-platelet therapy at different times on the effectiveness and safety after PCI, therefore providing a reference for clinical decisions.

MATERIALS AND METHODS

Materials

The reference selection criteria was based on randomized controlled clinical trials and observational studies (8). The study was divided into two groups according to the duration of receiving dual anti-platelet therapy after PCI therapy: a short-term treatment group (≤6 months) and a long-term treatment group (>6 months). The subjects of study were patients with coronary heart disease who received PCI. The search included comparison of dual anti-platelet including the comparison between the adverse cardiovascular events and bleeding events after PCI.

The short-term group, after the therapy, was treated with drugs of thiophene and pyridine (clopidogrel 75mg/d, or ticlopidine 5-10mg/d) for less than 6 months; the long-term group, after the therapy, was treated with drugs of thiophene and pyridine (clopidogrel 75mg/d, or ticlopidine 5-10mg/d) for more than 6 months. In the meantime, both groups took aspirin 82-325 mg/d until the end of the study.

Determining indicators of long-term efficacy and safety. The main therapeutic indicators were incidence of death or myocardial infarction, whilst the minor therapeutic indicators were the incidence of late stent thrombosis. The security indicators were the incidence of serious bleeding events.

Statistical analysis

The adopted references were meta-analyzed with RevMan5.1 software and STATA 9.0 software, which were provided by the Cochrane Collaboration. Firstly, we determined whether there was heterogeneity between the studies; χ^2 test was used to test the heterogeneity between the research results, the significance was set as $\alpha = 0.10$, that is, 95% CI. When statistical homogenity ($P>0.05$, $I^2<50\%$) existed in the study, the fixed effect model (FEM)

could be applied for analyzing; on the contrary, if the clinical heterogeneity was excluded, random effect model (REM) could be applied. The effect size applied the interval estimation and hypothesis test, related risk rate or odds ratio was used to describe the count data, the measurement data used the weighted mean difference (WMD). When the measurement methods or units had differences, or the mean difference was too large, we chose standard mean difference (SMD), 95% confidence interval (CI) was used to describe the effect size. Interval estimation applied 95% CI, hypothesis testing applied u to test and was represented by Z value and P value, the significance level was set as 0.05 (9). Hypothesis test results are listed in Fig. 1.

As the studies of a same meta-analysis vary from each other, we name the variations as heterogeneity, which can be can be interpreted as the estimated variation of curative effect between experiments; it is the direct result of diversity of clinical and methodology studies. Statistical heterogeneity is based on data, its principle is the bigger the confidence interval, the greater the possibility homogeneity exists between studies, on the contrary the smaller the confidence interval, the greater the possibility for heterogeneity to exist.

Search strategy

The search applied MEDICAL (Mesh) combined with free words. Advanced search in the data base according to Cochrane Reviewer's Handbook on RCT, applied manual searching in the Chinese Journal of Cardiology and also searched grey literature.

Methodological quality assessment

Methodological quality assessment was carried out by evaluating the quality of randomized controlled trials: such as random allocation method, whether allocation concealment is right, whether blind method was applied, whether the report was withdrawn, as well as applied intention-to-treat (ITT) analysis.

RESULTS

Methodological quality of literature search and inclusion research

The database assessed and searched ensured the recall ratio of the literature. By reading the abstracts and the full text, 8 studies were selected (10-17). Of these, 3 were randomized controlled trials [PCI-CURE2001, CREDO2002, Park2010 (10-12)], 4 were observational studies. Due to the limited number of relevant randomized controlled trials, we blended and analyzed the randomized controlled researches and observational studies; however, we may have increased the selection bias possibility.

Meta-analysis results of randomized controlled studies

Incidence rate of death or myocardial infarction

The follow-up of PCI-CURE2001, CREDO2002, Park2010 (10-12) research was 8 months, 12 months and 24 months, respectively. The mortality and incidence rate of myocardial infarction between the long-term group and short-term group which received anti-platelet therapy were compared; and as there was no statistical heterogeneity (I^2=0%, P=0.42) between the studies (Fig. 1), we combined the effect sizes applying fixed effect model. Meta-analysis showed that compared with the short-term group, in the long-term group the mortality and the incidence rate of myocardial infarction after PCI (OR = 0.74, 95% (0.56, 0.98), P < 0.0001) (Fig. 1) were reduced and the difference between these two groups was statistically significant.

Incidence rate of serious bleeding event

PCI-CURE2001, CREDO2002, P rk2010 (10-12) research trials reported the occurrence of serious bleeding events. As shown in Fig. 2, it was found that the heterogeneity test showed no significant heterogeneity between different studies (I^2=0%, P=0.62), therefore we applied the fixed effect model. The combined analysis results showed that the incidence rate of serious bleeding events in the short-term group was lower than in the long-term group, but the difference was not statistically significant (Fig. 2).

Meta-analysis results of observational studies

Incidence rate of death or myocardial infarction

The follow-up time of these four observational studies were as follows: literature (13-15), (17) were 24 months, 9 months, 24 months and 12 months, respectively. They all reported the incidence of death or myocardial infarction after PCI. There was statistical heterogeneity between the different studies (I^2=77%, P=0.004), so the combined effect size of random effect model was applied (Fig. 3). Meta-analysis result [OR=0.7, 95% CI (0.45, 1.08), P=0.11] showed that the incidence rate of death or myocardial infarction in the long-term group was

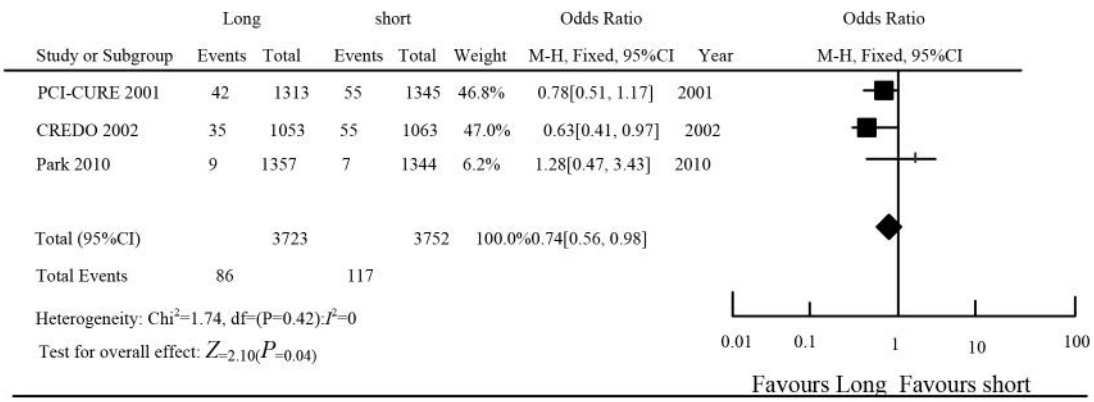

Fig. 1. *Meta-analysis of incidence rate of death or myocardial infarction in the long-term group and short-term group.*

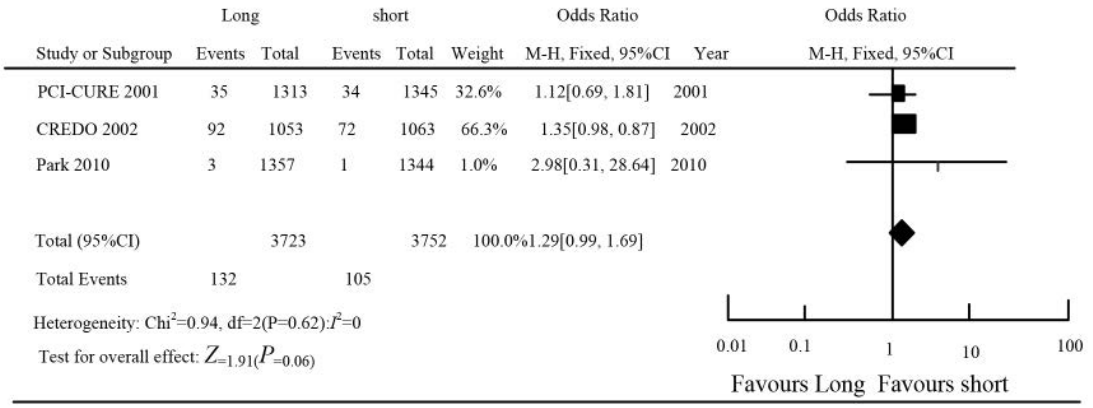

Fig. 2. *Meta-analysis of the incidence rate of serious bleeding event between long-term group and short-term group.*

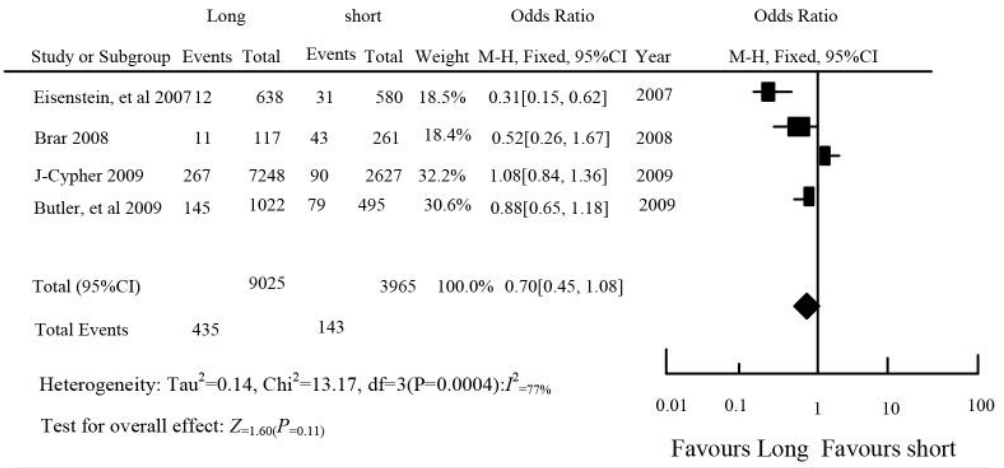

Fig. 3. *Meta-analysis of the incidence rate of death or myocardial infarction in the long-term group and short-term group.*

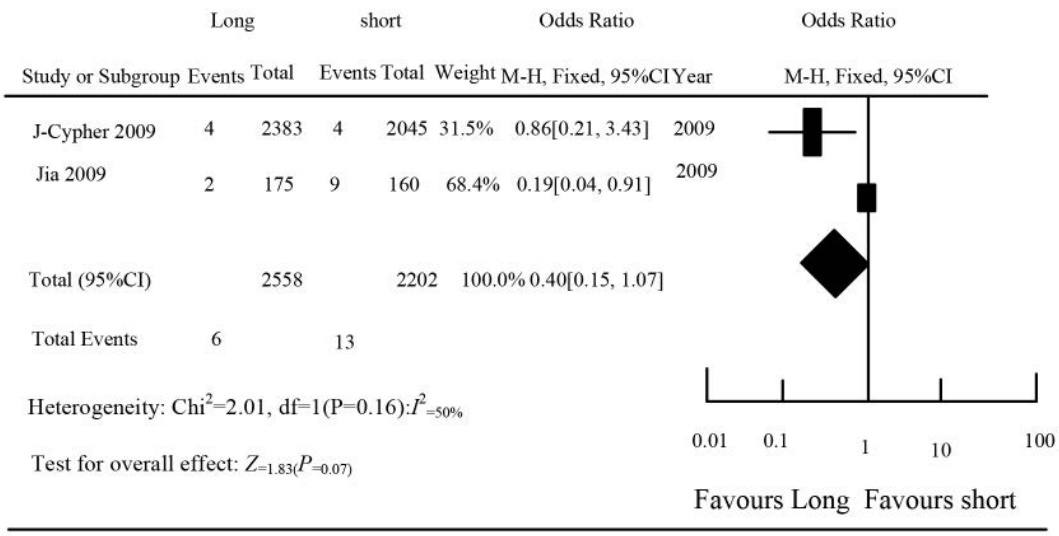

Fig. 4. *Meta-analysis of incidence rate of late stent thrombosis.*

lower than the short-term group, but the difference was not statistically significant.

Incidence rate of late stent thrombosis events

The follow-up periods of the two observational studies by literature (15, 16) were 24 months and 18 months, respectively. The occurrence was reported of late stent thrombosis event, and statistical heterogeneity existed in the different studies (I^2=50%, P=0.16), therefore the fixed effect model was applied (Fig. 4). The meta-analysis results [OR=0.40, 95% CI I (0.15, 1.07), P=0.07] showed that the incidence rate of late stent thrombosis in the long-term group was lower than the in the short-term group, but the differences were not statistically significant.

DISCUSSION

In this paper, 8 studies were selected for meta-analysis. Firstly, we studied 3 randomized controlled studies. The results showed that there was no heterogeneity, and then we performed the analysis applying fixed effect model. The results showed that in the patients in the long-term group who received dual anti-platelet therapy after PCI, the incidence rate of myocardial infarction was reduced (OR=0.74). The 5 observational studies showed that there was heterogeneity (I^2=77%, P=0.004), then we used the random effect model for analysis. The meta-analysis showed that the mortality and incidence rate of myocardial infarction in the long-term group (>6 months) was lower than in the short-term group (OR=0.7), but the difference was not statistically significant. In the randomized controlled trials and observational studies, we found that long-term dual anti-platelet therapy for more than 6 months can reduce the mortality and the incidence rate of myocardial infarction. Two observational studies (J-Cypher and Jia) reported the occurrence of late stent thrombosis events during the follow-up. There was no heterogeneity in these two observational studies, so we used the fixed effect model for analysis. Meta-analysis showed that the incidence rate of late stent thrombosis in the long-term subjects was lower than in the short-term subjects, but the difference was not statistically significant [OR=0.40, 95%CI (0.15, 1.07), P=0.07]. The formation of late stent thrombosis can be reduced by long-term treatment.

System evaluation collects and evaluates all the relevant studies around the world, and then comprehensive analysis and global assessment is performed by combining all the research results. The meta-analysis (a statistical method for quantitative

synthesis) is sometimes necessary to arrive at a comprehensive conclusion (valid, invalid and further studies), and gather scientific evidence. Eight clinical studies involved in the system evaluation evaluated the effect and safety of dual anti-platelet therapy after PCI with different treatment times. At present, drug therapy, PCI and coronary artery bypass graft surgery are the main methods of treating coronary atherosclerotic heart disease. As is well-known, the efficacy of PCI to treat coronary heart disease is definite, and has become the main method of treatment worldwide.

The drawbacks of this meta-analysis and research are: (i) the studies selected were all published in Chinese or English - the lack of literature in other languages might lead to discrepancies; (ii) the samples were small, and observational research was applied which made the assessment inexact; (iii) there is no international unified criterion for grouping, and clinical criteria may bring objective deviation.

In this paper, we used system evaluation and the latest clinical evidence, concluding that long-term (>6 months) dual anti-platelet treatment can reduce the incidence rate of death or myocardial infarction after PCI. Furthermore, long-term therapy can also reduce the tendency of late stent thrombosis. At the same time, long-term treatment did not increase the incidence rate of serious bleeding events. Therefore, the optimal strategies of dual anti-platelet therapy can be decided by the circumstances.

REFERENCES

1. Rezkalla SH, Dharmashankar KC, Abdalrahman IB, et al. No-reflow phenomenon following percutaneous coronary intervention for acute myocardial infarction: incidence, outcome, and effect of pharmacologic therapy. J Intervent Cardiol 2010; 23:429-36.
2. Zhang J, Jiang JG. Effects of intracoronary injections of tirofiban in acute coronary syndrome patients with no reflow phenomenon after percutaneous coronary intervention. Anhui Med J 2012; 33(2):155-7.
3. Zhang XM. Correlation between platelet factors as well as hs-CPR and no reflow in patients with ST-segment elevation myocardial infarction undergoing primary percutaneous coronary intervention. Hebei: Hebei Medical University 2013. http://cdmd.cnki.com.cn/Article/CDMD-10089-1013283437.htm
4. Park SJ, Park WD, Kim YH. Duration of dual antiplatelet therapy after implantation of drug-eluting stents. N Engl J Med 2010; 362:374-82.
5. Ndrepepa G, Tiroch K, Fusaro M, et al. Five-year prognostic value of no-reflow phenomenon after percutaneous coronary intervention in patients with acute myocardial infarction. Is Coll Cardiol 2010; 55:2383-9.
6. Xiong RC. Effect and safety research of dual anti-platelets with Aspirin and clopidogrel after percutaneous coronary intervention in old patients. Guangzhou: Southern Medical University 2010. ttp://cdmd.cnki.com.cn/Article/CDMD-90023-2010239819.htm
7. Ba B. System evaluation of dual anti-platelet therapy treatment time after percutaneous coronary intervention Xinjiang: Xinjiang Medical University 2012. http://cdmd.cnki.com.cn/Article/CDMD-10760-1012489403.htm
8. Friedland S, Eisenberg MJ, Shimony A, et al. Meta-analysis of randomized controlled trials of intracoronary versus intravenous administration of glycoprotein IIb/ IIIa inhibitors during percutaneous coronary intervention for acute coronary syndrome. Am J Cardiol 2011; 108(9):1244-51.
9. Li L. Assessment of benefit-risk of short term intravenous proton pump inhibitors during duplex anti-platelet treatment for acute myocardial infarction. Hunan Hengyang: Nanhua University 2011. http://cdmd.cnki.com.cn/Article/CDMD-10540-1011182907.htm
10. Mehta SR, Yusuf S, Peters RJ, et al. Effects of pretreatment with clopidogrel and aspirin followed by long-term therapy in patients undergoing percutaneous coronary intervention: the PCI-CURE study. Lancet 2001; 358:527-33.
11. Steinhubl SR, Berger PB, Mann JT 3rd. Early and sustained dual oral antiplatelet therapy following percutaneous coronary intervention. JAMA 2002; 288:2411-20.
12. Park SJ, Park WD, Kim YH. Duration of dual antiplatelet therapy after implantation of drug-eluting stents. N Engl J Med 2010; 362:1374-82.
13. Eisenstein EL, Anstrom KJ, Kong DF, et al. Clopidogrel use and long-term clinical outcomes after drug-eluting stent implantation. JAMA 2007; 297(2):159-68.

14. Brar SS, Kim J, Brar SK, Zadegan R, et al. Long-term outcomes by clopidogrel duration and stent type in a diabetic population with de novo coronary artery lesion. J Am Coll Cardiol 2006; 51(23):2220-27.
15. Kimura T, Morimoto T, Nakagawa Y, et al. Antiplatelet therapy and stent thrombosis after sirolimus-eluting stent implantation. Circulation 2009; 119(7):987-95.
16. Butler MJ, Eccleston D, Clark DJ, et al. The effect of intended duration of clopidogrel use on early and late mortality and major adverse cardiac events in patients with drug-eluting stents. Am Heart J 2009; 157(5):899-907.
17. Dean J, Yujie Z, Yingxin Z, et al. prolonged dual antiplatelet therapy improves clinical outcomes in high-risk patients implanted with sirolimus-eluting stents. Clin Cardiol 2009; 32(3):164-8.

LETTER TO THE EDITOR

RELATIONSHIP BETWEEN ADIPOQ GENE POLYMORPHISM AND LIPID LEVELS AND DIABETES

Y. SUN[1], DG. LI[2], Q. LI[3], L. HUANG[4], Z. HE[5], F. ZHANG[1] and CB. WANG[1]

[1]Department of Clinical Laboratory, the PLA General Hospital, Beijing, China; [2]Department of Nephrology, Chinese PLA General Hospital, Beijing, China; [3]Clinical Laboratory Center, Xiyuan Hospital, China Academy of Chinese Medical Sciences, Beijing, China; [4]Department of Clinical Laboratory Medicine, The Fifth People's Hospital of Chengdu, Chengdu, China; [5]Beijing Center for Physical and Chemical Analysis, Beijing, China

Received November 15, 2014 – Accepted February 10, 2015

The first two authors contributed equally to this paper

Metabolic syndrome (MS), a series of physiological and metabolic disorders caused by insulin resistance, combines clinical syndrome of abdominal obesity, diabetes or impaired glucose regulation, dyslipidemia, hypertension and other metabolic diseases. Several studies have found that multiple single nucleotide polymorphism (SNP) exists in adiponectin gene (ADIPOQ) and some unusual mutations might be related to hypoadiponectinemia and MS. This study aims to explore the relationship between ADIPOQ gene polymorphism and lipid levels and diabetes. A total of 1,049 confirmed MS cases were selected for research. From the perspective of potential functional SNPs of ADIPOQ gene, tag SNPs, combined with environmental factors, we studied the relationship between ADIPOQ gene polymorphism and phenotype (serum adiponectin level) and further analyzed the correlation of ADIPOQ gene polymorphism and metabolic syndrome components so as to clear the relationship between ADIPOQ gene polymorphism and lipid levels and diabetes and at the same time provide a scientific basis for preventing primarily MS etiology and screening high-risk groups.

In recent years the rate of global diabetes mellitus (DM) has risen sharply at an alarming rate. Up until 2013 international diabetes statistics indicated that the number of patients from 20 to 79 years of age reached 382 million, of whom type 2 DM patients (T2DM) were the majority. MS is a clinical syndrome which features the combined occurrence of central obesity, diabetes or impaired glucose tolerance, hypertension, dyslipidemia and hyperuricemia on a histopathological basis of insulin resistance, it induces the aggregation of various dangerous factors such as atherosclerosis and eventually leads to the occurrence and development of a variety of cardiovascular and cerebrovascular diseases (1, 2). At present, for the prevention of MS in the public health system the focus mainly lies in conducting

Key words: ADIPOQ gene, adiponectin, metabolic syndrome, blood lipid, blood glucose level

Mailing address: Dr Chengbin Wang,
Department of Clinical Laboratory,
The PLA General Hospital,
No.28, Fuxing Road, Haidian District,
Beijing, 100853, China
Tel.: +86-01 66936881 Fax: +86 01 68241369
e-mail: wcbjfjzyy@163.com

0393-974X (2015)

comprehensive prevention in the community, such as primary and secondary key prevention, thus restraining the current situation of type 2 DM and high incidence of cardio-cerebrovascular disease (3, 4). However, improvement in the standard of living and dietary habits have changed, leading to an increasing incidence of MS, also affecting the younger population. Common measures for prevention are those which adjust weight through a balanced diet, psychological measures and a better life-style. Western medicine mainly adopts active depressurization and controls blood lipid blood sugar in the treatment of MS, while the effect of traditional Chinese medicine is relatively weak with slower effects. The newly discovered adiponectin can improve insulin, anti-inflammatory, and anti-atherosclerosis resistance, which is the potential target for preventing insulin resistance syndrome. Other studies suggest that edmetabolic syndrome has a predictive effect on cardiovascular diseases and diabetes (1, 4, 5). The adiponectin encoding gene, ADIPOQ, is near the 3 q27 susceptibility loci, therefore is likely to be associated with the incidence of MS. We can further speculate that the relationship between the ADIPOQ gene and lipid levels are DM (6). Studies explored the role of the ADIPOQ gene in MS by observing the relevance of SNPs loci gene type and triglyceride, high density protein cholesterol, blood lipid emptiness, blood pressure and waistline level in patients before and after adjustment in order to clear the relationship between ADIPOQ gene polymorphism and lipid levels and diabetes.

MATERIALS AND METHODS

In our case group, we collected 1,049 confirmed MS cases (509 male and 540 female) (permanent residents of Han), ranging from 35 to 75 years of age, from the Endocrinology Department of Community Health and Physical Examination Centers of three areas in the Jiangsu province (Nanjing, Changzhou, Yizheng city) from the South Medical University's three affiliated hospitals (The First Hospital of Nanjing City, The Second Hospital of Changzhou City and The Third Affiliated Hospital) from March 2009 to September 2010. According to the temporary joint statement from a study conducted in 2009 of the International Diabetes Federation, the U.S. National Heart, Lung and Blood Institution, the American Heart Association, the World Heart Federation, the International Society for Atherosclerosis and the International Association For Obesity, the diagnostic criteria for MS was that it should at least meet three of the following five indicators: i) central obesity (male waist ≥90 cm, female waist ≥80 cm or higher); ii) rise of triglyceride levels: ≥150 mg/dL (1.7 mmol/L), or is being treated for lipids; iii) high density lipoprotein cholesterol: male <40 mg/dL (1.0 mmol/L), female <50 mg/dL (1.3 mmol/L), or is being treated for lipids; iv) increased blood pressure: systolic blood pressure≥150 mmHg (1 mmHg = 0.133 kPa) or diastolic blood pressure≥85 mmHg, or prior diagnosis of hypertension and is undergoing treatment; v) fasting glucose ≥100 mg/d or prior diagnosis of diabetes.

In the control group, we collected 1,092 cases (without endocrine metabolic medical history) in the same region at the same time for normal control in the physical examination center in which 491 were male, 601 were female (mean age 55.74±13.10). They matched the age and gender in the case group. The difference of average age and gender in the two groups had no statistical significance and in both groups all came from Han.

When agreeing and signing the informed consent a health status questionnaire was used for carrying out an epidemiological and health comparison investigation. Other details included general demographic characteristics, T2DM and other chronic medical history, family history, smoking and alcohol history and a general physical profile. Height, weight, blood pressure and waistline were measured, blood samples were collected and blood sugar was detected.

Blood specimen collection and genome DNA extraction

Vacuum blood tube was used for extracting 5 ml venous blood in each subject and anticoagulant was added. Specimens of white blood cells (blood clot was taken if part of the specimens were without anticoagulant) were taken and put in -20°C for preservation. Traditional phenol-chloroform extraction was applied in extracting genome DNA. Ultraviolet spectrophotometry (260/280 ratio) method was used for ensuring the purity of DNA, and the concentration of DNA was measured by OD260.

Gene loci SNPs selection

Four SNPs loci associated with MS, rs266729 (C>G), rs1063539 (G>C), rs16861205 (G>C) and rs7649121 (A>T) were selected, and the relevance of genotype of each locus in case group and MS component triglycerides, high density lipoprotein cholesterol, fasting blood glucose, blood pressure and waistline was further analyzed.

Genotyping

The measure of locus of ADIPOQ gene was through the extraction of genome DNA and considering it as the PCR template and performance of genetic typing for

locus of ADIPOQ gene associated Realtime PCR with Taqman-MGB probe. Samples were added according to the following method (5 μL method): 0.5 μl DNA template, 2.5 μl TaqMan® Universal PCR Master Mix, 0.25 μl Forward/Reverse Primers, 0.125 μl Probe 1/Probe 2 and 1.625 μl ddH2O. Reaction condition: 2 m 50°C, 10 m 95°C, 15 s 95°C, 1 m 60°C, 40 cycles. SDS2.0 software (ABI) was used for result observation. Every 384-well plate included 2 positive controls from the same sample.

Statistical analysis

All data was double-typed in by two people with EPIDATA3.0 software and then statistical analysis was used after checking and proofreading. Statistical analysis adopted SPSS. Measurement data was expressed as Mean±SD. Covariance analysis was used for comparing the MetS components level of each genotype on ADIPOQ gene. c^2 test was adopted in the enumeration data and the difference had statistical significance if $P<0.05$.

RESULTS

Correlation of SNPs loci genotype of ADIPOQ gene and triglyceride levels

After analyzing differences of average level of MS component triglycerides of different genotypes of four SNPs loci of ADIPOQ gene in case group and adjusting age, gender, high density lipoprotein cholesterol, fasting blood glucose, blood pressure, waistline, smoking, drinking and physical activity factors, we found that subjects average level of triglyceride (2.62±2.50 mmol/L) carrying hybrid type rs266729 CG was lower than subjects carrying wild type CC(2.96±2.71 mmol/L) and the difference had statistical significance (P=0.039). We had not found statistical significance in the differences of average level of triglycerides of different genotypes among other three SNP loci (P>0.05) (Table I).

Correlation of SNPs loci genotype of ADIPOQ gene and high density lipoprotein cholesterol

After analyzing differences of average level of MS components high density lipoprotein cholesterol of different genotypes of four SNPs loci of ADIPOQ gene in case group and adjusting age, gender, high density lipoprotein cholesterol, fasting blood-glucose, blood pressure, waistline, smoking, drinking, and physical activity factors, we found that the average level of triglyceride (1.20±0.49 mmol/L) of subjects carrying hybrid type rs266729

Table I. *Correlation of SNPs loci genotype of ADIPOQ gene and triglyceride levels.*

Loci	Genotype	Quantity	mean ± SD (mmol/L)	P Value	
				Before Adjustment	After Adjustment **
rs266729		845			
	CC	465	2.96±2.71	N/A	N/A
	CG	309	2.62±2.50	0.070	0.039a
	GG	75	2.42±1.41	0.089	0.122
rs1063539		843			
	GG	411	2.66±2.43	N/A	N/A
	GC	355	2.94±2.81	0.131	0.143
	CC	77	2.95±2.09	0.362	0.310
rs16861205		838			
	GG	571	2.80±2.71	N/A	N/A
	GA	247	2.83±2.33	0.877	0.841
	AA	20	2.74±1.70	0.907	0.941
rs7649121		845	2.61		
	AA	515	2.88±4.00	N/A	N/A
	AT	278	2.71±2.63	0.383	0.314

**: *Adjustment factors are age, gender, high density lipoprotein cholesterol, blood glucose, blood pressure, waistline, smoking, drinking, and physical activity; a: Covariance analysis of comparison on wild genotype CC.*

Table II. *Correlation of SNPs loci genotype of ADIPOQ gene and high density lipoprotein cholesterol.*

Loci	Genotype	Quantity	mean ± SD (mmol/L)	P Value	
				Before Adjustment	After Adjustment **
Rs266729		845			
	CC	465	2.96±2.71	N/A	N/A
	CG	309	2.62±2.50	0.070	0.039a
	GG	75	2.42±1.41	0.089	0.122
rs1063539		843			
	GG	411	2.66±2.43	N/A	N/A
	GC	355	2.94±2.81	0.131	0.143
	CC	77	2.95±2.09	0.362	0.310
rs16861205		838			
	GG	571	2.80±2.71	N/A	N/A
	GA	247	2.83±2.33	0.877	0.841
	AA	20	2.74±1.70	0.907	0.941
rs7649121		845	2.61		
	AA	515	2.88±4.00	N/A	N/A
	AT	278	2.71±2.63	0.383	0.314
	TT	52	2025±1.03	0.091	0.124

***: Adjustment factors are age, gender, high-density lipoprotein cholesterol, blood glucose, blood pressure, waistline, smoking, drinking, and physical activity; a: Covariance analysis of comparison on wild genotype CC.*

Table III. *Correlation of SNPs loci genotype of ADIPOQ gene and fasting blood glucose.*

Loci	Genotype	Quantity	mean ± SD (mmol/L)	P Value	
				Before Adjustment	After Adjustment **
rs266729		985			
	CC	551	8.99±3.87	N/A	N/A
	CG	350	8.88±4.13	0.670	0.723
	GG	74	8.11±4.62	0.081	0.201
rs1063539		989			
	GG	472	9.05±4.14	N/A	N/A
	GC	426	9.04±4.06	0.973	0.864
	CC	91	9.00±3.75	0.929	0.768
rs16861205		983			
	GG	675	9.04±4.04	N/A	N/A
	GA	285	9.15±4.21	0.688	0.528
	AA	23	8.28±3.22	0.028	0.019a
rs7649121		990			
	AA	615	9.12±4.00	N/A	N/A
	AT	309	8.85±4.10	0.338	0.383
	TT	66	9.80±4.59	0.195	0.222

***Adjustment factors are age, gender, high-density lipoprotein cholesterol, blood glucose, blood pressure, waistline, smoking, drinking, and physical activity; a) Covariance analysis of comparison on wild genotype CC.*

Table IV. *Correlation of SNPs loci genotype of ADIPOQ gene and blood pressure.*

Loci	Genotype	Quantity	Systolic Pressure			Diastolic Blood Pressure		
			mean ± SD (mmHg)	P Value Before Adjustment	P Value After Adjustment **	mean ± SD (mmHg)	P Value Before Adjustment	P Value After Adjustment **
rs266729		979						
	CC	548	137.11±19.60	N/A	N/A	84.98±11.85	N/A	N/A
	CG	348	138.56±20.00	0.281	0.489	84.93±10.98	0.946	0.887
	GG	83	135.52±17.83	0.491	0.529	84.93±11.60	0.968	0.990
rs1063539		984						
	GG	469	137.82±19.00	N/A	N/A	85.03±11.36	N/A	N/A
	GC	426	136.47±19.50	0.302	0.163	84.49±11.19	0.482	0.165
	CC	89	141.17±22.66	0.139	0.048a	88.02±13.60	0.025	0.013a
rs16861205		976						
	GG	670	138.08±20.26	N/A	N/A	85.19±11.82	N/A	N/A
	GA	284	137.42±18.29	0.635	0.712	85.24±10.91	0.958	0.799
	AA	22	128.68±15.51	0.027	0.028b	81.91±13.02	0.091	0.029b
rs7649121		984						
	AA	609	137.03±19.61	N/A	N/A	85.11±11.51	N/A	N/A
	AT	311	138.25±18.12	0.372	0.656	84.49±11.11	0.441	0.397
	TT	64	138.53±21.92	0.560	0.481	86.70±13.68	0.294	0.255

Adjustment factors are age, gender, high-density lipoprotein cholesterol, blood glucose, blood pressure, waistline, smoking, drinking, and physical activity; a) Covariance analysis of comparison on wild genotype GG; b) Covariance analysis of comparison on wild genotype GG.

Table V. *Correlation of SNPs loci genotype of ADIPOQ gene and waistline.*

Loci	Genotype	Male				Female			
		Quantity	mean ± SD	P Value Before Adjustment	P Value After Adjustment **	Quantity	mean ± SD	P Value Before Adjustment	P Value After Adjustment **
rs266729		478				490			
	CC	264	91.80±8.11	N/A	N/A	282	86.60±8.58	N/A	N/A
	CG	168	91.51±8.89	0.734	0.658	174	88.05±9.55	0.093	0.053
	GG	46	91.44±9.46	0.792	0.895	34	85.25±8.44	0.405	0.450
rs1063539		475				497			
	GG	227	92.70±8.50	N/A	N/A	233	87.20±9.54	N/A	N/A
	GC	202	90.94±9.02	0.065	0.051	222	86.59±8.18	0.461	0.500
	CC	46	89.53±6.45	0.052	0.068	42	88.32±9.23	0.455	0.417
rs16861205		471				493			
	GG	324	91.22±8.20	N/A	N/A	335	87.23±8.74	N/A	N/A
	GA	133	92.49±9.79	0.152	0.138	149	86.67±9.53	0.526	0.320
	AA	14	93.44±4.95	0.346	0.383	9	85.89±4.65	0.057	0.026a
rs7649121		475				498			
	AA	293	91.38±8.17	N/A	N/A	313	86.90±8.41	N/A	N/A
	AT	147	92.38±9.11	0.256	0.315	157	87.03±8.41	0.885	0.649
	TT	35	90.79±10.09	0.701	0.706	28	87.14±8.44	0.890	0.639

***Adjustment factors are age, gender, high-density lipoprotein cholesterol, blood glucose, blood pressure, waistline, smoking, drinking, and physical activity; a) Covariance analysis of comparison on wild genotype GG.*

CG was higher than subjects carrying wild type CC (1.13±0.37 mmol/L), and the difference had statistical significance (P=0.010). We had not found statistical significance in the differences of average level of high density lipoprotein cholesterol of different genotypes among other three SNP loci

(P>0.05) (Table II).

Correlation of SNPs loci genotype of ADIPOQ gene and fasting blood glucose level

After analyzing differences of average level of MS components fasting blood glucose of different genotypes of four SNPs loci of ADIPOQ gene in case group and adjusting age, gender, high density lipoprotein cholesterol, fasting blood-glucose, blood pressure, waistline, smoking, drinking, and physical activity factors, we found that the average level of fasting blood glucose (8.28±3.22 mmol/L) of subjects carrying hybrid type rs16861205 AA was lower than subjects carrying wild type GG (9.04±4.04 mmol/L) and the difference had statistical significance (P=0.019). We had not found statistical significance in the differences of average level of triglycerides of different genotypes among other three SNP loci (P>0.05) (Table III).

Correlation of SNPs loci genotype of ADIPOQ gene and blood pressure

After analyzing differences of average level of MS components blood pressure of different genotypes of four SNPs loci of ADIPOQ gene in case group and adjusting age, gender, high density lipoprotein cholesterol, fasting blood-glucose, blood pressure, waistline, smoking, drinking, and physical activity factors, we found that systolic pressure (141.17±22.66 mmHg) and diastolic blood pressure level (88.02±13.60 mmHg) of subjects carrying mutant typers1063539 CC was respectively higher than systolic pressure (137.82±19.00 mmHg) and diastolic blood pressure level (85.03±11.36 mmHg) of subjects carrying wild type GG; systolic pressure (128.68±15.51 mmHg) and diastolic blood pressure level (81.91±13.02 mmHg) of people carrying mutant typers16861205 AA was respectively higher than systolic pressure (138.08±20.26 mmHg) and diastolic blood pressure level (85.19±11.82 mmHg) of subjects carrying wild type GG and the difference had statistical significance (P=0.048, 0.013, 0.028, 0.029). We had not found statistical significance in the differences of average level of blood pressure of different genotypes among other two SNP loci (P>0.05) (Table IV).

Correlation of SNPs ADIPOQ gene loci genotype and waistline

After analyzing correlations of MS components waistline of different genotypes of four SNPs loci of ADIPOQ gene in case group and adjusting age, gender, high density lipoprotein cholesterol, fasting blood-glucose, blood pressure, waistline, smoking, drinking, and physical activity factors, we found that waistline of females carrying mutant type rs16810205 AA (85.89±4.65 cm) was lower than females carrying wild type GG (87.23±8.74 cm) and the difference had statistical significance (P=0.026). We had not found statistical significance in the differences of average level of triglyceride of different genotypes among other three SNP loci (P>0.05) (Table V).

DISCUSSION

At present pathogenesis of MS has not been fully illustrated. The American Heart Association, the American Heart, Lung and Blood Institution and The American Diabetes Association summarize the pathogeny into three aspects in its published clinical consensus: i) obesity and adipose tissue dysfunction; ii) insulin resistance; iii) high blood pressure, hypercoagulable state, aging of lipoprotein metabolism and dysfunction caused by a series of independent factors (such as hepatic cell, vascular endothelial cells, some molecules derived from immune cells) (7). Adipose tissue provides storage and energy, at the same time has endocrine function. Studies have shown that adiponectin can be considered as an important regulator and biomarker of the MS (6). In addition, high serum adiponectin level can regulate resistance of fat inflammation, insulin resistance and MS, especially in obese subjects. Serum adiponectin is influenced by environmental factors and regulated by ADIPOQ gene.

Mononuclear polymorphism of ADIPOQ gene is closely related to MS., From the perspective of four SNPs loci of ADIPOQ gene that are statistically associated with MS, this study analyzes the relationship between each SNPs loci and MS components in MS patients. Blood lipid refers to the general term of neutral fat (triglycerides and cholesterol) and lipoid (phospholipids, glycolipids, sterols and steroids) in plasma. In the case group, the average level of triglyceride in subjects carrying hybrid type rs26672 CG is lower than subjects carrying the wild type

CC after adjusting age, gender, smoking, drinking, and physical activity factors. But the average level of high density lipoprotein cholesterol in subjects is higher than people carrying wild type rs266729 CC and the difference had statistical significance. This suggests that rs266729 G-allele can reduce the blood lipid level in MS patients, and may reduce the risk of occurrence of MS. Ferguson et al. (8) found rs266729 G-allele could reduce the risk of dyslipidemia, which is in accordance with the results of the study. Marso et al. (9) once confirmed that the concentration of serum adiponectin was not only negatively correlated with triglyceride, total cholesterol levels and apolipoprotein B and E, but also positively correlated with serum high density lipoprotein cholesterol and apolipoprotein A-1. Furthermore, after comparing the average level of fasting blood pressure in the case group, the results show that the level of fasting plasma glucose of people carrying mutation type rs16861205 AA genotype is lower than people carrying wild type GG. This hints that rs16861205 A-allele can reduce the blood glucose level in MS patients, which is consistent with IR results that RS266729 C-allele can increase the risk of occurrence of T2DM discovered by Wang, Xizhen and Schwarz, et al (10, 11). This study also finds that rs1063539 C-allele can increase high blood pressure level in MS patients and the variation of ADIPOQ gene may be a genetic basis of obesity and related diseases (6, 12).

The study confirms that the main effects of ADIPOQ gene polymorphic loci in different sites are different in MS metabolic disorder. Rs266729 G-allele can reduce the blood lipid level in MS patients, and rs16861205 A-allele can reduce the blood glucose level in MS patients. In addition, rs1063539 C-allele can increase high blood pressure level in MS patients and the variation of ADIPOQ gene may be a genetic basis of obesity and related diseases.

REFERENCES

1. Li GR, Li LL, Wang JH. The research progress for type 2 diabetes drugs treatment. China Pharmacy 2008; 19(5):383.
2. Yao DS, Liu P, Hu YY, Sun MY. Research progress of Chinese medicine treatment of metabolic syndrome. Chinese archives of traditional Chinese medicine 2013; 31(5):1113-5.
3. Li JG. The research progress of metabolic syndrome. Chinese J of Nat Med, 2010; 12(1):74-6.
4. Duan J, He JB. The research progress of metabolic syndrome. chronic epidemiology magazine 2014; 15(1):58-62.
5. Zhang HY, Sun YN. Investigation progression on the relationship between adiponectin and insulin resistance. J of Jiaoning University of traditional Chinese medicine 2011; 13(12):218-20.
6. Du J. Epidemiological studies on ADIPOQ gene ecological and metabolic syndrome and its molecular components. Jiangsu, Nanjing Medical University 2012. http://cdmd.cnki.com.cn/Article/CDMD-10312-1012485709.htm.
7. Zhang JF. The pathogenesis and prevention strategies of metabolic syndrome. China healthcare innovation 2010; 5(5):10-11.
8. Ferguson JF, Phillips CM, Tierney AC, et al. Gene-nutrient interactions in the metabolic syndrome: single nucleotide polymorphisms in ADIPOQ and adipor1 interact with plasma saturated fatty acids to modulate insulin resistance. Am J Clin Nutr 2010; 91(3):794-801.
9. Marso SP, Mehta SK, Frutkin A, House JA, McCrary JR, Kulkarni KR. Low adiponectin levels are associated with atherogenic dyslipidemia and lipid-rich plaque in non-diabetic coronary arteries. Diabetes care 2008; 31(5):989-94.
10. Wang XZ, Zhang SZ, Chen YZ, et al. APM1 gene variants S11377C/G are associated respectively with obesity and with non-obesity in Chinese type 2 diabetes. Diabetes Res Clin Pract 2009; 84(3):205-10.
11. Schwarz PE, Govindarajalu S, Towers W, Schwanebeck U, Flscher S, Vasseur F, Bornsteln SR, Schulze J. haplotypes in the promoter region of the ADIPOQ gene are associated with increased diabetes risk in a German Caucasian population. Horm Metab Res 2006; 38(7):447-51.
12. Wang SJ, Jia WP, Bao YQ. Association of adiponectin gene polymorphism with obesity and adiponectin. J Clin Rehabilitative Tissue Eng Res 2008; 12(7):1295-9.

JOURNAL OF BIOLOGICAL REGULATORS & HOMEOSTATIC AGENTS Vol. 29, no. 1, 229-233 (2015)

LETTER TO THE EDITOR

CYTOGENETIC GENOTOXIC INVESTIGATION IN PERIPHERAL BLOOD LYMPHOCYTES OF SUBJECTS WITH DENTAL COMPOSITE RESTORATIVE FILLING MATERIALS

F. PETTINI[1], M. SAVINO[2], M. CORSALINI[1], S. CANTORE[2] and A. BALLINI[2]

[1]Department of Interdisciplinary Medicine, University of Bari "Aldo Moro" Bari, Italy;
[2]School of Medicine, University of Bari "Aldo Moro", Bari, Italy

Received November 3, 2014 – Accepted January 8, 2015

Dental composite resins are biomaterials commonly used to aesthetically restore the structure and function of teeth impaired by caries, erosion, or fracture. Residual monomers released from resin restorations as a result of incomplete polymerization processes interact with living oral tissues. The objective of this study was to evaluate the genotoxicity of a common dental composite material (Enamel Plus-HFO), in subjects with average 13 filled teeth with the same material, compared to a control group (subjects having neither amalgam nor composite resin fillings). Genotoxicity assessment of composite materials was carried out in vitro in human peripheral blood leukocytes using sister-chromatid exchange (SCE) and chromosomal aberrations (CA) cytogenetic tests. The results of correlation and multiple regression analyses confirmed the absence of a relationship between SCE/cell, high frequency of SCE (HFC) or CA frequencies and exposure to dental composite materials. These results indicate that composite resins used for dental restorations differ extensively *in vivo* in their cytotoxic and genotoxic potential and in their ability to affect chromosomal integrity, cell-cycle progression, DNA replication and repair.

Dental caries continues as the most prevalent malady in Dentistry despite remarkable advances in prevention over the past few decades. The long-lasting, ongoing controversy on the hazards for patients due to mercury exposure from amalgam has also increased the public interest in possible adverse effects caused by other dental restorative materials, like composite resins and resinous pit and fissure sealants (1).

During the last two decades, the use of resin composites for aesthetic restorative procedures has increased owing to improvements in adhesive systems and resin composite materials. Owing to advancement in filler technologies, the fillers in resin composites changed from macro or micro particles to hybrid or micro-hybrid particles (2) but no long-term clinical studies are available up today (3-5).

Monomers like triethylene glycol dimethacrylate (TEGDMA) or 2-hydroxylethyl methacrylate (HEMA) are cytotoxic via apoptosis, induce genotoxic effects, and delay the cell cycle (6). Monomers also influence the response of cells of the innate immune system, inhibit specific odontoblast cell functions, or delay the odontogenic differentiation and mineralization processes in pulp-derived cells including stem cells (7). The liberation of TEGDMA from resin restorations, therefore, should be minimized or prevented. Furthermore, it

Key words: sister-chromatid exchange, chromosomal aberrations, dental composite materials, cytotoxicity, genotoxicity

Mailing address: Dr Stefania Cantore,
School of Medicine,
University of Bari "Aldo Moro",
P.zza Giulio Cesare, 11,
70124, Bari, Italy
Tel./Fax: +39 0803430657
e-mail: stefaniacantore@pec.omceo.bari.it

0393-974X (2015)

DISCLOSURE: ALL AUTHORS REPORT NO CONFLICTS OF INTEREST RELEVANT TO THIS ARTICLE.

must be emphasized that there is no cell line which is consistently more sensitive compared with others (8). On the other hand, little is known however with respect to pharmacokinetics and toxicokinetics of degradation products of resin components. Some components of dental resin could have genotoxic effects on genomic DNA as potential target for chemical substances (1, 7).

As reported in Nature in 1975 (9), "The (SCE) test gives a very sensitive and rapid method for testing potential mutagenicity of chemical agents and provides a powerful method for detecting environmental mutagens" chromosome aberrations (CA) could be evaluated in conventional metaphase samples and in combination with the evaluation of SCE could provide a "first step" insight in the cytogenetic damage induced by various agents at very low concentrations (10).

Moreover, the determination of proliferation rates and mitotic indices in lymphocyte cultures has been proved to be a very useful and sensitive indicators as demonstrated by Barale and Norppa (11, 12). Namely, recent investigation demonstrated that elutes derived from three direct composite resins (Tetric Ceram / Ivoclar-Vivadent, Simile/Pentron, Filtek Z-250/3M ESPE) increased of sister-chromatid exchange and chromosomal aberrations frequencies (13).

The aim of this study was to evaluate *in vivo* the possible genotoxicity of a common dental composite material in a group of subjects with several teeth filled with the same substance respect to a control group.

MATERIALS AND METHODS

Patients, materials and cell culture

The participants in this study were divided into two groups.

Group I (Exposed): each independent experiment was carried out using blood of 20 different healthy donors (12 males and 8 females, Caucasians, aged 18-29 years (mean age 23.5 yrs), not on any medication) with a total of between 10 and 16 (average 13) teeth filled with the same dental composite materials (Enamel Plus-HFO Micerium S.p.A., Avegno, Italy) and with the absence of amalgam restorations.

Group II (Controls): twenty subjects (10 males and 10 females, Caucasians, aged 18-23 years (mean age 20.5 yrs) without exposure to dental composite materials (having neither amalgam nor composite resin fillings), were recruited from the students of the University of Bari "Aldo Moro" Dental School as controls. The subjects were, non-smokers, not alcohol consumers and not on any medication.

In this study group, 9 smokers were also enrolled, with a duration of the smoking habit from 1 to 9 years, and with a number of cigarettes per day from 5 to 10.

Written informed consent to participate in the research was obtained from all subjects, who were enrolled at the Dental Clinic, Operative Unit of Restorative Dentistry, during the daily practice routine.

Blood samples were collected, transported at room temperature and cultured for cytogenetic tests within 1 h from collection. The brands, types, manufacturer, and chemical compositions of the materials used in this study are listed in Table I. We performed at least two replicate cultures for each sample.

Cytogentic tests

The time of culture was 48 h for CA and 72 h, maintained in the dark with the addition of 5µg/ml 5-bromodeoxyuridine (BrdUrd) for SCE. The CA and SCE analyses were carried out using standard procedures (14) as previously described (15, 16). For CA analysis, in accordance with the International System for Human Cytogenetic Nomenclature (ISCN), at least 100 metaphases were counted and scored for each donor (ISCN 1978) (10); for SCE analysis, at least 25 metaphases of the second mitotic division were analyzed for each subject, and metaphases of the first (M1), second (M2) and third (M3) mitotic divisions were counted to calculate the proliferation rate index (PRI), according to the formula:

Table I. *Composite resin-based materials investigated in this study.*

Material (manufacturer)	Type of Material	Main Components	Curing method
Enamel Plus-HFO (Micerium S.p.A., Avegno, Italy)	micro-hybrid	bis-GMA, TEGDMA, UDMA resin 5.2% butandioldimethacrylate, 66.3 vol% strontium, aluminium, glass (silanized) 7.6 wt% siliciumoxide, 0.3 wt% pigments.	40 s Photo-polymerization, 650mW/cm^2 (bluepahse)

Table II. *SCE, HFC, CA and PRI in materials investigated in this study.*

		SCE/cell	HFC (%)	CA (%)	PRI
Controls (N=20)	Mean (SD) Median Min–max	5.6 (0.8) 5.5 4.4–7.6	6.4 (6.4) 4.0 0–20	1.9 (1.8) 2.0 0–8	2.7 (0.1) 2.7 2.5–2.9
Exposed (N=20)	Mean (SD) Median Min–max	5.9 (1.3) 5.6 4.1–8.6	6.7 (7.7) 4.0 0–20	1.7 (1.8) 1.7 0–8	2.7 (0.1) 2.7 2.6–2.9
Non-smokers (N=31)	Mean (SD) Median Min–max	5.5* (0.8) 5.3 4.1–7.5	5.2 (5.6) 4.0 0–20	1.9 (1.9) 2.0 0–8	2.7 (0.1) 2.7 2.5–2.9
Smokers (N=9)	Mean (SD) Median Min–max	6.6* (1.2) 6.3 4.5–8.6	9.9 (9.0) 8.0 0–20	1.4 (1.6) 1.0 0–5	2.7 (0.1) 2.7 2.5–2.8

**=SCE/cell: smokers vs non-smokers: t=3.66; p=0.001*

PRI=M1+2M2+3M3/100 (17). The threshold value to define high frequency of SCE (HFC) was calculated according to the procedure reported in Carrano and Moore (1982); cells with a minimum of 11 SCE (corresponding to the 95th percentile of the overall distribution) were considered as HFC (18).

Statistical analysis

The statistical analysis was performed using the Statistical Package for Social Sciences (SPSS, Version 12.0, Chicago, IL, USA). To compare groups, parametric procedures (Student's *t*-test) were used for normally distributed variables, in some cases after logarithmic transformation, while non-parametric procedures (Mann-Whitney U-test) were used for non-normally distributed variables. Correlations between variables were determined by the Spearman's test. Multiple regression models were used to analyze the relationship between different variables. A $p<0.05$ was considered significant.

RESULTS

No significant correlation between exposed subject and CA, SCE/cell, HFC frequencies or PRI (r=0.03, p=0.6; r=0.1, p=0.6; r=0.2, p=0.1; r=0.1, p=0.3; respectively) or between the number of cigarettes/day and CA or PRI (r=-0.1, p=0.3; r=0.01, p=0.8; respectively) was demonstrated. When subjects were classified as smokers *vs* nonsmokers (Table II), we observed no differences as regards CA frequency and PRI, while the mean frequency of SCE/cell was higher in smokers than in non-smokers (p=0.001), as reported in Table II. HFC frequency in the dental composite subject group (exposed) was higher in smokers than in non-smokers, but these differences did not reach statistical significance (p=0.1 for HFC and p=0.3 for exposed subjects).

However, a significant positive correlation was found between the number of cigarettes/day and both SCE/cell frequency (r=0.3, p=0.003) and HFC frequency (r=0.2, p=0.03). Further analyses were performed by multiple regression: two models were applied, considering both SCE/cell and HFC frequencies as dependent variables and age, exposition (yes/no), number of cigarettes/day, as independent variables. In both models, a significant relationship was observed between the number of cigarettes smoked per day and both SCE/cell (F=2.96; p=0.013) and HFC (F=11.73; p=0.001) frequencies.

DISCUSSION

To our knowledge the present study is the first with *in vivo* cytogenetic data derived from an hypothesis of exposure to dental restorations materials in subjects with a significant number of filled teeth. Biocompatibility of dental materials is an important consideration for the patient, clinician, laboratory technician, and manufacturer. Dental composite

resin materials degrade under the influence of saliva and other elements of the oral environment, and release harmful agents, thee general and local health risks of which are still under consideration (1, 6, 13). The general public has a substantial interest in the safety of dental restoration materials as indicated by the recent request of the European Commission to the Scientific Committee on Emerging and Newly Identified Health Risks (SCENIHR) to update, if appropriate, the opinion on this subject adopted in 2008 (19, 20). Ideally, a dental material that is to be used in the oral cavity should be harmless to all oral tissues, gingiva, mucosa, pulp, and bone. Furthermore, it should contain no toxic, leachable, or diffusible substances that can be absorbed into the circulatory system, causing systemic responses, including teratogenic or carcinogenic effects. The materials should also be free of agents that could elicit sensitization or an allergic response in a sensitized patient.

The results of correlation and multiple regression analyses confirmed the absence of a relationship between SCE/cell, HFC or CA frequencies and exposure to dental materials (average 13 teeth filled with the same dental composite). Our results also show the clear influence of cigarette smoking on some genotoxic endpoints, with a significant relationship between the number of cigarettes/day and both SCE/cell frequency ($p=0.003$) and HFC ($p=0.03$), in line with literature data (12). Moreover, many factors affect the toxicity of the components leached from the resin; in general, the monomers are more cytotoxic after 24 hours of aging and become less toxic with aging (21).

The results obtained in a recent *in vitro* investigation (mild to no toxic effects to the odontoblast-like MDPC-23 cells after light activation in contrast to intense cytotoxic effects when the resin-based material was not light-cured) suggested that any factor that limits or undermines the polymerization of resin materials such as low light intensity, short light-curing time, longer distance between material surface and light source, may contribute to increase significantly their cytotoxic effects to the pulp cells (22). Therefore, it is mandatory that the manufacturers' instructions of use are strictly followed regarding the adequate photoactivation of resin materials, which is inversely related to cytotoxicity (23). Furthermore, in a recent study, the Authors noted that expiry dates have a significant effect on the cytotoxicity of the composite materials and they concluded that expired composites presented lower cell viability than the non-expired composites over the three-day time period; the difference in survival rates between the expired and non-expired groups was statistically significant (24).

According to the evidence-based dentistry (25), taking into account that dental composite resins have an integral role in every day dental clinical practice, it is extremely important to encourage not only the development of less cytotoxic materials but also, as a future goal, the development of "biomimetic" materials or "biofillings", which will be effective in stimulating natural tissue repair and maintaining the vitality of the compromised oral tissues.

The combined efforts being made in the field on cellular toxicology of resin monomers and related future findings derived from cell biology will improve our understanding of possible systemic disorders as well as the identification of potential chronic local adverse effects caused by dental materials.

Further research is needed to investigate biochemical stability of composite resins in the oral cavity which will lead to a more concise definition of biocompatibility related to dental resin composites and risk assessment.

REFERENCES

1. Gupta SK, Saxena P, Pant VA, Pant AB. Release and toxicity of dental resin composite. Toxicol Int 2012; 19:225-34.
2. Ferracane JL. Resin composite—state of the art. Dent Mater 2011; 27:29-38.
3. Welbury RR. A clinical study of a microfilled composite resin for labial veneers. Int J Paediatr Dent 1991; 1:9-15
4. Meijering AC, Creugers NHJ, Roeters FJM, Mulder J. Survival of three types of veneer restorations in a clinical trial: a 2.5-year interim evaluation. J Dent 1998; 26:563-8.
5. Dietschi D, Ardu S, Krejci I. A new shading concept based on natural tooth color applied to direct composite restorations. Quintessence Int 2006; 37:91-102.

6. Krifka S, Spagnuolo G, Schmalz G, Schweikl H. A review of adaptive mechanisms in cell responses towards oxidative stress caused by dental resin monomers. Biomaterials 2013; 34:4555-63.
7. Paschalidis T, Bakopoulou A, Papa P, Leyhausen G, Geurtsen W, Koidis P. Dental pulp stem cells' secretome enhances pulp repair processes and compensates TEGDMA-induced cytotoxicity. Dent Mater. 2014 doi: 10.1016/j.dental.2014.08.377. Epub 2014 Sep 18.
8. Geurtsen W. Substances released from dental resin composites and glass ionomer cements. Eur J Oral Sci 1998; 106:687-95.
9. Perry P, Evans HJ. Cytological detection of mutagen-carcinogen exposure by sister chromatid exchange. Nature 1975; 258:121-5.
10. An international system for human cytogenetic nomenclature, (1978), ISCN (1978). Report of the Standing Committee on Human Cytogenetic Nomenclature. Birth Defects Orig Artic 1978; 14:313-404.
11. Norppa H, Bonassi S, Hansteen IL, et al. Chromosomal aberrations and SCEs as biomarkers of cancer risk. Mutat Res 2006; 600:37-45.
12. Barale R, Chelotti L, Davini T, et al. Sister chromatid exchange and micronucleus frequency in human lymphocytes of 1,650 subjects in an Italian population: II. Contribution of sex, age, and lifestyle. Environ Mol Mutagen 1998; 31:228–242
13. Bakopoulou A, Mourelatos D, Tsiftsoglou AS, Mioglou E, Garefis P Sister-chromatid exchange, chromosomal aberrations and delays in cell-cycle kinetics in human lymphocytes induced by dental composite resin eluates. Mutat Res 2008; 649:79-90.
14. Carrano AV, Natarajan AT. International Commission for Protection Against Environmental Mutagens and Carcinogens. ICPEMC publication no. 14. Considerations for population monitoring using cytogenetic techniques. Mutat Res 1988; 204:379–406.
15. Fracasso M, Doria D, Bartolucci GB, et al. Low air levels of benzene: correlation between biomarkers of exposure and genotoxic effects. Toxicol Lett 2010; 192:22-8.
16. Bukvic N, Lovreglio P, Fanelli M, et al. Influence of some detoxification enzyme polymorphisms on cytogenetic biomarkers between individuals exposed to very low doses of 1,3-butadiene. J Occup Environ Med 2009; 51:811-21.
17. Albertini RJ, Anderson D, Douglas GR, et al. IPCS guidelines for the monitoring of genotoxic effects of carcinogens in humans. International Programme on Chemical Safety. Mutat Res 2000;463:111-72.
18. Carrano AV, Moore DH. The rational methodology for quantifying sister-chromatid exchange in humans. In: Hendle JA (ed) New horizons in genetic toxicology. Academic Press, New York, 1982 pp 267–304.
19. http://ec.europa.eu/health/scientific_committees/emerging/docs/scenihr_q_034.pdf
20. Rothfuß A, Vonk R, Schweinfurth H. The evidence of genotoxic damage in the oral mucosa due to dental fillings is very questionable. Arch Toxicol 2013; 87:1155-6
21. Bouillaguet S, Shaw L, Gonzalez L, Kerjci I. Long term cytotoxicity of resin-based dental restorative materials. J Oral Rehab 2002; 29:7-13
22. Wisniewska-Jarosinska M, Poplawski T, Chojnacki CJ, Pawlowska E, Krupa R, Szczepanska J, Blasiak J. Independent and combined cytotoxicity and genotoxicity of triethylene glycol dimethacrylate and urethane dimethacrylate. Mol Biol Rep 2011; 38:4603-11.
23. Sigusch BW, Pflaum T, Völpel A, Gretsch K, Hoy S, Watts DC, et al. Resin-composite cytotoxicity varies with shade and irradiance. Dent Mater 2012; 28:312-9.
24. Bal BT, Sönmez N, Bavbek B, Akçaboy C. Cytotoxicity of composite resins before and after expiration date. Preliminary report. N Y State Dent J 2011; 77:31-5.
25. Ballini A, Capodiferro S, Toia M, Cantore S, Favia G, De Frenza G, Grassi FR. Evidence-based dentistry: what's new? Int J Med Sci. 2007; 4:174-8.

JOURNAL OF BIOLOGICAL REGULATORS & HOMEOSTATIC AGENTS Vol. 29, no. 1, 235-238 (2015)

LETTER TO THE EDITOR

ATRIAL NATRIURETIC PEPTIDE EXPRESSION IN HUMAN ARTICULAR CARTILAGE

L. LIPARI, A. GERBINO, A. LIPARI, R. BARONE and E. FARINA

Department of Experimental Biomedicine and Clinical Neurosciences (BioNeC), University of Palermo, Italy

Received November 5, 2014 – Accepted January 9, 2015

This immunohistochemical study aims to investigate the Atrial natriuretic peptide (ANP)-presence and localization in human articular cartilage. Fragments of articular cartilage covering the femoral head were removed from patients submitted to surgical operation after femoral neck fracture without joint disease. The samples were immunostained with anti-ANP antibody. The results demonstrate that ANP is present in chondrocytes in all the three zones of the articular cartilage. Superficial chondrocytes show strong ANP-immunopositivty. The presence of ANP in the articular cartilage suggests that ANP may play a role in cartilage metabolism by regulating transport of molecules through the different zones of the articular cartilage and in maintenance of its homeostasis; probably ANP could be also involved in the regulation of the balance between synovial fluid and the other body fluids.

Atrial natriuretic peptide (ANP) is a polypeptide hormone mainly synthesized and excreted by cardiomyocytes of the heart of mammals (dog, rabbit, man) and non mammalian vertebrates, such as amphibians (1) and tunicates (2). However, ANP is not only a cardiac hormone since it plays a role in the function of many different organs such as brain (3), kidney (4), turbinate (5), lung (6), pancreas (7) and salivary glands (8, 9). It has been widely demonstrated that ANP plays an important role in electrolyte composition and regulation of the homeostasis of body fluids, such as the *humor aqueous* in the eye, the cerebrospinal fluid in the brain, the blood plasma and the saliva. Therefore ANP may be also involved in the regulation of synovial fluid. Synovial fluid is synthesized by synovial membrane and is poured into the articular cavity. Synovial fluid is an essential nourishment to the metabolism of articular cartilage by a mutual, continuous transport of molecules between the articular cartilage and the synovial fluid. Therefore, the articular cartilage plays an important role in the turnover of the synovial fluid.

Considering the above-described roles of ANP and the metabolism of the articular cartilage, we hypothesized that this peptide may be present in the articular cartilage and contribute to the turnover of the synovial fluid. This immunohistochemical study aims to investigate the presence of ANP and its localization in human articular cartilage.

MATERIALS AND METHODS

Specimens of articular cartilage were removed from the head of the femur of patients who underwent joint surgery for femoral neck fracture with no history of joint disease. All samples were immediately fixed in Bouin‘s fluid, dehydrated in graded alcohol and embedded in paraffin. Histological sections, 5-μm thick, were dewaxed

Key words: human articular cartilage, ANP, immunohistochemistry

Mailing address: Dr Elvira Farina,
Dipartimento di Medicina Sperimentale
e Neuroscienze Cliniche (BioNec),
Via del Vespro 129,
90127 Palermo, Italy
Tel.: +39 091 6553585
e-mail: farina.elviravitt@tiscali.it

0393-974X (2015)

DISCLOSURE: ALL AUTHORS REPORT NO CONFLICTS OF INTEREST RELEVANT TO THIS ARTICLE.

in xylene**,** rehydrated in a graded series of alcohols and then transferred into distilled water for 5 min. Immunostaining was performed using the DakoCytomation EnVision + System-HRP (AEC) kit from Dako (Dako, Glostrup, Denmark). Briefly, the sections were covered with the Peroxidase block reagent and incubated for 5 min at room temperature. The samples were rinsed once in PBS buffer pH 7.2. The sections were covered with or without rabbit anti-ANP polyclonal antibody (Chemicon, Temecula, CA, USA) and incubated at 4°C overnight. The antibody was diluted 1:800 in PBS containing 0.1% BSA. The samples were rinsed twice in PBS pH 7.2 and then incubated with Peroxidase labelled polymer reagent for 30 min. The samples were rinsed twice in PBS pH 7.2, incubated with the Substrate-Chromogen reagent and immediately observed under a light microscope; the reaction was continued until staining appeared (2–10 min). Reaction was stopped by rinsing the slides in distilled water. Negative control samples were treated in the same way except for the omission of the primary antibody. The slides were coverslipped using Dako Cytomation Faramount aqueous mounting medium. Finally, the immunostained sections were observed and photographed under a Leica DM1000 light microscope.

RESULTS

The histological sections showed that the human articular cartilage was composed of chondrocytes immersed in an extracellular matrix constituting a morpho-functional unit. The superficial zone was a thin layer, composed of flattened ellipsoid chondrocytes and parallel arrangement of the fibrils. The transitional zone had lower cell density with predominantly spheroid-shaped cells embedded in abundant extracellular matrix. The radial zone had the lowest cell density: cells were arranged perpendicular to the surface and were spheroidal in shape. The mineralized cartilage zone contained small amounts of cells embedded in a calcified matrix.

The ANP-immunostained sections showed that ANP was present in the human articular cartilage. In particular, ANP-immunoreactivity was detectable in all the layers of the cartilage; the chondrocytes in the intermediate and in the inner layers were faintly ANP-immunoreactive, while the extracellular matrix was unstained (Fig. 1). The superficial layer showed marked ANP-immunoreactivity and the chondrocytes showed a strong ANP-immuno reactivity in their whole cytoplasm (Fig. 2). Control samples resulted ANP-immunonegative (Fig. 3).

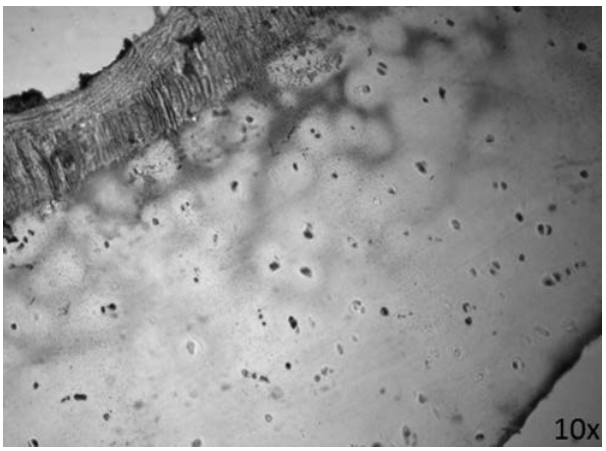

Fig. 1. *Human articular cartilage. ANP-immunopositive chondrocytes and ANP immunonegative matrix. Enhanced magnification 10X.*

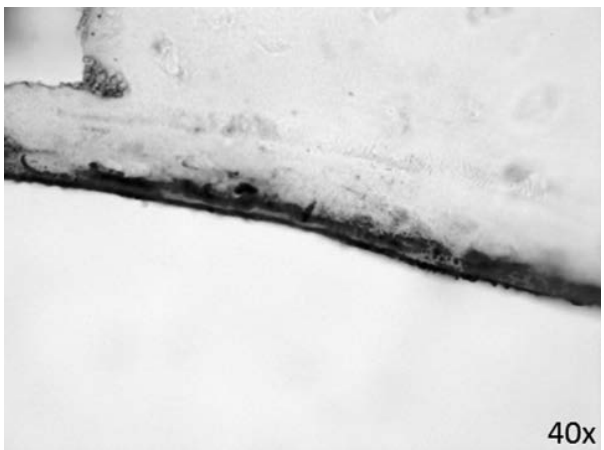

Fig. 2. *Human articular cartilage. Superficial layer with ANP-immunopositive chondrocytes. Enhanced magnification 40X.*

DISCUSSION

The articular cartilage covers the articular surfaces in bone ends. The articular cartilage is composed of chondrocytes included within an abundant extracellular matrix, which are responsible for the synthesis and maintenance of the extracellular matrix itself (10). The homeostasis of hyaline cartilage is

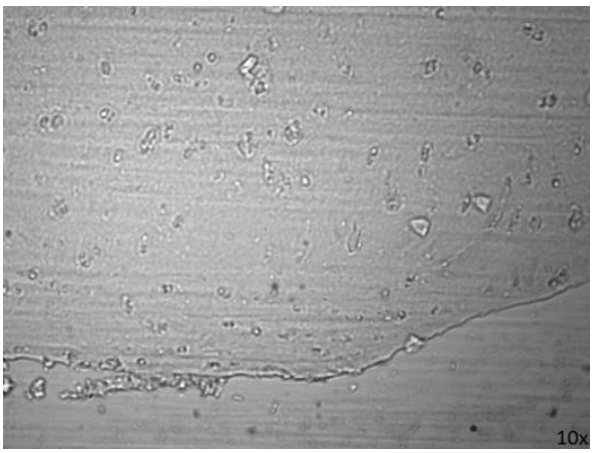

Fig. 3. *Human articular cartilage. Negative control is ANP-immunonegative. Enhanced magnification 10X.*

maintained mainly by chondrocytes through the interaction between collagen, proteoglycans, and interstitial fluid components (11).

The mechanical strength of the hyaline cartilage is determined by the marked hydrophylia of the extracellular matrix, the accumulation of interstitial fluid in the tissue and the balance between the macromolecular and aqueous phases.

The metabolic activity of chondrocytes is influenced by some physical and chemical factors, such as the ionic and osmotic environment of cartilage, which in turn alters the shape and volume of the resident cells (12). Chondrocytes respond to environmental changes in a well-coordinated and adaptive manner to changes in their environment. Ionic and osmotic changes in cartilage have been shown to alter cell morphology and affect the viscoelastic mechanical properties of these cells (13).

The mechanisms through which ionic and osmotic changes modulate the chondrocyte behavior are little known. Arg-vasopressin (VP) was found to be a stimulator of chondrocyte proliferation (14), while ANP was able to induce the synthesis of iNOS mRNA in human chondrocytes. Indeed, VP and ANP are known to be involved in the regulation of extracellular fluids and often co-exist in many organs playing antagonist roles.

This study first demonstrates that ANP immunoreactivity is present in human articular cartilage of the femoral head. The present results show that the whole superficial layer of the articular cartilage, including chondrocytes and extracelluar matrix, is strongly ANP-immunoreactive and that immunoreactive chondrocytes are localized in the middle and deep zone.

It has been widely demonstrated that ANP is involved in body fluid homeostasis and regulates the composition and metabolism of the secretive fluids, such as saliva (8, 9) and nasal mucus (5). We suggest that the presence of ANP in the articular cartilage could be correlated to its regulating role in the composition of extracellular fluids through the transport of ions and water from the cartilage to the synovial fluid and vice versa. Moreover, the presence of ANP could be involved in the modification of the permeability of the extracellular matrix, in the turn-over of the interstitial fluid and in the balance between the solid and liquid phases. Therefore, ANP could be capable of modifying both the electrolytic composition and concentration of articular cartilage and, consequently, to modulate its mechanical strength.

Since the articular cartilage is submitted to high working load, it may progressively degenerate and give rise to chronic degenerative joint disorders, such as osteoarthritis, characterized by the expression of extracellular matrix-degrading enzymes such as MMP-2 and MMP-9/gelatinases (15), it is possible that ANP could have an important role in both the prevention and treatment of these disorders. In this context, extrapolating the present findings, it is conceivable that ANP, and perhaps VP, may be involved in joint swelling and vasogenic edema and hydrarthrosis associated with synovial inflammation. Additional experiments are needed to determine whether the expression of these peptides may be altered in synovitis.

REFERENCES

1. Caso VH, Paz D, Ruiz G. Differentiation of endocrine myocardiocytes in developing heart of the toad (Bufo arenarum Hensel). Int J Dev Biol 1992; 36:537-42.
2. Lipari L, Gerbino A, Lipari D, Farina E. ANP (Atrial Natriuretic Peptide) presence in the heart of a tunicate, *Ciona intestinalis*. Folia Histochem Cytobiol 2010; 48(1):68-70.

3. Chriguer RS, Rocha MJ, Antunes-Rodrigues J, Franci CR. Hypothalamic atrial natriuretic peptide and secretion of oxytocin. Brain Res 2001; 889:239-42.
4. McKenzie JC, Scott J, Inagami T. Imunohistochemical localization of atrial natriuretic factor in the kidney, adrenal medulla, pituitary and atrium of rat. J Histochem Cytochem 1991; 33:928-32.
5. Valentino B, Lipari D, Restivo S, Speciale R, Gallina S, Farina Lipari E. Localization of the atrial natriuretic factor in the human inferior turbinates. An immunohistochemical study. Acta Otorhinolaryngol Ital 2003; 3:94-97.
6. Valentino B, Lipari D, Dieli F, Leone A, Farina E. Distribution of atrial natriuretic factor (ANF) in respiratory tract and lung showed by immunohistochemical and PCR methods. Dent Med Probl 2003; 40:17-22.
7. Chabot JG, Morel G, Kopelman H, Belles-isles M, Heisler S. Atrial natriuretic factor and exocrine pancreas autoradiographic localization of binding sites and ultrastructural evidence for internalization of endogenous ANF. Pancreas 1987; 2:404-13.
8. Carini F, Scardina GA, Lo Piccolo C, Lipari L, Ferrara S, Messina P. et al. ANF in the Parotid Gland in Rabbits. J Animal and veterinary advances 2012; 11(5):641-44.
9. Lipari L, Farina E, Buscemi M, Gerbino A. Atrial Natriuretic Peptide presence in parotid gland of human fetus at 13th week of development and in adult man. Folia Histochem Cytobiol 2013; 51(1):55-58.
10. Cohen NP, Foster RJ, Mow VC. Composition and dynamics of articular cartilage: structure, function, and maintaining healthy state. J Orthop Sports Phys Ther 1998; 28(4):203-15.
11. Tatari H. The structure, physiology, and biomechanics of articular cartilage: injury and repair. Acta Orthop Traumatol Turc 2007; 41(S):1-5.
12. Guilak F, Mow VC. The mechanical environment of the chondrocyte: a biphasic finite element model of cell-matrix interactions in articular cartilage. J Biomech 2000; 33(12):1663-73.
13. Trickey WR, Lee GM, Guilak F. Viscoelastic properties of chondrocytes from normal and osteoarthritic human cartilage. J Orthop Res 2000; 18(6):891-98.
14. Petersson M, Bucht E, Granbergz B, Stark A. Effects of arginine-vasopressin and parathyroid hormone-related protein (1e34) on cell proliferation and production of YKL-40 in cultured chondrocytes from patients with rheumatoid arthritis and osteoarthritis. OsteoArthritis and Cartilage 2006; 14:652e659.
15. Lipari L, Gerbino A. Expression of gelatinases (MMP-2,MM-9) in the human articular cartilage. Int J Immunopathol Pharmacol 2013; 26(3):817-23.

LETTER TO THE EDITOR

COMPARISON OF SALIVARY ANTIOXIDANT ENZYME ACTIVITY BETWEEN EX-SMOKERS AND SUBJECTS WHO HAD NEVER SMOKED

M.R. GIUCA[1], M. PASINI[1], S. D'ERCOLE[2], D. MARTINELLI[2], D. TRIPODI[2] and E. SPINAS[3]

[1]Department of Surgical, Medical, Molecular and Critical Area Pathology, University of Pisa, Pisa, Italy; [2]Department of Medical, Oral, and Biotechnological Sciences, Dental School, University "G. D'Annunzio" Chieti-Pescara, Chieti, Italy; [3]Department of Surgery Sciences, University of Cagliari, Italy

Received October 22, 2014 – Accepted February 4, 2015

Smoke contains oxidants such as oxygen-free radicals which are probably the major cause of damage to biomolecules. A decrease of salivary antioxidant enzymes was detected in habitual smokers. However, the effects of cigarette smoke on salivary antioxidant enzymes may persist after withdrawal from smoking. The objective of this study was to assess salivary superoxide dismutase (SOD) and glutathione peroxidase (GSH-Px) activity in ex-smokers in comparison with that of subjects who had never smoked. The test group included 25 ex-smokers (13 males and 12 females; mean age: 48±8 years) who had given up smoking for at least one year but for no more than 2 years, and a control group consisting of 25 subjects (14 males and 11 females; mean age: 50±12 years) who had never smoked. Salivary samples were collected and SOD and GSH-Px activity was measured. Student's *t*-test was used to evaluate differences between groups and significant differences were observed for $p < 0.05$. A significant decrease ($p< 0.05$) of GSH-Px (14.5±2) was observed in the test group compared to the control group (30±4). However, SOD was very similar in the two groups: 0.9±0.3 in the test group and 0.8±0.3 in the controls and no significant difference was detected ($p> 0.05$). Detoxification of hydrogen peroxide by the GSH-Px was altered even after withdrawal from smoking, while the production of hydrogen peroxide, that is mediated by SOD, was not modified.

Smoke consists of two states: the first is gas, and the second is aerosol. There are over four thousand chemicals in these fractions, including nicotine, carbon monoxide, tar (mixture of several substances, including nitrogen, oxygen, hydrogen, carbon dioxide, carbon monoxide, some polycyclic aromatic hydrocarbons, such as benzopyrene and dibenzantracene, and a wide range of volatile compounds) (1) .

Cigarette smoking is responsible for an extremely high proportion of deaths and chronic diseases in the western world, including coronary heart disease, emphysema, bronchitis and lung cancer (2-3).

Furthermore, smoking has various harmful effects on oral health including precancerous lesions and mouth cancer (4). Saliva is the first biological

Key words: cigarette smoke, saliva, antioxidants, enzymes

Mailing address: Dr Marco Pasini,
Department of Surgical, Medical,
Molecular and Critical Area Pathology,
University of Pisa,
Via Savi 10,
56126 Pisa, Italy
e-mail: dr.marcopasini@yahoo.it

0393-974X (2015)

fluid which comes into contact with inhaled cigarette smoke and has a highly protective function against deleterious agents such as microorganisms, toxins, and various oxidants (5) .

Smoke contains oxidants such as oxygen-free radicals and volatile aldehydes, which are probably the major cause of damage to biomolecules exposed to cigarette smoke (6). Free radicals are molecules or fragments of molecules characterized by the presence of an unpaired electron. (7) Therefore, they are highly reactive molecules, for their tendency to recover the doublet electronic link (8). At low concentrations, they function in physiological cell processes, but at high concentrations, they produce adverse modifications to cell components, such as proteins and DNA (9).

The human body has an antioxidant defense system able to counter the toxic activities of radical species. This system is formed by antioxidant enzymes such as superoxide dismutase, glutathione peroxidase and catalase, and non-enzymatic antioxidants like vitamins C and E, carotenoids, tiolic antioxidants including lipoic acid, glutathione and tioredoxine, flavonoids, and melatonin (10.)

The shift in balance between oxidant and antioxidant in favor of oxidants is called "oxidative stress" and may contribute to several pathological conditions such as periodontal disease and oral cancer (11).

It was observed that some salivary antioxidant enzymes were significantly lower in smokers than in non-smokers (12). However, the effects of cigarette smoke on salivary antioxidant enzymes may persist after withdrawal from smoking.

The objective of this study was to assess salivary superoxide dismutase (SOD) and glutathione peroxidase (GSH-Px) level in ex-smokers in comparison with that of subjects who had never smoked.

MATERIALS AND METHODS

Study population

In the present study, 50 healthy subjects were enrolled at the University Department of Odontostomatological Sciences. The aim of the study was explained to the patients and written consent was obtained after confirmation that they fully understood the survey. All procedures were conducted according to the principles expressed in the Declaration of Helsinki; this study was approved by the Ethics Committee. All recruited patients fulfilled the following criteria for participation in this study: absence of systemic disease and oral diseases, absence of metal or metal-ceramic crowns and fixed metal ceramic bridge prostheses, because of the possible release of metal ions into saliva.

The test group included 25 ex-smokers (13 males and 12 females; mean age: 48±8 years) who had given up smoking for at least 1 year but for no more than 2 years. These subjects were previously heavy smokers (they smoked at least 20 cigarettes per day).

The control group consisted of 25 subjects (14 males and 11 females; mean age: 50±12 years) who had never smoked in their entire life and were not exposed to passive smoke.

Salivary analysis

The saliva collection was performed by the same researcher and for each patient 3 cc of non-stimulated saliva was collected inside a test tube. We collected unstimulated whole saliva in order to minimize problems that may originate due to differences in the composition of saliva from the various salivary glands or as a result of changes that may occur with stimulation. Presence of oral injuries, oral diseases and blood contamination in saliva was excluded before collecting the salivary samples.

Sample collection was carried out at standardized times (at 9 A.M.) as salivary components have been observed to have independent diurnal rhythms (13). The samples were placed on ice, immediately after collection and then were centrifuged in the clinical analysis laboratory (14).

Enzyme activity was measured according to a specific assay: glutathione peroxidase enzyme activity was determined with test reagents of Randox RANSEL, while superoxide dismutase activity was measured by using the RANSOD kit.

Statistical analysis

Statistical package SPSS 15.0 was used for statistical analysis. Mean and standard deviation (SD) of superoxide dismutase and glutathione peroxidase activity were measured in the test and in the control groups. The student's *t*-test was used to evaluate differences between groups and significant differences were observed for $p < 0.05$.

RESULTS

The results of the present study showed a significant decrease of glutathione peroxidase enzyme activity in the test group of ex-smokers

compared to the control group (Table I).

In fact, in the test group the GSH-Px activity mean value was 14.5±2 while in the control group it was 30±4 and a significant difference of GSH-Px activity between the ex-smokers and persons who had never smoked was detected ($p< 0.05$). However, the superoxide dismutase activity was very similar in the two groups: 0.9±0.3 in the test group and 0.8±0.3 in the controls.

No significant difference of SOD activity was observed between the ex-smokers and the subjects who had never smoked ($p> 0.05$).

We next studied whether the enzyme activity differed according to sex. The GHS-Px activity in the test group did not show significant difference ($p> 0.05$) between males (14.4±3) and females (14.7±1.9). Furthermore, the mean values of GSH-Px in the males (29.9±3.4) and in the females (30.1±4.9) of the control group were very similar and no significant difference between the two subgroups was observed ($p> 0.05$) (Table II).

The salivary samples collected from the test group did not show a significant difference of the SOD activity between males (1±0.3) and females (0.8±0.2) ($p> 0.05$).

Also in the control group, no significant difference of SOD ($p> 0.05$) was detected between males (0.9±0.4) and females (0.7±0.2) (Table III).

DISCUSSION

Cigarette smoke is the major source of toxic materials, including oxygen free radicals, reactive species, that cause serious systemic damage and oral diseases such as oral carcinoma (3-4). However, the human body has defence systems against radicals, the so-called antioxidizing systems, which include enzymes such as glutathione peroxidase and

Table I. *Evaluation of GSH-Px and SOD activity in both groups.*

SALIVARY ENZYME	TEST GROUP	CONTROL GROUP	P VALUE
GSH-Px	14.5 ± 2	30 ± 4	< 0.05
SOD	0.9 ± 0.3	0.8 ± 0.3	N.S.

N.S: not significant

Table II. *Comparison of salivary GHS-Px activity between males and females of the two groups.*

GSH-PX	MALES	FEMALES	P VALUE
TEST	14.4±3	14.7±1.9	N.S.
CONTROLS	29.9±3.4	30.1±4.9	N.S.

N.S: not significant

Table III. *Comparison of salivary SOD activity between males and females of the two groups.*

SOD	MALES	FEMALES	P VALUE
TEST	1 ± 0.3	0.8 ± 0.2	N.S.
CONTROLS	0.9 ± 0.4	0.7 ± 0.2	N.S.

N.S: not significant

superoxide dismutase, which are found within the blood cells, in the plasma and in the saliva (15).

Oxidative stress occurs when the balance between antioxidants and reactive oxygen species (ROS) are disrupted, because of either depletion of antioxidants or accumulation of ROS. When oxidative stress occurs, cells attempt to counteract the oxidant effects and restore the redox balance by activation or silencing of genes encoding defensive enzymes, transcription factors, and structural proteins (16).

Most of the studies that have investigated the relationship between cigarette smoke and antioxidizing enzymes have focused on samples of plasma, red blood cells and white blood corpuscles, and agree in showing that cigarette smoke causes an alteration of antioxidant enzymes (17-18).

Recently, however, the antioxidizing enzyme system present in the saliva has attracted the attention of many researchers, since this is a very important defence mechanism for the oral cavity, especially against attack by free radicals due to cigarette smoke (19).

In some studies it was found that the mean levels of salivary superoxide dismutase and glutathione peroxidase were significantly lower in smokers than in non-smokers (20-21). In other studies a significant decrease was found of GHS-Px in smoking patients in comparison to non-smoking subjects but a significantly higher SOD level in non-smokers in comparison to the smokers. To explain this result, the authors suggested that the increased activity of superoxide dismutase acts as a defence system against oxidative stress generated during inflammation and this causes an overproduction of H_2O_2 (22-23). In the present study we found that the effects of cigarette smoke on salivary GSH-Px are still evident even after withdrawal from smoking. Thus, cigarette smoke may alter the detoxification of hydrogen peroxide by the GSH-Px even in ex-smokers (16). The GSH-Px catalyzes the reduction of hydrogen peroxide in the presence of glutathione; during the detoxification of H2O2 by GSH-Px, there is an increase in the consumption of reduced glutathione, which could therefore no longer be sufficient for the detoxification of the H_2O_2 in excess. H_2O_2 cannot be converted into water and the overproduction of H_2O_2 leads to an oxidative stress that is involved in a large number of diseases, such as cardiovascular diseases and neoplastic lesions (20-21). However, it is important to consider that the GHS-Px levels measured in previous studies in habitual smokers are lower than the levels measured in the ex- smokers of this study (24). This means that the effects of cigarette smoke on salivary antioxidant enzymes slightly decrease after withdrawal from smoking and maybe the benefits become more evident with the passage of time.

The main limitation of this study was the limited number of samples analyzed; for this reason, further studies are needed in order to increase the number of patients involved in the survey. According to the results found in this study, the level of activity of GSH-Px was significantly lower in the saliva of ex-smokers compared to non-smokers. Instead, no significant difference of SOD activity was observed between ex-smokers and non-smokers and no significant differences were observed between males and females of the two groups. It was observed that detoxification of hydrogen peroxide by the GSH-Px is altered even after withdrawal from smoking, while the production of hydrogen peroxide that is mediated by SOD is not modified. Moreover, a decrease of salivary antioxidants may lead to an oxidative stress that is involved in a large number of diseases, including precancerous and neoplastic lesions of the oral cavity.

REFERENCES

1. Baker RR, Pereira da Silva JR, Smith G. The effect of tobacco ingredients on smoke chemistry. Part I: Flavourings and additives. Food Chem Toxicol 2004; 42:S3-37.
2. Giuca MR, Pasini M, Tecco S, Giuca G, Marzo G. Levels of salivary immunoglobulins and periodontal evaluation in smoking patients. BMC Immunol 2014; 15:1-5.
3. Begum S. Molecular changes in smoking-related lung cancer. Expert Rev Mol Diagn 2012; 12:93-106.
4. Sasco AJ, Secretan MB, Straif K. Tobacco smoking and cancer: a brief review of recent epidemiological evidence. Lung Cancer 2004; 45:S3-9.
5. Cho HY, Reddy SP, Kleeberge SR. Nrf2 defends the lung from oxidative stress. Antioxid Redox Signal

2006; 8:76-87.
6. Edirisinghe I, Arunachalam G, Wong C, Yao H, Rahman A, Phipps RP, Jin ZG, Rahman I. Cigarette-smoke-induced oxidative/nitrosative stress impairs VEGF- and fluid-shear-stress-mediated signaling in endothelial cells. Antioxid Redox Signal 2010; 12:1355-69.
7. Aizenbud D, Peri-Front Y, Nagler RM. Salivary analysis and antioxidants in cleft lip and palate children. Arch Oral Biol 2008; 53:517-22.
8. Ekuni D, Endo Y, Irie K, Azuma T, Tamaki N, Tomofuji T, Morita M. Imbalance of oxidative/anti-oxidative status induced by periodontitis is involved in apoptosis of rat submandibular glands. Arch Oral Biol 2010; 55:170-76.
9. Watson J. Oxidants, antioxidants and the current incurability of metastatic cancers. Open Biol 2013; 3:120-44.
10. Moore S, Calder ACK, Miller JN, Rice-Evans AC. Antioxidant activity of the saliva and periodontal disease. Free Radic Res 1994; 21:417-25.
11. Giuca MR, Pasini M, Nastasio S, D' Ercole S, Tripodi D. Dental and periodontal complications of labial and tongue piercing. J Biol Regul Homeost Agents 2012; 26:553-60.
12. Nagler R, Lischinsky S, Diamond E, Drigues N, Klein I, Reznick A. Effects of cigarette smoke on salivary proteins and enzyme activities. Arch Bioch Bioph 2000; 379:229-36.
13. Chiappelli F, Iribarren FJ, Prolo P. Salivary biomarkers in psychobiological medicine. Bioinformation 2006; 29:331-34.
14. Gröschl M. Current status of salivary hormone analysis. Clin Chem 2008; 54:1759-69.
15. Bolzan AD, Bianchi MS, Bianchi NO. Superoxide dismutase, catalase and glutathione peroxidase activities in human blood: influence of sex, age and cigarette smoking. Clin Biochem 1997; 30:449-54.
16. Birben E, Sahiner UM, Sackesen C, Erzurum S, Kalayci O. Oxidative stress and antioxidant defense. World Allergy Organ J 2012; 5:9-19.
17. Kocyigit A, Erel O, Gur S. Effects of tobacco smoking on plasma selenium, zinc, copper and iron concentrations and related antioxidative enzyme activities. Clin Biochem 2001; 34:629-33.
18. Karincaoglu Y, Batcioglu K, Erdem T, Esrefoglu M, Genc M. The levels of plasma and salivary antioxidants in the patients with recurrent aphthous stomatitis. J Oral Pathol Med 2005; 34:7-12.
19. Yoshino F, Yoshida A, Wada-Takahashi S, et al. Assessments of salivary antioxidant activity using electron spin resonance spectroscopy. Arch Oral Biol 2012; 57:654-62.
20. Kanehira T, Shibata K, Kashiwazaki H, Inoue N, Morita M. Comparison of antioxidant enzymes in saliva of elderly smokers and non-smokers. Gerodontology 2006; 23:38-42.
21. Abdolsamadi HR, Goodarzi MT, Mortazavi H, Robat M, Ahmadi-Motemaye F. Comparison of salivary antioxidants in healthy smoking and non-smoking men. Chang Gung Med J 2011; 34:607-11.
22. Saggu TK, Masthan KMK, Dudanakar MP, Nisa SUI, Patil S. Evaluation of salivary antioxidant enzymes among smokers and nonsmokers. World J Dent 2012; 3:18-21.
23. Baharvand M, Maghami AG, Azimi S, Bastani H, Ahmadieh A, Taghibakhsh M. Comparison of superoxide dismutase activity in saliva of smokers and nonsmokers. South Med J 2010; 103:425-27.
24. Giuca MR, Giuggioli E, Metelli MR, Pasini M, Iezzi G, D'Ercole S, Tripodi D. Effects of cigarette smoke on salivary superoxide dismutase and glutathione peroxidase activity. J Biol Regul Homeost Agents 2010; 24:359-66.

LETTER TO THE EDITOR

WESTERN BLOT EXPRESSION OF 5-LIPOXYGENASE IN THE BRAIN FROM STRIPED DOLPHINS (*STENELLA COERULEOALBA*) AND BOTTLENOSE DOLPHINS (*TURSIOPS TRUNCATUS*) WITH OR WITHOUT ENCEPHALITIS/ MENINGO-ENCEPHALITIS OF INFECTIOUS NATURE

G. DI GUARDO[1], A. FALCONI[1], A. DI FRANCESCO[1], S. MAZZARIOL[2], C. CENTELLEGHE[2], C. CASALONE[3], A. PAUTASSO[3], C. COCUMELLI[4], C. ELENI[4], A. PETRELLA[5], C.E. DI FRANCESCO[1], A. SABATUCCI[6], L. LEONARDI[7], A. SERRONI[8], L. MARSILI[9], M.M. STORELLI[10] and R. GIACOMINELLI-STUFFLER[1]

[1]Faculty of Veterinary Medicine, University of Teramo, Teramo, Italy; [2]Department of Comparative Biomedicine and Food Science, University of Padova, AGRIPOLIS, Legnaro, Padua, Italy; [3]Istituto Zooprofilattico Sperimentale (IZS) del Piemonte, Liguria e Valle d'Aosta, Turin, Italy; [4]IZS del Lazio e della Toscana "M. Aleandri", Rome, Italy; [5]IZS della Puglia e della Basilicata, Foggia, Italy; [6]Faculty of Biosciences and Technology for Food, Agriculture and Environment, University of Teramo, Mosciano S. Angelo, Teramo, Italy; [7]Department of Biopathological Sciences and Hygiene of Animal and Alimentary Productions, University of Perugia, Italy; [8]IZS dell'Umbria e delle Marche, Perugia, Italy; [9]Department of Physical Sciences, Earth and Environment,University of Siena, Italy; [10]Department of Pharmaco-Biology, University of Bari, Italy

Received November 24, 2014 – Accepted January19, 2015

***Dolphin Morbillivirus* (DMV), *Toxoplasma gondii* and *Brucella ceti* are pathogens of major concern for wild cetaceans. Although a more or less severe encephalitis/meningo-encephalitis may occur in striped dolphins (*Stenella coeruleoalba*) and bottlenose dolphins (*Tursiops truncatus*) infected by the aforementioned agents, almost no information is available on the neuropathogenesis of brain lesions, including the neuronal and non-neuronal cells targeted during infection, along with the mechanisms underlying neurodegeneration. We analyzed 5-lipoxygenase (5-LOX) expression in the brain of 11 striped dolphins and 5 bottlenose dolphins, affected or not by encephalitic lesions of various degrees associated with DMV, *T. gondii* and *B. ceti*. All the 8 striped dolphins with encephalitis showed a more consistent 5-LOX expression than that observed in the 3 striped dolphins showing no morphologic evidence of brain lesions, with the most prominent band intensity being detected in a *B. ceti*-infected animal. Similar results were not obtained in *T. gondii*-infected vs *T. gondii*-uninfected bottlenose dolphins. Overall, the higher 5-LOX expression found in the brain of the 8 striped dolphins with infectious neuroinflammation is of interest, given that 5-LOX is a putative marker for neurodegeneration in human patients and in experimental animal models. Therefore, further investigation on this challenging issue is also needed in stranded cetaceans affected by central neuropathies.**

Key words: 5-lipoxygenase, neuroinflammation, infectious agents, striped dolphin, bottlenose dolphin

Mailing address:
Prof. Giovanni Di Guardo, DVM, Dipl. ECVP,
University of Teramo,
Faculty of Veterinary Medicine,
Piazza Aldo Moro 45, 64100 Teramo, Italy
Tel: +39 (0)861 266933 Fax: +39 (0)861 266865
e-mail: gdiguardo@unite.it

0393-974X (2015)

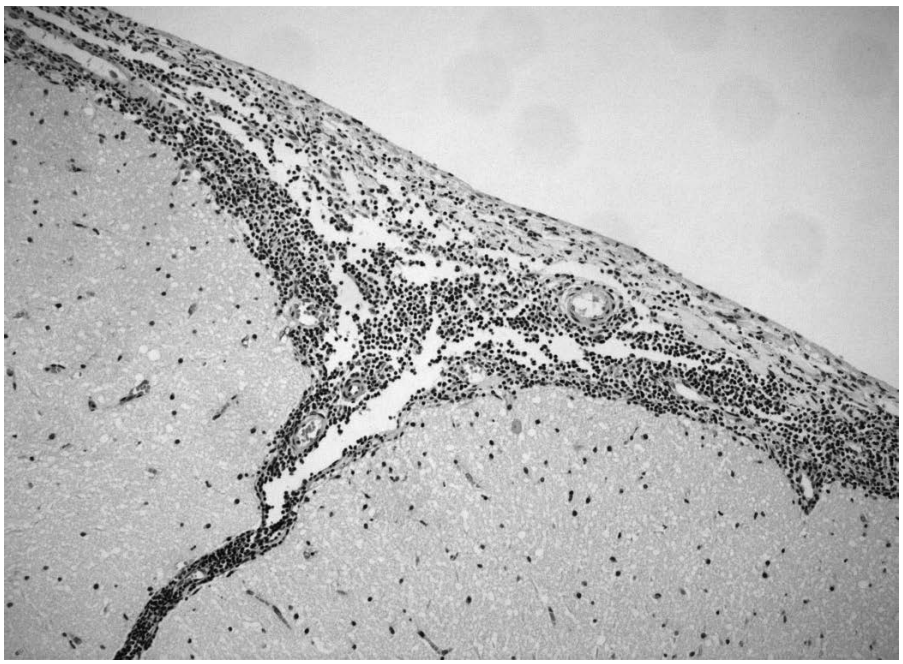

Fig. 1. *Striped dolphin (Stenella coeruleoalba). Brain. Brucella ceti infection (animal corresponding to WB lane 4 in Fig. 2). A prominent leptomeningeal, non-purulent inflammatory infiltrate is clearly shown. Haematoxylin and eosin (H&E) stain (20x objective; final magnification x 250).*

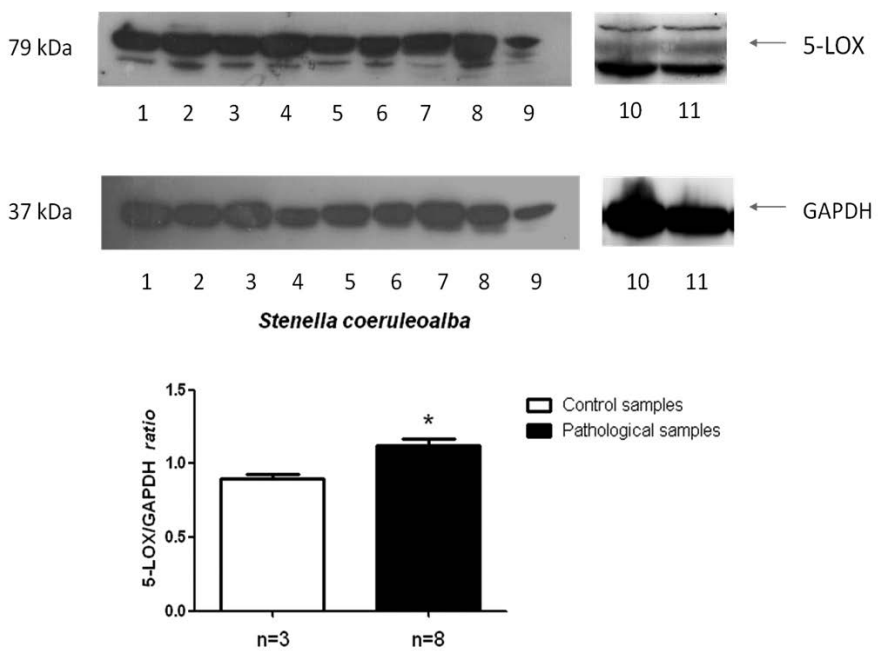

Fig. 2. *Western blot analysis of 5-LOX in brain tissue homogenates from striped dolphins (S. coeruleoalba). GAPDH was used as protein loading control. A greater intensity of 5-LOX bands is present in all the 8 animals affected by central infectious neuropathies (with special emphasis on the B. ceti-infected dolphin, lane 4), compared to the 3 unaffected control dolphins under study (lanes 1, 3, 10). The 5-LOX/GAPDH ratio is shown in the two histograms below, with a statistically significant difference (* $P < 0.05$) existing between the pathological and the control samples.*

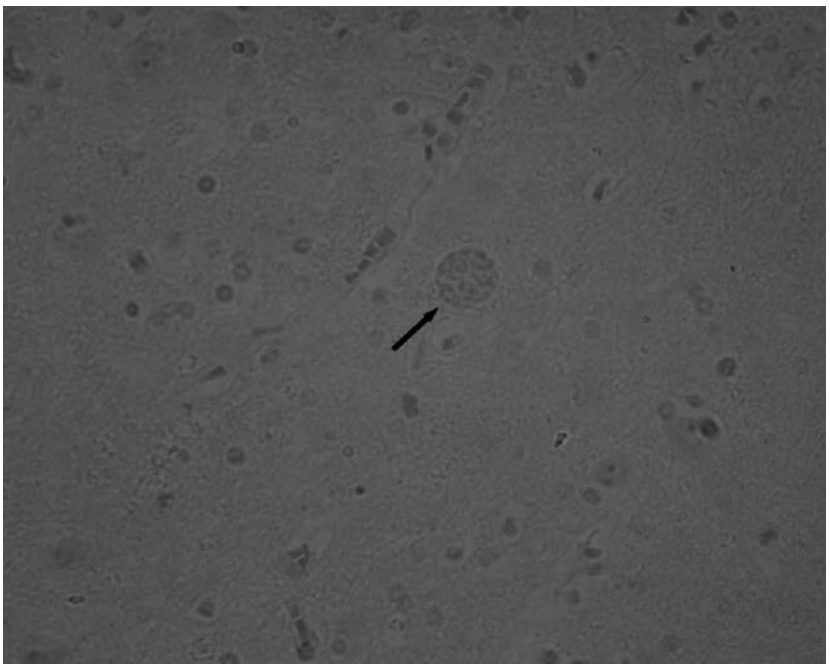

Fig. 3. *Bottlenose dolphin (Tursiops truncatus). Brain Toxoplasma gondii infection. (animal corresponding to WB lane 2 in Fig. 4). A mature protozoan cyst is shown (arrow), with no evidence of inflammatory reaction being observed in the surrounding cerebral parenchyma. H&E stain (40x objective; final magnification x 500).*

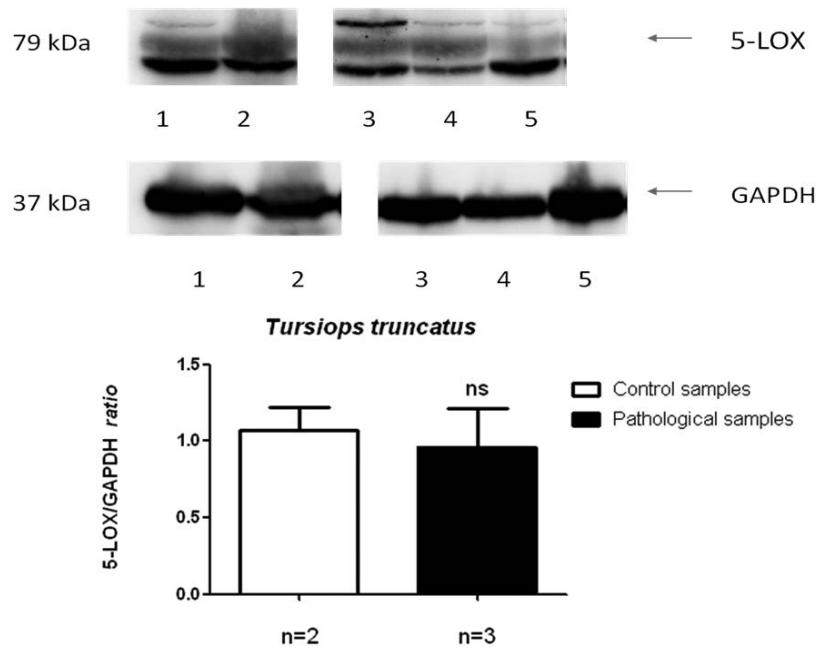

Fig. 4. *Western blot analysis of 5-LOX in brain tissue homogenates from bottlenose dolphins (T. truncatus). Differently from striped dolphins, no significant differences were found between T. gondii-infected (lanes 2, 4) and T. gondii-uninfected animals (lanes 1, 3, 5), as shown in the two histograms below. This likely represents the consequence of the much milder brain lesions seen in T. gondii-infected bottlenose dolphins, in comparison to T. gondii-infected striped dolphins.*

Dolphin Morbillivirus (DMV), *Toxoplasma gondii* and *Brucella ceti* are regarded as pathogens of major concern for both free-ranging striped dolphins (*Stenella coeruleoalba*) and bottlenose dolphins (*Tursiops truncatus*) (1). Although a more or less severe encephalitis/meningo-encephalitis is known to occur in striped dolphins and, to a lesser degree, in bottlenose dolphins infected by the aforementioned agents, very little information is available on the neuropathogenesis of brain lesions, including the neuronal and non-neuronal cells targeted during infection and the molecular mechanisms leading to neurodegeneration (2, 3).

With this in mind, we investigated by Western blot (WB) the expression of 5-lipoxygenase (5-LOX) - a key-enzyme in the pathogenesis of mammalian infections, such as porcine enzootic pneumonia and pleuropneumonia (4), and equine cyathostominosis (5) - in the brain tissue from 11 striped dolphins and 5 bottlenose dolphins, with 3 of the striped dolphins (corresponding to WB lanes 1, 3 and 10 in Fig. 2) and 3 of the bottlenose dolphins (corresponding to WB lanes 1, 3 and 5 in Fig. 4) under study showing no morphologic evidence of central neuroinflammation. The remaining 8 striped dolphins and 2 additional bottlenose dolphins exhibited encephalitic/meningo-encephalitic lesions of various extension and degree, ranging from focal to multifocal as well as from mild to severe, associated with DMV (1 striped dolphin, corresponding to WB lane 8 in Fig. 2), *T. gondii* (5 striped dolphins, corresponding to WB lanes 2, 5, 6, 7 and 11 in Fig. 2, along with 2 bottlenose dolphins, corresponding to WB lanes 2 and 4 in Fig. 4, respectively) and *B. ceti* (1 striped dolphin, corresponding to WB lane 4 in Fig. 2) infection, as well as with DMV-*T. gondii* coinfection (1 striped dolphin, corresponding to WB lane 9 in Fig. 2).

For WB analysis, total cell lysates were prepared by homogenizing 0.3 g of brain tissue from all dolphins in T-PER lysis buffer (PIERCE, Rockford, Il, USA) containing 1% NP-40 detergent solution, 5% glycerol, 1mM EDTA and 0.1% protease inhibitor cocktail (Sigma-Aldrich, Milan, Italy). Samples were sonicated and then centrifuged at 5,000 rpm for 30 min at 4°C. Protein concentrations were measured by the Bradford method. Equal amounts of total extracts (70 µg of protein) were electrophoresed on 9% acrylamide gels and transferred to PVDF membranes (Amersham Biosciences, Psicataway, NJ, USA). Membranes were saturated with a blocking solution of 5% non-fat dry milk and subsequently incubated with a purified mouse anti-5-LOX monoclonal antibody (MoAb) (1:1,000 in blocking solution; BD Biosciences, San Jose, Ca, USA) and a rabbit anti-GAPDH MoAb (1:5,000 in blocking solution; Cell Signaling, Danvers, Ma, USA). GAPDH was used to normalize samples. Finally, membranes were incubated with the following, horseradish peroxidase-conjugated, secondary Abs: anti-mouse Ab for 5-LOX (1:10,000 in blocking solution; Santa Cruz Biotechnology Inc., Ca, USA) and anti-rabbit Ab for GAPDH (1:2,000 in blocking solution; Santa Cruz Biotechnology Inc.). The antigen-antibody complex was detected by enhanced chemiluminescence reagents (Amersham Biosciences), with the intensities of immunoreactive bands being subsequently quantified by densitometric analysis through the ImageJ software (NIH, Bethesda, Maryland, USA). Data were expressed as mean ± SEM of 16 experiments. To determine statistical significance, Student's t-test was used for comparing the pathological and the control brain samples. P values less than or equal to 0.05 were considered to be statistically significant.

All the 8 striped dolphins affected by encephalitis/meningo-encephalitis (Fig. 1) showed an intensity of 5-LOX WB bands which was more pronounced than that observed in the 3 dolphins without any morphologic evidence of neuroinflammation, with a statistically significant difference ($P < 0.05$) existing between the pathological and the control samples and with the most prominent band intensity being detected in the *B. ceti*-infected animal (Fig. 2), which showed a severe meningitis. The same was not true for *T. gondii*-infected (Fig. 3) as compared to *T. gondii*-uninfected bottlenose dolphins, 1 of which had the most consistent 5-LOX band intensity (Fig. 4). Malacic areas, associated or not with cholesterol clefts, were seen scattered throughout this animal's brain (data not shown).

Based upon the results presented herein, the finding related to a higher expression of 5-LOX enzyme in the brain tissue of the 8 striped dolphins affected by infectious encephalitis/meningo-encephalitis appears to be of interest. In this respect, the positive correlation observed between the brain

inflammation's intensity and the expression levels of 5-LOX, as distinctly shown by the *B. ceti*-infected animal, which had a severe meningitis associated with the most prominent band intensity among the 8 striped dolphins under study, could be explained by a pathogen-driven, increased production of a set of cytokines playing a crucial role in host's anti-microbial immune response. Nevertheless, cell-mediated immune response to infectious agents needs to be properly controlled, in order to avoid damage to body tissues. Cytokines, such as interleukin (IL)-12, interferon (IFN)-gamma and tumour necrosis factor (TNF), albeit critical for host's resistance to a huge number of intracellular pathogens, may become harmful when expressed in an uncontrolled fashion (6). This is clearly exemplified, among others, by experimental models of *T. gondii* infection, in which IL-12-dependent production of IFN-gamma in immunocompetent mice is of key relevance for the control of both acute and chronic infection. Furthermore, prominent tissue damage associated with overproduction of the aforementioned proinflammatory cytokines has been observed in IL-10-deficient mice, in a similar manner to what reported in 5-LOX-deficient mice exposed to *T. gondii*, which, differently from *T. gondii*-infected wild-type mice, develop a lethal and severe form of encephalitis (7). While this information about the host's immune response to experimental *T. gondii* infection in mice is of concern, it is also of interest that, in the 8 encephalitis/meningo-encephalitis-affected striped dolphins investigated herein, we found a positive and statistically significant correlation between the occurrence of inflammatory lesions and the expression levels of 5-LOX, with an apparent correlation likely existing between the intensity of neuroinflammation and the densitometry values of the 5-LOX WB bands observed in the brain parenchyma of these animals. This appears to be true also for the 5 *T. gondii*-infected striped dolphins under study; a plausible explanation for such striking differences between the murine (7) and the natural model of *T. gondii* infection in the above cetaceans is missing. On the other hand, we believe it is of additional interest that the results obtained in our striped dolphins were not paralleled by a simultaneous increase of 5-LOX expression in the brain from *T. gondii*-infected in comparison to *T. gondii*-uninfected bottlenose dolphins. This most likely reflects the mutual host-parasite adaptation/coevolution existing in the bottlenose dolphin, a "coastal" species frequently exposed to *T. gondii*, as compared to the striped dolphin, a "pelagic" species much less commonly encountering such protozoan agent (8).

Notwithstanding the above, it should be emphasized that, albeit original, the results reported in the present work do not allow us to draw any definitive conclusion, which is mainly due to the limited number of brain lesion-affected and control animals included in our study.

Therefore, since 5-LOX - besides its crucial role in the pathogenesis of mammalian infections (4, 5) - is being increasingly regarded as a promising biomarker for neurodegeneration both in human patients (9) and in experimental animal models (10), further investigation on this challenging issue is also warranted in stranded cetaceans affected by central neuropathies.

ACKNOWLEDGEMENTS

We would like to thank the "Mediterranean Marine Mammals' Tissue Bank" (University of Padua; Scientific coordinator: Prof. Bruno COZZI) for kindly providing us with part of the brain tissue samples investigated herein.

This work was supported by a grant from the Italian Ministry for the Environment, in the framework of the Research Project entitled "Contaminanti ambientali e relativi effetti sul sistema nervoso centrale e sul sistema immunitario nei cetacei spiaggiati, le sentinelle del mare" (Scientific coordinator: Prof. Giovanni DI GUARDO).

REFERENCES

1. Van Bressem MF, Raga JA, Di Guardo G, et al. Emerging infectious diseases in cetaceans worldwide and the possible role of environmental stressors. Dis Aquat Organ 2009; 86:143-57.
2. Di Guardo G. *Morbillivirus*-host interaction: lessons from aquatic mammals. Front Microbiol 2012; 3:431 (doi:10.3389/fmicb.2012.00431).
3. Di Guardo G, Mazzariol S. *Dolphin Morbillivirus*: a lethal but valuable infection model. Emerg Microbes

Infect 2013; 2(11):e74 (doi:10.1038/emi.2013.74).
4. Giacominelli-Stuffler R, Marruchella G, Storelli MM, Sabatucci A, Angelucci CB, Maccarrone M. 5-lipoxygenase and cyclooxygenase-2 in the lungs of pigs naturally affected by enzootic pneumonia and porcine pleuropneumonia. Res Vet Sci 2012; 93:898-903.
5. Giacominelli-Stuffler R, Frangipane di Regalbono A, Traversa D, et al. The expression and activity of 5-LOX in the large intestine of horses with cyathostominosis. Vet Parasitol 2014; 203(1-2):96-101.
6. Shevach EM, Chang JT, Segal BM. The critical role of IL-12 and the IL-12R beta 2 subunit in the generation of pathogenic autoreactive Th1 cells. Springer Semin Immunopathol 1999; 21:249-62.
7. Aliberti J, Serhan C, Sher A. Parasite-induced lipoxin A4 is an endogenous regulator of IL-12 production and immunopathology in *Toxoplasma gondii* infection. J Exp Med 2002; 196:1253-62.
8. Di Guardo G, Mazzariol S. *Toxoplasma gondii*: clues from stranded dolphins. Vet Pathol 2013; 50:737.
9. Di Francesco A, Arosio B, Gussago G, Dainese E, Mari D, D'Addario C, Maccarrone M. Involvement of 5-lipoxygenase in Alzheimer's disease: a role for DNA methylation. J Alzheimers Dis 2013; 37:3-8.
10. Chu J, Giannopoulos PF, Ceballos-Diaz C, Golde TE, Pratico D. Adeno-associated virus-mediated brain delivery of 5-lipoxygenase modulates the AD-like phenotype of APP mice. Mol Neurodegener 2012; 7(1):1 (doi:10.1186/1750-1326-7-1).

LETTER TO THE EDITOR

SYSTEMIC EFFECTS OF LOCALLY INJECTED PLATELET RICH PLASMA IN A RAT MODEL: AN ANALYSIS ON MUSCLE AND BLOODSTREAM

P. BORRIONE[1], L. GRASSO[1], S. RACCA[2], G. ABBADESSA[2], V. CARRIERO[2], F. FAGNANI[1], F. QUARANTA[1] and F. PIGOZZI[1]

[1]Department of Movement, Human and Health Science, University of Rome "Foro Italico", Rome, Italy; [2]Department of Clinical and Biological Sciences, University of Turin, Turin, Italy

Received August 4, 2014 – Accepted February 5, 2015

Abundant evidence suggests that growth factors, contained in platelets alpha granules, may play a key role in the early stages of the muscle healing process with particular regard to the inflammatory phase. Although the contents of the platelet-rich plasma preparations have been extensively studied, the biological mechanisms involved as well as the systemic effects and the related potential doping implications of this approach are still largely unknown. The aim of the present study was to investigate whether local platelet-rich plasma administration may modify the levels of specific cytokines and growth factors both in treated muscle and bloodstream in rats. An additional aim was to investigate more deeply whether the local platelet-rich plasma administration may exert systemic effects by analyzing contralateral lesioned but untreated muscles. The results showed that platelet-rich plasma treatment induced a modification of certain cytokines and growth factor levels in muscle but not in the bloodstream, suggesting that local platelet-rich plasma treatment influenced directly or, more plausibly, indirectly the synthesis or recruitment of cytokines and growth factors at the site of injury. Moreover, the observed modifications of cytokine and growth factor levels in contralateral injured but not treated muscles, strongly suggested a systemic effect of locally injected platelet-rich plasma.

The repair response of musculoskeletal tissue generally starts with the formation of a blood clot and the following degranulation of platelets, which release locally growth factors (GFs) and cytokines (1). This microenvironment results in chemotaxis of inflammatory cells as well as activation and proliferation of local progenitor cells. Alpha granules are storage units within platelets, which contain pre-packaged GFs in an inactive form. Abundant evidence suggest that GFs, contained in platelet alpha granules, may play a key role in the early stages of the healing process with particular regard to the inflammatory phase being able to modulate the recruitment, duplication, activation and differentiation of the cells involved in the healing process (2-6). The efficacy of those GFs should be, in theory, directly proportional to their local concentration. This hypothesis is at the base of the use of platelet-rich plasma (PRP) in several circumstances, all of them characterized by the need of activating, modulating, speeding up or ameliorating the process of tissue repair.

With regard to sport medicine, doping related issues are still a matter of debate when considering this therapeutic approach for the treatment of sport-

Key words: platelet rich plasma, muscle injury, systemic effect, inflammatory phase

Mailing address: Dr. Paolo Borrione,
Department of Movement, Human and Health Science,
University of Rome "Foro Italico",
Piazza Lauro De Bosis 15,
00194 Rome, Italy
Tel.: +39 06 36733253, Fax: +39 06 36733344
e-mail: paolo.borrione@uniroma4.it

0393-974X (2015)

DISCLOSURE: ALL AUTHORS REPORT NO CONFLICTS OF INTEREST RELEVANT TO THIS ARTICLE.

related injuries, in particular because of the Insulin-like growth factor-1 (IGF-1) content in the platelet alpha granules as well as the blood manipulation procedures. With particular regard to the muscle injection of platelet-derived GFs, several issues still need to be clarified. Assuming that this procedure, as has been demonstrated by several studies, is able to ameliorate the muscle tissue repair processes, it is still unclear whether the locally injected concentrated amount of GFs may exert systemic effects. Indeed, although the contents of the PRP preparations themselves have been extensively studied (7-12), the biological mechanisms involved in treatment with PRP as well as its systemic effect with the related potential doping implications are largely unknown. In this regard, it has to be underlined that the World Anti-Doping Agency (WADA) prohibited the use of intramuscular injection of PRP in the 2010 list (13), then allowed its use in the 2012 list (14). This modification was introduced despite the suggested systemic effect of locally injected GFs described by some authors (7, 15). Banfi et al. measured the levels of some cytokines and GFs in the serum obtained from five male subjects 30 minutes, three hours and 24 hours after the treatment with PRP in order to evaluate the eventual systemic effect of this local injection. The authors reported significant modifications of Vascular Endothelial Growth Factor (VEGF), Epidermal Growth Factor (EGF) and Chemokine (C-C motif) Ligand 2 (CCL2) levels 30 minutes after the treatment, followed by a gradual return near to basal values 24 hours after the injection (15). Wasterlain et al. measured the levels of some GFs in the serum obtained from 25 subjects treated with leukocyte-rich PRP (LR-PRP). The authors reported significant increases of Insulin-like Growth Factor 1 (IGF-1), basic Fibroblast Growth Factor (bFGF) and VEGF levels following the local PRP injection (7).

With the exception of these two studies, the possible systemic effect of locally injected PRP is largely unknown. Conceivably, the systemic effect should be studied observing whether the treatment with PRP is able to modify the healing process in contralateral, but untreated with PRP, injured muscle, as suggested by Borrione et al. in a recent study (2).

The aim of the present study was to investigate whether the local PRP administration may modify the levels of specific cytokines and GFs both in treated muscle and bloodstream. The hypothesis at the base of this speculation was that the injection of cytokines and GFs naturally present in platelets and included in the WADA prohibited list could generate an increase of normal function, strength and capacity in non-injured muscles if a systemic effect is actually present.

MATERIALS AND METHODS

Animals and surgery

Adult male Wistar rats (n=60), 8-9 weeks old, weighing approximately 250 g, were used. Twenty-seven animals were sacrificed 2 days after surgery: seven rats were subjected to muscle injury on the right flexor muscles and immediately treated with PRP (treated group: TR); eight animals, used as controls, were subjected to the same muscle injury and left untreated (untreated group: UT); seven rats were subjected to muscle injury in both anterior limbs: the right limb was treated with PRP while the injury on the left limb remained untreated (contralateral group: CL). Five rats, left untreated and uninjured, were used as controls (C). Twenty-five animals were sacrificed 5 days after surgery (seven treated, seven untreated, six contralaterals and five controls). Eight animals were analyzed 30 days after surgery (two treated, two untreated, two contralaterals and two controls).

The animals were kept in cages in a room with controlled temperature and humidity, with light/dark cycle of 12/12h, and fed with food and water *ad libitum*. Animals underwent surgery under general anesthesia by intramuscular injection of tiletamine + zolazepam (Zoletil) 3mg/kg. The decision to treat all animals with Finadyne administered at a dose of 2.5 mg/kg/12h, independently of the presence of signs of suffering, was determined by the intention of obtaining the same condition in the different experimental settings since the use of anti-inflammatory drugs may affect both the healing process and the first inflammatory response (16). The surgical procedures were performed with the aid of a surgical microscope (Zeiss OPMI7, Jena, Germany). A longitudinal incision was performed on the right leg (or both legs) from the knee region to the ankle in order to access the flexor sublimis muscles of the upper joint of the digits. The muscle was then injured transversely and medially using a scalpel. The wedge-shaped lesion had a length of approximately 3 mm, a width of 2 mm and a depth of 3 mm. After the incision, the injury sites of the treated animals were immediately filled with PRP. The flexor muscles were withdrawn after 2, 5 or 30 days and analyzed. Animals were monitored daily to assess their state of wellbeing, to prevent self-

mutilation, skin ulcers, muscle contractures and suffering. All procedures were carried out in accordance with the Local Ethics Committee and the European Communities Council Directive of 24 November 1986 (86/609/EEC). All procedures were approved by the local Animal Care Committee and supervised by a veterinary physician.

Blood collection and PRP preparation

Blood was collected by intracardiac drawing. Briefly the needle (21G) was inserted at the base of the sternum at a 20° angle just lateral of the midline; 3-3.5 ml of blood were slowly aspirated in a syringe containing 1 ml of 3.8% sodium citrate as anticoagulant in order to avoid platelet activation and subsequent degranulation. Blood was then transferred in sterile tubes containing sodium citrate and underwent a first centrifugation at 220 g for 15 min. The top layer plasma was transferred, in another sterile tube without anticoagulant. To objectively determine the number of platelets and investigate the presence of other cells, before proceeding with the second centrifugation, a complete blood count was performed using a cell counter ADVIA 2021 (Bayer, Leverkusen, Germany) on a small amount of the plasma layer obtained after the first spin centrifugation (platelets content: 361.43±32.48 $x10^3/\mu l$; white blood cells content: 0.01±0.082 $x10^3/\mu L$). A second centrifugation at 1270 g for 5 min allowed the platelets to fall to the bottom of the tube. Most of the acellular plasma was removed and discarded. The pellet was re-suspended in 100 µL of plasma to obtain a concentration 4 times greater than the initial condition. This platelet-enriched preparation was activated with 20 µL of 10% calcium chloride (Braun, Melsungen, Germany, 1000 IE / ml CaCl2-2SG) at room temperature, and after jellification was immediately inserted using tweezers into the injured muscle of the same animals from which the blood had been drawn. The wound was then sutured and washed with saline solution (17-18).

Cytokines and growth factors

Blood samples were collected before surgery and animal sacrifice. Muscle samples (200-300 mg) were lysed in RIPA buffer (25 mmol/L Tris-HCl pH 7.6, 150 mmol/L NaCl, 1% NP-40, 1% sodium deoxycholate, and 0.1% SDS; Sigma Aldrich) supplemented with Halt™Protease Inhibitor Cocktail (Sigma Aldrich). Plasma and muscle tissue samples were analyzed by Milliplex plus kit (Millipore, Billerica, Massachusetts, USA) to quantify the levels of the following 10 molecules: Granulocyte-colony stimulating factor (G-CSF), Granulocyte-macrophage colony-stimulating factor (GM-CSF), Epidermal growth factor (EGF), Tumor necrosis factor alpha (TNF-α), Interleukin 1 alpha (IL1-α), Interleukin 4 (IL-4), Interleukin 5 (IL-5), Interleukin 6 (IL-6), Interleukin 10 (IL-10), Interleukin 13 (IL-13).

Statistical analysis

Cytokines and growth factors data were analyzed by two-way ANOVA analysis. Multiple comparisons were further performed with Bonferroni's post hoc test. The effects of the time for each cytokine and growth factor in each experimental condition were analyzed by one-way ANOVA. Differences were considered statistically significant when p-value < 0.05. All data are presented as mean ± SD. The small variation of the number of rats in the 2 day group and the 5 day group depended on accidental deaths, probably caused by intracardiac drawing or anesthesia.

RESULTS

Cytokines and growth factors analysis

In blood samples, the levels of all the investigated molecules remained unmodified in all the experimental conditions as well as in all the time points considered (data not shown).

IL-4, IL-6, IL-10, IL-1α, TNF-α and EGF showed significant modifications in treated and contralateral muscle samples. On the contrary, G-CSF, GM-CSF, IL-5 and IL-13 showed no modifications when compared to basal values.

IL-4

At day 2, TR, CL and UT showed lower values in comparison to C. The reduction was statistically significant only in TR (Table I). At days 5 and 30, TR showed a significant increase of IL-4 levels when compared to C and UT (Table I) while cytokine values in CL and UT remained lower in comparison to C. The increase in time of IL-4 levels in TR was statistically significant ($p<0.05$, one way-ANOVA).

The evaluation of data was supported by two-way ANOVA analysis that revealed significant effects for interaction ($F=5.975$; $p<0.001$), treatment ($F=7.346$; $p<0.001$) and time ($F=8.064$; $p<0.001$).

IL-10

Two days after surgery, IL-10 showed a significant peak in TR (Table I). The cytokine in CL showed a behavior similar to that observed in TR with higher values when compared to C, but the difference was not statistically significant. At 2 days, TR and CL values were higher in comparison to UT, whereas UT

Table I. *Cytokines and growth factors in muscles at 2, 5 and 30 days after surgery.*

IL-4	2 days	5 days	30 days	IL-10	2 days	5 days	30 days
C	4.05±0.95	4.13±0.33	3.96±1.7	C	0.63±0.34	0.64±0.34	0.60±0.23
UT	2.30±0.61*	3.41±0.72	3.29±1.33	UT	0.06±0.05**	0.02±0.01	0.30±0.03
TR	1.77±0.45*	6.24±1.92*##	7.06±2.78*##	TR	1.09±0.41**##	0.46±0.21	0.61±0.04
CL	3.45±0.61*	3.63±0.91	2.78±0.82	CL	0.93±0.26*##	0.16±0.08*	0.29±0.17
IL-1α	2 days	5 days	30 days	IL-6	2 days	5 days	30 days
C	0.96±0.21	0.74±0.24	1.20±0.20	C	6.08±2.17	6.07±3.1	5.99±1.9
UT	0.14±0.08	0.23±0.08	1.32±0.06	UT	17.53±4.61	1.59±0.53	0.85±0.5
TR	6.66±1.33**##	3.41±0.51**##	1.27±0.07	TR	327.02±40.9**##	165.22±65.11**##	0.69±0.43
CL	1.32±0.54	0.94±0.38	1.05±0.18	CL	298.51±6.4**##	1.55±0.93**	0.47±0.39
TNF- α	2 days	5 days	30 days	EGF	2 days	5 days	30 days
C	0.11±0.03	0.10±0.03	0.12±0.02	C	1.66±0.05	1.66±0.07	1.65±0.06
UT	0.03±0.01*	0.09±0.03	0.02±0.02*	UT	1.19±0.12**	1.14±0.18**	0.88±0.07**
TR	0.13±0.03#	0.31±0.10**##	0.02±0.02*	TR	0.73±0.08**##	0.86±0.11**	1.16±0.11**
CL	0.09±0.05	0.14±0.08	0.06±0.02	CL	0.79±0.13**##	0.94±0.12**	0.75±0.06**

*C: control group; UT: untreated group; TR: treated group; CL: contralateral group. Multiple comparison Bonferroni's test: * $p<0.05$ vs C; ** $p<0.01$ vs C; # $p<0.05$ vs UT; ## $p<0.01$ vs UT*

showed lower values when compared to C (Table I).

At day 5, IL-10 levels in TR and CL decreased, showing values lower than C (significant difference in CL). UT continued to show values lower than C (Table I).

Interestingly, IL-10 showed a trend, even if not statistically significant, toward a progressive increase in TR, CL and UT from day 5 to day 30 after surgery. Two-way ANOVA analysis showed significant effects for interaction ($F=5.618$; $p<0.001$), treatment ($F=20.39$; $p<0.0001$) and time ($F=13.14$; $p<0.0001$).

IL-1α

IL-1α showed a significant peak level at day 2 in TR in comparison to all the other groups. UT showed values lower than C while CL revealed values similar to C (Table I).

At 5 days after surgery, IL-1α levels decreased in TR maintaining otherwise higher values when compared to all the other groups (Table I).

At day 30 IL-1α values in TR reached the values found in C. The decrease of IL-1α values from day 2 to day 30 was statistically significant ($p<0.05$, one way-ANOVA). Two-way ANOVA analysis confirmed significant effects for interaction ($F=49.17$; $p<0.001$), treatment ($F=146.0$; $p<0.0001$) and time ($F=30.40$; $p<0.0001$).

IL-6

IL-6 showed a significant peak in TR and CL at day 2 when compared to C and UT respectively (Table I). IL-6 values in UT did not differ from those observed in C.

At day 5, the values in TR remained higher than in C and UT (Table I).

At 30 days after surgery, the cytokine values in TR decreased, showing values similar to all the other groups. The IL-6 decrease in TR and CL from day 2 to day 30 was statistically significant ($p<0.05$, one way-ANOVA). The evaluation of data was supported by two-way ANOVA analysis that showed significant effects for interaction ($F=95.24$; $p<0.001$), treatment ($F=179.2$; $p<0.0001$) and time ($F=277.0$; $p<0.0001$).

At day 2, TNF-α showed UT levels lower than in C ($p<0.05$). At day 5 TNF-α in TR was characterized by a significant peak level when compared to the other experimental groups. At day 30, UT, TR and CL presented values lower than in C (Table I). The variations in time of the values of TNF-α in TR and UT resulted significant ($p<0.05$, one way-ANOVA). Two-way ANOVA analysis showed significant effects for interaction ($F=11.16$; $p<0.001$), treatment ($F=14.72$; $p<0.0001$) and time ($F=29.07$; $p<0.0001$).

EGF levels in all injured muscles were significantly lower when compared to C values in all considered time points. In particular, at day 2 TR, CL and UT presented values lower than in C. UT levels were higher than those observed in TR and CL (Table I).

At day 5, the values detected in all injured muscles continued to remain lower than those observed in C without significant differences among them. These results were still present 30 days after surgery (Table I).

The comparison between EGF values in time in TR and UT groups showed two different trends. The UT values at day 30 were lower than those observed at days 2 and 5 ($p<0.01$, one way-ANOVA). On the contrary, EGF values in TR presented a progressive increase in the same time interval ($p<0.001$, one way-ANOVA). Two-way ANOVA analysis confirmed significant effect for interaction ($F=3.422$; $p<0.01$), treatment ($F=51.74$; $p<0.0001$) but not for the time.

DISCUSSION

The results of the present study showed that PRP treatment induced a modification of certain cytokines and GFs in muscle but not in the bloodstream, suggesting that local PRP treatment influenced directly or, more plausibly, indirectly the synthesis or recruitment of cytokines and GFs in the site of injury.

Since cytokines and GFs have a short half-life (15), we can hypothesize that cytokines and GFs present in the site of injury after 2, 5 and 30 days from PRP application, were not directly derived from PRP application (data confirmed by the absence of relevant data in bloodstream). Conceivably, the variation of cytokine and GF concentrations observed in muscles resulted from biosynthetic activity of other cells (e.g. macrophages/monocytes) recruited in the site of injury.

Moreover, the observed modifications of cytokine and GF levels in contralateral injured but not treated muscles strongly suggested a systemic effect of locally injected PRP. Indeed, several of the analyzed molecules, namely IL-1α, IL-4, IL-6, IL-10, TNF-α and EGF, showed a different behavior in the three different experimental conditions: treated, untreated and contralateral. In particular IL-1α, IL-4, IL-6, IL-10 and TNF-α showed a significant modification 2 and 5 days after PRP treatment.

The local increase of cytokines can be determined by different factors. It is known that the muscle healing process progresses through a constant series of overlapping phases (degeneration and inflammation, regeneration, remodelling) resulting in the restoration of the anatomic continuity and function (19). The first stage usually starts with the formation of a blood clot followed by the degranulation of platelets that release locally GFs and cytokines. The following phases are controlled by complex and dynamic molecular mechanisms involving local and systemic factors interacting with many different cell types recruited to the site of injury from the surrounding tissues and/or circulation (1). Generally, during the acute phase following a muscle injury, polymorphonucleated leukocytes are the most abundant cells present at the lesion site (19-22) and they are replaced by monocytes within the first days. Monocytes are then activated into macrophages and involved in the proteolysis and phagocytosis of the necrotic material (19, 23, 24). Previous studies demonstrated that PRP treatment increases the leukocyte infiltration in the injured

muscle (2). Conceivably, the higher concentration of macrophages in the muscles treated with PRP may easily explain the observed increased concentration of IL-1α in the treated group (25, 26). These data were confirmed by a recent study carried out by our group in which a significant increase was observed of NF-κB-p65 at 2-day post-injury. On the contrary, at 5-day post-injury, while in the PRP group the level of NF-κB-p65 was still significantly higher than in the C group, in the UT group the NF-κB-p65 protein returned to approximately the same level as in the C group. The trend of NF-κB-p65 was directly correlated to the IL-1α trend (18).

The amplification and modulation of the first inflammatory phase induced by PRP treatment may also be explained by the observed reduction of IL-10 levels following PRP injection. Indeed, the reduction of IL-10 levels results in an increased macrophage recruitment, consequently enhancing the inflammatory condition during the first 2 days following the treatment (27).

The observed increase of IL-4 and TNF-α levels at day 5 is a direct consequence of the amplification of the early inflammatory response. Indeed, macrophages recruited in the site of injury are subsequently activated, producing additional chemoattractors, thus resulting in an increased leukocyte recruitment in the site of injury. Conceivably, when considering the short half life of these cytokines, it could be assumed that the observed increased levels of IL-4 and TNF-α at day 5 after PRP treatment is the result of the synthesis of these cytokines by the leukocytes recalled in the site of injury. This hypothesis may explain the persistence of high levels of cytokines until 30 days after the treatment. Indeed, IL-4 is able to protect lymphoid cells from apoptosis (28, 29), thus favoring the persistence of the amplified inflammatory response. Furthermore, IL-6 levels were found increased only in treated and contralateral muscles but not in untreated samples. Conceivably, this finding supports the hypothesis of a stimulated IL-6 production by infiltrating lymphocytes and excludes its lesioned muscle origin. This observation strongly supports the conclusions of previous studies indicating that PRP injection induces an amplification and modulation of the early inflammatory response resulting in an increase of the inflammatory infiltration in the site of injury, data further confirmed by the present study (2, 18). Indeed, changes in cytokine values were predominantly recorded at day 2 and day 5 with gradual reduction at day 30 after surgery with the exception of IL-4 in the treated group. This evidence suggests that the inflammatory response in the treated group continued beyond 30 days after surgery, though to a lesser extent.

The hypothesis of a possible systemic effect of locally injected PRP preparation was also effectively confirmed by the results of the present study since several analyzed molecules such as IL-10, IL-6, TNF-α and EGF in contralateral muscles showed an intermediate behavior between treated and untreated samples. The observation that none of the analyzed molecules showed any statistically significant modification in the bloodstream following PRP local administration reinforces the hypothesis that certain, not yet identified, locally produced molecules may exert systemic effects capable of modifying the inflammatory response of contralateral injured but not treated muscles. The peculiarity of this investigation was to analyze "contralateral" muscles (the same animal was injured on both limbs and only one was treated with PRP while the other, the contralateral one, was left untreated) and observe whether the treatment with locally injected PRP, may influence the healing process even far from the site of injury. The results obtained using this experimental model strongly suggested that local PRP treatment may influence inflammatory responses even far from the site of injection. When considering its application on athletes, no evidence supports the hypothesis of possible action on non-injured muscles, thus excluding possible muscle performance enhancing properties. Certainly, the issue of the systemic effect of locally injected PRP preparation needs further investigation.

In conclusion, the results of the present study confirmed that PRP treatment influences the early inflammatory phase of the healing process. This observation may have an immediate clinical translation. Indeed, the demonstrated modulation of the inflammatory response may explain the pain reduction usually observed after PRP administration and accounting for the early mobilization of the patients (30). Moreover, it suggests that an early treatment after the injury may results in better clinical responses.

In literature, PRP has been studied *in vitro* and *in vivo* in the field of maxillofacial surgery and general surgery, and more recently in muscle and tendon healing but little is known about a possible systemic effect derived from the local use of PRP. Further experimental studies are needed in order to understand the biological mechanisms at the base of the inflammatory process following the local treatment with PRP preparations, focusing on which mediators exert systemic effect. For example, a microarray analysis could be useful to investigate how IL-1α, IL-4, IL-6, IL-10, TNF-α, EGF, IL-5 and IL-13 expression could be modulated in muscles. The easy reproducibility achieved in this study has allowed us to create a solid foundation on which future studies will be carried out in order to deeply understand the molecular dynamics of the inflammatory process modulated by PRP administration. A potential limitation of the present study was represented by the low number of animals analyzed 30 days after surgery (2 animals in each experimental condition). These data should be considered the result of a pilot study carried out in order to obtain useful indications for future analysis aimed to analyze the long-term effects of PRP preparations.

The little variation of number of rats in the 2 day group and the 5 day group depended on accidental deaths probably caused by intracardiac drawing or anesthesia.

ACKNOWLEDGEMENTS

This study was supported by a grant from World Anti-Doping Agency (WADA) and from the Italian Ministry of Health, Commission for the surveillance of Doping (CVD).

REFERENCES

1. Chargé SBP, Rudnicki MA. Cellular and molecular regulation of muscle regeneration. Physiol Rev 2004; 84:209-38.
2. Borrione P, Grasso L , Chierto E, et al. Experimental model for the study of the effects of platelet-rich plasma on the early phases of muscle healing. Blood Transfus 2014; 12(S):s221-8.
3. Foster TE, Puskas BL, Mandelbaum BR, Gerhardt MB, Rodeo SA. Platelet-rich plasma: from basic science to clinical applications. Am J Sports Med 2009; 37:2259-72.
4. Schnabel LV, Mohammed HO, Miller B, McDermott WG, Jacobson MS, Santangelo KS, Fortier LA. Platelet rich plasma (PRP) enhances anabolic gene expression patterns in flexor digitorum superficialis tendons. J Orthop Res 2007; 25:230-40.
5. Schmidt MB, Chen HE, Lynch SE. A review of the effects of insulin-like growth factor and platelet derived growth factor on in vivo cartilage healing and repair. Osteoarthr Cartil 2006; 14:403-12.
6. Best TM, Shehadeh SE, Leverson G, Michel JT, Corr DT, Aeschlimann D. Analysis of changes in RNA levels of myoblast and fibroblast-derived gene products in healing skeletal muscle using quantitative reverse transcription-polymerase chain reaction. J Orthop Res 2001; 19:565-72.
7. Wasterlain AS, Braun HJ, Harris AHS, Kim H-J, Dragoo JL. the systemic effects of platelet-rich plasma injection. Am J Sports Med 2013; 41:186.
8. Castillo TN, Pouliot MA, Kim HJ, Dragoo JL. Comparison of growth factor and platelet concentration from commercial platelet-rich plasma separation systems. Am J Sports Med 2011; 39(2):266-71.
9. Dragoo JL, Braun HJ, Durham JL, Ridley BA, Odegaard JI, Luong R, Arnoczky SP. Comparison of the acute inflammatory response of two commercial platelet-rich plasma systems in healthy rabbit tendons. Am J Sports Med 2012; 40(6):1274-81.
10. Eppley BL, Woodell JE, Higgins J. Platelet quantification and growth factor analysis from platelet-rich plasma: implications for wound healing. Plast Reconstr Surg 2004; 114(6):1502-8.
11. Harrison S, Vavken P, Kevy S, Jacobson M, Zurakowski D, Murray MM. Platelet activation by collagen provides sustained release of anabolic cytokines. Am J Sports Med 2011; 39(4):729-34.
12. Wasterlain AS, Braun HJ, Dragoo JL. Contents and formulations of platelet-rich plasma. Oper Techn Orthop 2012; 22(1):33-42.
13. WADA 2010. The World Antidoping Code. The 2010 Prohibited List. World Antidoping Agency. Montreal. Available at: http:// www.wada-ama.org/rtecontent/document/2010_prohibited_list_final_en_web.pdf. Accessed on 12/09/2012 .

14. WADA 2012. The World Antidoping Code. The 2012 Prohibited List. World Antidoping Agency. Montreal. Available at: http://www.wada-ama.org/Documents/World_ Anti Doping_Program/WADP-Prohibited-list/2012/WADA_Prohibited_List_2012_EN.pdf. Accessed on 12/09/2012.
15. Banfi G, Corsi MM, Volpi P. Could platelet rich plasma have effects on systemic circulating growth factors and cytokine release in orthopedic applications? Br J Sport Med 2006; 40:816.
16. Paoloni JA, Orchard JW. The use of therapeutic medications for soft-tissue injuries in sports medicine. Med J Aust 2005; 183:384-8.
17. Liu Y, Zhou Y, Feng H, Ma GE, Ni Y. Injectable tissue-engineered bone composed of human adipose-derived stromal cells and platelet-rich plasma. Biomaterials 2008; 29(23):3338-45.
18. Dimauro I, Grasso L, Fittipaldi S, et al. Platelet-rich plasma and skeletal muscle healing: a molecular analysis of the early phases of the regeneration process in an experimental animal model. PLoS One 2014; 23:9(7).
19. Hurme T, Kalimo H, Lehto M, Järvinen M. Healing of skeletal muscle injury: an ultrastructural and immunohistochemical study. Med Sci Sports Exerc 1991; 23:801-10.
20. Brickson S, Hollander J, Corr DT, Ji LL, Best TM. Oxidant production and immune response after stretch injury in skeletal muscle. Med Sci Sports Exerc 2001;33:2010-15.
21. Brickson S, Ji LL, Schell K, Olabisi R, St Pierre Schneider B, Best TM. M1/70 attenuates blood-borne neutrophil oxidants, activation and myofiber damage following stretch injury. J Appl Physiol 2003; 95:969-76.
22. Schneider BS, Sannes H, Fine J, Best T. Desmin characteristics of CD11b-positive fibers after eccentric contractions. Med Sci Sports Exerc 2002; 34:274-81.
23. Best TM, Hunter KD. Muscle injury and repair. Phys Med Rehabil Clin N Am 2000; 11:251-66.
24. Farges MC, Balcerzak D, Fisher BD, Attaix D, Bechet D, Ferrara M, Baracos VE. Increased muscle proteolysis after local trauma mainly reflects macrophage-associated lysosomal proteolysis. Am J Physiol Endocrinol Metab 2002; 282:E326-E335.
25. Hirsiger S, Simmen HP, Werner CM, Wanner GA, Rittirsch D. Danger signals activating the immune response after trauma. Mediators Inflamm 2012; 2012:315941.
26. Serrano AL, Mann CJ, Vidal B, Ardite E, Perdiguero E, Muñoz-Cánoves P. Cellular and molecular mechanisms regulating fibrosis in skeletal muscle repair and disease. Curr Top Dev Biol 2011; 96:167-201.
27. Li Y-H, Brauner A, Jonsson B, van der Ploeg I, Söder O, Holst M, Jensen J, Lagercrantz H, Tullus K. Inhibition of macrophage proinflammatory cytokine expression by steroids and recombinant IL-10 Biol Neonate 2001;80:124-32.
28. Zamorano J, Rivas M.D., Perez-G M. Interlukin-4 multifunctional cytokine. Immunologia 2003; 22:215-24.
29. Illera VA1, Perandones CE, Stunz LL, Mower DA Jr, Ashman RF. Apoptosis in splenic B lymphocytes. Regulation by protein kinase C and IL-4. J Immunol 1993 Sep 15; 151(6):2965-73.
30. Asfaha S, Cenac N, Houle S, et al. Protease-activated receptor-4: a novel mechanism of inflammatory pain modulation. Br J Pharmacol 2007; 150:176-85.

JOURNAL OF BIOLOGICAL REGULATORS & HOMEOSTATIC AGENTS Vol. 29, no. 1, 259-264 (2015)

LETTER TO THE EDITOR

THE HEME OXYGENASE/BILIVERDIN REDUCTASE SYSTEM IN SKIN CANCERS

V. ARENA[1], I. PENNACCHIA[1], G. GUERRIERO[2] and C. MANCUSO[3]

[1]Institute of Pathology, Catholic University School of Medicine, Rome, Italy; [2]Institute of Dermatology, Catholic University School of Medicine, Rome, Italy; [3]Institute of Pharmacology, Catholic University School of Medicine, Rome, Italy

Received September 24, 2014 – Accepted December 12, 2014

The heme oxygenase/biliverdin reductase (HO/BVR) pathway enhances cell stress response by degrading excess heme or producing antioxidant and cytoprotective molecules. Recently, members of the HO/BVR system have been proposed as biomarkers for the early diagnosis of free radical-related diseases. In this study, the presence of both the inducible and constitutive HO isoforms (HO-1 and HO-2, respectively) and BVR was evaluated by immunohistochemistry in human skin cancer samples. Moderate/strong immunoreactivities against HO-1, HO-2 and BVR were detected in 100% of the nodular malignant melanoma samples, whereas in basal cell carcinoma specimens these figures were 62%, 88% and 60%, respectively, with a faint/moderate degree of expression. Faint/moderate HO-1, HO-2 and BVR immunoreactivities were detected in 33%, 66% and 100% of melanocytic nevi samples, respectively. In conclusion, HO-1 and HO-2 and BVR were expressed in the cytosols of skin cancer cells, whereas perilesional normal epidermis showed only faint staining, thus leading to the hypothesis that the HO/BVR system is activated in skin cancers.

Heme oxygenase (HO) is a microsomal enzyme and catalyzes the oxidation of the alpha-meso-carbon bridge of heme moieties generating equimolar amounts of carbon monoxide, ferrous iron, and biliverdin. Two main isoforms of HO have been described, the first inducible (HO-1) and involved in the adaptive response to oxidative stress, the second constitutive (HO-2) and responsible for the physiologic turn-over of heme (1). Heme oxygenase is functionally coupled to the cytosolic enzyme biliverdin reductase (BVR), which reduces biliverdin to bilirubin, an endogenous molecule with strong antioxidant features (1).

Free radical generation is a common pathogenetic mechanism in skin diseases. An increased production of reactive oxygen species (ROS) was demonstrated in allergic contact dermatitis, psoriasis, acne and in skin cancers (2-4).

In recent years, HO-1 has been extensively studied as a disease-modifying protein in several free radical-induced diseases, including certain types of tumors (5, 6). Keeping this in mind, we decided to explore whether or not HO-1 is expressed in malignant skin cancers, such as basal cell carcinoma and nodular malignant melanoma. As a comparison, the more frequent benign skin lesions, such as melanocytic nevi, were studied. A qualifying feature of this work was the extension of the study also to HO-2 and BVR, the roles of which in free radical-induced diseases has not been completely explored

Key words: basal cell carcinoma, biliverdin reductase, heme oxygenase, nodular melanoma

Mailing address: Cesare Mancuso M.D., Ph.D.
Institute of Pharmacology,
Catholic University School of Medicine,
Largo F. Vito, 1 00168 Roma, Italy
Tel.: +39 06 30154367
Fax: +39 06 3050159
e-mail: cmancuso@rm.unicatt.it

0393-974X (2015)

DISCLOSURE: ALL AUTHORS REPORT NO CONFLICTS OF INTEREST RELEVANT TO THIS ARTICLE.

to date.

MATERIALS AND METHODS

Paraffin embedded skin samples from patients who underwent biopsy for nodular malignant melanoma (N=5, 4M/1F, average age 54 years), basal cell carcinoma (N=8, 4M/4F, average age 72 years) and melanocytic nevi (N=3, 2M/1F, average age 39 years) were obtained from the diagnostic Library of the Institute of Pathology of the Catholic University School of Medicine in Rome and analyzed for HO-1, HO-2 and BVR by standard immunohistochemistry. The following rabbit polyclonal antibodies were used: anti-HO-1 or anti-HO-2 (Enzo Life Sciences, Vinci-Biochem, Italy) both diluted 1:200 or anti-BVR (Sigma-Aldrich, Milan, Italy) diluted 1:400. Binding was visualised using biotinylated secondary antibody and the streptavidin-biotin peroxidase complex was developed with diaminobenzidine. Endogenous biotin was saturated using a commercial kit (Vector Laboratories; Burlingame, CA, USA). Finally, slides were counterstained with hematoxylin. Each sample was evaluated for HO-1, HO-2 and BVR expressions by two blinded pathologists and the intensity of immunostaining was expressed by the following scores: 0= absent; 1= faint; 2= moderate; 3= strong.

The procedure was performed in accordance with the Helsinki Declaration of 1975 and updates. Data were analyzed omitting subjects' identity and the results were referred only to accession numbers given in the laboratory, thus, the data was completely anonymous.

RESULTS

Heme oxygenase-1 was detected in 100% of nodular malignant melanoma and 62% of basal cell carcinoma samples analyzed. Of the 5 melanoma samples analyzed, HO-1 immunostaining was faint in 1 and moderate/strong in 4, whereas the signal was faint in the 5 basal cell carcinoma specimens positive for HO-1 (Figs. 1 and 2).

On the other hand, HO-2 was detected in 100% and 88% of nodular malignant melanoma and basal

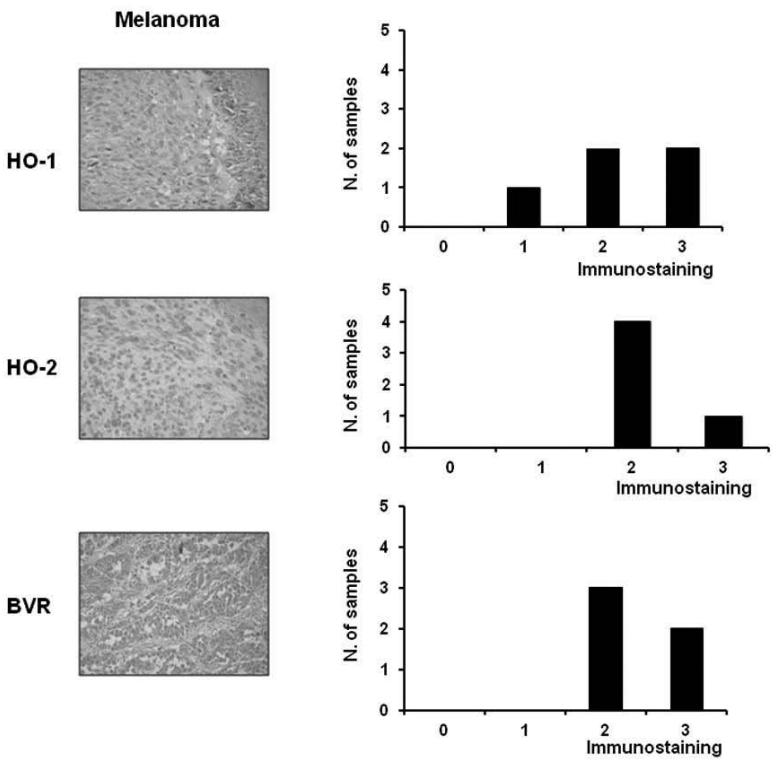

Fig. 1. *A representative panel showing diffuse cytoplasmic staining for HO-1, HO-2 and BVR in nodular malignant melanoma. Perilesional normal epidermis showed only faint staining. On the right, graphics with the semiquantitative scoring for HO-1, HO-2 and BVR.*

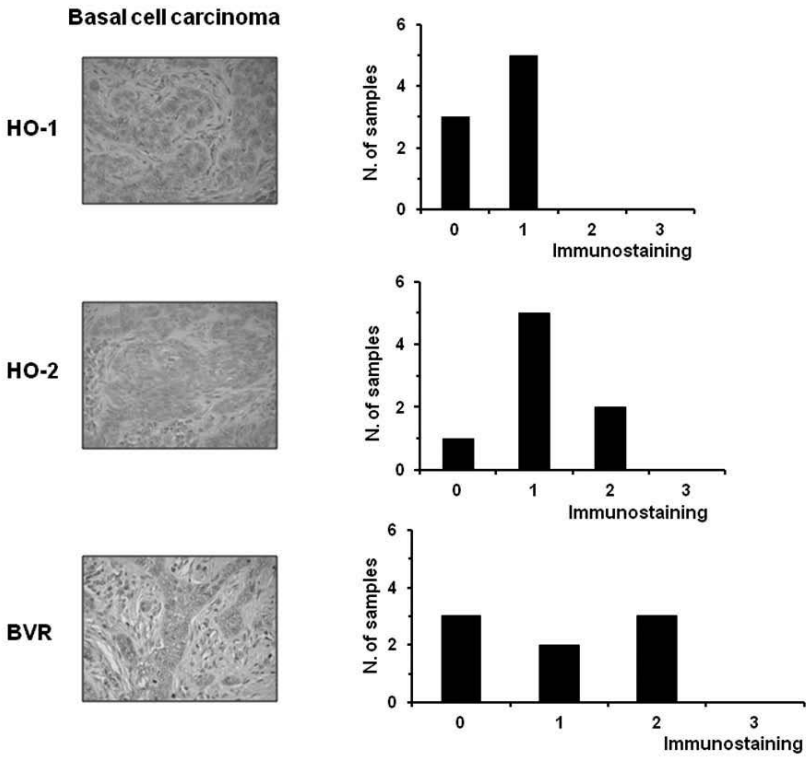

Fig. 2. *A representative panel showing diffuse cytoplasmic staining for HO-1, HO-2 and BVR in basal cell carcinoma. On the right, graphics with the semiquantitative scoring for HO-1, HO-2 and BVR.*

cell carcinoma specimens, respectively. Heme oxygenase-2 immunostaining was moderate in 4 out of 5 and strong in 1 out of 5 melanoma samples analyzed, but a faint signal (5 out of 8 samples) prevailed in basal cell carcinoma specimens (Figs. 1 and 2).

Finally, a similar pattern of expression was found for BVR, the enzyme being detected in 100% and 60% nodular malignant melanoma and basal cell carcinoma samples, respectively. Biliverdin reductase immunostaining detected a moderate/strong signal in all the melanoma samples analyzed, whereas in basal cell carcinoma the signal resulted faint or moderate in 2 out of 8 and 3 out of 8 specimens, respectively (Figs. 1 and 2). For melanocytic nevi, a faint HO-1 immunostaining was detected in 33% (1 out of 3) of specimens and a moderate HO-2 signal was found in 66% of samples (2 out of 3), respectively, whereas a faint/moderate BVR immunostaining was detected in all samples (Fig. 3). Indeed, HO-1, HO-2 and BVR immunoreactivity was primarily localized within the cytosolic compartment in all the specimens assayed (Figs. 1-3). A faint immunostaining for HO-1, HO-2 and BVR was observed in the perilesional normal epidermis.

Cytologically speaking, all nodular melanomas (Fig. 1) were characterized by a roundish collection of atypical melanocytes in the dermis with little or no adjacent intraepithelial components**.** Variable pagetoid spread of atypical melanocytes in the epidermis was seen, but it did not extend beyond the margins of the neoplasms. The dermal component was typified by a cohesive nodule or smaller nests of tumor cells that showed a pushing or expansive pattern of growth. A high mitotic rate was evident throughout the neoplasms and the cytological atypia was also remarkable. Basal cell carcinoma samples were composed of islands or nests of basaloid cells, with peripheral palisading and a haphazard arrangement of the more central cells; numerous mitotic figures, sometimes atypical, were

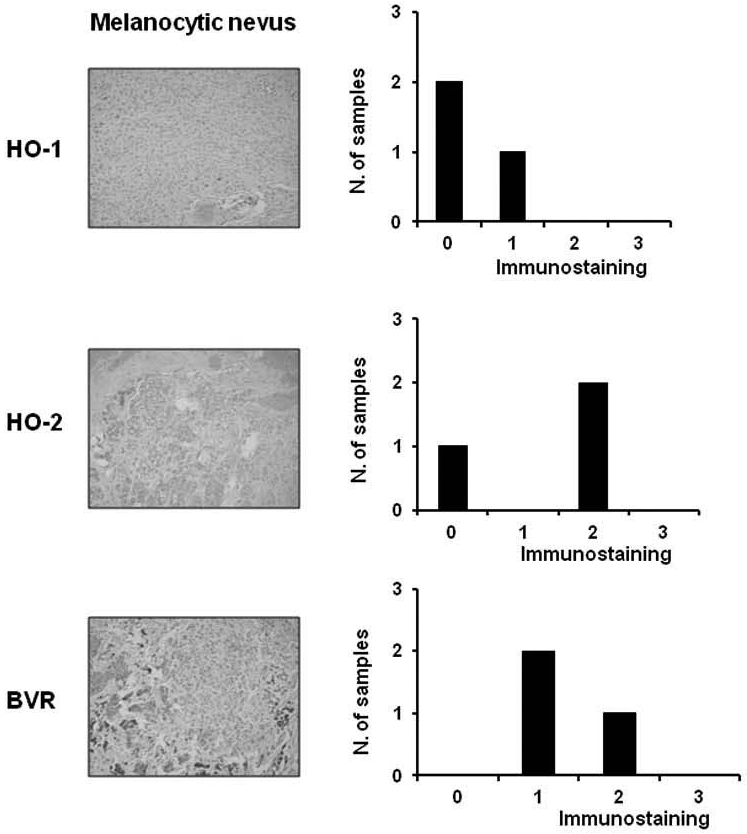

Fig. 3. *A representative panel showing diffuse cytoplasmic staining for HO-1, HO-2 and BVR in melanocytic nevi. On the right, graphics with the semiquantitative scoring for HO-1, HO-2 and BVR.*

seen throughout the neoplasms (Fig. 2). Tumor cells had a hyperchromatic nucleus with relatively scant and poorly defined cytoplasm (Fig. 2). All nevi consisted of a sharply defined proliferation of melanocytes arranged in nests and sheets both at the dermoepidermal junction and in the dermis (Fig. 3). Cells were monomorphous with small round nuclei, inconspicuous nucleoli and scant cytoplasm. Neither mitotic figures nor any other feature indicating malignancy were seen.

DISCUSSION

The data described in this study suggest that the HO/BVR axis could have a role in human skin cancers. As mentioned above, ROS production was shown to have a pathogenetic role in the onset and development of skin diseases, including melanoma and basal cell carcinoma (2, 4). In this light, it is arguable to hypothesize that the moderate/strong overexpression of both HO-1 and BVR detected in all the melanoma samples analyzed in the current research is secondary to an excessive free radical generation. Whether the up-regulation of HO-1/BVR system can affect the tumorigenesis or it is only an epiphenomenon in skin cancers is still matter of study. Was et al. (7) linked HO-1 up-regulation with melanoma neoplastic potential in mice, and Okamoto et al. (8) found a significant up-regulation of HO-1 in the neoplastic tissue of individuals suffering from malignant melanoma. This evidence is in good agreement with the results shown in this study in which moderate/strong HO-1 immunoreactivity was detected in all the nodular malignant melanoma samples analyzed (Fig. 1). This finding does not contradict the results of Jin et

al. (9) who found reduced HO-1 immunoreactivity in superficial spreading type, acral lentiginous type, lentigo maligna type and metastatic melanomas and it could reflect a different expression of HO-1 in tumor cells depending on the melanoma histological type. On the other hand, Shipp et al. (10) showed that HO-1 expression in the neoplastic tissue correlated with improved survival in patients affected by metastatic melanomas.

With regard to basal cell carcinoma, a faint/moderate HO-1/BVR up-regulation was found in about 60% of specimens tested. This result could imply a lower activation of the HO-1/BVR system, perhaps due to a milder free radical formation, in this type of cancer. The study of a possible correlation between free radical generation and HO-1/BVR activation in both nodular melanoma and basal cell carcinoma samples was fascinating, but was out of the aims of this paper because of technical difficulties due to the nature of the specimens available, these latter being paraffin-embedded tissues.

In this paper, also HO-2 was detected in basal cell carcinoma and nodular malignant melanoma samples and this evidence is rather novel. Dysregulation of the main metabolic pathways leading to porphyrin/heme biosynthesis was found in both preclinical and clinical experimental settings related to skin cancer research (11-13). On the basis of these findings, the detection of HO-2 in almost all the specimens of human malignant melanoma and basal cell carcinoma assayed, even if with a different degree of expression (moderate/strong in melanoma and faint in basal cell carcinoma samples, respectively), could reflect the main metabolic activity of HO-2 to degrade heme and, consequently, to prevent the formation of heme-driven secondary free radical species.

The presence of a faint expression of the HO-1/BVR system in melanocytic nevi was not a surprise and deals with the evidence that melanin synthesis is *per se* a potential source of ROS (14, 15). Therefore, the low degree of expression of both HO-1 and BVR in melanocytic nevi could be considered as an adaptive response of melanocytes to a "basic" free radical generation.

The limited number of samples analyzed does not allow us to conclude that overexpression of the HO-1/BVR system can be considered as a consistent biomarker for skin cancers. Although a larger number of samples should be necessary for such a conclusion together with *ad hoc* designed clinical studies, this paper has to be considered as a pilot study to put forth the possible role of both HO-1 and HO-2 and BVR in skin cancers. In addition, the adjuvant use of drugs which potentiate the up-regulation of the HO/BVR pathway (1) is a novel and promising approach to fight against skin cancers.

ACKNOWLEDGEMENTS

The Authors thank Paola Lanza for the precious technical support. This work was supported by 'Fondi Ateneo' to C.M. The authors state that they have no conflict of interest associated with this study.

REFERENCES

1. Mancuso C, Barone E. The heme oxygenase/biliverdin reductase pathway in drug research and development. Curr Drug Metab 2009; 10:579-94.
2. Belli R, Amerio P, Brunetti L, Orlando G, Toto P, Proietto G, Vacca M, Tulli A. Elevated 8-isoprostane levels in basal cell carcinoma and in UVA irradiated skin. Int J Immunopathol Pharmacol 2005; 18:497-502.
3. Bickers DR, Athar M. Oxidative stress in the pathogenesis of skin disease. J Invest Dermatol 2006; 126:2565-75.
4. Fruehauf JP, Trapp V. Reactive oxygen species: an Achilles' heel of melanoma? Expert Rev Anticancer Ther 2008; 8:1751-57.
5. Was H, Dulak J, Jozkowicz A. Heme oxygenase-1 in tumor biology and therapy. Curr Drug Targets 2010; 11:1551-70.
6. Zu X, Fan WG, Li DP, Lin MC, Kung H. Heme oxygenase-1 system and gastrointestinal tumors. World J Gastroenterol 2010; 16:2633-37.
7. Was H, Cichon T, Smolarczyk R, et al. Overexpression of heme oxygenase-1 in murine melanoma: increased proliferation and viability of tumor cells, decreased survival of mice. Am J Pathol 2006; 169:2181-98.
8. Okamoto I, Krögler J, Endler G, et al. A microsatellite polymorphism in the heme oxygenase-1 gene promoter is associated with risk for melanoma. Int J Cancer 2006; 119:1312-15.

9. Jin SA, Park JJ, Lee JB, Lee SC, Yun SJ. Decreased heme oxygenase-1 expression distinguishes human melanomas from melanocytic nevi. Pigment Cell Melanoma Res 2010; 23:841-44.
10. Shipp C, Weide B, Derhovanessian E, Pawelec G. Hsps are up-regulated in melanoma tissue and correlate with patient clinical parameters. Cell Stress Chaperones 2013; 18:145-54.
11. Fritsch C, Abels C, Goetz AE, Stahl W, Bolsen K, Ruzicka T, Goerz G, Sies H. Porphyrins preferentially accumulate in a melanoma following intravenous injection of 5-aminolevulinic acid. Biol Chem 1997; 378:51-57.
12. Lang K, Bolsen K, Stahl W, Ruzicka T, Sies H, Lehmann P, Fritsch C. The 5-aminolevulinic acid-induced porphyrin biosynthesis in benign and malignant cells of the skin. J Photochem Photobiol B 2001; 65:29-34.
13. Peng Q, Soler AM, Warloe T, Nesland JM, Giercksky KE. Selective distribution of porphyrins in skin thick basal cell carcinoma after topical application of methyl 5-aminolevulinate. J Photochem Photobiol B 2001; 62:140-45.
14. Pavel S, van Nieuwpoort F, van der Meulen H, Out C, Pizinger K, Cetkovská P, Smit NP, Koerten HK. Disturbed melanin synthesis and chronic oxidative stress in dysplastic naevi. Eur J Cancer 2004; 40:1423-30.
15. Smit NP, van Nieuwpoort FA, Marrot L, Out C, Poorthuis B, van Pelt H, Meunier JR, Pavel S. Increased melanogenesis is a risk factor for oxidative DNA damage--study on cultured melanocytes and atypical nevus cells. Photochem Photobiol 2008; 84:550-55.